



MONASH University

**Concise Access to Heteroacenes and Cyclopentanoids through
Alkyne Activation: sp to sp^2 to sp^3 Conversions**

Hanson Yu Leuk Law
BPharmSc(Hons)

A thesis submitted for the degree of (*Doctor of Philosophy*) at
Monash University in 2019
Medicinal Chemistry, Monash Institution of Pharmaceutical Science

Copyright notice

© The author (2019).

I certify that I have made all reasonable efforts to secure copyright permissions for third-party content included in this thesis and have not knowingly added copyright content to my work without the owner's permission.

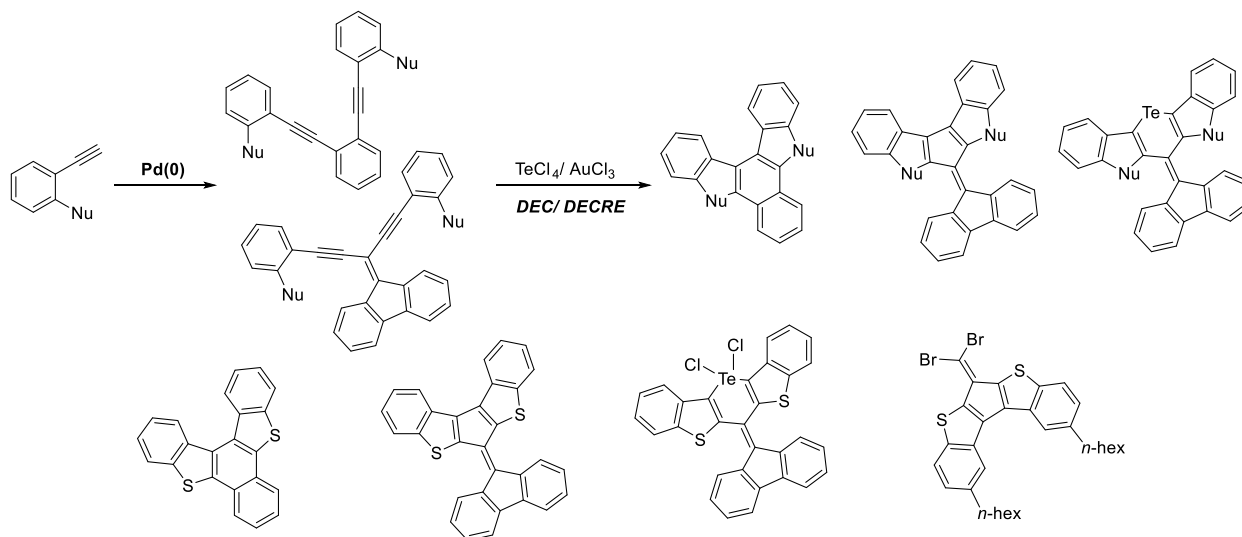
Table of Contents

Abstract.....	iii
Declaration.....	v
Acknowledgements.....	vi
Abbreviation and acronyms.....	vii
1. Introduction.....	1
1.1 Simple alkyne as building blocks to both sp^2 - and sp^3 -rich products	1
1.2 π -Rich heteroacenes and their contribution towards materials science	2
1.3 Electrophilic cyclization of activated alkynes	3
1.3.1 The recent emergence of electrophilic cyclization on activated alkynes.....	3
1.3.2 The development of Double-Electrophilic Cyclization (DEC).....	6
1.3.3 Transition metal directed electrophilic cyclization	8
1.4 Aim 1: The elaboration of DECRE reaction, towards complex angular heteroacenes	15
1.5 Conversion of alkyne to multiple 4° -stereocentres containing compounds in drug discovery	17
1.5.1 Interest in sp^3 -rich compound synthesis	17
1.5.2 Synthesis of compounds containing contiguous all-carbon 4° -stereocentres.....	19
1.5.3 Synthetic strategies towards sp^3 -rich compounds.....	20
1.6 The Nazarov cyclization.....	21
1.6.1 Promoting the Nazarov reaction	22
1.6.2 Auxiliary groups as master controllers of reactivity and torquoselectivity	24
1.6.3 Chiral catalysis.....	29
1.6.4 The interrupted Nazarov cyclization	31
1.7 Aim 2: Synthesis of sp^3 -rich cyclopentanoids via torquoselective asymmetric Nazarov cyclization	35
2. Result and discussion: Synthesis of angular heteroacenes via Double-Electrophilic Cyclization Reductive Elimination (DECREE) reaction	36
2.1. Preliminary study	38
2.2. $AuCl_3$ -induced tandem-cyclization reductive elimination	41
2.3. Application of DECRE and DEC in the synthesis of fulvalene derivatives.....	46
2.4. Synthesis of extended angular heteroacenes	49
2.5 Conclusion and future work	56
3. Result and discussion: Chiral oxazolidinone promoted Nazarov cyclization, towards the formation of multiple all-carbon 4°-stereocentres containing cyclopentanoids.....	58
3.1 The enantioselective synthesis of the bridged-cyclopentanoids.....	60
3.2 Preparation and the Nazarov cyclization of highly substituted Nazarov substrates.....	64

3.3 The synthesis of fully substituted divinyl ketones and the Nazarov cyclization to form vicinal 4°-stereocentres.....	68
3.4 The formation of fused-bridged ring structure via [4+3]-cycloaddition	80
3.5 Conclusion and future work	85
4. Experimental	87
4.1 Experimental for Chapter 2.....	89
4.2. Experimental for Chapter 3.....	105
4.3 X-ray crystallography structure.....	133
5. References	135
6. Appendices.....	140
6.1 Appendices A- NMR data	140
6.2 Appendix B- published journal article	229
6.3 Appendices C- X-ray crystallography data.....	246

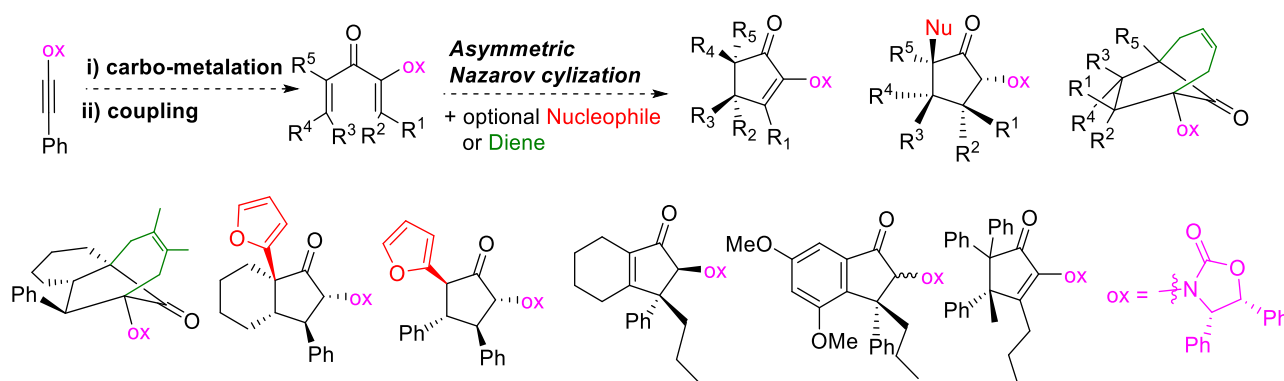
Abstract

The current research within materials and medicinal science rely on convergent synthesis towards sp^2 - and sp^3 -rich molecules to improve the productivity towards multi kilogram-scale synthesis of related materials. This thesis, therefore, expands the synthetic scope towards π -rich and sp^3 -rich molecules, via Double-Electrophilic Cyclization Reductive Elimination (**DECRe**) and asymmetric Nazarov cyclization, respectively.



Scheme 1. The investigation of angular heteroacenes synthesis via **DECRE** (**Chapter 2**).

Angular heteroacenes serve as the important source of active photonic materials in materials science area of research. **Chapter 2** of this thesis describes the elaboration of our newly developed novel chemistry, Double-Electrophilic Cyclization Reductive Elimination (**DECRe**), using AuCl₃. In this investigation, we were able to address the limitation and scope in the synthesis of angular heteroacenes using our DECRe approach (**Scheme 1**).



Scheme 2. The investigation of bridged cyclopentanoids synthesis via the torquoselective asymmetric Nazarov cyclization (**Chapter 3**).

The Nazarov cyclization is a convenient reaction that allows access into sp^3 -rich cyclopentanoids. Previous examples from our group have demonstrated the enantioselective synthesis of multiple all-carbon 4°-stereocentres containing cyclopentanoids, via the torquoselective asymmetric Nazarov cyclization. However, the enantioselective synthesis of bridged cyclopentanoids remains to be a challenge and has yet to be explored. **Chapter 3** of this thesis provides a detailed investigation in the enantioselective synthesis of multiple all-carbon 4°-stereocentres containing bridged cyclopentanoids, with the aid of chiral auxiliary oxazolidinone (ox) to provide torquoselectivity during the Nazarov cyclization.

Declaration

This thesis is an original work of my research and contains no material which has been accepted for the award of any other degree or diploma at any university or equivalent institution and that, to the best of my knowledge and belief, this thesis contains no material previously published or written by another person, except where due reference is made in the text of the thesis.

Signature:

Print Name:Yu Leuk Law.....

Date:06/11/2019.....

Acknowledgements

First, I would like to thank Associate Professor Bernard Flynn, who has taken me under his supervision, providing such a fantastic and valuable opportunity to work in his laboratory. The guidance he has provided, including the knowledge in chemistry, is something that I would not be able to obtain from elsewhere. He has been incredibly supportive along my PhD journey, his solutions to problem-solving have been exceptionally inspiring, meanwhile building up my confidence at synthetic and medicinal chemistry.

I want to express my gratefulness to my girlfriend, Alexa Wong, who has supported me throughout my whole PhD journey. Her support has gotten me through things that I thought were impossible to accomplish. I am very thankful for her embracement with my mood swing, and always believe and support every decision that I've made so far. I could not have reached where I am now without her love and mental support.

To my sisters Penn and Denise Law, they have been the most important people that my life has given me. Thank you for always believing in me, allowing myself to chase after my ambition. Special thanks to my parents Vincent Law and Shirley Lai, for all the mental and financial support along my life journey, and having faith in me, allowing myself to chase after my dream without hesitation. For that, I am incredibly grateful.

To all the current and previous members within our group, Cassandra, Giang, Akhil, Carmen, Murray, Xu, Annaliese, Bai, Caely, Vanessa, Dorothy, Ahmad, Rajinder and Shu Xin. Thank you for all the patience and help you have given. I would like to particularly thank Dr Rohan Volpe for teaching me all the knowledge in chemistry and experimental skills, where it has been the most valuable and indispensable skills for my future.

And to the PhD cohort, Cassandra Yong, Jisook Lee, Mitchell Silk and Mathew Bentley. You have made my PhD journey very enjoyable. And I sincerely appreciate all the support and suggestions you have given. Special thanks to Cassandra Yong, who provided a tremendous amount of assistance in organizing my thesis.

Last but not least, I would like to send my gratitude to my co-supervisor, Dr Lou Aurelio, as well as panel members, Dr Ben Capuano, A/Prof Bim Graham and Prof. Philip Thompson. The advice they have provided has undoubtedly made a positive impact on my work around my thesis. I would also like to appreciate Prof. Jonathan White for obtaining X-ray crystallography, Dr Elizabeth Krenske for related computational study and Dr Jason Dang for all analytical data support and giving exceptional guidance in compound assignment.

Abbreviation and acronyms

[O]	oxidation
α	alpha
β	beta
σ	sigma
π	pi
μL	microlitres
μM	micromolar
δ	chemical shift
$^{\circ}\text{C}$	degrees Celsius
^{13}C NMR	carbon nuclear magnetic resonance
^1H NMR	hydrogen (proton) nuclear magnetic resonance
^{125}Te NMR	tellurium nuclear magnetic resonance
^{19}F NMR	fluorine nuclear magnetic resonance
2D NMR	two-dimensional nuclear magnetic resonance
3D	three dimensional
1 $^{\circ}$	primary
2 $^{\circ}$	secondary
3 $^{\circ}$	tertiary
4 $^{\circ}$	quaternary
aq.	aqueous
Ac	acetyl
ADME	absorption, distribution, metabolism, excretion
Au	gold
br	broad
Boc	<i>tert</i> -butoxycarbonyl
Bu	butyl
calcd.	calculated
conc.	concentrated
CuTC	copper(I)-thiophene-2-carboxylate
d	doublet
dppf	1,1'-Bis(diphenylphosphino)ferrocene
dr	diastomeric ratio

DCE	1,2-dichloroethane
DCM	dichloromethane
DFT	density functional theory
DIPA	diisopropylamine
DIPEA	<i>N,N</i> -diisopropylethylamine
DMAc	dimethylacetamide
DMF	dimethylformamide
DMP	Dess-Martin Periodinane
DMSO	dimethylsulfoxide
e ⁻	electron
eq.	equivalents
ee	enantiomeric ratio
Et	ethyl
EDG	electron donating group
EWG	electron withdrawing group
Fsp ³	fraction of sp ³ -hybridized centres in a molecule
g	grams
Ge	germanium
h	hours
hex	hexyl
HOMO	highest occupied molecular orbital
HPLC	high performance liquid chromatograph
HRMS	high resolution mass spectrometry
<i>i</i> -Pr	<i>iso</i> -propyl
LCMS	liquid chromatography mass spectrometry
LDA	lithium diisopropylamide
LUMO	lowest unoccupied molecular orbital
LiNp	lithium naphthalenide
<i>m</i> -CPBA	<i>meta</i> -Chloroperoxybenzoic
mg	milligrams
min	minutes
mL	millilitres
mmol	millimoles
M	molar
Me	methyl

MP	melting point
Ms	methanesulfonyl
MeSO ₃ H	methanesulfonic acid
Nu	nucleophile
NBS	N-bromosuccinimide
NEt ₃	triethylamine
nOe	nuclear Overhauser effect
NOESY	nuclear Overhauser enhancement spectroscopy
<i>o</i>	<i>ortho</i>
TBS	<i>tert</i> -butyldimethylsilyl
Tf	trifluoromethanesulfonyl
p	pentet
Pd	palladium
Ph	phenyl
Pr	propyl
PivOH	pivalic acid
Pyr	pyridine
PMP	para-methoxyphenyl
PS	petroleum spirits
ppm	parts per million
q	quartet
rt	room temperature
R _f	retardation factor
s	singlet
<i>s</i> -Bu	<i>sec</i> -butyl
sext	sextet
Se	selenium
t	triplet
<i>t</i> -Bu	<i>tert</i> -butyl
<i>t</i> _R	retention time
Te	tellurium
THT	tetrahydrothiophene
TBAB	tetra- <i>n</i> -butylammonium bromide
THF	tetrahydrofuran
THIQ	tetrahydroisoquinoline

TLC	thin-layer chromatography
TMS	trimethylsilyl
TS	transition state
UV	ultraviolet

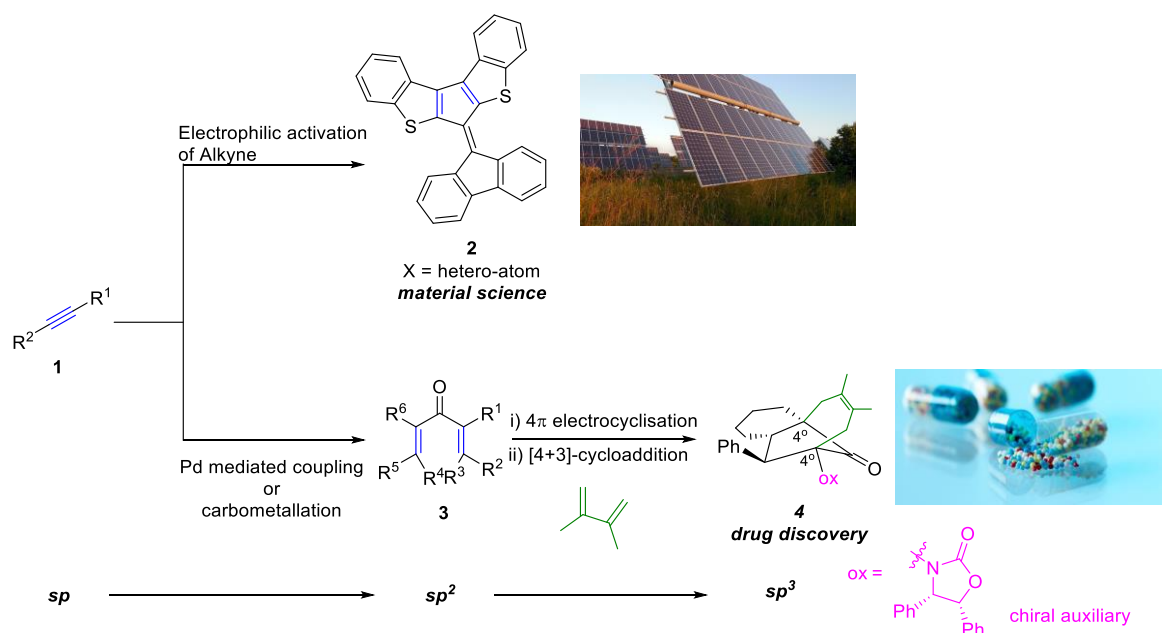
Nb. All chemical reagents are given by standard chemical formulas

Chapter 1

1. Introduction

1.1 Simple alkyne as building blocks to both sp^2 - and sp^3 -rich products

Alkyne is widely known as the smallest and simplest building block in synthetic organic chemistry, which provides access to an array of synthetic targets.^{1,2} Chemistry around activating alkynes continues to grow, where alkynes undergo various transformations to form diverse sp^2 -rich (e.g. arenes and heteroarenes) or sp^3 -rich structures (e.g. saturated carbocycles).³⁻⁵ These methods enable the *ab initio* design and synthesis of valuable new products, ranging from novel functional materials to medicinal therapies. In this thesis, we present research towards new approaches in the electrophilic activation of alkynes to form extended heteroacenes (e.g. **2**), with potential applications on photo-electronic devices (**Scheme 1**). Also, presented are convergent approaches to sp^2 -rich pentadienone structures **3** from sp -hybridized ynamide **1** (ox = chiral oxazolidinone), followed by chiral-oxazolidinone promoted asymmetric cyclization to form a range of sp^3 -rich cyclopentanoids with multiple all-carbon quaternary (4°) stereogenic centres, e.g. **4**. These chemistries illustrate a broader synthetic paradigm of gaining increasing structural complexity through exploiting π -bonds in organic synthesis by facile sp to sp^2 to sp^3 conversion.



Scheme 1. Divergent synthesis from sp -hybridized alkyne into complexed sp^2 - and sp^3 - structures.

1.2 π -Rich heteroacenes and their contribution towards materials science

Materials science has experienced major advances over the past 10-15 years, where the area of organic photonics has significantly evolved.⁶ Organic chemistry has provided remarkable contributions to materials science through the development of functional π -systems that interact with light or electricity or both. These include new and emerging photonic products, such as organic light-emitting diodes (OLEDs), organic photovoltaics (OPVs), semi-conductors and bio-imaging agents.⁶⁻¹⁰ The incorporation of heteroatoms, such as sulfur, into π -rich systems enhancing photonic activity of heteroacenes. Sulfur-based heteroacenes, provide a useful platform for S-S, S- π and π - π inter-molecular interaction, therefore allowing enhancement of charge transferring efficiency.^{6,11} Meanwhile, the insertion of other heteroatoms such as O, N, Se, Ge, Te ,etc. provides alternative photonic properties. Tellurium in particular has been extensively studied previously and proved to have two to three-folds extended conductivity due to the Te-Te inter-molecular contact.¹²

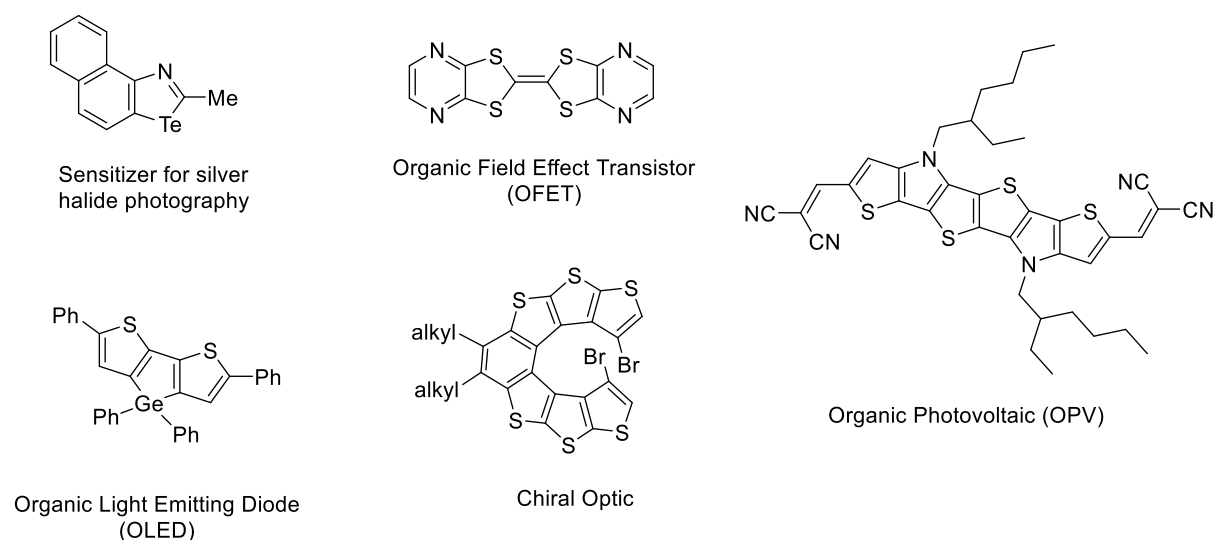
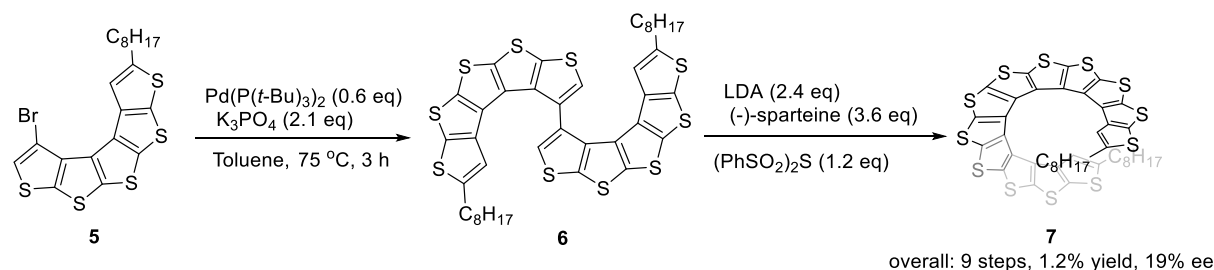


Figure 1. Examples of current organic compounds with materials science.

Moreover, the properties of heteroacenes can be tuned by varying fusion patterns, heteroatomic content and substitution patterns. Further exploration of photonic materials and their mass production in devices is highly dependent on gaining ready synthetic access to these chemicals.¹³ To date the synthesis of heteroacenes relies heavily on the stepwise introduction of new rings and new heteroatoms. For example, **Scheme 2** shows a recent synthesis towards carbon-sulfur helicities **7** by Miyasaka and co-workers.¹⁴ Though elegant, the low yielding reaction highlights the deficiency in current synthetic strategies towards sp^2 -rich heteroacenes.



Scheme 2. Synthesis of Carbon-Sulfur helicene by Miyasaka and co-workers, though low yield was obtained.

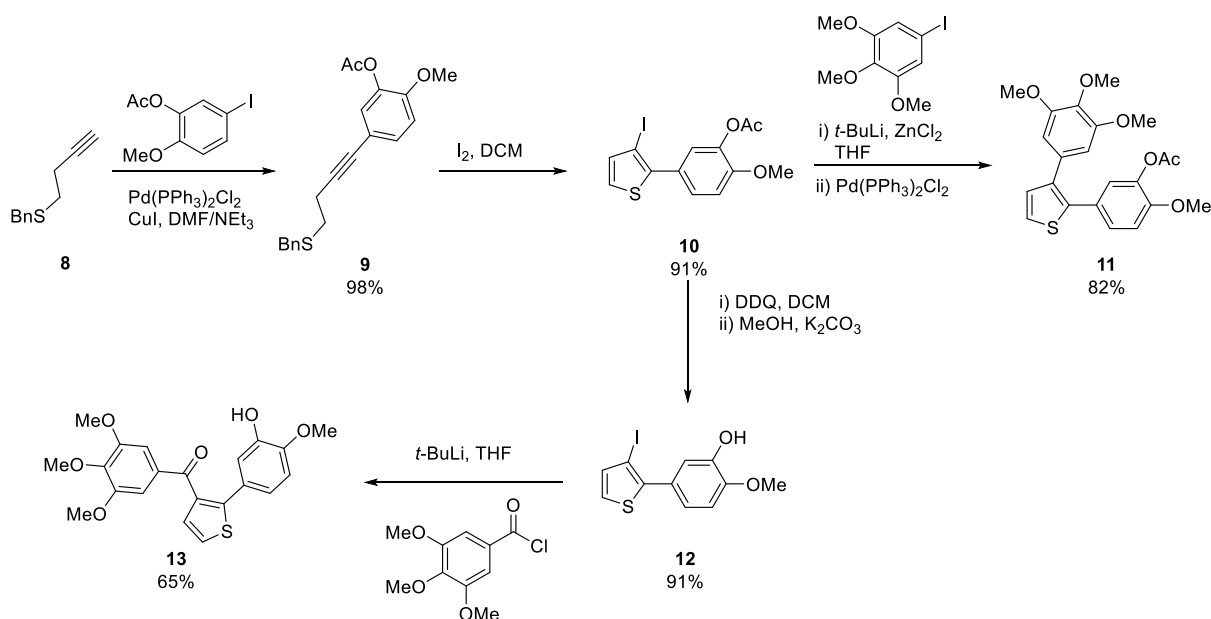
Moreover, the introduction of an increasing number of heterocycles into highly conjugated systems is an onerous achievement.¹⁵ If we could improve these syntheses, the efficiency in photonic materials exploration would make a tremendous advancement.

1.3 Electrophilic cyclization of activated alkynes

1.3.1 The recent emergence of electrophilic cyclization on activated alkynes

Heteroaromatic scaffolds synthesis towards benzothiophene, benzofuran or indole has been an area of huge interest in drug discovery and materials science.¹⁶⁻¹⁸ The synthetic methods towards these materials are predominantly dependent on the use of transition metals, where the most notable example would be palladium.

In the last 20 years, electrophilic cyclization has rapidly emerged in organic synthesis.¹⁹⁻²¹ The development of electrophilic cyclization has been truly exquisite, considering the capacity to adjust the functionalities on the core scaffold, providing opportunities to install a variety of functionalities. Flynn and co-workers were able to highlight the potential of the electrophilic cyclization by the synthesis of tubulin-binding analogues **11** and **13** via the iodo-cyclization approach, yielding compounds with improved activity (**Scheme 3**).²²

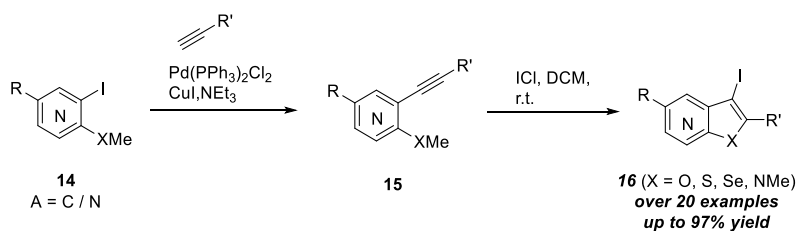


Scheme 3. Synthesis of Tubulin binding analogues via iodo-cyclization by Flynn and co-workers.

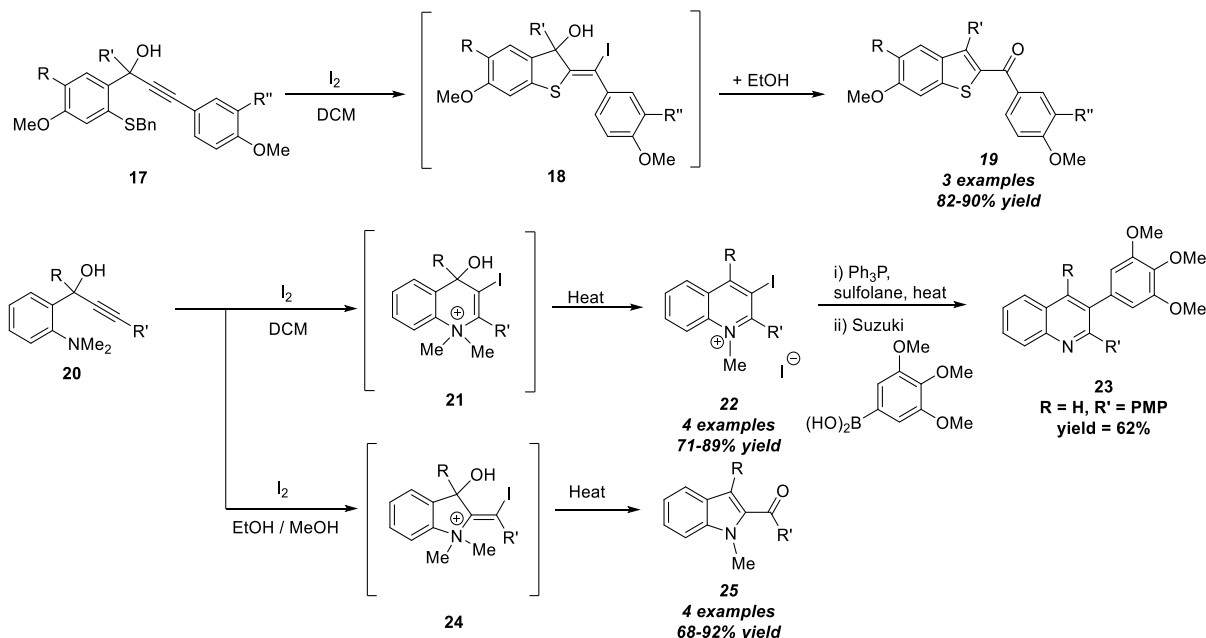
Both Flynn's and Larock's research groups have both been extensively studied on the iodo-cyclization of alkynes, forming a diverse array of heteroaromatic scaffolds (**Scheme 4**).²³⁻²⁵ Iodo-cyclization holds immense power in providing a route for further elaboration, as the iodo-heteroaromatic compound resulting from the cyclization can undergo subsequent Pd-mediated coupling or related substitution reactions. **Scheme 4** shows both Larock and Flynn's group effort towards heteroaromatic scaffold, where Flynn and co-workers discovered the solvent effect on the same substrate to divergently produce quinoline salt **22** via *endo-dig* cyclization, and *exo-dig* cyclization to yield indole derivatives **25**, selectively, with the use of DCM and alcoholic solvents, respectively. Note that iodo-quinoline salt **22** could further undergo Pd-mediated coupling for further elaboration.²⁶⁻²⁸

Chapter 1

Larock and Flynn's work

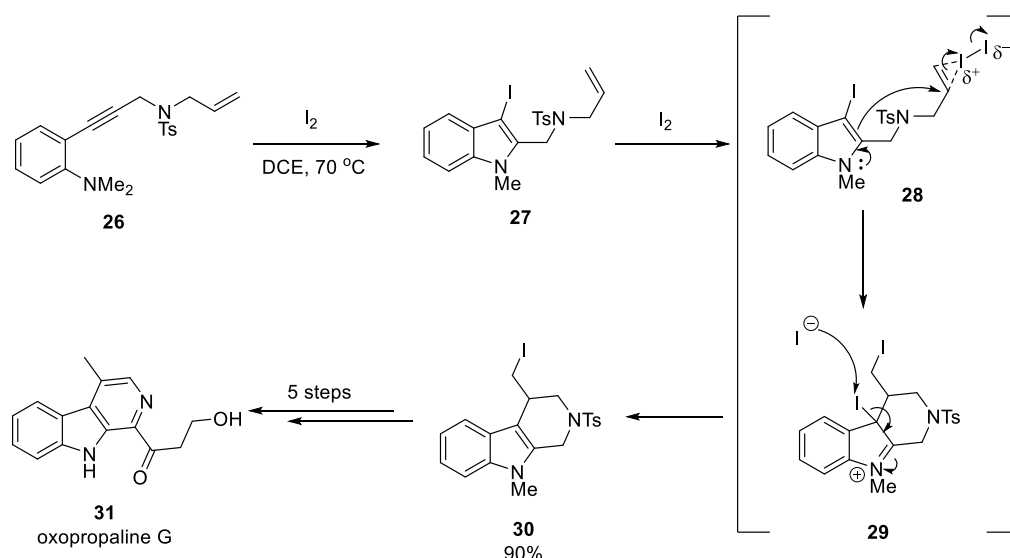


Flynn's work



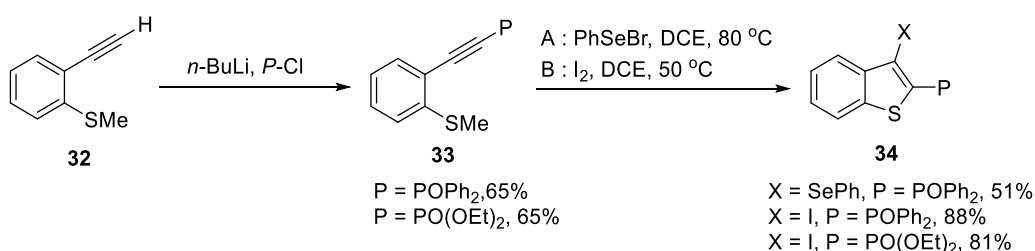
Scheme 4. Iodo-cyclization towards benzofuran, benzothiophene, quinoline and indole scaffolds by Larock and Flynn's research groups.

Only recently, Wang and co-workers synthesized oxopropaline G **31**, an anti-cytocidal natural product, via a much shorter route than the first total synthesis.²⁹⁻³⁰ The involvement of iodo-cyclization in this total synthesis is majestic, with the enablement of two continuous *in situ* iodo-cyclization cascades to form iodo species **30**, followed by five further steps to furnish the natural product synthesis, which is half as many steps as compared to the first total synthesis (**Scheme 5**).



Scheme 5. The total synthesis of oxopropaline G by Wang and co-workers via iodo-cyclization cascade.

Notwithstanding the extensive effort towards iodo-cyclization, iodine is not the only electrophile that can facilitate electrophilic cyclization. Flynn and co-workers were also able to use PhSeBr as the electrophile during the cyclization to form Se containing compound **34** (X = SePh, P = POPh₂) (**Scheme 6**).³¹

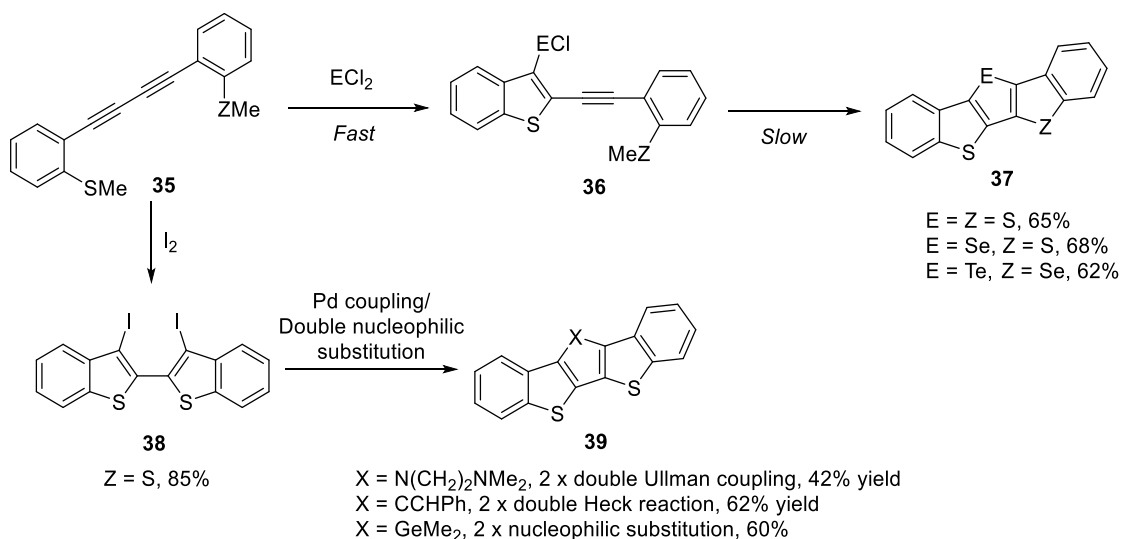


Scheme 6. Electrophilic cyclization using PhSeBr as an electrophile.

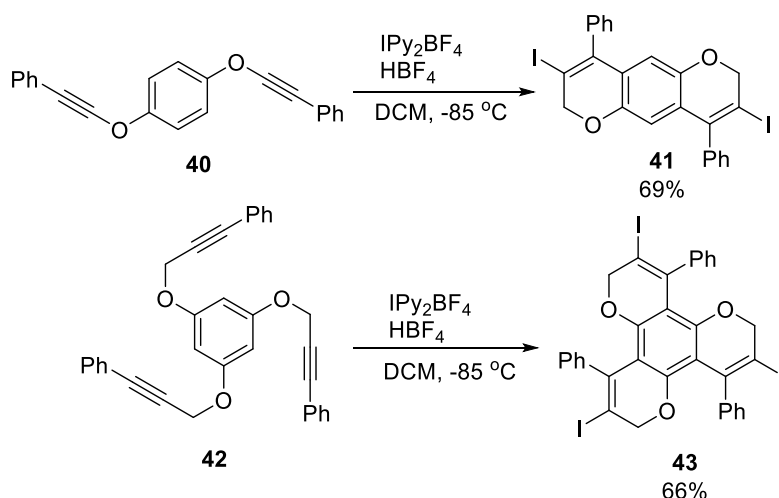
1.3.2 The development of Double-Electrophilic Cyclization (DEC)

The electrophilic cyclization has been intensively studied as mentioned. Gupta and Flynn have also developed the double-electrophilic cyclization (DEC) reaction, where linear heteroacenes were obtained in a one-pot process. The DEC reaction is performed in the presence of suitable electrophiles, such as SeCl_2 , SCl_2 and TeCl_4 , where it provides access to the first example of three chalcogens (S, Se, Te) in fused heteroacene **37** (E = Te, Z = Se, **Scheme 7**). The DEC reaction offers a significant opportunity to improve heteroacene synthesis. It can also be performed with the use of iodine, forming bis-iodo benzothiophene **38** in excellent yield. The formation of **38** was followed by a subsequent Pd-mediated coupling or nucleophilic substitution to give linear heteroacene **39**, with the incorporation of different elements such as N, O, and Ge (**Scheme 7**).³¹⁻³² This chemistry could

provide great utility towards materials science, in particular the incorporation of tellurium and germanium has proven useful in generating photonic activity.¹² In other work, González and co-workers were also able to show double and triple iodo-arylation with the Barluenga's reagent (IPy₂BF₄), forming iodo-substituted poly-benzofused aromatic **41** and **43** in moderate yields (**Scheme 8**).³³



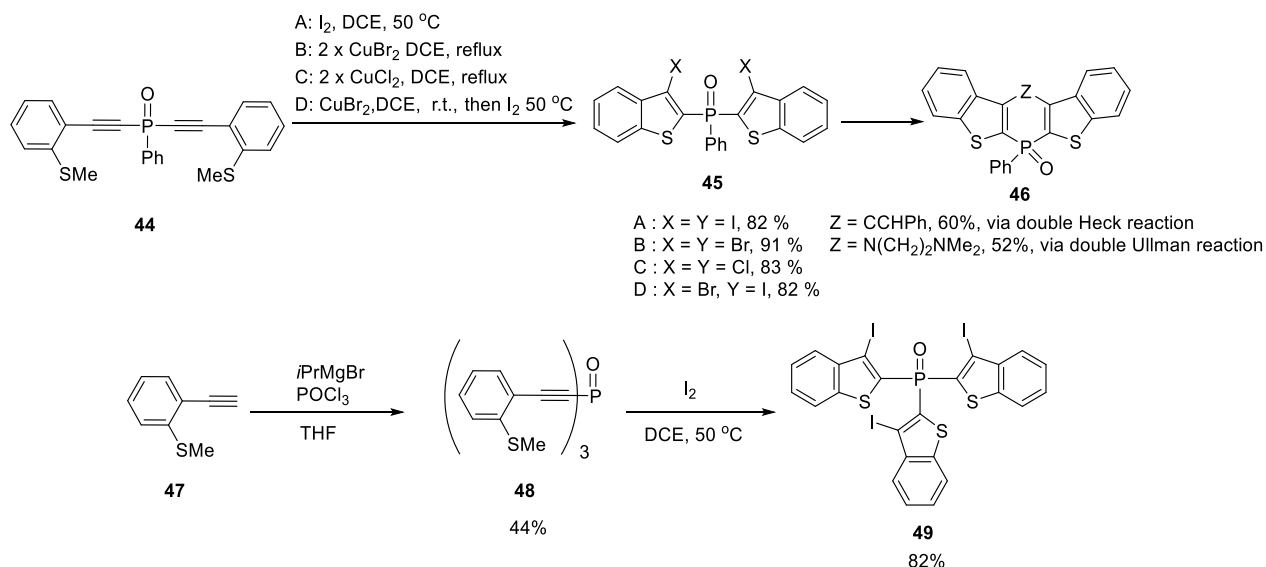
Scheme 7. Double electrophilic cyclization towards linear heteroacenes **37** and **39** incorporation with rare elements.



Scheme 8. Iodo-arylation by González and co-workers.

To further elaborate on the DEC reaction, Flynn and co-workers performed the double and triple halogen mediated electrophilic cyclization on P-centred alkynes **44** and **48**, forming **45** and **49** in good yield, respectively. Cyclized materials **45** underwent further Pd-mediated coupling reaction to form highly conjugated heteroacenes **46** (**Scheme 9**).³¹ P-centred compounds have played an important role within materials and medicinal science. The research on the use of these electrophiles

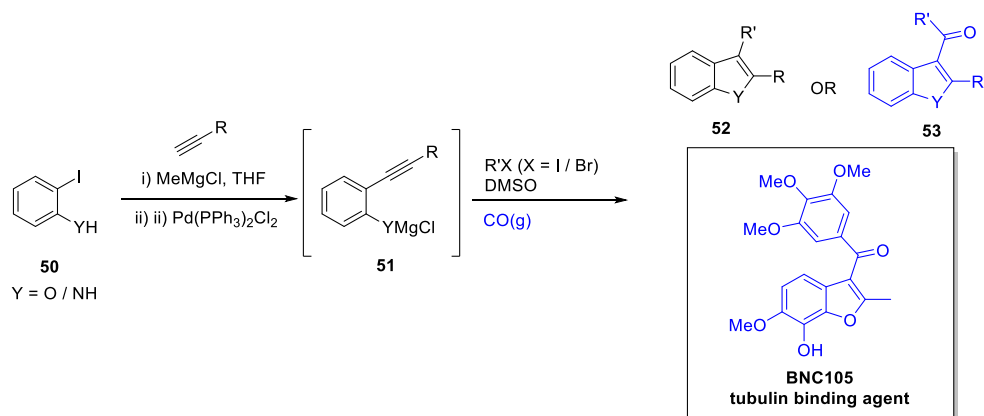
within alkyne cyclization has given materials science a huge opportunity to evolve, therefore increasing the efficiency of mass production of photonic products.



Scheme 9. Work towards P-centred benzothiophene derivatives.

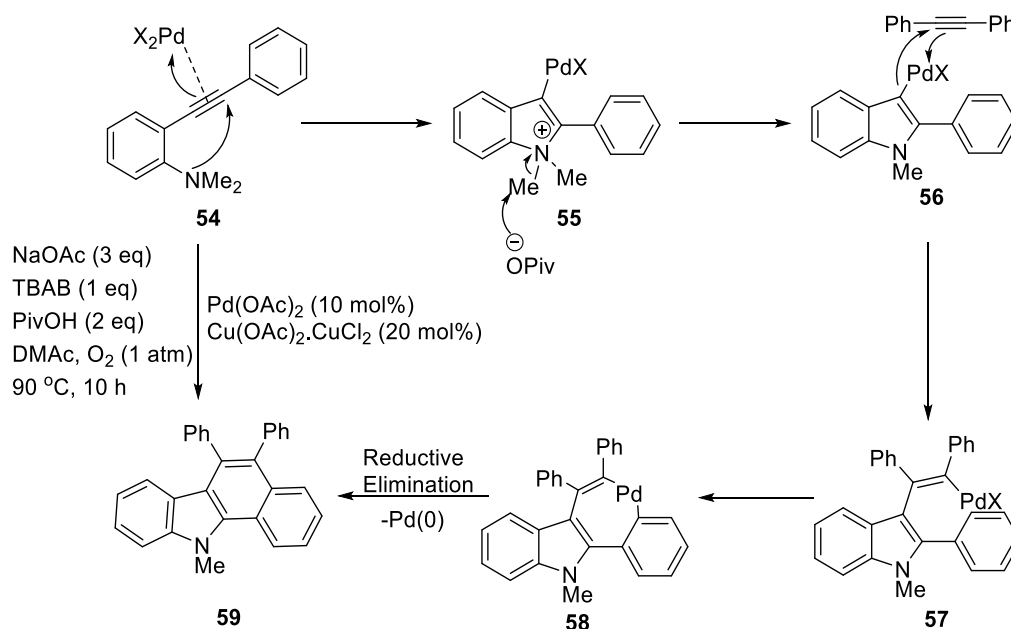
1.3.3 Transition metal directed electrophilic cyclization

The early development of transition metal-directed alkyne cyclization was predominantly around the use of Pd. Chaplin and Flynn developed an efficient synthetic method for benzofuran and indole scaffolds via the initial deprotonation of phenol or aniline and terminal alkyne, followed by addition of a Pd catalyst to form *o*-alkynyl phenolate as an intermediate.³⁴ The dilution of DMSO and addition of coupling partner then yields a 2,3-di-substituted benzofuran or indole in excellent yield. The presence of CO gas in the second stage allowed access into ketone derivatives, broadening the synthetic utility of this strategy (**Scheme 10**). The anticancer drug, **BNC105** (currently in clinical trials) is manufactured on kilogram scale, using this multi-component coupling reaction approach.³⁵



Scheme 10. Multi-component cyclization and coupling reaction approach towards benzofuran and indole scaffolds.

The development of multi-component coupling reaction towards benzofuran and indole demonstrated great scope in the scaffold-divergent synthesis, meanwhile envisions the ability of functionality manipulation.

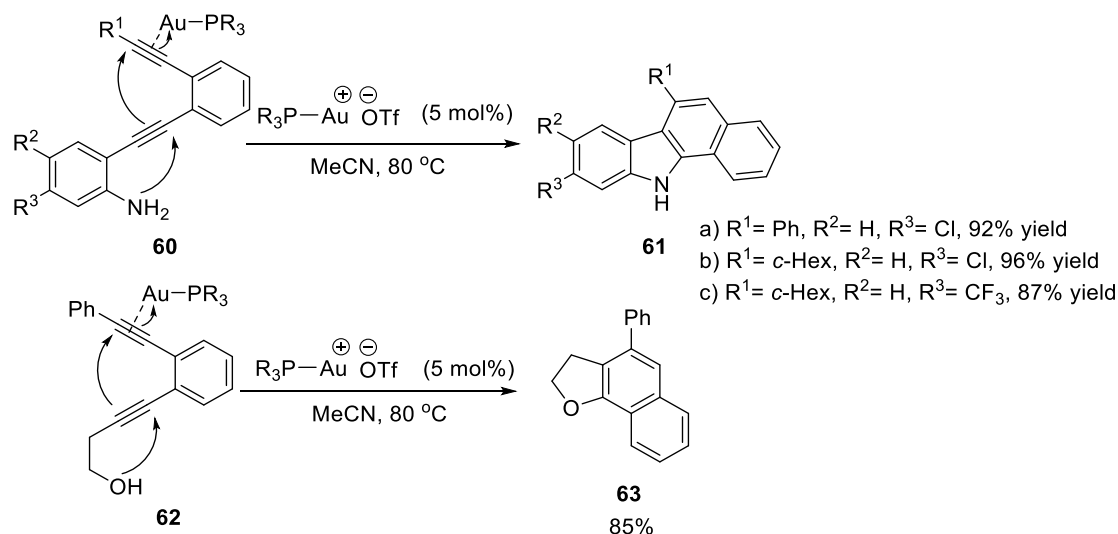


Scheme 11. Pd-mediated tandem cyclization towards extended indole scaffolds.

A later study by Xiao and co-workers investigated the formation of polyaromatic functionalized indole via Pd-mediated tandem alkyne cyclization (**Scheme 11**).³⁶ The formation of described extended indole **59** involves the initial Pd-mediated cyclization of alkyne **54**, followed by tandem inter-molecular cyclization with alkynyl additive, wherein most of the cases described to be diphenylacetylene. The seven-membered Pd-containing intermediate **58** then undergoes reductive elimination of Pd(0) to yield indole derivative **59**. Another transition metal showing excellent utility in alkyne activation is gold (Au).

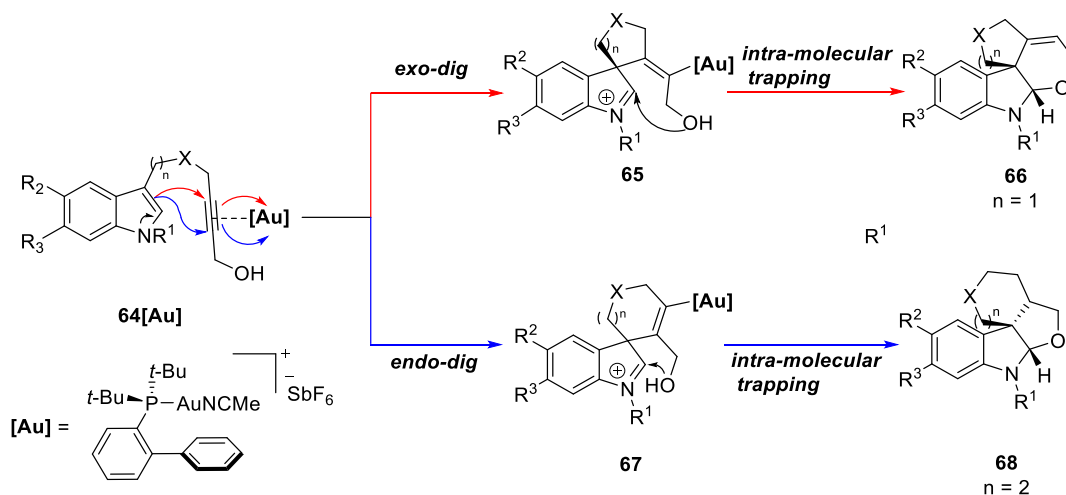
Previous research on gold includes gold oxidative coupling,³⁷ and especially gold induced Sonogashira coupling, have identified its similarity to copper.³⁸ All previous efforts have provided its current value within the area of alkyne cyclization. Earlier, gold was considered an inert element, where it was neglected until the recent 10-15 years. Over the past decade, there has been ongoing research on gold chemistry and now has become one of the most widely used transition metals within synthetic chemistry. The application of gold nowadays has provided a significant impact on the synthesis towards heterocyclic or hetero-aromatic compounds. The following examples in **Scheme 12** demonstrate the ability of gold to promote alkyne cyclization, forming extended indole derivatives **61**.³⁹ Although **Schemes 11** and **12** both demonstrate the synthesis towards similar indole derivatives,

gold cyclization bears the advantage of using less additive, allowing a more convenient and cost-efficient method in the synthesis of heteroacenes.



Scheme 12. Au induced cyclization by Hirano and co-workers.

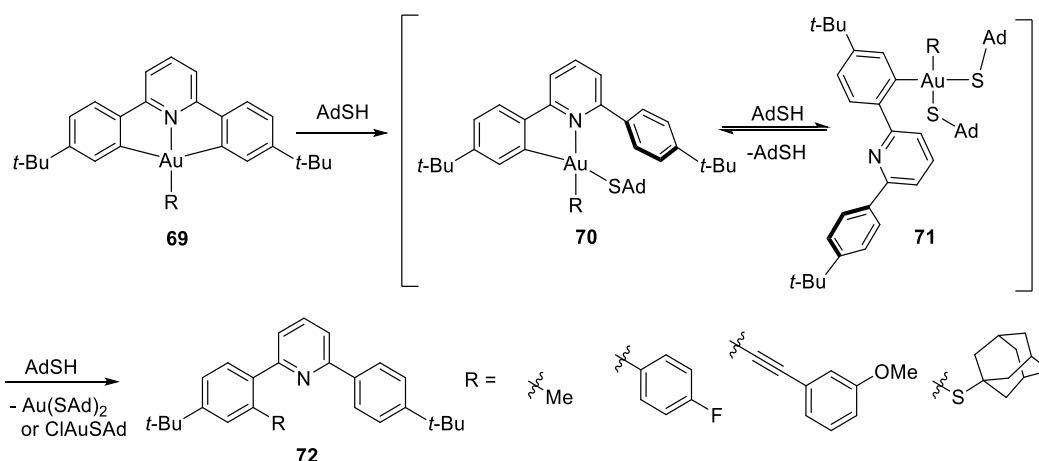
Gianpiero and co-workers were able to utilize chiral gold catalyst to perform alkyne cyclization, followed by the intramolecular nucleophilic trapping by *in situ* allylic alcohol **65** and **67**, yielding a range of indoline scaffolds **66** and **68** in a stereoselective manner, where the enantioselectivity was induced by the presence of the chiral ligand [Au] (**Scheme 13**).⁴⁰



Scheme 13. Enantioselective synthesis of indoline **66** and **68**.

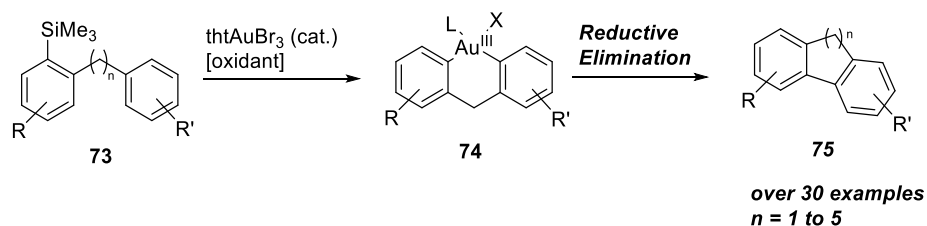
Under normal circumstances, gold intermediates undergo proto-deauration, giving protonated cyclic or aromatic material. Alternatively, it can be trapped by electrophiles, such as iodine, to form similar scaffold with iodide as additional functionality.⁴¹ Recent studies by Lucy and co-workers have shown the formation of C-C and C-S bond from the reductive elimination of Au-S and Au-C bond, respectively.⁴² In the same study, they also described the rate of gold reductive elimination between

carbon in different hybridization state, where aryl has a superior reductive elimination aptitude followed by alkyl and alkynyl species (**Scheme 14**).



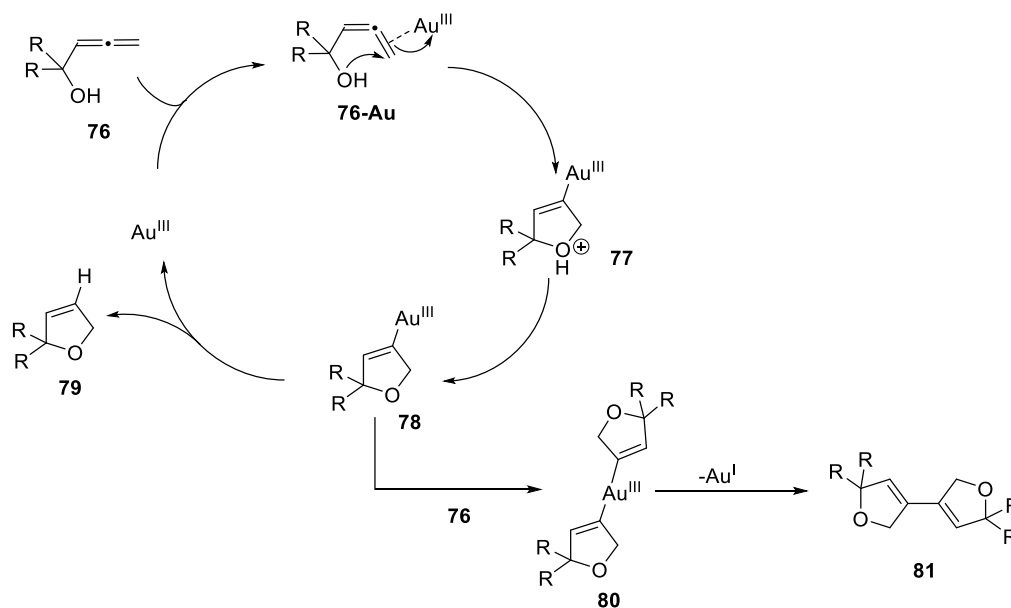
Scheme 14. Reductive Elimination of Au intermediate, forming C-S bond.

In addition to the gold chemistry, Tom and co-workers had shown the ability to form a range of five to nine-membered rings via gold-catalyzed biaryl coupling. This reaction involves the initial C-Si and C-H auration, followed by the crucial Au(I) reductive elimination of **74** to afford fused ring scaffolds **75** in various ring sizes (**Scheme 15**).⁴³ It was concluded that the rate of reductive elimination is dependent on the nature of aryl, where electron-rich aryl favours a more rapid reductive elimination. Meanwhile, they also observed an increased rate of reductive elimination when linker between aryl involves two or more carbons, in which the participation of ether linker seems to retain the stability and reactivity towards the ring formation and reductive elimination of gold.



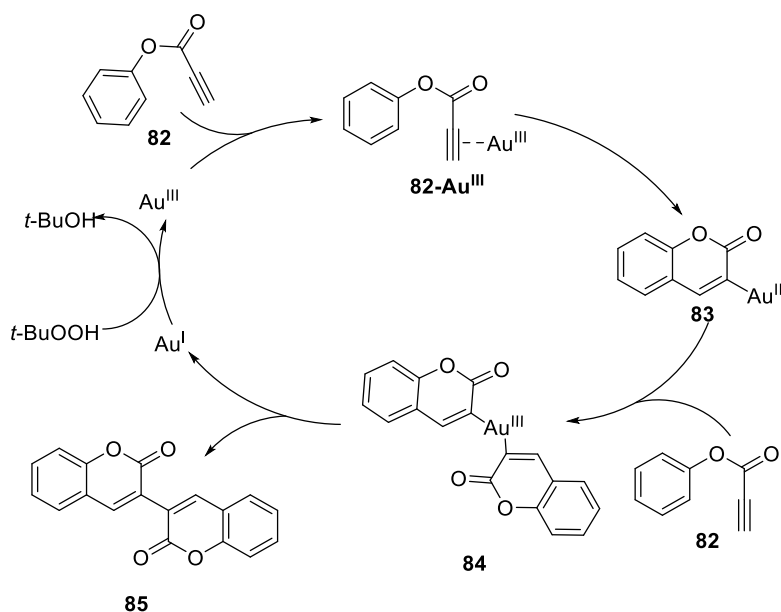
Scheme 15. The formation of fused ring **75** via reductive elimination of gold.

In 2006, Hashmi and co-workers discovered gold-induced cyclization-dimerization of allenyl carbinols **76**, producing dimerized material **81** as a side product via a gold reductive elimination process.⁴⁴ **Scheme 16** shows the mechanism Hashmi deduced, where **76** first undergoes gold-induced cyclization, followed by the removal of proton of **77**, to give gold intermediate **78**. Intermediate **78** then undergoes proto-deauration to yield **79** as the main cyclized product. The formation of **78** also induces the cyclization of **76**, forming gold dimerized intermediate **80**, which rapidly undergoes reductive elimination of Au(I) to yield **81**. Despite the effort on the mechanistic proposal by Hashmi *et al.*, the existence of gold intermediate was yet to be physically characterized.



Scheme 16. The initial discovery of gold induced dimerization.

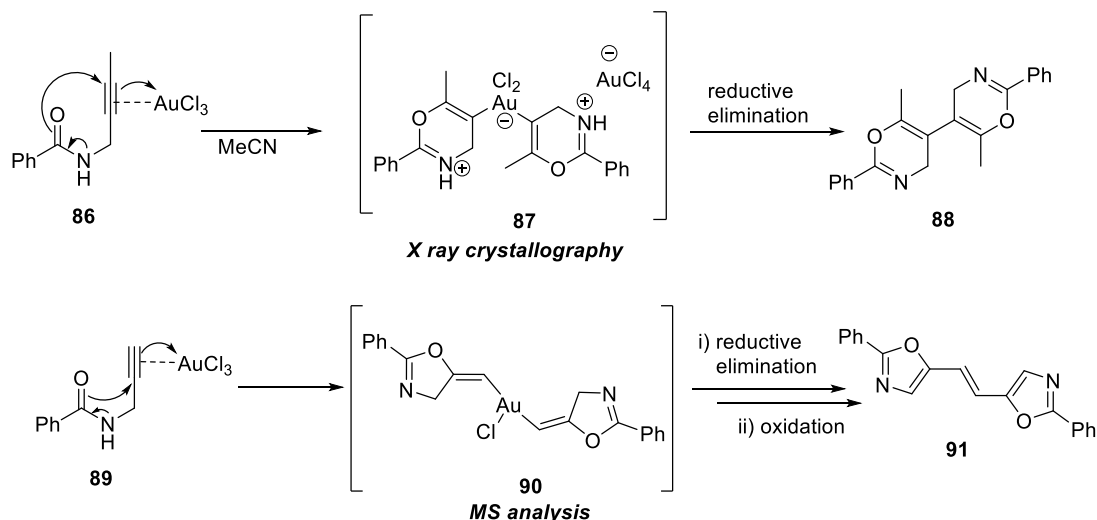
Hermann and co-workers in 2008, found the occurrence of the same dimerization process in the production of **85**.⁴⁵ They argued that the use of catalytic HAuCl₄ undergoes oxidation upon reductive elimination of Au(I), wherein the presence of suitable oxidant (*t*-BuOOH) to return Au(III), forming a catalytic cycle of the dimerization process (**Scheme 17**). This process effectively reduced the amount of Au in the reaction, offering an enhancement in synthetic and manufacturing efficiency.



Scheme 17. Catalytic cyclization cycle proposed by Hermann and co-workers.

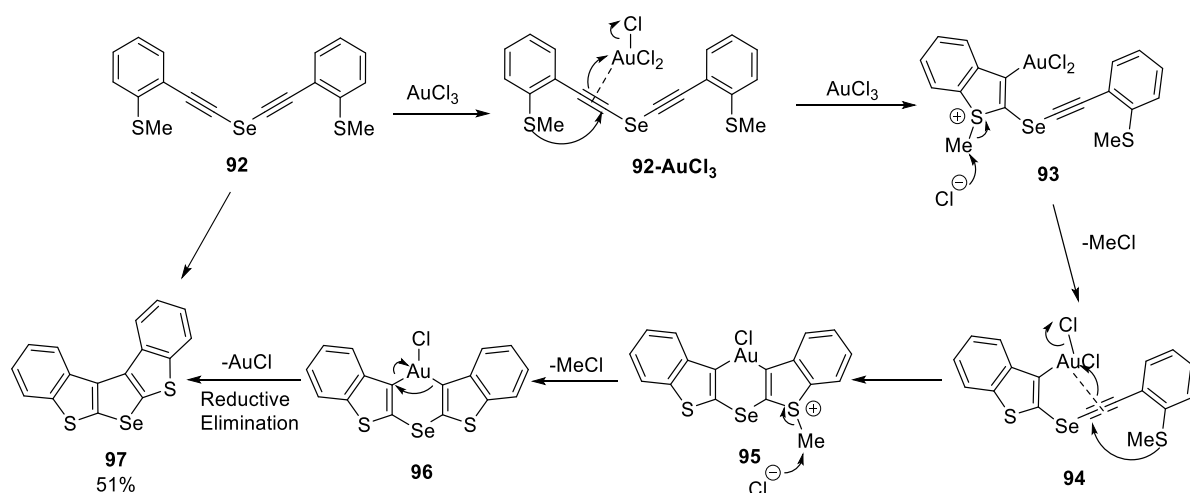
A later study by Olga and co-workers further confirmed the gold dimerization process by extensive x-ray crystallography and mass spectrometry analysis.⁴⁶ In the dimerization process, they captured

the formation of Au(III) cyclized intermediate **87** as a zwitterionic intermediate by the formation of crystal during the reaction. Using substrate **89**, they also observed the formation of gold(III) intermediate **90** by mass spectrometry (**Scheme 18**). Therefore, it further confirmed the dimerization mechanism Hashmi and Hermann proposed, in which gold(III) dimerized intermediate undergoes reductive elimination to form dimerized product explicitly.



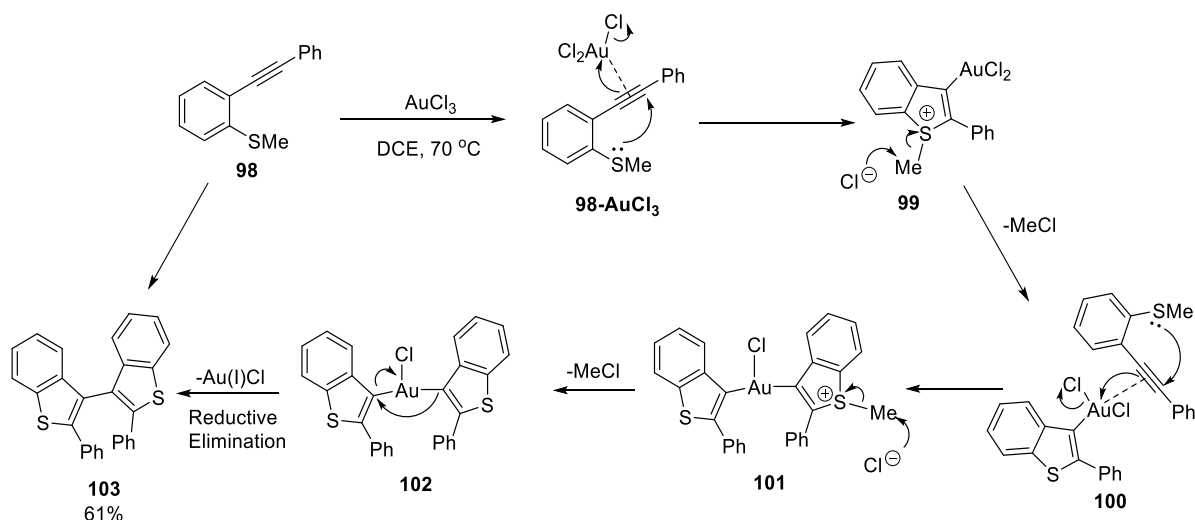
Scheme 18. The capture of Au(III) intermediate **87** and **90**.

The discovery and confirmation of Au cyclization-dimerization process was truly a fascinating find. Notwithstanding the effort that was spent on the intermolecular gold induced cyclization-dimerization process, the intra-molecular cyclization-reductive elimination process has also emerged. The properties of gold that are mentioned above inspired Flynn and co-workers to investigate on the intramolecular cyclization-reductive elimination reaction, which was later dubbed double-electrophilic cyclization reductive elimination (DECRE) reaction.³² The benefit of applying the DECRE reaction is that the formation of angular heteroacenes could be achieved in a one-pot process. Such angular heteroacenes have been proven to exert valuable photonic activities. Using the DECRE approach, we anticipate furnishing the synthetic protocols towards organo-photonic materials, reducing the number of synthetic steps towards multi-chalcogen containing heteroacenes, providing access into a diverse array of highly conjugated sp^2 -rich materials.



Scheme 19. DECARE proof of concept by Flynn and co-workers.

In 2017, Flynn and co-workers had proven the concept of DECARE, by generating a sulfur and selenium-containing angular heteroacenes **97** in 51% yield (**Scheme 19**).³² Gold is an extremely reactive electrophile, which induces the nucleophilic attack of sulfur to the alkyne, resulting in an *endo-dig* electrophilic cyclization. Cationic intermediate **93** is then concomitant with the expulsion of electrofugal methyl, resulting in the formation of mono-cyclized intermediate **94**. The other alkyne on intermediate **94** would then cyclize intra-molecularly, forming the 6-membered Au(III) containing intermediate **95**. This process is then followed by the elimination of methyl once again, yielding **96** as an intermediate. As a highly reactive intermediate, **96** spontaneously undergoes reductive elimination to remove Au(I)Cl, yielding the novel multi-chalcogen containing angular heteroacene **97** (**Scheme 19**).

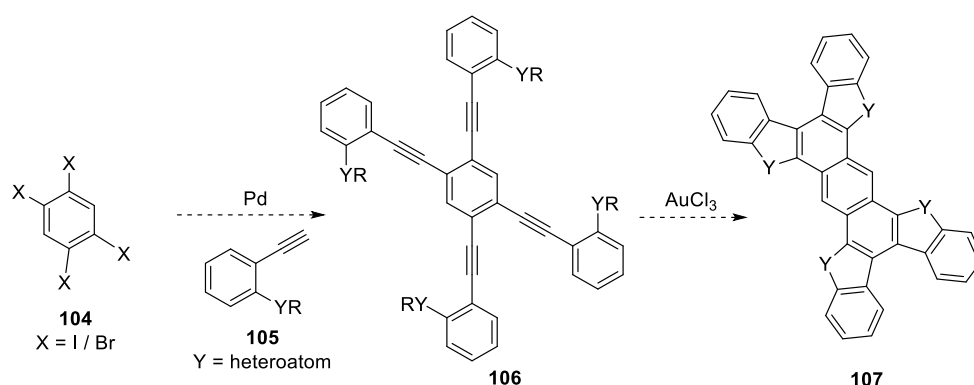


Scheme 20. Inter-molecular DECARE reaction.

Similar to the DECARE reaction mechanism proposed in **Scheme 19**, alkyne **98** also undergoes DECARE, but in an inter-molecular fashion. Alkyne **98** first undergoes electrophilic cyclization,

followed by the removal of MeCl to give gold(III) benzothiophene intermediate **100**. A second molecule of **98** then undergoes gold mono-cyclized intermediate-dependant cyclization to give cationic intermediate **101**, followed by the removal of MeCl to give bis-benzothiophene gold(III) intermediate **102**, which then ultimately undergoes Au(I)Cl reductive-elimination to yield bis-benzothiophene product **103** (Scheme 20).

Notwithstanding, the efforts on generating these examples, there is a demand in expanding the scope of this reaction as the current example within DECRE process is rather limited. We anticipate that the use of AuCl₃ would allow access into various extended heteroacenes such as **107**, via a bidirectional DECRE. Such chemistry will enable the further exploration of extended heteroacenes in photonic materials.



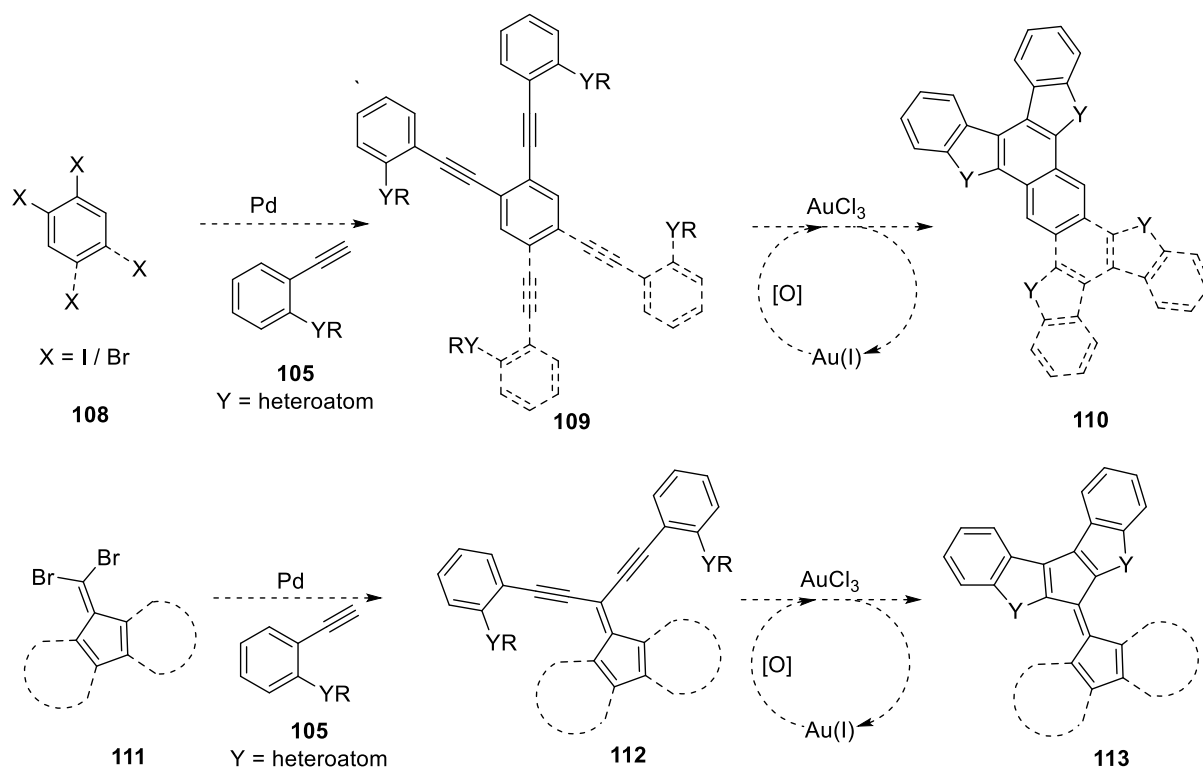
Scheme 21. Synthetic proposal towards angular heteroacenes.

1.4 Aim 1: The elaboration of DECRE reaction, towards complex angular heteroacenes

The objective in the synthesis of angular heteroacenes involves the use of double-electrophilic cyclization reductive elimination (DECARE) process, where effort would direct to the elaboration of angular heteroacene synthesis using AuCl₃. We anticipate that the use of AuCl₃ would lead to the formation of extended heteroacene **110** via DECRE. The synthesis of described angular heteroacenes involves the initial formation of alkynyl substrates **109** via Sonogashira coupling, where the early investigation should involve two alkynes per molecule. The resulting substrate would then be subjected to the DECRE reaction to yield expected angular heteroacenes **110**, forming either three or six (bidirectional) new rings (Scheme 22).

Fulvalene type molecules have been discovered to contain superior electronic properties, thus leading to the interest in the formation of novel fulvalene type compounds.⁴⁷ The synthetic protocol would be similar to the formation of angular heteroacene **110**, which involves the initial Sonogashira coupling between geminal dibromide **111** and related terminal alkyne **105**, forming substrate **112**. **112** would then be subjected to the DECRE reaction to yield fulvalene derivatives **113** (Scheme 22).

An additional objective in the elaboration of the DECRE reaction is the use of a catalytic amount of AuCl_3 , where the Au(I) that is reductively eliminated during the reaction could be re-oxidized to Au(III) , allowing a catalytic DECRE reaction cycle with the use of suitable oxidant. We expect our recently developed DECRE would allow access into a diverse array of angular heteroacenes, including those highly extended systems, therefore improving current synthetic protocols towards organo-photonic materials.



Scheme 22. The synthetic route towards proposed angular heteroacenes.

1.5 Conversion of alkyne to multiple 4°-stereocentres containing compounds in drug discovery

In addition to our aims for converting alkynes into sp^2 -rich heteroacenes, this thesis work has also been directed to the new methods for converting alkynes into multi-stereocentres containing carbocycles, in particular multi 4°-stereocentre containing cyclopentanoids.

1.5.1 Interest in sp^3 -rich compound synthesis

The synthesis of sp^3 -rich compounds holds an enormous impact on both current and future drug discovery. This impact is attributable to the capacity of sp^3 -rich molecules to project binding motifs into 3D space, improving their capacity to act as ligands for proteins. Over the past decades, sp^2 -rich molecule syntheses have dominated medicinal chemistry for the reason of synthetic tractability. Notwithstanding the advance made in the synthesis of π -rich molecules, the importance of generating sp^3 -rich molecules has received less attention and may contribute to the recent decrease in productivity of pharmaceutical industry.⁴⁸⁻⁴⁹ The inability to readily synthesize sp^3 -rich molecules has potentially contributed to the decline in the pharmaceutical companies ability to identify suitable molecules from library screening, which has a tremendous influence on the failure of clinical trials. Therefore, improving our capacity to generate sp^3 -rich molecules should improve the drug discovery outcomes. This has already been evidenced in the significance of stereogenic molecules within drug discovery.⁵⁰⁻⁵²

sp^3 -Rich compounds are indeed extremely attractive in drug discovery due to their superior projection of functionalities into 3D space, while sp^2 -rich compounds only project motifs on the same plane. **Figure 2** exemplifies the superiority of sp^3 -rich scaffolds in projecting substituents (protein binding elements) into 3D space. While sp^3 -molecules can install twice the number of functionalities compared to planar sp^2 benzene, this reflects high ligand efficiency in sp^3 -rich molecules, which in turn can improve their ADME (Absorption, Distribution, Metabolism, Excretion) profile, hence leading to better drug candidates.

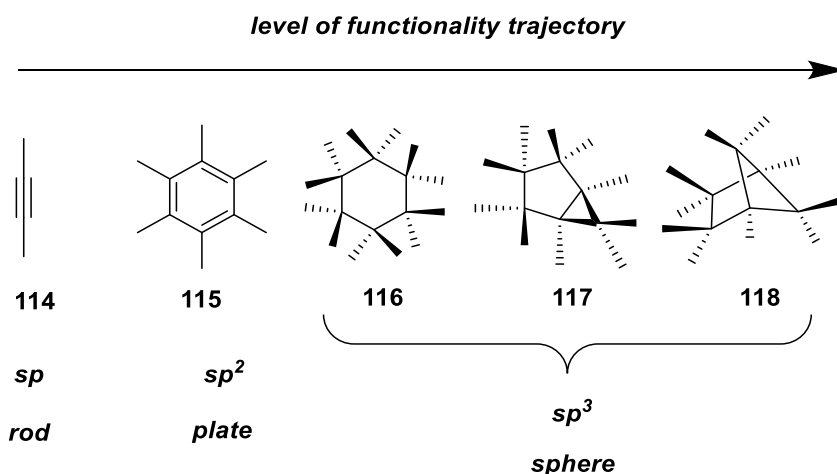


Figure 2. The increasing level of functionality trajectory from sp - to sp^3 -hybridized carbon.

Various studies by different pharmaceutical research groups have identified the significance of sp^3 -rich molecules.⁵³⁻⁵⁴ Lipinski and others were able to predict the drug likeliness by comparing molecular weight, number of hydrogen bond donors and acceptors, number of rotatable bonds, polar surface area and lipophilicity with statistical data.⁵⁵ Lovering *et al.* utilized a similar approach to show the value of sp^3 -rich molecules. As anticipated, F_{sp^3} (Fraction sp^3) of drug out in the market was reasonably higher than molecules that were still at the preclinical stage, concluding stereogenic molecules hold tremendous potential in modulating specific protein targets.⁵⁶ An interesting discovery also by Lovering *et al.* was that melting point increases as F_{sp^3} decreases, pointing out compounds that have lower melting point genuinely possess much better solubility, which also seems to be very consistent with Thomas and Yalkowsky and co-worker's discovery.⁵⁷ These researches undoubtedly demonstrated the worthiness of sp^3 -rich molecules, where ADME properties are improved.

Currently, the synthesis of sp^3 -rich compounds remains to be a challenge in the pharmaceutical industry because of there so called "poor synthetic tractability". This poor synthetic tractability is due to the difficulties in controlling the enantio- and diastereoselectivity of reactions and explains the bias towards the use of sp^2 -rich compounds in drug discovery. 2D compounds are easily accessible due to the efficiency of Pd-mediated C-C bond formation in synthetic chemistry.⁵⁸ Most of these Pd-reactions bear the properties of being convergent, modular, chemo- and regioselective. However, controlling the enantio- and diastereoselectivity has always been a huge limitation for the synthesis of sp^3 -rich compounds. Therefore, overcoming this barrier would be a breakthrough in the synthesis of extremely potent molecules, enabling chemistry and especially drug discovery to reach a new level of therapeutic efficiency.

1.5.2 Synthesis of compounds containing contiguous all-carbon 4°-stereocentres

Over recent years, chemistry and drug discovery have unquestionably witnessed the increased interest in multiple stereocentres containing compounds. Although multiple research groups have been developing stereoselective synthesis towards natural products and natural product-like compounds to better accommodate the nature of binding to proteins, all-carbon 4°-stereocentres have proven particularly challenging to generate, stereoselectively (enantio- and diastereoselectively). Since sp^3 -stereocentres are either 3° or 4°, the lack of efficient production of 4°-stereocentres excludes a significant component of the theoretically available sp^3 -rich molecular diversity. **Figure 3** shows natural products that contain >1 all-carbon 4° stereocentres, showing the significance in the synthesis of sp^3 -rich compounds and their relationship with natural products.⁵⁹⁻⁶³

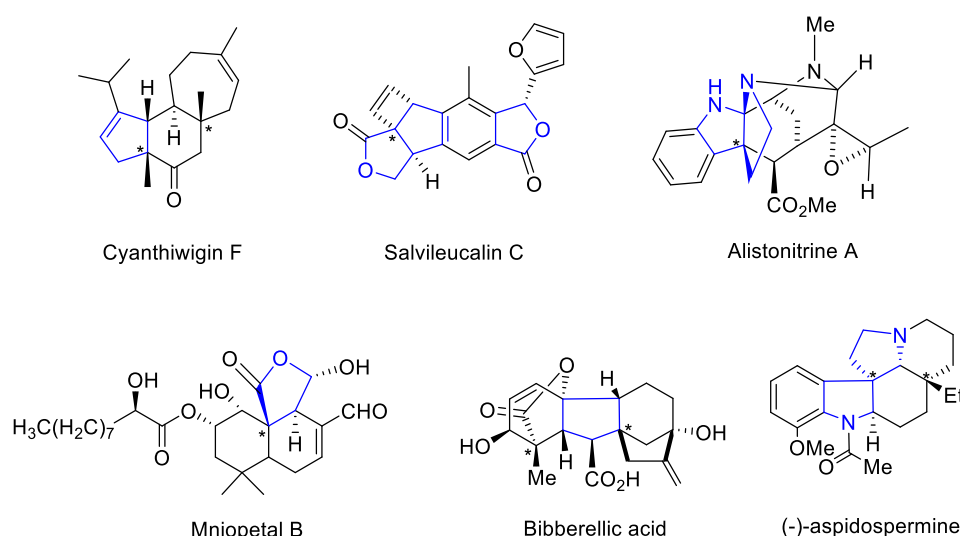
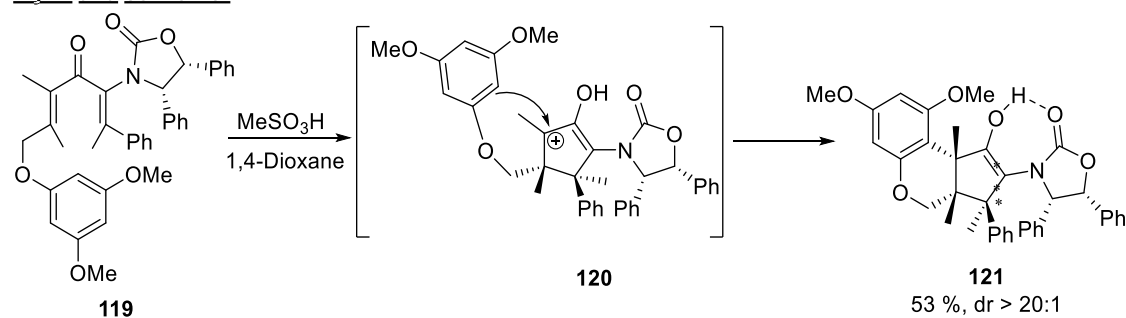
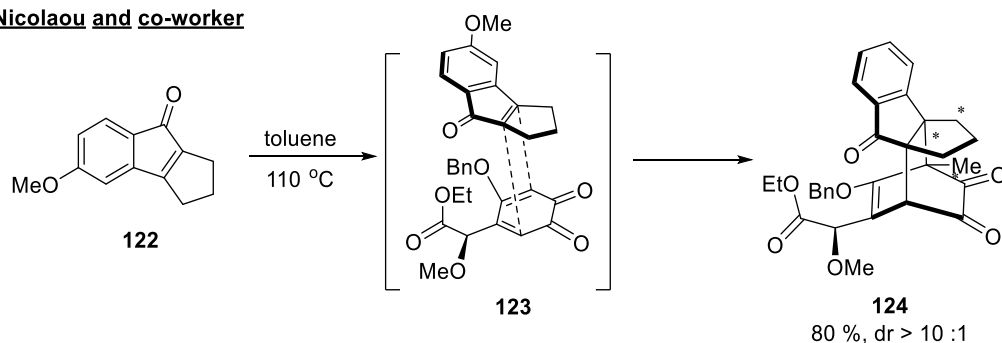


Figure 3. Natural compounds that contain >1 all-carbon containing 4°-stereocentres.

The formation of all-carbon 4°-stereocentres has already proven to be an impediment to synthetic chemistry due to the difficulty in controlling the enantio- and diastereoselectivity in the C-C bond formation step.⁶⁴ The stereoselective formation of one or two stereogenic centres is proven to be difficult. To control enantio- and diastereoselectivity of multiple all carbon 4°- stereogenic centres during the formation of C-C bond appears to be extremely challenging. To date there are only two examples we know of within organic chemistry, that has produced compounds that contain three contiguous all-carbon 4°-stereogenic centres in a single step, enantioselectively. These are Flynn's and Nicolaous' examples **121** and **124** (**Scheme 23**), where they were synthesized through torquoselective Nazarov cyclization and Diels-Alder reaction, respectively.⁶⁵⁻⁶⁶ Despite the synthesis of multiple all-carbon 4°-stereocentres containing compounds being a major challenge within organic chemistry, we could undeniably open the new horizon, and find the key to upcoming synthetic problems as we continue the development of sp^3 -rich compounds.

Flynn and co-worker**Nicolaou and co-worker****Scheme 23.** Formation of three contiguous all-carbon containing 4° -stereocentres.

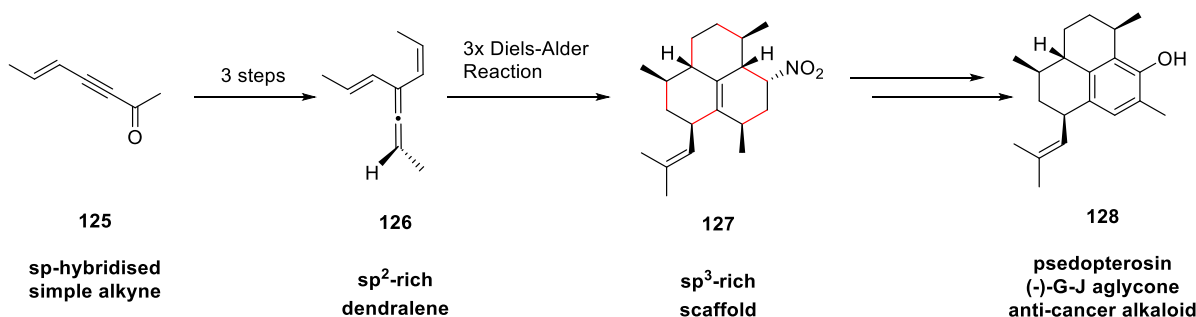
Thus, one of the major topics in this thesis is the synthesis of complex cyclopentanoid scaffolds with multiple all-carbon vicinal 4° -stereocentres.

1.5.3 Synthetic strategies towards sp^3 -rich compounds

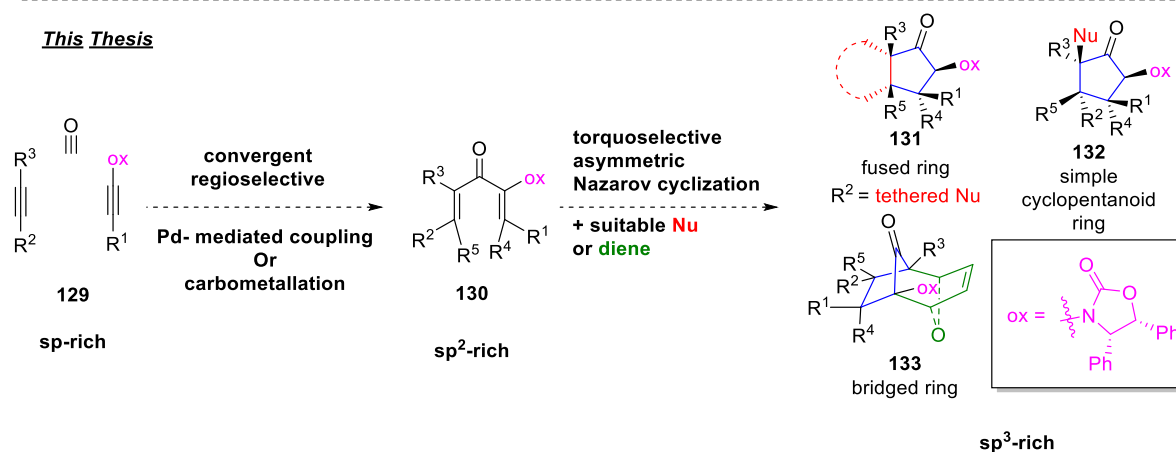
As mentioned, controlling enantio- and diastereoselectivity in sp^3 -rich molecules synthesis remains a challenge, where Pd-mediated coupling reaction dominates in sp^2 C-C bond formation.⁵⁸ However, these coupling reactions could nevertheless provide an excellent platform for the formation of sp^3 -rich compounds. The most familiar and well-known sp^3 C-C bond forming reaction would be the Diels-Alder reaction. However, the formation of sp^3 -rich cyclopentyl rings is less well established. Cyclopentanoids are the second most frequently observed all-carbon scaffolds in nature.⁶⁷ The Nazarov cyclization is a reaction with excellent potential in the synthesis of cyclopentanoids. It is important to address the formation of cyclopentyl systems as they frequently appear within natural products. The frequent appearance of cyclopentyl scaffolds in nature also highlights the relationship between sp^3 -rich C-C bond formation and natural products synthesis. The Nazarov reaction is an acid promoted electrocyclization of sp^2 -rich pentadienone structure **130**, providing access into sp^3 -rich cyclopentanoids diastereospecifically.⁶⁸ **Scheme 24** contains an example from Sherburn and co-workers, demonstrating a strategy towards sp^3 -rich scaffold **127**, via Diels-Alder reaction.⁶⁹ This thesis presents a synthetic protocol that bases on the convergent and modular synthesis of sp^2 -rich divinyl ketone **130**, from simple accessible sp -hybridized alkynes **129**, then performing the Nazarov

cyclization to yield a range of sp^3 -rich cyclopentanoids **131-133** torquoselectively, in the presence of chiral auxiliary oxazolidinone **ox** (**Scheme 24**). The aim of this thesis section is to synthesize complexed cyclopentanoids via the Nazarov cyclization with chiral oxazolidinone **ox** to provide torquoselectivity control, therefore, the removal of chiral auxiliary is not included in this work.

Sherburn's Work



This Thesis

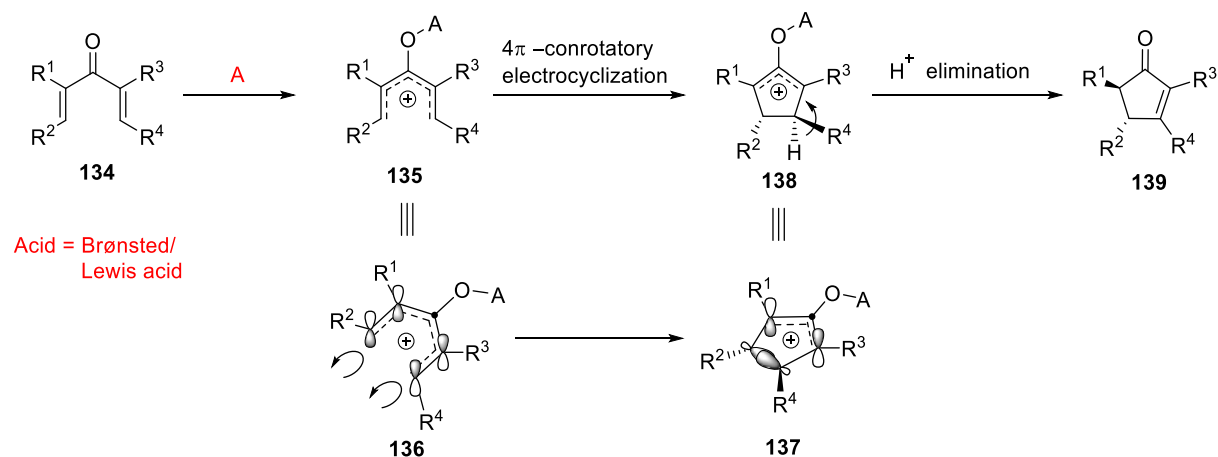


Scheme 24. The conversion of alkynes into sp^3 -rich complex cyclopentanoids in this thesis.

1.6 The Nazarov cyclization

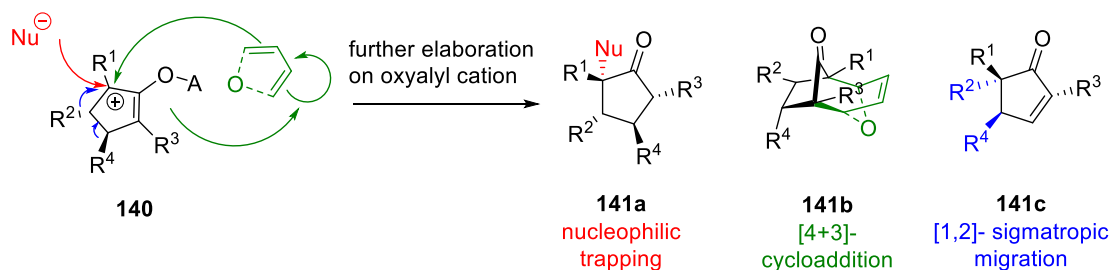
Of interest to our group is to gain ready access into sp^3 -rich cyclopentanoids that contains multiple all-carbon 4° -stereogenic centres. The Nazarov cyclization is an excellent path to form such stereogenic cyclopentanoids diastereoselectively.

The Nazarov cyclization was first reported by Ivan Nikilawvich Nazarov in 1942.⁷⁰ It is an acid promoted 4π -electrocyclization of sp^2 -rich pentadienone **134**, forming sp^3 -rich cyclopentanoid **139**. When dienone **134** is treated with an acid, it forms pentadienyl cation **135**. According to Woodward-Hoffmann rules, pentadienyl cation **136** must undergo conrotatory electrocyclicization to preserve orbital symmetry, hence forming the oxyallyl cation **138**, diastereospecifically. Oxyallyl cation **138** resulted from cyclization would then undergo β -proton elimination to give cyclopentanoid **139** with two stereocentres (**Scheme 25**).



Scheme 25. The mechanism of the Nazarov cyclization.

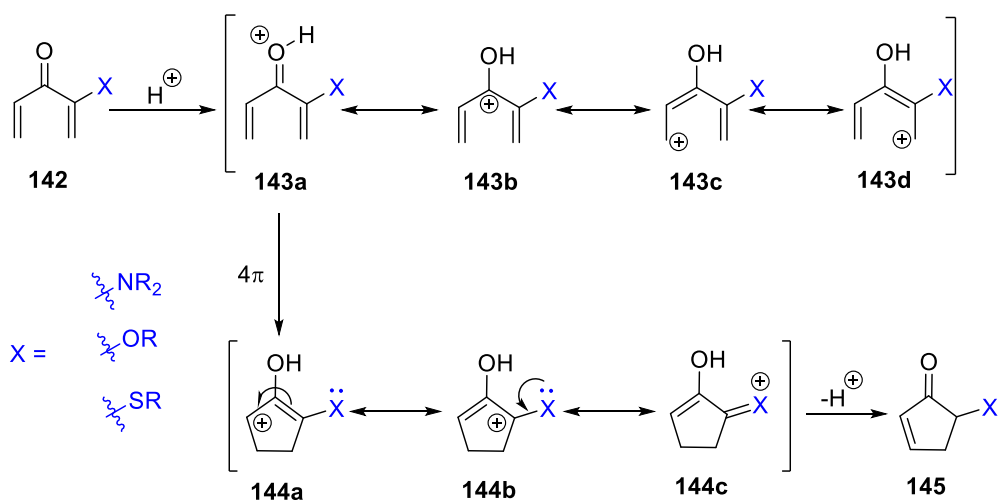
While the Nazarov cyclization is known to yield cyclopentanoids with two stereocentres, further elaborations on the oxyallyl cation **140** provide pathways into structurally diverse 3D compounds. Examples from numerous groups, including West, Frontier, Burnell and Flynn's group, have identified the utility of nucleophile, diene and 1,2-sigmatropic migration during the Nazarov reaction, yielding sp^3 -rich cyclopentanoids with multiple stereocentres (**Scheme 26**).⁷¹ Further mechanism and examples will be shown in later of this chapter. Such complex structures are exceptionally compelling, which could serve to advance both diversity-oriented synthesis and drug discovery.



Scheme 26. Elaboration of the oxyallyl cation intermediate **140**.

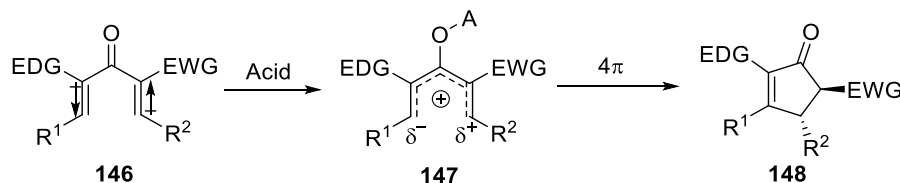
1.6.1 Promoting the Nazarov reaction

While the Nazarov reaction is promoted by both Lewis and Brønsted acid, without the appropriate functionality, it often requires extreme conditions for the pentadienyl cation to undergo cyclization. Simple divinyl ketone that has typical alkyl or aromatic group often encounters slow and inefficient cyclization, therefore, forming multiple diastereomers over an extended period. Therefore, a strong electron-donating group (X) is preferable for efficient Nazarov cyclization.



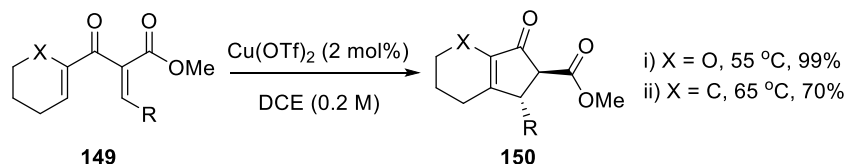
Scheme 27. Delocalization of positive charge in presence of strong electron donor **X**.

Heteroatoms are great examples of electron-donating group that promotes the Nazarov reaction. It facilitates the cyclization by donating its lone pair to stabilize the oxyallyl cation (**144a-c**, **Scheme 27**).⁷²⁻⁷³ This stabilization allows the oxyallyl cation to undergo a variety of trapping cascade, yielding a range of complexed sp^3 -rich cyclopentanoid scaffolds. Therefore, the electron-donating group must be at α position of pentadienone to provide resonance stability.



Scheme 28. The proposed polarized Nazarov reaction by Frontier *et al.*

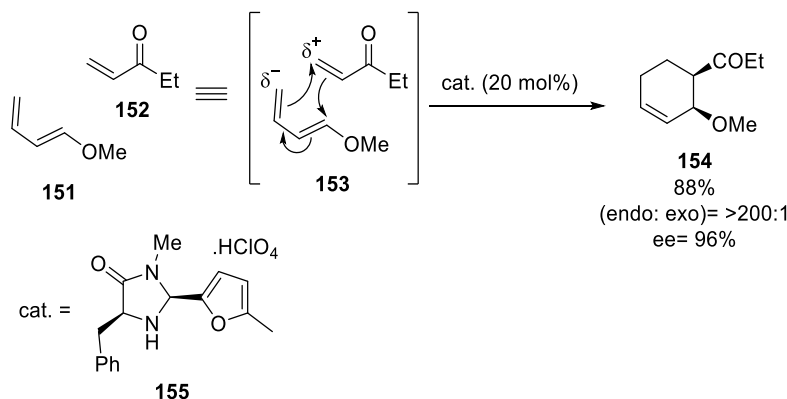
Meanwhile, previous studies by Frontier group have also indicated the presence of both electron-donating and electron-withdrawing group on α and α' positions facilitate the Nazarov reaction, known as the polarized Nazarov cyclization (**Scheme 28**).⁷⁴⁻⁷⁵



Scheme 29. Examples of the polarized Nazarov reaction by Frontier *et al.*

The idea was originated from the most classical pericyclic reaction, the Diels-Alder reaction. Similar to the Nazarov reaction, in the absence of activating groups, the Diels-Alder reaction requires harsh conditions to form simple cyclohexene from an alkene and 1,3-butadiene. However, the installation of electron-donating and electron-withdrawing group on diene and dienophile respectively, increases the rate of reaction rapidly by delocalizing partial charges, promoting the movement of electrons in

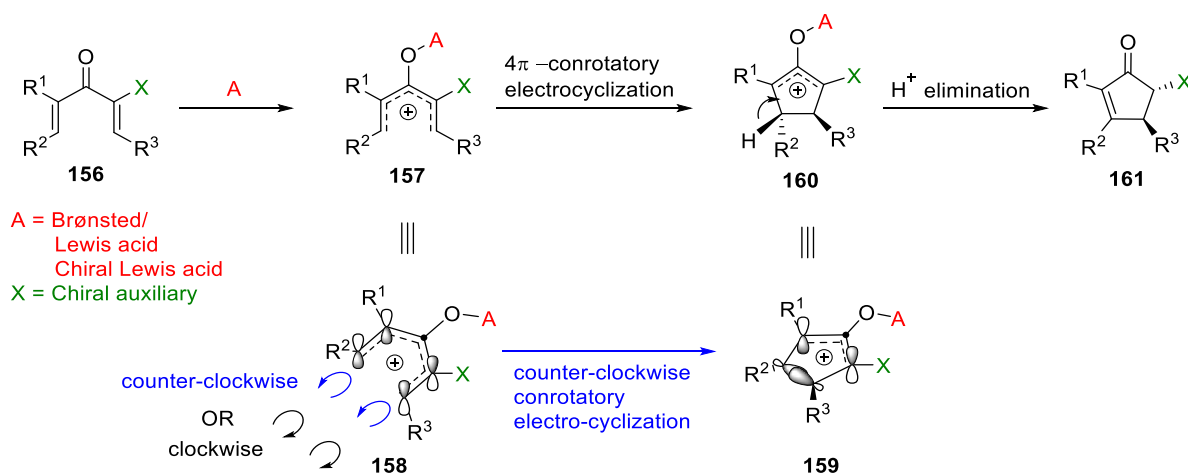
favourable directions, hence leading to spontaneous electrocyclization. The example in **Scheme 30** demonstrates the utility of polarization in the Diels-Alder reaction.⁷⁶ Besides, the employment of chiral imidazolidinone perchloric acid salt **155** in this example yielded excellent enantioselectivity, which also indicates the significance in controlling the enantioselectivity.



Scheme 30. Chiral catalyst induced Diels-Alder reaction.

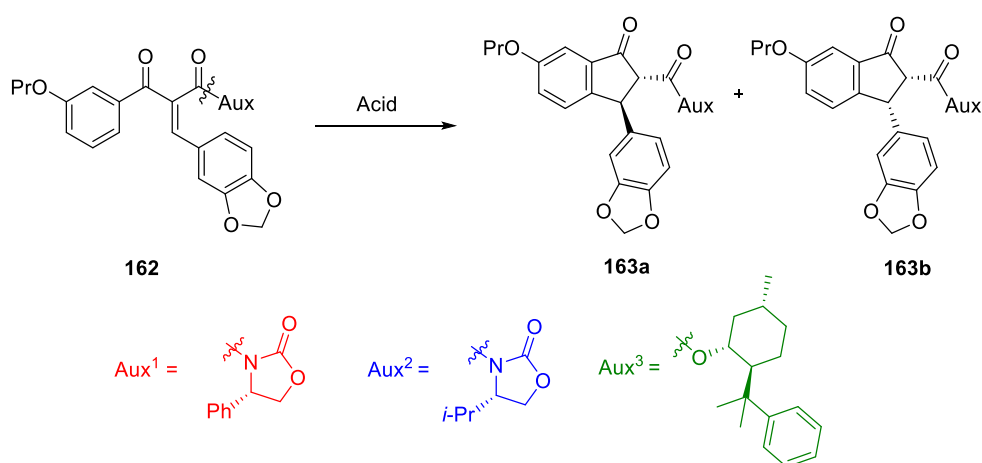
1.6.2 Auxiliary groups as master controllers of reactivity and torquoselectivity

Undoubtedly, the Nazarov cyclization emerges as a powerful pericyclic reaction that forms sp^3 -rich cyclopentanoids. Despite the diastereospecificity of this reaction, chemists often observed unexpected stereochemical outcomes. As mentioned before, the Nazarov reaction undergoes conrotatory electrocyclization, giving diastereospecific outcome (**Scheme 31**). However, the direction of the bond or orbital rotation during the cyclization is extremely important to predict the stereochemical outcome, and the control of specific bond rotation is named torquoselectivity. Controlling the torquoselectivity has been a popular area of research over the past decade, where several different approaches have been applied, with the most common approaches being the installation of chiral auxiliary or chiral acid loading.



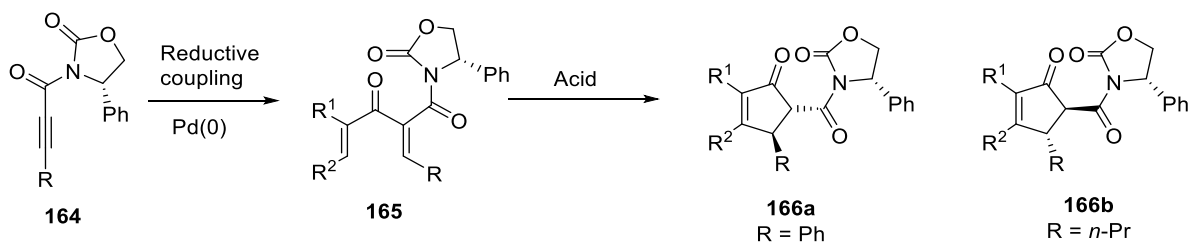
Scheme 31. Chiral auxiliary/ chiral acid-induced torquoselective Nazarov cyclization.

Chiral auxiliaries are powerful stereochemical inducers that provide steric interaction with reaction substrate, therefore giving coherent torquoselectivity. This technology has been a useful tool within synthetic chemistry. Currently, the architecture and utility of these auxiliaries are improving rapidly. An early chiral auxiliary for the Nazarov reaction was proposed by Pridgen and co-workers, where they attempted the asymmetric synthesis of endothelin receptor antagonists SB 209670 and SB 217242 via the Nazarov reaction.⁷⁷ These different auxiliaries were examined, where 8-phenylmenthol (**Aux³**, **Scheme 32**) found to be the most selective in the presence of catalytic amount of SnCl₄. However, when phenyl oxazolidinone (**Aux¹**, **Scheme 32**) was installed, it yielded a more stereoselective outcome due to the predominant formation of one specific epimer **163a** and ease in purification.



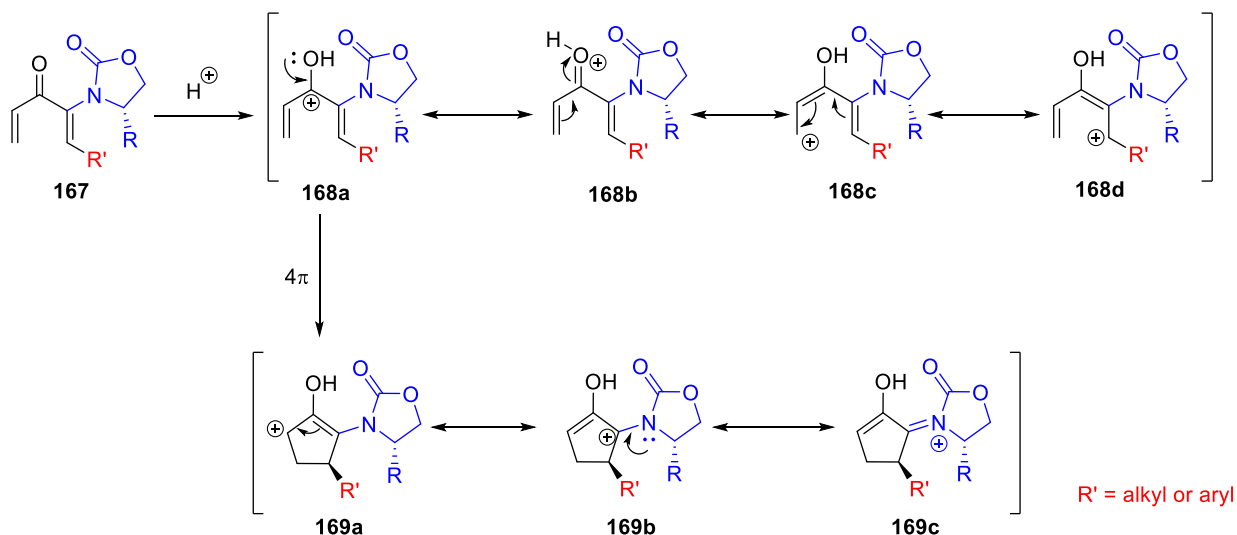
Scheme 32. First chiral auxiliary for Nazarov reaction by Curtis *et. al.*

Over the past 17 years, Flynn's group has been undertaking extensive research on the utility of chiral oxazolidinone, to control absolute torquoselectivity in the Nazarov reaction. Due to the lack of substrates examination by Pridgen and co-workers, Flynn's group extensively studied on the carboxy oxazolidinone directed torquoselective Nazarov cyclization. Substrates prepared by Flynn and co-workers were differentiated by having R = *n*-Pr or Ph. The investigation suggested that having alkyl or aryl switches the torquoselectivity, where aryl bias towards the formation of **166a**, and alkyl bias towards the formation of **166b** (**Scheme 33**).⁷⁸⁻⁷⁹



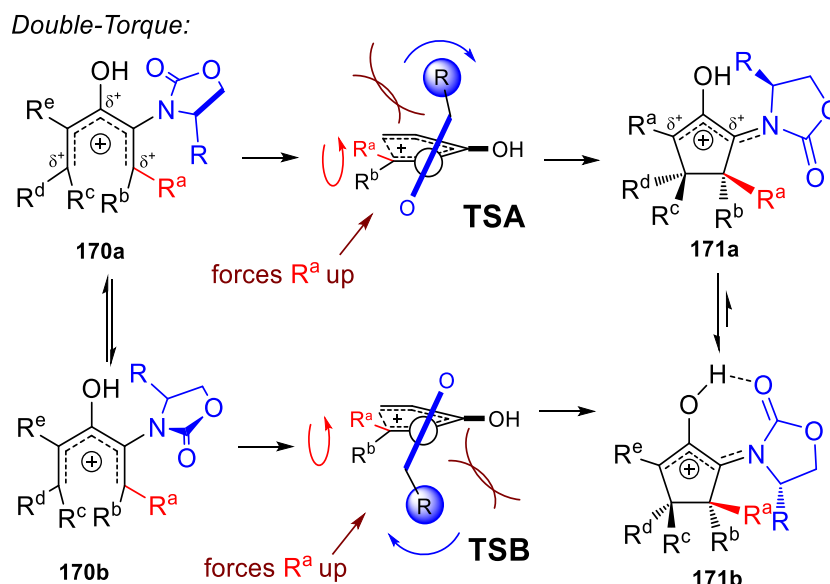
Scheme 33. The examination on carboxy-oxazolidinone directed Nazarov cyclization

Later investigation of chiral auxiliary within Flynn's group remains around oxazolidinone, where carboxy linker was removed. The direct attachment of chiral oxazolidinone serves as an electron-donating group. The donation of lone pair from nitrogen stabilizes oxyallyl cation **169a-c**, reduces the energy barrier for electrocyclization, hence increases the rate of reaction (**Scheme 34**). The oxyallyl cation stabilization also facilitates further reactions on oxyallyl cation **169a-c**, providing divergency to the Nazarov reaction, meanwhile controlling torquoselectivity.⁸⁰



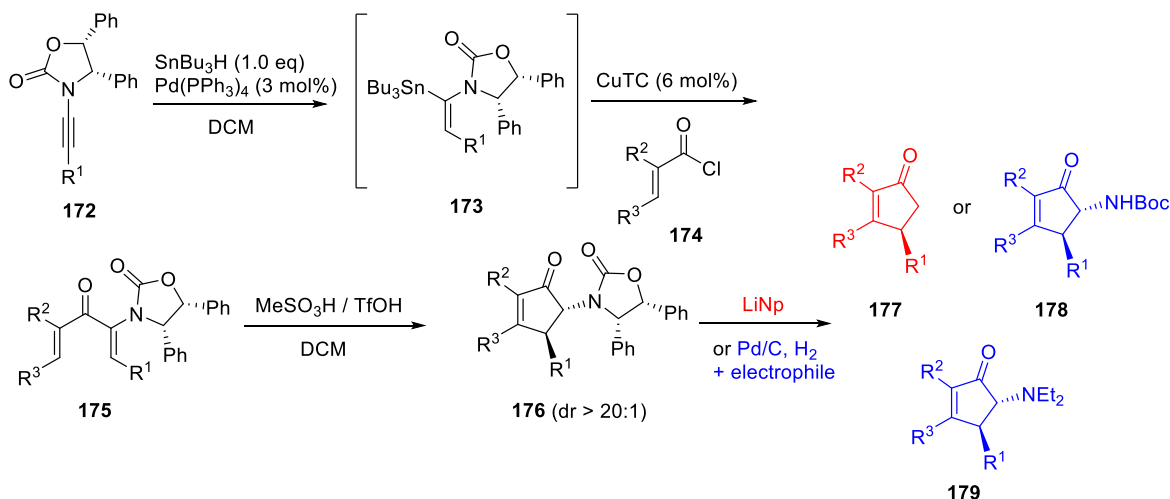
Scheme 34. Oxazolidinone stabilizes oxyallyl cation **169a-c**.

To interpret the mechanism of chiral induction from oxazolidinone, Flynn's group collaborated with Dr Elizabeth Krenske to perform a computational study. Density functional theory (DFT) has indicated the “double-torque mechanism” of oxazolidinone, which provides outstanding stereinduction. DFT calculations reveal to pentadienyl cations **170a** and **170b** of similar energy where the oxazolidinone has opposite conformations. In both of these conformations, the lone pair of electrons on the nitrogen of the oxazolidinone is out of conjugation with the pentadienyl cation. As the pentadienyl cation approaches the transition state of cyclization **170a** \rightarrow **TSA** and **170b** \rightarrow **TSB**, the oxazolidinone rotates to increase overlap of the lone-pair of the *N*-group with the pentadienyl cation, reaching coplanarity in intermediates **171a** and **171b**, respectively. In this rotation of the oxazolidinone, R (blue sphere) is position on the trailing face of the oxazolidinone for steric relief. This forces *O*-group in **TSA** and the C-H group in **TSB** to sterically clash with **R^a**, forcing it up. Thus, both conformation of **164** (**a** and **b**) rotate the auxiliary in a clockwise direction and **R^a** & **R^b** in a counter-clockwise direction, affording **171a/b** with excellent stereo-induction (**Scheme 35**).⁸⁰⁻⁸¹



Scheme 35. Density functional theory calculation, “double torque” mechanism, achieving the same torquoselectivity.

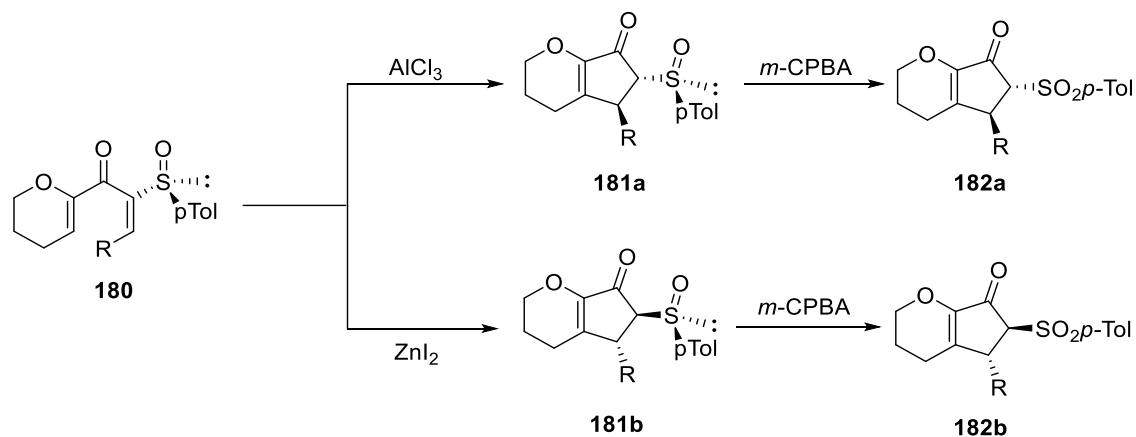
Flynn’s group has published many articles on the oxazolidinone promoted Nazarov cyclization. In **Scheme 36**, ynamide **172** undergoes reductive Stille coupling to give pentadienone structure **175** in a range of 60–91% yield, followed by the Nazarov cyclization by treatment of Brønsted acid, yielding cyclopentanoids **176** enantio- and diastereoselectively. Oxazolidinone could be cleaved using lithium naphthalenide forming **177**, designated the possibility of it being synthetically elaborated.⁸² Diphenyl oxazolidinone also acts as a masked amine, where it could be hydrogenated into protected amine **178** and **179** in the presence of Boc anhydride or aldehydes (reductive amination) during the hydrogenation (**Scheme 36**).



Scheme 36. Example of chiral oxazolidinone promoted torquoselective Nazarov cyclization.

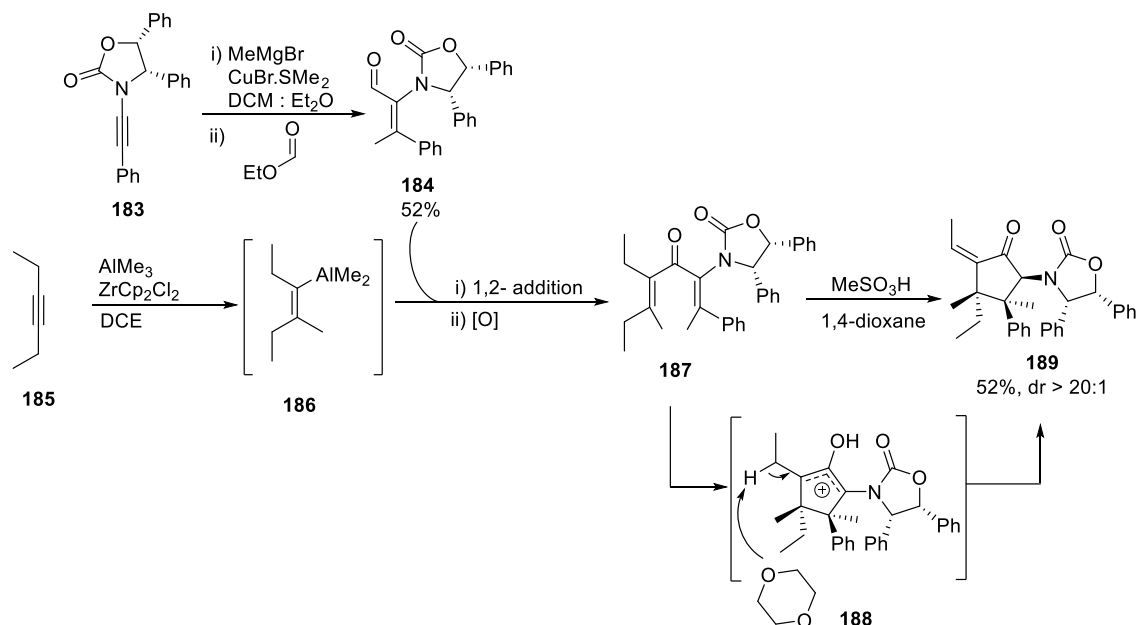
More recently, Xavier and co-workers have also published the torquoselective Nazarov reaction by having chiral sulfoxide to promote chiral induction (**Scheme 37**).⁸³ They took advantage of the

polarized Nazarov reaction, where oxygen on the dihydropyran and sulfoxide act as electron-donating and electron-withdrawing group, respectively. Interestingly, chiral sulfoxide responded differently to different Lewis acid, yielded two different diastereomers torquoselectively (**181a-b**, Scheme 37). Chiral sulfoxide was further translated into sulfonyl moiety, yielding **182a** and **182b** enantioselectively.



Scheme 37. Chiral sulfoxide induced torquoselective Nazarov cyclization.

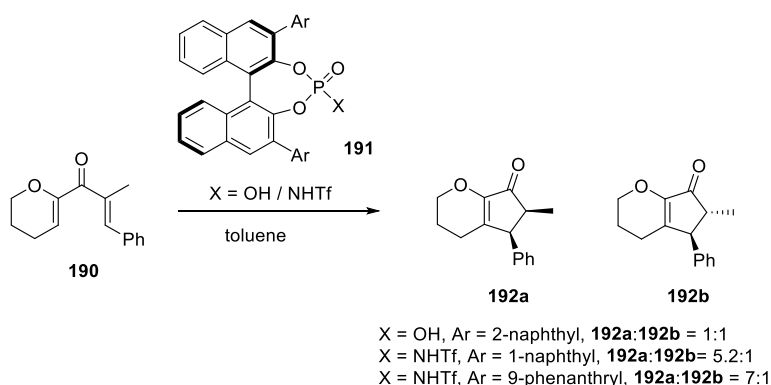
A later study by Volpe and Flynn has further demonstrated the convergent access into fully substituted divinyl ketone **187**, via 1,2-addition of preformed vinyl alanate **186** to oxazolidinone containing aldehyde **184**, followed by oxidation. The treatment of acid in basic solvent, 1,4-dioxane, provided access into two all-carbon 4°-stereocentres containing cyclopentanoid **189**, enantioselectively. The formation of **189** has shown the broad utility of chiral oxazolidinone, in attaining excellent torquoselectivity in the cyclization of fully substituted Nazarov substrates (**Scheme 38**).⁶⁵



Scheme 38. Torquoselective synthesis of **189** containing two contiguous 4°-stereocentres.

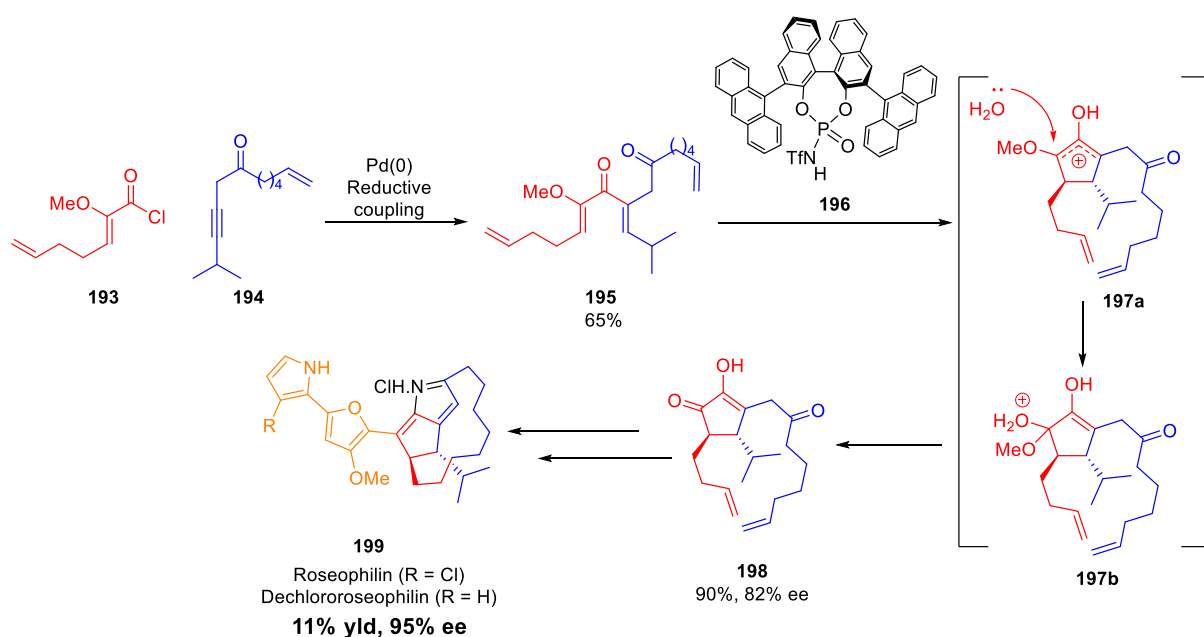
1.6.3 Chiral catalysis

While chiral auxiliary has proven its utility in controlling the torquoselectivity in the Nazarov cyclization, chiral acid has also been indicated to be one of the major prospects in stereo-induction. Scientists, in general, have been invariably investigating methods to induce enantioselectivity, using numerous reagents such as chiral ionic solvent⁸⁴, chiral auxiliary,^{67,80,81,83,85} or chiral phase-transfer catalyst.⁸⁶ Notwithstanding the effort that was spent in this area, the utility of chiral catalysts that have been developed is genuinely substrate-specific. Hence there is a serious demand for the development of chiral catalyst, expanding the capability to control enantioselectivity.



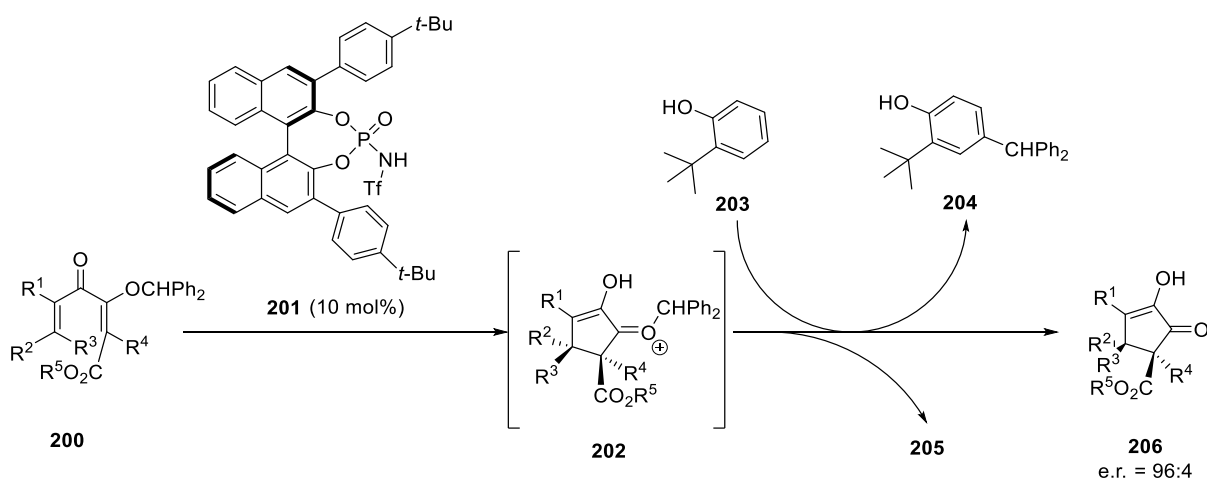
Scheme 39. Rueping study on chiral phosphoric acid and *N*-trifly phosphoramidate

Rueping and co-workers were the first to explore the utility of chiral Brønsted acid in stereo-induction of activated Nazarov precursor.⁸⁷ Although Rueping anticipated that phosphoric acid **191** ($X = \text{OH}$, **Scheme 39**) to give better control in torquoselectivity, when phosphoric acid was replaced with *N*-trifly phosphoramidate ($X = \text{NHTf}$), enantiomeric excess was increased to 87% (**Scheme 39**). Flynn's group utilized a similar *N*-trifly phosphoramidate in the synthesis of natural product, roseophillin **199**, an anti-cancer alkaloid.⁷³ Flynn and co-workers approached roseophillin synthesis using Pd-catalyzed reductive Stille coupling, forming divinyl ketone **195**. Nazarov reaction was attempted with catalytic load of chiral *N*-trifly phosphoramidate **191** ($\text{Ar} = \text{phenanthracene}$, **Scheme 39**) that was studied by Rueping and co-workers. However, result did not meet satisfactory as only a modest ee was obtained. This as well highlights the high substrate specificity of chiral catalyst in the Nazarov reaction. However, a modification to the aryl group by substituting phenanthracenyl groups for anthracenyl groups (**196**, **Scheme 40**), enantiomeric excess of **198** was improved from 60% to 82% (**Scheme 40**).



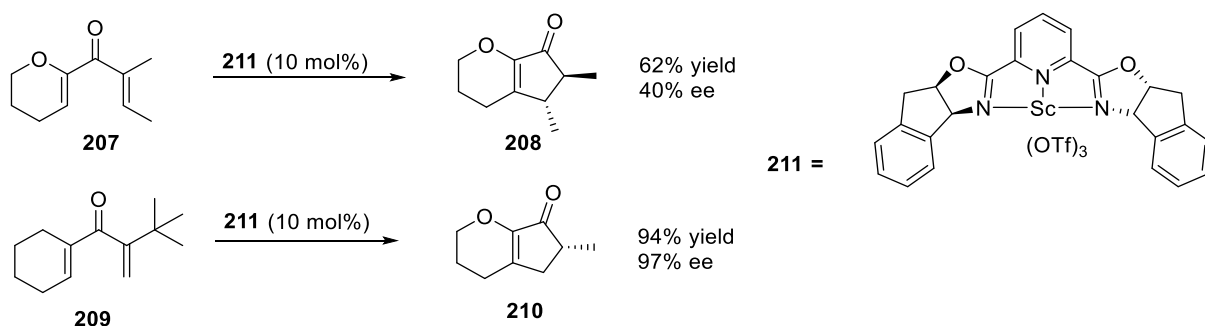
Scheme 40. Enantioselective synthesis of roseophilin **199**.

The latest modification of *N*-trifly phosphoramidate was made by Tius and co-workers, where they found that **201** yielded the best enantioselectivity.⁸⁸ 2-*tert*-butylphenol **203** in this specific example serves as nucleophile that removes benzyl group from stabilized cation **202**, which avoided the possibility of Wagner-Meerwein rearrangement. The significance of this investigation was that the Nazarov reaction was able to perform on fully substituted divinyl ketone, giving cyclopentanoids **206** in excellent enantiomeric ratio (**Scheme 41**).



Scheme 41. Development of *N*-trifly phosphoramidate **201** by Tius *et al.*

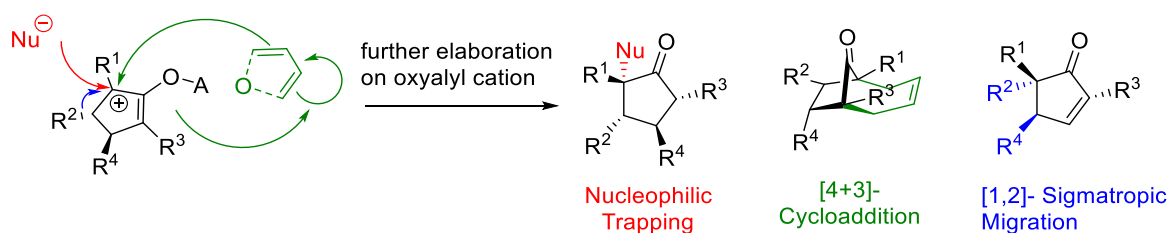
Nevertheless, *N*-trifly phosphoramidate is not the only chiral acid to have been examined. Trauner and co-workers employed chiral Lewis acid **211** where pentadienone was activated while coordinated to bidendate ligand (**Scheme 42**).⁸⁹



Scheme 42. Investigation of Chiral bidendate lewis acid **211** promoted Nazarov cyclization

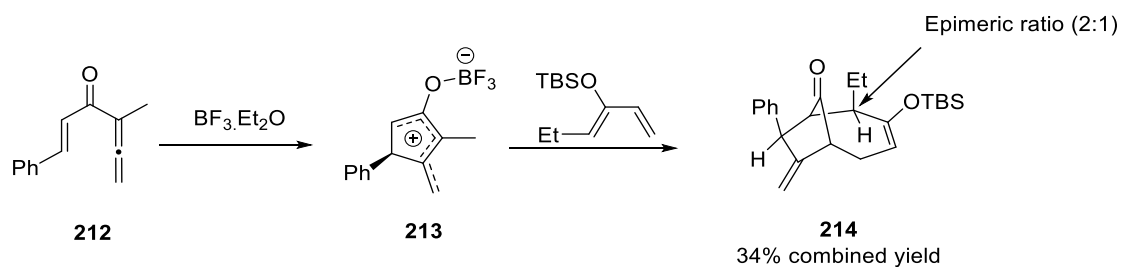
While a few different chiral acids used in specific circumstances, the compatibility of chiral acid needs to be further developed, as the current limitation of chiral catalysis yields inconsistent chiral induction with different Nazarov reaction substrates.

1.6.4 The interrupted Nazarov cyclization



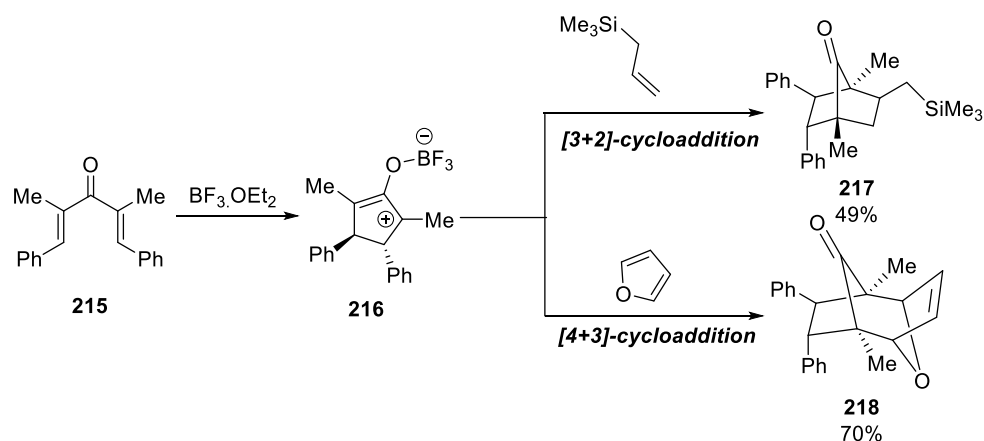
Scheme 43. Elaboration of oxyallyl cation intermediate

In addition to the introduction of asymmetric Nazarov reaction, another major innovation has been the interrupted Nazarov reaction. The interrupted Nazarov cyclization is an excellent method to further extend this diastereospecific pericyclic reaction, where the oxyallyl cation is captured by a nucleophile or diene, forming additional stereocentres, including 4°-stereocentres, avoiding β -proton elimination. Burnell was able to form cycloadduct **214** by interrupting the Nazarov reaction with the addition of siloxy substituted diene (**Scheme 44**).⁹⁰ Regardless of the modest yield, this reaction demonstrated the ability to form bridged ring structure in a one-pot process.



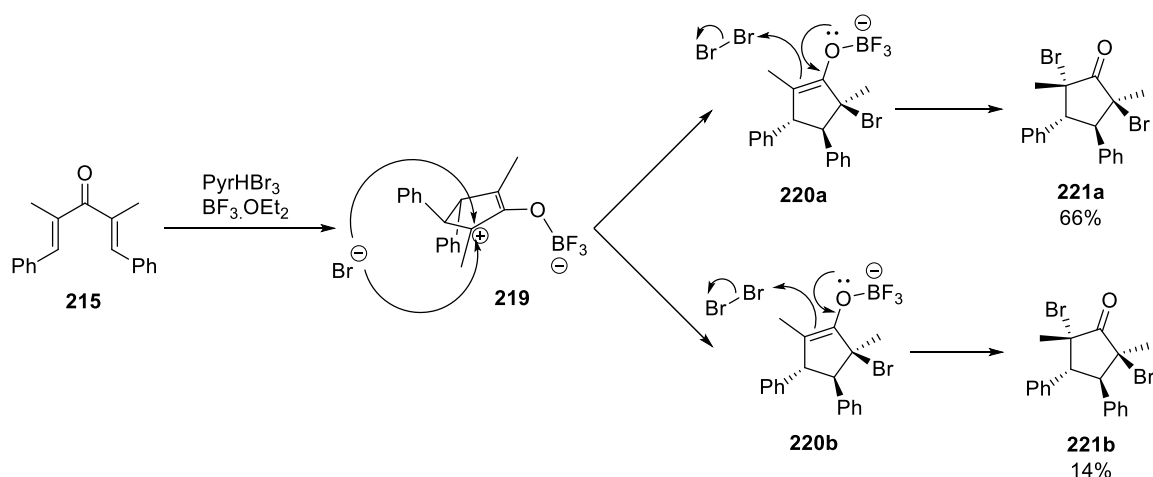
Scheme 44. Burnell's investigation on cycloaddition in the presence of diene

Other examples had also shown the formation of bridged ring structures when alkene or furan was used as an additive during the Nazarov cyclization, forming **217** and **218**, via [3+2] and [4+3]-cycloaddition, respectively (**Scheme 45**).⁹¹⁻⁹² The construction of these bridged ring structures are particularly valuable within organic chemistry, as the formation of two further bonds, and two all-carbon 4°-stereogenic centres are something that is proven to be extremely difficult to achieve.



Scheme 45. Formation of bridged rings **217** and **218** via [3+2]- and [4+3]-cycloaddition.

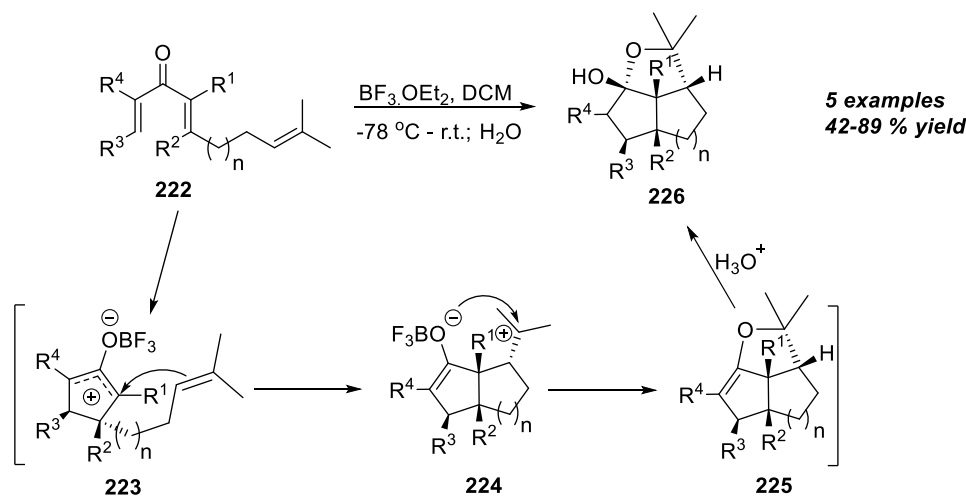
A recent publication by West and co-workers also indicated the possibility to use brominated reagent to trap oxyallyl cation **219**, forming α, α' -dibromo cyclopentanoid **221a** and **221b** (**Scheme 46**).⁹³ Halogenated species are known to be one of the most widely used functionalities within synthetic chemistry. Further elaboration on such stereogenic and halogenated species could yield extremely valuable compounds.



Scheme 46. Bromine trapping example by West and co-workers.

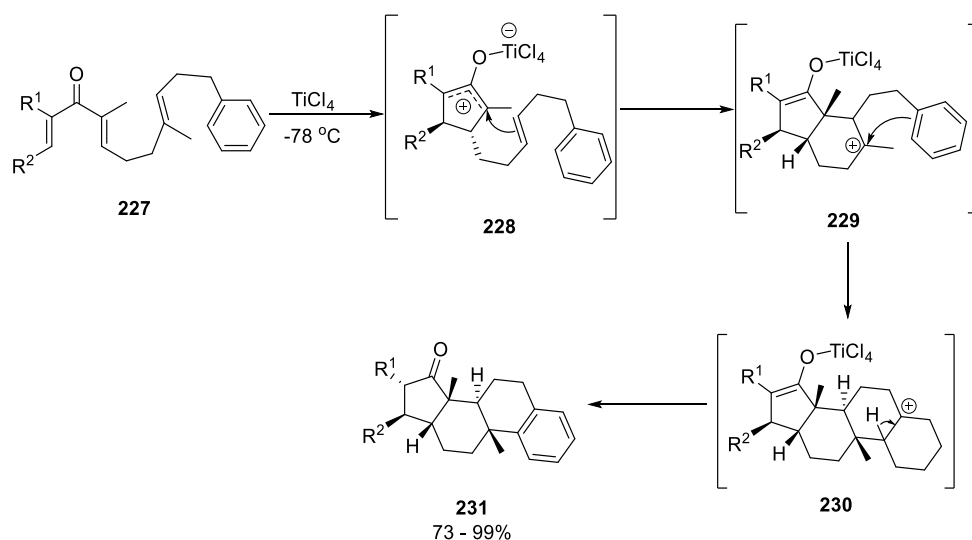
Notwithstanding the excellent achievement on yielding bromine trapped cyclopentanoids, tricyclic structures, diquinanes **226** could also be formed in the presence of tethered olefin, where oxyallyl

cation **223** was trapped with tethered alkene in a 5-*exo* cyclization fashion, followed by the final ring closure to afford hemiketal **226** diastereoselectively, in a range of 42-89% yield (**Scheme 47**).⁹⁴



Scheme 47. Diquinanes **226** formation via interrupted Nazarov cyclization by West *et al.*

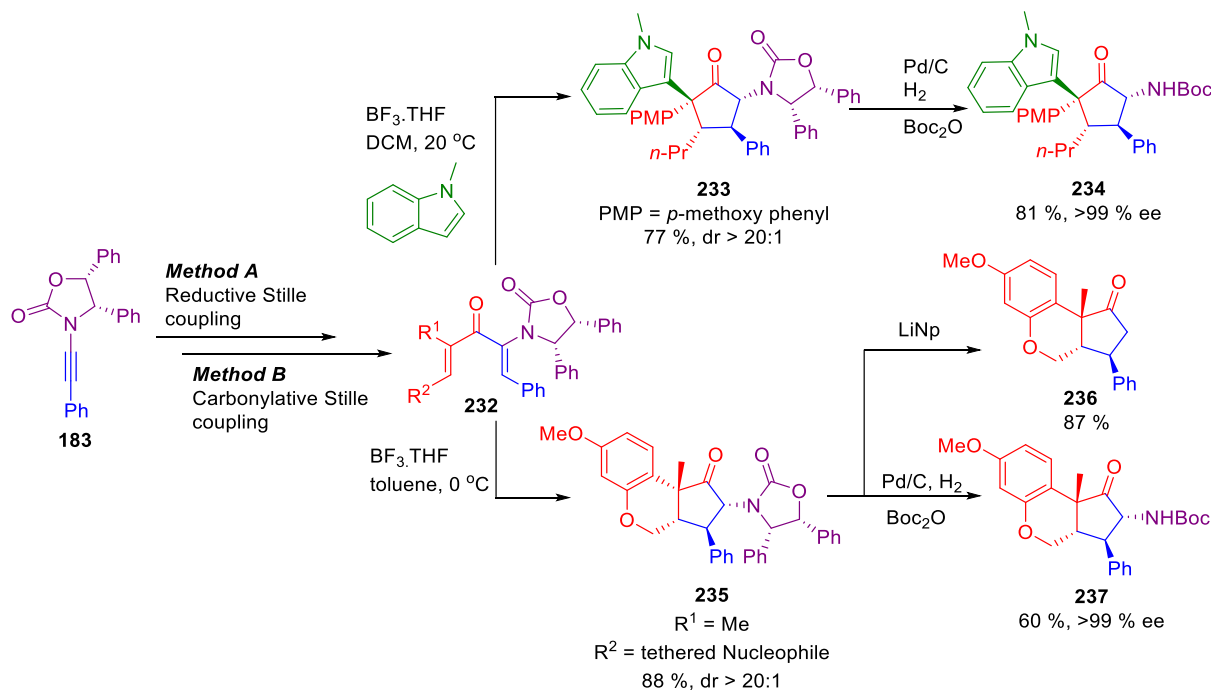
The formation of polycyclic compound **231** shows great scope in the synthesis of sterol scaffolds.⁹⁵ Tethered olefin on substrate **227** plays a major role in this cationic polycyclization, where the oxyallyl cation **228** was trapped by tethered alkene, followed by nucleophilic attack from aryl ring to form a sterol skeleton in a diastereoselective fashion. The formation of six stereocentres including two all-carbon 4°-stereocentres in a one-step has explained the divergence arises from the Nazarov cyclization (**Scheme 48**).



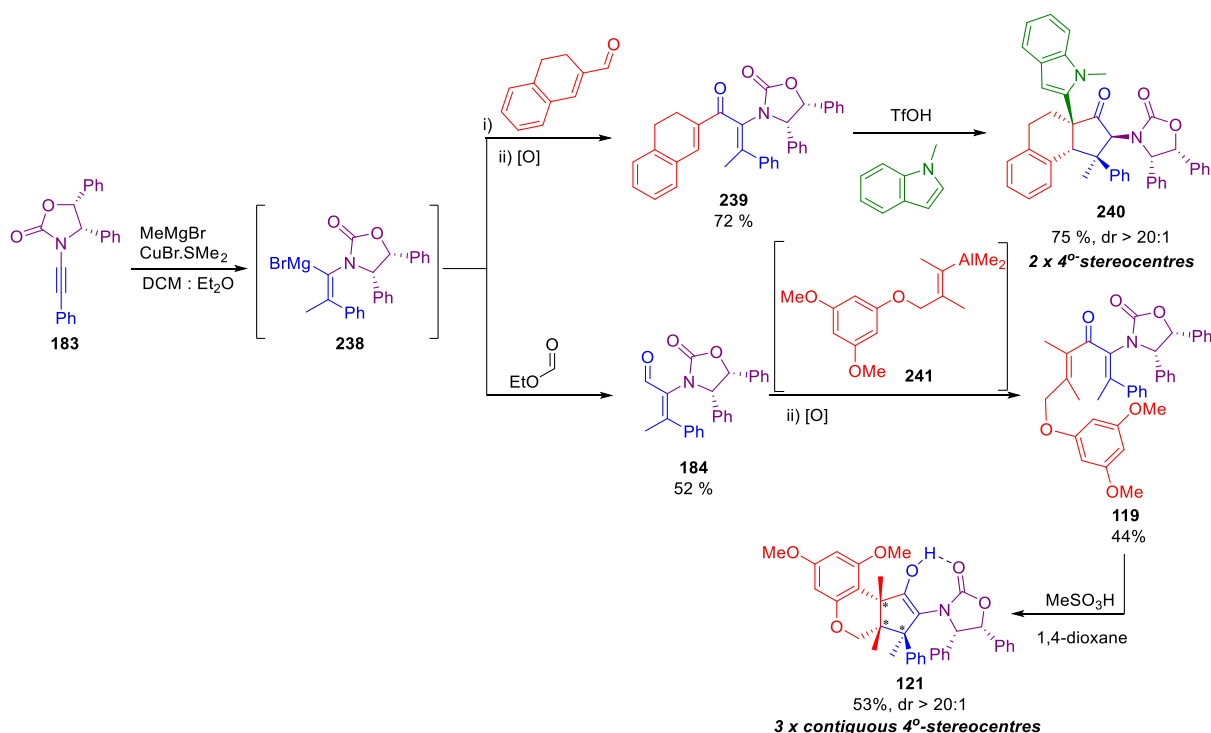
Scheme 48. The cationic poly-cyclization towards sterol scaffold **231**.

Flynn and coworkers have demonstrated the excellent utility of the oxazolidinone-controlled Nazarov reaction in nucleophilic trapping. In addition to promoting the Nazarov and inducing stereo-control, the oxazolidinone group drives the regio- and stereochemical placement of the nucleophile, as

exemplified in the formation of **233** and **235**. The oxazolidinone group can be conveniently removed to give C-H (LiNp) or an amine functionality (hydrogenation) (**234**, **236-237**, **Scheme 49**).⁸¹ The powerful Nazarov promoting properties of the oxazolidinone, combined with trapping enabled fully substituted divinyl ketone **119** to be cyclized to form up to three new 4°-stereocentres (**Scheme 50**).⁶⁵

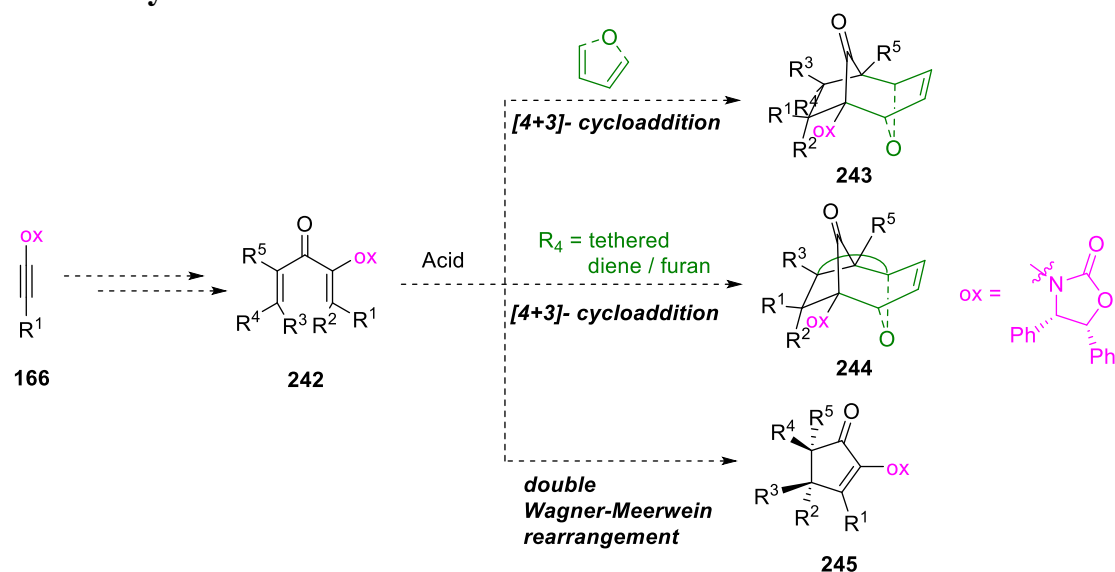


Scheme 49. Formation of sp³-rich cyclopentanoids with aid of chiral auxiliary.



Scheme 50. The formation of cyclopentanoids **121** and **240**, containing up to three 4°-stereocentres.

1.7 Aim 2: Synthesis of sp^3 -rich cyclopentanoids via torquoselective asymmetric Nazarov cyclization



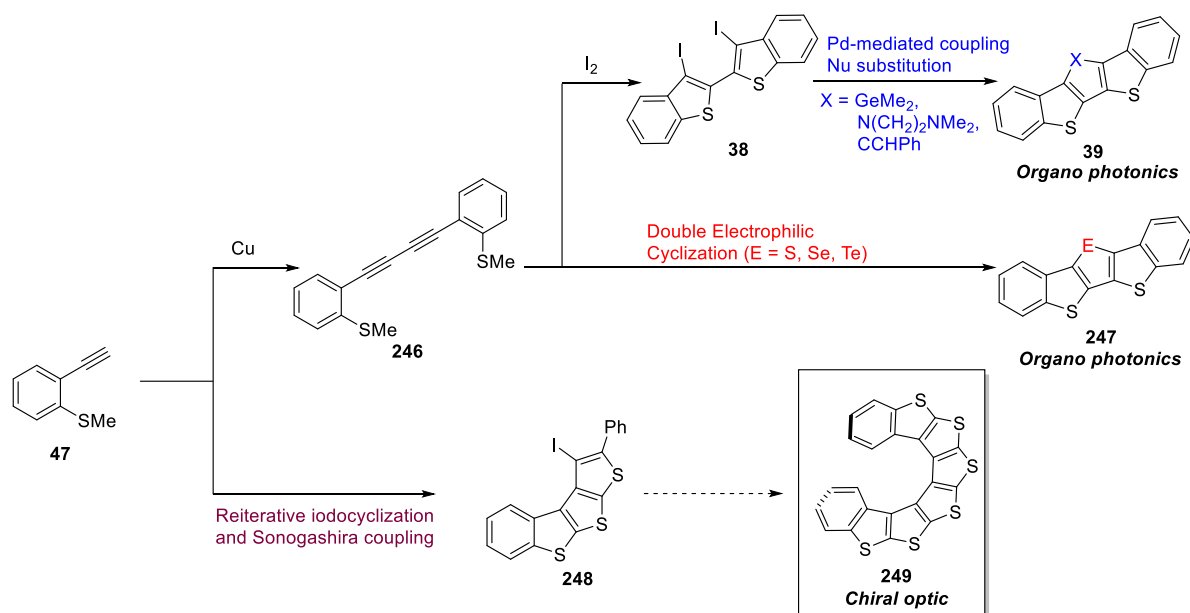
Scheme 51. Synthetic protocol towards complexed cyclopentanoids.

In this part of the project, we will be studying chiral oxazolidinone (ox) directed Nazarov cyclization, forming a variety of multiple all-carbon 4° -stereocentres containing cyclopentanoids. The synthetic protocol towards mentioned cyclopentanoids involves the initial formation of highly substituted Nazarov precursor **242** from ynamide **172**. Dienone **242** then undergoes the torquoselective Nazarov cyclization involving other reaction cascades, such as inter- or intramolecular [4+3]-cycloaddition, or double Wagner-Meerwein rearrangement to yield bridged **243**, fused-bridged **244** or normal cyclopentanoids **245** that contain multiple all-carbon 4° -stereogenic centres (**Scheme 51**).

Chapter 2

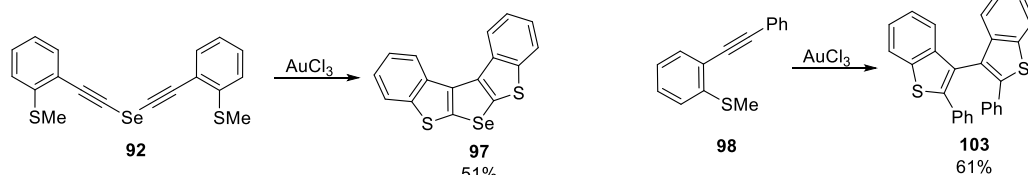
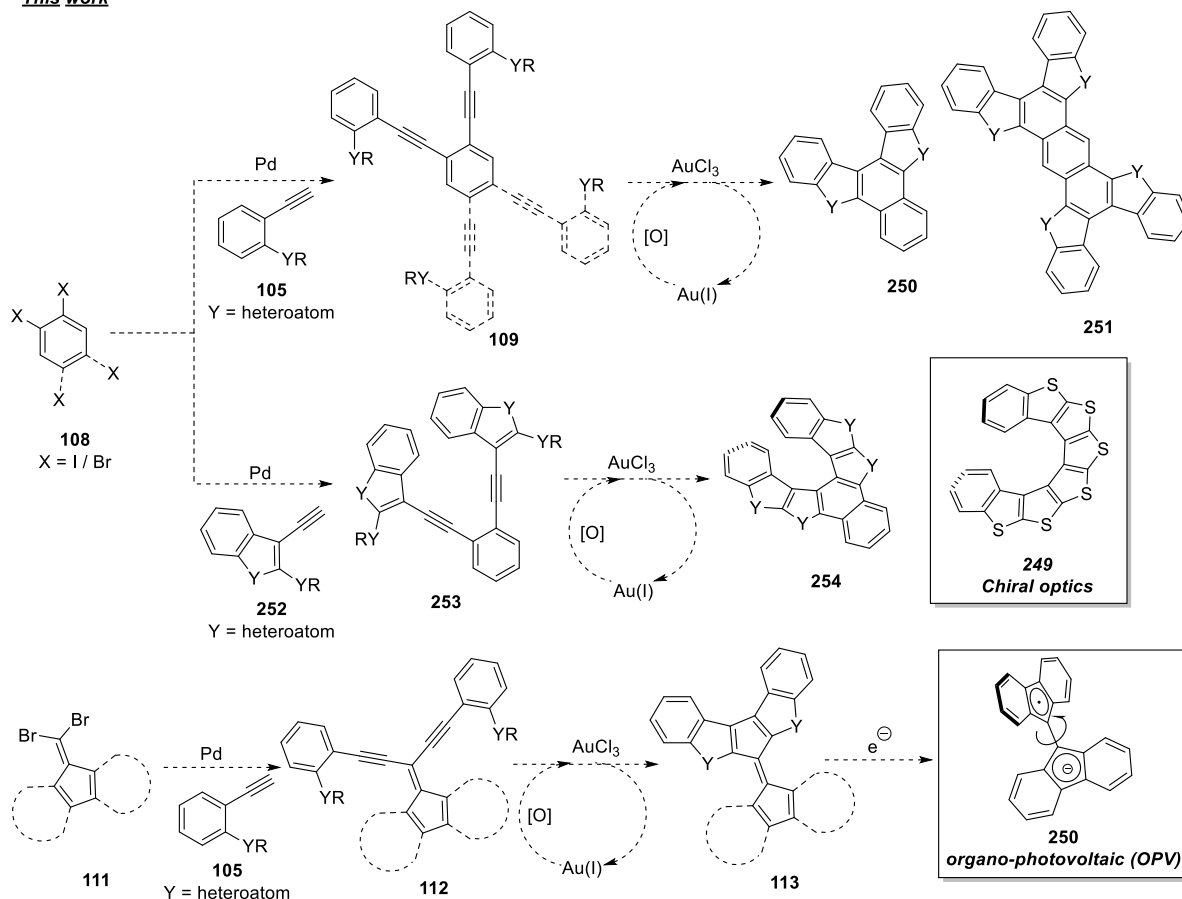
2. Result and discussion: Synthesis of angular heteroacenes via Double-Electrophilic Cyclization Reductive Elimination (DECREE) reaction

As discussed in **Chapter 1**, our group has developed the Double- Electrophilic Cyclization (DEC) reaction, where electrophiles such as iodine and ECl_2 ($\text{E} = \text{S}, \text{Se}, \text{TeCl}_2$) were used, to give either linear bis-iodobenzothiophene **38** and heteroacene **247**, respectively. The further elaboration of **38** then furnished the synthesis of linear heteroacene **39**, where unusual elements such as germanium were incorporated (**Scheme 52**).³¹⁻³² The formation of iodo-substituted benzothiophene scaffold **248** via reiterative iodo-cyclization and Sonogashira coupling reaction also helps exploring the scope in the formation of chiral optic **249**.²⁴



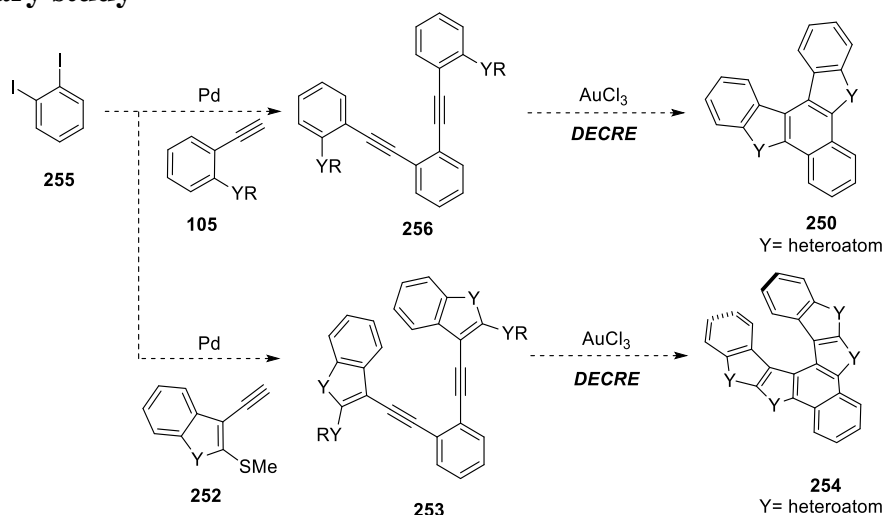
Scheme 52. Iodo-cyclization and double-electrophilic cyclization, towards heteroacenes **39**, **247**, and **248**.

The unique ability of gold to promote cyclization provides a great utility in the formation of polycyclic or heteroaromatic compounds.⁹⁶ Recently, our group proposed the Double-Electrophilic Cyclization Reductive Elimination (DECREE) reaction.³² The development of the DECREE reaction yielded selenium and sulfur containing compound **97** in 51% yield (**Scheme 53**). However, due to the limited number of examples generated from the DECREE reaction, in this thesis, we propose the elaboration on the synthesis of angular heteroacenes, via the DECREE reaction. We expect that the development of the DECREE reaction would allow access into a diverse array of extended heteroacenes, including **250**, **251**, **254** and **113**, where the formation of **254** and **113** could potentially be used as chiral optics and organo-photovoltaics, respectively.

Previous work from Flynn's group*This work***Scheme 53.** Synthetic strategies towards target compounds.

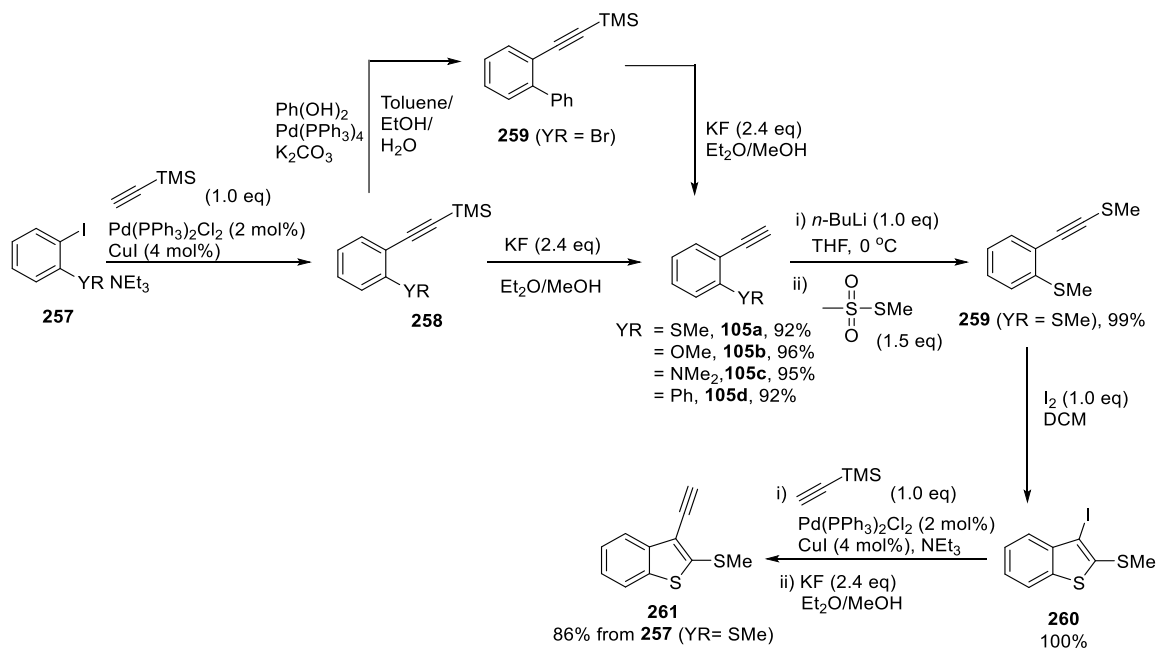
To initiate the study of our novel DECARE chemistry, we devised a general synthetic route. This protocol involves an initial Pd-mediated Sonogashira coupling reaction, from either 1,2-di or 1,2,4,5-tetra halogenated benzene **108** with electron-rich terminal alkynes **105** and **252** (Scheme 53). The resultant bis/tetra alkyne species **109** and **253** would then undergo DECARE with the addition of AuCl_3 to yield heteroacene **250**, **251** and **254**, forming three or six new rings (bidirectional). Additionally, we will also be investigating the synthesis of fulvalene derivative **113**. The synthesis initiates with Sonogashira coupling reaction on geminal dibromide **111**, yielding diyne **112**, followed by the DECARE reaction, yielding multi-chalcogen containing fulvalene derivative **113**. We will also investigate on the catalytic usage of AuCl_3 , where the presence of a suitable oxidant should oxidize the reductively eliminated Au(I) back to AuCl_3 .

2.1. Preliminary study

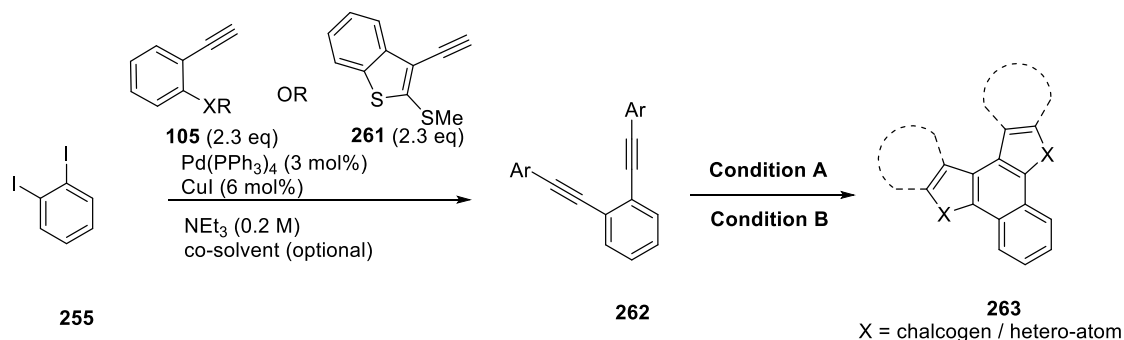


Scheme 54. Synthetic targets.

Our DECARE study was based on the cyclization of substrates **256** and **253** to corresponded **250** and **254**, respectively (Scheme 54). The synthesis of related terminal alkynes (**105a-d** and **261**, Scheme 55) are required for the formation of substrates **256** and **253**. Scheme 55 details the general synthetic route towards terminal alkyne **105a-c**. The preparation starts with Sonogashira coupling of TMS acetylene with aryl iodide **257**, followed by silyl deprotection to give **105a-c**. The Suzuki coupling between **258** (YR = Br, Scheme 55) and phenyl boronic acid, followed by silyl deprotection to yield **105d**. The synthesis of **261** initiated with lithiation of **105a** and nucleophilic substitution to give **259**. This is followed by the iodo-cyclization of **259** to give **260** in quantitative yield. **260** Then undergoes the Sonogashira coupling and silyl deprotection to yield **261**.²⁴

Scheme 55. Synthesis of terminal alkynes **105a-d**, **261**.

Diyne **262a-e** were all obtained in moderate to good yield (41-94%) via the Sonogashira coupling to diiodobenzene **255** (Table 1). With the obtained substrates **262a-e**, we first investigated the addition of AuCl₃ to **262a-e**, where **262a** was anticipated to react most rapidly. It is reasonable to expect the formation of **263a-e** resulted from the treatment of **262a-e** with AuCl₃, as this has been previously observed with similar selenium type product **97** from our research group (see Page 14, Scheme 19).



Scheme 56. Condition A: AuCl₃ (1.1 eq), DCE (0.1 M) rt; Condition B: **262** in DCE (0.1 M), slow addition into AuCl₃ (1.1 eq) in 1,4-Dioxane (0.1 M) at 70 °C over 3 h.

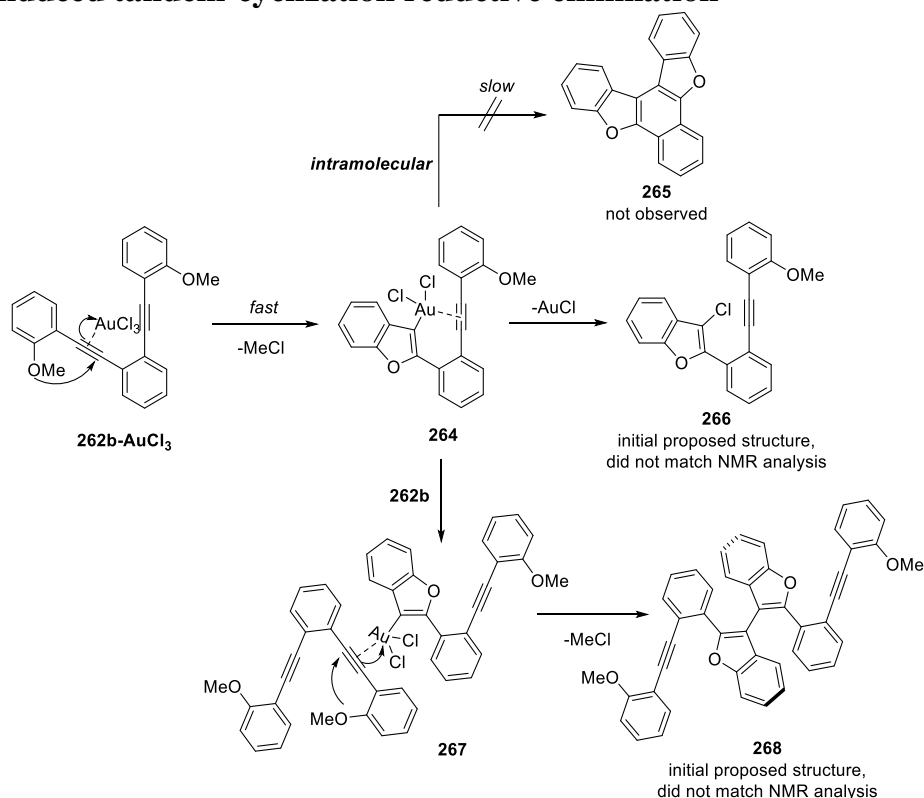
Table 1. Synthesis of di-yne substrates and gold cyclization

Entry	105/ 261	255 → 262 (yield%)	262 → 263 (yield%)
1	 105a (XR= SMe)	262a (82%)	 263a (60%) [Condition A]
2	 105b (XR= OMe)	262b (72%)	Unknown 262b - (1 x Me) + Cl [262b - (1 x Me)] x 2 [Condition B]
3	 105c (XR= NMe ₂)	262c (94%)	complex mixture (polymerization)
4	 105d (XR= Ph)	262d (41%)	complex mixture (polymerization)
5	 261	262e (89%)	Unknown 262e - (1 x Me) + Cl [262e - (1 x Me)] x 2 [Condition B]

The results obtained from NMR and mass spectroscopic analysis confirmed the formation of **263a** (60%), which was the expected outcome from the DECRE reaction. The loss of methyl resonance on

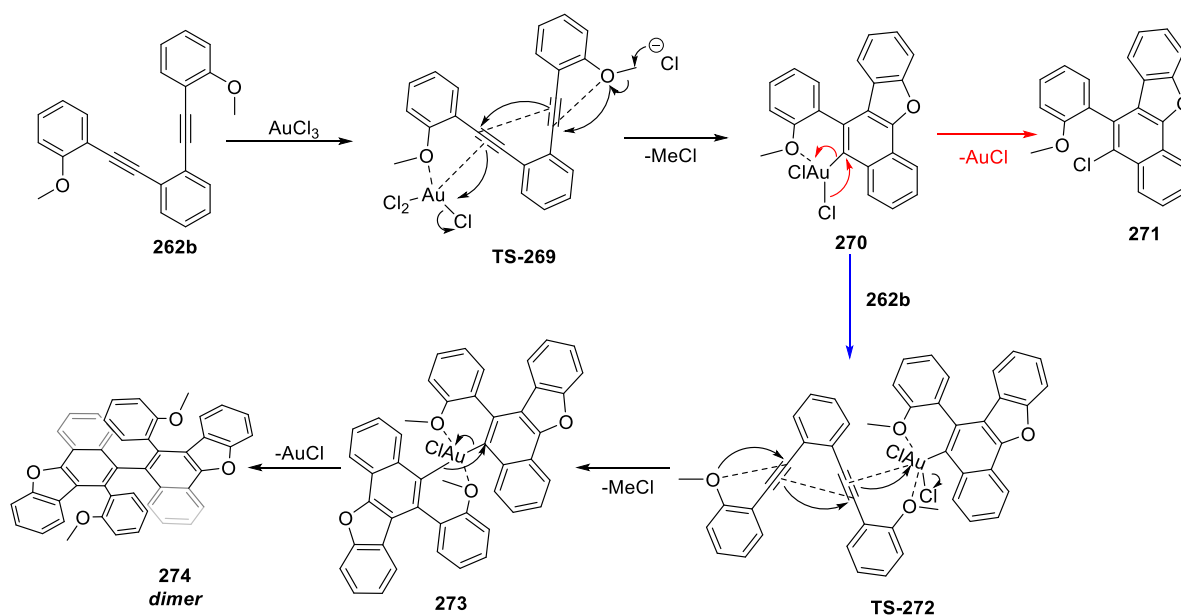
the NMR spectrum was indicative of the formation of **263a**. The related reaction mechanism of the formation of **263a** is explained in **Scheme 19** (**Page 14, Chapter 1.3.3**).

Given the success in the synthesis of **263a**, we then looked at performing the same reaction with substrate **262b**, which contains oxygen instead of the sulfur as the nucleophile. Substrate **262b** was not as reactive as **262a**, as polymerization was observed with the oxygen atom (**Condition A, Scheme 56**). This issue was resolved through the use of a slow addition technique (**Condition B, Scheme 56**). Even though polymerization was minimized from the slow addition process, the expected oxygen equivalent of **263a** (**263**, X = O) did not form. ¹H NMR and high-resolution mass spectrometry (HRMS) indicated to the formation of two unknown products, which indicate either a loss of 1 x *Me*-group and an installation of *Cl*-group ([**262b** - (1 x *Me*) + Cl]), and a dimeric product of **262b** which also has a loss of 1 x *Me* per monomeric unit ([**262b** - (1 x *Me*)] x 2). The investigation of DECRE was continued with the cyclization of **262c** and **262d**, where a NMe₂ or Ph group were used as the nucleophiles, respectively. Unfortunately, polymerization was observed with both substrates, even with slow addition of reaction substrates to AuCl₃. In the case of **262d**, Na₂CO₃ was used as an additive to quench HCl that was produced during the cyclization. Despite this, polymerization remained persistent, resulting in a complex product mixture (**Table 1**). For the cyclization of substrate **262e**, we also observed a similar outcome as the treatment of **262b** with AuCl₃ ([**262e** - (1 x *Me*) + Cl]), and ([**262e** - (1 x *Me*)] x 2). The insight of this observation will be described below in **Chapter 2.2**.

2.2. AuCl₃-induced tandem-cyclization reductive elimination

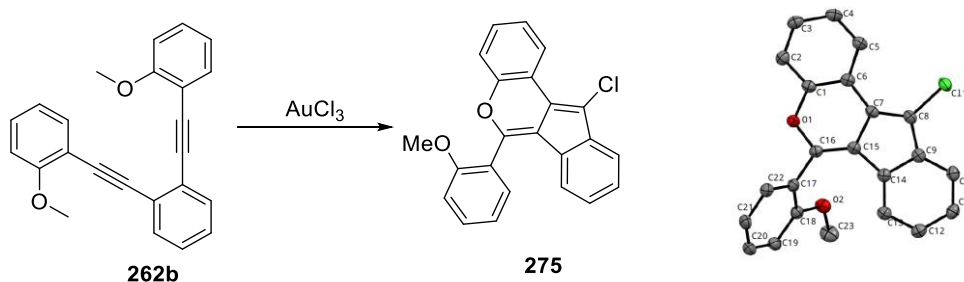
Scheme 57. Initial proposed products **266** and **268**.

In **Section 2.1**, we described the formation of unexpected products from the treatment of **262b** and **262e** with AuCl₃. The initial ¹H NMR analysis shows *OMe*-group related resonance, which indicates the reaction did not yield expected product **265** (**Scheme 57**). Meanwhile, the ¹H NMR analysis also points towards where one of the *OMe*-group is consumed. We then proposed that either chloride **266** or alkynyl dimer **268** has formed. However, ¹³C NMR shows full consumption of alkyne resonances, indicates that both **266** and **268** are not the obtained products. Since one *OMe*-group remained, both alkynes consumed, and a chloro and dimer product detected in the mass spectrometry (MS), we proposed a tandem cyclization pathway that gives both **271** and **274**. However, we could not discern which was the major product (**271** or **274**) as both were present and assignable to the NMR spectra.



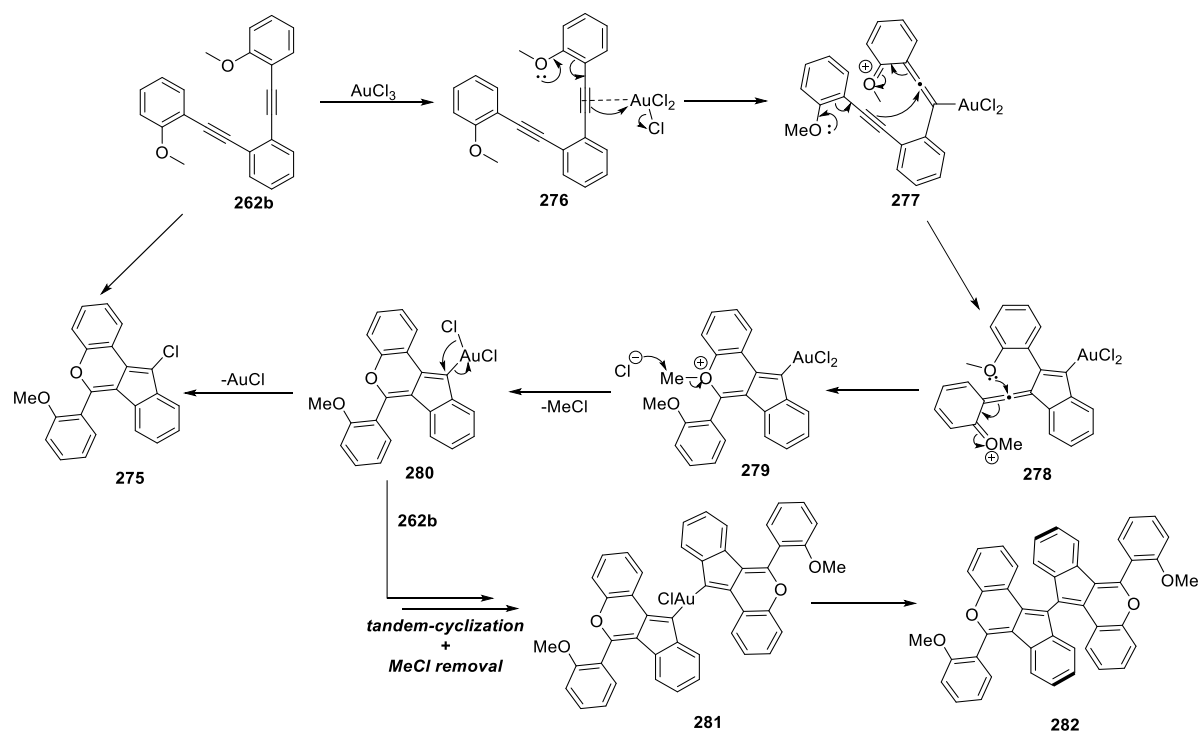
Scheme 58. Explanation in the formation of proposed structures **271** and **274**.

Eventually, recrystallization yielded pure material, which was used in X-ray crystallography. Surprisingly, this gave structure **275** as the product (isomer of **271**). Accordingly, we adjusted our mechanistic proposal for the conversion of **262b** into chloride **275** and dimer **282**.



Scheme 59. X-ray crystallography of obtained product **275**.

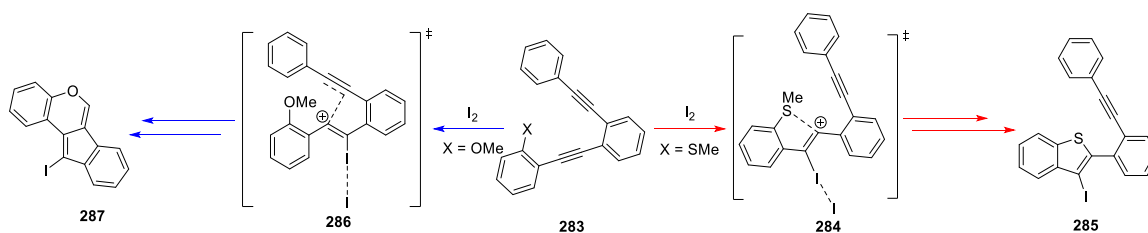
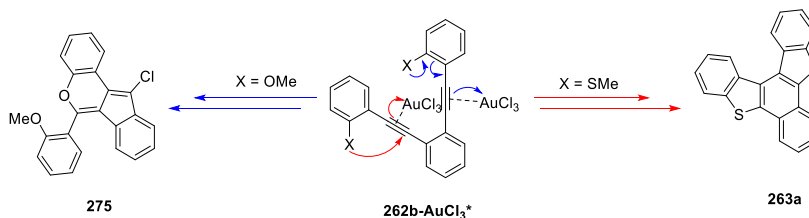
We suggest that AuCl_3 coordinates to triple bond electrophilically activates the alkyne forming allenyl oxonium cation **277** (**Scheme 60**). The presence of another alkyne on intermediate **277** then traps this electrophilic allenyl oxonium ion, allows an intramolecular cyclization to form intermediate **278**. The *OMe*-group in **278** then undergoes nucleophilic attack the electrophilic allene intermediate, forming intermediate **279**. Intermediate **279** then undergoes MeCl removal, followed by AuCl reductive elimination to give chloride **275**. In the ms analysis, we also observed that there is small amount of dimerized material **282**, which its abundance is significantly lower than chloride **275**. Although relative ratio from ms analysis does not give indicative conclusion of whether chloride **275** or dimer **282** is the major product (ability of ionization between compounds can vary), x-ray crystallography has confirmed that chloride **275** is the major product.



Scheme 60. Explanation to the formation of **275** and **282**.

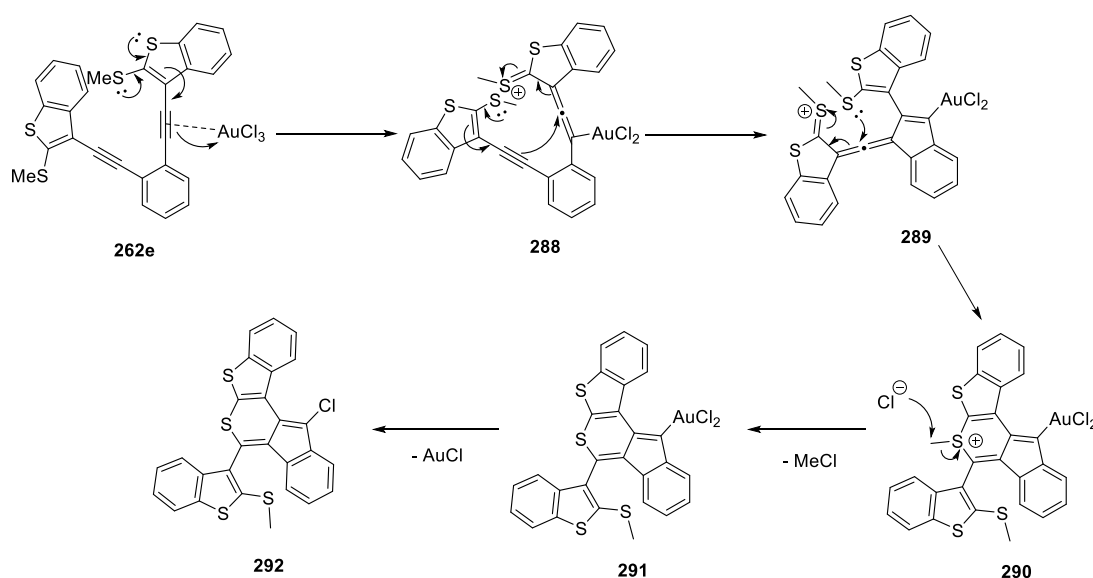
The predominant formation of chloride **275** comparing to dimer **282** involves two major factors. Firstly, the reaction was carried out using one equivalent of AuCl_3 due to our initial expectation upon the intramolecular DECRE reaction of **262b**. With one equivalent of AuCl_3 , all diyne **262b** is expected to be converted to chloride **275**, therefore no remaining diyne **262b** can undergo intermediate **280** dependant electrophilic cyclization to form dimer **282**. Meanwhile, the reaction was also carried under heating, in which the rate of C-Cl bond formation from reductive elimination was enhanced, leading to a faster C-Cl bond formation from AuCl reductive elimination.

While the initial formation of sulfur-containing **263a** has proven the ability of intramolecular DECRE to access fused angular heteroacenes, expected oxygen-containing product **265** was not observed. A similar investigation was done by Chin *et al.*, where it was concluded that *SMe* promotes the formation of benzothiophene **285** and *OMe* promotes the tandem cyclization process, forming **287**.⁹⁷

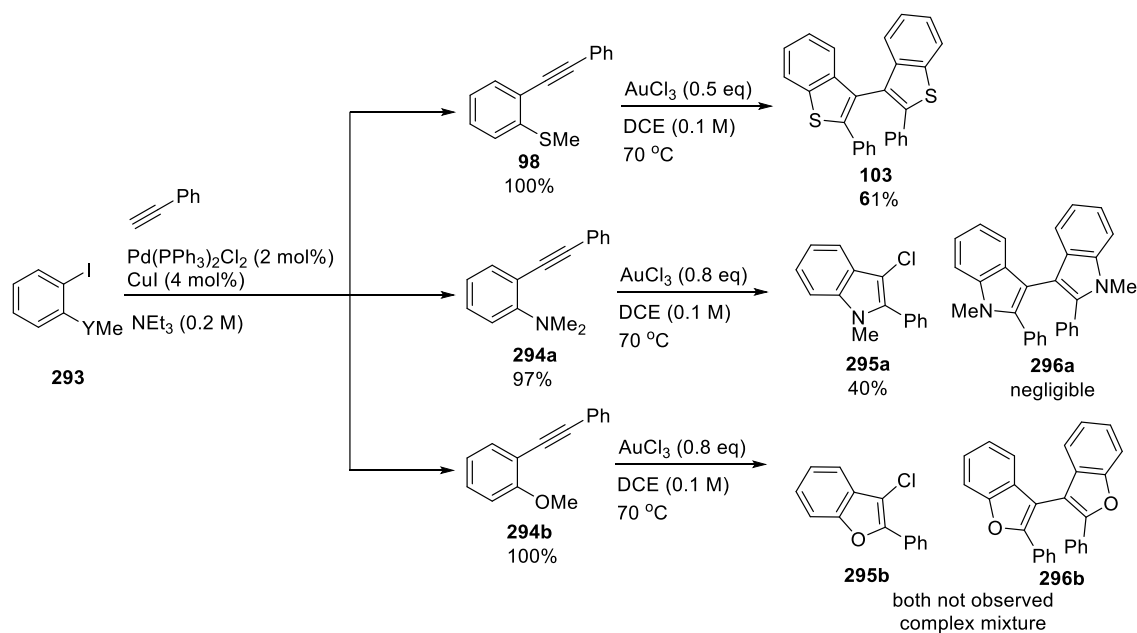
Chin's work*This work*

Scheme 61. Supported data from Chin's work.

A similar product chloride **292** was also obtained from the cyclization of **262e**. Although *SMe*-substituted diyne is described to undergo heteroatomic addition to alkyne in the discussion above, in the case of **262e**, the electron-rich benzothiophene ring and also the presence of *SMe*-group promote the formation of intermediate **288** (Scheme 62). This is then followed by the nucleophilic attack from triple bond to electrophilic allenyl intermediate, forming **289**. *SMe*-group on **289** acts as nucleophile, attacks electrophilic allenyl intermediate, forming cation **290**. Cation intermediate **290** then undergoes MeCl removal and reductive elimination of AuCl, giving **292** exclusively.

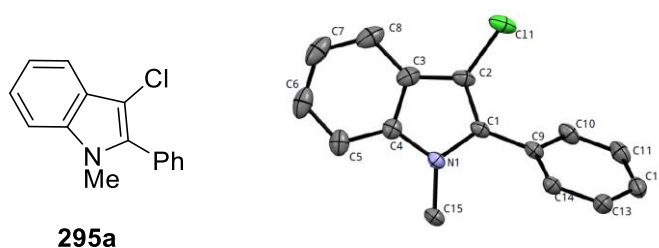
Scheme 62. The formation of product **292**.

We then also focused our synthetic efforts on alkynes **98** and **294** and subjected them to $AuCl_3$ -mediated cyclization to confirm the aforementioned dimerization concept (Scheme 63).



Scheme 63. Synthesis of simple alkyne and AuCl_3 cyclization.

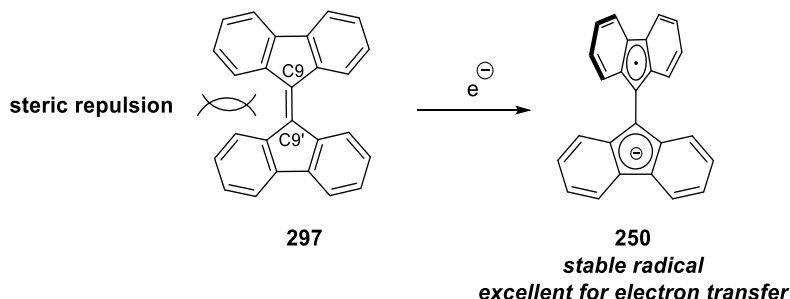
Alkyne **98** and its resultant dimerized product **103** were prepared and published within our group (**Scheme 63**).³² The cyclization of *N* containing alkyne **294a** though gave chloride **295a**, which is consistent with the previously discussed formation of chloride **275** and **292**, where a crystal structure of chloro-indole **295a** was also obtained through x-ray crystallography (**Scheme 64**). The formation of chloro-indole **295a** again signifies that the formation of dimer could be obtained if the amount of AuCl_3 is reduced to 0.5 equivalent, where unreacted alkyne could undergo dimerization to form dimer **296a**. Unfortunately, the treatment of *OMe*-substituted alkyne **294b** with AuCl_3 resulted in a complex mixture, where both chloride **295b** and dimer **296b** were not observed.



Scheme 64. X-ray crystal structure of chloro-indole **296a**.

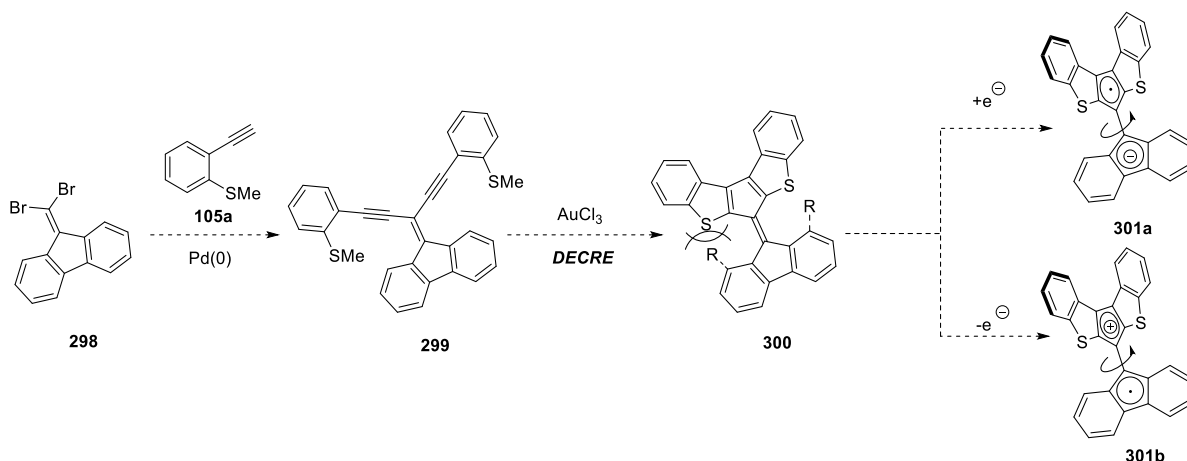
2.3. Application of DECRE and DEC in the synthesis of fulvalene derivatives

A recent investigation by Brunetti *et al.* suggested that bis-fulvalene structures contains superior ability in charge transfer, becoming an extremely interesting prospect within materials science, especially for the development of organic photovoltaic (OPV).⁴⁷



Scheme 65. Formation of stable radical species **250**.

9,9'-Bifluorenylidene **297** at ground state should remain co-planar. However, due to the steric repulsion that arises from H1 – H1' and H8 – H8', it allows a “twist” along the C9 - C9' double bond, and results in the capability of accepting an electron to form stable radical **250**. This radical is highly stable as it forms a 14 π aromatic intermediate, therefore allowing better electron transportation (**Scheme 65**). The formation of radical species can also act as photo-redox catalyst in organic synthesis.⁹⁸⁻⁹⁹ Therefore, the formation of fulvalene derivatives could potentially benefit future organic photovoltaic (OPV) technology and also photo-redox chemistry.



Scheme 66. The synthetic strategy towards fulvalene derivative **300**.

The synthesis of fulvalene derivative **300** involves the initial Sonogashira coupling between alkyne **105a** and alkenyl geminal dibromide **298**, forming geminal di-yne **299**. Diyne **299** then undergoes DECRE to yield chalcogen-containing fulvalene **300** (**Scheme 66**). We anticipate that the formation of **300** contains the ability to either gain or loss an electron, to form either radical **301a** or **301b**.

Therefore, we expect the DECRE reaction would allow access into a range of photoactive fulvalene derivatives with the co-operation of heteroatoms.

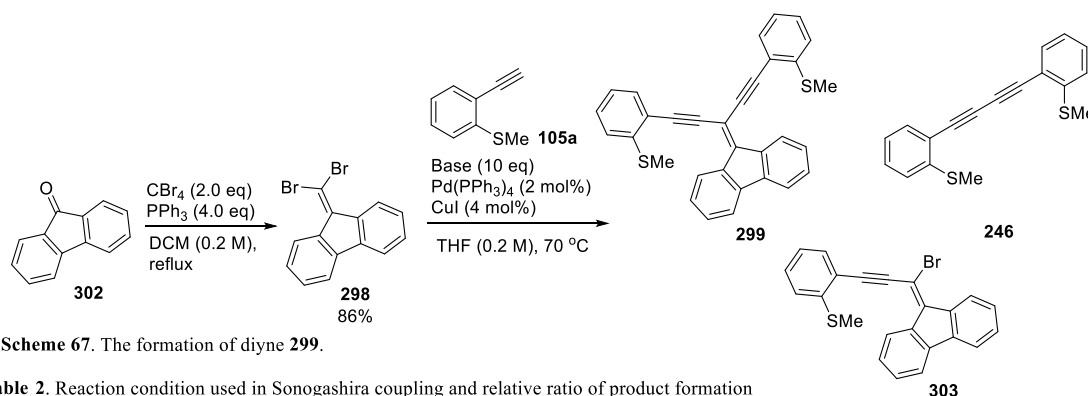
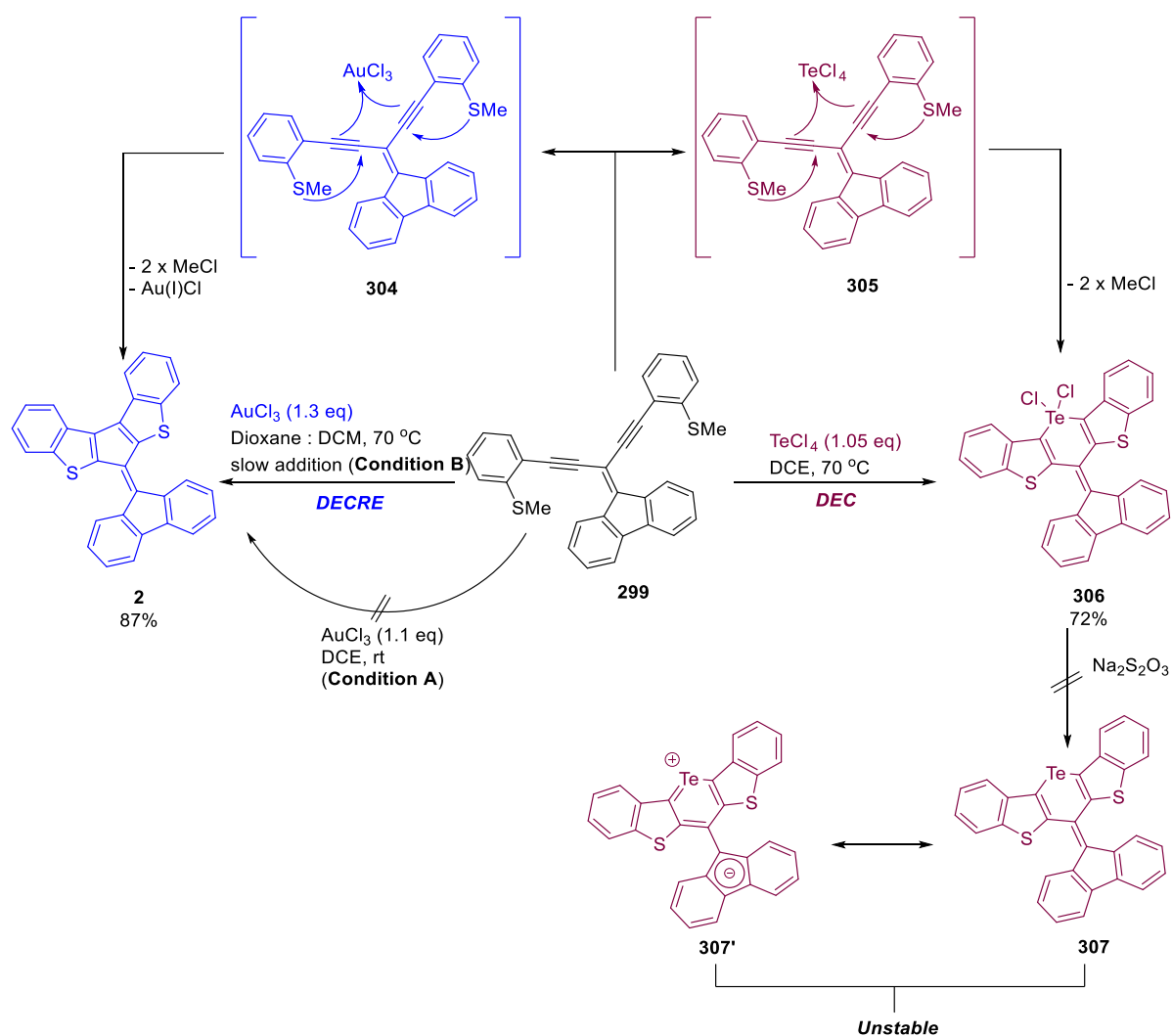


Table 2. Reaction condition used in Sonogashira coupling and relative ratio of product formation

Entry	105a (eq)	Base	Temp	298 → 299 (% conversion) 298 : 303 : 299	Note
1	3 eq	NEt ₃	r.t.	23% : 21% : 64%	Competitive formation of 246
2	3.5 eq	NEt ₃	40 °C	- : - : 100%	Competitive formation of 246 , difficulties with purification
3	2.3 eq	DIPA	50 °C	- : - : 100%	Formation of 246 minimized
4	2.5 eq	DIPEA	50 °C	- : 45% : 55%	Reduced rate of Sonogashira reaction, competitive formation of 246

The synthesis initiated with *gem*-dibromomethenylation of fluorenone **302** via Wittig type reaction, forming **298** (**Scheme 67**). *Gem*-dibromide **298** was then subjected to Sonogashira coupling with alkyne **105a**. Initially, NEt₃ was used as the base for this reaction, where 64% conversion of **298** to diyne **299** was observed, with unreacted **298** and mono-coupled material **303** still present in the resultant product mixture (**Table 2, Entry 1**). The formation of **246** was also observed. When the temperature was raised to 40 °C, even though there was full conversion to **299**, the formation of **246** was extremely competitive, resulting in difficulties with purification (**Table 2, Entry 2**). The use of DIPA reduced the formation of **246** significantly, giving high conversion towards **299** (**Table 2, Entry 3**). Sonogashira coupling in the presence of DIPEA was attempted, but the rate in the formation of **299** reduced drastically, and formation of **246** increased (**Table 2, Entry 4**). It was then concluded that DIPA gave the best outcome, particularly in the Sonogashira coupling reaction, giving expected **299** in 49% isolated yield. The inconsistency between the percentage conversion and the yield obtained was due to chromatographic issues, as the part of the products were degraded upon column chromatography.

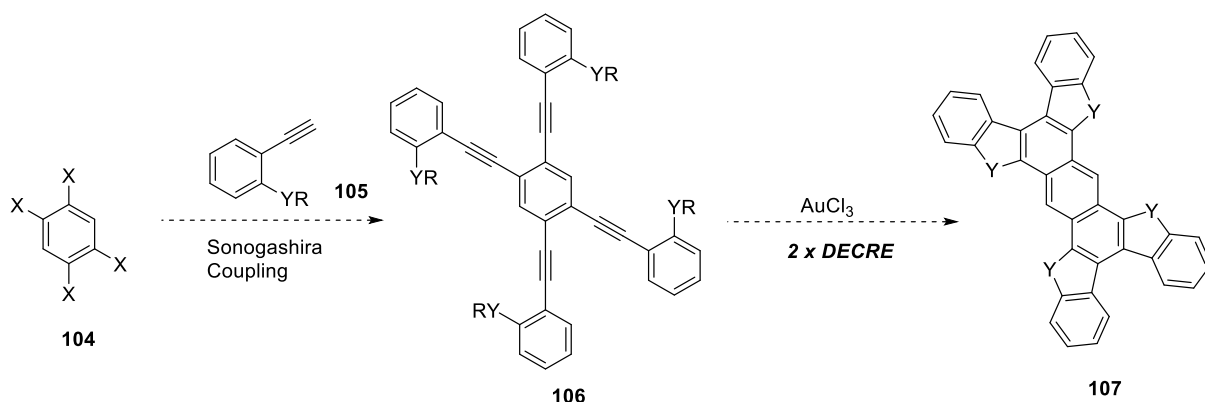


Scheme 68. Divergent synthesis of fulvalene type materials **2** and **306** via DECREASE and DEC.

Considering the success in the formation of **299**, we then investigated the formation of fulvalene derivative **2** via the DECREASE reaction. Although the synthesis appeared to be reasonably straightforward, we observed inconsistencies between various different attempts. When subjected to the normal condition (**Scheme 68, Condition A**), we anticipated the formation of expected fulvalene **2**, though one persistent by-product was observed in all our attempts. Isolation of this product was unsuccessful due to the instability issue. However, the formation of this by-product was diminished with slow addition technique (**Scheme 68, Condition B**), and had successfully furnished **2** in 87% yield (**Scheme 68**). With further explored other derivatives, by conducting the DEC reaction with TeCl_4 , successfully yielding telluroene dichloride **306** in 72% yield. The treatment of $\text{Na}_2\text{S}_2\text{O}_4$ on telluroene dichloride **306** was unable to yield **307**, where a complex reaction mixture was obtained, presumably due to the electron-rich nature of **307**. The electron-rich **307** can possibly allow further elaboration, due to the reaction resonance contributor **307'**. Nevertheless, we successfully exemplified the formation of fulvalene derivatives **2** and **306** via DECREASE and DEC reaction, respectively.

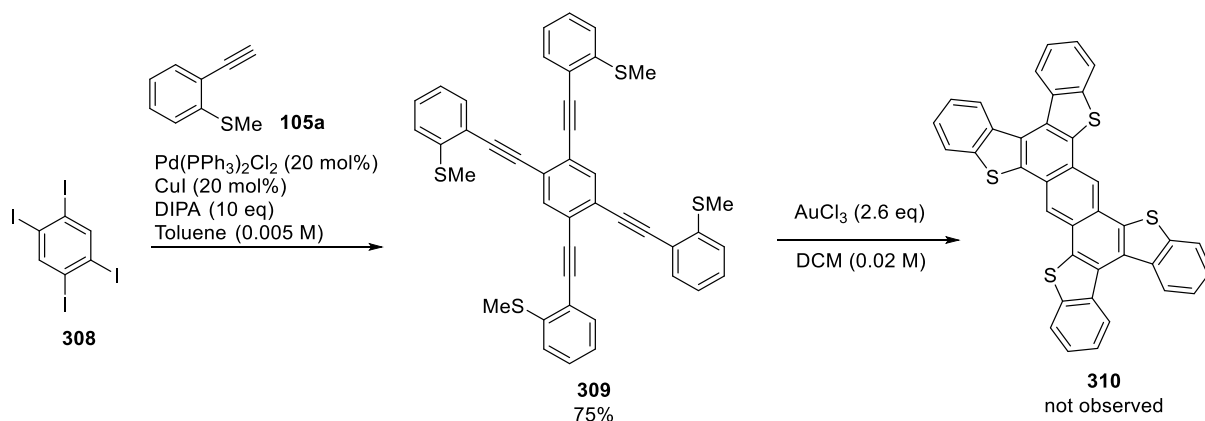
2.4. Synthesis of extended angular heteroacenes

With the successful attempts in DECRE, we then proposed the synthesis of extended systems using a bidirectional strategy (**Scheme 69**).



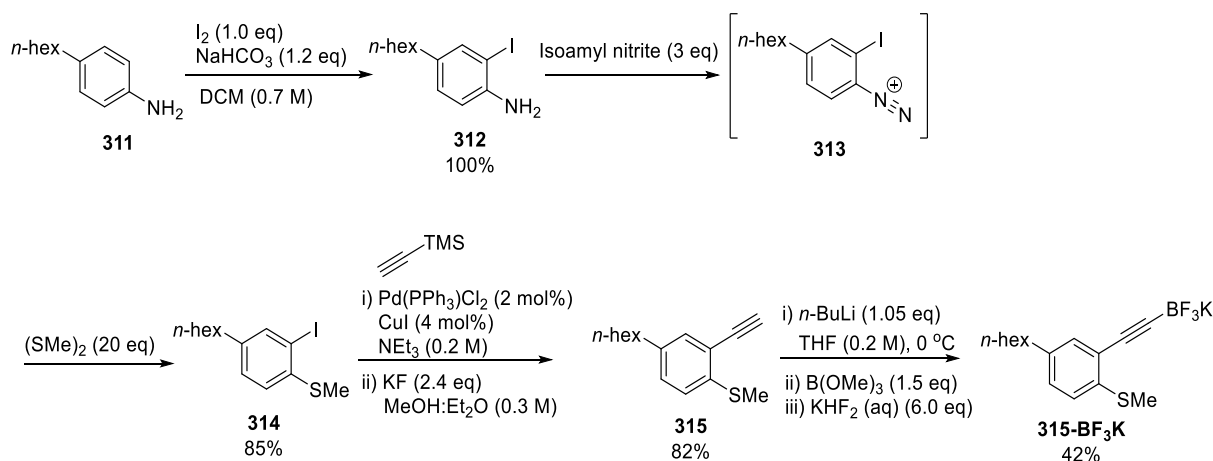
Scheme 69. Approach to extended angular heteroacene **107**.

In the study of extended heteroacene synthesis, we anticipated that Sonogashira reaction between alkyne **105a** and preformed 1,2,4,5-tetraiodobenzene **308** to give tetrayne **309** would perform very well (**Scheme 70**). However, due to the solubility issue of tetraiodobenzene **308**, a few conditions including DMSO as the reaction solvent was attempted, however, we were unable to achieve the desired **309**. Eventually, a successful attempt was achieved by conducting the reaction under an extremely diluted environment while having an increased amount of catalyst to yield **309** in 75% yield. The condition for the formation of tetrayne **309** was adapted from a literature procedure with the formation of a similar tetrayne.¹⁰⁰ Notwithstanding the effort in synthesizing **309**, we were unable to perform the DECRE reaction due to solubility issues of **309**. An attempt of DECRE was performed in an extremely diluted environment, though this resulted in a complex mixture, where expected product **310** was not observed (**Scheme 70**). We then decided to install a hexyl group for increased solubility.



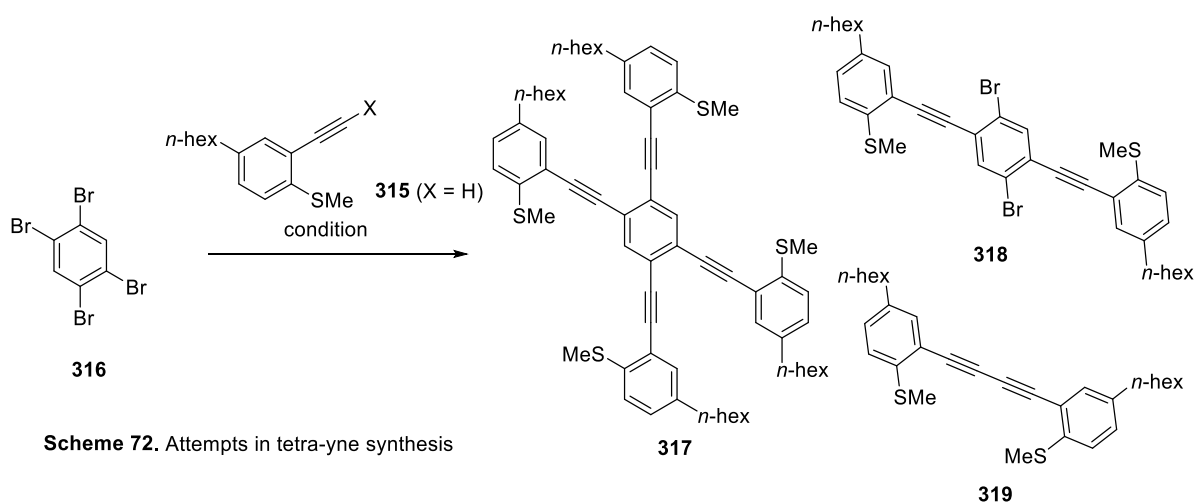
Scheme 70. An unsuccessful attempt in the DECRE reaction.

The synthesis of hexyl substituted terminal alkyne **315** involves initial selective *ortho*-iodination of *n*-hexyl aniline **311**, giving **312** in quantitative yield. Iodoaniline **312** is diazotized, giving intermediate **313**, which was further treated with dimethyl disulfide to yield *n*-hexyl substituted iodothioanisole **314** (85%). Sonogashira coupling of **314** with TMS acetylene, followed by silyl deprotection gave terminal alkyne **315** in 82% yield. Potassium trifluoroborate salt **315-BF₃K** was also formed in preparation for the Suzuki type coupling reaction (Table 3).



Scheme 71. Synthesis of *n*-hexyl substituted alkyne **315** and **315-BF₃K**.

A series of coupling reactions were attempted to obtain *n*-hexyl substituted tetrayne **317** (Scheme 72). The use of 1,2,4,5-diiodobenzene **308** was abandoned due to the solubility issues, where soluble tetrabromobenzene **316** was used instead. We initially attempted the Sonogashira reaction, which is our typical approach towards alkynyl species. However, the formation of **319** was very competitive, even with a large excess of terminal alkyne **315**. As an alternative approach, we attempted Suzuki type coupling with the pre-formed alkynyl potassium trifluoroborate salt **315-BF₃K** (X = BF₃K, Table 3, Entries 2 & 3). Unfortunately, the conversion towards **317** was hampered by the hydrodeboration of **315-BF₃K**, returning **315** (X = H) as terminal alkyne. Elevation in temperature resulted in more rapid hydrodeboration, but did give some di-coupled material **318** as major product. We next attempted InCl₃-mediated coupling reaction that was developed by Kang and co-workers, which provided significant improvement in the conversion towards **317**.¹⁰¹ The absence of copper could potentially be beneficial to similar alkyne coupling reactions. Utilizing InCl₃ mediated coupling, **317** was obtained in 50% isolated yield. (Table 3, Entry 4)

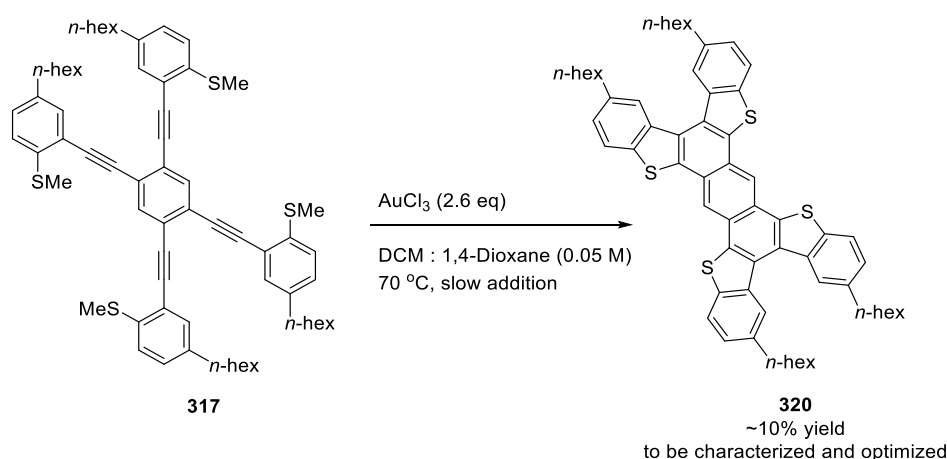


Scheme 72. Attempts in tetra-yne synthesis

Table 3. condition used in the synthesis of **317**.

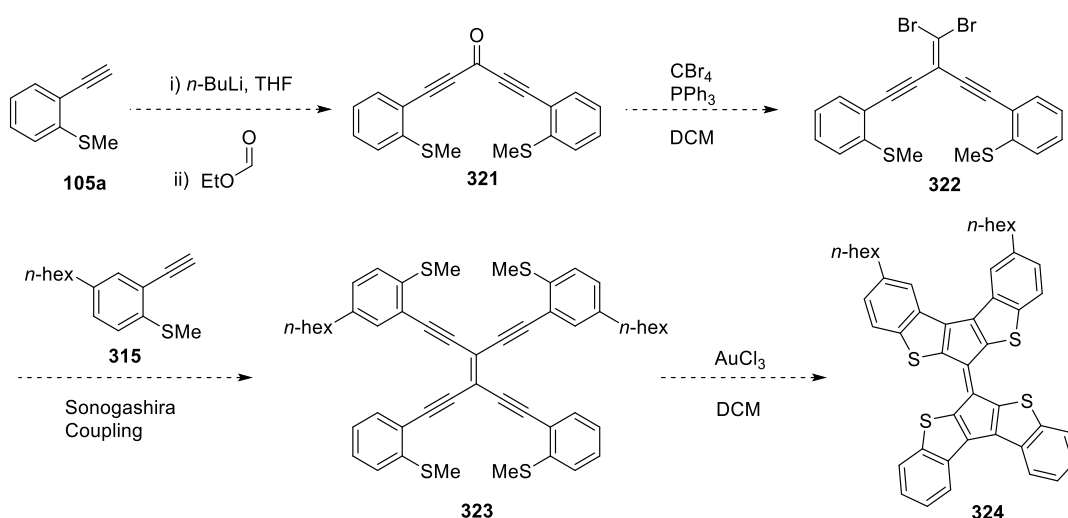
Entry	Alkyne 315	Condition	Products observed
1	X = H, 8 eq	Pd(PPh ₃) ₄ (3 mol%) CuI (6 mol%) DIPA (10 eq), 70 °C	317 (< 10%) : 319 (major)
2	X = BF ₃ K, 6 eq	Pd(dppf)Cl ₂ (5 mol%) CsF (3 eq) THF, rt	- mono, di, tri coupled material isolated - hydro-deboronation, 315 recovered
3	X = BF ₃ K, 6 eq	Pd(dppf)Cl ₂ (5 mol%) CsF (3 eq) THF, 50 °C	- di-coupled material 318 (major) - 315 recovered
4	X = InCl ₂ , 8 eq	i) 315 , <i>n</i> -BuLi (8.0 eq) THF, 0 °C ii) InCl ₃ (2.0 eq) 0 °C - rt iii) Pd(dppf)Cl ₂ (4 mol%) reflux	317 (50% isolated yield, major)

With the obtained tetrayne **317**, we then proceeded to the formation of extended heteroacene **320** via DECRE (Scheme 73). These attempts were conducted via slow addition process, to avoid polymerization as mentioned in the earlier discussion. However, due to the time constraint, the result is yet to be fully characterized and optimized, where the formation of **320** requires re-synthesis from hexylaniline **311**.



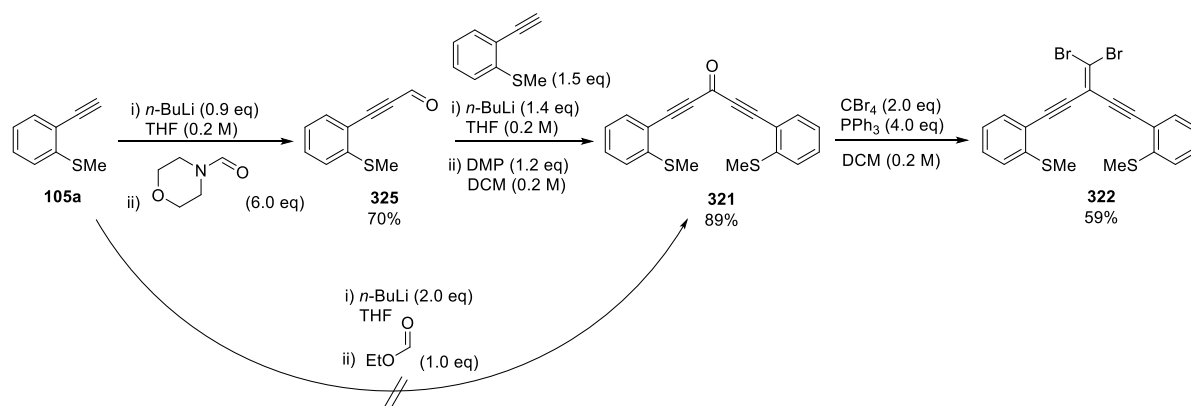
Scheme 73. An attempt in the synthesis of extended heteroacene **320** with *n*-hexyl to aid solubility.

In parallel with our attempts towards **320**, we also sought to extend our bidirectional approach to bisfulvalenes, e.g. **324** (**Scheme 74**). The proposed synthesis of **324** starts with the formation of ketone **321**, via the addition of alkynyl lithium towards ethyl formate. Ketone **321** is then to be converted to alkenyl geminal dibromide **322**, followed by Sonogashira coupling with alkyne **315** to yield H-shape tetrayne **323**, which then finally undergoes 2 x DECRE to yield the extended fulvalene **324** (**Scheme 74**).



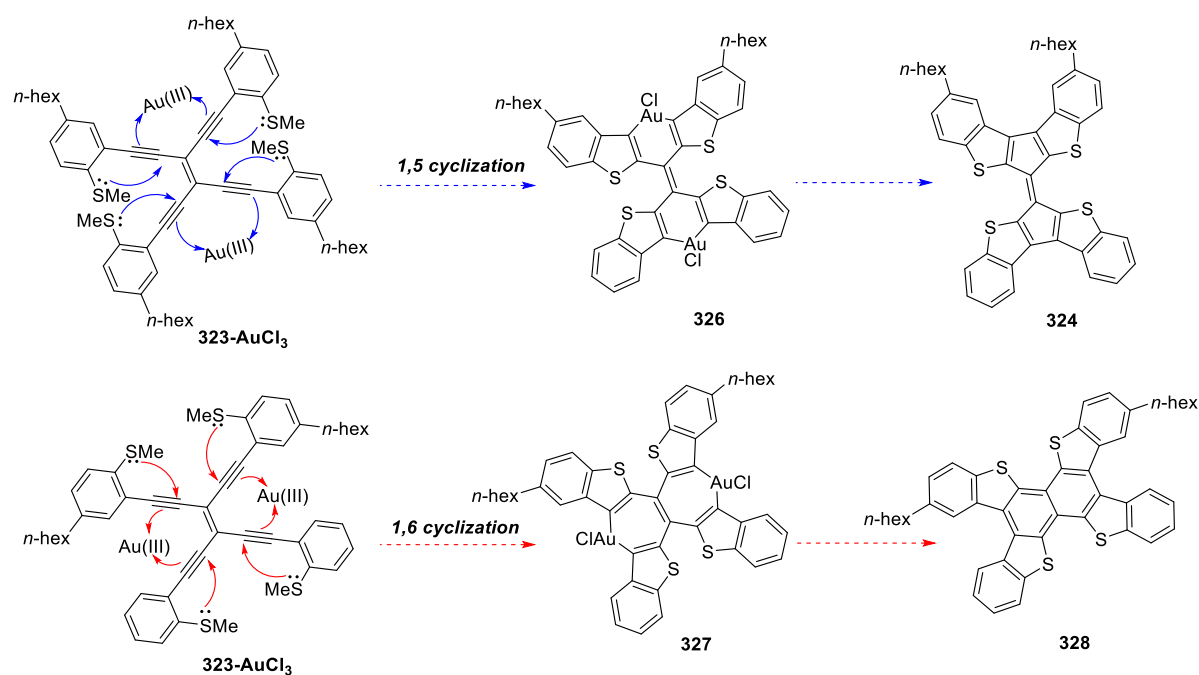
Scheme 74. A proposed route towards extended fulvalene **324**.

An initial study in the synthesis of **321** via double-1,2-addition onto ethyl formate was unsuccessful (**Scheme 75**), whereupon our interest migrated towards the formation of aldehyde **325**. Aldehyde **325** could possibly provide opportunities in co-operation with alkyne that contains other heteroatoms, leading to un-symmetrical angular heteroacenes. Aldehyde **325** was obtained in 70% isolated yield, where it was brought through to the formation of ketone **321** via 1,2-addition and oxidation, followed by the formation of *gem*-dibromide **322** in 59% yield (**Scheme 75**).



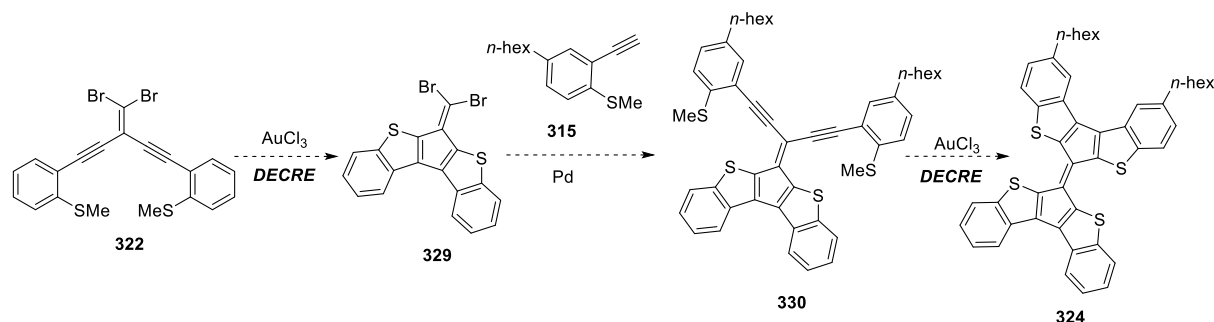
Scheme 75. The synthesis towards **322**.

However, considering the structure of proposed tetrayne **323**, there could be two possible outcomes upon DECARE reaction, which involves 1,5- or 1,6- cyclization, forming gold containing 6 or 7 membered ring intermediates **326** and **327**, which then lead to a rapid reductive elimination of Au(I)Cl, yielding either the desired product **324**, or alternative product **328** (**Scheme 76**).



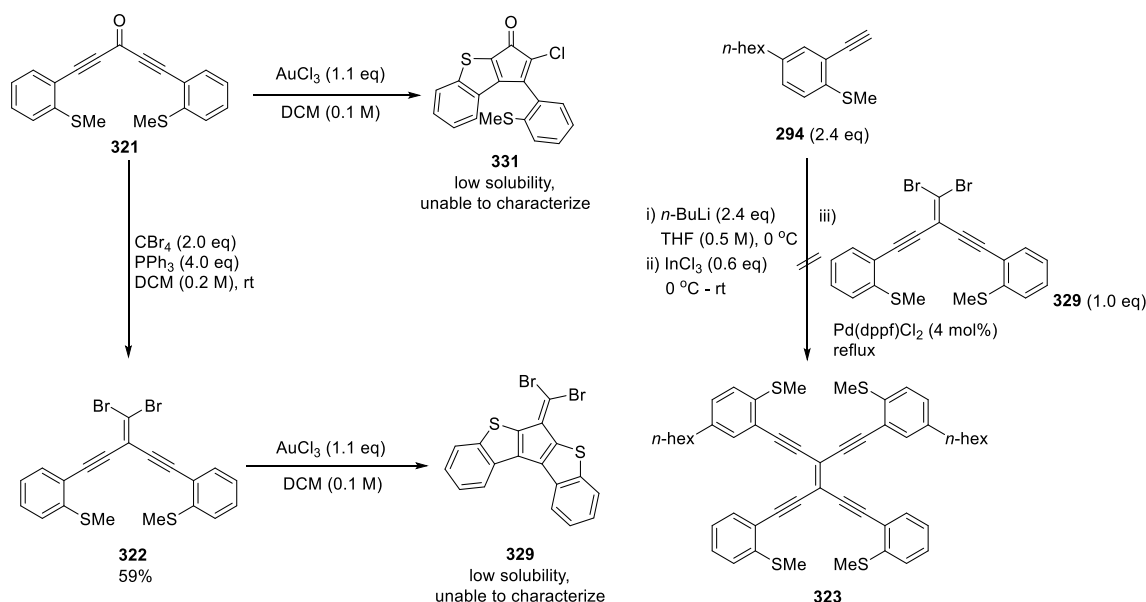
Scheme 76. Proposed cyclization mechanisms, possibility in the formation of **324** and **328**.

It is challenging to discern the possibility of bias formation towards either product. Therefore, we proposed a prolonged route towards **324**, where the formation of **328** could be avoided. We anticipated that *gem*-dibromide **322** we obtained could first undergo DECARE to gain access to **329**, which could then be coupled to alkyne **315** to yield di-yne **330**, followed by the DECARE to form **324** (**Scheme 77**).



Scheme 77. The selective prolonged route towards **324**.

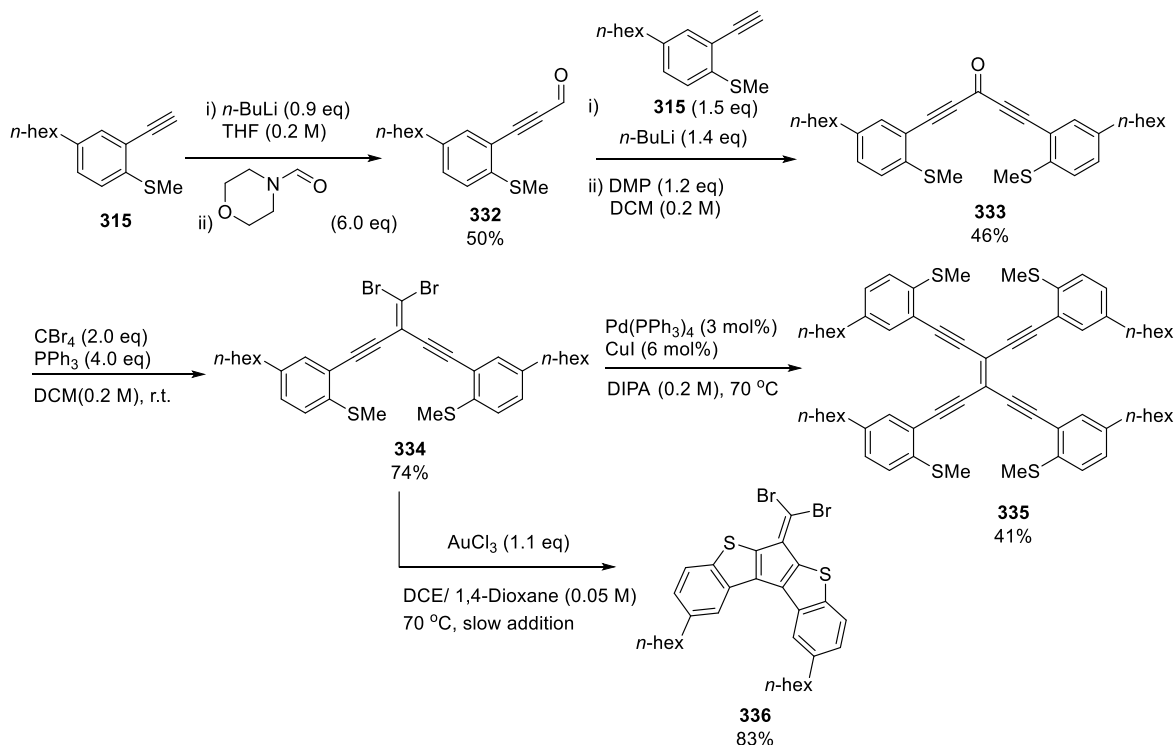
Both **321** and **322** were subject to DECARE, where cyclization of **321** appears to give chloride **331** according to ^1H NMR analysis. The formation of chloride **331** instead of related dimerized product is due to the use of stoichiometric amount of AuCl_3 , where all starting material **321** should be consumed. Though **331** could not be fully characterized due to low solubility. ^1H NMR analysis also suggested that the cyclization of **322** yielded expected product **329**, as no methyl related resonances were observed. Similar to **331**, **329** encountered solubility issues, where only ^1H NMR were obtained as both **331** and **329** were partially soluble in various NMR solvents. Due to the solubility issues we encountered, compound **331** and **329** could not be fully characterized (**Scheme 78**). We have also attempted an InCl_3 -mediated coupling to form tetrayne **323**, where **323** could possibly lead to the formation of compound **324**. Unfortunately, the InCl_3 -mediated coupling resulted in a complexed reaction mixture, where no sign of tetrayne **323** was observed.



Scheme 78. The attempted cyclization of **321** and **322**.

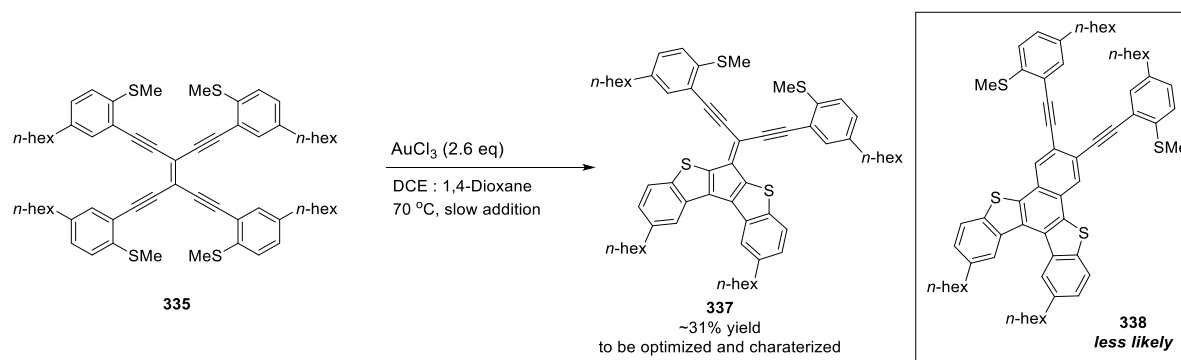
As mentioned above, the formation of tetrayne **317** (**Scheme 73**) exemplifies that the use of *n*-hexyl enhances the solubility of highly conjugated systems. Therefore, we attempted the synthesis of **336**,

anticipating that *n*-hexyl substituent would increase solubility. Aldehyde **332** was initially synthesized via formylation, followed by the formation of ketone **333**, then *gem*-dibromide **334**. Diyne **334** was subjected to the DECRE reaction, where cyclized product **336** was obtained in 83% yield, with improved solubility (**Scheme 79**). *n*-Hexyl substituted tetrayne **335** was also obtained in 41% yield through Sonogashira coupling, which **335** was subjected to the DECRE reaction.



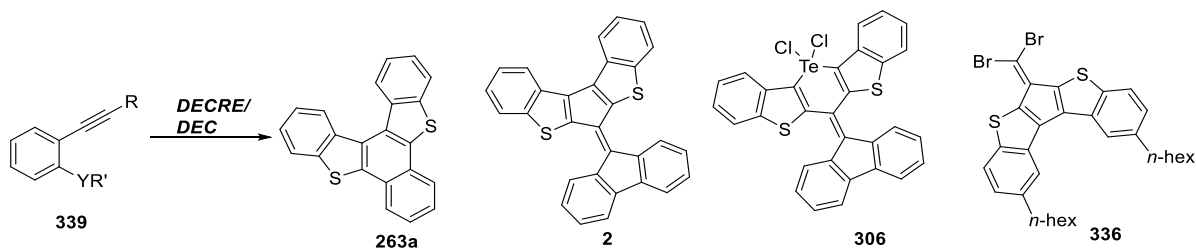
Scheme 79. Formation of tetrayne **335** and cyclized product **336**.

A trial DECRE reaction was attempted on substrate **335**, where the formation of partially cyclized product **337** was observed (**Scheme 80**). The result was discerned by ^1H NMR. However, **337** was not fully characterized due to rapid degradation. The instability characteristic allows us to believe that the formation of **337** is more likely the case instead of the formation of **338**, due to the weak double bond of **337**. The result is yet to be fully characterized, due to time constraint within candidature.



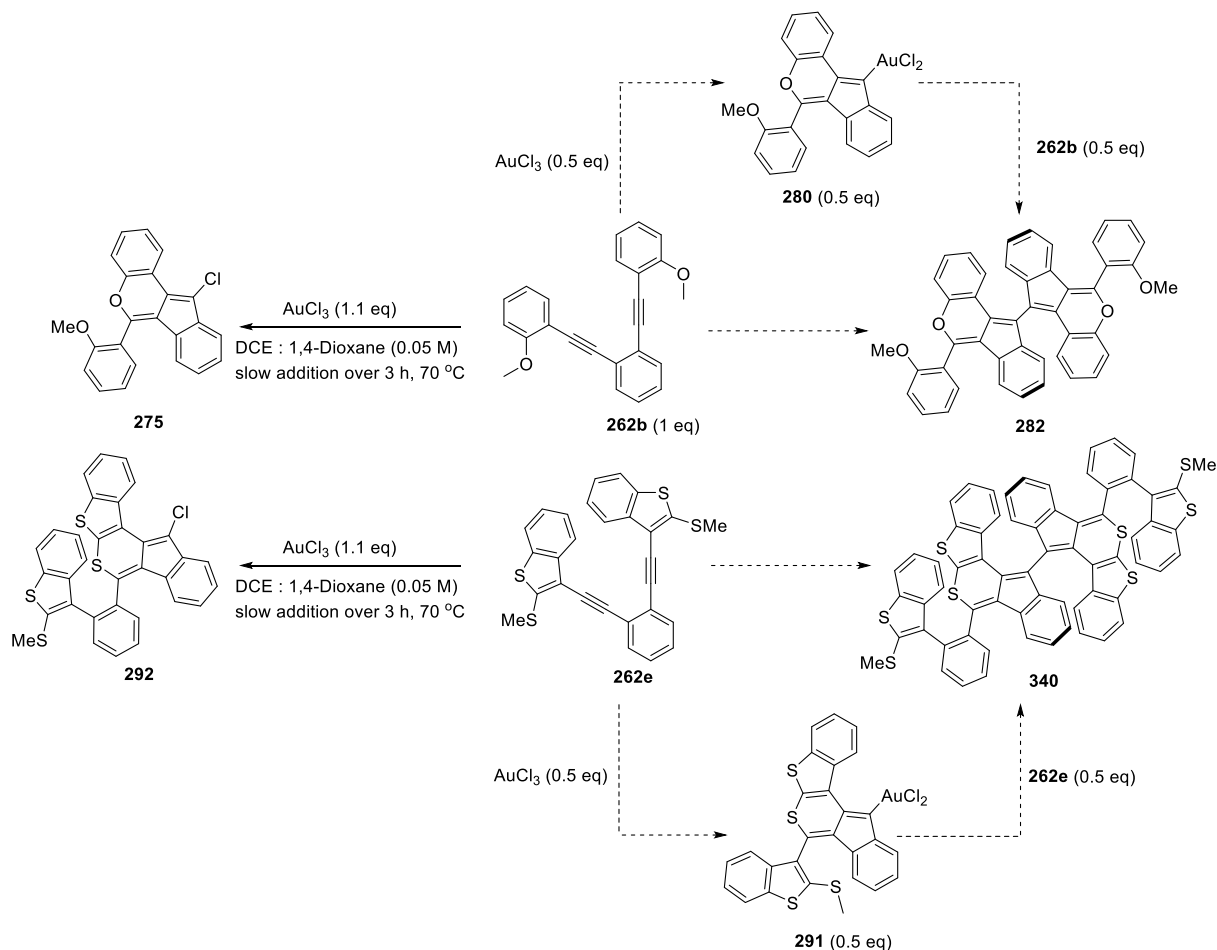
Scheme 80. The formation of partial-cyclized product **337**.

2.5 Conclusion and future work



Scheme 81. Intramolecular DECARE products described in **Chapter 2**.

Within this chapter, we have described the elaboration and limitation of the angular heteroacene synthesis via DECARE. The obtained heteroacene **263a** and fulvalene type molecules, **2** and **336** were also synthesized, via DECARE, where telluroene dichloride **306** was synthesized via DEC, by the addition of TeCl_4 .

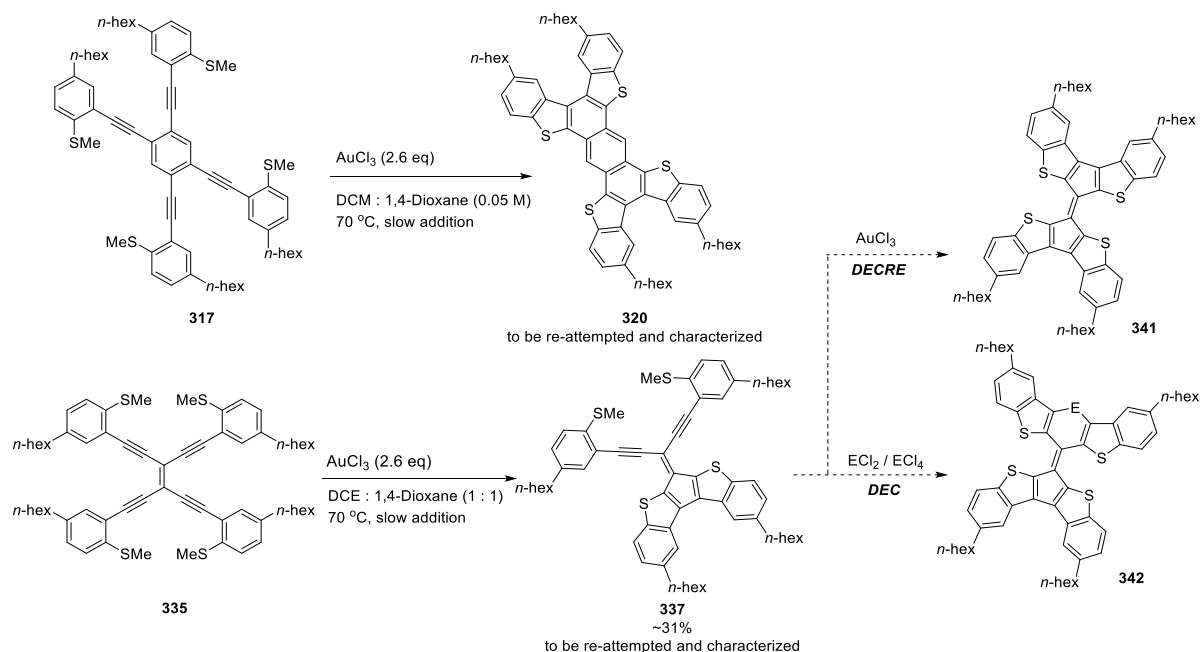


Scheme 82. The observed unexpected product **275** and **292**, resulted from tandem DECARE.

We have also obtained unexpected cyclized products **275** and **292**, where the structure of compound **275** was determined by X-ray crystallography. The cyclization pathway towards products **275** and **292** were directed by the strong EDG (i.e. *OMe* and benzofuran), and our mechanistic proposal of the formation of compounds **275** and **292** is also supported by Chin's work.⁹⁷ We also expect that the

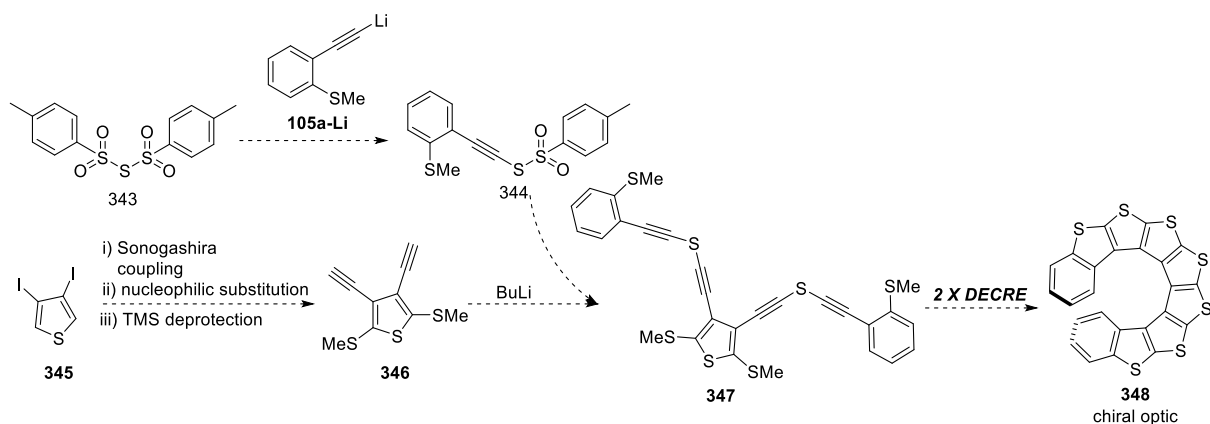
reduce amount of AuCl_3 catalyst (0.5 eq) could potentially produce dimeric structures **282** and **340** selectively, where only half an equivalent of **262b** or **262e** are anticipated to react with AuCl_3 , forming gold intermediate **280** or **291**. The remaining 0.5 equivalent of diyne **262b** or **262e** could then react with intermediate **280** or **291**, forming dimerized product **282** or **340** selectively.

In the synthesis of extended heteroacenes (bidirectional), the result in the formation of **299** is undergoing further characterization and optimization. Meanwhile, the formation of **316** was observed from ^1H NMR analysis, but yet fully characterized, due to the instability of the compound.



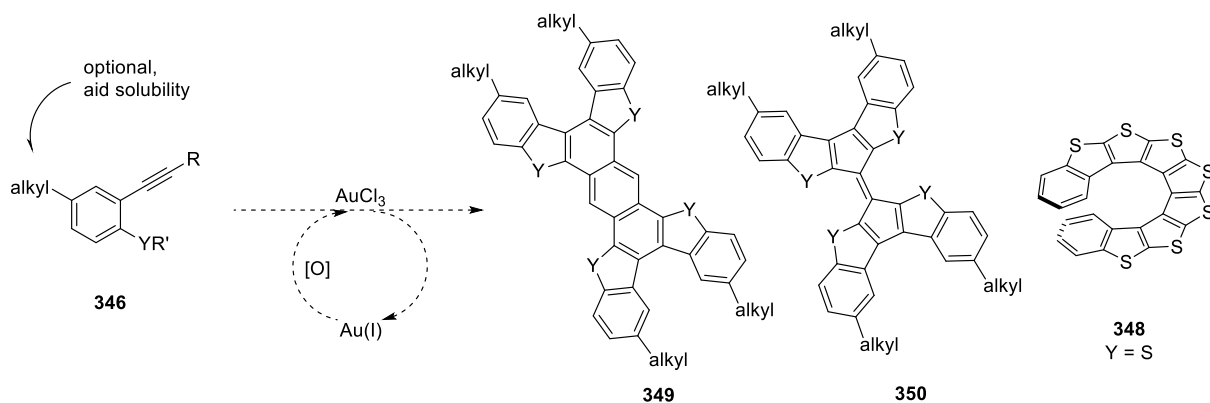
Scheme 83. Work to be optimized and possible elaboration of structure **335**.

Diyne **316** could undergo further elaboration to give **341** (angular) and **342** (linear), via DEC and DEC, respectively. Meanwhile, extended heteroacene **342** could potentially involve various heteroatoms or chalcogens, including sulfur, selenium and tellurium (**Scheme 83**).



Scheme 84. Future work, synthesis of chiral optic **348** via DEC.

As a future direction, the formation of chiral optic **348** is visible through the DECRE reaction of tetrayne **347**. The involvement of electron-rich thiophene unit and sulfur linkers should remove the electron bias effect, therefore diminishing the merit in the cyclization pattern that is explained in **Scheme 82**.



Scheme 85. Future investigation in catalytic DECRE

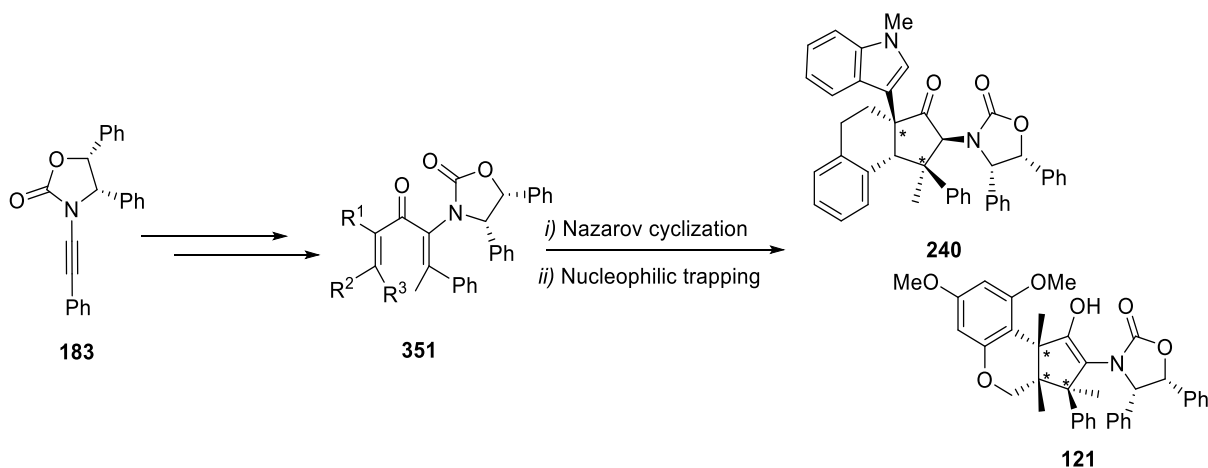
To improve the cost efficiency of the synthesis of angular fused heteroacenes, we will also investigate the use of suitable oxidant to perform catalytic DECRE reaction, allowing a more efficient way to produce photonic materials (**Scheme 85**).

Chapter 3

3. Result and discussion: Chiral oxazolidinone promoted Nazarov cyclization, towards the formation of multiple all-carbon 4°-stereocentres containing cyclopentanoids

The power of chiral oxazolidinone to control torquoselectivity during the Nazarov cyclization is demonstrated by numerous of examples generated within our group.^{65,79-81} The involvement of intermolecular or tethered nucleophile (e.g. arenes), facilitated stereoselective intra- or intermolecular nucleophilic trapping. A recent investigation within our group had shown the ability to sustain such torquoselectivity on the cyclization of highly substituted Nazarov precursor **351**.⁶⁵ The tandem nucleophilic trapping cascade allows the enantioselective formation of complex cyclopentanoids, which contain up to three contiguous all-carbon 4°-stereocentres (**Scheme 86**).

Previous work



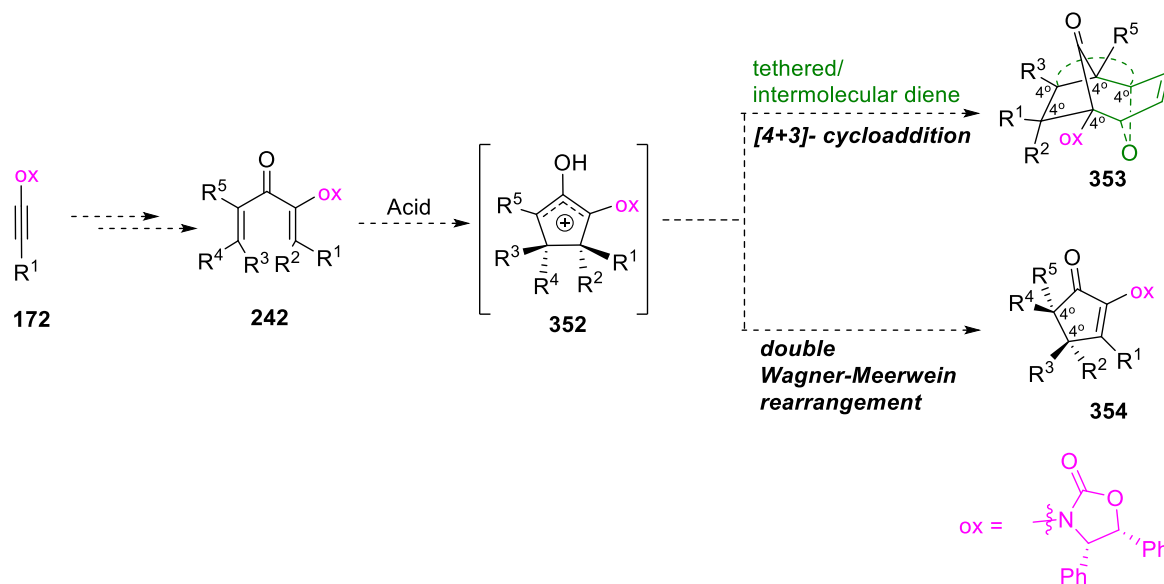
Scheme 86. Enantioselective formation of multiple 4°-stereocentres containing cyclopentanoids **121** and **234**.

A captivating elaboration of the oxyallyl cation intermediate that results from the acid treatment of the Nazarov precursor would be the [4+3]-cycloaddition. The formation of bridged cyclopentanoids via cycloaddition provides a significant enhancement in the capacity to project functionalities into 3D space. The formation of two extra C-C bonds and 4°-stereocentres during the cycloaddition is particularly powerful. Although there are precedented reports on the formation of cycloadduct during the Nazarov reaction, those examples were all generated racemically.⁹⁰⁻⁹² To date, there has not been any reported study showing the ability to control torquoselectivity during the [4+3]-cycloaddition process. Therefore, we foresee the potential and possibility in the formation of bridged ring cyclopentanoids enantioselectively, with the aid of chiral oxazolidinone.

The objective in this part of the project is the formation of multiple all-carbon 4°-stereocentres containing bridged or fused-bridged ring cyclopentanoids **353**, via the chiral oxazolidinone promoted

asymmetric Nazarov reaction, followed by tandem [4+3]-cycloaddition. We will also investigate the formation of cyclopentanoids **354**, that contains two all-carbon 4°-stereocentres, via the Nazarov cyclization induced double Wagner-Meerwein rearrangement (**Scheme 87**).

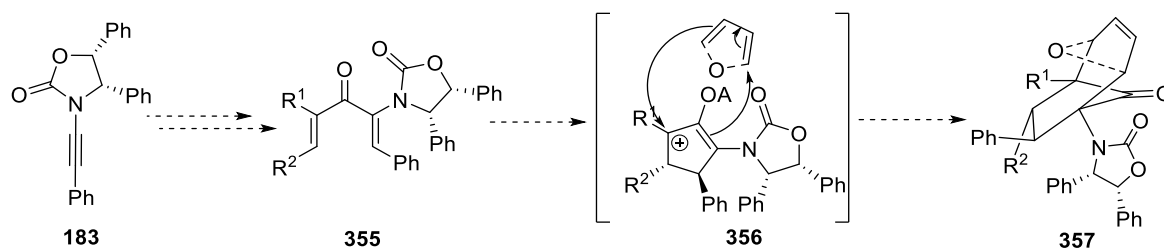
This work



Scheme 87. A synthetic proposal in the formation of multiple all-carbon 4°-stereogenic centres containing cyclopentanoids.

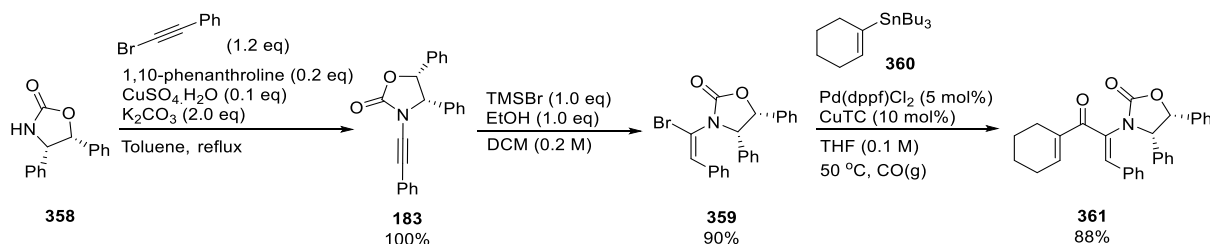
3.1 The enantioselective synthesis of the bridged-cyclopentanoids

Our early investigation in the [4+3]-cycloaddition involves the synthesis of Nazarov precursor **355** from ynamide **183**. In the presence of acid and diene then promotes the formation of oxyallyl cation **356**, followed by the [4+3]-cycloaddition to form the bridged ring structure **357** enantioselectively (Scheme 88).



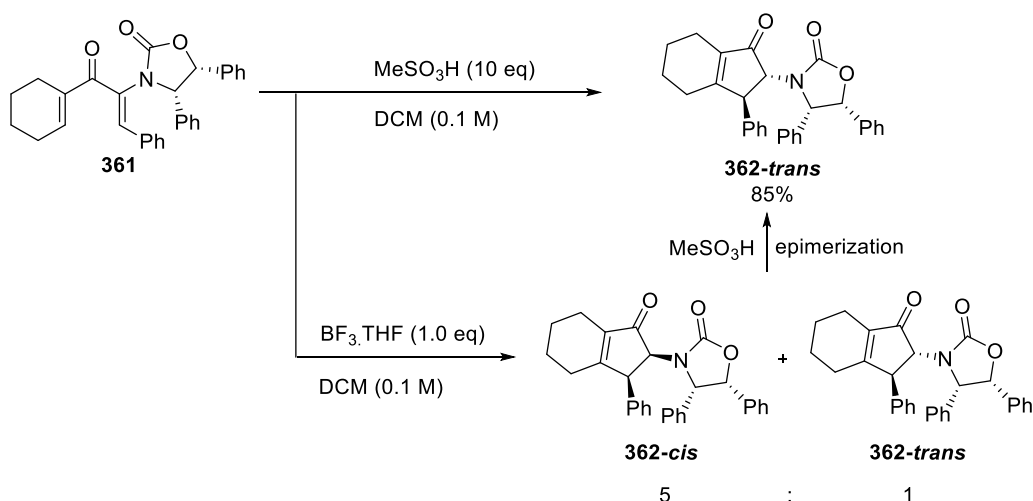
Scheme 88. Proposed synthesis towards bridged ring **357**.

Ynamide **183** was initially formed via Cu^{II}-coupling method,⁷⁹ and obtained in quantitative yield. **183** then undergoes regio- and stereoselective *syn*-HBr addition with TMSBr/EtOH to yield vinyl bromide **359** (90%). This was followed by the carbonylative Stille coupling with cyclohexenyl stannane **360** to form divinyl ketone **361** in 88% yield (Scheme 89).



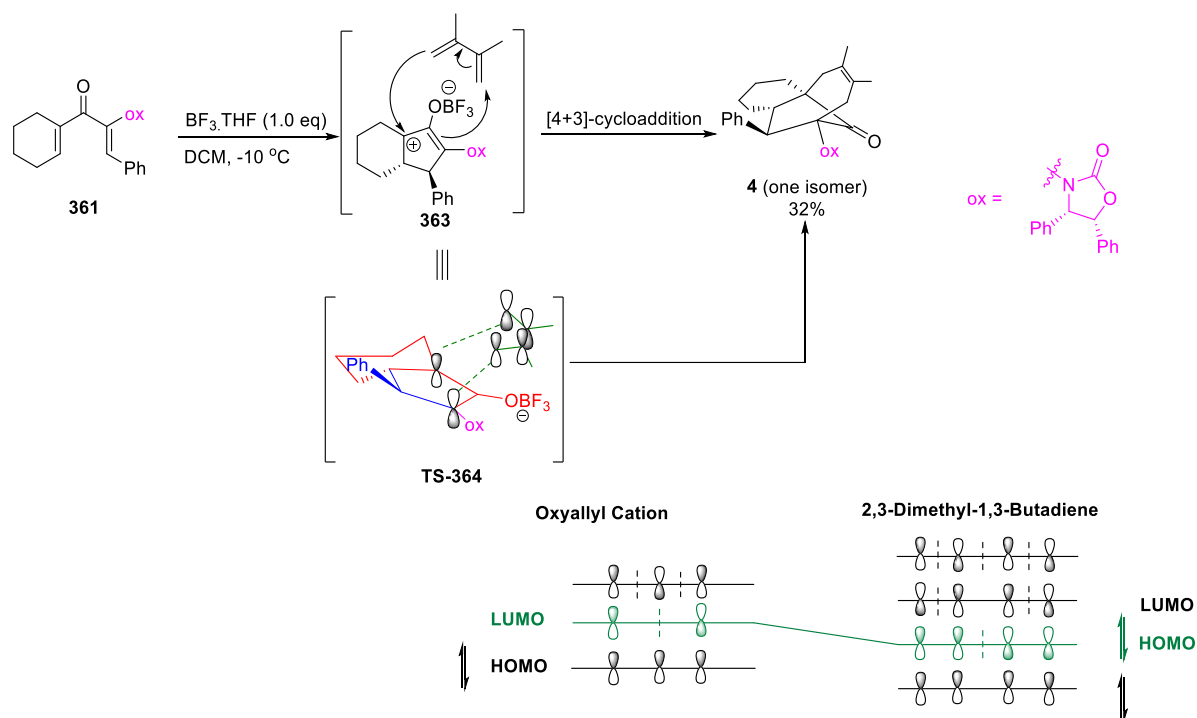
Scheme 89. Formation of divinyl ketone **361**.

We then performed a conventional (no trapping) Nazarov cyclization on divinyl ketone **361** by treatment of Lewis acid BF₃·THF to give a mixture of **362-cis** and **362-trans** in a 5:1 ratio, in which the ratio was determined by NMR analysis. With the use of excess MeSO₃H, **362-trans** was obtained exclusively in 85% isolated yield (Scheme 90).



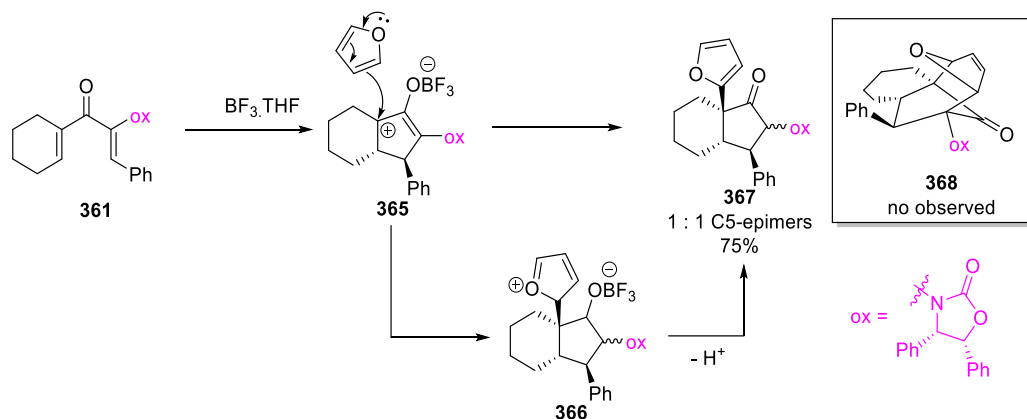
Scheme 90. The Nazarov cyclization towards cyclopentanoid **362-trans**.

We then investigated the synthesis of bridged-ring structure **4** in the presence of 2,3-dimethyl-1,3-butadiene. With several attempts, we concluded that the formation of bridged-ring structure **4** was best achieved at $-10\text{ }^\circ\text{C}$, giving it in 32% yield. The [4+3]-cycloaddition can be explained by the Woodward-Hoffmann rules, where the oxyallyl cation's LUMO reacts with butadiene's HOMO (**Scheme 91**, **TS-364**), allowing a concerted tandem [4+3]-cycloaddition. Despite the modest yield, this is a relatively efficient process from the perspective of number of new bond formation (3), number of stereocentre formation (4 stereocentres, including 2 x 4°) and stereoselectivity (100%).



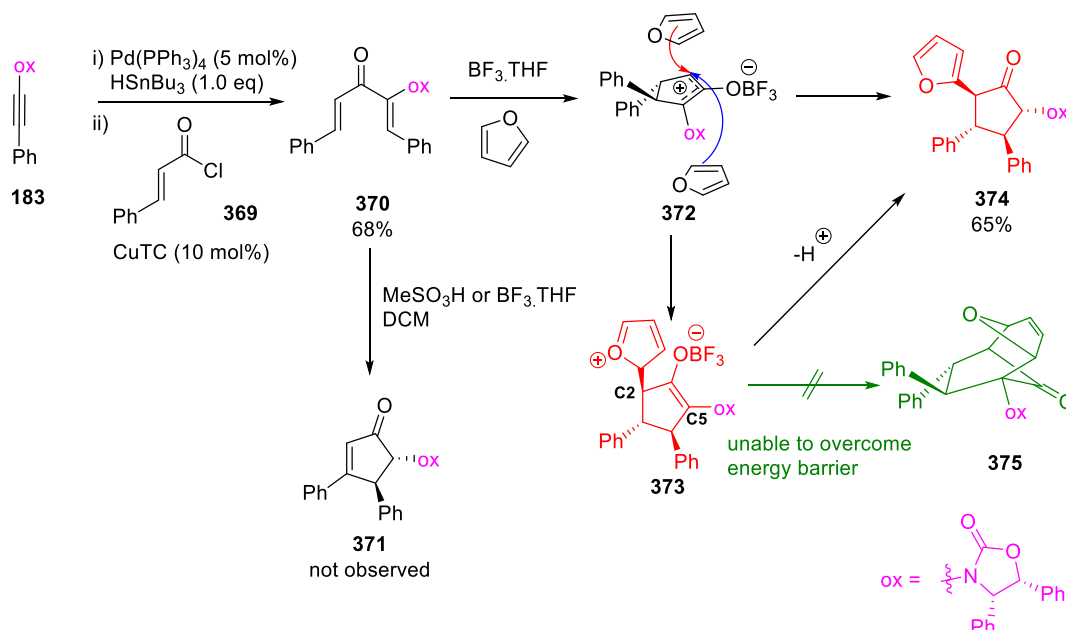
Scheme 91. The enantioselective formation of bridged ring **4**.

We also anticipated that a furan may participate in the [4+3]-cycloaddition process. However, the formation of **367** shows that furan prefers to undergo nucleophilic trapping instead. The addition of furan during the Nazarov cyclization of **361** yielded **367** as epimers.



Scheme 92. The formation of nucleophilic trapped product **367**.

A less congested Nazarov substrate **370** was formed as an alternative cycloaddition partner (**Scheme 93**). Dienone **370** was formed using our previously developed reductive-coupling procedure, involving one-pot Pd-mediated hydrostannylation of ynamide and acid chloride cross-coupling.⁷⁵ Further investigation with the use of furan as diene was performed on the Nazarov precursor **370**. Accordingly, ynamide **183** was coupled to cinnamoyl chloride **369** to give **370** in 68% isolated yield. Dienone **370** was subjected to Nazarov cyclization, however, a complex mixture was obtained, where cyclized product **371** was not observed. Interestingly, however, treatment of dienone **370** with acid in the presence of furan yielded nucleophilic trapped product **374** in 65% isolated yield.



Scheme 93. Formation of nucleophilic trapped product **374**.

The formation of **374** rather than **375** has been rationalized using density functional theory (DFT), where the DFT was performed by Dr. Elizabeth Krenske. The DFT reveals that furan first undergoes nucleophilic trapping with oxyallyl cation **372**, where nucleophilic attack is favoured from the top face, forming zwitterion **373** (**Figure 4**). The bias formation of **TSD** (furan attacks from the top face) rather than **TSE** (furan attacks from the bottom face) is due to the furan C-H and **ox**-Ph group interaction in space (distance between furan C-H and **ox**-Ph group = 2.79 Å, **TSD**, **Figure 4**) is closer than furan C-H and C3-Ph group of **TSE** (distance between furan C-H and C3-Ph group = 3.04 Å, **TSE**, **Figure 4**). The formation of CH- π interaction between furan CH and **ox**Ph in **TSD** then allows the formation of zwitterion **373**, as **TSD** is lower in energy, therefore explains such stereoselectivity. The stabilizing interaction between furan and C5 of zwitterion **373** also allows us to believe in the formation of bridged structure **375**. However, DFT again proves that the formation of nucleophilic trapped product **374** is favoured. This is due to the initial bond formation between furan and oxyallyl cation C2 contains a lower energy barrier (15.6 kcal/mol) than second bond formation in the expected cycloaddition process (21.3 kcal/mol), which has a difference of 5.7 kcal/mol, favouring the proton elimination of zwitterion **373**, forming **374** selectively.⁷⁸

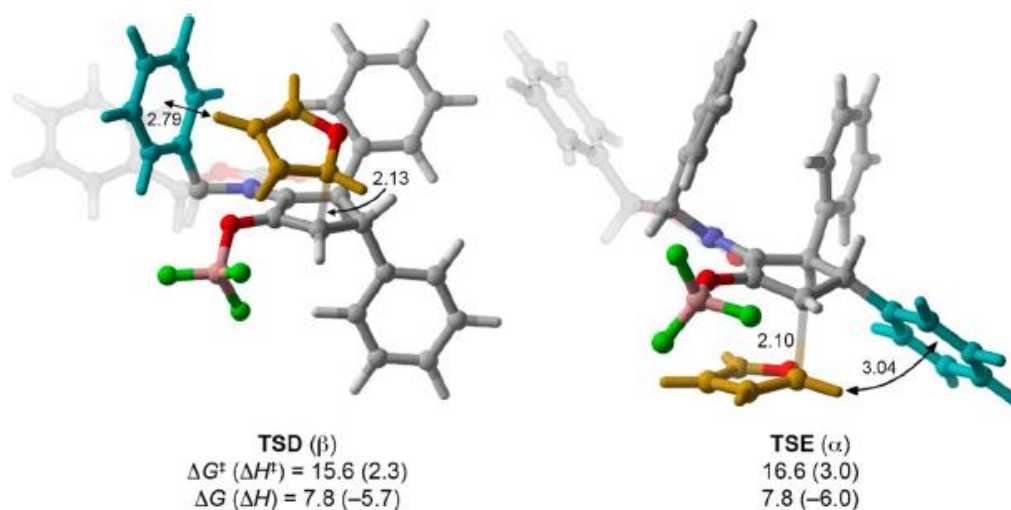
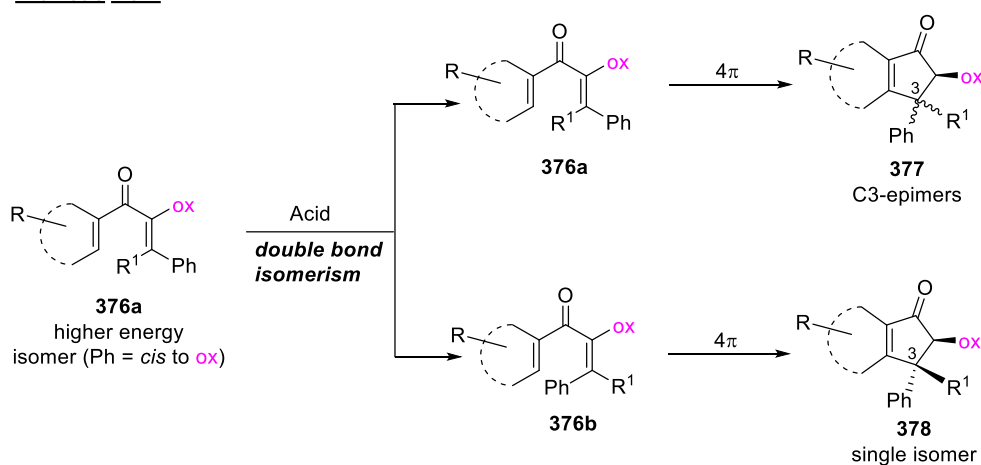


Figure 4. DFT calculation of **TSD** and **TSE** (ΔH^\ddagger in kcal).

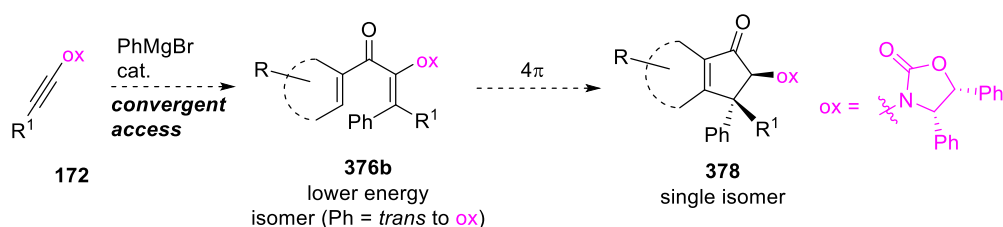
3.2 Preparation and the Nazarov cyclization of highly substituted Nazarov substrates

Previous studies within our group have identified that dienone **376a** (Ph = *cis* to ox, **Scheme 94**) to undergo partial double bond isomerism upon acid treatment. As a result, Nazarov cyclization of **376a** using acid leads to the formation of C3-epimers **377**. Our group was also able to isolate dienone **376b**, which upon the Nazarov cyclization, only produced one stereoisomer **378**. In this part of the project, we hypothesize that the stereoselective access into the lower energy dienone **376b** (Ph = *trans* to ox) from ynamides **172** would allow access to cyclopentanoid **378** selectively without double bond isomerism of dienone upon acid treatment.

Previous work

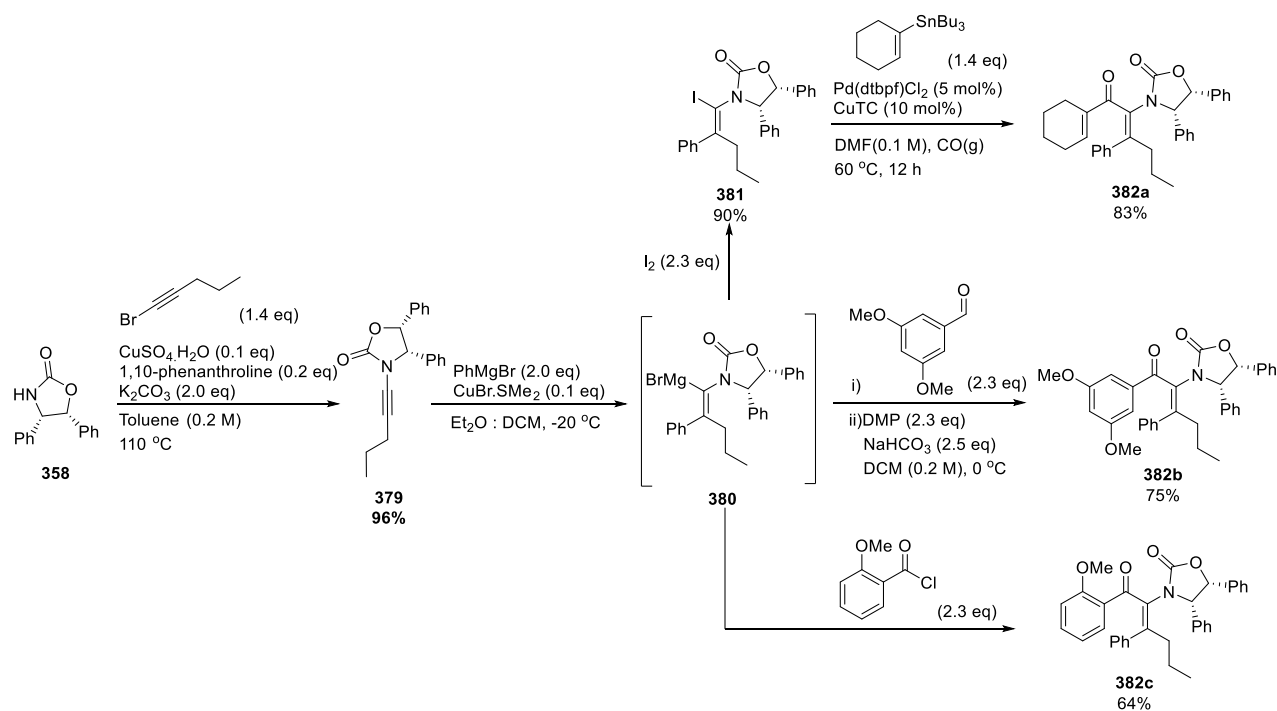


This work



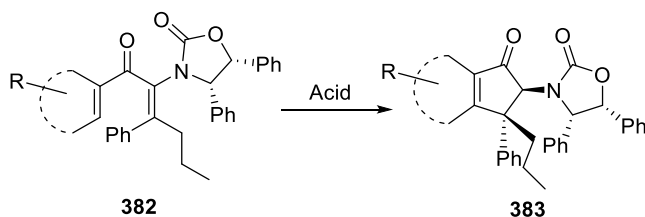
Scheme 94. The proposed convergent access from ynamide **172** to cyclopentanoid **378**.

The initial synthesis of precursor ynamide **379** was prepared via Cu^{II}-coupling method.⁷⁹ We then prepared one divinyl ketone and two aryl vinyl ketones via three different methods. To synthesize the Nazarov precursors **382a-c**, carbo-magnesiation was performed on ynamide **379** using PhMgBr in the presence of CuBr·SMe₂, forming vinyl Grignard **380** via *syn*-addition, with Ph group added as an internal substituent (**Scheme 95**).



Scheme 95. The conversion towards **382a-c**.

Vinyl Grignard **380** and vinyl iodide **381** were converted into three different Nazarov substrates via three different methods (**Scheme 95**). The first method involves the conversion of **380** into vinyl iodide **381**, followed by the carbonylative Stille coupling reaction to yield divinyl ketone **382a** in 83% yield. The synthesis of aryl vinyl ketone **382b** via 1,2-addition, followed by DMP oxidation was achieved in 75% yield. The last method was the nucleophilic acyl substitution of **380** with *o*-methoxybenzoyl chloride, giving **382c** in 64% yield.



Scheme 96. Nazarov cyclization of substrate **382a-c**.

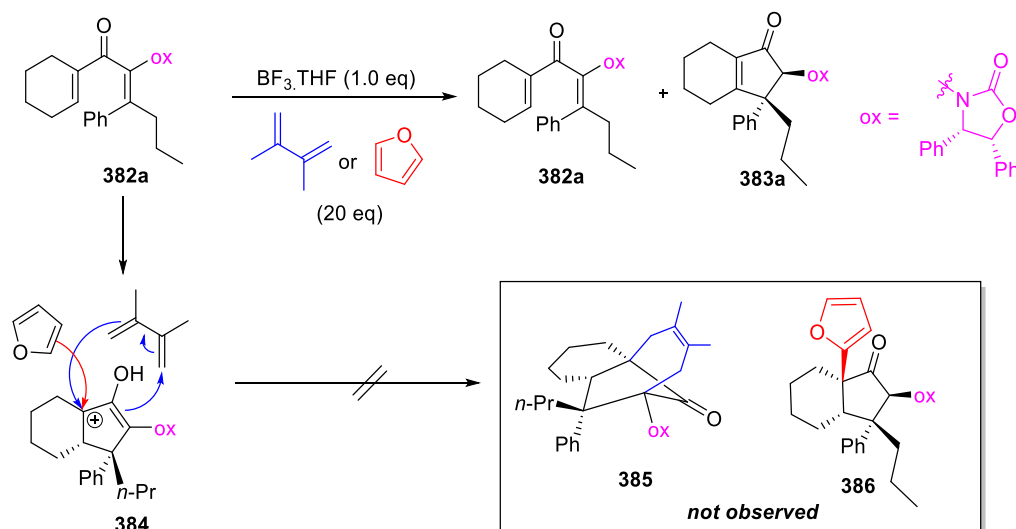
Table 4. The formation of products **383a-c**.

382a \longrightarrow 383a (dr)	382b \longrightarrow 383b (dr)	382c \longrightarrow 383c (dr)
<p>383a 82%^b (>20:1) R = cyclohexenyl</p>	<div style="display: flex; justify-content: space-around;"> <div> <p>383b-2S, 51%^b (>20:1) R = 3,5-dimethoxyphenyl</p> </div> <div> <p>383b-2R, 43%^b (>20:1) R = 3,5-dimethoxyphenyl</p> </div> </div> <div style="text-align: center; margin-top: 10px;"> <p>383b^{a,c} R = 3,5-dimethoxyphenyl</p> </div>	<p>383c^d R = o-methoxyphenyl</p>

a) observation from ^1H NMR analysis, degradation upon purification, b) the reaction was conducted with $\text{BF}_3 \cdot \text{THF}$ as catalyst
c) the reaction was conducted with TiCl_4 as catalyst, d) the reaction was conducted with TfOH as catalyst

We then performed the Nazarov cyclization on dienone **382a-c**. Satisfyingly, the cyclization of **382a** with $\text{BF}_3 \cdot \text{THF}$ yielded **383a** in 82% yield as a single stereoisomer. Interestingly, the use of TiCl_4 on **382b** formed enol-cyclized material **383b'**. However, due to the instability of **383b'** upon chromatography, chiral auxiliary oxazolidinone was cleaved, leading to degradation. Though the cyclization of **382b** with $\text{BF}_3 \cdot \text{THF}$ allowed the formation of epimers **383b-2S** and **383b-2R** in a combined yield of 94%. Previous results from our groups had shown convergent access into specific epimer with the treatment of excess MeSO_3H (as shown in **Scheme 90, Chapter 3.1**). A similar method could be applied in the scenario of **383b-2S** and **383b-2R**, to obtain one specific epimer. Also, the cleavage of C2-oxazolidinone epimers has been previously demonstrated to give single enantiomer.⁶³ The treatment of **382c** with $\text{BF}_3 \cdot \text{THF}$ required extended reaction time, which led to a slightly complexed mixture. TfOH was then used for the cyclization of **382c**, which allowed complete consumption of **382c** in 2 h. However, 2D NMR analysis indicated that acid treatment of **382c** led to double bond deconjugation, forming **383c**, where no cyclized product was observed (**Scheme 96, Table 4**). The formation **383c** is consistent with the previous report on such double bond

deconjugation, where *p*-methoxyphenyl was used.⁶³ These examples have proven that the *ortho* and *para* methoxy groups are not as activating as *meta* ones.

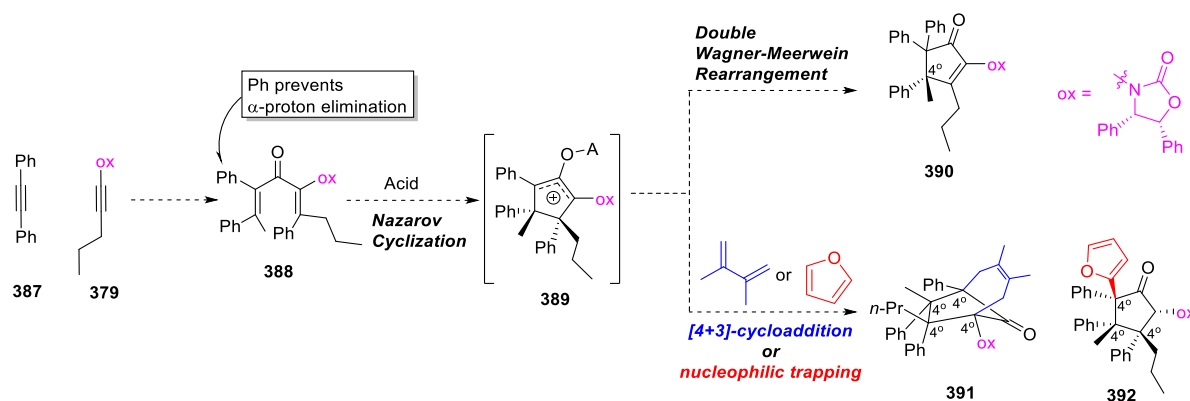


Scheme 97. Attempt in the formation of **385** and **386**.

We also investigated the synthesis of bridged ring structure **385** and furan trapped product **386** in the presence of butadiene and furan, respectively. However, reactions were not successful and yielded normal (not trapped) cyclized product **383a**, or the recovery of starting material **382a** (**Scheme 97**). Further exploration of the trapping of oxyallyl cation **384** with more powerful nucleophiles is yet to be undertaken.

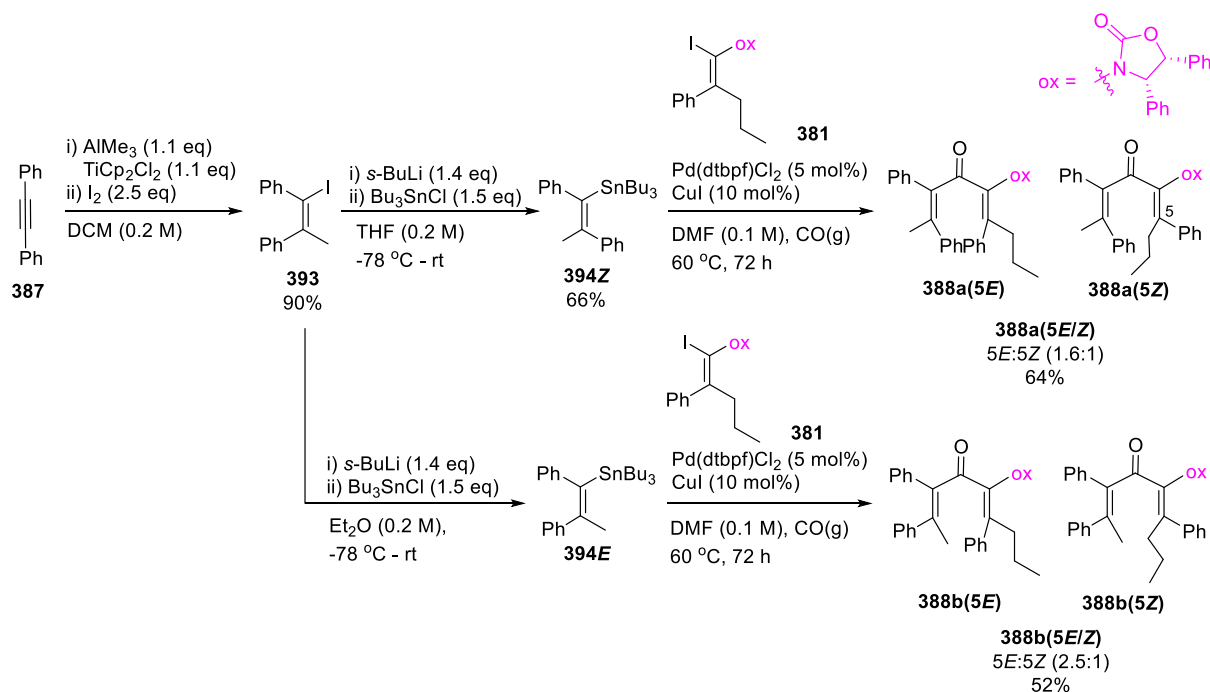
3.3 The synthesis of fully substituted divinyl ketones and the Nazarov cyclization to form vicinal 4°-stereocentres

We then investigated the Nazarov cyclization on a series of fully substituted divinyl ketones, while examining the ability to undergo inter- and intramolecular interrupted Nazarov cyclization. With Ph group installed at the α -carbon, proton elimination from **388** is not possible, increasing the chance for tandem nucleophilic trapping or cycloaddition cascade. We anticipated that the acid treatment of tetra-substituted divinyl ketone **388** should yield **390**, via double Wagner-Meerwein rearrangement.^{65,102} In the presence of diene or furan during the cyclization, we also expect the formation of **391** and **392** via [4+3]-cycloaddition and nucleophilic trapping, respectively (**Scheme 98**).



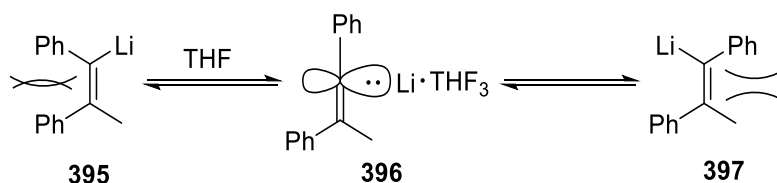
Scheme 98. The proposed route towards the synthesis of cyclopentanoids **390** - **392**.

The synthesis of the divinyl ketone **388** initiated with *syn*-carboalumination of diphenyl acetylene **387**, followed by the addition of iodine to give vinyl iodide **393** in 90% yield, regio- and stereoselectively (**Scheme 99**). Vinyl iodide **393** was then converted into vinyl stannane **394Z** (66%), followed by carbonylative Stille coupling with vinyl iodide **381** to yield expected divinyl ketone **388a(5E/Z)** in 64% yield as *E/Z* isomers (1.6:1).



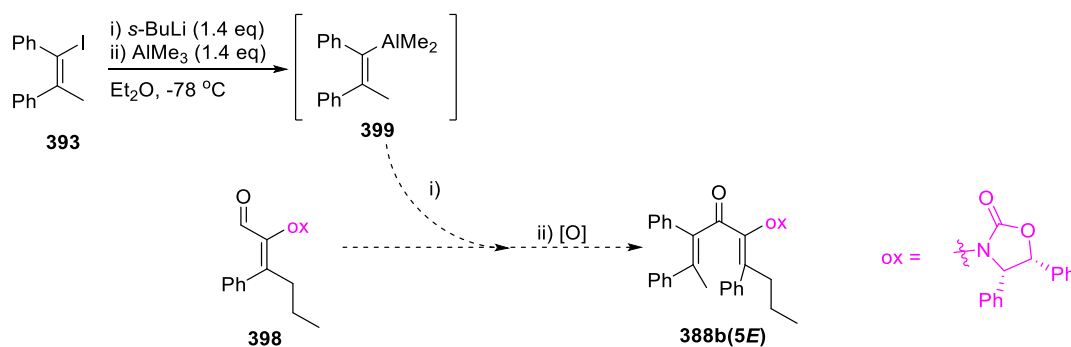
Scheme 99. Synthesis of the Nazarov precursors **388a(5E/Z)** and **388b(5E/Z)**.

Surprisingly, the conversion of the vinyl iodide **393** into a vinyl stannane **394** gave different isomers in different solvents. In THF, **394Z** was obtained, where the vinyl lithium species **365** undergoes rapid isomerism. However, **394E** was obtained where Et_2O was used. According to the investigation by Knorr *et al.*, when Ph group is geminal to vinyl lithium, the sterically encumbered alkene undergoes rapid isomerism, which was directed by THF solvation (see structure **396**, **Scheme 100**). However, it was also indicated that non-THF ethereal solvent such as Et_2O is not as effective in directing such isomerism.¹⁰³ **394E** was also brought forward to the carbonylative Stille coupling to form divinyl ketone double bond isomers **388b(5E/Z)** as *E/Z*-isomers in 2.5:1 ratio (**Scheme 99**).



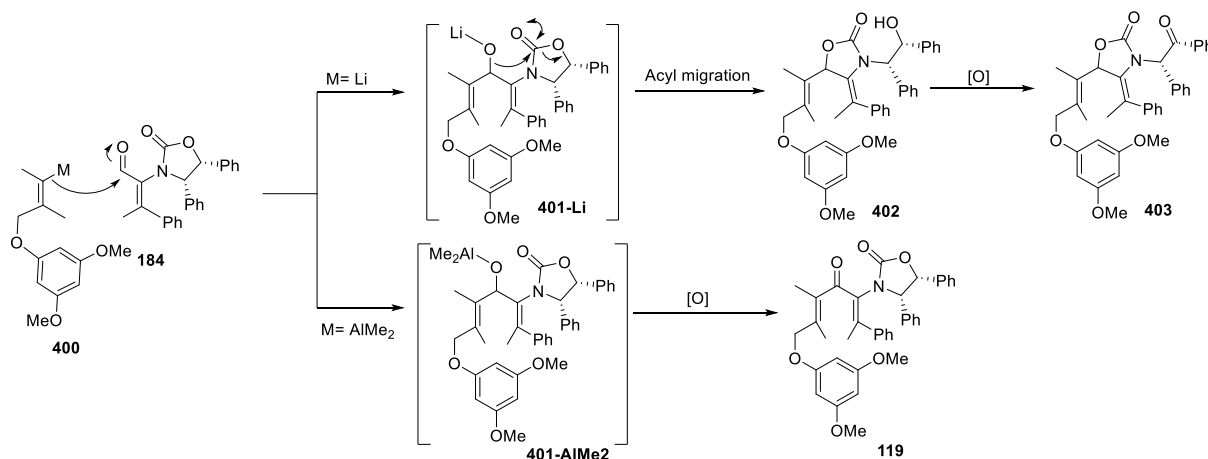
Scheme 100. Double bond isomerism of **395** directed by THF solvation.

We also attempted to access stereochemically pure divinyl ketone isomer **388b(5E)** via alanate **399** addition to aldehyde **398**, where alanate **399** is generated by lithiation of vinyl iodide **393**, followed by the addition of AlMe_3 (**Scheme 101**). The formation of vinyl alanate **399** can only be performed in Et_2O , where vinyl lithium generated from lithiation does not undergo *in situ* rearrangement, explaining the expected stereochemical outcome from the addition of alanate **399** to aldehyde **398** (**388b(5E)**, **Scheme 101**).



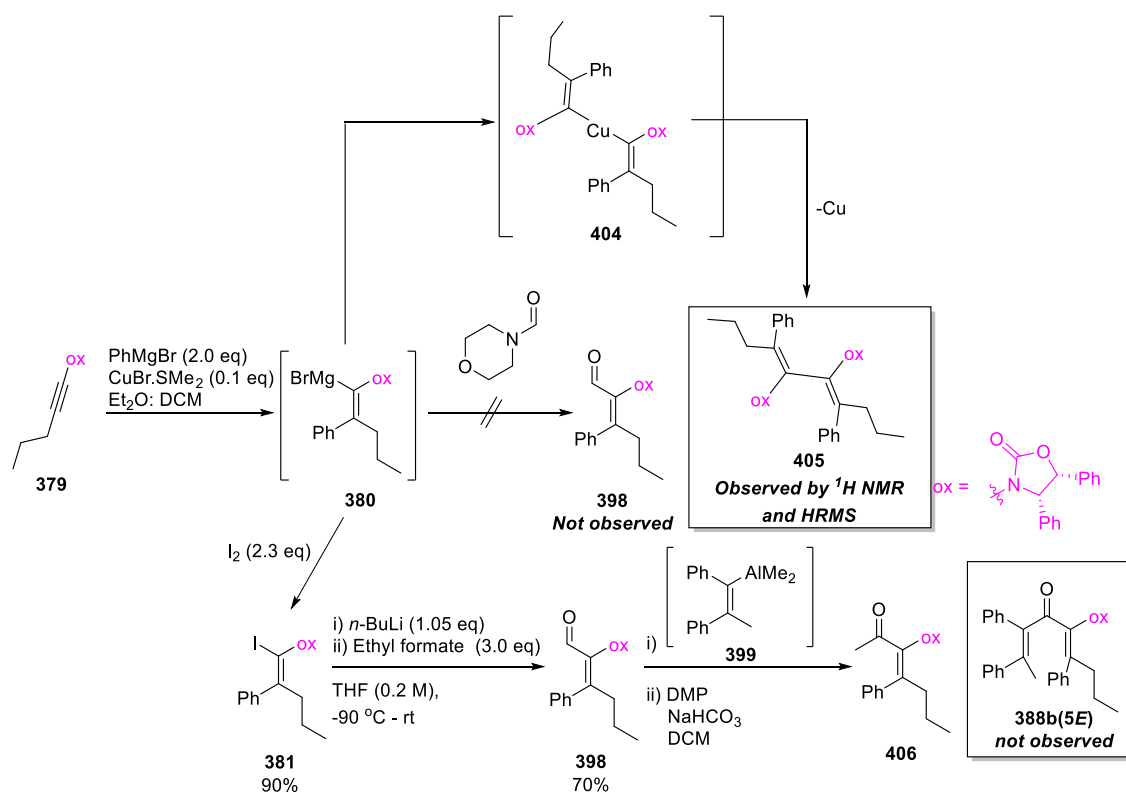
Scheme 101. The proposed formation of **388b(5E)**.

The use of vinyl alanate **399** in the proposed formation of **388b(5E)** is due to the previously observed acyl migration phenomenon, where the formation of **403** was observed when *in situ* **401-Li** was generated (**Scheme 102**).⁶⁵ The formation of **403** was avoided when *in situ* **401-AlMe₂** was generated, giving dienone **119** selectively.



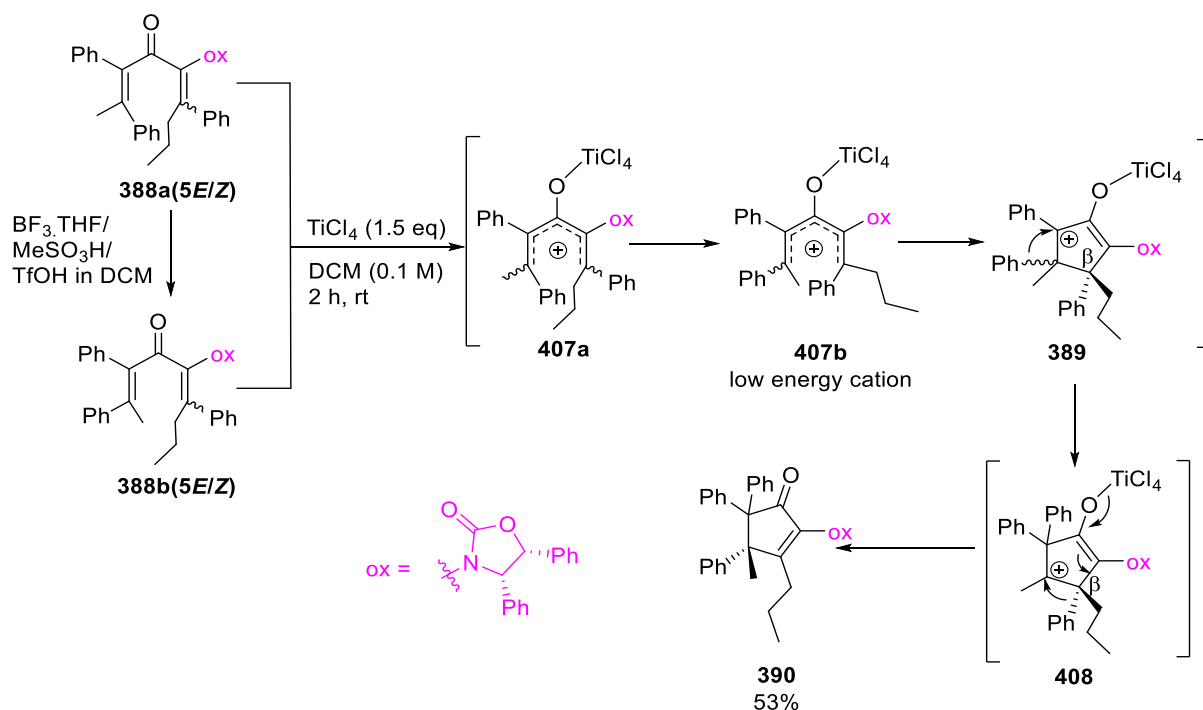
Scheme 102. The previously observed formation of **403** via lithium alkoxide **401-Li**.

The initial formation of aldehyde **398** appeared to be problematic as there had been a persistent formation of dimer **405** via copper-mediated reductive elimination of **404** (**Scheme 103**), which was detected by both ¹H NMR and HRMS. The unsuccessful formation of **398** via Grignard intermediate **380** was possibly due to the sterically hindered nature of **380**, and the usage of comparatively less reactive *N*-formylmorpholine as the electrophile. Nevertheless, the formation of **398** was successful via the lithiation of vinyl iodide **381**, followed by the addition of ethyl formate. Despite the success in the formation of **398**, the synthesis of divinyl ketone **388b(5E)** was unsuccessful, where the formation of methyl ketone **406** was observed by mass spectrometry.



Scheme 103. Unsuccessful attempt stereoselective synthesis of divinyl ketone **388b(5E)**.

Nevertheless, we then attempted the cyclization of **388a(5E/Z)** and **388b(5E/Z)**. The treatment of divinyl ketone **388a(5E/Z)** with various acid including $\text{BF}_3\cdot\text{THF}$, MeSO_3H and TfOH , give full conversion to divinyl ketone isomers **388b(5E/Z)** without cyclization. Surprisingly, TiCl_4 was the only acid that induces the cyclization of both **388a(5E/Z)** and **388b(5E/Z)**, yielding **390** as one enantiomer (**Scheme 104**). The stereochemistry of compound **390** was confirmed by X-ray crystallography, which was performed by Prof. Jonathan White (**Figure 5**). This result indicates that the formation of pentadienyl cation **407a** rapidly undergoes TiCl_4 -mediated pre-equilibration, forming thermodynamically stable pentadienyl cation **407b**. Upon the Nazarov cyclization of **407b**, oxyallyl cation **389** was formed, where Ph group at β carbon points down, due to the torquoselectivity provided by chiral auxiliary oxazolidinone. This is followed by the initial Ph group migration, giving cation **408**. The Ph group at β carbon possesses a much greater migrating aptitude than Pr group, which then allows Ph to migrate from bottom face, forming **390** enantioselectively.¹⁰⁴ The stereoselective formation of **390** shows that TiCl_4 is able to provide access to thermodynamically stable pentadienyl cation from resistant Nazarov precursors, which then allows the enantioselective formation of cyclopentanoid via Nazarov cyclization and double Wagner-Meerwein rearrangement from highly substituted divinyl ketones.



Scheme 104. Enantioselective synthesis of **390** via double Wagner-Meerwein rearrangement.

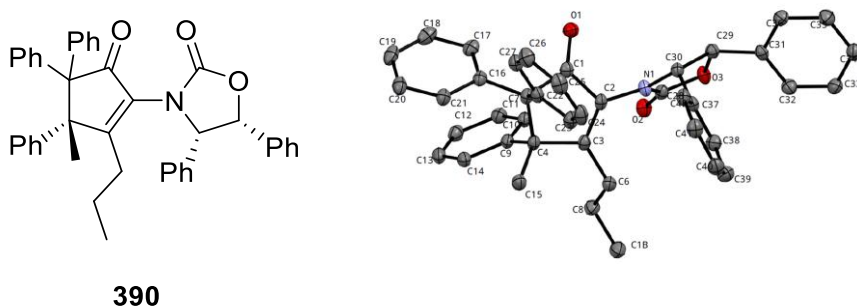
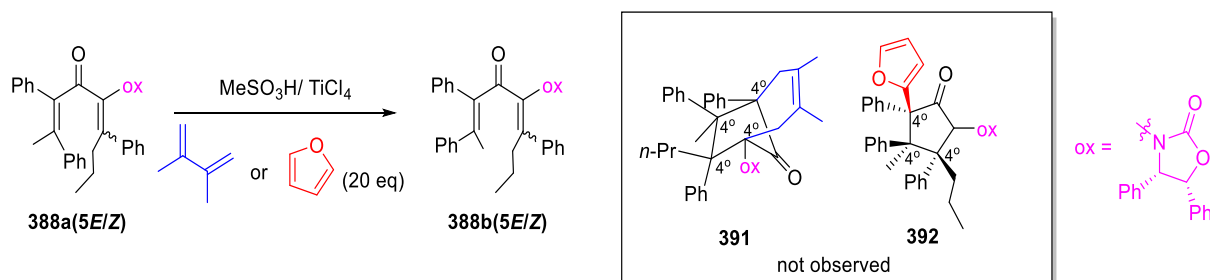


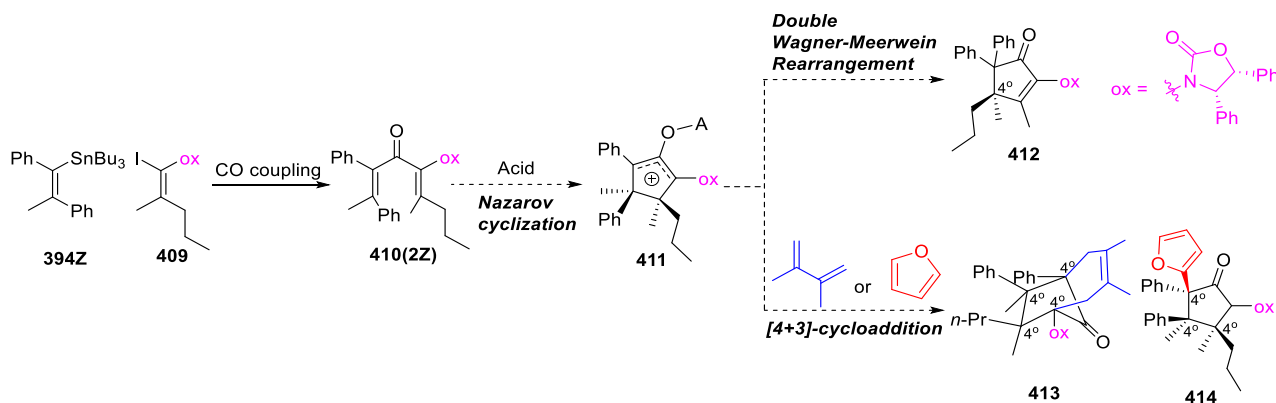
Figure 5. X-ray crystal structure of **390**.

We also attempted the [4+3]-cycloaddition on **388a(5E/Z)**, in the presence of furan or diene with MeSO_3H or TiCl_4 . However, only double bond isomerism towards **388b(5E/Z)** was observed (**Scheme 105**).



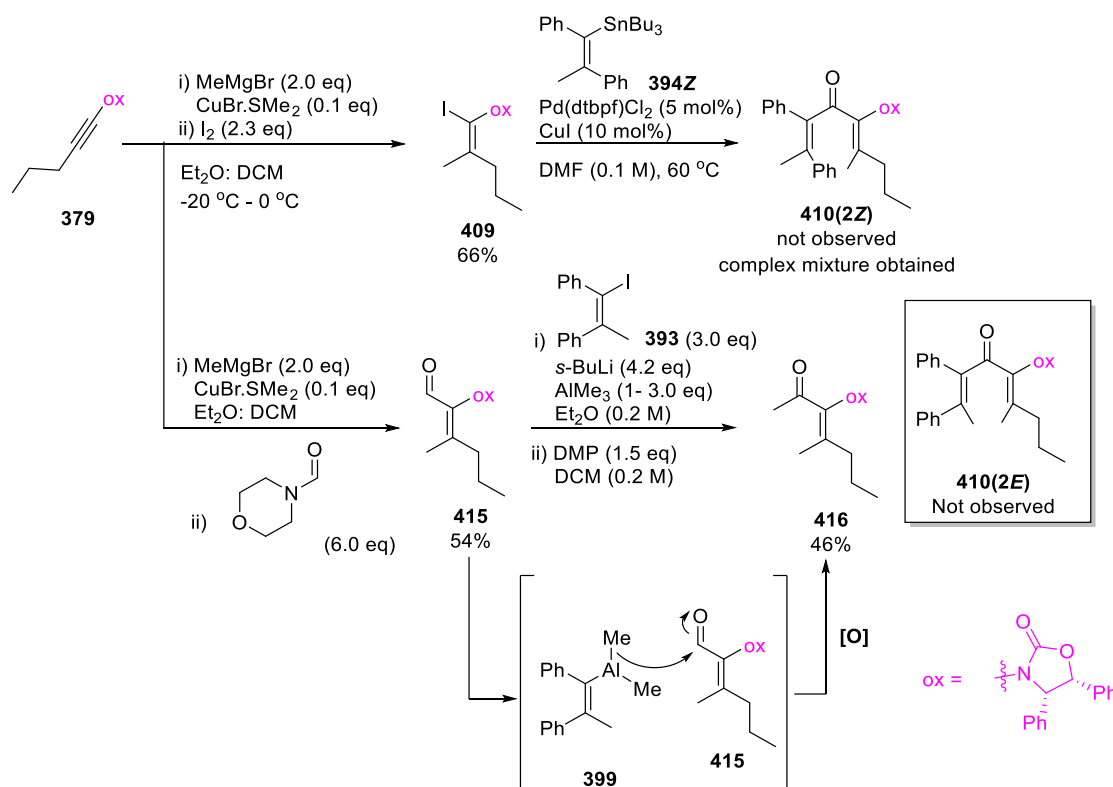
Scheme 105. The attempted formation of **391** and **392**.

We next targeted an alternative substitution pattern of the divinyl ketone, **410(2Z)**. Dienone **410(2Z)** formation via CO-coupling is anticipated to perform without isomerism as alkyl substituents at β -carbon should slow down the rate of isomerism. **Scheme 106** shows the proposed synthesis of divinyl ketone **410(2Z)** and subsequent cyclopentanoids **412-414**, which are anticipated to result from double Wagner-Meerwein rearrangement, [4+3]-cycloaddition and nucleophilic trapping, respectively.



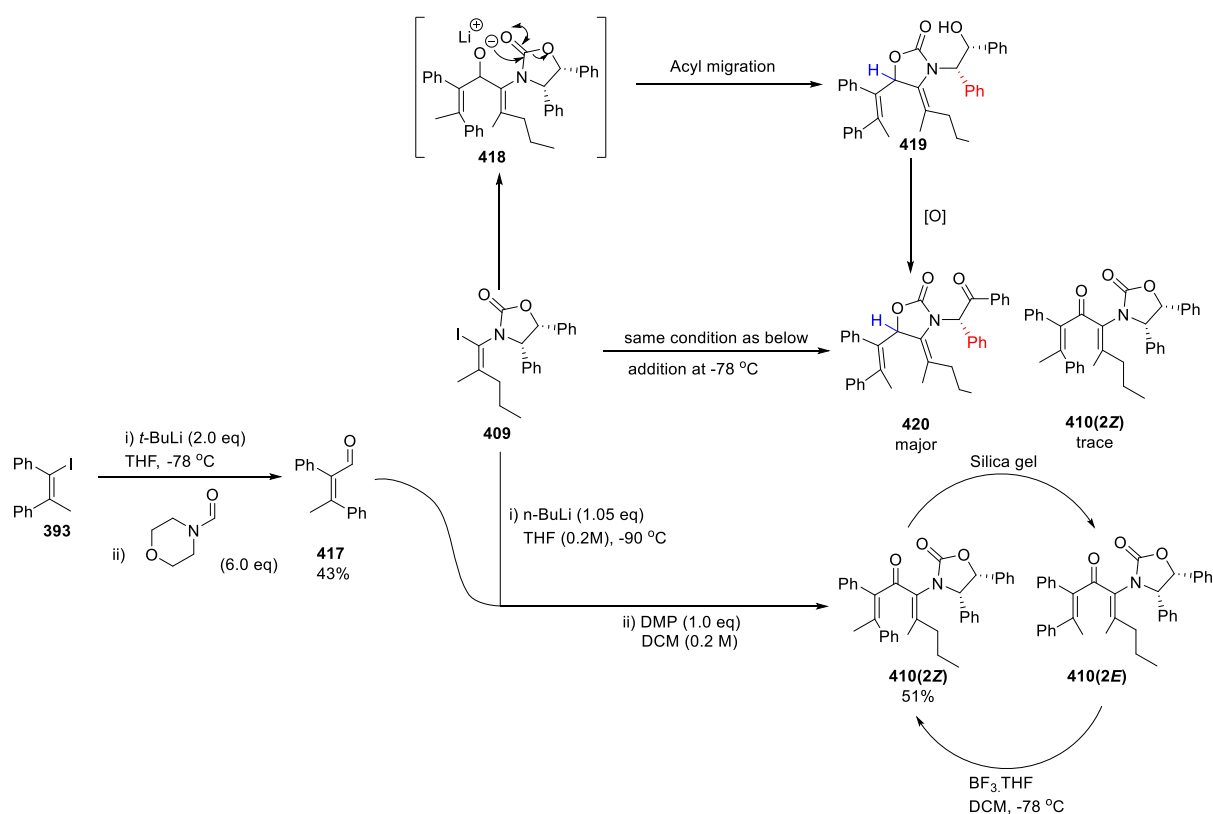
Scheme 106. A proposed formation of cyclopentanoids **412-414**.

The synthesis of vinyl iodide **409** from ynamide **379** was reasonably straight forward, giving **409** in 66% yield (**Scheme 107**). However, the carbonylative coupling between **409** and vinyl stannane **394Z** was unsuccessful, where multiple products were observed. We also attempted 1,2-addition of *in situ* formed alanate **399** to aldehyde **415**, followed by oxidation, where the intention for the use of alanate **399** and the resulting stereochemistry were explained in **Scheme 102 (Page.74)**. Unfortunately, this method produced methyl ketone **416**, where methyl transfer from alanate **399** was again observed (**Scheme 107**).



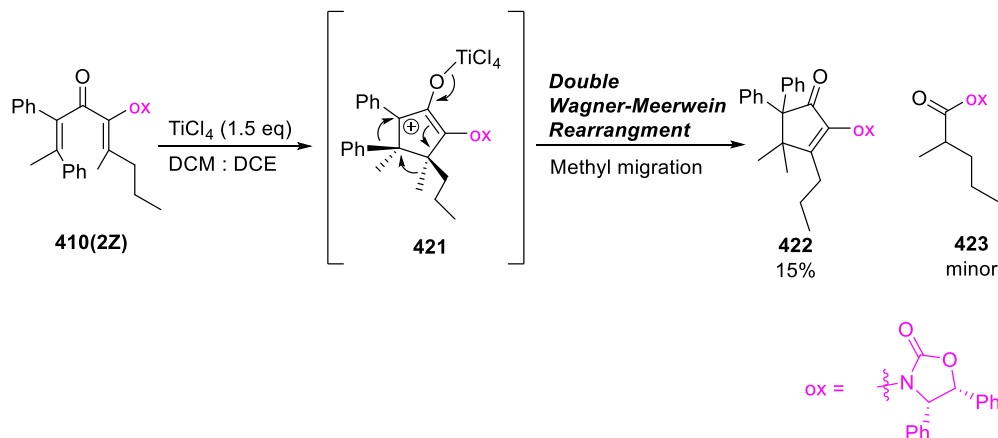
Scheme 107. An unsuccessful attempt in the formation of **410(2E)**.

To further pursue the proposed divinyl ketone **410(2Z)**, we attempted the lithiation of vinyl iodide **409** and addition across to aldehyde **417**, where **417** was prepared via formylation of **393** with *in situ* rearrangement of the vinyl lithium in THF (**Scheme 108**). The addition process conducted at -78°C produced acyl migrated product **420**, where lithium alkoxide of **418** attacks carbonyl on oxazolidinone, causing oxazolidinone ring-opening, forming alcohol **419**, followed by oxidation to give **420** as the major product (**Scheme 108**). The formation of side product **420** is also consistent with the earlier discussed acryl migration (**Scheme 102, Page. 74**). As expected, Ph groups of compound **419** and **420** (highlighted in red) retain their stereochemistry. However, we were not able to determine the stereochemistry of the proton (highlighted in blue), as it is too far in space to produce any NOE (Nuclear Overhauser Effect) interaction. Hence, the only method to determine the stereochemistry of compound **419** and **420** is by X-ray crystallography, however, no suitable sample was obtained for this specific analysis.



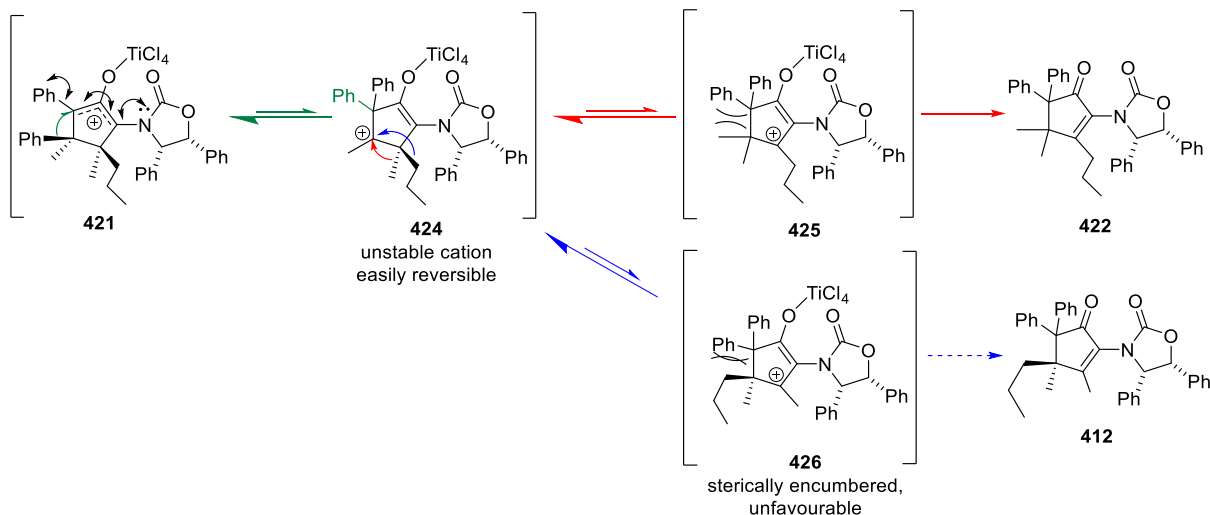
Scheme 108. The formation of divinyl ketones **410(2Z)** and **410(2E)** as an isomeric mixture.

The reaction efficiency was significantly improved when reaction conducted at -90 °C, where the formation of **420** was completely avoided, giving **410(2Z)** initially as the only isomer. However, chromatography on silica gel gave 51% yield of **410(2Z)** and **410(2E)** in 1.4:1 ratio (**Scheme 108**). Accordingly, efficient conversion to stereochemically pure **410(2Z)** can be accessed by treating a chromatographed mix of **410(2Z/E)** with BF₃·THF at -78 °C, to give **410(2Z)** in overall 51% yield. The treatment of **410(2Z)** with TiCl₄ yielded **422** (**Scheme 109**). Product **422** has resulted from double Wagner-Meerwein rearrangement, where the Me group shifted from β-carbon instead of the expected Pr group, produced a rather unexpected result. The formation of **422** contradicts with known migrating aptitude: Ph > 4°-carbon > 3°-carbon > 2°-carbon > 1°-carbon > hydride.¹⁰⁴



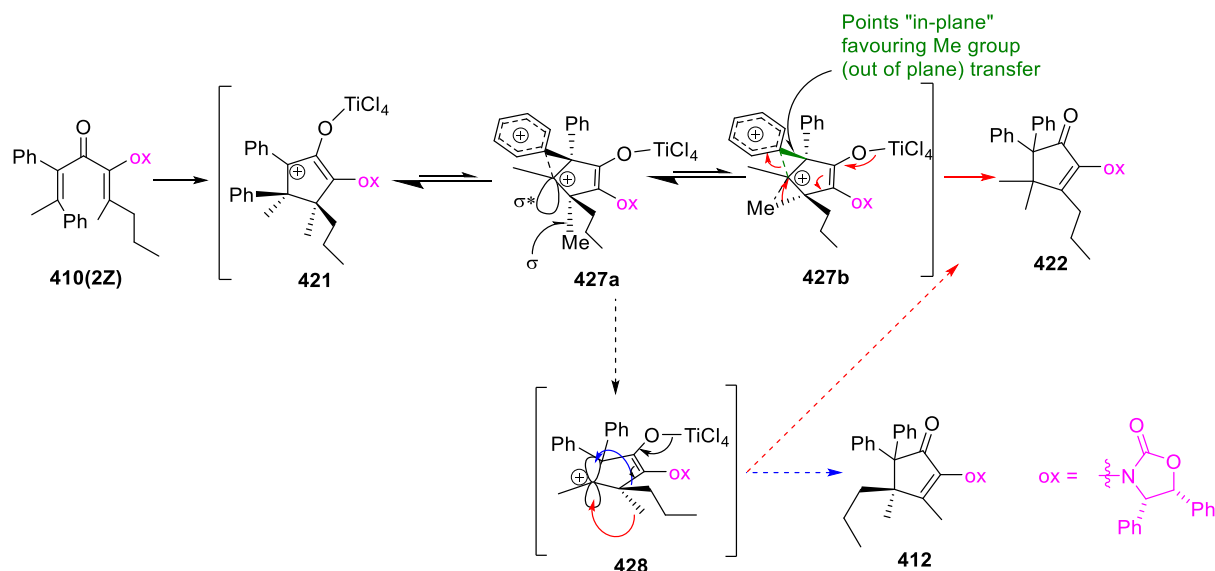
Scheme 109. The formation of **422** from Nazarov cyclization and minor hydrolyzed product **423**.

Therefore, we propose two mechanistic explanation for the formation of **422**. Our first proposal is that the formation of cation **426** is disfavoured relative to **425** (**Scheme 110**). This is due to the steric clash between Ph and Pr group in cation **426**. However, when Me group shifts, it reduces this steric hindrance, as the Me group is less bulky than the Pr group.



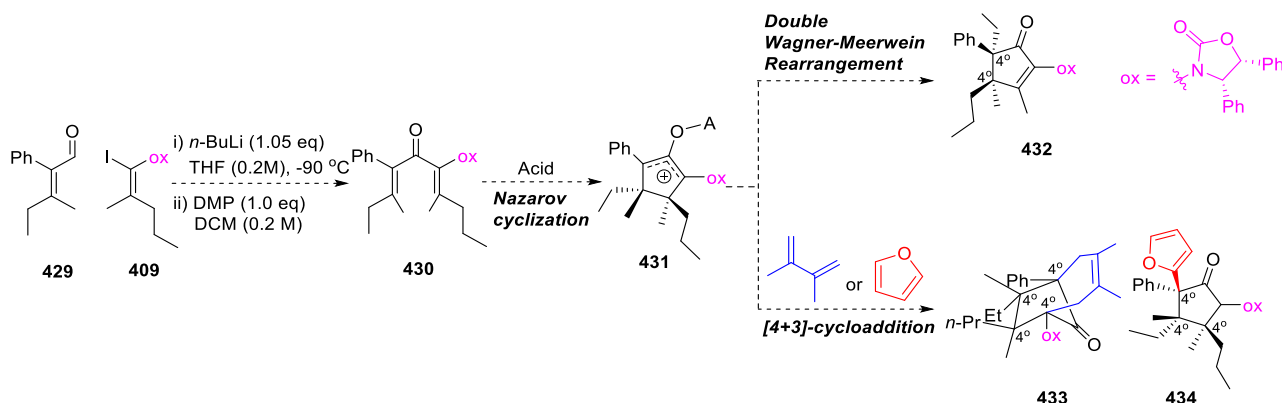
Scheme 110. Sterically clash between Ph and Pr group in intermediate **426**, formation of **412** disfavoured.

A second mechanistic proposal is shown in **Scheme 111**. As divinyl ketone **410(2Z)** cyclizes, the enantioselective formation of oxyallyl cation **421**, where the β -Ph group points in-plane, then forms the intermediate **427a**. The formation of this intermediate **427a** (and also **427b**) then allows a concerted rearrangement, where the Me group (out of plane) attacks from the bottom face, as the cyclopropyl-Ph cationic intermediate points in-plane. The σ -orbital between β -carbon and Me group in **427a** also interacts with the antibonding σ^* -orbital, therefore providing the observed methyl migration. Alternatively, as the Ph group migrates, the σ^* -orbital slowly becomes vacant π -orbitals, forming cation **428** (non-concerted). The formation of cation **428** then allows either Pr or Me group migration from top or bottom face. Although we expected to obtain a mixture of **412** and **422** from the non-concerted rearrangement of cation **428**, the result has indicated that the concerted formation of **422** from intermediate **427b** is more favourable.



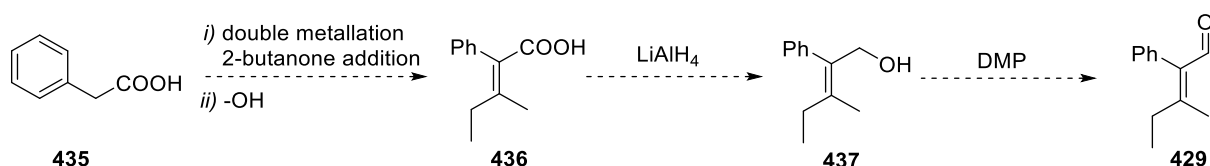
Scheme 111. A Proposed detailed mechanism of the Wagner-Meerwein rearrangement.

Notwithstanding the failure in the formation of **412**, we then moved forward to the synthesis of divinyl ketone structure **430**. The proposed Nazarov precursor **430** should undergo a slower double Wagner-Meerwein rearrangement, due to the all-alkyl substituents at both β and β' positions. The formation of stabilized oxyallyl cation **431** resulted from the Nazarov cyclization is anticipated to increase the probability of [4+3]-cycloaddition and nucleophilic trapping, giving **433** and **434** (Scheme 112).



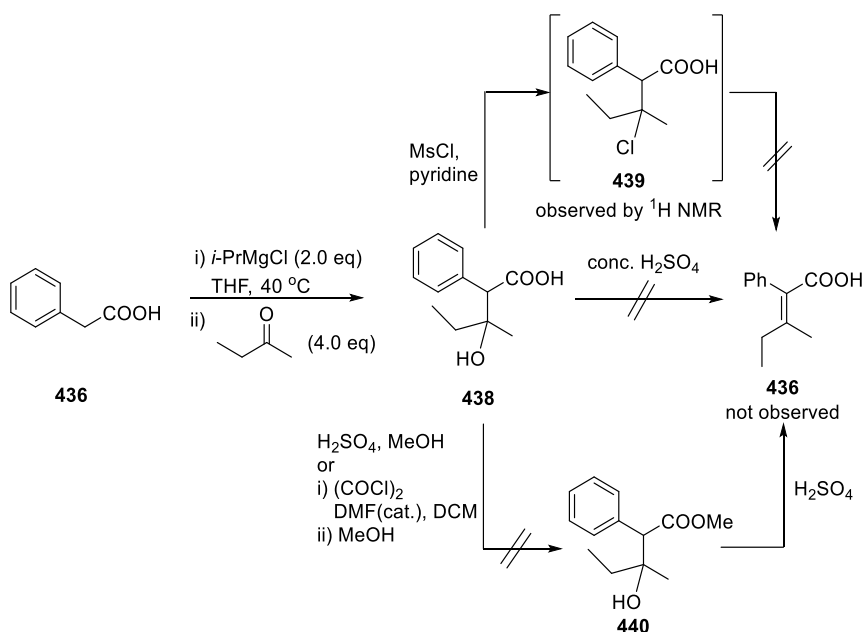
Scheme 112. Design of new divinyl ketone **430**, and the proposed formation of **432-434**.

The initial study on the synthesis of dienone **430** involves the formation of proposed aldehyde **429**. We anticipated that the formation of **429** involves 1,2-addition of α -metallated phenylacetic acid **435** to 2-butanone, followed by dehydration to give carboxylic acid **436**. Acid **436** could then be reduced to alcohol **437**, followed by subsequent oxidation to yield expected aldehyde **429**. Although the synthesis is seemingly straightforward, the formation of acid **436** proved rather challenging (Scheme 113).



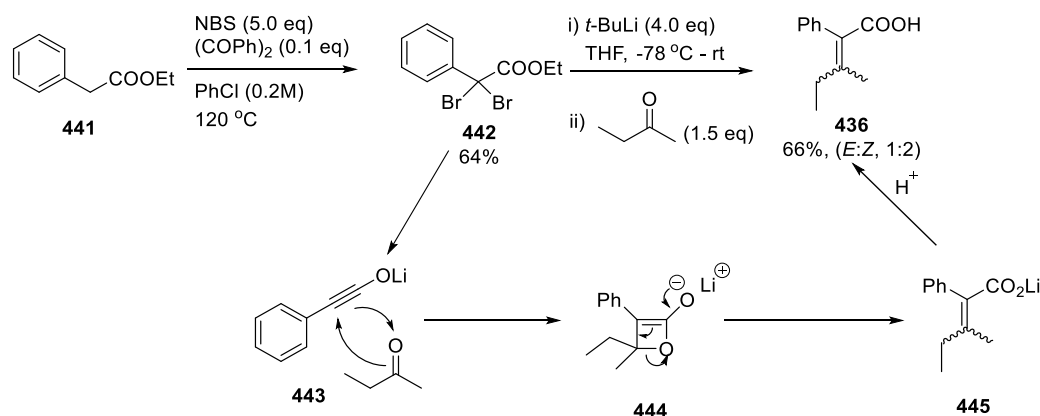
Scheme 113. A proposed synthetic route towards **429**.

The formation of alcohol **438** was very successful, though subsequent dehydration proved to be problematic, where numerous conditions were applied (**Scheme 114**). We first attempted dehydration of **438** with addition of conc. H_2SO_4 , however, a complex mixture was obtained and acid **436** was not observed. Later attempts including the elimination of chloride group of *in situ* formed **439** using pyridine were not successful. The dehydration from ester **440** is expected to provide more stability upon treatment with conc. H_2SO_4 , due to the absence of acid functionality. An attempt in the esterification of **438** did not give expected ester **440**, therefore did not allow us to perform the subsequent dehydration of ester **440**.



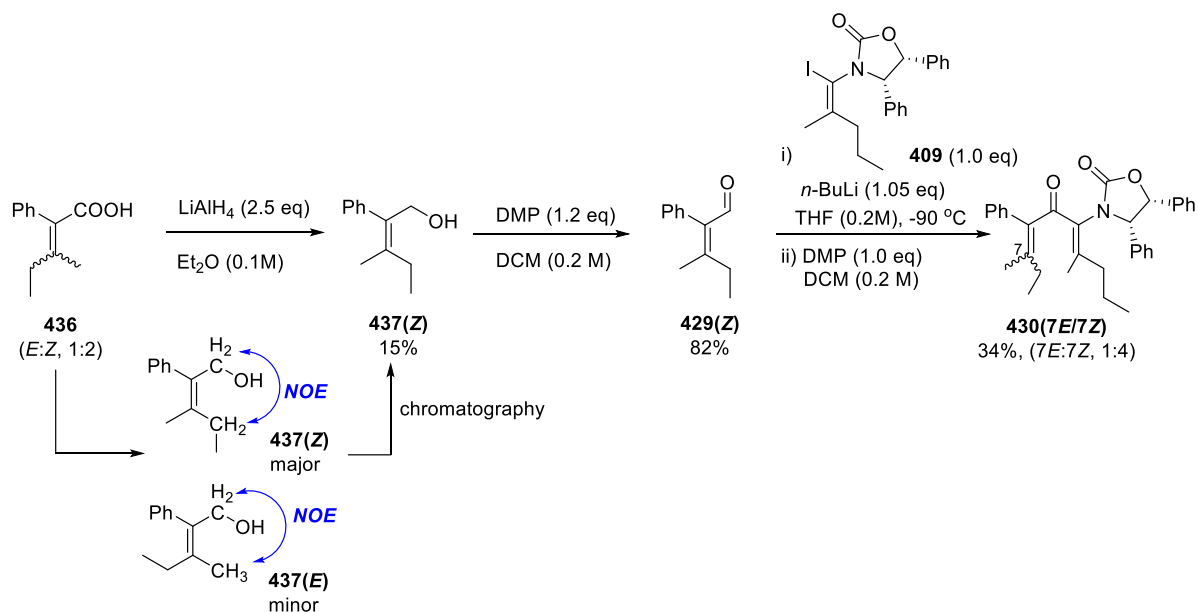
Scheme 114. Unsuccessful attempts in the formation of acid **436**.

We decided to re-route the synthesis of carboxylic acid **436** using an olefination devised by Mitsuru and co-workers.¹⁰⁵ We first synthesized di-bromo phenyl acetate **442** via radical bromination, forming dibromide **442** in 64% yield. Dibromide **442** was then treated with four equivalence of *t*-BuLi to yield lithium ynolate **443**, where the addition of 2-butanone further reacted with **443** to form the cyclobutene intermediate **444** (non-concerted [2+2]-cycloaddition). Intermediate **444** then undergoes electrocyclic ring-opening, followed by acidic workup to yield carboxylic acid **436** as *E:Z* double bond isomers in good yield (**Scheme 115**).



Scheme 115. Mechanism in the formation of **436** via electrocyclic reaction.

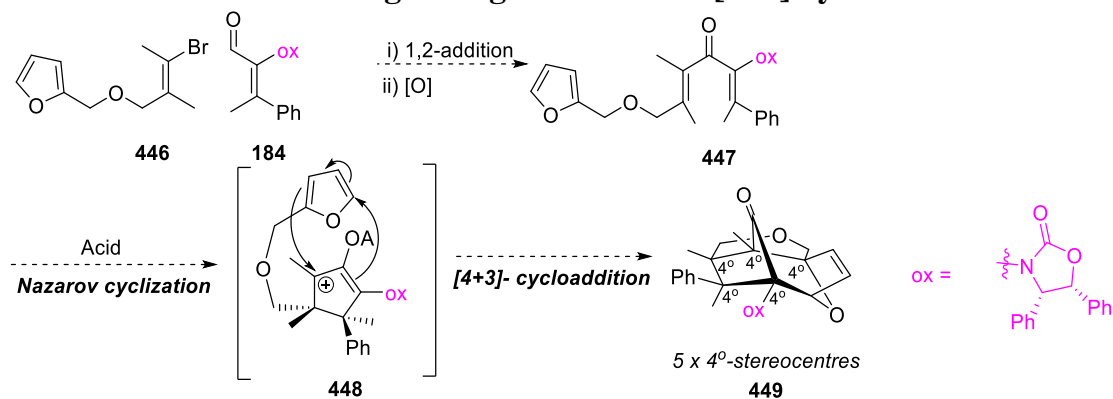
However, due to the difficulty in the separation between the double bond isomers of acid **436**, chromatography was performed on the subsequently formed alcohol **437**, where a notable amount of **437** degraded through purification. This purification process has not yet been optimized. Characterization of **437(Z)** shows that acid **436(Z)** is the major isomer obtained from olefination (*NOE* analysis). Alcohol **437(Z)** was then oxidized to give aldehyde **429(Z)** in excellent yield. The 1,2-addition of lithiated vinyl iodide **409** to aldehyde **429(Z)**, followed by oxidation, yielded **430(7E/7Z)** as a double bond isomeric mixture in 1:4 ratio (34% yield) (**Scheme 116**).



Scheme 116. Formation of divinyl ketone **430(7E/7Z)**.

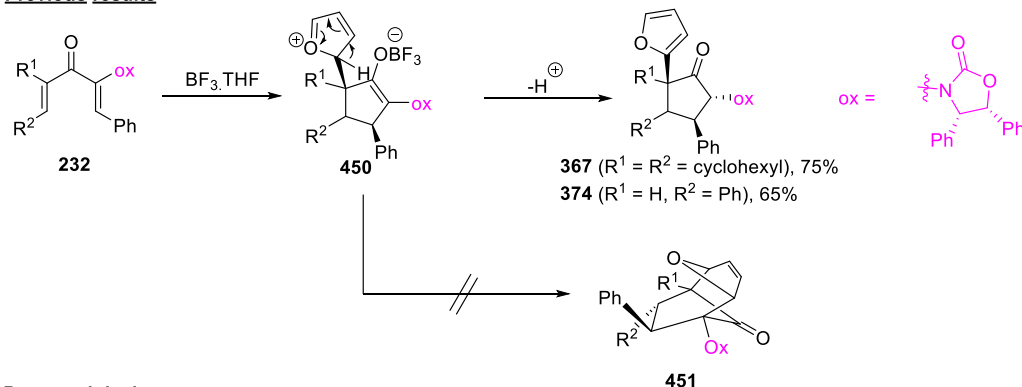
Despite the successful formation of divinyl ketone **430(7E/7Z)**, we were unable to perform the Nazarov reaction due to time constraint, which requires the re-synthesis of precursor **430(7E/7Z)** to evaluate the Nazarov cyclization.

3.4 The formation of fused-bridged ring structure via [4+3]-cycloaddition

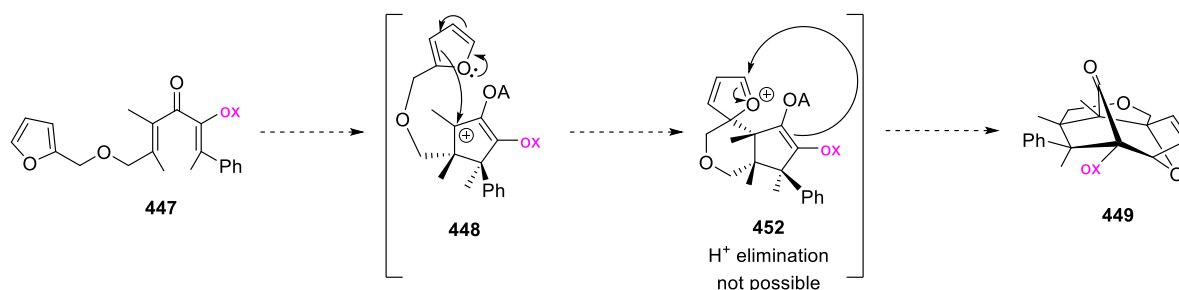
Scheme 117. Proposed enantioselective synthesis of bridged ring **449**.

One of our main objectives is the formation of the fused-bridged ring structure **449**, which involves the intra-molecular [4+3]-cycloaddition of *in situ* oxyallyl cation **448** that bears a tethered furan. The formation of the fused-bridged ring structure **449** involves the formation of fully substituted Nazarov precursor **447** (Scheme 117). Dienone **447** is anticipated to undergo Nazarov cyclization to give cation **448** that then undergoes a non-concerted cycloaddition to the furan: **448**→**452**→**449** (Scheme 118). The proposed product **449** is notable as it generates 6 new stereocentres enantioselectively, 5 of which are 4°-stereocentres.

Previous results



Proposed design

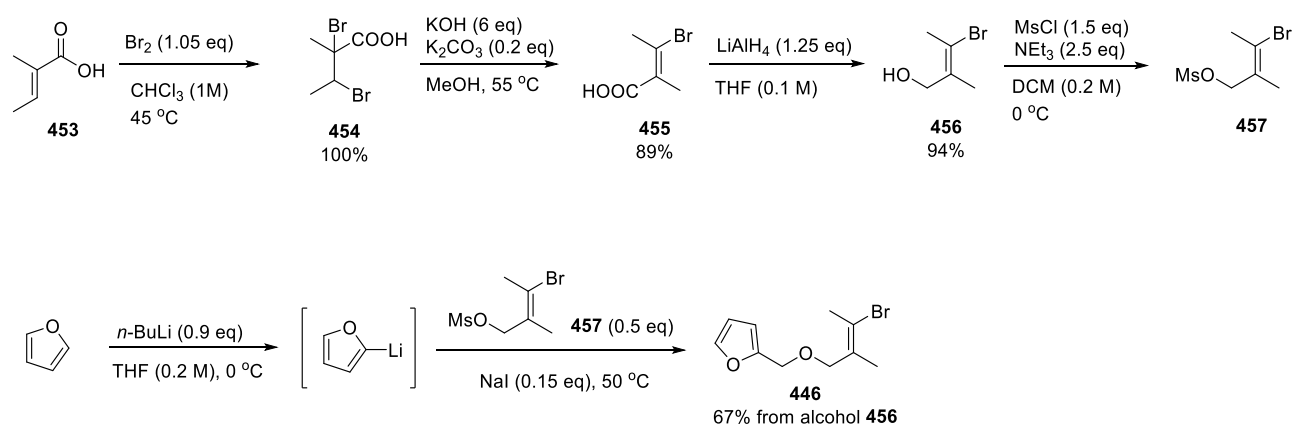


Scheme 118. Absence of proton on tethered furan, improving the probability of cycloaddition.

The formation of **367** and **374** have shown that furan undergoes nucleophilic trapping, as DFT explains which the proton elimination step has a slightly lower energy barrier than the formation of

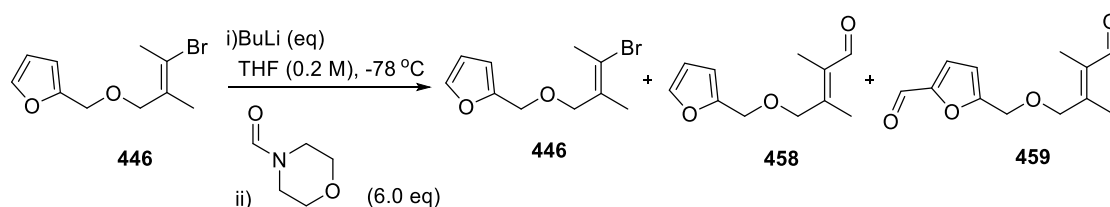
the bridged ring structure **451** (Scheme 118). In this part of the investigation, we expect that the installation of a tethered furan will diminish the proton elimination process due to the absence of proton on tethered furan that is prone to elimination. Therefore, we predict that there is a high possibility of **447** to undergo double intramolecular pericyclic reaction to yield fused-bridged ring structure **449**, enantioselectively.

The preparation of **447** involved the formation of vinyl bromide **446**, where the synthesis initiated with bromination of tiglic acid **453**, forming dibromo alkane **454** (100%). Dibromide **454** then undergoes elimination to give **455** (89%), followed by subsequent reduction, mesylation and nucleophilic substitution to yield furanyl vinyl bromide **446** in 65% yield from alcohol **456** (Scheme 119).



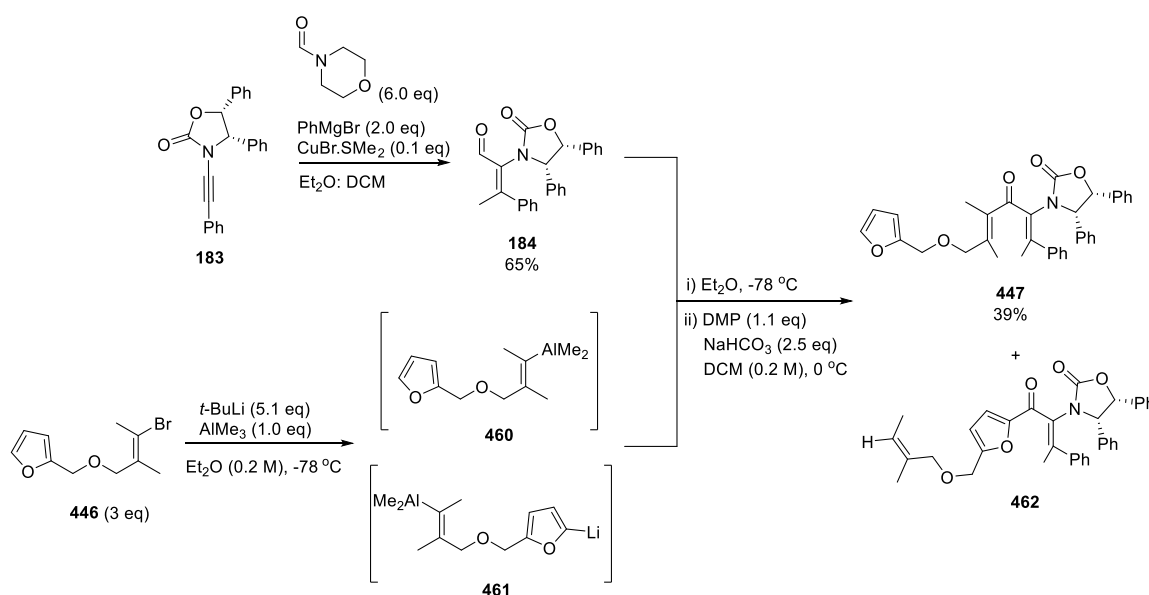
Scheme 119. Synthesis towards vinyl bromide **446**.

Due to the presence of the acidic proton that locates at the C5 of tethered furan, we performed a series of investigation on the stoichiometric equivalence of BuLi that is required to complete only the halogen-metal exchange process, without lithiation of furan (Scheme 120). *N*-formylmorpholine was used in the formation of aldehyde **458** (Scheme 120). Using *s*- BuLi , we observed the formation of double-formylated product **459**, while **446** wasn't completely consumed (Table 5, Entry 1). One equivalent of *t*- BuLi did not give complete consumption of **446** as well, even though the formation of **458** and **459** were both observed (Table 5, Entry 2). Further attempts concluded that 1.7 eq of *t*- BuLi yielded the best result, with complete consumption of **446** and a minimal formation of **459** (Table 5, Entry 5).

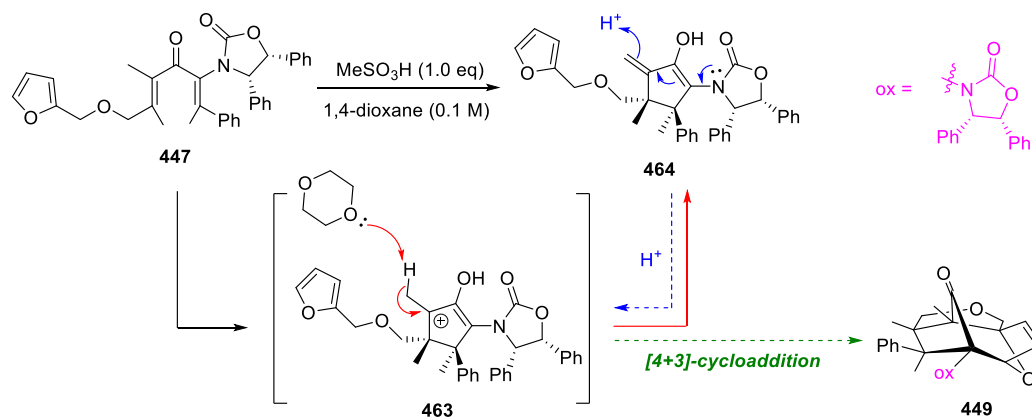
Scheme 120. Formation of aldehyde **458**.Table 5. Ratio in the formation of **458** and **459**.

entry	BuLi (eq)	ratio (446 : 458 : 459)
1	<i>s</i> -BuLi (1.0 eq)	7 : 4 : 1
2	<i>t</i> -BuLi (1.0 eq)	5 : 5 : 1
3	<i>t</i> -BuLi (1.5 eq)	3 : 21 : 1
4	<i>t</i> -BuLi (1.6 eq)	- : 13 : 1
5	<i>t</i> -BuLi (1.7 eq)	- : 32 : 1
6	<i>t</i> -BuLi (2.0 eq)	- : 2 : 1

The formation of fully substituted dienone **447** was obtained via 1,2-addition of preformed *in situ* vinyl alanate **460** to aldehyde **184**, where **184** was synthesized through carbo-magnesiation of **183**, followed by the addition of *N*-formylmorpholine. Despite the success in the formation of **447**, 1,2-addition of alanate species appeared to be substrate-specific, as this approach often yields the formation of methyl ketone, similar to the formation of **416** (Scheme 107, Page 78, Chapter 3.3). A side product **462** was also observed during the formation of **447**, where furan was lithiated and added to aldehyde **184** (Scheme 121).

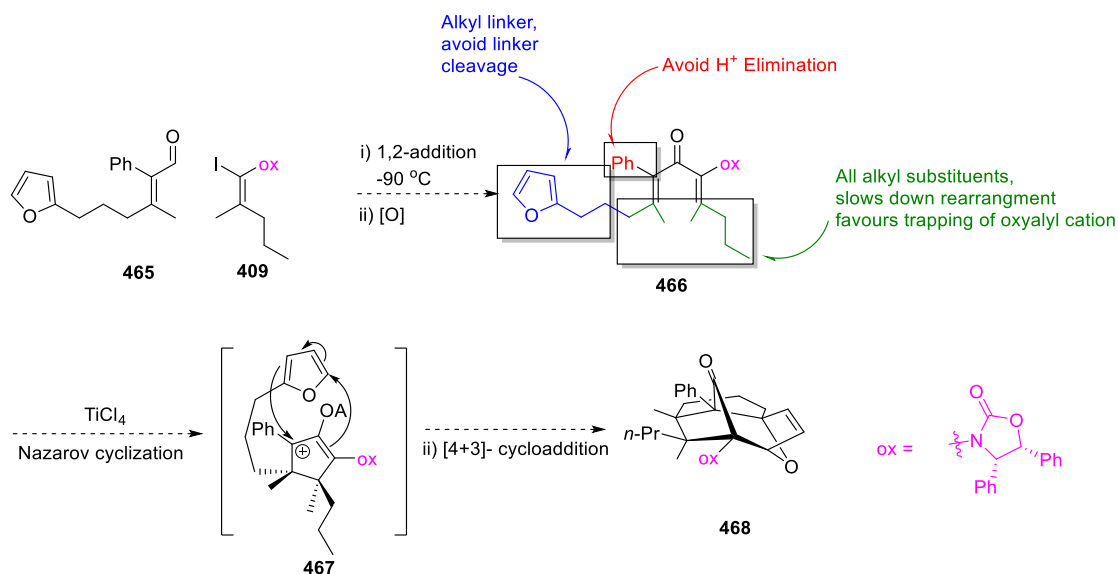
Scheme 121. Synthesis of divinyl ketone **447**.

Dienone **447** was subjected to the Nazarov reaction, where MeSO_3H was used with 1,4-dioxane as the solvent. We observed the formation of enol cyclized material **464**, where no cycloadduct **449** was obtained (**Scheme 122**). However, previous DFT calculation indicates that α -proton elimination is reversible with protic acid, where α -methylene can easily re-accept proton due to the presence of electron-rich oxazolidinone.⁸⁰ Therefore, we expect that the re-subjection of **464** with acid could gain a proton to re-form **463**, ultimately forming cycloadduct **449**.



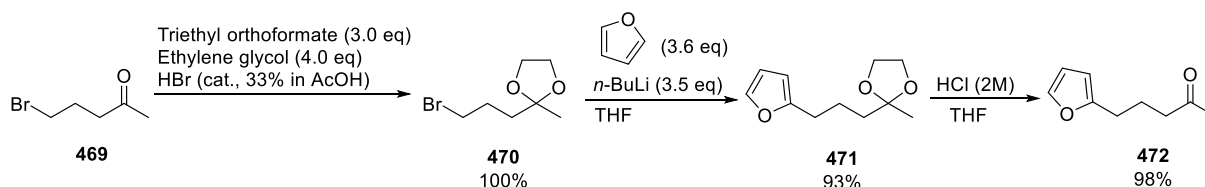
Scheme 122. Observed enol-cyclized product **464** formation.

Due to the proton elimination of α -methyl, we then designed a new tethered furanyl substrate **466**. We propose that having Ph group at α -position could avoid the proton elimination process. The substitution of a tethered ether into a tethered alkyl linker could diminish the cleavage of furan moiety. Finally, the all-alkyl β -substituents are designed to slow down the Wagner-Meerwein rearrangement. This proposed structure **466** is anticipated to yield fused-bridged ring structure **468** selectively, where all the modifications are designed to enhance the ability in the tandem [4+3]-cycloaddition (**Scheme 123**).



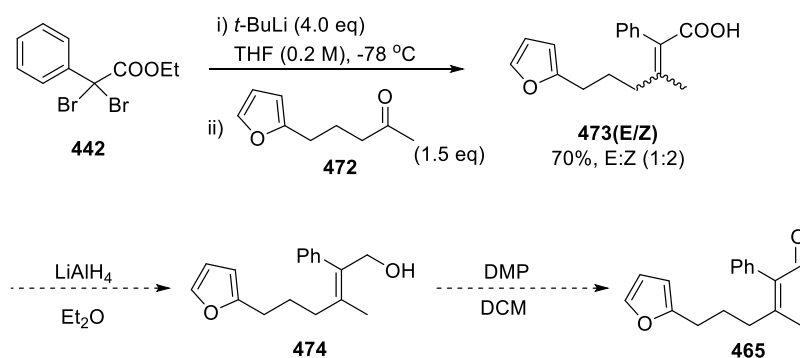
Scheme 123. A new proposal in the formation of **468**.

We initially prepared furanyl ketone **472** to aid in the synthesis of acid **473** through the non-concerted [2+2]-cycloaddition process, as described in the earlier synthesis of carboxylic acid **436** (Scheme 115, Page 83). We first protected 5-bromopentan-2-one **469** with acetal group to avoid 1,2-addition of lithiated furan to ketone. **470** was obtained in 100% yield. The nucleophilic substitution of **470** with furanyl lithium gave **471** in 93% yield. This was followed by the deprotection of **471** using aq. HCl to give furanyl ketone **472** (98%).



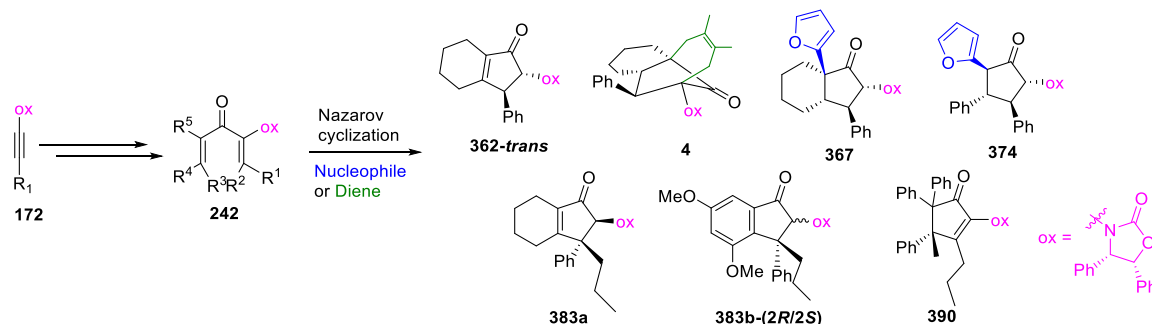
Scheme 124. The synthesis of furanyl ketone **472**.

We then synthesized carboxylic acid **473**, where it was obtained as a mixture of E:Z isomers (1:2) in 70% yield. The purification proved to be problematic due to the persistent co-elution of both isomers of **473** upon chromatography. Due to the time constraints, alcohol **474** and aldehyde **465** were not obtained (Scheme 123). Therefore we were unable to bring this through to the formation of divinyl ketone **466**, as well as a trial formation of the fused-bridged structure **468**.



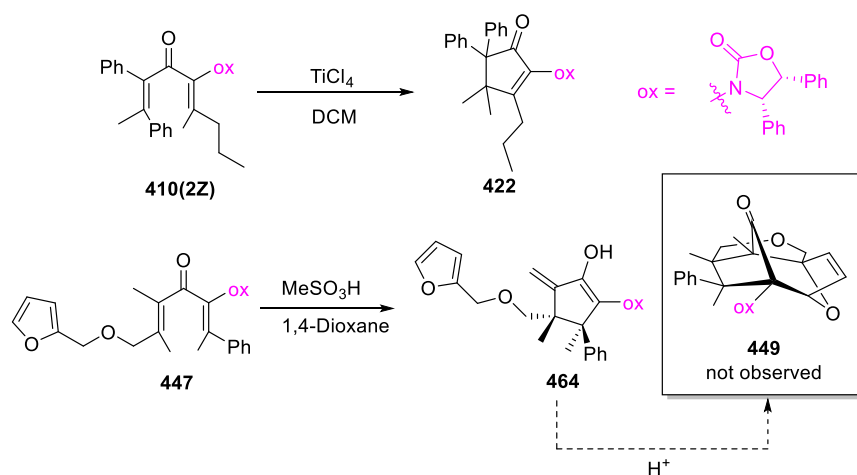
Scheme 125. Formation of carboxylic acid **473(E/Z)**.

3.5 Conclusion and future work



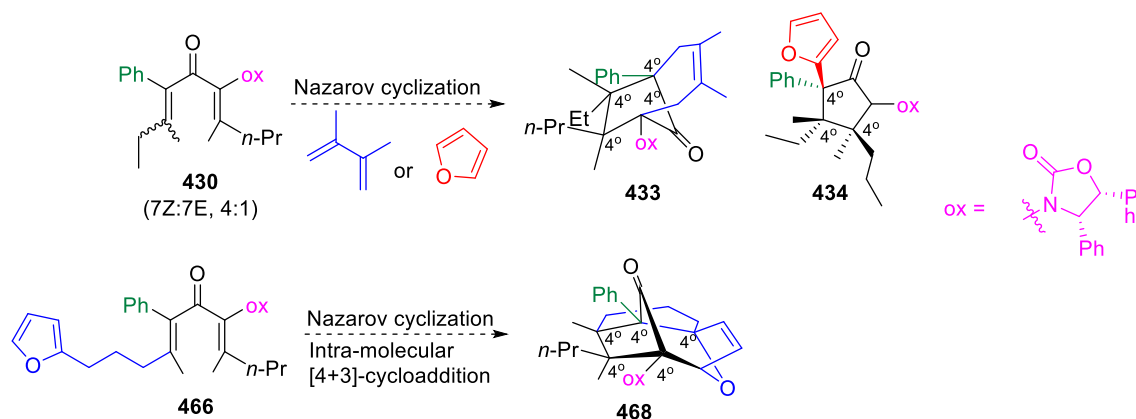
Scheme 126. Formation of cyclopentanoids described in Chapter 3.

In this part of the project, we have described various methods in the synthesis of Nazarov precursors that contain different substitution levels from simple ynamide, where divinyl ketone could contain up to two substituents per vinylic carbon (fully substituted). The Nazarov precursors that were described in Chapter 3.1 and Chapter 3.2 undergo efficient Nazarov cyclization, giving **362-trans**, **383a** and **383b(2R/S)**. The synthesis of **383a** and **383b(2R/S)** also signifies the ability to access specific stereoisomer in two steps from simple ynamide. Chapter 3.1 also describes the elaborations on the Nazarov cyclization, such as the formation of all-carbon 4°-stereocentres containing furan trapped cyclopentanoids (**367** and **374**) and bridged cyclopentanoid (**4**), in the presence of nucleophile (furan) and diene respectively. Later investigation on the Nazarov cyclization of fully substituted divinyl ketone yielded cyclopentanoid **390** enantioselectively, where stereochemistry was confirmed by x-ray crystallography (Scheme 126). It was also observed that TiCl_4 is the only acid that promotes the cyclization of resistant fully substituted Nazarov substrates.

Scheme 127. Formation of unexpected **422** and **464**.

The formation of **422** resulted from unexpected methyl shift during the double Wagner-Meerwein rearrangement, in which explanations are proposed in the earlier discussion in Chapter 3.3. The formation of fused-bridged ring **449** was unsuccessful due to the α -proton elimination of α -Me group,

giving **464**. though we expect that the further treatment of enol **464** with protic acid could potentially lead to the formation of **449**, due to the presence of electron-rich oxazolidinone (**Scheme 127**).



Scheme 128. Future work

Nonetheless, we have designed dienone structures **430** and **466**, specifically for the formation of bridged and fused-bridged ring structure **433** and **468**, respectively. The presence of α -Ph group is anticipated to avoid α -proton elimination, and the all β -alkyl substituents are designed to increase the likelihood in the cycloaddition process, by reducing the rate of Wagner-Meerwein rearrangement. However, due to the time constraint, investigation on the synthesis of **433**, **434**, **466** and **468** were not completed. Nevertheless, the ability in the enantioselective formation of 4-5 contiguous 4° -stereocentres containing compounds has never been achieved. Therefore, if we could generate these structures, it would allow a major breakthrough within organic chemistry. Further experimental work will be continued in our laboratory.

Chapter 4

4. Experimental

General Experimental

All reactions were performed under an inert atmosphere of anhydrous N₂ in glassware dried with heating under vacuum, unless otherwise stated. DCM, Et₂O, EtOH, toluene, dimethylsulfoxide (DMSO) and *N,N*-dimethylformamide (DMF) were dried using a commercial solvent purification system. Tetrahydrofuran (THF) and 1,4-dioxane (dioxane) were purchased in an anhydrous form and stored under nitrogen. Solvents used in reaction extractions and chromatography and all other reagents were used as supplied by commercial vendors without further purifications or drying. Purchased reagents were used as supplied unless otherwise indicated. PS refers to commercial petroleum spirits with a boiling point range of 40-60 °C. Column (flash) chromatography was performed on silica gel (40-63 µm) unless otherwise indicated. Analytical TLC was performed using aluminium backed 0.2 mm thick silica gel 60 GF254 plates (Merck). The TLC plates were visualised using a 254 nm UV lamp, and/or stained using reagent solutions of KMnO₄ (1.5 g of KMnO₄, 10 g K₂CO₃, and 1.25 mL 10% NaOH in 200 mL water) or phosphomolybdic acid [phosphomolybdic acid: 95% ethanol (4 g:100 mL)] followed by heating. ¹H NMR spectra were recorded at 400 MHz, ¹³C NMR at 101 MHz for selected compounds the number of attached hydrogens to each carbon atom was determined using Distortionless Enhancement by Polarization Transfer with detection of quaternary carbons (DEPT-Q 135), as indicated. ¹²⁵Te NMR spectra was recorded at 126 MHz and ¹⁹F NMR was recorded at 377 MHz. Chemical shifts were calibrated using residual nondeuterated solvent as an internal reference and are reported in parts per million (δ) relative to trimethylsilane (δ = 0). High-resolution mass spectra (HR-ESI or HR-APCI) were recorded on a time of flight mass spectrometer fitted with an electrospray (ESI) or atmospheric pressure chemical ionization (APCI) ion source, the capillary voltage was 2400 V. All data was acquired and mass corrected using a dual-spray Leucine Enkephaline reference sample. Melting points were measured using an electrothermal melting point apparatus.

The following materials were prepared according to literature procedures: (2-ethynylphenyl)(methyl)sulfane (**105a**),²⁴ 1-ethynyl-2-methoxybenzene (**105b**),²⁴ 2-ethynyl-*N,N*-dimethylaniline (**105c**),²⁴ 2-ethynyl-1,1'-biphenyl (**105d**),¹⁰⁶ 3-ethynyl-2-(methylthio)benzo[b]thiophene (**261**),²⁴ (4*S*,5*R*)-4,5-diphenyloxazolidin-2-one (**328**),⁶³ (4*S*,5*R*)-4,5-diphenyloxazolidin-2-one **358**,⁶³ 1-bromopent-1-yne.¹⁰⁷

For the experimental details of following compounds, please refer to **Chapter 7, appendix B** (published journal article): (4*S*,5*R*)-3-((4*aR*,9*R*,10*R*,10*aS*)-6,7-dimethyl-11-oxo-10-phenyl-1,2,3,4,5,8,10,10*a*-octahydro-9*H*-4*a*,9-methanobenzo[8]annulen-9-yl)-4,5-diphenyloxazolidin-2-one (**4**), (4*S*,5*R*)-4,5-diphenyl-3-(phenylethynyl)oxazolidin-2-one (**183**), (4*S*,5*R*)-3-((*Z*)-3-(cyclohex-1-en-1-yl)-3-oxo-1-phenylprop-1-en-2-yl)-4,5-diphenyloxazolidin-2-one (**361**), (4*S*,5*R*)-3-((2*R*,3*S*)-1-

oxo-3-phenyl-2,3,4,5,6,7-hexahydro-1H-inden-2-yl)-4,5-diphenyloxazolidin-2-one (**362-trans**), (4S,5R)-3-((1R,2R/S,3aS,7aS)-3a-(furan-2-yl)-3-oxo-1-phenyloctahydro-1H-inden-2-yl)-4,5-diphenyloxazolidin-2-one (**367**), (4S,5R)-3-((1Z,4E)-3-oxo-1,5-diphenylpenta-1,4-dien-2-yl)-4,5-diphenyloxazolidin-2-one (**370**) and (4S,5R)-3-((1R,3S,4S,5R)-3-(furan-2-yl)-2-oxo-4,5-diphenylcyclopentyl)-4,5-diphenyloxazolidin-2-one (**374**).

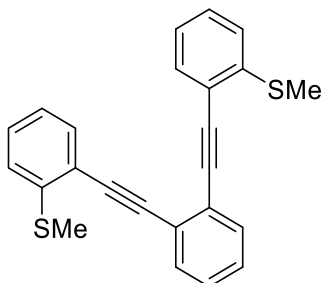
4.1 Experimental for Chapter 2

General Procedure A- Sonogashira Coupling Reaction

To a dried flask with NEt₃ (or optional base/co-solvent) was added aryl/ vinyl halide and CuI (4-6 mol%). This mixture was evacuated and backfilled with N₂ three times. To this dried mixture was added indicated Pd-catalyst (2-5 mol%). A solution of indicated terminal alkyne in indicated anhydrous solvent was injected slowly into the reaction mixture via syringe pump over 1-2 h period at indicated temperature. Upon complete consumption of aryl/ vinyl halide, the reaction was filtered through Celite, rinsed with Et₂O, dried over MgSO₄ and concentrated under reduced pressure. The resulting crude reaction mixture was chromatographed utilizing indicated eluent system.

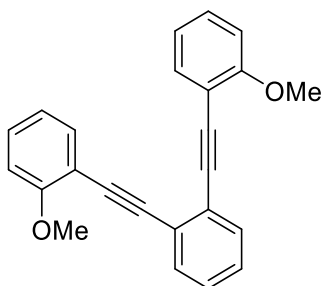
General Procedure B- DECRE reaction

To a dried schlenk tube with AuCl₃ in anhydrous 1,4-dioxane, was injected slowly a solution of indicated reaction substrate in anhydrous DCE via syringe pump over 4 h at 70 °C. The reaction mixture was then filtered, rinsed with DCM, dried over MgSO₄ and concentrated under reduced pressure. The resulting crude reaction mixture was passed through short silica gel plug utilizing indicated eluent system.



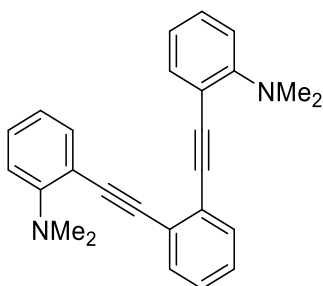
1,2-bis((2-(methylthio)phenyl)ethynyl)benzene (262a)

Synthesized according to General Procedure A. Prepared from 1,2-diiodobenzene **255** (0.2 mL, 1.53 mmol), **105a** (0.49 g, 3.33 mmol), Pd(PPh₃)₄ (0.04 g, 0.03 mmol), CuI (0.01 g, 0.06 mmol), NEt₃ (8 mL). The resulting crude reaction mixture was chromatographed (15% - 25% DCM in PS, 5% step gradient), yielding **262a** (0.46 g, 82%) as light-green solid; ¹H NMR (401 MHz, CDCl₃) δ 7.63 (dd, *J* = 5.8, 3.4 Hz, 2H), 7.56 (dd, *J* = 7.6, 1.4 Hz, 2H), 7.32 (dd, *J* = 5.8, 3.3 Hz, 2H), 7.29 (td, *J* = 7.7, 1.3 Hz, 2H), 7.17 (d, *J* = 7.4 Hz, 2H), 7.09 (td, *J* = 7.5, 1.2 Hz, 2H), 2.43 (s, 6H). Spectra conforms to previously reported data.¹⁰⁸



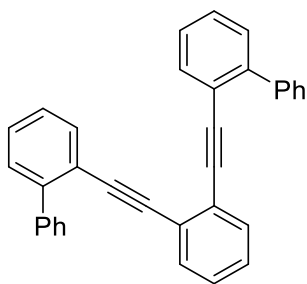
1,2-bis((2-methoxyphenyl)ethynyl)benzene (**262b**)

Synthesized according to General Procedure A. Prepared from 1,2-diiodobenzene **255** (0.12 mL, 1.003 mmol), **105b** (0.32 g, 2.40 mmol), Pd(PPh₃)₄ (0.03 g, 0.02 mmol), CuI (0.01 g, 0.02 mmol), NEt₃ (6 mL); The resulting crude reaction mixture was chromatographed (15% EtOAc in PS), yielding **262b** (0.23 g, 72%) as brown syrup. ¹H NMR (401 MHz, CDCl₃) δ 7.59 (dd, *J* = 5.8, 3.3 Hz, 2H), 7.56 (dd, *J* = 7.6, 1.6 Hz, 2H), 7.30 (dt, *J* = 9.2, 1.8 Hz, 2H), 7.28 (dd, *J* = 5.8, 3.3 Hz, 2H), 6.91 (td, *J* = 7.5, 1.0 Hz, 2H), 6.89 (d, *J* = 8.3 Hz, 2H), 3.81 (s, 6H). Spectra conforms to previously reported data.¹⁰⁸



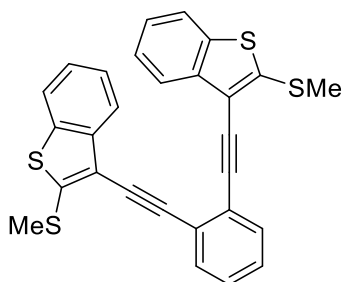
2,2'-(1,2-phenylenebis(ethyne-2,1-diyl))bis(N,N-dimethylaniline) (**262c**)

Synthesized according to General Procedure A. Prepared from 1,2-diiodobenzene **255** (0.14 mL, 1.03 mmol), **105c** (0.33 g, 2.27 mmol), Pd(PPh₃)₄ (0.02 g, 0.02 mmol), CuI (0.01 g, 0.04 mmol), NEt₃ (5 mL). The resulting crude reaction mixture was chromatographed (55% DCM in PS), yielding **262c** (0.28 g, 73%) as dark brown syrup. *R*_f = 0.26 (50% DCM in PS); ¹H NMR (401 MHz, CDCl₃) δ 7.57 (dd, *J* = 5.8, 3.4 Hz, 2H), 7.54 (dd, *J* = 7.6, 1.6 Hz, 2H), 7.29 (dd, *J* = 5.8, 3.4 Hz, 2H), 7.24 (dt, *J* = 7.4, 2.1 Hz, 2H), 6.91 (d, *J* = 8.2 Hz, 2H), 6.85 (t, *J* = 7.5 Hz, 2H), 2.97 (s, 12H); ¹³C NMR (101 MHz, CDCl₃) δ 154.8, 135.0, 131.9, 129.5, 127.8, 126.1, 120.3, 116.8, 114.9, 93.8, 93.0, 43.6. HRMS (ESI) calcd. for C₂₆H₂₅N₂ (M+H)⁺: 365.2012, found 365.2021.



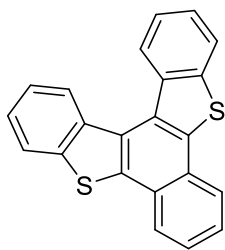
1,2-bis([1,1'-biphenyl]-2-ylethynyl)benzene (**262d**)

Synthesized according to General Procedure A. Prepared from 1,2-diiodobenzene **255** (0.07 mL, 0.57 mmol), **105d** (0.20 g, 1.14 mmol), Pd(PPh₃)₄ (0.03 g, 0.03 mmol), CuI (0.01 g, 0.06 mmol), NEt₃ (3 mL). The resulting crude reaction mixture was chromatographed (1% Et₂O in PS), yielding **262d** (0.10 g, 41%) as light brown wax. *R*_f = 0.44 (30% DCM in PS); ¹H NMR (401 MHz, CDCl₃) δ 7.68 (dt, *J* = 8.2, 1.8 Hz, 4H), 7.64 (ddd, *J* = 7.7, 1.3, 0.6 Hz, 2H), 7.46 – 7.41 (m, 4H), 7.40 – 7.34 (m, 4H), 7.31 (m, 4H), 7.24 (dt, *J* = 6.8, 3.6 Hz, 2H), 7.19 (dt, *J* = 5.4, 3.6 Hz, 2H). ¹³C NMR (101 MHz, CDCl₃) δ 143.9, 140.5, 133.5, 132.1, 129.6, 129.5, 128.8, 128.0, 127.9, 127.6, 127.1, 125.7, 93.2, 91.1. HRMS (ESI) calcd. for C₃₄H₂₃ (M+H)⁺: 431.1794, found 431.1782.

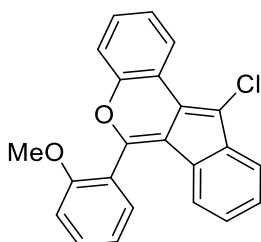


1,2-bis((2-(methylthio)benzo[b]thiophen-3-yl)ethynyl)benzene (**262e**)

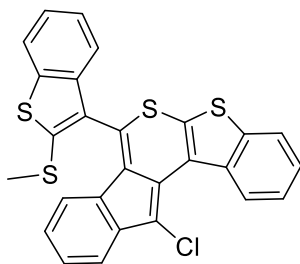
Synthesized according to general procedure A. Prepared from 1,2-diiodobenzene **255** (0.12 mL, 10.9 mmol), **261** (0.43 g, 2.11 mmol), Pd(PPh₃)₄ (0.02 g, 0.02 mmol), CuI (0.01 g, 0.04 mmol), NEt₃ (5 mL) and THF (2 mL). The resulting crude reaction mixture was chromatographed (20% DCM in PS), yielding **262e** (0.39 g, 89%) as brown wax. *R*_f = 0.41 (30% DCM in PS); ¹H NMR (401 MHz, CDCl₃) δ 7.91 (d, *J* = 7.9 Hz, 2H), 7.72 (dd, *J* = 5.8, 3.3 Hz, 2H), 7.68 (d, *J* = 8.0 Hz, 2H), 7.38 (dd, *J* = 5.8, 3.3 Hz, 2H), 7.25 – 7.19 (m, 2H), 7.06 – 7.01 (m, 2H), 2.55 (s, 6H); ¹³C NMR (101 MHz, CDCl₃) δ 144.8, 140.1, 138.1, 132.4, 128.2, 125.7, 125.0, 124.5, 122.9, 121.6, 117.5, 95.7, 86.4, 18.9. HRMS (ESI) calcd. for C₂₈H₁₉S₄ (M+H)⁺: 483.0364, found 483.0372.

**(263a)**

To a dried 10 mL flask with **262a** (0.11 g, 0.28 mmol) in anhydrous DCE (3.0 mL) was added AuCl_3 (0.09 g, 0.28 mmol) and allowed to stir overnight at rt. The reaction mixture was filtered and rinsed with DCM (5 mL), dried over MgSO_4 and concentrated under reduced pressure. The resulting crude reaction mixture was passed through a short plug of silica gel (60% DCM in PS), yielding **263a** (0.06 g, 60%) as off white solid; $R_f = 0.70$ (30 % DCM in PS); MP= 204-207 °C; ^1H NMR (401 MHz, CDCl_3) δ 8.93 (dd, $J = 6.1, 2.8$ Hz, 2H), 8.22 (dd, $J = 6.1, 3.2$ Hz, 2H), 8.04 (dd, $J = 5.9, 3.0$ Hz, 2H), 7.65 (dd, $J = 6.2, 3.2$ Hz, 2H), 7.53 (p, $J = 7.5$ Hz, 4H); ^{13}C NMR (101 MHz, CDCl_3) δ 139.3, 137.2, 136.4, 129.1, 127.7, 127.3, 126.0, 125.4, 125.3, 123.9, 123.3. HRMS (APCI) calcd. for $\text{C}_{22}\text{H}_{12}\text{S}_2$ (M) $^+$: 340.0375, found 340.0356.

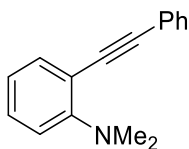
**11-chloro-6-(2-methoxyphenyl)indeno[1,2-c]chromene (275)**

Synthesized according to General Procedure B. Prepared from **262b** (0.07 g, 0.22 mmol), AuCl_3 (0.09 g, 0.28 mmol), DCE (2 mL) and 1,4-dioxane (2 mL). The resulting crude reaction mixture was passed through a short plug of silica gel (40% DCM in PS), yielding **275** (0.05 g, 63%) as neon yellow syrup. $R_f = 0.56$ (30% DCM in PS); ^1H NMR (400 MHz, CDCl_3) δ 8.90 – 8.86 (m, 1H), 7.71 – 7.68 (m, 1H), 7.62 (ddd, $J = 8.4, 7.5, 1.8$ Hz, 1H), 7.57 (dd, $J = 7.5, 1.7$ Hz, 1H), 7.52 – 7.48 (m, 1H), 7.47 – 7.41 (m, 3H), 7.15 (dtd, $J = 8.3, 7.4, 1.0$ Hz, 3H), 7.03 – 6.99 (m, 1H), 3.77 (s, 3H). ^{13}C NMR (101 MHz, CDCl_3) δ 158.0, 150.5, 150.0, 140.5, 132.3, 131.5, 128.9, 128.4, 126.9, 125.4, 124.7, 123.7, 122.4, 122.0, 121.3, 121.0, 119.4, 118.1, 117.8, 116.9, 114.3, 111.9, 55.9. HRMS (APCI) calcd. for $\text{C}_{23}\text{H}_{16}\text{ClO}_2$ ($\text{M}+\text{H}$) $^+$: 359.0833, found 359.0847.



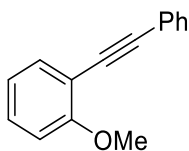
12-chloro-7-(2-(methylthio)benzo[b]thiophen-3-yl)benzo[4,5]thieno[2,3-b]indeno[2,1-d]thiopyran (292)

Synthesized according to General Procedure B. Prepared from **262e** (0.04 g, 0.09 mmol), AuCl₃ (0.03 g, 0.10 mmol), DCE (1 mL) and 1,4-dioxane (1 mL). The resulting crude reaction mixture was passed through a short plug of silica gel (40% DCM in PS), yielding **292** (0.04 g, 89%) as neon orange wax; $R_f = 0.58$ (30% DCM in PS); ¹H NMR (401 MHz, CDCl₃) δ 8.99 (d, $J = 7.9$ Hz, 1H), 7.89 (t, $J = 9.7$ Hz, 2H), 7.73 (d, $J = 7.7$ Hz, 1H), 7.57 (ddd, $J = 8.3, 7.2, 1.2$ Hz, 1H), 7.47 (ddd, $J = 8.2, 7.2, 1.2$ Hz, 1H), 7.44 (td, $J = 7.6, 1.0$ Hz, 1H), 7.41 – 7.34 (m, 2H), 7.26 (td, $J = 7.6, 1.0$ Hz, 1H), 7.02 (td, $J = 7.8, 1.1$ Hz, 1H), 6.64 (dt, $J = 7.8, 0.7$ Hz, 1H), 2.50 (s, 3H); ¹³C NMR (101 MHz, CDCl₃) δ 141.5, 140.0, 139.8, 138.7, 138.2, 136.1, 134.4, 133.4, 129.6, 128.2, 128.2, 127.8, 127.6, 125.6, 125.3, 125.2, 125.2, 124.9, 124.5, 124.4, 122.4, 122.2, 121.9, 121.8, 118.2, 117.9, 19.8. HRMS (APCI) calcd. for C₂₇H₁₆ClO₂ (M+H)⁺: 502.9818, found 502.9825.



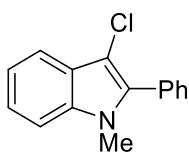
N,N-dimethyl-2-(phenylethynyl)aniline (294a)

Synthesized according to General Procedure A. Prepared from 2-iodo-N,N-dimethylaniline (1.50 g, 6.07 mmol), phenylacetylene (0.8 mL, 7.29 mmol), Pd(PPh₃)₂Cl₂ (0.09 g, 0.12 mmol), CuI (0.05 g, 0.24 mmol), NEt₃ (30 mL). The resulting crude reaction mixture was chromatographed (0% - 5% EtOAc in PS, 5% step gradient), yielding **295a** (1.27 g, 99%) as yellow oil. ¹H NMR (401 MHz, CDCl₃) δ 7.54 (d, $J = 7.2$ Hz, 2H), 7.49 (d, $J = 5.7$ Hz, 1H), 7.31-7.37 (m, 3H), 7.25 (t, $J = 6.3$ Hz, 1H), 6.88-6.94 (m, 2H), 3.01 (s, 6H). Spectra conforms to previously reported data.¹⁰⁹



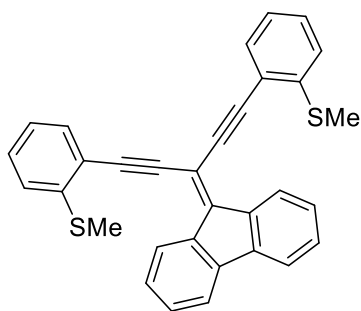
1-methoxy-2-(phenylethynyl)benzene (**294b**)

Synthesized according to General Procedure A. Prepared from 2-iodoanisole (0.83 mL, 6.41 mmol), phenylacetylene (0.84 mL, 7.69 mmol), Pd(PPh₃)₂Cl₂ (0.09 g, 0.13 mmol), CuI (0.05 g, 0.26 mmol), NEt₃ (32 mL). The resulting crude reaction mixture was chromatographed (0% - 4% EtOAc in PS, 2% step gradient), yielding **295c** (1.30 g, 98%) as yellow oil. ¹H NMR (400 MHz, CDCl₃) δ 7.59 – 7.53 (m, 2H), 7.50 (dd, *J* = 7.6, 1.7 Hz, 1H), 7.39 – 7.28 (m, 4H), 6.94 (td, *J* = 7.6, 1.1 Hz, 1H), 6.91 (d, *J* = 8.4 Hz, 1H), 3.92 (s, 3H). Spectra conforms to previously reported data.¹¹⁰



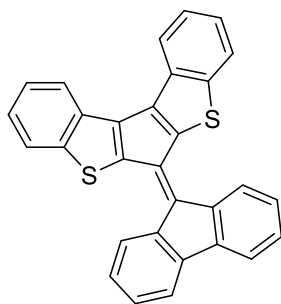
3-chloro-1-methyl-2-phenyl-1H-indole (**295a**)

To a dried 10 mL flask with **294a** (0.12 g, 0.52 mmol) in anhydrous DCE (5 mL), was added AuCl₃ (0.13 g, 0.41 mmol) and allowed to stir for 72 h at 75 °C. The reaction was filtered, rinsed with DCM (10 mL), dried over MgSO₄ and concentrated under reduced pressure. The resulting crude reaction mixture was passed through a short silica gel plug (40% DCM in PS), yielding **295a** (0.05 g, 40%) as yellow syrup; *R*_f = 0.61 (30% DCM in PS); ¹H NMR (401 MHz, CDCl₃) δ 7.69 (dt, *J* = 1.9, 1.3 Hz, 1H), 7.53 (d, *J* = 4.1 Hz, 4H), 7.51 – 7.44 (m, 1H), 7.38 (dt, *J* = 8.5, 1.1 Hz, 1H), 7.32 (ddd, *J* = 8.2, 6.9, 1.2 Hz, 1H), 7.24 (ddd, *J* = 8.0, 6.9, 1.2 Hz, 1H), 3.68 (s, 3H); ¹³C NMR (101 MHz, CDCl₃) δ 136.3, 130.7, 129.9, 128.7, 128.6, 125.8, 123.0, 120.5, 118.4, 109.8, 103.6, 31.6; HRMS (ESI) calcd. for C₁₅H₁₃ClN (M+H)⁺: 242.0731, Found: 242.0722.



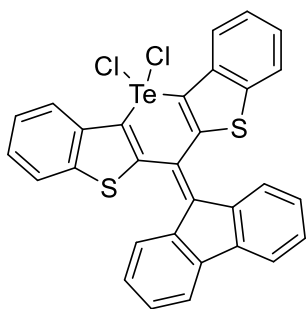
((3-(9H-fluoren-9-ylidene)penta-1,4-diyne-1,5-diyl)bis(2,1-phenylene))bis(methylsulfane) (299**)**

Synthesized according to General Procedure A. Prepared from **298** (0.60g, 1.80 mmol), **105a** (0.61 g, 4.13 mmol), Pd(PPh₃)₄ (0.06 g, 0.05 mmol), CuI (0.02 g, 0.11 mmol), DIPA (2.5 mL, 18.0 mmol) and THF (9 mL). **105a** in anhydrous THF (4 mL) was slowly added into the reaction mixture at 70 °C over 3 h, then allowed to stir at 70 °C overnight. The resulting crude reaction mixture was chromatographed (15% - 30% DCM in PS, 5% step gradient), yielding **299** (0.42 g, 49%) as bright orange solid. R_f = 0.35 (30% DCM in PS); MP = 116-118 °C; ¹H NMR (401 MHz, CDCl₃) δ 8.98 (d, J = 7.6 Hz, 2H), 7.67 (d, J = 7.2 Hz, 2H), 7.64 (dd, J = 7.6, 1.3 Hz, 2H), 7.37 (td, J = 7.4, 1.1 Hz, 2H), 7.36 (ddd, J = 8.0, 7.5, 1.5 Hz, 2H), 7.31 (td, J = 7.6, 1.3 Hz, 2H), 7.27 (d, J = 7.4 Hz, 2H), 7.19 (td, J = 7.5, 1.2 Hz, 2H), 2.56 (s, 6H); ¹³C NMR (101 MHz, CDCl₃) δ 144.7, 142.3, 140.4, 137.6, 133.2, 129.7, 129.6, 127.6, 126.0, 125.3, 124.8, 121.8, 119.6, 101.3, 96.3, 94.9, 15.8. HRMS (ESI) calcd. for C₃₂H₂₃S₂ (M+H)⁺: 471.1236, Found: 471.1239.

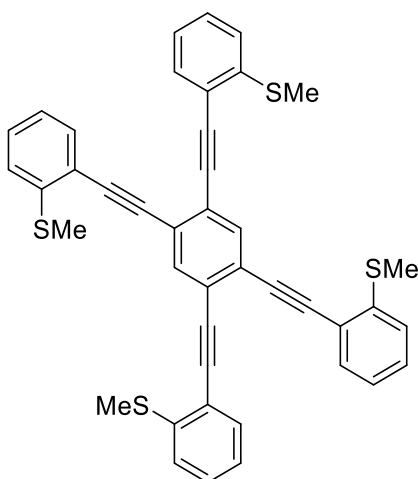


(2)

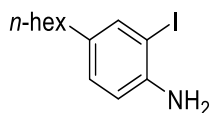
Synthesized according to General Procedure B. Prepared from **299** (0.06 g, 0.12 mmol), AuCl₃ (0.04 g, 0.13 mmol), DCE (1 mL) and 1,4-dioxane (1 mL). The resulting crude reaction mixture was passed through a short plug of silica gel (60% DCM in PS) to yield **2** (0.05 g, 87%) as dark brown wax; R_f = 0.61 (30% DCM in PS); ¹H NMR (401 MHz, CDCl₃) δ 9.01 (d, J = 7.8 Hz, 2H), 8.32 (d, J = 8.1 Hz, 2H), 7.78 (d, J = 8.1 Hz, 2H), 7.65 (d, J = 7.4 Hz, 2H), 7.48 (ddd, J = 8.1, 7.2, 1.0 Hz, 2H), 7.40 (td, J = 7.5, 0.9 Hz, 2H), 7.34 (ddd, J = 8.2, 7.3, 0.9 Hz, 2H), 7.29 (dd, J = 7.7, 1.0 Hz, 2H); ¹³C NMR (101 MHz, CDCl₃) δ 144.6, 143.1, 142.3, 141.3, 138.4, 137.7, 131.9, 131.1, 127.6, 125.4, 125.4, 125.2, 123.7, 123.6, 120.3. HRMS (APCI) calcd. for C₃₀H₁₇S₂ (M+H)⁺: 441.0766, found 441.0767.

**(306)**

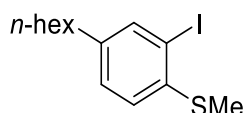
To a dried 10 mL flask with **299** (0.05 g, 0.11 mmol) in anhydrous DCE (1 mL) was added TeCl_4 (0.03 g, 0.12 mmol), and allowed to stir for 2.5 h at 70 °C. The reaction mixture was then cooled to rt, filtered, rinsed with DCM (5 mL) and concentrated under reduced pressure, yielding **306** (0.05 g, 72%) as dark powder; MP = 285-287 °C; ^{125}Te NMR (126 MHz, CDCl_3) δ 84.29; ^1H NMR (401 MHz, CDCl_3) δ 8.01 (d, J = 7.8 Hz, 2H), 7.79 (d, J = 7.9 Hz, 2H), 7.54 (t, J = 7.5 Hz, 4H), 7.49 (ddd, J = 8.2, 7.1, 1.0 Hz, 2H), 7.42 (ddd, J = 8.1, 7.3, 1.1 Hz, 2H), 7.24 (td, J = 7.4, 1.0 Hz, 2H), 6.95 (td, J = 7.7, 1.2 Hz, 2H); ^{13}C NMR (101 MHz, CDCl_3) δ 146.8, 142.4, 139.5, 138.2, 136.8, 130.8, 128.3, 126.8, 126.5, 125.9, 124.6, 124.1, 123.2, 120.1.

**1,2,4,5-tetrakis((2-(methylthio)phenyl)ethynyl)benzene (309)**

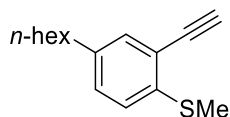
Synthesised according to General Procedure A. Prepared from 1,2,4,5-tetraiodobenzene **308** (0.19 g, 0.32 mmol), **105a** (0.21 g, 1.40 mmol), $\text{Pd}(\text{PPh}_3)_2\text{Cl}_2$ (0.05 g, 0.06 mmol), CuI (0.01 g, 0.06 mmol), DIPA (16 mL, 114 mmol), and anhydrous toluene (60 mL). **105a** in DIPA was slowly added into 1,2,4,5-tetraiodobenzene mixture at 75 °C over 3 h, then allowed to stir at 75 °C overnight. The resulting crude reaction mixture was chromatographed (20% toluene in PS), yielding **309** (0.19 g, 89%) as orange wax; R_f = 0.35 (30% DCM in PS); ^1H NMR (401 MHz, CDCl_3) δ 7.88 (s, 2H), 7.57 (dd, J = 7.6, 1.3 Hz, 4H), 7.34 – 7.29 (m, 4H), 7.18 (d, J = 7.5 Hz, 4H), 7.10 (td, J = 7.5, 1.1 Hz, 4H), 2.44 (s, 12H); ^{13}C NMR (101 MHz, CDCl_3) δ 142.4, 135.9, 133.1, 129.2, 125.2, 124.3, 124.3, 121.4, 93.9, 93.0, 15.2. HRMS (ESI) calcd. for $\text{C}_{42}\text{H}_{30}\text{S}_4$ ($\text{M}+\text{H}^+$): 663.1303, found 663.1303.

**4-hexyl-2-iodoaniline (312)**

To a solution of 4-hexylaniline **311** (11 mL, 56.4 mmol) in DCM (56 mL) was added 11 M aq. NaHCO_3 (6 mL), followed by the addition of I_2 (14.3 g, 56.4 mmol) and allowed to stir overnight. Sat. aq. $\text{Na}_2\text{S}_2\text{O}_3$ (50 mL) was added, extracted with Et_2O (2 x 50 mL), dried over MgSO_4 and concentrated under reduced pressure to give **312** (17.0 g, 100%) as black oil, which was used in the next reaction without purification. ^1H NMR (401 MHz, CDCl_3) δ 7.46 (d, $J = 1.9$ Hz, 1H), 6.95 (dd, $J = 8.1, 2.0$ Hz, 1H), 6.68 (d, $J = 8.1$ Hz, 1H), 4.38 (brs, 2H), 2.45 (t, $J = 16.0, 8.0$ Hz, 2H), 1.60 – 1.48 (m, 2H), 1.38 – 1.24 (m, 6H), 0.88 (t, $J = 6.7$ Hz, 3H). ^{13}C NMR (101 MHz, CDCl_3) δ 144.6, 138.6, 135.0, 129.5, 114.8, 84.5, 34.6, 31.8, 31.7, 29.0, 22.7, 14.2. HRMS (ESI) calcd. for $\text{C}_{12}\text{H}_{19}\text{IN}$ ($\text{M}+\text{H}$) $^+$: 304.0557, found 304.0556.

**(4-hexyl-2-iodophenyl)(methyl)sulfane (314)**

To a dried 250 mL flask with isopentyl nitrite (23 mL, 172 mmol) and dimethyl disulfide (103 mL, 1.15 mol) was added **312** (17.4 g, 57.3 mmol). The reaction mixture was allowed to stir for 2 h at 80 °C. The reaction was cooled to rt, 1M aq. HCl (100 mL) was added, extracted with Et_2O (2 x 150 mL), dried over MgSO_4 and concentrated under reduced pressure. The resulting crude reaction mixture was passed through a short plug of silica gel (1% EtOAc in PS), giving **314** (17.9 g, 93%) as dark red oil. $R_f = 0.66$ (1% EtOAc in PS); ^1H NMR (401 MHz, CDCl_3) δ 7.63 (d, $J = 1.8$ Hz, 1H), 7.15 (dd, $J = 8.1, 1.9$ Hz, 1H), 7.04 (d, $J = 8.1$ Hz, 1H), 2.51 (t, $J = 16.0, 8.0$ Hz, 2H), 2.45 (s, 3H), 1.60 – 1.53 (m, 2H), 1.34 – 1.26 (m, 6H), 0.88 (t, $J = 6.8$ Hz, 3H). ^{13}C NMR (101 MHz, CDCl_3) δ 141.6, 139.7, 139.4, 129.1, 125.5, 98.2, 35.0, 31.8, 31.4, 29.0, 22.7, 17.4, 14.2. HRMS (APCI) calcd. for $\text{C}_{13}\text{H}_{19}\text{IS}$ (M) $^+$: 334.0247, found 334.0238.

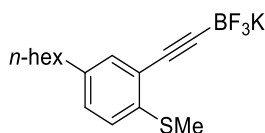
**(2-ethynyl-4-hexylphenyl)(methyl)sulfane (315)**

Synthesized according to general procedure A, followed by potassium fluoride induced deprotection. Sonogashira reaction condition (**General procedure A**) as following:

314 (5.12 g, 15.3 mmol), TMS acetylene (2.5 mL, 18.3 mmol), Pd(PPh₃)₂Cl₂ (0.22 g, 0.31 mmol), CuI (0.12 g, 0.611 mmol), NEt₃ (76 mL). The Crude intermediate **((5-hexyl-2-(methylthio)phenyl)ethynyl)trimethylsilane** was then used in the next step without further purification;

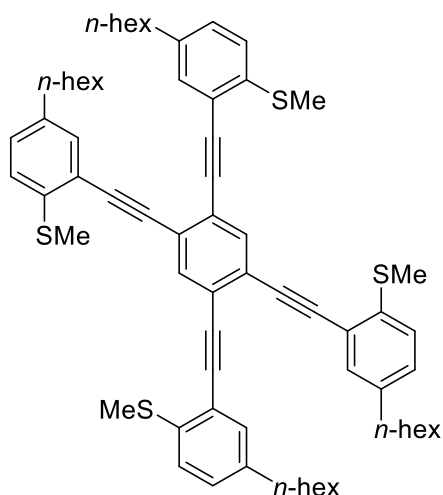
¹H NMR (401 MHz, CDCl₃) δ 7.26 (s, 1H), 7.09 (dd, *J* = 8.2, 1.9 Hz, 1H), 7.06 (d, *J* = 8.1 Hz, 1H), 2.55 – 2.49 (t, *J* = 16.04, 8.02, 2H), 2.47 (s, 3H), 1.61 – 1.50 (m, 2H), 1.33 – 1.25 (m, 6H), 0.95 – 0.81 (m, 3H), 0.28 (s, 9H). ¹³C NMR (101 MHz, CDCl₃) δ 139.3, 138.6, 132.9, 129.5, 124.7, 121.4, 102.7, 100.8, 35.2, 31.8, 31.4, 29.0, 22.7, 15.4, 14.2, 0.1.

To a solution of crude reaction mixture in Et₂O (25 mL) and MeOH (25 mL), was added KF (2.13 g, 36.7 mmol) at 0 °C. The reaction mixture was allowed to stir overnight at rt. The reaction was diluted with water (50 mL), extracted with Et₂O (2 x 50 mL), dried over MgSO₄ and concentrated under reduced pressure. The resulting crude reaction mixture was then passed through a short plug of silica gel (20% DCM in PS) to yield **315** (3.07 g, 86%) as dark oil. *R*_f = 0.56 (30% DCM in PS); ¹H NMR (401 MHz, CDCl₃) δ 7.30 (d, *J* = 1.6 Hz, 1H), 7.14 (dd, *J* = 8.2, 1.8 Hz, 1H), 7.10 (d, *J* = 8.1 Hz, 1H), 3.43 (s, 1H), 2.54 (t, *J* = 16.04, 8.02 Hz, 2H), 2.49 (s, 3H), 1.61 – 1.53 (m, 2H), 1.34 – 1.23 (m, 6H), 0.88 (t, *J* = 6.8 Hz, 3H). ¹³C NMR (101 MHz, CDCl₃) δ 139.6, 138.5, 133.4, 129.8, 125.2, 120.6, 83.0, 35.2, 31.8, 31.3, 29.0, 22.7, 15.7, 14.2. HRMS (ESI) calcd. for C₁₅H₂₁S (M+H)⁺: 233.1358, found 233.1355.



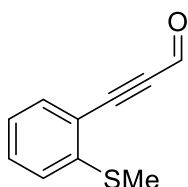
trifluoro((5-hexyl-2-(methylthio)phenyl)ethynyl)-14-borane, potassium salt (315-BF₃K**)**

To a dried 50 mL flask with **315** (0.58 g, 2.47 mmol) in anhydrous THF (12 mL), was added *n*-BuLi (1.0 mL, 2.5 M in hexane, 2.47 mmol) at 0 °C and allowed to stir for 1.5 h. B(OMe)₃ (0.41 mL, 3.71 mmol) was added at 0 °C and stirred for 1 h then 1 h at rt. The reaction mixture was then cooled to 0 °C and sat. aq. KHF₂ (1.16 g, 14.8 mmol) was added dropwise and allowed stir overnight at rt. The reaction mixture was then concentrated under reduced pressure to remove solvent and water. The resulting crude reaction mixture was triturated with hot acetone and filtered. The filtrate was concentrated under reduced pressure. The resulting concentrate was then triturated again with Et₂O, filtered, yielding **315-BF₃K** (0.35 g, 42%) as white solid. ¹H NMR (401 MHz, DMSO) δ 7.07 (s, 1H), 7.04 (d, *J* = 1.5 Hz, 2H), 2.48 (t, *J* = 6.8 Hz, 2H), 2.38 (s, 3H), 1.60 – 1.46 (m, 2H), 1.34 – 1.15 (m, 6H), 0.84 (t, *J* = 6.7 Hz, 3H). ¹³C NMR (101 MHz, DMSO) δ 138.0, 137.1, 131.8, 127.5, 123.8, 123.1, 34.2, 31.1, 30.8, 28.2, 22.0, 14.2, 13.9. ¹⁹F NMR (377 MHz, DMSO) δ -131.5. HRMS (ESI) calcd. for C₁₅H₁₉BF₃KS (M): 377.0524, found 377.0526.



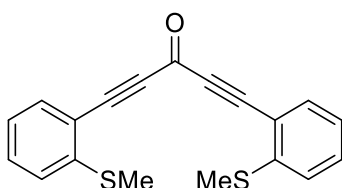
1,2,4,5-tetrakis((5-hexyl-2-(methylthio)phenyl)ethynyl)benzene (**317**)

To a dried 25 mL flask with **315** (0.48 g, 2.07 mmol) in anhydrous THF (4 mL) was added *n*-BuLi (0.84 mL, 2.45 M in hexane, 2.07 mmol) at 0 °C and allowed to stir for 1.5 h. A solution of InCl₃ (0.11 g, 0.52 mmol) in anhydrous THF (2 mL) was added into reaction mixture at -78 °C and allowed to stir for 0.5 h then 0.5 h at rt. To this reaction was added Pd(dppf)Cl₂ (0.01 g, 0.01 mmol) and 1,2,4,5-tetrabromobenzene **316** (0.10 g, 0.26 mmol) then heated to reflux overnight. Sat. aq. NaHCO₃ (5 mL) was added, diluted with water (5 mL), extracted with Et₂O (2 x 5 mL), dried over MgSO₄ and concentrated under reduced pressure. The resulting crude reaction mixture was chromatographed (17.5% - 30% DCM in PS, 2.5% step gradient) to yield **317** (0.13 g, 48%) as yellow syrup. *R*_f = 0.23 (25% DCM in PS); ¹H NMR (401 MHz, CDCl₃) δ 7.87 (s, 2H), 7.42 (s, 4H), 7.12 (s, 8H), 2.52 (t, *J* = 7.7 Hz, 8H), 2.44 (s, 12H), 1.56 (dt, *J* = 14.9, 7.5 Hz, 8H), 1.37 – 1.22 (m, 24H), 0.88 (t, *J* = 6.5 Hz, 12H). ¹³C NMR (101 MHz, CDCl₃) δ 139.4, 138.8, 135.7, 133.2, 129.5, 125.2, 125.0, 121.6, 93.5, 93.4, 35.3, 31.9, 31.4, 29.1, 22.8, 15.7, 14.3. HRMS (APCI) calcd. for C₆₆H₇₉S₄ (M+H)⁺: 999.5059, found 999.5057.



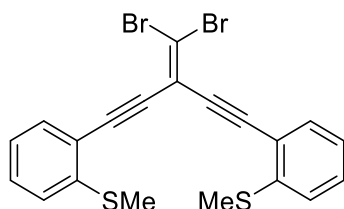
3-(2-(methylthio)phenyl)propionaldehyde (**325**)

To a dried 100 mL flask with **105a** (0.90 g, 6.07 mmol) in anhydrous THF (30 mL), was added *n*-BuLi (2.4 mL, 2.42 M in hexane, 5.76 mmol) at 0 °C dropwise. The reaction mixture was allowed to stir for 30 min at 0 °C, then *N*-formylmorpholine (3.7 mL, 36.4 mmol) was added and stir for 1 h at 0 °C. Sat. aq. NH₄Cl (30 mL) was added, extracted with EtOAc (2 x 30 mL), dried over MgSO₄ and concentrated under reduced pressure. The resulting crude reaction mixture was chromatographed (5% – 10% EtOAc in PS, 5% step gradient) to yield **325** (0.82 g, 76%) as yellow syrup. ¹H NMR (401 MHz, CDCl₃) δ 9.49 (s, 1H), 7.55 (dd, *J* = 7.7, 1.5 Hz, 1H), 7.43 (ddd, *J* = 8.1, 7.6, 1.5 Hz, 1H), 7.22 (d, *J* = 8.0 Hz, 1H), 7.15 (td, *J* = 7.6, 1.1 Hz, 1H), 2.53 (s, 3H). ¹³C NMR (101 MHz, CDCl₃) δ 176.7, 144.8, 134.7, 131.8, 124.7, 124.7, 117.6, 94.2, 92.4, 15.3. HRMS (ESI) calcd. for C₁₀H₉OS (M+H)⁺: 177.0369, found 177.0362.



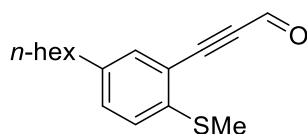
1,5-bis(2-(methylthio)phenyl)penta-1,4-diyne-3-one (**321**)

To a dried 25 mL flask with **105a** (0.31 g, 2.10 mmol) in anhydrous THF (11 mL), was added *n*-BuLi (0.9 mL, 2.13 M in hexane, 2.01 mmol) at 0 °C dropwise. The reaction mixture was allowed to stir for 30 min at 0 °C, then a solution of **325** (0.26 g, 1.48 mmol) in anhydrous THF (2 mL) was added and allowed to stir for 1.5 h at 0 °C. Sat. aq. NH₄Cl (15 mL) was added, extracted with Et₂O (2 x 15 mL), dried over MgSO₄ and concentrated under reduced pressure. To a solution of crude reaction mixture in DCM (11 mL) was added Dess-Martin periodinane (0.69 g, 1.62 mmol) and allowed to stir for 2 h. Sat. aq. NaHCO₃ (10 mL) was added, diluted with water (10 mL), extracted with DCM (2 x 10 mL), dried over MgSO₄ and concentrated under reduced pressure. The resulting crude reaction mixture was chromatographed (5% - 10% EtOAc in PS, 5% step gradient), yielding **321** (0.38 g, 79%) as dark oil. R_f = 0.1 (40% DCM in PS); ¹H NMR (401 MHz, CDCl₃) δ 7.56 (dd, *J* = 7.7, 1.2 Hz, 2H), 7.40 (ddd, *J* = 8.1, 7.6, 1.5 Hz, 2H), 7.20 (d, *J* = 7.9 Hz, 2H), 7.12 (td, *J* = 7.6, 1.0 Hz, 2H), 2.50 (s, 6H). ¹³C NMR (101 MHz, CDCl₃) δ 160.4, 145.2, 134.6, 131.6, 124.7, 124.5, 117.7, 95.2, 89.5, 15.2. HRMS (ESI) calcd. for C₁₉H₁₅OS₂ (M+H)⁺: 323.0559, Found: 323.0566.



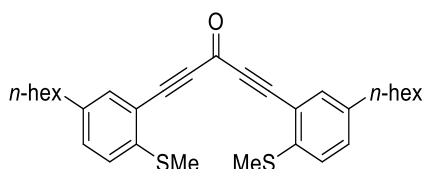
((3-(dibromomethylene)penta-1,4-diyne-1,5-diyl)bis(2,1-phenylene))bis(methylsulfane) (321)

To a dried 50 mL flask with CBr_4 (1.66 g, 5.02 mmol) in anhydrous DCM (13 mL) was added PPh_3 (2.63 g, 10.0 mmol) and allowed to stir for 5 min. To this reaction mixture was added a solution of **321** (0.81 g, 2.51 mmol) in anhydrous DCM (3 mL) and allowed to stir overnight at rt. The reaction mixture was then diluted with water (15 mL), extracted with DCM (2 x 15 mL), dried over MgSO_4 and concentrated under reduced pressure. The resulting crude reaction mixture was then passed through short silica plug (15% EtOAc in PS) to yield **322** (0.71 g, 59%) as light yellow wax. $R_f = 0.56$ (40% DCM in PS); ^1H NMR (401 MHz, CDCl_3) δ 7.51 (dd, $J = 7.7, 1.2$ Hz, 2H), 7.33 (td, $J = 8.0, 1.4$ Hz, 2H), 7.19 (d, $J = 7.8$ Hz, 2H), 7.11 (td, $J = 7.6, 1.0$ Hz, 2H), 2.51 (s, 6H). ^{13}C NMR (101 MHz, CDCl_3) δ 142.5, 133.0, 129.7, 124.7, 124.5, 120.6, 114.5, 108.1, 93.5, 92.1, 15.4. HRMS (APCI) calcd. for $\text{C}_{20}\text{H}_{15}\text{Br}_2\text{S}_2$ ($\text{M}+\text{H}^+$): 478.8956, found 478.8973.



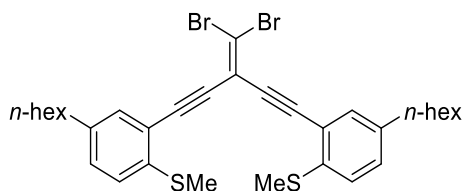
3-(5-hexyl-2-(methylthio)phenyl)propionaldehyde (332)

To a dried 50 mL flask with **315** (0.86 g, 3.69 mmol) in anhydrous THF (19 mL), was added $n\text{-BuLi}$ (1.4 mL, 2.50 M in hexane, 3.51 mmol) at 0 °C dropwise. The resulting reaction mixture was allowed to stir for 1.5 h at 0 °C, then N -formylmorpholine (2.2 mL, 22.2 mmol) was added and allowed to stir for 1 h at 0 °C. Sat. aq. NH_4Cl (20 mL) was added, diluted with water (10 mL), extracted with EtOAc (2 x 20 mL), dried over MgSO_4 and concentrated under reduced pressure. The resulting crude reaction mixture was chromatographed (4% EtOAc in PS) to yield **332** (0.48 g, 50%) as yellow syrup. ^1H NMR (401 MHz, CDCl_3) δ 9.48 (s, 1H), 7.39 (d, $J = 1.9$ Hz, 1H), 7.25 (dd, $J = 9.2, 1.6$ Hz, 1H), 7.15 (d, $J = 8.2$ Hz, 1H), 2.56 (t, $J = 7.2$ Hz, 2H), 2.51 (s, 3H), 1.58 (dt, $J = 15.5, 7.6$ Hz, 2H), 1.34 – 1.24 (m, 6H), 0.88 (t, $J = 6.7$ Hz, 3H). ^{13}C NMR (101 MHz, CDCl_3) δ 176.7, 141.3, 139.9, 134.7, 132.3, 125.4, 117.8, 93.8, 93.0, 35.1, 31.8, 31.2, 28.9, 22.7, 15.6, 14.2. HRMS (ESI) calcd. for $\text{C}_{16}\text{H}_{21}\text{OS}$ ($\text{M}+\text{H}^+$): 261.1308, Found: 261.1299.



1,5-bis(5-hexyl-2-(methylthio)phenyl)penta-1,4-diyn-3-one (**333**)

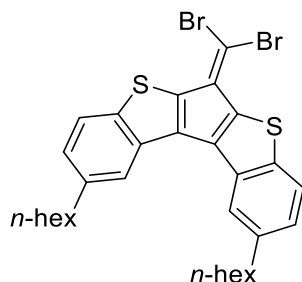
To a dried 25 mL flask with **315** (0.48 g, 1.85 mmol) in anhydrous THF (14 mL), was added *n*-BuLi (1.1 mL, 2.42 M in hexane, 2.68 mmol) at 0 °C dropwise. The resulting reaction was allowed to stir for 1.5 h at 0 °C, then a solution of **332** (0.26 g, 1.48 mmol) in anhydrous THF (2 mL) was added and allowed to stir for 1.5 h at 0 °C. Sat. aq. NH₄Cl (15 mL) was added, diluted with water (15 mL), extracted with Et₂O (2 x 15 mL), dried over MgSO₄ and concentrated under reduced pressure. To a solution of crude reaction mixture in DCM (14 mL), was added Dess-Martin periodinane (1.18 g, 2.78 mmol) and allowed to stir for 2 h at rt. Sat. aq. NaHCO₃ (15 mL) was added, diluted with water (15 mL), extracted with DCM (2 x 15 mL), dried over MgSO₄ and concentrated under reduced pressure. The resulting crude reaction mixture was chromatographed (5% EtOAc in PS), yielding **333** (0.42 g, 46%) as dark oil. *R*_f = 0.19 (30% DCM in PS); ¹H NMR (401 MHz, CDCl₃) δ 7.42 (d, *J* = 1.9 Hz, 2H), 7.23 (dd, *J* = 8.2, 2.0 Hz, 2H), 7.15 (d, *J* = 8.2 Hz, 2H), 2.56 (t, *J* = 7.3 Hz, 4H), 2.51 (s, 6H), 1.62 – 1.53 (m, 4H), 1.35 – 1.23 (m, 12H), 0.88 (t, *J* = 6.7 Hz, 6H). ¹³C NMR (101 MHz, CDCl₃) δ 160.6, 141.7, 139.8, 134.6, 132.1, 125.6, 118.2, 94.9, 90.0, 35.1, 31.8, 31.2, 28.9, 22.7, 15.8, 14.2. HRMS (ESI) calcd. for C₃₁H₃₉OS₂ (M+H)⁺: 491.24347, Found: 491.2441.



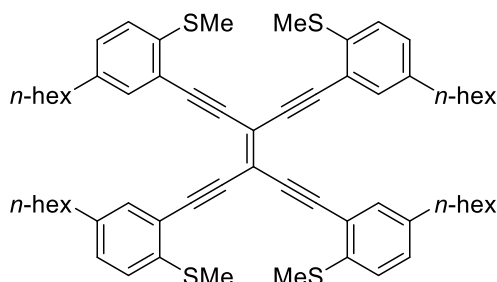
((3-(dibromomethylene)penta-1,4-diyn-1,5-diyl)bis(4-hexyl-2,1-phenylene))bis(methylsulfane) (**334**)

To a dried 25 mL flask with CBr₄ (0.57 g, 1.70 mmol) in anhydrous DCM (4 mL) was added PPh₃ (0.89 g, 3.41 mmol) and allowed to stir for 5 min. To this reaction mixture was added a solution of **333** (0.42 g, 0.85 mmol) in anhydrous DCM (4 mL) and allowed to stir for 4 h at rt. Water (5 mL) was added, extracted with DCM (2 x 5 mL), dried over MgSO₄ and concentrated under reduced pressure. The resulting crude reaction mixture was passed through a silica plug (30% DCM in PS), yielding **334** (0.41 g, 74%) as orange wax. *R*_f = 0.50 (30% DCM in PS); ¹H NMR (401 MHz, CDCl₃) δ 7.34 (d, *J* = 1.4 Hz, 2H), 7.15 (dd, *J* = 8.2, 1.8 Hz, 2H), 7.12 (d, *J* = 8.1 Hz, 2H), 2.56 (t, *J* = 8.0 Hz, 4 H), 2.50 (s, 6H), 1.59 (p, *J* = 8.0 Hz, 4H), 1.36 – 1.25 (m, 12H), 0.88 (t, *J* = 6.8 Hz, 6H). ¹³C NMR (101 MHz, CDCl₃) δ 139.7, 139.0, 133.0, 130.1, 125.5, 120.9, 114.6, 107.7, 93.9, 91.6, 35.2, 31.8,

31.4, 29.0, 22.7, 15.9, 14.2. HRMS (APCI) calcd. for $C_{32}H_{39}Br_2S_2$ ($M+H$)⁺: 647.0836, found 647.0858.

**(336)**

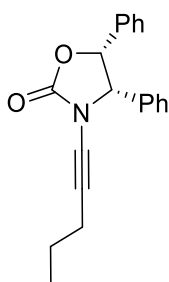
Synthesized according to General Procedure B. Prepared from **334** (0.06 g, 0.09), $AuCl_3$ (0.03 g, 0.10 mmol), DCE (1 mL) and 1,4-dioxane (1mL). The resulting crude material was passed through short silica gel plug (30% DCM in PS) to yield **336** (0.05 g, 83%) as dark red needle. R_f = 0.80 (40% DCM in PS); 1H NMR (401 MHz, $CDCl_3$) δ 8.11 (s, 2H), 7.72 (d, J = 8.3 Hz, 2H), 7.20 (dd, J = 8.3, 1.3 Hz, 2H), 2.83 (t, J = 8.0 Hz, 4H), 1.79 (dt, J = 15.4, 7.5 Hz, 4H), 1.41 – 1.33 (m, 12H), 0.91 (t, J = 7.1 Hz, 6H). ^{13}C NMR (101 MHz, $CDCl_3$) δ 141.8, 140.1, 139.3, 138.4, 136.7, 131.9, 125.9, 123.4, 122.8, 96.5, 36.3, 32.0, 31.4, 29.2, 22.8, 14.2.



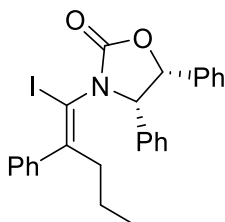
((3-(1,5-bis(5-hexyl-2-(methylthio)phenyl)penta-1,4-diyn-3-ylidene)penta-1,4-diyne-1,5-diyl)bis(4-hexyl-2,1-phenylene))bis(methylsulfane) (335)

Synthesized according to general procedure A. Prepared from **334** (0.13 g, 0.26 mmol), **315** (0.18 g, 0.79 mmol), $Pd(PPh_3)_4$ (0.01 g, 0.01 mmol), CuI (0.01 g, 0.02 mmol), DIPA (2 mL). The resulting crude reaction mixture was chromatographed (10% - 15% DCM in PS, 5% step gradient), yielding **335** (0.10 g, 41%) as brown wax; R_f = 0.25 (30% DCM in PS); MP = 80–82 °C; 1H NMR (401 MHz, $CDCl_3$) δ 7.41 (s, 4H), 7.12 (s, 8H), 2.52 (t, J = 8.0 Hz, 8H), 2.42 (s, 12H), 1.61 – 1.51 (m, 8H), 1.35 – 1.21 (m, 24H), 0.88 (t, J = 6.8 Hz, 12H). ^{13}C NMR (101 MHz, $CDCl_3$) δ 139.4, 139.2, 133.4, 129.7, 125.4, 121.7, 116.6, 97.0, 93.3, 35.3, 31.8, 31.4, 29.1, 22.7, 15.8, 14.2. HRMS (APCI) calcd. for $C_{62}H_{77}S_4$ ($M+H$)⁺: 949.4903, found 949.4908.

4.2. Experimental for Chapter 3

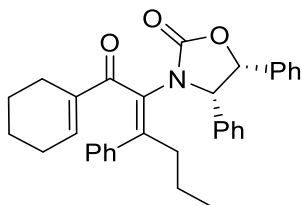
**(4*S*,5*R*)-3-(pent-1-yn-1-yl)-4,5-diphenyloxazolidin-2-one (379)**

A dried 250 mL flask with (4*S*,5*R*)-4,5-diphenyloxazolidin-2-one **358** (3.01 g, 12.6 mmol), 1-bromopent-1-yne¹¹⁰ (2.77 g, 18.8 mmol), 1,10-phenanthroline (3.01 g, 2.51 mmol), CuSO₄·H₂O (0.22 g, 1.26 mmol) and K₂CO₃ (3.47 g, 25.1 mmol) in anhydrous toluene (63 mL) was heated to reflux for 72 h. The reaction mixture was then cooled to rt, filtered, diluted with water (70 mL), extracted with DCM (70 mL), washed with 10% aq. citric acid (70 mL) and brine (70 mL), dried over MgSO₄ and concentrated under reduced pressure to give **379** (3.70 g, 96%) as brown solid. MP = 114-116 °C; R_f = 0.65 (20% EtOAc in PS); ¹H NMR (401 MHz, CDCl₃) δ 7.15 – 7.06 (m, 6H), 6.95 – 6.86 (m, 4H), 5.91 (d, *J* = 8.2 Hz, 1H), 5.30 (d, *J* = 8.2 Hz, 1H), 2.16 (t, *J* = 7.0 Hz, 2H), 1.47 – 1.34 (sxt, *J* = 14.4, 7.2 Hz, 2H), 0.80 (t, *J* = 7.4 Hz, 3H). ¹³C NMR (101 MHz, CDCl₃) δ 156.7, 133.7, 133.0, 128.6, 128.5, 128.3, 128.1, 127.6, 126.2, 80.8, 72.4, 69.8, 67.3, 22.2, 20.4, 13.2. HRMS (ESI) calcd. for C₂₀H₂₀NO₂ (M+H)⁺: 306.1489, found 306.1486.

**(4*S*,5*R*)-3-((*Z*)-1-iodo-2-phenylpent-1-en-1-yl)-4,5-diphenyloxazolidin-2-one (381)**

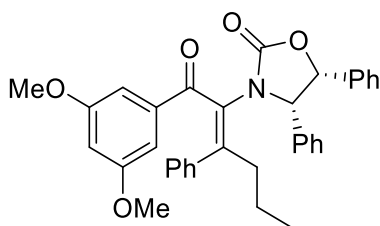
To a dried 250 mL flask with anhydrous DCM (11 mL) and Et₂O (67 mL) was added **379** (1.02 g, 3.35 mmol) and CuBr·SMe₂ (0.07 g, 0.34 mmol). This mixture was cooled to -40 °C and PhMgBr (2.2 mL, 3.0 M in Et₂O, 6.69 mmol) was added dropwise. The resulting brown reaction mixture was warmed to -20 °C and allowed to stir for 45 min. At -78 °C, a solution of I₂ (1.95 g, 7.70 mmol) in anhydrous Et₂O (10 mL) was added and allowed to stir overnight at rt. Sat. aq. NH₄Cl (25 mL) and sat. aq. Na₂S₂O₃ (25 mL) were added, diluted with water (25 mL), extracted with Et₂O (2 x 60 mL), dried over MgSO₄ and concentrated under reduced pressure. The resulting crude reaction mixture was then chromatographed (10% -15% EtOAc in PS, 5% step gradient), yielding **381** as orange syrup (1.57 g, 92%). R_f = 0.30 (10% EtOAc in PS). ¹H NMR (401 MHz, CDCl₃) δ 7.30 – 7.25 (m, 3H),

7.22 – 7.17 (m, 4H), 7.13 (t, $J = 7.3$ Hz, 2H), 7.04 – 6.94 (m, 4H), 6.90 (d, $J = 7.3$ Hz, 2H), 5.89 (d, $J = 8.5$ Hz, 1H), 5.40 (d, $J = 8.5$ Hz, 1H), 2.49 (dddd, $J = 37.6, 13.8, 11.0, 5.3$ Hz, 2H), 1.38 – 1.28 (m, 1H), 1.00 – 0.89 (m, 1H), 0.81 (t, $J = 7.2$ Hz, 3H). ^{13}C NMR (101 MHz, CDCl_3) δ 155.4, 154.1, 143.2, 135.1, 132.8, 128.9, 128.8, 128.5, 128.3, 128.2, 128.2, 127.8, 126.1, 92.1, 79.5, 68.1, 37.8, 20.9, 14.3. HRMS (ESI) calcd. for $\text{C}_{26}\text{H}_{25}\text{INO}_2$ ($\text{M}+\text{H}$) $^+$: 510.0924, found 510.0928.



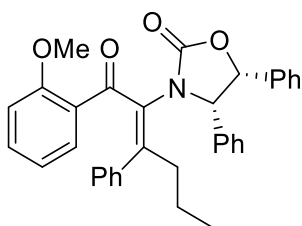
(4*S*,5*R*)-3-((*E*)-1-(cyclohex-1-en-1-yl)-1-oxo-3-phenylhex-2-en-2-yl)-4,5-diphenyloxazolidin-2-one (382a)

To a dried 25 mL flask was added **381** (0.15 g, 0.30 mmol), tributyl(cyclohex-1-en-1-yl)stannane **360**⁶³ (0.13 g, 0.34 mmol), $\text{Pd}(\text{dtbpf})\text{Cl}_2$ (0.01 g, 0.02 mmol), CuTC (0.01 g, 0.03 mmol) and dissolved in anhydrous DMF (3 mL). The resulting mixture was then evacuated and backfilled with $\text{CO}(\text{g})$ three times, then allowed to stir overnight at 50 °C. After which TLC indicated full consumption **381**, the reaction was diluted with water (5 mL), extracted with EtOAc (2 x 5 mL), dried over MgSO_4 and concentrated under reduced pressure. The crude reaction mixture was then chromatographed (15% – 25% EtOAc in PS, 5% step gradient), yielding **382a** (0.12 g, 83%) as green syrup. $R_f = 0.31$ (20% EtOAc in PS); ^1H NMR (401 MHz, CDCl_3) δ 7.19 – 7.14 (m, 6H), 7.11 – 7.01 (m, 5H), 6.95 – 6.90 (m, 4H), 5.90 (d, $J = 8.5$ Hz, 1H), 5.83 (s, 1H), 5.42 (d, $J = 8.5$ Hz, 1H), 2.65 (ddd, $J = 13.8, 10.8, 4.8$ Hz, 1H), 2.45 (ddd, $J = 13.8, 11.3, 4.9$ Hz, 1H), 1.89 (d, $J = 17.3$ Hz, 1H), 1.66 – 1.53 (m, 3H), 1.42 (ddd, $J = 19.0, 10.1, 6.2$ Hz, 1H), 1.19 – 1.03 (m, 4H), 0.96 – 0.87 (m, 1H), 0.84 (t, $J = 6.9$ Hz, 3H). ^{13}C NMR (101 MHz, CDCl_3) δ 196.2, 156.7, 149.6, 143.4, 139.9, 139.1, 135.4, 134.6, 128.9, 128.4, 128.4, 128.3, 128.1, 128.1, 128.0, 127.9, 126.1, 79.7, 65.6, 36.2, 25.9, 23.0, 21.6, 21.3, 20.7, 14.7. HRMS (ESI) calcd. for $\text{C}_{33}\text{H}_{34}\text{INO}_3$ ($\text{M}+\text{H}$) $^+$: 492.2533, found 492.2538.



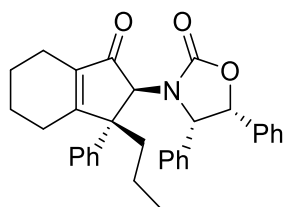
(4*S*,5*R*)-3-((*E*)-1-(3,5-dimethoxyphenyl)-1-oxo-3-phenylhex-2-en-2-yl)-4,5-diphenyloxazolidin-2-one (382b)

To a dried 50 mL flask with anhydrous DCM (2 mL) and Et₂O (13 mL) was added **379** (0.20 g, 0.66 mmol) and CuBr.SMe₂ (0.01 g, 0.07 mmol). This mixture was cooled to -40 °C and PhMgBr (0.44 mL, 3.0 M in Et₂O, 1.31 mmol) was added dropwise. The resulting brown reaction mixture was warmed to -20 °C and allowed to stir for 45 min. At -78 °C, 3,5-dimethoxybenzaldehyde (0.24 g, 1.44 mmol) was added and allowed to stir for 1 h at rt. Sat. aq. NH₄Cl (10 mL) was added, diluted with water (10 mL), extracted with Et₂O (2 x 15 mL), dried over MgSO₄ and concentrated under reduced pressure. To a solution of crude reaction mixture in DCM (3.2 mL) was added NaHCO₃ (0.17 g, 1.97 mmol), cooled to 0 °C and Dess-Martin Periodinane (0.33 g, 0.79 mmol) was added, then allowed to stir for 2 h. Sat. aq. NaHCO₃ (5 mL) was added, diluted with water (5 mL), extracted with DCM (2 x 5 mL), dried over MgSO₄ and concentrated under reduced pressure. The resulting crude reaction mixture was then chromatographed (15% – 25% EtOAc in PS, 5% step gradient) to yield **382b** (0.27 g, 75%) as pale-yellow solid. *R*_f = 0.29 (20% EtOAc in PS); MP = 174-177 °C; ¹H NMR (401 MHz, CDCl₃) δ 7.18 – 7.14 (m, 3H), 7.11 – 7.06 (m, 3H), 7.03 – 6.99 (m, 5H), 6.97 – 6.93 (m, 2H), 6.91 – 6.87 (m, 2H), 6.44 (d, *J* = 2.3 Hz, 2H), 6.30 (t, *J* = 2.3 Hz, 1H), 5.87 (d, *J* = 8.5 Hz, 1H), 5.37 (d, *J* = 8.5 Hz, 1H), 3.58 (s, 6H), 2.75 (ddd, *J* = 13.7, 11.1, 4.9 Hz, 1H), 2.52 (ddd, *J* = 13.7, 11.3, 5.2 Hz, 1H), 1.56 – 1.42 (m, 1H), 1.08 – 0.96 (m, 1H), 0.90 (t, *J* = 7.2 Hz, 3H). ¹³C NMR (101 MHz, CDCl₃) δ 194.1, 160.0, 156.6, 151.0, 139.6, 138.1, 135.2, 134.1, 128.9, 128.8, 128.6, 128.4, 128.3, 128.2, 128.1, 128.1, 128.0, 126.1, 106.4, 106.0, 79.7, 65.5, 55.5, 36.6, 20.6, 14.7. HRMS (ESI) calcd. for C₃₅H₃₄NO₅ (M+H)⁺: 548.2431, found 548.2437.



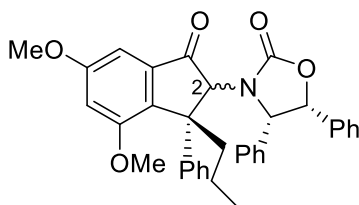
(4*S*,5*R*)-3-((*E*)-1-(2-methoxyphenyl)-1-oxo-3-phenylhex-2-en-2-yl)-4,5-diphenyloxazolidin-2-one (382c)

To a dried 50 mL flask with anhydrous DCM (5 mL) and Et₂O (29 mL) was added **379** (0.45 g, 1.48 mmol) and CuBr.SMe₂ (0.03 g, 0.15 mmol). This mixture was cooled to -40 °C and PhMgBr (0.98 mL, 3.0 M in Et₂O, 2.95 mmol) was added dropwise. The resulting brown reaction mixture was warmed to -20 °C and allowed to stir for 45 min. At -78 °C, *o*-methoxybenzoyl chloride (0.50 mL, 3.39 mmol) was added and allowed to stir for 1h at rt. Sat. aq. NH₄Cl (20 mL) was added, diluted with water (20 mL), extracted with DCM (2 x 20 mL), dried over MgSO₄ and concentrated under reduced pressure. The resulting crude reaction mixture was chromatographed (20% – 22.5% EtOAc in PS, 2.5% step gradient), yielding **382c** (0.52 g, 64%) as yellow syrup. *R*_f = 0.20 (20% EtOAc in PS); ¹H NMR (401 MHz, CDCl₃) δ 7.11 – 7.06 (m, 3H), 7.06 – 6.99 (m, 3H), 6.98 – 6.94 (m, 2H), 6.91 – 6.80 (m, 6H), 6.76 (dd, *J* = 7.9, 1.6 Hz, 2H), 6.44 (d, *J* = 6.7 Hz, 1H), 6.34 (td, *J* = 7.5, 0.8 Hz, 1H), 6.28 (d, *J* = 8.2 Hz, 1H), 5.87 (d, *J* = 8.5 Hz, 1H), 5.46 (d, *J* = 8.5 Hz, 1H), 3.35 (s, 3H), 2.63 (ddd, *J* = 13.5, 11.0, 4.8 Hz, 1H), 2.35 (ddd, *J* = 13.5, 11.4, 4.9 Hz, 1H), 1.49 – 1.31 (m, 1H), 0.92 – 0.81 (m, 1H), 0.78 (t, *J* = 7.0 Hz, 3H). ¹³C NMR (101 MHz, CDCl₃) δ 193.2, 157.3, 156.8, 154.4, 138.4, 135.5, 134.6, 132.1, 131.2, 129.61, 129.6, 129.1, 128.9, 128.6, 128.4, 128.3, 128.1, 128.0, 127.8, 127.4, 126.2, 119.3, 110.4, 80.0, 65.4, 54.89, 37.7, 20.6, 14.8. HRMS (ESI) calcd. for C₃₄H₃₂NO₄ (M+H)⁺: 518.2326, found 518.2339.



(4*S*,5*R*)-3-((1*R*,2*R*)-3-oxo-1-phenyl-1-propyl-2,3,4,5,6,7-hexahydro-1*H*-inden-2-yl)-4,5-diphenyloxazolidin-2-one (383a)

To a dried 5 mL flask with **382a** (0.17 g, 0.34 mmol) in anhydrous DCM (3 mL) was added $\text{BF}_3 \cdot \text{THF}$ (0.04 mL, 0.34 mmol) at -78°C and allowed to stir for 1 h at rt. Sat. aq. NaHCO_3 (1 mL) was added, diluted with water (1 mL), extracted with DCM (2 x 5 mL), dried over MgSO_4 and concentrated under reduced pressure. The resulting crude reaction mixture was chromatographed (15% – 20% EtOAc in PS, 5% step gradient) to yield **383a** (0.14 g, 82%) as clear wax. $R_f = 0.17$ (20% EtOAc in PS); ^1H NMR (401 MHz, CDCl_3) δ 7.29 (t, $J = 7.5$ Hz, 2H), 7.21 (t, $J = 7.3$ Hz, 1H), 7.08 – 7.02 (m, 5H), 6.99 – 6.89 (m, 5H), 6.75 (brs, 2H), 5.90 (d, $J = 8.6$ Hz, 1H), 4.76 (d, $J = 8.6$ Hz, 1H), 3.45 (s, $J = 9.7$ Hz, 1H), 2.43 (dt, $J = 17.0, 4.8$ Hz, 1H), 2.36 – 2.17 (m, 3H), 2.14 (t, $J = 5.6$ Hz, 2H), 1.77 (dq, $J = 11.7, 5.8$ Hz, 2H), 1.72 – 1.63 (m, 1H), 1.60 – 1.46 (m, 2H), 1.40 – 1.25 (m, 1H), 1.01 (t, $J = 7.2$ Hz, 3H). ^{13}C NMR (101 MHz, CDCl_3) δ 198.0, 173.8, 156.4, 143.9, 139.0, 134.9, 133.4, 129.1, 128.4, 128.1, 128.0, 127.9, 126.8, 126.5, 126.2, 79.9, 71.4, 66.9, 56.6, 35.3, 26.5, 22.5, 21.6, 20.4, 19.3, 15.4. HRMS (ESI) calcd. for $\text{C}_{33}\text{H}_{34}\text{NO}_3$ ($\text{M}+\text{H}$) $^+$: 492.2533, found 492.2536.



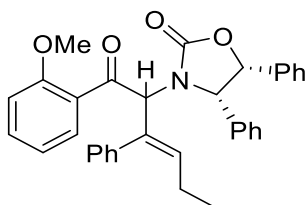
(4*S*,5*R*)-3-((1*R*,2*S*)-5,7-dimethoxy-3-oxo-1-phenyl-1-propyl-2,3-dihydro-1*H*-inden-2-yl)-4,5-diphenyloxazolidin-2-one (383b-2*S*/2*R*)

In a dried 10 mL flask with **382b** (0.15 g, 0.28 mmol) in anhydrous DCE (3 mL) was added $\text{BF}_3 \cdot \text{THF}$ (0.03 mL, 0.28 mmol) at -78°C and allow to stir for 24 h at 45°C . Sat. aq. NaHCO_3 (1 mL) was added, diluted with water (1 mL), extracted with DCM (2 x 5 mL), dried over MgSO_4 and concentrated under reduced pressure. The resulting reaction mixture was chromatographed (17.5% EtOAc in PS) to yield **383b-2*S*** as yellow syrup (0.08 g, 51%).

383b-2*S*: $R_f = 0.15$ (22.5% EtOAc in PS); ^1H NMR (401 MHz, CDCl_3) δ 7.29 – 7.19 (m, 3H), 7.14 (d, $J = 6.9$ Hz, 3H), 7.08 – 7.03 (m, 3H), 7.00 – 6.88 (m, 6H), 6.73 (brs, 1H), 6.66 (d, $J = 2.1$ Hz, 1H), 5.95 (d, $J = 8.5$ Hz, 1H), 4.70 (d, $J = 8.5$ Hz, 1H), 3.85 (s, 3H), 3.68 (s, 1H), 3.53 (s, 3H), 2.57 (ddd, $J = 16.6, 13.8, 7.8$ Hz, 1H), 2.11 (ddd, $J = 22.5, 16.1, 10.1$ Hz, 1H), 1.30 – 1.22 (m, 2H), 0.90 (t, $J = 7.2$, 3H). ^{13}C NMR (101 MHz, CDCl_3) δ 196.3, 161.6, 158.2, 156.4, 145.4, 137.4, 137.1, 134.9, 133.6, 128.6, 128.5, 128.1, 127.9, 126.4, 126.2, 125.8, 106.8, 97.4, 79.9, 74.2, 67.1, 55.9, 55.4, 54.3, 37.2, 19.2, 15.1. HRMS (ESI) calcd. for $\text{C}_{35}\text{H}_{34}\text{NO}_5$ ($\text{M}+\text{H}$) $^+$: 548.2431, found 548.2436.

383b-2*R*: Isolated as the minor epimer (0.07 g, 43%). $R_f = 0.14$ (22.5% EtOAc in PS); ^1H NMR (401 MHz, CDCl_3) δ 7.44 – 7.40 (m, 3H), 7.26 (brs, 2H), 7.09 – 7.03 (m, 2H), 7.03 – 6.93 (m, 5H), 6.73 (d, $J = 2.2$ Hz, 1H), 6.67 (d, $J = 2.2$ Hz, 1H), 6.60 (dd, $J = 7.4, 1.7$ Hz, 2H), 5.12 (brs, 1H), 4.52 (d, $J = 6.9$ Hz, 1H), 3.79 (s, 3H), 3.70 (s, 3H), 3.65 (brs, 1H), 2.57 (t, $J = 10.5$ Hz, 1H), 2.45 (td, $J = 12.7, 4.4$ Hz, 1H), 1.16 – 1.08 (m, 1H), 0.91 (t, $J = 7.4$ Hz, 3H), 0.81 (ddd, $J = 12.4, 9.8, 6.0$ Hz, 1H). ^{13}C NMR (101 MHz, CDCl_3) δ 198.6, 161.9, 159.4, 158.2, 143.8, 138.3, 137.1, 135.4, 134.0, 128.5, 128.0, 128.0, 127.8, 127.7, 127.5, 126.1, 107.2, 96.5, 81.3, 67.3, 64.7, 55.9, 55.8, 39.1, 18.4, 14.7. HRMS (ESI) calcd. for $\text{C}_{35}\text{H}_{34}\text{NO}_5$ ($\text{M}+\text{H}$) $^+$: 548.2431, found 548.2443.

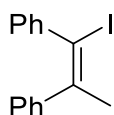
383b-2*R* (Additional NMR was performed in $\text{DMSO}-d_6$ at 70°C , resolved oxazolidinone C-H peaks). ^1H NMR (401 MHz, DMSO) δ 7.42 – 7.36 (m, 3H), 7.15 – 7.01 (m, 8H), 6.94 (d, $J = 2.2$ Hz, 1H), 6.73 (d, $J = 6.8$ Hz, 2H), 6.67 (d, $J = 2.2$ Hz, 1H), 6.64 – 6.59 (m, 2H), 4.95 (d, $J = 7.4$ Hz, 1H), 4.59 (s, 1H), 4.22 (d, $J = 7.0$ Hz, 1H), 3.84 (s, 3H), 3.67 (s, 3H), 2.35 – 2.24 (m, 1H), 2.20 – 2.11 (m, 1H), 1.51 – 1.39 (m, 1H), 1.34 – 1.22 (m, 1H), 0.73 (t, $J = 4.3$ Hz, 3H).



(4*S*,5*R*)-3-((*E*)-1-(2-methoxyphenyl)-1-oxo-3-phenylhex-3-en-2-yl)-4,5-diphenyloxazolidin-2-one (383c)

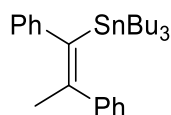
Formed in the reaction using **382c** in DCM using TfOH, obtained after 2 h at rt. Minor unknown product co-eluted with **383c**.

^1H NMR (401 MHz, CDCl_3) δ 7.66 (d, $J = 7.2$ Hz, 1H), 7.63 (d, $J = 7.0$ Hz, 0.28H), 7.51 – 7.36 (m, 1.8H), 7.10 (ddd, $J = 19.3, 10.1, 1.0$ Hz, 11H), 6.98 – 6.86 (m, 5H), 6.80 (t, $J = 6.1$ Hz, 2H), 6.59 (dd, $J = 7.2, 1.4$ Hz, 0.76H), 6.54 (t, $J = 7.4$ Hz, 1H), 6.42 (dt, $J = 6.6, 3.7$ Hz, 2H), 5.69 (bs, 1H), 5.60 (d, $J = 8.5$ Hz, 0.38H), 5.06 (d, $J = 8.3$ Hz, 1H), 4.84 (d, $J = 8.5$ Hz, 0.38H), 3.86 (bs, 3H), 3.57 (s, 1H), 2.98 – 2.76 (m, 2.67H), 1.28 (t, $J = 7.5$ Hz, 3H), 1.19 (t, $J = 7.5$ Hz, 1.13H). ^{13}C NMR (101 MHz, CDCl_3) δ 219.8, 157.7, 157.3, 141.8, 141.5, 138.4, 135.3, 135.2, 133.9, 133.7, 133.0, 131.3, 130.4, 130.0, 128.4, 128.2, 128.2, 128.0, 128.0, 127.9, 127.7, 127.6, 127.0, 126.9, 126.0, 126.0, 125.7, 125.6, 123.7, 123.5, 122.3, 122.1, 121.2, 121.2, 120.6, 111.0, 80.1, 79.9, 66.7, 55.2, 23.1, 23.0, 14.1, 14.0.

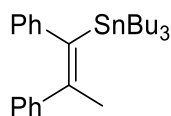


(*E*)-(1-iodoprop-1-ene-1,2-diyl)dibenzene (393)

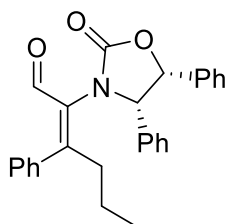
To a dried 250 mL flask with TiCp_2Cl_2 (6.71 g, 26.9 mmol) in anhydrous DCM (112 mL), was added AlMe_3 (13.5 mL, 2.0 M in toluene, 26.9 mmol) and allowed to stir for 30 min. To this mixture was added diphenylacetylene **387** (4.02 g, 22.4 mmol) and allowed to stir for 5 h. A solution of I_2 (14.2 g, 56.1 mmol) in anhydrous Et_2O (50 mL) was then added at -78°C and allowed to stir for 30 min. The reaction mixture was filtered through Celite, rinsed with Et_2O (200 mL), washed with sat. aq. NaHCO_3 (2 x 150 mL), sat. aq. $\text{Na}_2\text{S}_2\text{O}_3$ (2 x 150 mL), brine (2 x 150 mL), dried over MgSO_4 , concentrated under reduced pressure to afford **393** (6.69 g, 93%) as brown oil. $R_f = 0.66$ (30% DCM in PS); ^1H NMR (401 MHz, CDCl_3) δ 7.14 – 7.03 (m, 8H), 7.02 – 6.98 (m, 2H), 2.50 (s, 3H). ^{13}C NMR (101 MHz, CDCl_3) δ 144.8, 144.6, 141.0, 130.1, 128.7, 128.0, 127.8, 127.2, 126.8, 100.2, 32.6. HRMS (APCI) calcd. for $\text{C}_{15}\text{H}_{13}\text{I}$ (M^+): 320.0056, found 320.0052.

**(Z)-tributyl(1,2-diphenylprop-1-en-1-yl)stannane (394Z)**

To a dried 50 mL flask with **393** (1.51 g, 6.70 mmol) in anhydrous THF (16 mL) was added *s*-BuLi (5.4 mL, 1.18 M in hexane, 6.33 mmol) at -78 °C and allowed to stir for 5 min. ClSnBu₃ (1.2 mL, 6.56 mmol) was added and allowed to stir overnight at rt. Sat. aq. K₂CO₃ (10 mL) was added, diluted with water (10 mL), extracted with Et₂O (2 x 15 mL), dried over MgSO₄ and concentrated under reduced pressure. The crude reaction mixture was chromatographed (100% PS), yielding **394Z** (1.49 g, 66%) as clear oil. *R*_f = 0.60 (100% PS). ¹H NMR (401 MHz, CDCl₃) δ 7.41 – 7.27 (m, 7H), 7.12 (tt, *J* = 7.8, 1.2, 1H), 7.01 (dd, *J* = 8.2, 1.2 Hz, 2H), 1.96 (s, 3H), 1.32 – 1.09 (m, 12H), 0.82 (t, *J* = 7.2 Hz, 9H), 0.45 (t, *J* = 11.0 Hz, 6H). ¹³C NMR (101 MHz, CDCl₃) δ 148.2, 147.5, 146.9, 145.0, 128.3, 128.2, 127.9, 127.4, 127.0, 124.8, 29.1, 27.4, 22.6, 13.8, 11.3. HRMS (ESI) calcd. for C₂₇H₄₀SnNa (M+Na)⁺: 503.204, found 503.194.

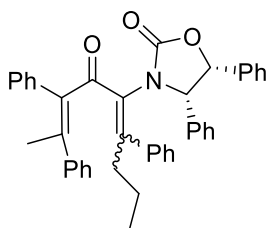
**(E)-tributyl(1,2-diphenylprop-1-en-1-yl)stannane (394E)**

To a dried 50 mL flask with **393** (0.55 g, 1.73 mmol) in anhydrous Et₂O (6 mL) was added *s*-BuLi (2.3 mL, 1.00 M in hexane, 2.34 mmol) at -78 °C and allowed to stir for 5 min. ClSnBu₃ (0.46 mL, 2.43 mmol) was added and allowed to stir overnight at rt. Sat. aq. K₂CO₃ (5 mL) was added, diluted with water (5 mL), extracted with Et₂O (2 x 10 mL), dried over MgSO₄ and concentrated under reduced pressure, yielded **394E** (0.84 g) as brown oil, which was used in next reaction without further purification. *R*_f = 0.60 (100% PS); ¹H NMR (401 MHz, CDCl₃) δ 7.11 – 6.95 (m, 7H), 6.91 (tt, *J* = 7.2, 1.5 Hz, 1H), 6.72 (dd, *J* = 8.2, 1.3 Hz, 2H), 2.27 (s, 3H), 1.51 – 1.42 (m, 6H), 1.37 – 1.24 (m, 9H), 0.96 – 0.84 (m, 18H). ¹³C NMR (101 MHz, CDCl₃) δ 146.5, 146.4, 143.9, 143.8, 128.7, 128.3, 127.6, 127.5, 125.8, 124.1, 29.4, 28.8, 27.8, 27.5, 13.8, 11.4.



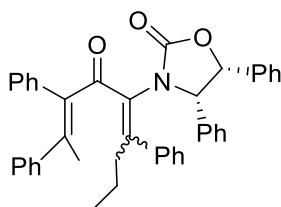
(*E*)-2-((4*S*,5*R*)-2-oxo-4,5-diphenyloxazolidin-3-yl)-3-phenylhex-2-enal (398**)**

To a dried 10 mL flask with **381** (0.48 g, 0.94 mmol) in anhydrous THF (5.0 mL), was added *n*-BuLi (0.49 mL, 2.27 M in hexane, 1.13 mmol) at -90 °C and stirred for 5 min. Ethyl formate (0.46 mL, 5.67 mmol) was then added and allowed to stir for 1.5 h at -78 °C. 10% aq. citric acid (5 mL) was added, diluted with water (5 mL), extracted with EtOAc (2 x 8 mL), dried over MgSO₄ and concentrated under reduced pressure. The resulting crude reaction mixture was chromatographed (20% - 25% EtOAc in PS, 5% step gradient), yielding **398** (0.27 g, 70%) as yellow syrup. *R*_f = 0.40 (25% EtOAc in PS); MP = 128-130 °C; ¹H NMR (401 MHz, CDCl₃) δ 9.12 (s, 1H), 7.38 – 7.30 (m, 3H), 7.19 – 7.14 (m, 3H), 7.13 – 7.04 (m, 7H), 6.89 (d, *J* = 6.8 Hz, 2H), 6.09 (d, *J* = 8.6 Hz, 1H), 5.75 (d, *J* = 8.5 Hz, 1H), 2.66 (ddd, *J* = 13.7, 10.7, 5.2 Hz, 1H), 2.54 (ddd, *J* = 15.9, 8.9, 3.4 Hz, 1H), 1.35 – 1.19 (m, 2H), 0.83 (m, 3H). ¹³C NMR (101 MHz, CDCl₃) δ 188.7, 156.9, 136.0, 135.3, 134.3, 132.2, 131.6, 129.3, 128.9, 128.8, 123.6, 128.5, 128.1, 128.1, 128.1, 126.1, 80.3, 37.8, 20.6, 14.6. HRMS (ESI) calcd. for C₂₇H₂₆NO₃ (M+H)⁺: 412.1907, found 412.1914 .



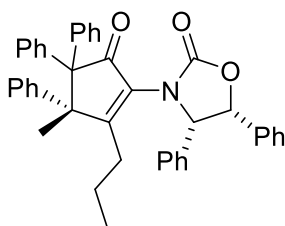
(4*S*,5*R*)-3-((2*Z*,5*E/Z*)-4-oxo-2,3,6-triphenylnona-2,5-dien-5-yl)-4,5-diphenyloxazolidin-2-one (388a(5*E/Z*))

To a dried 50 mL flask was added **381** (0.32 g, 0.63 mmol), **394Z** (0.43 g, 0.89 mmol), Pd(dtbpf)Cl₂ (0.02 g, 0.03 mmol), CuI (0.01 g, 0.06 mmol) and dissolved in anhydrous DMF (6 mL). The resulting mixture was then evacuated and backfilled with CO(g) three times, then heated to 60 °C and allowed to stir for 72 h. After which TLC indicated full consumption of **381**, the reaction was diluted with water (10 mL), extracted with EtOAc (2 x 10 mL), dried over MgSO₄ and concentrated under reduced pressure. The resulting crude reaction mixture was then chromatographed (10% – 15% EtOAc in PS, 5% step gradient), yielding **388a(5*E/Z*)** (0.24 g, 66%) as double bond isomers in 1.6:1 ratio (E : Z). R_f = 0.57 (20% EtOAc in PS); ¹H NMR (401 MHz, CDCl₃) δ 7.43 (dd, *J* = 8.2, 1.3 Hz, 2.4H), 7.40 – 7.21 (m, 20H), 7.16 – 6.99 (m, 26H), 6.98 – 6.89 (m, 13H), 6.86 – 6.75 (m, 11H), 6.66 – 6.60 (m, 6.5H), 6.56 (dd, *J* = 6.8, 1.5 Hz, 2.2H), 6.48 (dd, *J* = 8.1, 1.1 Hz, 4.4H), 6.04 (dd, *J* = 8.2, 1.0 Hz, 2H), 5.75 (d, *J* = 8.4 Hz, 2.2H), 5.18 (d, *J* = 8.7 Hz, 1H), 4.42 (d, *J* = 8.4 Hz, 2.2H), 4.11 (d, *J* = 8.7 Hz, 1H), 2.55 (ddd, *J* = 14.0, 11.1, 4.6 Hz, 1H), 2.23 (ddd, *J* = 13.9, 10.7, 5.0 Hz, 1H), 2.11 (s, 3H), 2.02 (ddd, *J* = 13.8, 11.7, 4.9 Hz, 2.2H), 1.86 (ddd, *J* = 13.8, 11.5, 5.0 Hz, 2.2H), 1.79 (s, 6.6H), 1.33 – 1.24 (m, 2.2H), 0.77 – 0.71 (m, 2H), 0.65 – 0.57 (m, 3H), 0.47 (t, *J* = 7.3 Hz, 6.6H), 0.27 – 0.13 (m, 2.2H). ¹³C NMR (101 MHz, CDCl₃) δ 194.1, 193.6, 156.2, 154.3, 142.7, 141.7, 139.8, 138.0, 135.6, 135.4, 134.8, 130.2, 130.1, 129.4, 129.0, 128.8, 128.8, 128.5, 128.5, 128.4, 128.3, 128.3, 128.1, 128.0, 128.0, 127.7, 127.7, 127.6, 127.6, 127.5, 127.4, 127.4, 80.1, 79.6, 66.2, 65.8, 38.2, 37.0, 23.8, 23.6, 21.2, 20.2, 14.3, 14.1. HRMS (ESI) calcd. for C₄₂H₃₈NO₃ (M+H)⁺: 604.2846, Found: 604.2835.



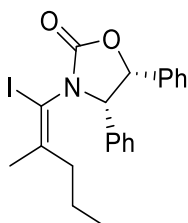
(4*S*,5*R*)-3-((2*E*,5*E/Z*)-4-oxo-2,3,6-triphenylnona-2,5-dien-5-yl)-4,5-diphenyloxazolidin-2-one (388b(5*E/Z*))

To a dried 50 mL flask was added **381** (0.23 g, 0.45 mmol), **394E** (0.31 g, 0.63 mmol), Pd(dtbpf)Cl₂ (0.01 g, 0.02 mmol), CuI (0.01 g, 0.04 mmol) and dissolved in anhydrous DMF (5 mL). The resulting mixture was then evacuated and backfilled with CO(g) three times, then heated to 60 °C and allowed to stir for 72 h. After which TLC indicated full consumption of **381**, the reaction was diluted with water (10 mL), extracted with EtOAc (2 x 10 mL), dried over MgSO₄ and concentrated under reduced pressure. The resulting crude reaction mixture was then chromatographed (10% – 15% EtOAc in PS, 5% step gradient), yielding **388b(5*E/Z*)** (0.24 g, 66%) as double bond isomers in 2.5:1 ratio (E:Z). R_f = 0.54 (20% EtOAc in PS); ¹H NMR (401 MHz, CDCl₃) δ 7.39 – 7.33 (m, 6.5H), 7.29 (t, *J* = 7.4 Hz, 7.5H), 7.21 – 6.91 (m, 60H), 6.88 – 6.80 (m, 7H), 6.62 (dd, *J* = 10.4, 4.8 Hz, 10H), 6.46 (d, *J* = 7.3 Hz, 2H), 6.09 (d, *J* = 7.3 Hz, 5H), 6.05 (d, *J* = 8.5 Hz, 2.5H), 5.61 (d, *J* = 8.5 Hz, 2.5H), 5.48 (d, *J* = 8.8 Hz, 1H), 4.49 (d, *J* = 8.8 Hz, 1H), 2.83 (ddd, *J* = 14.0, 10.2, 5.9 Hz, 1H), 2.69 (ddd, *J* = 13.9, 10.1, 5.9 Hz, 1H), 2.53 (ddd, *J* = 15.7, 10.9, 4.7 Hz, 2.5H), 2.38 (s, 3H), 2.21 (ddd, *J* = 15.8, 11.2, 4.4 Hz, 2.5H), 2.09 (s, 7.5H), 1.36 – 1.28 (m, 2.5H), 1.20 – 1.07 (m, 2.5H), 0.79 (t, *J* = 7.3 Hz, 3H), 0.77 – 0.67 (m, 9.5H). ¹³C NMR (101 MHz, CDCl₃) δ 195.0, 194.5, 157.7, 156.4, 144.6, 142.4, 142.4, 140.7, 139.9, 139.4, 139.3, 138.5, 136.1, 135.4, 135.4, 135.3, 135.0, 133.6, 131.7, 131.2, 130.7, 130.4, 129.4, 129.1, 128.9, 128.7, 128.6, 128.5, 128.5, 128.4, 128.3, 128.2, 128.0, 128.0, 128.0, 127.9, 127.8, 127.8, 127.7, 127.7, 127.5, 127.4, 127.4, 127.1, 126.9, 126.8, 126.5, 126.3, 126.2, 80.3, 80.2, 66.1, 65.7, 39.2, 37.0, 24.4, 23.6, 21.7, 20.6, 14.6, 14.4. HRMS (ESI) calcd. for C₄₂H₃₈NO₃ (M+H)⁺: 604.2846, Found: 604.2859.



(4*S*,5*R*)-3-((*S*)-3-methyl-5-oxo-3,4,4-triphenyl-2-propylcyclopent-1-en-1-yl)-4,5-diphenyloxazolidin-2-one (390)

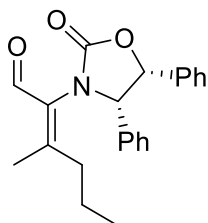
To a dried 5 mL flask with **388a**(*5E/Z*) (0.06 g, 0.09 mmol) in anhydrous DCM (0.9 mL) was added TiCl_4 (0.02 mL, 0.14 mmol) at -78°C and allowed to stir for 2.5 h at rt. Sat. aq. NaHCO_3 (1 mL) was added, diluted with water (1 mL), extracted with EtOAc (2 x 5 mL), dried over MgSO_4 and concentrated under reduced pressure. The resulting crude reaction mixture was chromatographed (3% EtOAc in 1:1 toluene : PS), yielding **390** (0.03 g, 53%) as clear oil. ^1H NMR (401 MHz, CDCl_3) δ 7.19 – 7.11 (m, 4H), 7.09 (d, $J = 7.8$ Hz, 2H), 7.06 – 6.98 (m, 8H), 6.97 – 6.89 (m, 6H), 6.85 (d, $J = 8.4$ Hz, 3H), 6.83 – 6.78 (m, 2H), 6.09 (d, $J = 8.7$ Hz, 1H), 5.82 (d, $J = 8.7$ Hz, 1H), 2.55 (ddd, $J = 12.8, 12.4, 4.6$ Hz, 1H), 2.41 (ddd, $J = 13.2, 12.0, 4.9$ Hz, 1H), 1.55 – 1.41 (m, 1H), 1.08 – 0.96 (m, 1H), 0.91 (t, $J = 7.2$ Hz, 3H). ^{13}C NMR (101 MHz, CDCl_3) δ 201.8, 175.4, 156.3, 143.3, 140.5, 139.3, 135.3, 135.1, 134.7, 130.4, 129.9, 128.7, 128.2, 128.1, 128.0, 128.0, 127.7, 127.7, 127.2, 126.4, 126.4, 126.1, 80.5, 70.4, 63.8, 58.6, 31.8, 21.6, 18.7, 15.5. HRMS (ESI) calcd. for $\text{C}_{42}\text{H}_{38}\text{NO}_3$ ($\text{M}+\text{H}$) $^+$: 604.2846, found 604.2861.



(4*S*,5*R*)-3-((*E*)-1-iodo-2-methylpent-1-en-1-yl)-4,5-diphenyloxazolidin-2-one (409)

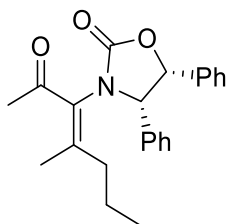
To a dried 250 mL flask with anhydrous DCM (6 mL) and Et_2O (36 mL) was added **379** (0.55 g, 1.82 mmol) and $\text{CuBr}\cdot\text{SMe}_2$ (0.04 g, 0.18 mmol). This mixture was cooled to -40°C and MeMgBr (1.2 mL, 3.0 M in Et_2O , 3.63 mmol) was added dropwise. The resulting brown reaction mixture was warmed to -20°C and allowed to stir for 1 h. At -78°C , a solution of I_2 (1.06 g, 4.18 mmol) in anhydrous Et_2O (20 mL) was added and allowed to stir for 20 min at 0°C . Sat. aq. $\text{Na}_2\text{S}_2\text{O}_3$ (30 mL) and sat. aq. NH_4Cl (30 mL) were added, diluted with water (25 mL), extracted with Et_2O (2 x 60 mL) and dried over MgSO_4 . The resulting crude reaction mixture was then chromatographed (10% EtOAc in PS), affording **409** as yellow solid (0.54 g, 66%). $R_f = 0.57$ (20% EtOAc in PS); MP = $95\text{--}98^\circ\text{C}$;

^1H NMR (401 MHz, CDCl_3) δ 7.18 – 7.11 (m, 4H), 7.06 (t, J = 7.4 Hz, 2H), 6.98 – 6.94 (m, 2H), 6.82 (d, J = 7.1 Hz, 2H), 5.84 (d, J = 8.6 Hz, 1H), 5.31 (d, J = 8.6 Hz, 1H), 2.22 (qdd, J = 13.4, 11.0, 5.3 Hz, 2H), 1.79 (s, 3H), 1.60 – 1.46 (m, 1H), 1.13 – 0.97 (m, 1H), 0.86 (t, J = 7.3 Hz, 3H). ^{13}C NMR (101 MHz, CDCl_3) δ 155.9, 148.4, 135.1, 132.9, 129.0, 128.7, 128.4, 128.1, 126.0, 90.9, 79.4, 67.8, 37.0, 25.9, 21.0, 14.4. HRMS (ESI) calcd. for $\text{C}_{21}\text{H}_{23}\text{INO}_2$ ($\text{M}+\text{H}$) $^+$: 448.0768, found 448.0767.



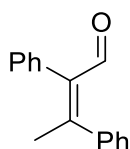
(Z)-3-methyl-2-((4S,5R)-2-oxo-4,5-diphenyloxazolidin-3-yl)hex-2-enal (415)

To a dried 50 mL flask with anhydrous DCM (3 mL) and Et_2O (20 mL) was added **379** (0.30 g, 0.98 mmol) and $\text{CuBr}\cdot\text{SMe}_2$ (0.02 g, 0.10 mmol). This mixture was cooled to $-40\text{ }^\circ\text{C}$ and MeMgBr (0.66 mL, 3.0 M in Et_2O , 1.97 mmol) was added dropwise. The resulting brown reaction mixture was warmed to $-20\text{ }^\circ\text{C}$ and allowed to stir for 1 h. At $-78\text{ }^\circ\text{C}$, *N*-formylmorpholine (0.59 mL, 5.60 mmol) was added to the reaction mixture and allowed to stir for 1 h at $0\text{ }^\circ\text{C}$. Sat. aq. NH_4Cl (20 mL) was added, diluted with water (20 mL), extracted with EtOAc (2 x 20 mL), dried over MgSO_4 and concentrated under reduced pressure. The resulting crude reaction mixture was chromatographed (25% - 30% EtOAc in PS, 5% step gradient), yielding **415** (0.19 g, 54%) as light brown wax. R_f = 0.26 (20% EtOAc in PS); ^1H NMR (401 MHz, CDCl_3) δ 9.88 (s, 1H), 7.17 – 7.11 (m, 3H), 7.10 – 7.05 (m, 2H), 7.05 – 6.99 (m, 3H), 6.83 (dd, J = 8.0, 1.3 Hz, 2H), 6.08 (d, J = 8.6 Hz, 1H), 5.55 (d, J = 8.5 Hz, 1H), 2.28 (dd, J = 8.6, 7.7 Hz, 2H), 2.17 (s, 3H), 1.58 – 1.46 (m, 2H), 0.86 (t, J = 7.1 Hz, 3H). ^{13}C NMR (101 MHz, CDCl_3) δ 186.3, 157.2, 135.3, 134.5, 130.4, 128.8, 128.5, 128.1, 128.0, 127.9, 126.0, 80.2, 38.2, 20.3, 16.8, 14.5. HRMS (ESI) calcd. for $\text{C}_{22}\text{H}_{24}\text{NO}_3$ ($\text{M}+\text{H}$) $^+$: 350.1751, found 350.1762.



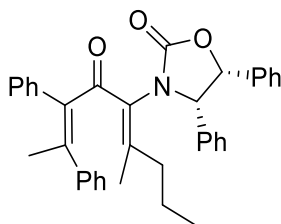
(4*S*,5*R*)-3-((*Z*)-4-methyl-2-oxohept-3-en-3-yl)-4,5-diphenyloxazolidin-2-one (416)

Obtained as the major product from 1,2-addition of alanate **399** to **415** follow by DMP oxidation. ^1H NMR (401 MHz, CDCl_3) δ 7.16 – 7.09 (m, 3H), 7.09 – 7.05 (m, 2H), 7.05 – 6.99 (m, 3H), 6.81 (d, J = 7.0 Hz, 2H), 6.01 (d, J = 8.4 Hz, 1H), 5.14 (d, J = 8.5 Hz, 1H), 2.17 (s, 3H), 2.19 – 2.12 (m, 2H), 1.91 (s, 3H), 1.53 – 1.39 (m, 1H), 1.06 – 0.98 (m, 1H), 0.85 (t, J = 7.3 Hz, 3H). ^{13}C NMR (101 MHz, CDCl_3) δ 198.0, 156.8, 151.9, 134.9, 133.7, 129.5, 128.9, 128.7, 128.1, 128.0, 128.0, 125.8, 79.6, 66.7, 53.5, 37.8, 29.8, 20.3, 19.1, 14.5. HRMS (ESI) calcd. for $\text{C}_{23}\text{H}_{26}\text{NO}_3$ ($\text{M}+\text{H}$) $^+$: 364.1907, found 364.1911.



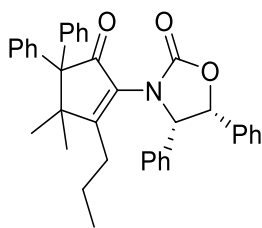
(*Z*)-2,3-diphenylbut-2-enal (417)

To a dried 25 mL flask with **393** (0.52 g, 1.61 mmol) in anhydrous THF (8.0 mL), was added *t*-BuLi (2.2 mL, 1.44 M in pentane, 3.22 mmol) at -78 °C and allowed to stir for 15 min. At -78 °C. *N*-formylmorpholine (1.3 mL, 12.9 mmol) was added and allowed to stir for 1 h. Sat. aq. NH_4Cl (8 mL) was added, diluted with water (8 mL), extracted with Et_2O (2 x 10 mL), dried over MgSO_4 and concentrated under reduced pressure. The resulting crude reaction mixture was chromatographed (7.5% – 10% EtOAc in PS, 2.5% step gradient), yielding **417** (0.16 g, 43%) as yellow powder. R_f = 0.1 (30% DCM in PS); ^1H NMR (401 MHz, CDCl_3) δ 9.66 (s, 1H), 7.47 – 7.42 (m, 5H), 7.40 – 7.34 (m, 3H), 7.21 (dd, J = 8.2, 1.4 Hz, 2H), 2.21 (s, 3H). ^{13}C NMR (101 MHz, CDCl_3) δ 192.9, 159.5, 140.5, 139.6, 135.4, 130.1, 129.0, 128.6, 128.4, 127.8, 24.9. HRMS (ESI) calcd. for $\text{C}_{16}\text{H}_{15}\text{O}$ ($\text{M}+\text{H}$) $^+$: 223.1117, found 223.1122.



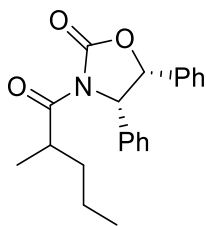
(4*S*,5*R*)-3-((2*Z*,5*Z*)-6-methyl-4-oxo-2,3-diphenylnona-2,5-dien-5-yl)-4,5-diphenyloxazolidin-2-one (410(2*Z*))

To a dried 10 mL flask with **409** (0.21 g, 0.46 mmol) in anhydrous THF (2.3 mL) was added *n*-BuLi (0.21 mL, 2.32 M in hexane, 0.48 mmol) at -90 °C and allowed to stir for 10 min. At -90 °C, **417** (0.21 g, 0.92 mmol) was added and allowed to stir for 1 h while temperature was maintained at -90 °C. Sat. aq. NH₄Cl (5 mL) was added, diluted with water (5 mL), extracted with Et₂O (2 x 5 mL), dried over MgSO₄ and concentrated under reduced pressure. To a solution of the crude reaction mixture in DCM (2 mL) was added Dess-Martin Periodinane (0.22 g, 0.46 mmol) at 0 °C and allowed to stir for 1 h. Sat. aq. NaHCO₃ (5 mL) was added, diluted with water (5 mL), extracted with DCM (2 x 5 mL), dried over MgSO₄ and concentrated under reduced pressure. The resulting crude reaction mixture was chromatographed (5% - 10% EtOAc in PS, 5% step gradient), giving **410(2*E/Z*)** (0.13 g, 51%) as a 1:1.4 mixture of *E/Z* isomers. To a solution of **410(2*E/Z*)** (0.15 g, 0.28 mmol) in anhydrous DCM (3 mL) was added BF₃·THF (0.03 mL, 0.28 mmol) at -78 °C and allowed to stir for 30 min. Sat. aq. NaHCO₃ (0.5 mL) was added, diluted with water (0.5 mL), extracted with DCM (2 x 2 mL), dried over MgSO₄ and concentrated under reduced pressure, yielded **410(2*Z*)** (0.13 g, 51% from **409**) as stereochemically pure double bond isomer. *R*_f = 0.53 (20% EtOAc in PS); ¹H NMR (401 MHz, CDCl₃) δ 7.44 – 7.27 (m, 10H), 7.12 – 7.04 (m, 3H), 7.01 – 6.87 (m, 5H), 6.63 (d, *J* = 6.9 Hz, 2H), 5.61 (d, *J* = 8.5 Hz, 1H), 4.47 (d, *J* = 8.5 Hz, 1H), 2.17 (s, 3H), 1.89 (qdd, *J* = 13.5, 10.8, 5.4 Hz, 2H), 1.68 (s, 3H), 0.75 – 0.72 (m, 1H), 0.55 (t, *J* = 7.2 Hz, 3H), 0.45 – 0.35 (m, 1H). ¹³C NMR (101 MHz, CDCl₃) δ 195.3, 156.6, 154.7, 142.2, 140.4, 140.3, 136.0, 135.4, 135.0, 130.4, 129.6, 128.9, 128.6, 128.5, 128.5, 128.1, 128.0, 127.9, 127.7, 127.6, 125.8, 79.6, 65.9, 38.2, 23.1, 20.2, 19.0, 14.2. HRMS (ESI) calcd. for C₃₇H₃₆NO₃ (M+H)⁺: 542.2690, found 542.2709.



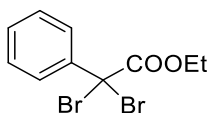
(4*S*,5*R*)-3-(3,3-dimethyl-5-oxo-4,4-diphenyl-2-propylcyclopent-1-en-1-yl)-4,5-diphenyloxazolidin-2-one (422)

To a dried 5 mL flask with **410(2Z)** (0.09 g, 0.16 mmol) in anhydrous DCM (2.0 mL) was added TiCl_4 (0.03 mL, 0.24 mmol) at -78°C and allowed to stir for 2 h at rt. Anhydrous DCE (1.6 mL) was added and allowed to stir for 24 h. Sat. aq. NaHCO_3 (1 mL) was added, diluted with water (1 mL), extracted with EtOAc (2 x 2 mL), dried over MgSO_4 and concentrated under reduced pressure. The resulting crude reaction mixture was purified by preparative reverse phase HPLC (10% - 100% MeCN in H_2O gradient over 30 minutes, 10 mL min^{-1} , Luna $5\mu\text{m}$ C8(2) 100 \AA $250 \times 21.2\text{ mm}$ column, UV detection at 254 nm, $t_R=23.0\text{ min}$), yielding **422** (0.02 g, 12%) as light yellow syrup. $R_f = 0.54$ (20% EtOAc in PS); ^1H NMR (401 MHz, CDCl_3) δ 7.34 – 7.30 (m, 10H), 7.25 (t, $J = 7.4\text{ Hz}$, 3H), 7.08 (dd, $J = 8.4, 1.3\text{ Hz}$, 2H), 7.04 (dt, $J = 2.2, 1.5\text{ Hz}$, 1H), 6.96 (t, $J = 7.7\text{ Hz}$, 2H), 6.79 (d, $J = 7.4\text{ Hz}$, 2H), 5.46 (d, $J = 8.3\text{ Hz}$, 1H), 5.34 (d, $J = 8.3\text{ Hz}$, 1H), 2.69 (td, $J = 12.7, 4.8\text{ Hz}$, 1H), 2.41 (td, $J = 12.6, 4.8\text{ Hz}$, 1H), 1.79 (tdd, $J = 12.3, 7.3, 5.0\text{ Hz}$, 1H), 1.37 (tdd, $J = 12.4, 7.2, 5.0\text{ Hz}$, 1H), 1.12 (s, 3H), 1.10 (t, $J = 7.6, 3\text{ Hz}$), 0.87 (s, 3H). ^{13}C NMR (101 MHz, CDCl_3) δ 201.2, 181.6, 155.4, 139.7, 139.6, 137.2, 136.9, 131.3, 130.3, 130.1, 129.2, 129.1, 128.9, 128.3, 128.0, 127.8, 127.0, 126.5, 126.2, 84.3, 69.6, 67.2, 50.4, 31.6, 30.6, 22.2, 21.6, 15.6. HRMS (ESI) calcd. for $\text{C}_{37}\text{H}_{36}\text{NO}_3$ ($\text{M}+\text{H}$) $^+$: 542.2690, found 542.2699.



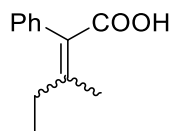
(4*S*,5*R*)-3-(2-methylpentanoyl)-4,5-diphenyloxazolidin-2-one (423)

Obtained as a side product from synthesis of **422** as a transparent syrup (0.01 g, 6%). ^1H NMR (401 MHz, CDCl_3) δ 7.10 (ddd, $J = 6.4, 3.0, 1.8$ Hz, 6H), 7.00 – 6.95 (m, 2H), 6.89 – 6.85 (m, 2H), 5.90 (d, $J = 7.7$ Hz, 1H), 5.69 (d, $J = 7.7$ Hz, 1H), 3.89 (h, $J = 6.8$ Hz, 1H), 1.78 – 1.68 (m, 1H), 1.37 – 1.30 (m, 1H), 1.26 (dt, $J = 15.0, 7.4$ Hz, 2H), 1.20 (d, $J = 6.8$ Hz, 3H), 0.87 (t, $J = 7.3$ Hz, 3H). ^{13}C NMR (101 MHz, CDCl_3) δ 176.8, 153.6, 134.9, 133.1, 128.5, 128.4, 128.3, 128.2, 126.8, 126.2, 80.1, 63.1, 47.6, 37.6, 35.7, 20.1, 19.3, 16.9, 14.1. HRMS (ESI) calcd. for $\text{C}_{21}\text{H}_{24}\text{NO}_3$ ($\text{M}+\text{H}$) $^+$: 338.1751, found 338.1749.



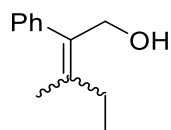
ethyl 2,2-dibromo-2-phenylacetate (442)

To a 500 mL flask with ethyl phenylacetate **441** (4.9 mL, 30.45 mmol) in chlorobenzene (150 mL) was added *N*-bromosuccinimide (24.4 g, 137 mmol) and benzoyl peroxide (1.05 g, 3.04 mmol, contains 30% H_2O content). This reaction mixture was heated to reflux overnight. The reaction was cooled and sat. aq. $\text{Na}_2\text{S}_2\text{O}_3$ (100 mL) was added, diluted with water (100 mL), extracted with EtOAc (250 mL), dried over MgSO_4 and concentrated under reduced pressure. The resulting crude reaction mixture was chromatographed (10% - 20% DCM in PS, 5% step gradient) to yield **442** (6.28 g, 64%) as clear liquid. ^1H NMR (600 MHz, CDCl_3) δ 7.71 – 7.69 (m, 2H), 7.38 – 7.34 (m, 3H), 4.35 (q, $J = 7.1$ Hz, 2H), 1.31 (t, $J = 7.1$ Hz, 3H). Spectra conform to previously reported data.¹¹¹



3-methyl-2-phenylpent-2-enoic acid (**436**)

To a dried 50 mL flask with **442** (0.73 g, 2.27 mmol) in anhydrous THF (11 mL) was added *t*-BuLi (6.0 mL, 1.51 M in pentane, 9.09 mmol) at -78 °C dropwise and allowed to stir for 1 h. The reaction was then warmed up to 0 °C and stirred for 30 min. 2-butanone (0.31 mL, 3.41 mmol) was then added and allowed to stir for 1 h at rt. 1M aq. HCl (20 mL) was added, extracted with EtOAc (2 x 20 mL), dried over MgSO₄ and concentrated under reduced pressure. The resulting crude reaction mixture was then chromatographed (20% EtOAc in PS) to yield **436** (0.29 g, 66%) as yellow wax in a 1:2 mixture of *E*:*Z* isomers. *R*_f = 0.26 (20% EtOAc in PS); ¹H NMR (401 MHz, CDCl₃) δ 7.35 (m, 7.5H), 7.32 – 7.25 (m, 4.5H), 7.20 – 7.16 (m, 7.5H), 2.59 (q, *J* = 7.5 Hz, 5H), 2.21 (s, 3H), 1.97 (q, *J* = 7.5 Hz, 2H), 1.68 (s, 7.5H), 1.15 (t, *J* = 7.5 Hz, 7.5H), 0.96 (t, *J* = 7.5 Hz, 3H). ¹³C NMR (101 MHz, CDCl₃) δ 173.6, 173.4, 156.0, 155.4, 138.5, 138.2, 129.7, 129.7, 128.8, 128.3, 128.3, 127.2, 127.2, 30.6, 29.3, 21.7, 20.2, 13.1, 12.5. HRMS (ESI) calcd. for C₁₂H₁₅O₂ (M+H)⁺: 191.1067, found 191.1072.

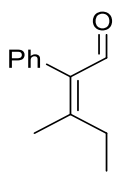


(*E/Z*)-3-methyl-2-phenylpent-2-en-1-ol (**437**(*E/Z*))

To a dried 100 mL flask with **436** (1.37 g, 6.72 mmol) in anhydrous Et₂O (34 mL) was added slowly LiAlH₄ (0.64 g, 16.8 mmol) at 0 °C. The resulting reaction mixture was warmed to rt and allowed to stir for 3 h. Water was added (30 mL), followed by Et₂O (30 mL). The organic layer was separated and washed with 1M aq. HCl (30 mL), dried over MgSO₄ and concentrated under reduced pressure. The resulting crude reaction mixture was then chromatographed (15% - 20% EtOAc in PS, 2.5% step gradient) to yield main product **437**(*Z*) (0.18 g, 15%) as opaque oil. *R*_f = 0.18 (20% EtOAc in PS); ¹H NMR (401 MHz, CDCl₃) δ 7.34 (t, *J* = 7.3 Hz, 2H), 7.25 (t, *J* = 7.4 Hz, 1H), 7.18 (dt, *J* = 8.0, 1.7 Hz, 2H), 4.40 (d, *J* = 0.6 Hz, 2H), 2.29 (q, *J* = 7.6 Hz, 2H), 1.60 (s, 3H), 1.38 (brs, 1H), 1.10 (t, *J* = 7.6 Hz, 3H). ¹³C NMR (101 MHz, CDCl₃) δ 141.6, 138.4, 134.4, 129.3, 128.4, 126.7, 63.1, 27.2, 19.9, 13.8. HRMS (ESI) calcd. for C₁₂H₁₄ONa (M+Na)⁺: 199.1093, found 199.1095.

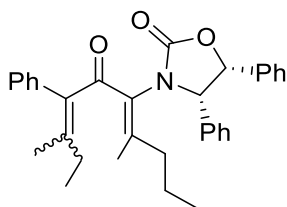
437(*E*) (0.044 g, 4 %) was obtained as a minor isomer. *R*_f = 0.17 (20% EtOAc in PS); ¹H NMR (401 MHz, CDCl₃) δ 7.34 (tt, *J* = 8.1, 1.5 Hz, 2H), 7.25 (t, *J* = 7.4 Hz, 1H), 7.16 (dt, *J* = 8.0, 2.4 Hz, 2H), 4.38 (s, 2H), 1.92 (q, *J* = 7.7 Hz, 2H), 1.89 (s, 3H), 1.44 (brs, 1H), 0.94 (t, *J* = 7.5 Hz, 3H). ¹³C NMR

(101 MHz, CDCl₃) δ 141.5, 137.8, 134.5, 129.1, 128.4, 126.7, 63.7, 28.7, 17.0, 13.0.



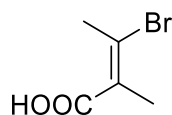
(Z)-3-methyl-2-phenylpent-2-enal (429Z)

To a solution of **437(Z)** (0.15 g, 0.85 mmol) in DCM (4 mL) was added Dess-Martin Periodinane (0.54 g, 1.28 mmol) at 0 °C and allowed to stir for 1 h. Sat. aq. NaHCO₃ (5 mL) was added, diluted with water (5 mL), extracted with Et₂O (2 x 5 mL), dried over MgSO₄ and concentrated under reduced pressure. The resulting crude reaction mixture was triturated with PS (10 mL) and filtered. The filtrate was concentrated under reduced pressure, yielding **429Z** (0.12 g, 82%) as yellow syrup. R_f = 0.42 (20% EtOAc in PS); ¹H NMR (401 MHz, CDCl₃) δ 10.25 (s, 1H), 7.37 (tt, J = 8.1, 1.7 Hz, 2H), 7.30 (tt, J = 2.8, 1.6 Hz, 1H), 7.04 (dt, J = 7.1, 1.5 Hz, 2H), 2.76 (q, J = 7.6 Hz, 2H), 1.84 (s, 3H), 1.27 (t, J = 7.6 Hz, 4H). HRMS (ESI) calcd. for C₁₂H₁₅O (M+H)⁺: 175.1117, found 175.1119. Result is not fully characterized due to insufficient quantity obtained.

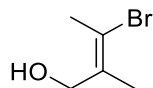


(4*S*,5*R*)-3-((4*Z*,7*Z*/*E*)-4,8-dimethyl-6-oxo-7-phenyldeca-4,7-dien-5-yl)-4,5-diphenyloxazolidin-2-one (430(7*E*/7*Z*))

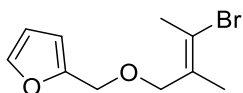
To a dried 10 mL flask with **409** (0.13 g, 0.29 mmol) in anhydrous THF (2 mL) was added *n*-BuLi (0.13 mL, 2.40 M in hexane, 0.30 mmol) at -90 °C and allowed to stir for 10 mins. At -90 °C, a solution of **429(Z)** (0.100 g, 0.56 mmol) in anhydrous THF (1 mL) was added and allowed to stir for 1 h while temperature was maintained at -90 °C. Sat. aq. NH₄Cl (2 mL) was added, diluted with water (2 mL), extracted with Et₂O (2 x 5 mL), dried over MgSO₄ and concentrated under reduced pressure. To a solution of the crude reaction mixture in DCM (1.4 mL), Dess-Martin Periodinane (0.22 g, 0.46 mmol) was added at 0 °C and allowed to stir for 1 h. Sat. aq. NaHCO₃ (2 mL) was added, diluted with water (2 mL), extracted with DCM (2 x 5 mL), dried over MgSO₄ and concentrated under reduced pressure. The resulting crude reaction mixture was purified through reversed phase chromatography (C18 silica gel, 10% - 90% MeOH in H₂O), yielding a 1:4 mixture of **430(7*E*)**:**430(7*Z*)** (0.05 g, 34%) as clear wax. *R*_f = 0.57 (20% EtOAc in PS); ¹H NMR (401 MHz, CDCl₃) δ 7.25 – 7.20 (m, 4.5H), 7.16 – 7.07 (m, 7.5H), 7.04 – 6.92 (m, 8H), 6.76 – 6.71 (m, 2.5H), 5.92 (d, *J* = 8.6 Hz, 0.25H), 5.91 (d, *J* = 8.6 Hz, 1H), 5.11 (d, *J* = 8.6 Hz, 1H), 5.06 (d, *J* = 8.6 Hz, 0.25H), 2.29 – 2.14 (m, 5H), 2.04 (s, 0.75H), 2.03 (s, 3H), 1.87 (s, 0.75H), 1.82 (s, 3H), 1.09 (t, *J* = 7.5 Hz, 4H), 0.70 – 0.61 (m, 5H). ¹³C NMR (101 MHz, CDCl₃) δ 195.0, 156.6, 155.2, 144.7, 138.8, 135.9, 135.5, 134.9, 130.3, 129.4, 128.7, 128.3, 128.3, 128.0, 128.0, 127.8, 127.5, 125.9, 79.6, 65.7, 38.5, 29.4, 28.4, 20.3, 19.5, 19.4, 19.4, 19.2, 14.5, 14.2, 12.9, 12.6. HRMS (ESI) calcd. for C₃₃H₃₆NO₃ (M+H)⁺: 494.2690, found 494.2695.

**(E)-3-bromo-2-methylbut-2-enoic acid (453)**

Bromine (8.1 mL, 157 mmol) was slowly added to a stirring solution of tiglic acid **453** (15.0 g, 150 mmol) in CHCl_3 (150 mL) at 45 °C under N_2 . The resulting reaction mixture was stirred for 1.5 h then cooled and sat. aq. NaHCO_3 (160 mL) was added. The organic layer was separated and washed with sat. aq. NaHCO_3 (2 x 90 mL). The combined aq. layer was then acidified with 37% aq. HCl (200 mL), cooled to 4 °C overnight and filtered to give **454** in quantitative yield. ^1H NMR (400 MHz, CDCl_3) δ 4.85 (q, $J = 6.7$ Hz, 1H), 1.99 (s, 3H), 1.91 (d, $J = 6.8$ Hz, 3H). Spectra conform to previously reported data.⁶³ **454** (31.3 g, 120 mmol) was dissolved in MeOH (17 mL) and 129 g of a 25% KOH in MeOH solution (42.5 g, 758 mol) was added slowly with a dropping funnel at 0 °C. K_2CO_3 (3.33 g, 24.1 mmol) was added and reaction was heated to 55 °C for 2h at which point the reaction mixture was poured into a 6M aq. HCl (135 mL) and diluted with H_2O (408 mL). The mixture was then cooled to 0 °C overnight and filtered to yield **455** (19.3 g, 89 %) as white crystalline. ^1H NMR (400 MHz, CDCl_3) δ 2.76 (q, $J = 1.6$ Hz, 1H), 2.12 (q, $J = 1.6$ Hz, 1H). Spectra conform to previously reported data.¹¹²

**(E)-3-bromo-2-methylbut-2-en-1-ol (456)**

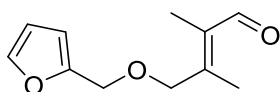
To a dried 250 mL flask with **455** (3.01g, 16.9 mmol) in anhydrous THF (170 mL) was added LiAlH_4 (0.80 g, 20.9 mmol) at 0 °C. The reaction mixture was then allowed to stir for 5 h at rt. Water (0.8 mL) was added dropwise, followed by 3M aq. NaOH (0.8 mL). The reaction mixture was filtered and rinsed with Et_2O (2 x 100 mL). The combined organic layer was washed with water (100 mL) and brine (100 mL), dried over MgSO_4 and concentrated under reduced pressure to give **456** (2.59 g, 94%) as white solid. ^1H NMR (401 MHz, CDCl_3) δ 4.11 (s, 2H), 2.31 (d, $J = 1.5$ Hz, 3H), 1.89 (q, $J = 1.5$ Hz, 3H). Spectra conform to previously reported data.¹¹³



(*E*)-2-(((3-bromo-2-methylbut-2-en-1-yl)oxy)methyl)furan (446**)**

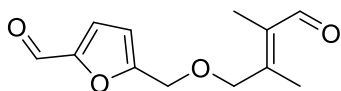
To a dried 250 mL flask with **456** (2.81 g, 17.0 mmol) and NEt₃ (4.7 mL, 3.40 mmol) in anhydrous DCM (85 mL), was added MsCl (2.0 mL, 25.5 mmol) at 0 °C. The resulting mixture was allowed to stir for 10 min at 0 °C. Ice was added to the reaction mixture, followed by the addition of water (80 mL), DCM (80 mL) and sat. aq. NaHCO₃ (80 mL). The resulting organic layer was washed with brine (80 mL), dried over MgSO₄, filtered and concentrated under reduced pressure, yielding mesylate **457**, which was used in the next step without further purification. ¹H NMR (400 MHz, CDCl₃) δ 4.79 – 4.71 (s, 2H), 3.03 – 2.97 (s, 3H), 2.44 (dd, *J* = 2.9, 1.3 Hz, 3H), 1.97 (q, *J* = 1.5 Hz, 3H). Spectra conform to previously reported data.⁶³

To a dried 250 mL flask with furfural alcohol (2.4 mL, 27.8 mmol) in anhydrous THF (70 mL), was added *n*-BuLi (11.4 mL, 2.37 M in pentane, 27.1 mmol) dropwise at 0 °C. The resulting reaction mixture was allowed to stir for 1.5 h. A solution of mesylate **457** (3.29 g, 13.5 mmol) in anhydrous THF was added into the reaction mixture at 0 °C and allowed to stir overnight at rt. NaI (0.61 g, 4.06 mmol) was added then allowed to stir overnight at 50 °C. Sat. aq. NH₄Cl (50 mL) was added, diluted with water (50 mL), extracted with EtOAc (2 x 70 mL), dried over MgSO₄ and concentrated under reduced pressure. The resulting crude reaction mixture was then chromatographed (30% DCM in PS), yielding **446** (2.23 g, 67%) as yellow oil. *R*_f = 0.25 (30% DCM in PS, stains black in PMA dip). ¹H NMR (401 MHz, CDCl₃) δ 7.41 (dd, *J* = 1.8, 0.8 Hz, 1H), 6.35 (dd, *J* = 3.2, 1.8 Hz, 1H), 6.32 (d, *J* = 3.1 Hz, 1H), 4.40 (s, 2H), 4.03 (s, 2H), 2.34 (d, *J* = 1.5 Hz, 3H), 1.91 (q, *J* = 1.5 Hz, 3H). ¹³C NMR (101 MHz, CDCl₃) δ 151.8, 143.1, 131.4, 122.6, 110.4, 109.6, 69.1, 63.6, 25.3, 21.6. HRMS (ESI) calcd. for C₁₀H₁₄BrO₂ (M+H)⁺: 245.0172, found 245.0163.



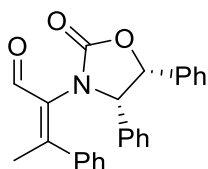
(E)-4-(furan-2-ylmethoxy)-2,3-dimethylbut-2-enal (458)

To a dried 50 mL flask with **446** (0.34 g, 1.38 mmol) in anhydrous THF (7 mL), was added *t*-BuLi (1.5 mL, 1.58 M in pentane, 2.35 mmol) at -78 °C and allowed to stir for 30 min. *N*-formylmorpholine (0.42 mL, 4.14 mmol) was then added and allowed to stir for 1 h at -78 °C. Sat. aq. NH₄Cl (5 mL) was added, diluted with water (5 mL), extracted with Et₂O (2 x 10 mL), dried over MgSO₄ and concentrated under reduced pressure. The resulting crude reaction mixture was then chromatographed (10% EtOAc in PS) to yield **458** as yellow oil (0.29 g, 55%). *R*_f = 0.30 (20% EtOAc in PS); ¹H NMR (401 MHz, CDCl₃) δ 10.14 (s, 1H), 7.40 (dd, *J* = 1.8, 0.9 Hz, 1H), 6.33 (tdd, *J* = 3.2, 2.0, 1.1 Hz, 2H), 4.45 (s, 2H), 4.18 (s, 2H), 2.19 (d, *J* = 1.4 Hz, 3H), 1.71 (ddd, *J* = 2.1, 1.4, 0.7 Hz, 3H). ¹³C NMR (101 MHz, CDCl₃) δ 191.7, 153.0, 151.4, 143.1, 133.2, 110.5, 109.9, 70.8, 64.6, 14.4, 10.5. HRMS (ESI) calcd. for C₁₁H₁₄O₃Na (M+Na)⁺: 217.0835, found 217.0838.



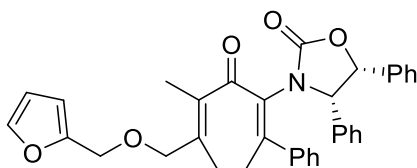
(E)-5-(((2,3-dimethyl-4-oxobut-2-en-1-yl)oxy)methyl)furan-2-carbaldehyde (459)

Obtained as the side product from the formation of **458**, when slight excess of *t*-BuLi was added to the reaction. *R*_f = 0.19 (20% EtOAc in PS); ¹H NMR (401 MHz, CDCl₃) δ 10.17 (s, 1H), 9.63 (s, 1H), 7.22 (d, *J* = 3.5 Hz, 1H), 6.55 (d, *J* = 3.5 Hz, 1H), 4.56 (s, 2H), 4.26 (s, 2H), 2.23 (d, *J* = 1.4 Hz, 3H), 1.76 – 1.72 (m, 3H). ¹³C NMR (101 MHz, CDCl₃) δ 191.6, 177.8, 157.8, 151.9, 133.5, 111.7, 71.8, 64.9, 14.4, 10.6. HRMS (ESI) calcd. for C₁₂H₁₅O₄ (M+H)⁺: 223.0965, found 223.0971.



(Z)-2-((4S,5R)-2-oxo-4,5-diphenyloxazolidin-3-yl)-3-phenylbut-2-enal (184)

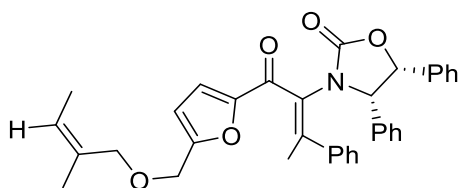
To a dried 50 mL flask with anhydrous DCM (5 mL) and Et₂O (30 mL) was added **183** (0.51 g, 1.50 mmol) and CuBr.SMe₂ (0.03 g, 0.15 mmol). This mixture was cooled to -40 °C and MeMgBr (1.0 mL, 3.0 M in Et₂O, 2.94 mmol) was added dropwise and allowed to stir for 30 min. At -78 °C, *N*-formylmorpholine (0.44 mL, 4.42 mmol) was added to the reaction mixture and allowed to stir for 1 h at rt. Sat. aq. NH₄Cl (20 mL) was added, diluted with water (20 mL), extracted with EtOAc (2 x 30 mL), dried over MgSO₄ and concentrated under reduced pressure. The resulting crude reaction mixture was chromatographed (25% - 30% EtOAc in PS, 5% step gradient), yielding **184** (0.39 g, 68%) as orange syrup. ¹H NMR (400 MHz, CDCl₃) δ 10.02 (s, 1H), 7.51 – 7.42 (m, 3H), 7.30 – 7.26 (m, 2H), 7.08 – 6.95 (m, 4H), 6.83 (dd, *J* = 9.8, 5.0 Hz, 4H), 6.34 (d, *J* = 7.5 Hz, 2H), 5.59 (d, *J* = 8.8 Hz, 1H), 4.71 (brd, *J* = 7.9 Hz, 1H), 2.42 (s, 3H). Spectra conform to previously reported data.⁶⁵



(4S,5R)-3-((2Z,5E)-7-(furan-2-ylmethoxy)-5,6-dimethyl-4-oxo-2-phenylhepta-2,5-dien-3-yl)-4,5-diphenyloxazolidin-2-one (447)

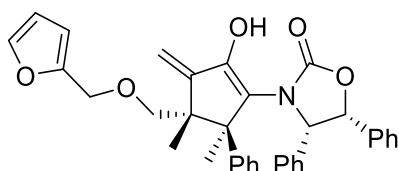
To a dried 25 mL flask with **446** (0.17 g, 0.70 mmol) in anhydrous Et₂O (4 mL), was added *t*-BuLi (0.80 mL, 1.48 M in hexane, 0.70 mmol) at -78 °C and allowed to stir for 30 min. To this reaction mixture was added AlMe₃ (0.19 mL, 2.0 M in toluene, 0.38 mmol), followed by a solution of **184** (0.15 g, 0.38 mmol) in anhydrous Et₂O (4 mL), then allowed to stir for 15 min at -78 °C. Sat. aq. NaHCO₃ (3 mL) was added, diluted with water (3 mL), extracted with Et₂O (2 x 5 mL), dried over MgSO₄ and concentrated under reduced pressure. To a solution of the crude reaction mixture in DCM (2 mL) was added NaHCO₃ (0.07, 0.85 mmol), followed by Dess-Martin periodinane (0.15 g, 0.34 mmol) at 0 °C and allowed to stir for 2 h. The reaction mixture was then diluted with water (2 mL), extracted with DCM (2 x 3 mL), dried over MgSO₄ and concentrated under reduced pressure. The resulting crude reaction mixture was chromatographed (22.5% EtOAc in PS), yielding **447** (0.08 g, 37%) as yellow syrup. ¹H NMR (401 MHz, CDCl₃) δ 7.45 – 7.40 (m, 4H), 7.17 (dd, *J* = 6.7, 3.0 Hz, 2H), 7.08 – 6.99 (m, 5H), 6.91 (t, *J* = 7.6 Hz, 2H), 6.88 – 6.79 (m, 2H), 6.59 (d, *J* = 7.2 Hz, 2H), 6.36

(dd, $J = 3.1, 1.8$ Hz, 1H), 6.34 (d, $J = 2.8$ Hz, 1H), 5.56 (d, $J = 8.8$ Hz, 1H), 4.56 (d, $J = 8.7$ Hz, 1H), 4.44 (s, 2H), 4.09 (s, 2H), 2.09 (s, 3H), 1.98 (s, 3H), 1.97 (s, $J = 1.4$ Hz, 3H).. Result is not fully characterized due to insufficient quantity obtained.



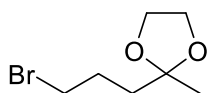
(4*S*,5*R*)-3-((*Z*)-1-(5-((((*Z*)-2-methylbut-2-en-1-yl)oxy)methyl)furan-2-yl)-1-oxo-3-phenylbut-2-en-2-yl)-4,5-diphenyloxazolidin-2-one (462)

Obtained alongside with **447** when slight excess of *t*-BuLi was added to the reaction. ^1H NMR (401 MHz, CDCl_3) δ 7.42 (dd, $J = 3.9, 2.5$ Hz, 5H), 7.36 (d, $J = 3.5$ Hz, 1H), 7.22 (dd, $J = 6.6, 3.0$ Hz, 3H), 7.05 – 6.97 (m, 6H), 6.90 (t, $J = 7.6$ Hz, 3H), 6.80 (dd, $J = 7.3, 1.9$ Hz, 3H), 6.67 – 6.62 (m, 2H), 6.49 (d, $J = 3.5$ Hz, 1H), 5.53 (d, $J = 8.6$ Hz, 1H), 5.48 (dd, $J = 13.9, 7.0$ Hz, 1H), 4.67 (d, $J = 8.5$ Hz, 1H), 4.47 (s, 2H), 4.07 (s, 2H), 1.88 (s, 3H), 1.74 (dt, $J = 2.9, 1.4$ Hz, 3H), 1.62 (dd, $J = 6.9, 1.4$ Hz, 3H). ^{13}C NMR (101 MHz, CDCl_3) δ 180.5, 158.3, 156.8, 152.5, 141.7, 140.0, 134.8, 133.1, 132.0, 128.9, 128.8, 128.7, 128.2, 128.0, 127.9, 127.9, 127.5, 126.2, 124.7, 121.8, 111.3, 80.7, 68.9, 65.9, 63.9, 22.9, 22.3, 21.7, 14.3, 13.5.



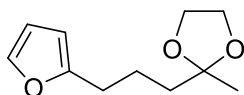
(4*S*,5*R*)-3-((4*S*,5*S*)-4-((furan-2-ylmethoxy)methyl)-2-hydroxy-4,5-dimethyl-3-methylene-5-phenylcyclopent-1-en-1-yl)-4,5-diphenyloxazolidin-2-one (464)

To a dried 5 mL flask with **447** (0.06 g, 0.11 mmol) in anhydrous 1,4-dioxane (1 mL) was added MeSO₃H (0.01 mL, 0.15 mmol) and allowed to stir overnight. Sat. aq. NaHCO₃ (1 mL) was added, diluted with water (1 mL), extracted with DCM (2 x 2 mL), dried over MgSO₄ and concentrated under reduced pressure. The resulting crude reaction mixture was chromatographed (15% – 20% EtOAc in PS, 5% step gradient) to yield **464** (0.01 g, 17%) as clear syrup. ¹H NMR (401 MHz, CDCl₃) δ 7.89 (s, 1H), 7.39 – 7.32 (m, 6H), 7.11 – 6.99 (m, 6H), 6.77 (dd, *J* = 8.3, 1.3 Hz, 2H), 6.75 – 6.70 (m, 2H), 6.29 (dd, *J* = 3.2, 1.9 Hz, 1H), 6.18 (d, *J* = 3.1 Hz, 1H), 5.49 (d, *J* = 7.9 Hz, 1H), 5.30 (s, 1H), 4.76 (d, *J* = 7.9 Hz, 1H), 4.69 (s, 1H), 4.32 (d, *J* = 13.0 Hz, 1H), 4.21 (d, *J* = 13.0 Hz, 1H), 3.49 (d, *J* = 9.4 Hz, 1H), 3.30 (d, *J* = 9.4 Hz, 1H), 1.26 (s, 3H), 0.73 (s, 3H). HRMS (ESI) calcd. for C₃₅H₃₄NO₅ (M+H)⁺: 548.2431, found 548.2432. Result is not fully characterized due to insufficient quantity obtained.



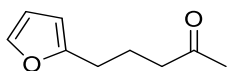
2-(3-bromopropyl)-2-methyl-1,3-dioxolane (470)

To a 50 mL flask with 5-bromo-pentanone **469** (5.51 g, 33.4 mmol), triethyl orthoformate (17 mL, 100 mmol) and ethylene glycol (7.5 mL, 133 mmol), was added aq. HBr solution (1 drop, 33% in acetic acid). The resulting reaction mixture was stirred for 10 min. Sat. aq. NaHCO₃ (5 mL) was added, diluted with water (5 mL), extracted with PS (2 x 10 mL), dried over MgSO₄ and concentrated under reduced pressure, giving **470** (7.0 g, quantitative). ¹H NMR (401 MHz, CDCl₃) δ 3.98 – 3.90 (m, 4H), 3.44 (t, *J* = 6.8 Hz, 2H), 2.04 – 1.93 (m, 2H), 1.84 – 1.73 (m, 2H), 1.32 (s, 3H). Spectra conform to previously reported data.¹¹⁴



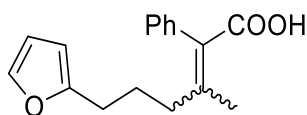
2-(3-(furan-2-yl)propyl)-2-methyl-1,3-dioxolane (**471**)

To a dried 500 mL 2-necked flask with furan (5.0 mL, 68.9 mmol) in anhydrous THF (230 mL), was added *n*-BuLi (26.8 mL, 2.50 M in hexane, 67.0 mmol) dropwise at 0 °C. This reaction mixture was allowed to stir for 1.5 h, then a solution of **470** (4.01 g, 19.2 mmol) in anhydrous THF (20 mL) was added at 0 °C. The reaction mixture was allowed stir overnight at rt. Sat. aq. NH₄Cl (200 mL) was added, diluted with water (150 mL), extracted with Et₂O (200 mL), dried over MgSO₄ and concentrated under reduced pressure to yield **471** (3.50 g, 93%) as a dark liquid. *R*_f = 0.26 (10% EtOAc in PS, stains black in PMA dip); ¹H NMR (401 MHz, CDCl₃) δ 7.29 (dd, *J* = 1.8, 0.8 Hz, 1H), 6.26 (dd, *J* = 3.1, 1.9 Hz, 1H), 5.98 (dd, *J* = 3.1, 0.8 Hz, 1H), 3.99 – 3.85 (m, 4H), 2.63 (t, *J* = 7.0 Hz, 2H), 1.83 – 1.62 (m, 4H), 1.31 (s, 3H). ¹³C NMR (101 MHz, CDCl₃) δ 156.2, 140.9, 110.16, 110.08, 104.9, 64.8, 38.7, 28.1, 24.0, 22.7. HRMS (ESI) calcd. for C₃₁H₃₉OS₂ (M+H)⁺: 491.24347, Found: 491.2441.



5-(furan-2-yl)pentan-2-one (**472**)

To a 250 mL flask with **471** (3.50 g, 17.8 mmol) in THF (77 mL) was slowly added 2M aq. HCl (77 mL) at 0 °C. This reaction mixture was allowed to stir for 2 h. The reaction mixture was diluted with water (100 mL), extracted with Et₂O (2 x 100 mL), dried over MgSO₄ and concentrated under reduced pressure to give **472** (2.66 g, 98%) as dark liquid. *R*_f = 0.12 (30% DCM in PS); ¹H NMR (401 MHz, CDCl₃) δ 7.29 (dd, *J* = 1.8, 0.8 Hz, 1H), 6.27 (dd, *J* = 3.1, 1.9 Hz, 1H), 5.99 (dd, *J* = 3.1, 0.8 Hz, 1H), 2.64 (t, *J* = 7.2 Hz, 2H), 2.46 (t, *J* = 7.3 Hz, 2H), 2.12 (s, 3H), 1.91 (p, *J* = 7.4 Hz, 2H). ¹³C NMR (101 MHz, CDCl₃) δ 208.7, 155.4, 141.1, 110.2, 105.4, 42.8, 30.1, 27.2, 22.2.



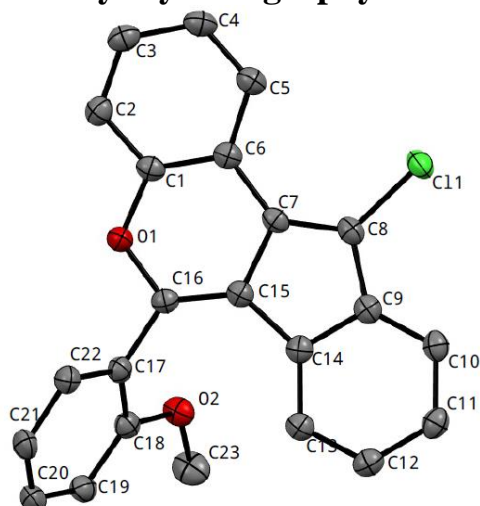
(*E/Z*)-6-(furan-2-yl)-3-methyl-2-phenylhex-2-enoic acid (473**(*E/Z*))**

To a dried 25 mL flask with **442** (0.34 g, 1.06 mmol) in anhydrous THF (5 mL) was added *t*-BuLi (2.7 mL, 1.59 M in pentane, 4.22 mmol) at -78 °C dropwise and allowed to stir for 1 h. The reaction mixture was then warmed up to 0 °C and allowed to stir for 30 min. A solution of **472** (0.27 g, 1.58 mmol) in anhydrous THF (1 mL) was added and allowed reaction to stir for 1 h at rt. 1M aq. HCl (5 mL) was added, diluted with water (5 mL), extracted with EtOAc (2 x 10 mL), dried over MgSO₄ and concentrated under reduced pressure. The resulting crude reaction mixture was then chromatographed (20% EtOAc in PS) to yield **473**(*E/Z*) (0.20, 70%) as brown wax in 1:2 ratio of *E*:*Z* isomers.

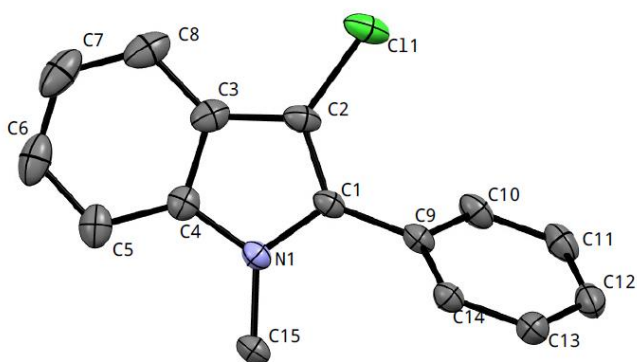
473E: *R*_f = 0.29 (20% EtOAc in PS); ¹H NMR (401 MHz, CDCl₃) δ 7.37 – 7.28 (m, 3H), 7.23 (dd, *J* = 1.8, 0.8 Hz, 1H), 7.17 – 7.13 (m, 2H), 6.21 (dd, *J* = 3.1, 1.9 Hz, 1H), 5.82 (dd, *J* = 3.1, 0.8 Hz, 1H), 2.46 (t, *J* = 7.5 Hz, 2H), 2.20 (s, 3H), 2.04 – 1.99 (m, 2H), 1.72 (ddd, *J* = 15.4, 12.4, 6.4 Hz, 2H). ¹³C NMR (101 MHz, CDCl₃) δ 172.9, 155.9, 153.5, 141.0, 138.3, 129.7, 129.7, 128.4, 127.4, 116.8, 110.2, 105.1, 35.6, 28.1, 26.9, 22.2. HRMS (ESI) calcd. for C₁₇H₁₉O₃ (M+H)⁺: 271.1329, found 271.1328.

473Z: *R*_f = 0.22 (20% EtOAc in PS); ¹H NMR (401 MHz, CDCl₃) δ 7.36 (tt, *J* = 7.8, 1.6 Hz, 2H), 7.30 (dt, *J* = 3.8, 1.5 Hz, 1H), 7.28 (dd, *J* = 1.8, 0.7 Hz, 1H), 7.17 (dd, *J* = 8.1, 1.3 Hz, 2H), 6.26 (dd, *J* = 3.1, 1.9 Hz, 1H), 6.02 (dd, *J* = 3.1, 0.7 Hz, 1H), 2.71 (t, *J* = 7.6 Hz, 2H), 2.67 – 2.61 (m, 2H), 1.92 (dt, *J* = 15.3, 7.7 Hz, 2H), 1.68 (s, 3H). ¹³C NMR (101 MHz, CDCl₃) δ 172.9, 155.9, 153.5, 141.0, 138.3, 129.7, 129.7, 128.4, 127.4, 116.8, 110.2, 105.1, 35.6, 28.1, 26.9, 22.2. HRMS (ESI) calcd. for C₁₇H₁₉O₃ (M+H)⁺: 271.1329, found 271.1330.

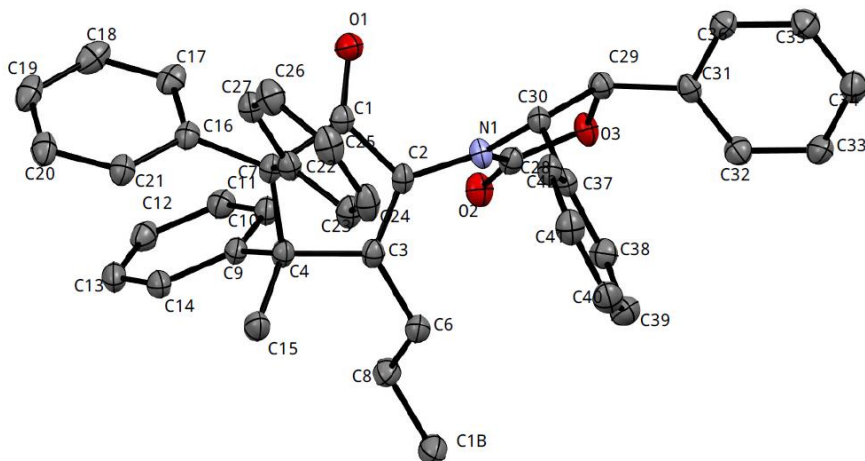
4.3 X-ray crystallography structure



Crystal data for **275**. $C_{23}H_{15}ClO_2$, $M = 358.80$, $T = 100.0(10)$ K, $\lambda = 1.54184$ Å, Monoclinic, space group P 21/c, $a = 8.11170(10)$ Å, $b = 14.62620(10)$ Å, $c = 14.5010(2)$ Å, $V = 1693.18(3)$ Å³, $Z = 4$, $D_c = 1.408$ mg M⁻³, $\mu(\text{Mo-K}\alpha) = 2.109$ mm⁻¹, $F(000) = 744$, crystal size 0.313 x 0.218 x 0.184 mm³, $\theta_{\text{max}} = 77.12^\circ$, 20393 reflections measured, 3552 independent reflections [$R(\text{int}) = 0.0514$], the final $R = 0.0412$ [$I > 2\sigma(I)$] and $wR(F^2) = 0.111$ (all data), GOOF = 1.082.



Crystal data for **295a**. $C_{15}H_{12}ClN$, $M = 241.71$, $T = 100.0(10)$ K, $\lambda = 0.71073$ Å, Monoclinic, space group P 21/n, $a = 11.9505(3)$ Å, $b = 10.1422(3)$ Å, $c = 19.8545(7)$ Å, $V = 2405.18(13)$ Å³, $Z = 8$, $D_c = 1.335$ mg M⁻³, $\mu(\text{Mo-K}\alpha) = 0.292$ mm⁻¹, $F(000) = 1008$, crystal size 0.584 x 0.349 x 0.293 mm³, $\theta_{\text{max}} = 37.24^\circ$, 30215 reflections measured, 11191 independent reflections [$R(\text{int}) = 0.0408$], the final $R = 0.0481$ [$I > 2\sigma(I)$] and $wR(F^2) = 0.117$ (all data), GOOF = 1.054.



Crystal data for **390**. $C_{42}H_{37}NO_3$, $M = 603.72$, $T = 100.0(1)$ K, $\lambda = 1.54184$ Å, Triclinic, space group P 1, $a = 9.4983(2)$ Å, $b = 11.1047(2)$ Å, $c = 16.2802(3)$ Å, $V = 1617.36(6)$ Å³, $Z = 2$, $D_c = 1.240$ mg M⁻³ $\mu(\text{Mo-K}\alpha) = 0.604$ mm⁻¹, $F(000) = 640$, crystal size 0.500 x 0.352 x 0.206 mm³. $\theta_{\text{max}} = 78.19^\circ$, 57926 reflections measured, 12942 independent reflections [$R(\text{int}) = 0.040$], the final $R = 0.0339$ [$I > 2\sigma(I)$] and $wR(F^2) = 0.091$ (all data), GOOF = 1.049, Absolute structure parameter -0.07(6)

Chapter 5

5. References

1. H. Yin, N. Shan, S. Wang, Z. Yao, *J. Org. Chem.*, 2014, **79**, 9748.
2. G. Zeni, R. C. Larock, *Chem. Rev.*, 2004, **104**, 2285.
3. A. Furstner, P. W. Davies, *Chem. Commun.*, 2005, 2307
4. U. S. Gunay, B. Ozsoy, H. Durmaz, G. Hizal, U. Tunca, *J. Polym. Sci., Part A : Polym. Chem*, 2013, **51**, 4667.
5. B. Godoi, R. F. Schumacher, G. Zeni, *Chem. Rev*, 2011, **111**, 2937.
6. W. Jiang, Y. Li, Z. Wang, *Chem. Soc. Rev.*, 2013, **42**, 6113.
7. A. Mishra, C. Ma, P. Bäuerle, *Chem. Rev.*, 2009, **109**, 1141.
8. P. Josse, L. Favereau, C. Shen, S. Dabos-Seignon, P. Blanchard, C. Cabanetos, J. Crassous, *Chem. Eur. J.*, 2017, **23**, 6277.
9. Q. Wang, D. Ma, *Chem. Soc. Rev.*, 2010, **39**, 2387.
10. P. Gu, Z. Wang, Q. Zhang, *J. Mater. Chem. B.*, 2016, **4**, 7060.
11. T. Ren, J. Xiao, W. Wang, W. Xu, S. Wang, X. Zhang, X. Wang, H. Chen, J. Zhao, L. Jiang, *Chem. Asian J.*, 2014, **9**, 1194.
12. M. E. Detty, M. B. O'Regan, *Chem. Heterocycl. Compd.(N.Y.)*, 1994, **53**, 1.
13. G. T. Jason, E. N. Fokoua, J. S. Shrimpton, D. J. Richardson, F. Poletti, *Opt. Exp*, 2015, 23.
14. M. Miyasaka, A. Rajca, M. Pink, S. Rajca, *J. Am. Chem. Soc.*, 2005, **127**, 13806.
15. P. Gu, J. Gao, C. Wang, Q. Zhang, *RSC Adv.*, 2015, **5**, 80307.
16. S. F. Kirsch, *Synthesis*, 2008, **20**, 3183.
17. R. Mancuso, B. Gabriele, *Molecules*, 2014, **19**, 15687.
18. J. Schlosser, E. Johannes, M. Zindler, J. Lemmerhirt, B. Sommer, M. Schütt, C. Peifer, *Tetrahedron Lett*, 2015, **56**, 89.
19. B. Godoi, R. F. Schumacher, G. Zeni, *Chem. Rev*, 2011, **111**, 2937.
20. Y. Unoh, K. Hirano, M. Miura, *J. Am. Chem. Soc.*, 2017, **139**, 6106.
21. X. Zhou, Z. Jiang, L. Xue, P. Lu, Y. Wang, *Eur. J. Org. Chem.*, 2015, **2015**, 5789.
22. B. L. Flynn, P. V. Pinard, E. Hamel, *Org. Lett.*, 2001, **3**, 651
23. S. Mehta, J. P. Waldo, R. C. Larock, *J. Org. Chem.* 2009, **74**, 1141.
24. L. Aurelio, R. Volpe, R. Halim, P. J. Scammells, B. L. Flynn, *Adv. Synth. Catal.*, 2014, **356**, 1974.
25. S. Mehta, R. C. Larock, *J. Org. Chem.*, 2010, **75**, 1652.
26. K. O. Hessian, B. L. Flynn., *Org. Lett.*, 2006, **8**, 243.
27. K. O. Hessian, B. L. Flynn., *Org. Lett.*, 2003, **5**, 4377.

28. C.Cho, B. Neuenswander, G. H. Lushington, R. C. Larock, *J. Comb. Chem.*, 2008, **10**, 941.
29. H. Song, Y. Liu, Q. Wang, *Org. Lett.*, 2013, **15**, 3274.
30. T. Choshi, Y. Matsuya, M. Okita, K. Inada, W. Sugino, S. Hibino, *Tetrahedron Lett.*, 1988, **39**, 2341.
31. A. Gupta, B. L. Flynn, *J. Org. Chem*, 2016, **81**, 4012.
32. A. Gupta, B. L. Flynn, *Org. Lett.*, 2017, **19**, 1939.
33. J. Barluenga, M. Trincado, M. Marco-Arias, A. Ballesteros, E. Rubio, J. M. González, *Chem. Commun.*, 2005, 2008.
34. J. H. Chaplin, B. L. Flynn, *Chem. Commun.*, 2001, 1594.
35. G. Kremmidiotis, A. F. Leske, T. C. Lanvranos, D. Beaumont, J. Gasic, A. Hall, M. O’Callaghan, C. A. Matthews, B. Flynn, *Mol. Cancer Ther.*, 2010, **9**, 1562.
36. X. Xia, N. Wang, L. Zhang, X. Song, X. Liu, Y. Liang, *J. Org. Chem.*, 2012, **77**, 9163.
37. A. Kar, N. Mangu, H. M. Kaiser, M. Beller, M. K. Tse, *Chem. Commun.*, 2008, 386.
38. C. González-Arellano, A. Abad, A. Corma, H. García, M. Iglesias, F. Sánchez, *Angew. Chem. Int. Ed.*, 2007, **46**, 1536.
39. K. Hirano, Y. Inaba, N. Takahashi, M. Shimano, S. Oishi, N. Fujii, H. Ohno, *J. Org. Chem.*, 2011, **76**, 1212.
40. G. Cera, P. Crispino, M. Monari, M. Bandini, *Chem. Commun.*, 2011, **47**, 7803.
41. A. S. K. Hashmi, M. Rudolph, *Chem. Soc. Rev.*, 2008, **37**, 1766.
42. L. Currie, L. Rocchigiani, D. L. Hughes, M. Bochmann, *Dalton Trans*, 2018, **47**, 6333
43. T. J. A. Corrie, L. T. Ball, C. A. Russell, G. C. Lloyd-Jones, *J. Am. Chem. Soc.*, 2017, **139**, 245.
44. A. S. K. Hashmi, M. C. Blanco, D. Fischer, J. W. Bats, *Eur. J. Org. Chem.*, 2006, 1387.
45. H. A. Wegner, S. Ahles, M. Neuburger, *Chem. Eur. J.*, 2008, **14**, 11310.
46. O. A. Egorova, H. Seo, Y. Kim, D. Moon, Y. M. Rhee, K. H. Ahn, *Angew. Chem. Int. Ed.*, 2011, **50**, 11446.
47. F. G. Brunetti, X. Gong, M. Tong, A. J. Heeger, F. Wedl, *Angew. Chem. Int. Ed.*, 2010, **49**, 532.
48. F. Pammolli, L. Magazzini and M. Riccaboni, *Nat. Rev. Drug Discov.*, 2011, **10**, 428.
49. F. Lovering, *Med. Chem. Commun*, 2013, **4**, 515.
50. T. E. Nielsen, S. L. Schreiber, *Angew. Chem. Int. Ed.*, 2008, **47**, 48.
51. S. Tokoshima, M. Ishikawa, Y. Beniyama, T. Fukuyama, *Chem. Pharm. Bull.*, 2016, **64**, 1528.
52. D. H. Drewry, R. Macarron, *Curr. Opin. Chem. Biol.*, 2010, **14**, 289.

53. A. Karawajczyk, F. Giordanetto, J. Benningshof, D. Hamza, T. Kalliokoski, K. Pouwerm R. Morgentin, A. Nelson, G. Müller, A. Piechot, D. Tzalis. *Drug Discov. Today*, 2015, **20**, 1310.
54. Y. Zhu, J. Han, J. Wang, N. Shibata, M. Sodeoka, V. A. Soloshonok, J. A. S. Coelho, F. D. Toste. *Chem. Rev.*, 2018, **118**, 3887.
55. D. F. Veber., S. R. Johnson, H. Y. Cheng, B. R. Smith, K. W. Ward, K. D. Kopple, *J. Med. Chem.*, 2002, **45**, 2615.
56. F. Lovering, J. Bikker and C. Humblet, *J. Med. Chem.*, 2009, **52**, 6752
57. K. A. Chu, S. H. Yalkowsky, *Int. J. Pharm.*, 2009, **24**, 373.
58. S. D. Roughley, A. M. Jordan, *J. Med. Chem.*, 2011, **54**, 3451.
59. B. Halford, *Chem. Eng. News Archive*, 2008, **86**, 11.
60. C. Fu, Y. Zhang, J. Xuan, C. Zhu, B. Wang, H. Ding, *Org. Lett.*, 2014, **16**, 3376.
61. J. Yang, J. Fu, X. Liu, Z. Jiang, G. Zhu, *Fitoterapia*, 2018, **124**, 73.
62. Y. Suzuki, K. Takao, K. Tadano, *Stud. In Nat. Prod. Chem.*, 2003, **29**, 127.
63. A. H. Hoveyda, S. J. Malcolmson, S. J. Meek, A. R. Zhudralin, *Angew. Chem. Int. Ed.*, 2010, **49**, 34.
64. P. Starkov, J. T. Moore, D. C. Duquette, B. M. Stoltz, I. Marek, *J. Am. Chem. Soc.*, 2017, **139**, 9615.
65. R. Volpe, R. J. Lepage, J. M. White, W. H. Krenske, B. L. Flynn, *Chem. Sci.*, 2018, **9**, 4644.
66. K. C. Nicolaous, J. Wang, Y. Tang, L. Botta, *J. Am. Chem. Soc.*, 2010, **132**, 11350.
67. J. D. Padwal, D. V. Filippov, B. D. Narhe, S. Aertssen, R. J. Beuving, J. C. J. Benningshof, G. A. van der Marel, H. S. Overkleeft, M. van der Stelt, *Bioorg. Med. Chem.*, 2015, **23**, 2650
68. M. G. Vinogradov, O. V. Turova, S. G. Zlotin, *Org. Biomol. Chem.*, 2017, **15**, 8245.
69. C. G. Newton, M. S. Sherburn, *Nat. Prod. Rep.*, 2015, **32**, 865.
70. K. L. Habermas, S. E. Denmark. *Org. React.*, 1994, **45**, 1-158.
71. D. R. Wenz, J. R. d. Alaniz, *Eur. J. Org. Chem.*, 2014, **2015**, 23.
72. J. A. Malona, K. Carious, A. J. Frontier, *J. Am. Chem.*, 2009, **131**, 7560.
73. D. J. Kerr, B. L. Flynn, *Org. Lett.*, 2012, **14**, 1740.
74. W. He, X. Sun, and A. J. Frontier, *J. Am. Chem. Soc.* 2003, **125**, 14278.
75. A. Jolit, S. Vazquez-Rodriguez, G. O. A. Yap, M. A. Tius, *Angew. Chem. Int. Ed.*, 2013, **52**, 11102.
76. R. Merino, E. M López, T. Tejero, R. P. Herrera, *Synthesis*, 2010, **1**, 1.
77. L. N. Pridgen, K. Huang, S. Shilcrat, A. T. Eldridge, C DeBross, R. C. Haltiwanger, *Synlett.*, 1999, **10**, 1612.
78. D. J. Kerr, J. M. White, B. L. Flynn, *J. Org. Chem.*, 2010, **75**, 7073.
79. J. H. Chaplin, K. Jackson, J. M. White, B. L. Flynn, *J. Org. Chem.*, 2014, **79**, 3659.

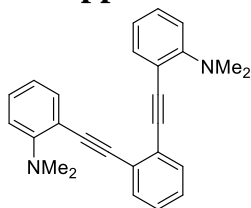
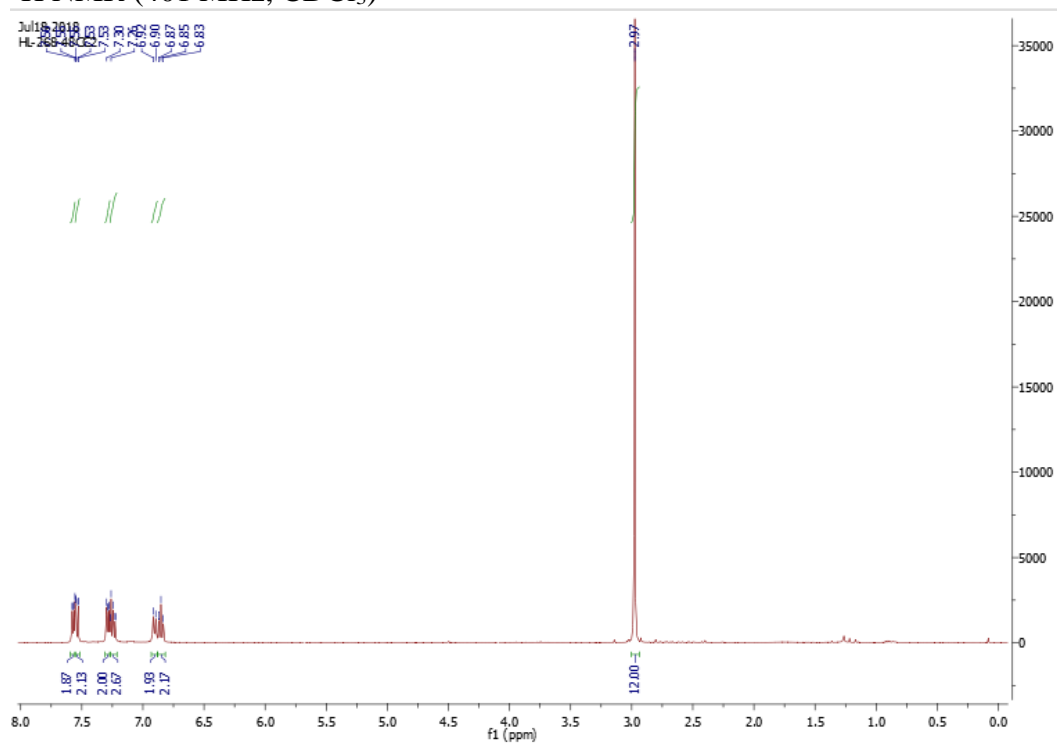
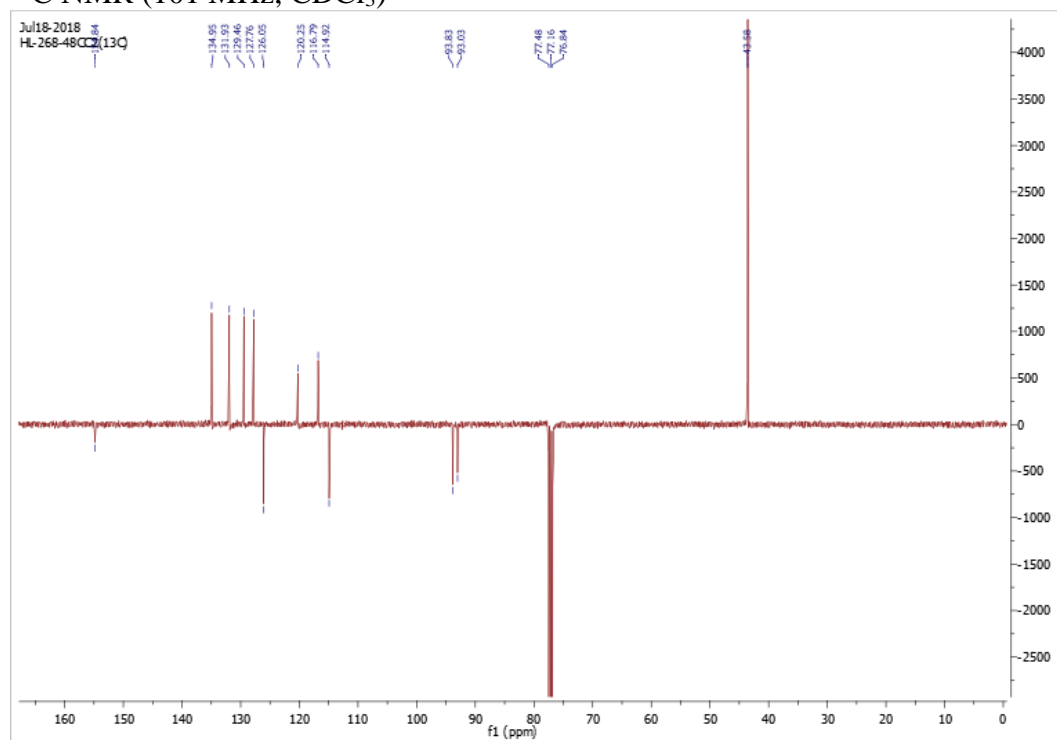
80. B. L. Flynn, N. Manchala, E. H. Krenske, *J. Am. Chem. Soc.* 2013, **135**, 9156.
81. N. Manchala, H. Y. L. Law, D. J. Kerr, R. Volpe, R. J. Lepage, J. M. White, E. H. Krenske, B. L. Flynn. *J. Org. Chem.* 2017, **82**, 6511.
82. D. J. Kerr, M. Miletic, J. H. Chaplin, J. M. White, B. L. Flynn. *Org. Lett.*, 2012, **14**.
83. E. Grenet, J. Martínez, X. J. Salom-Roig, *Chem. Eur. J.* 2016, **22**, 16770
84. Y. Suzuki, J. Wakatsuki, M. Tsubaki, M. Sato, *Tetrahedron*, 2013, **69**, 9690.
85. D. J. Kerr, M. J. H. Chaplin, J. M. White, B. L. Flynn, *Org. Lett.*, 2012, **14**, 1732.
86. S. Shirakawa, K. Liu, K. Maruoka, *J. Am. Chem. Soc.*, 2012, **134**, 916.
87. M. Rueping, W. Ieawsuwan, A. P. Antonchick, B. J. Nachtsheim. *Angew. Chem. Int. Ed.* 2007, **46**, 2097.
88. A. Jolit, P. M. Walleser, G. P. A. Yap, M. A. Tius. *Angew. Chem. Int. Ed.*, 2014, **53**, 6180.
89. G. Liang and D. Trauner, *J. Am. Chem. Soc.* 2004, **126**
90. F. M. LeFort, V. Mishra, G. D. Dexter, T. D. R. Morgan, and D. J. Burnell, *J. Org. Chem.* 2015, **80**, 5877.
91. Y. Wang, B. D. Schill, A. M. Arif, F. G. West, *Org. Lett.*, 2003, **5**, 2747.
92. Y. Wu, C. R. Dunbar, R. McDonald, M. J. Ferguson, F. G. West, *J. Am. Chem. Soc.*, 2014, **136**, 14903.
93. D. J. Schatz, Y. Kwon, T. W. Scully, and F. G. West, *J. Org. Chem.* 2016, **81**, 12494.
94. J. A. Bender, A. E. Blize, C. C. Browder, S. Giese, F. G. West, *J. Org. Chem.*, 1998, **63**, 2430.
95. J. A. Bender, A. M. Arif, F. G. West, *J. Am. Chem. Soc.*, 1999, **121**, 7443.
96. B. Alcaide, P. Almendros, J. M. Alonso, *Molecules*, 2011, **16**, 7815.
97. C. Chen, M. Wu, H. Chen, M. Wu, *J. Org. Chem.* 2017, **82**, 6071.
98. J. Xuan, W. Xiao, *Angew. Chem. Int. Ed.*, 2012, **51**, 6828.
99. J. M. R. Narayanam, C. R. J. Stephenson, *Chem. Soc. Rev.*, 2011, **40**, 102
100. H. Yan, S. I. Lim, Y. Zhang, Q. Chen, D. Mott, W. Wu, D. An, S. Zhou, C. Zhong, *Chem. Commun.*, 2010, **46**, 2218.
101. D. Kang, D. Eom, H. Kim, P. H. Lee, *Eur. J. Org. Chem.*, 2010, 2330.
102. D. Leboeuf, V. Gandon, J. Ciesielski, A. J. Frontier, *J. Am. Chem. Soc.*, 2012, **134**, 6296.
103. R. Knoww, C. Behringer, M. Knittl, U. v. Roman, E. Lattke, *J. Am. Chem. Soc.*, 2017, **139**, 4690.
104. S. Maoulay, *Chem. Educ. Res. Pract.*, 2002, **3**, 33.
105. M. Shindo, Y. Sato, Takashi Yoshikawa, R. Koretsune, K. Shishido, *J. Org. Chem*, 2004, **69**, 3912.
106. K. Naveen, A. Nandakumar, P. T. Perumal, *Synthesis*, 2015, **47**, 1633.
107. X. Nie, G. Wang, *J. Org. Chem.*, 2006, **71**, 4734.

108. C. Lin, Y. Lo, M. Hsieh, Y. Chen, J. Wang, M. Wu, *Bioorg. Med. Chem.*, 2005, **13**, 3565.
109. D. Yue, T. Yao, R. C. Larock, *J. Org. Chem.*, 2006, **71**, 62.
110. K. G. Thakur, G. Sekar, *Synthesis*, 2009, **16**, 2785.
111. S. Umezū, G. d. P. Gomes, T. Yoshinaga, M. Sakae, K. Matsumoto, T. Iwata, I. Alabugin, M. Shindo, *Angew. Chem. Int. Ed*, 2016, **56**, 1298.
112. N. E. Campbell and G. M. Sammis, *Angew. Chemie Int. Ed.*, 2014, **53**, 6228.
113. D. P. Curran and S.-C. Kuo, *Tetrahedron*, 1987, **43**, 5653.
114. S. Umezū, G. d. P. Gomes, T. Yoshinaga, M. Sakae, K. Matsumoto, T. Iwata, I. Alabugin, M. Shindo, *Angew. Chem. Int. Ed*, 2016, **56**, 1298.

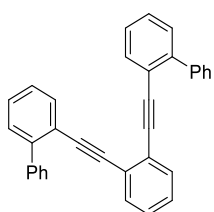
Chapter 6

6. Appendices

6.1 Appendices A- NMR data

**262c** ^1H NMR (401 MHz, CDCl_3) ^{13}C NMR (101 MHz, CDCl_3)

Chapter 6

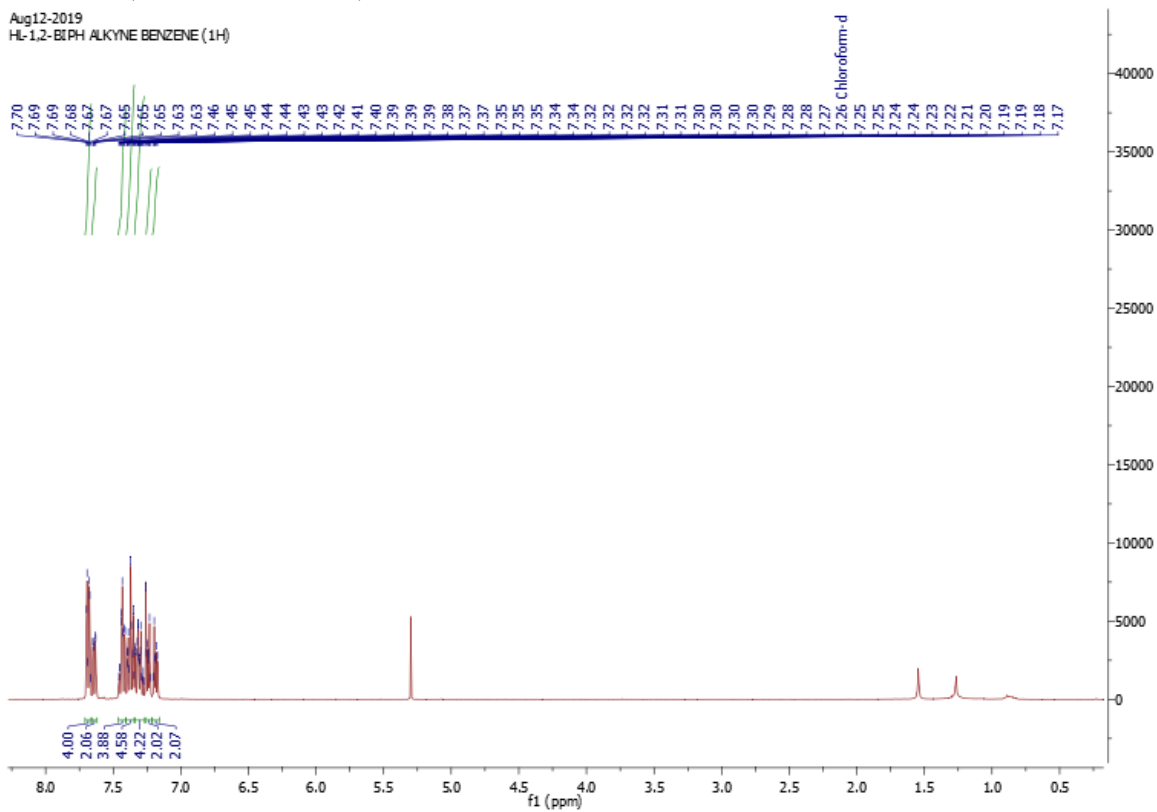


262d

^1H NMR (401 MHz, CDCl_3)

Aug12-2019

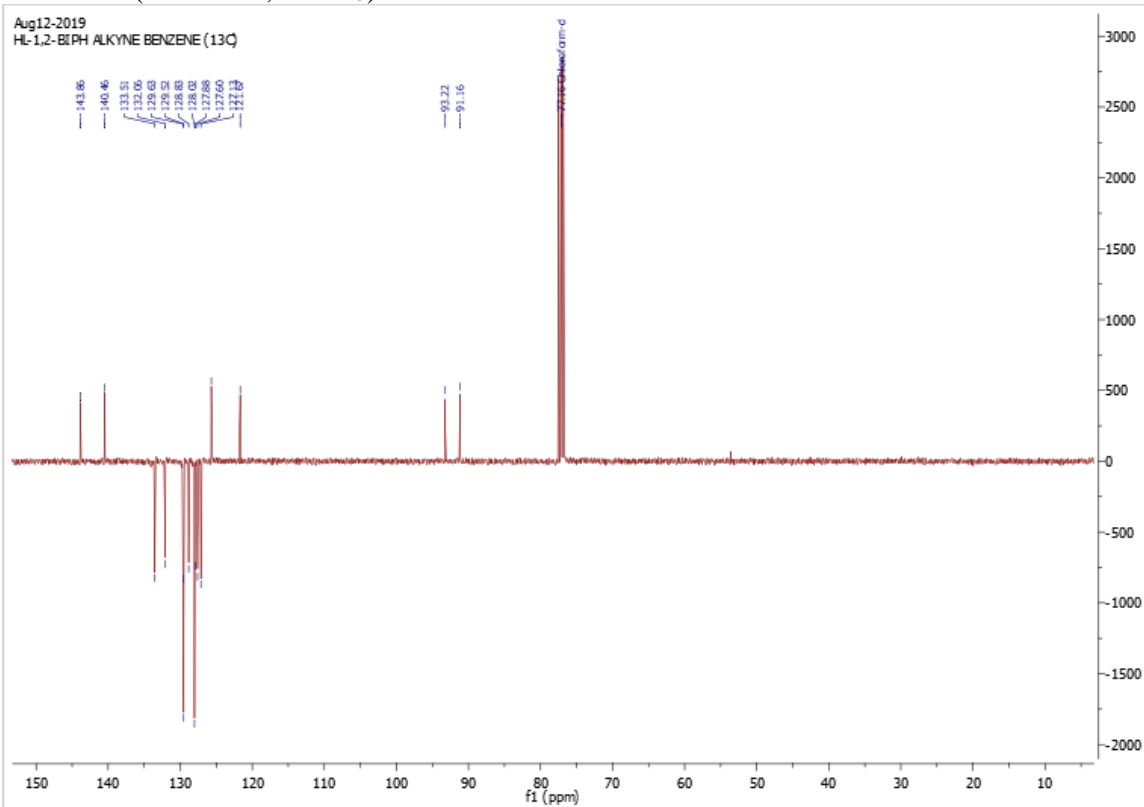
HL-1,2-BIPH ALKYNE BENZENE (1H)



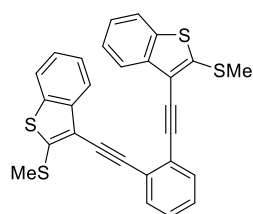
^{13}C NMR (101 MHz, CDCl_3)

Aug12-2019

HL-1,2-BIPH ALKYNE BENZENE (13C)

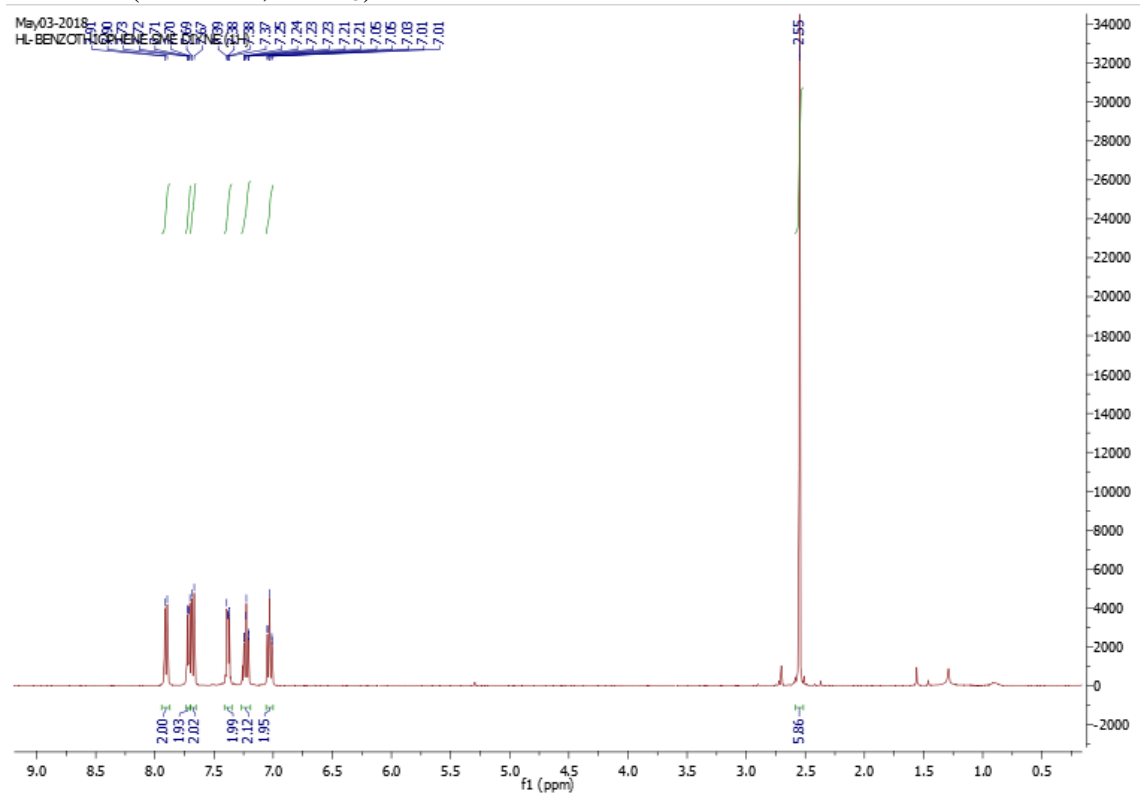


Chapter 6

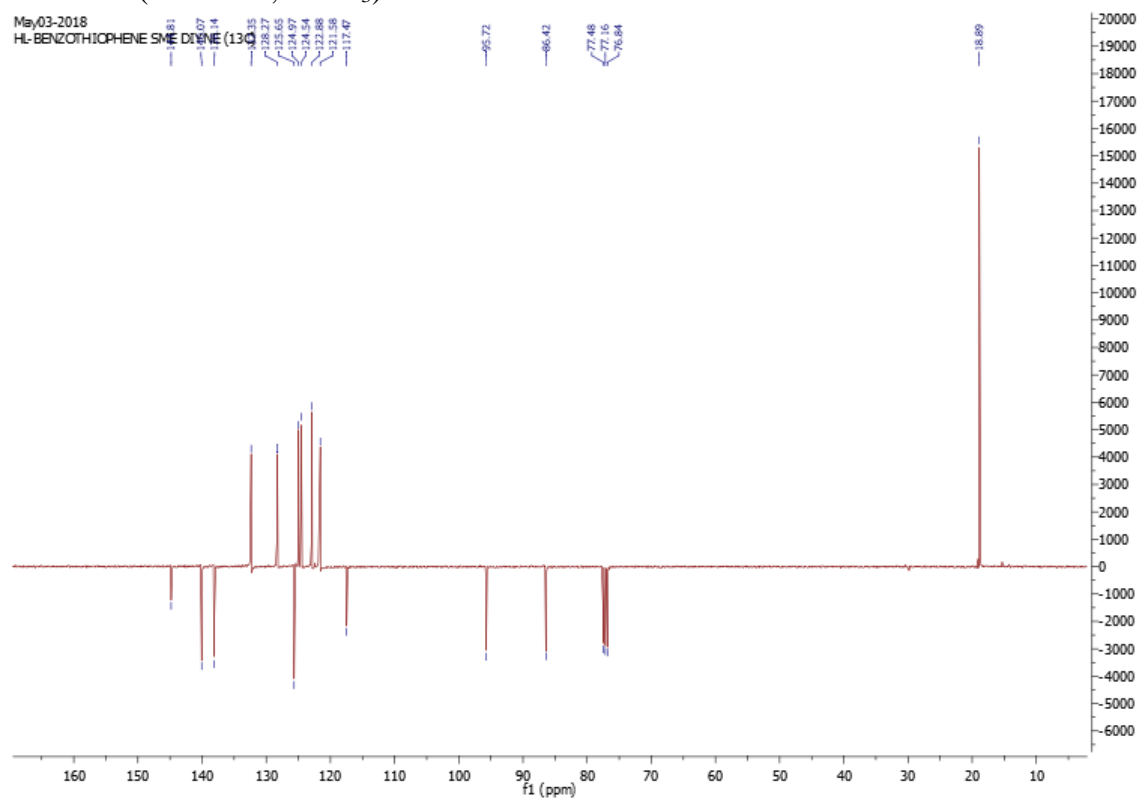


262e

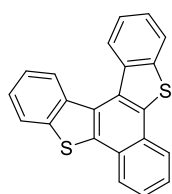
^1H NMR (401 MHz, CDCl_3)



^{13}C NMR (101 MHz, CDCl_3)

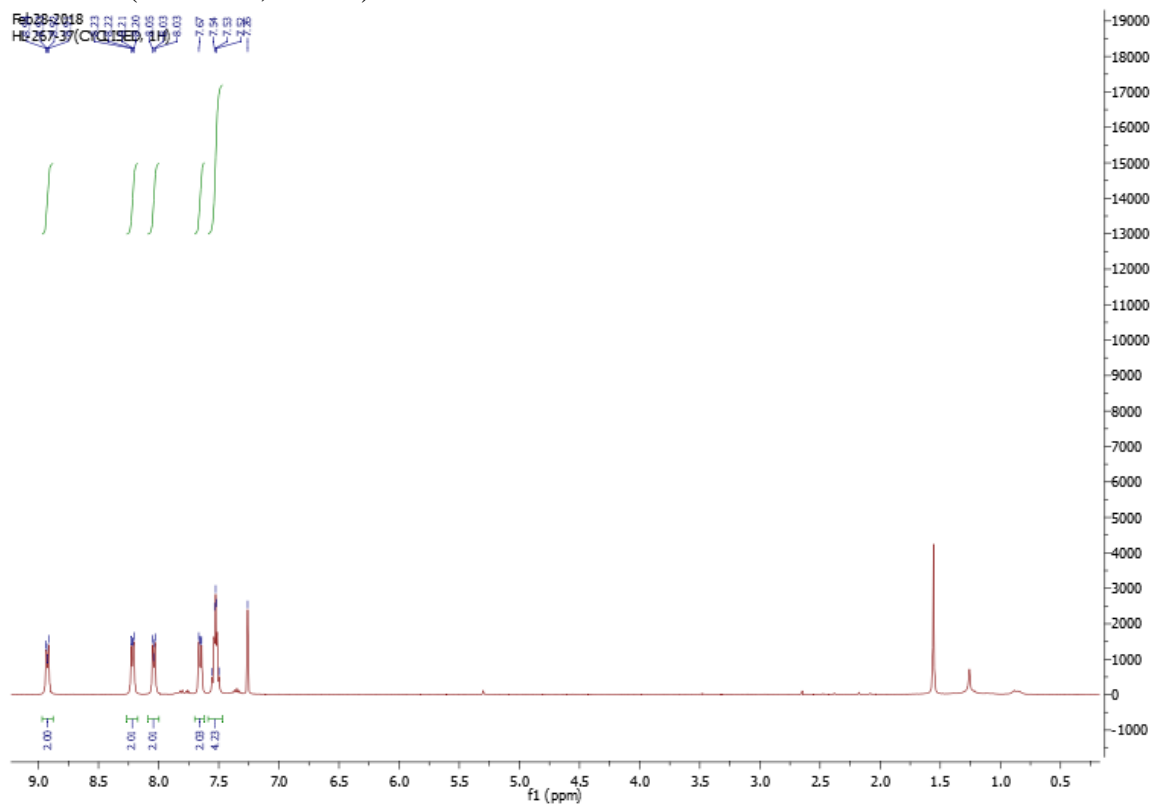


Chapter 6

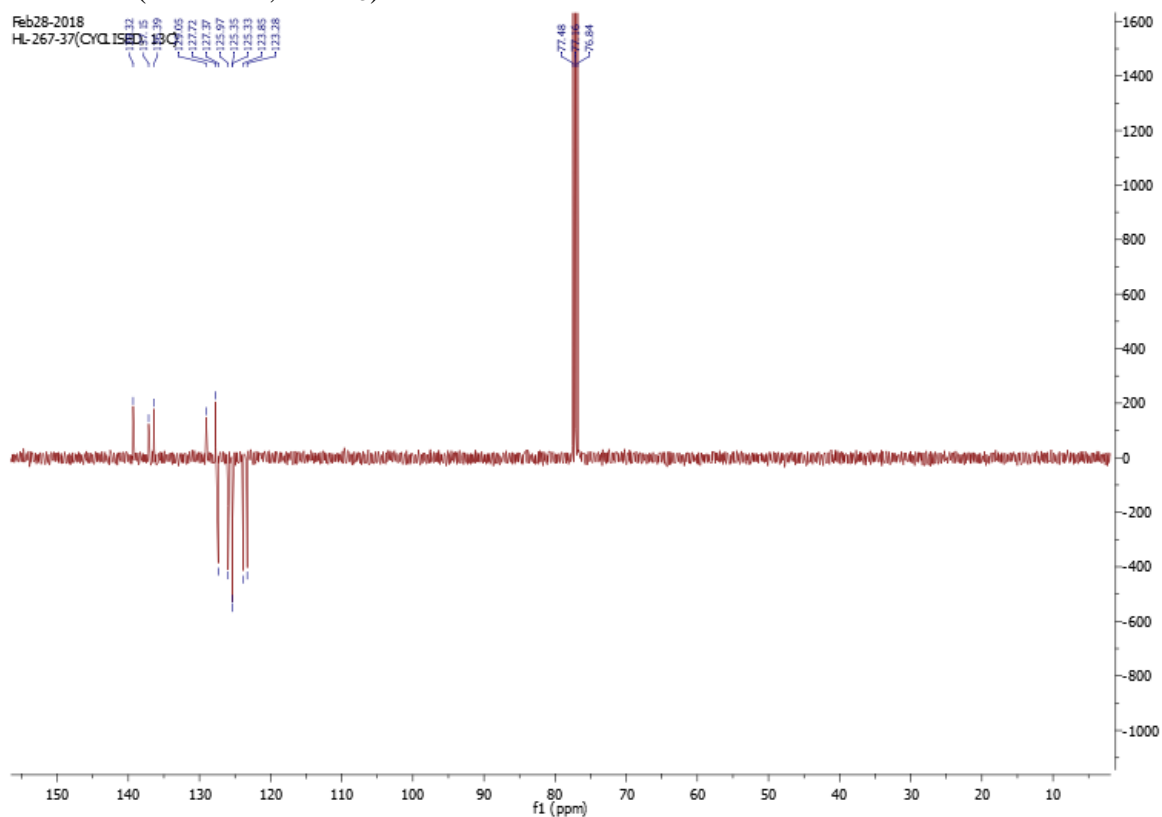


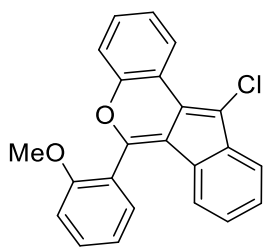
263a

^1H NMR (401 MHz, CDCl_3)

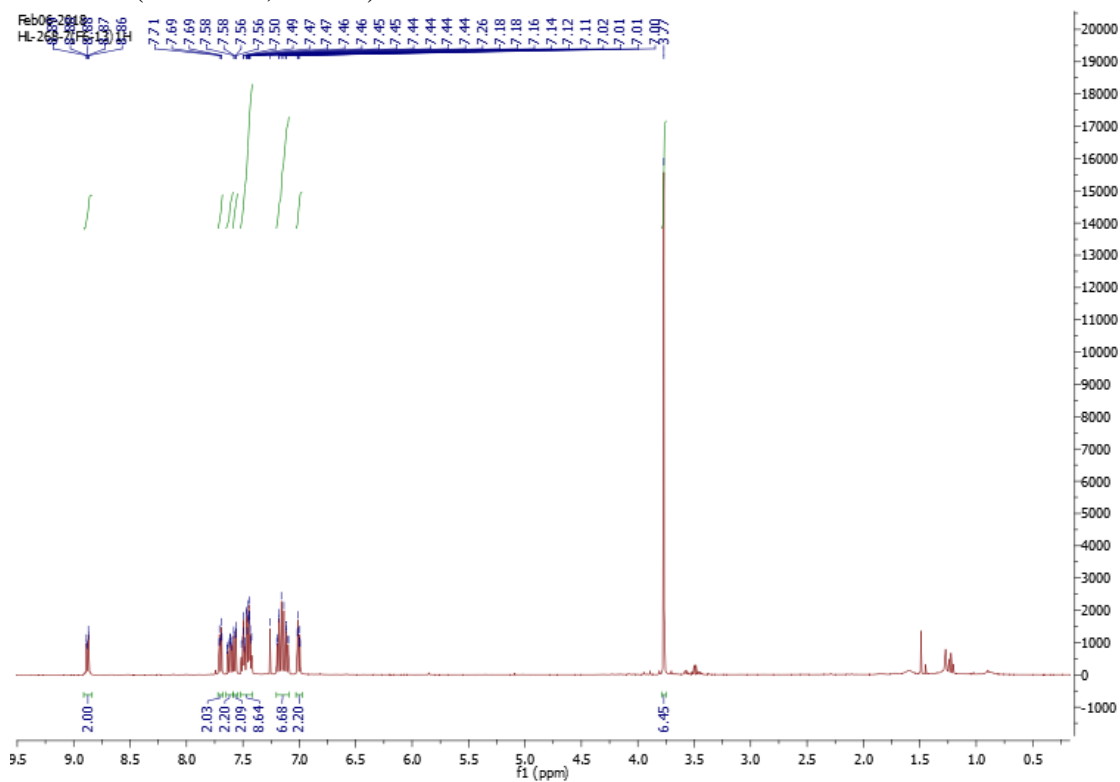
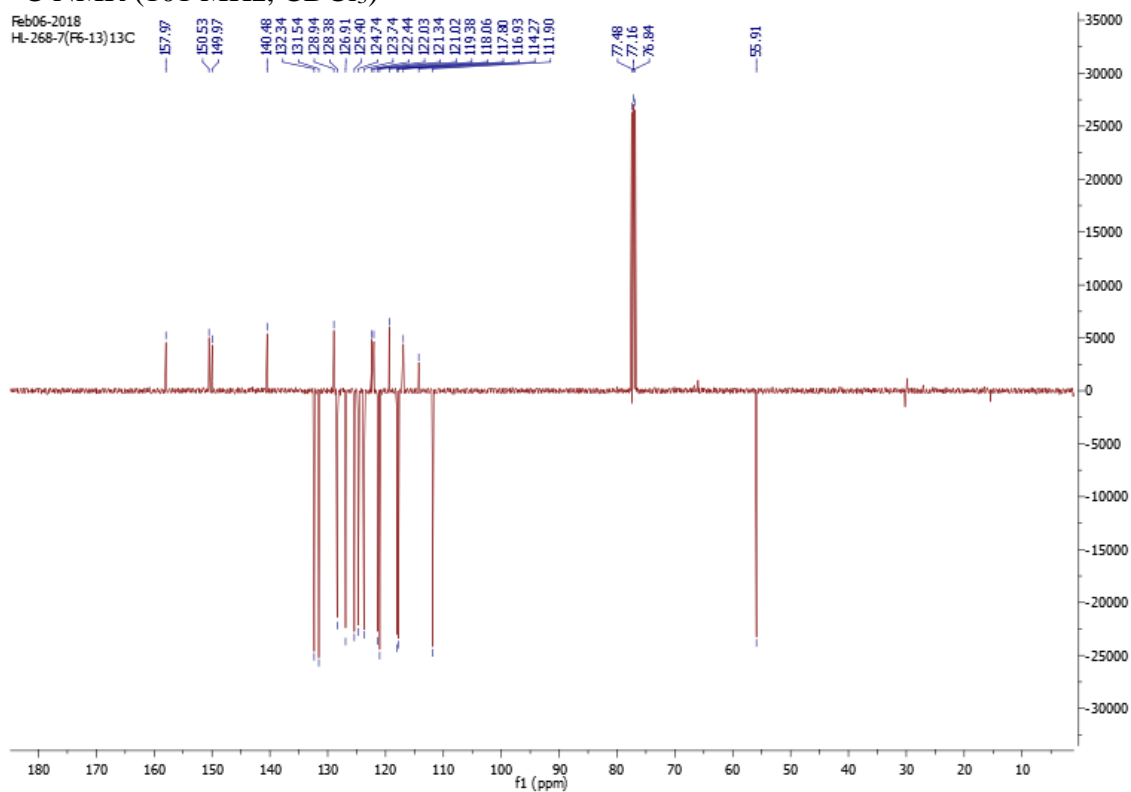


^{13}C NMR (101 MHz, CDCl_3)

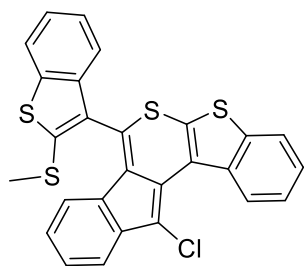




275

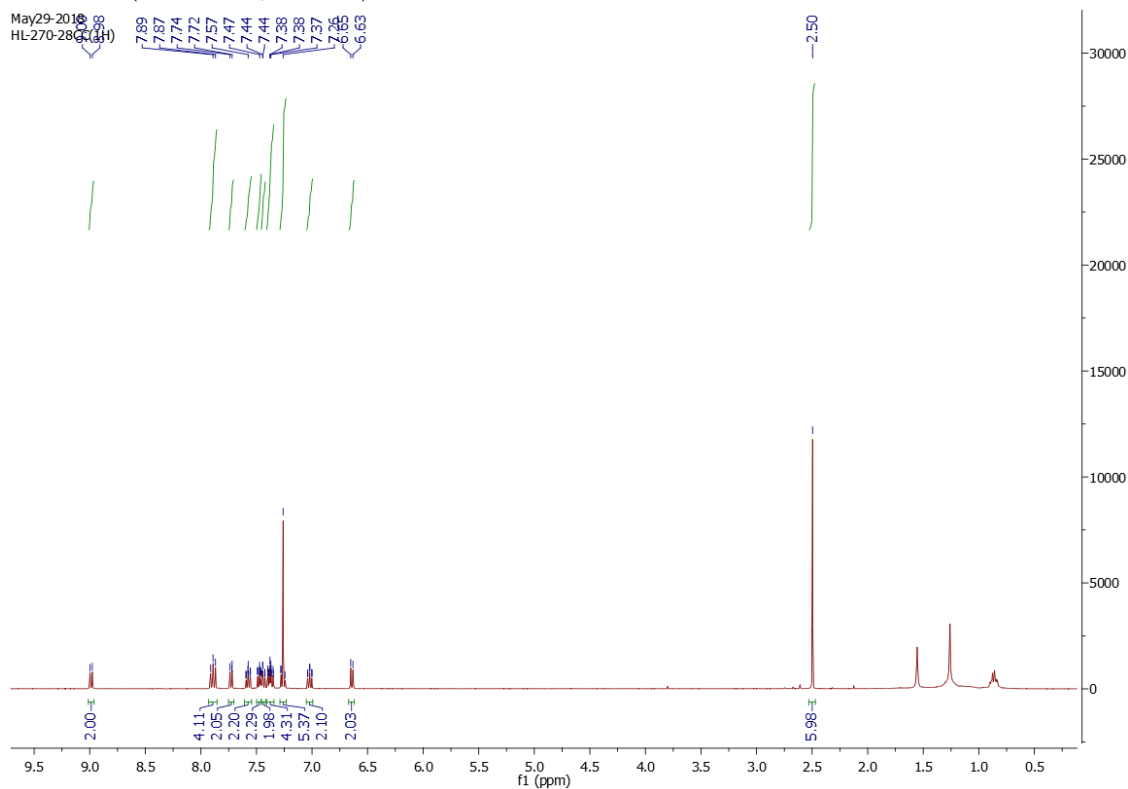
 ^1H NMR (401 MHz, CDCl_3) ^{13}C NMR (101 MHz, CDCl_3)

Chapter 6

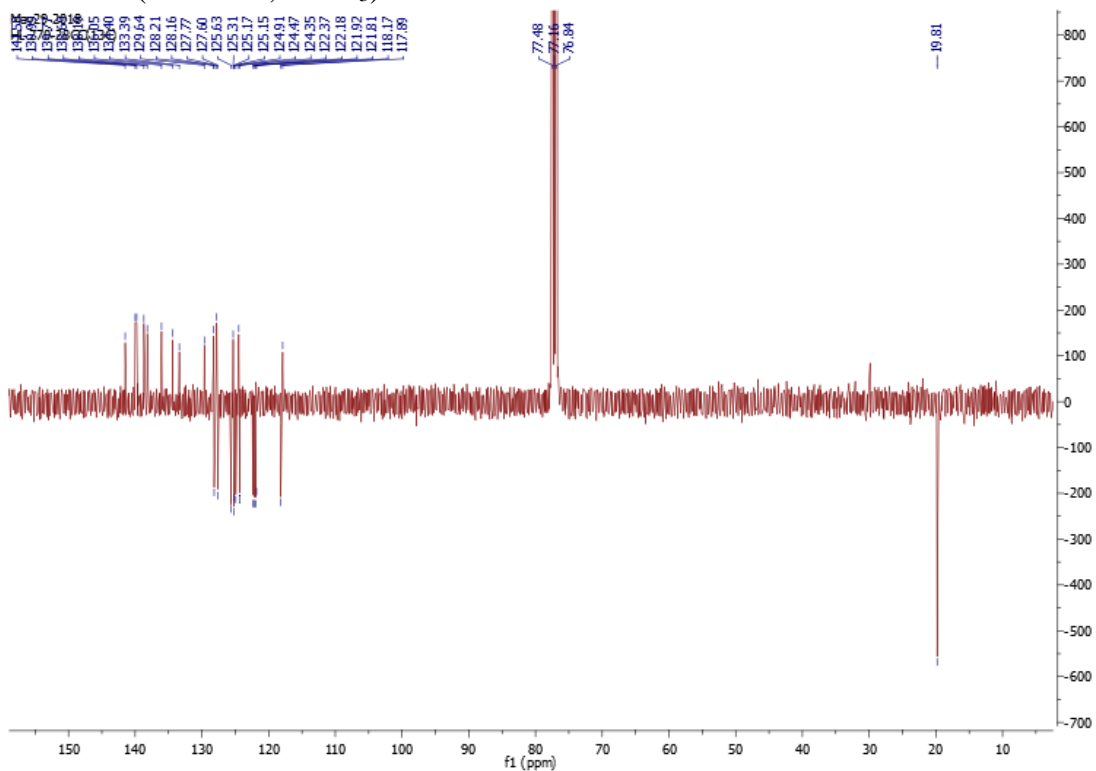


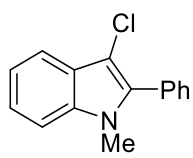
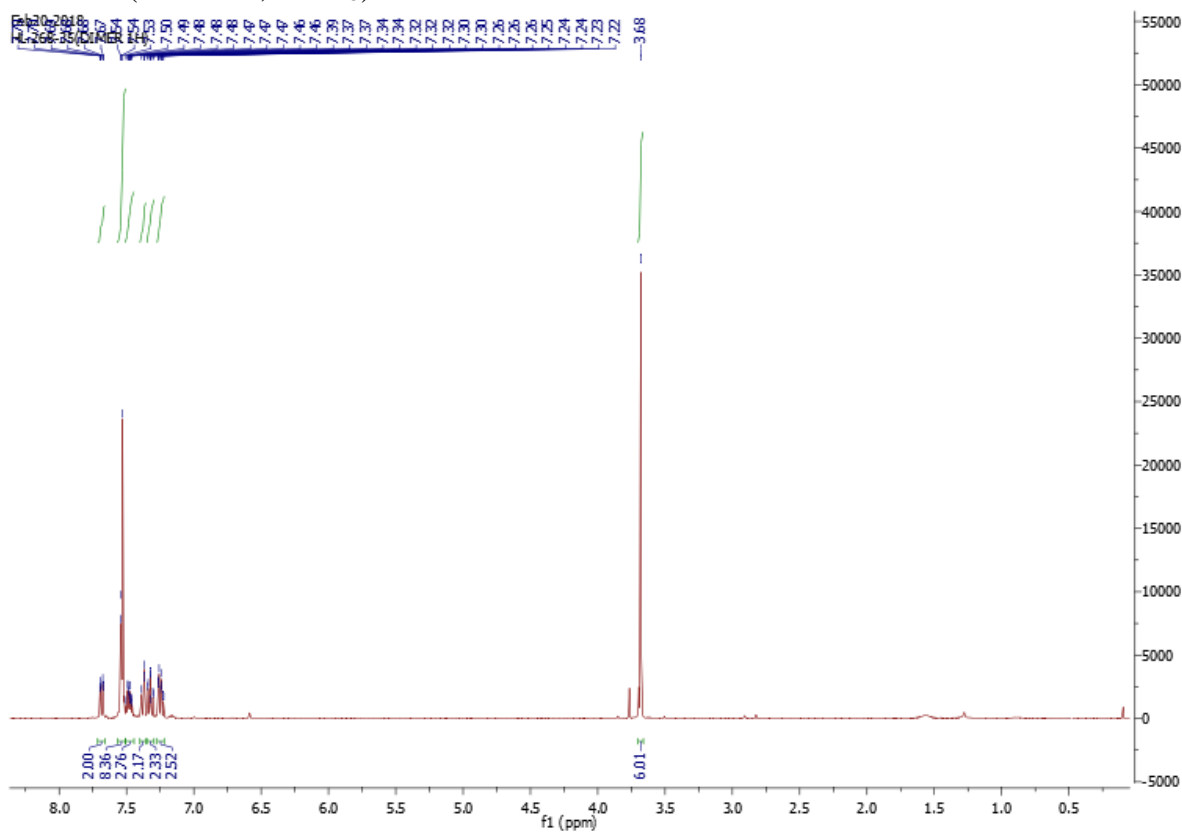
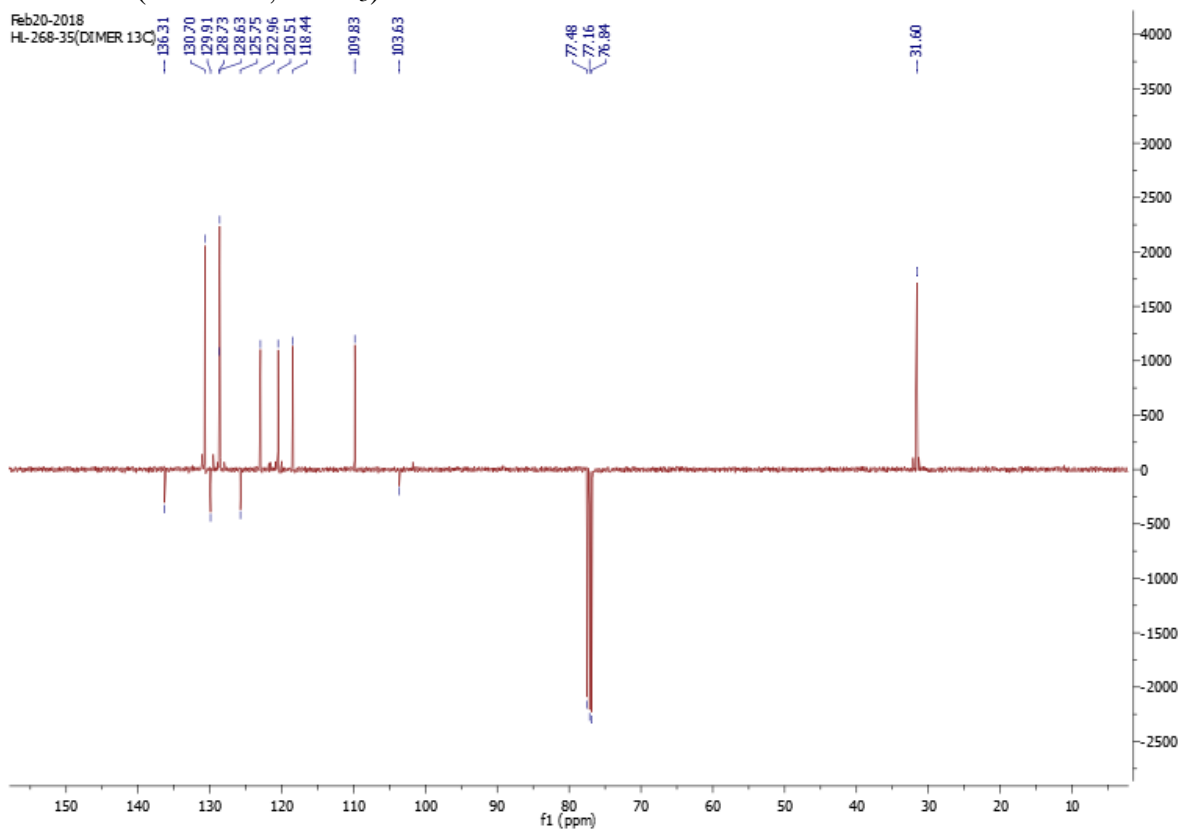
292

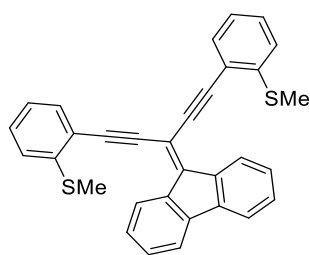
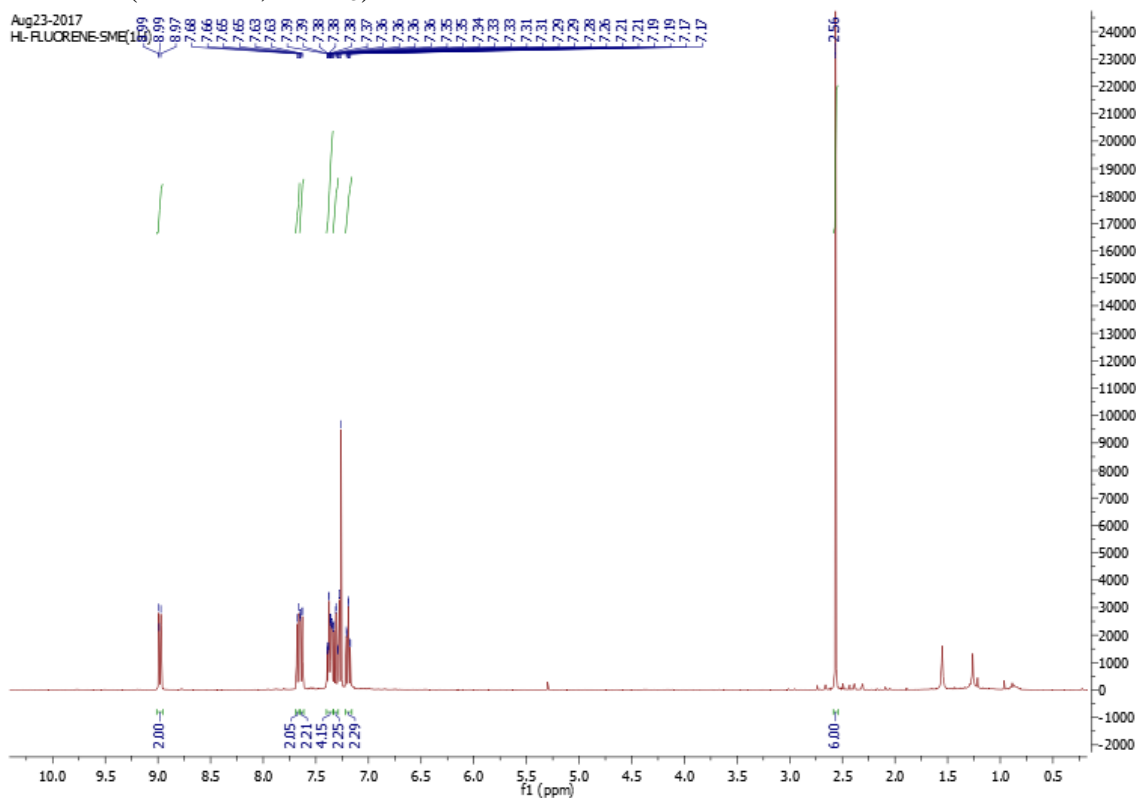
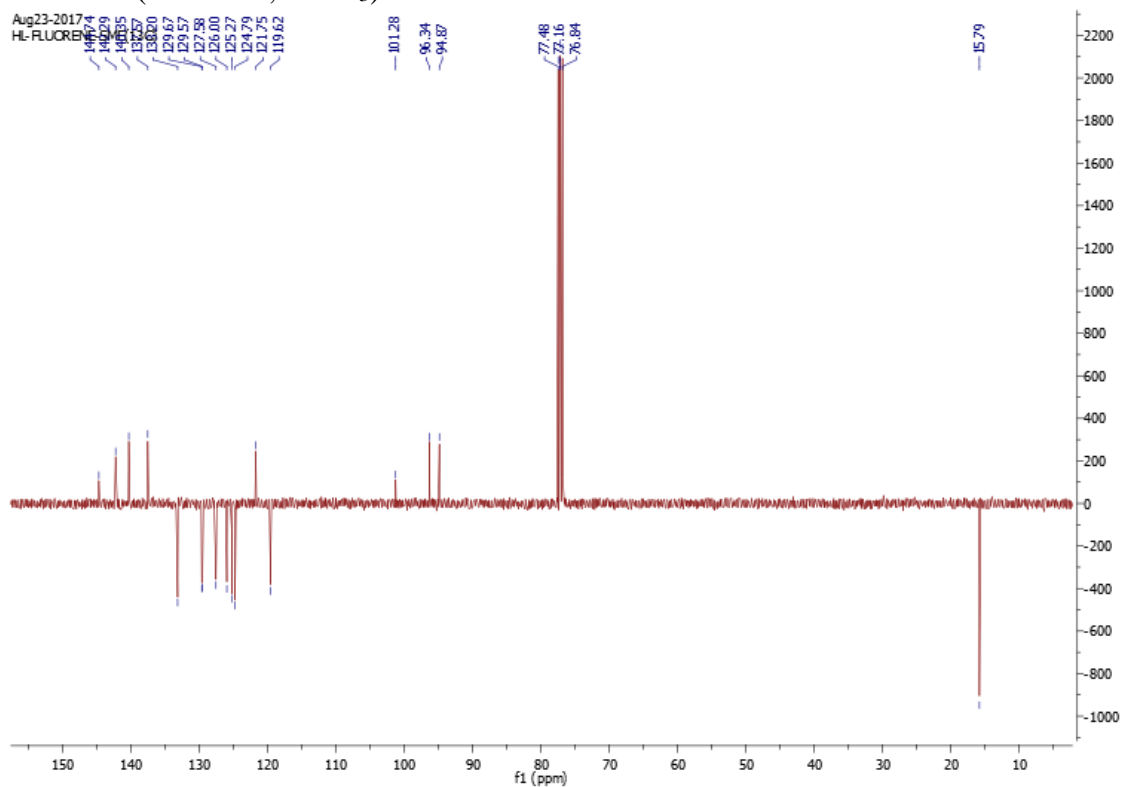
^1H NMR (401 MHz, CDCl_3)



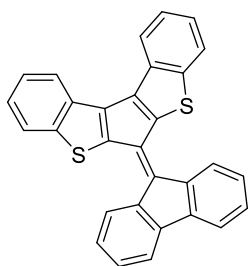
^{13}C NMR (101 MHz, CDCl_3)



**295a** ^1H NMR (401 MHz, CDCl_3) ^{13}C NMR (101 MHz, CDCl_3)

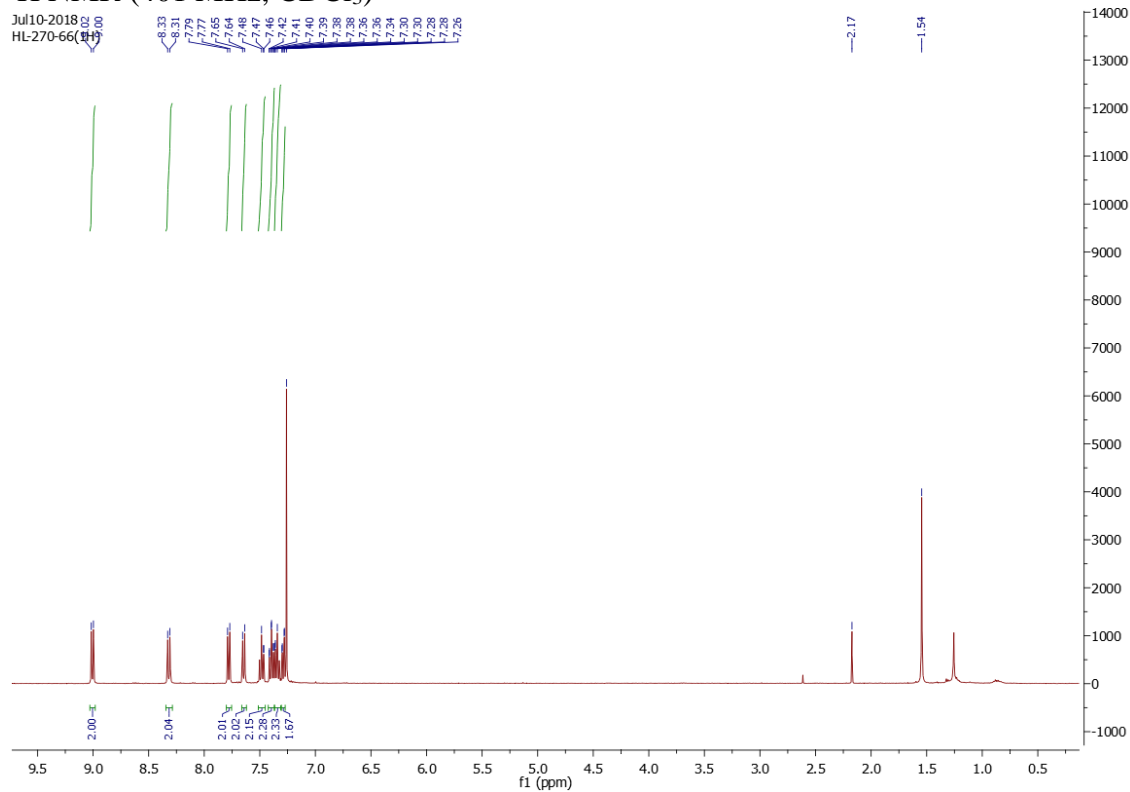
**299** ^1H NMR (401 MHz, CDCl_3) ^{13}C NMR (101 MHz, CDCl_3)

Chapter 6

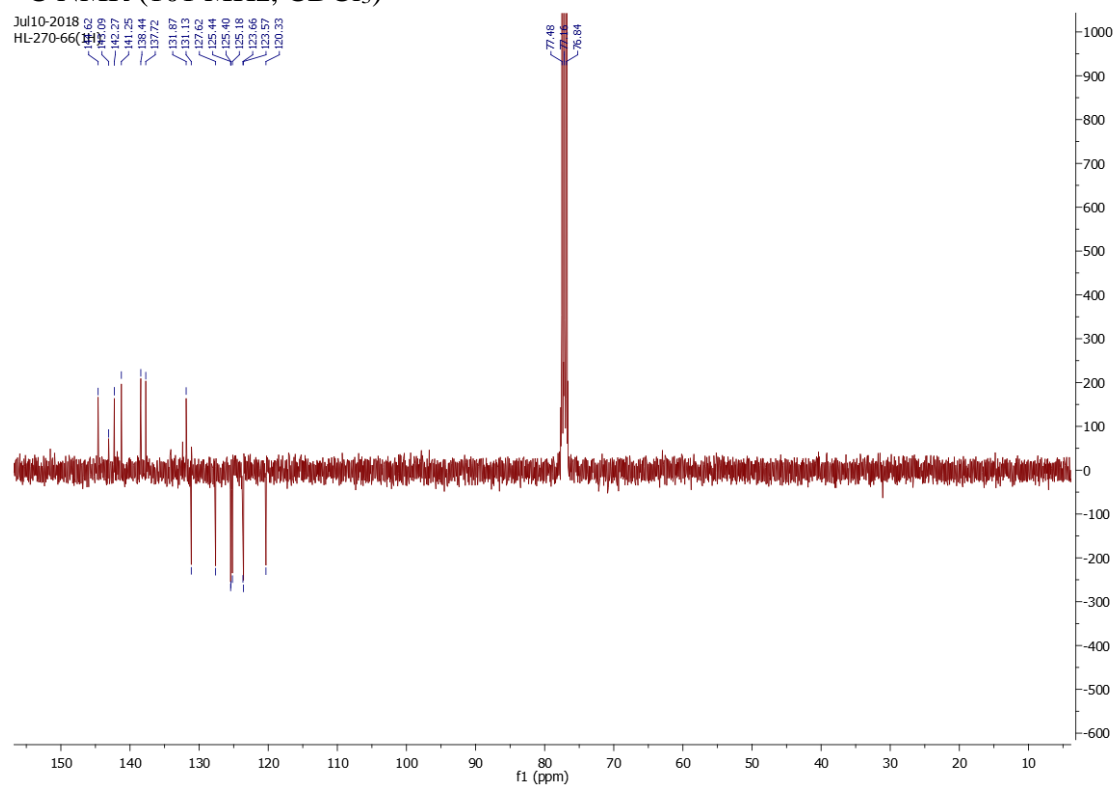


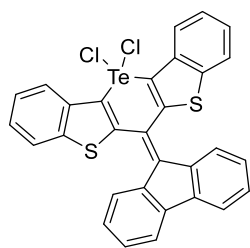
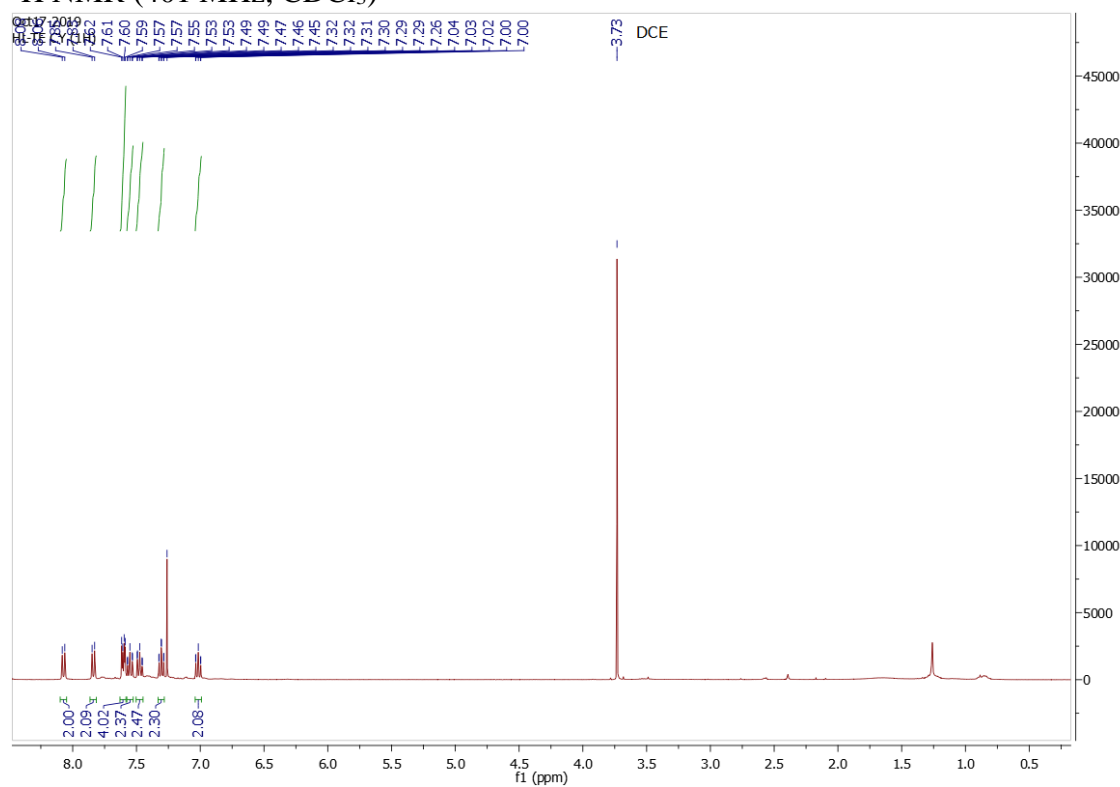
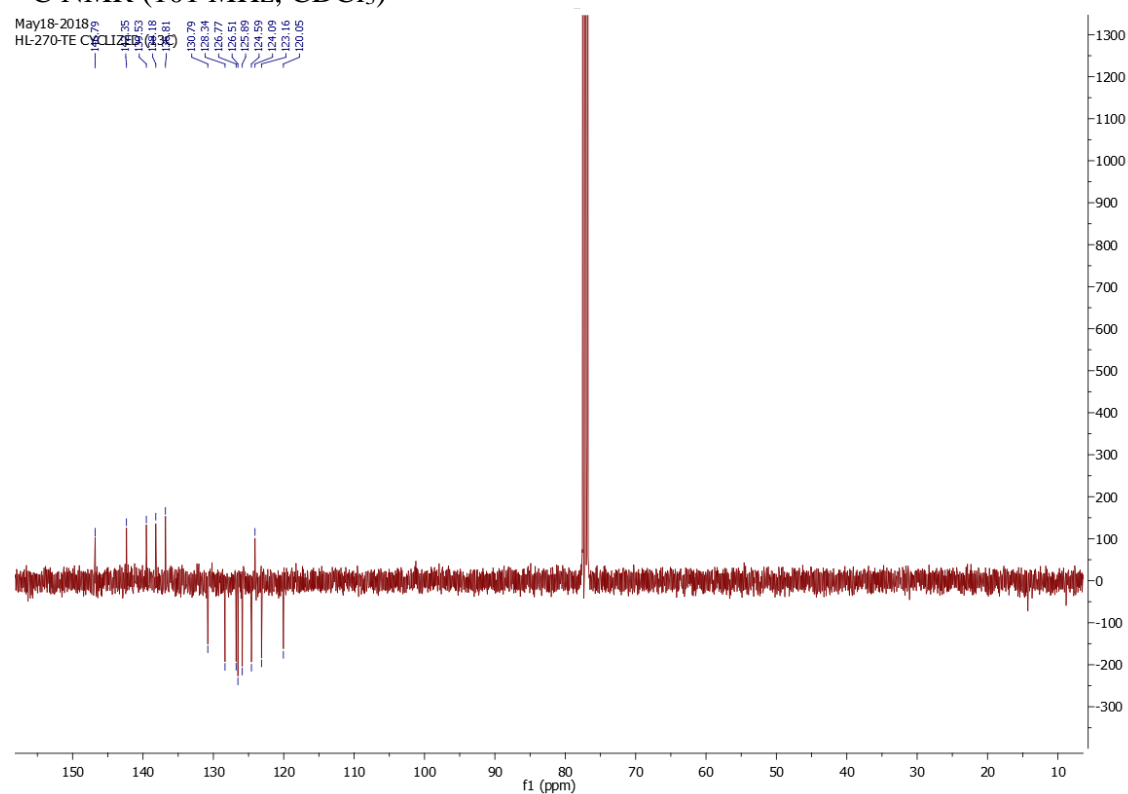
2

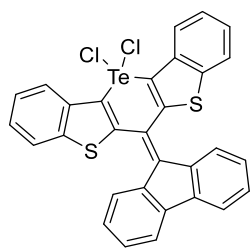
^1H NMR (401 MHz, CDCl_3)



^{13}C NMR (101 MHz, CDCl_3)

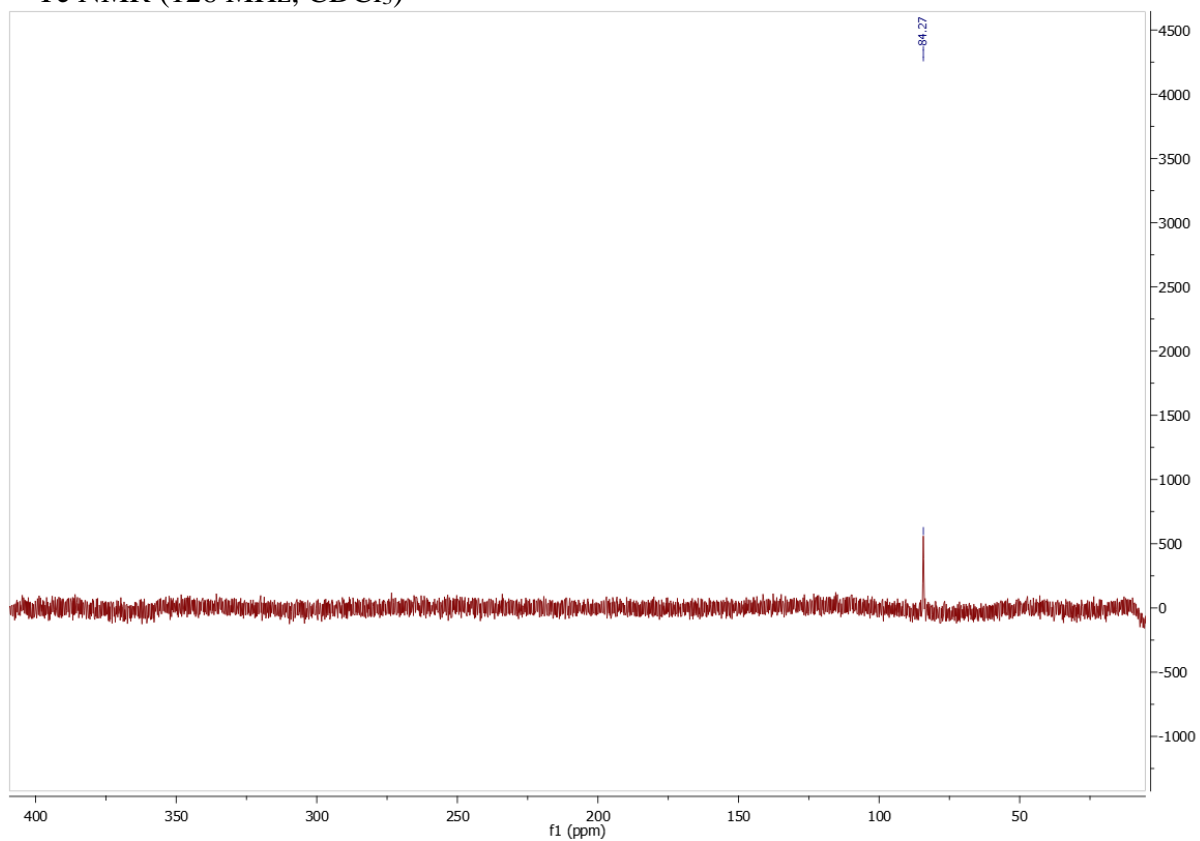


**306** ^1H NMR (401 MHz, CDCl_3) ^{13}C NMR (101 MHz, CDCl_3)

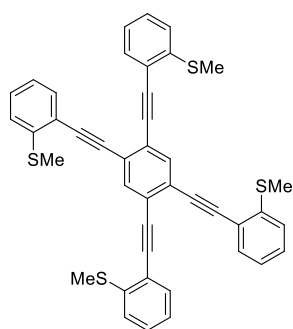


306

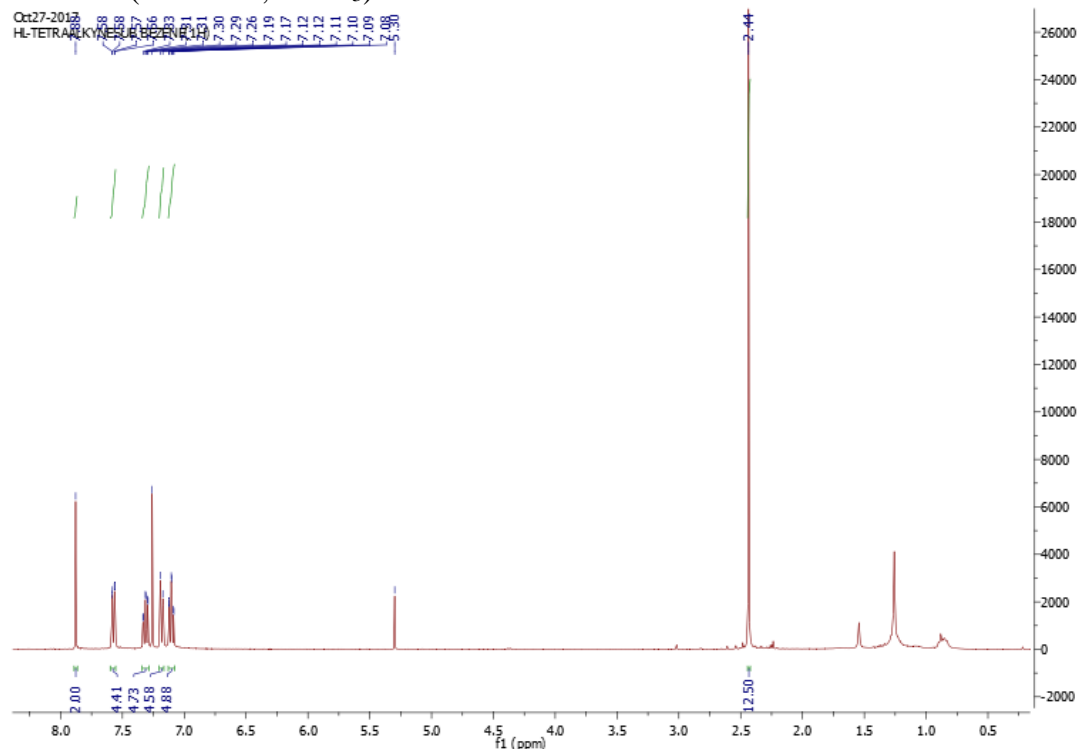
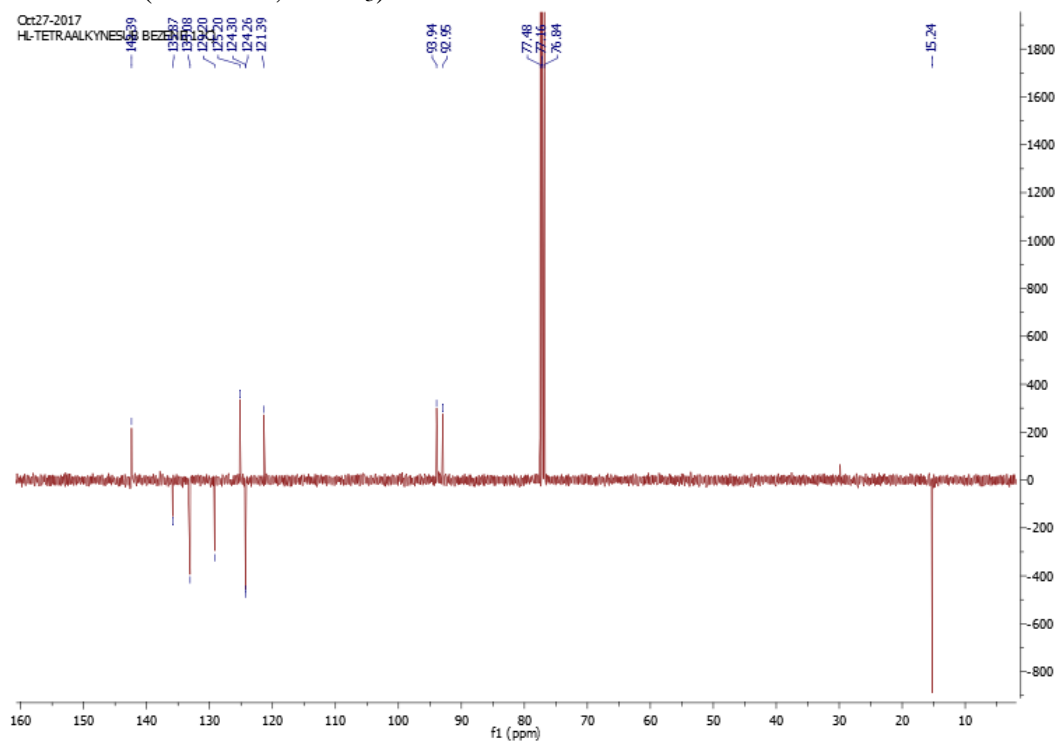
^{125}Te NMR (126 MHz, CDCl_3)



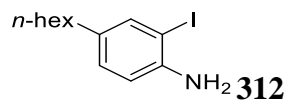
Chapter 6



309

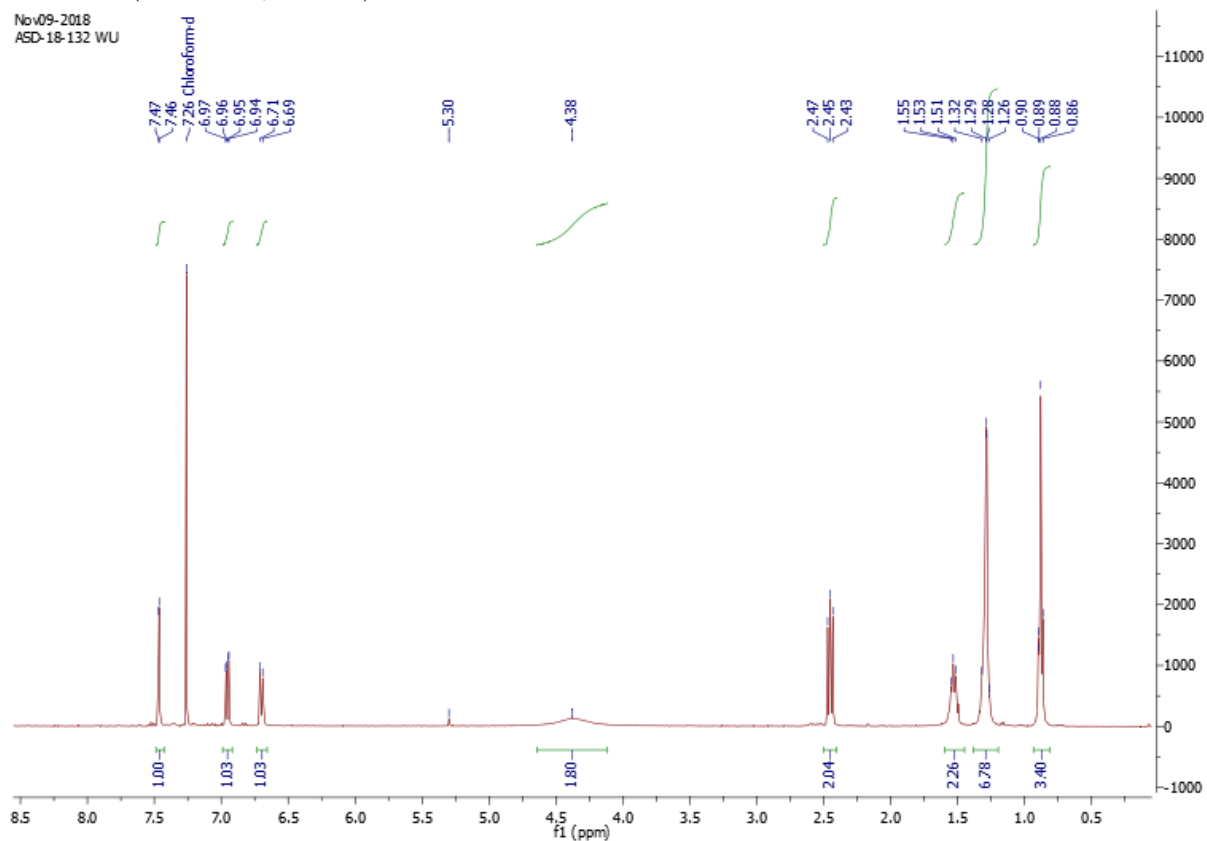
¹H NMR (401 MHz, CDCl₃) ^{13}C NMR (101 MHz, CDCl_3)

Chapter 6



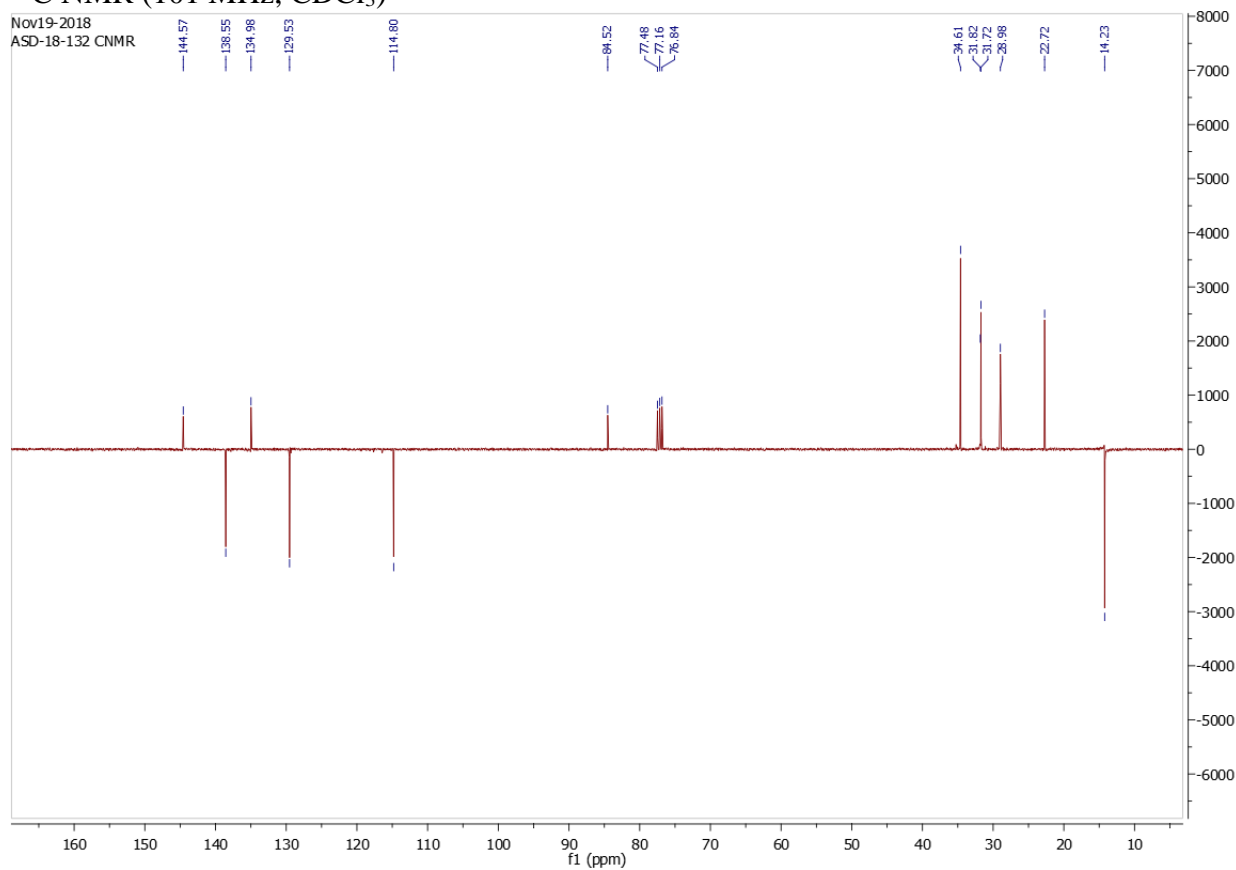
^1H NMR (401 MHz, CDCl_3)

Nov09-2018
 ASD-18-132 WU

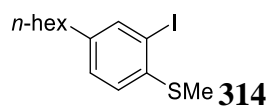


^{13}C NMR (101 MHz, CDCl_3)

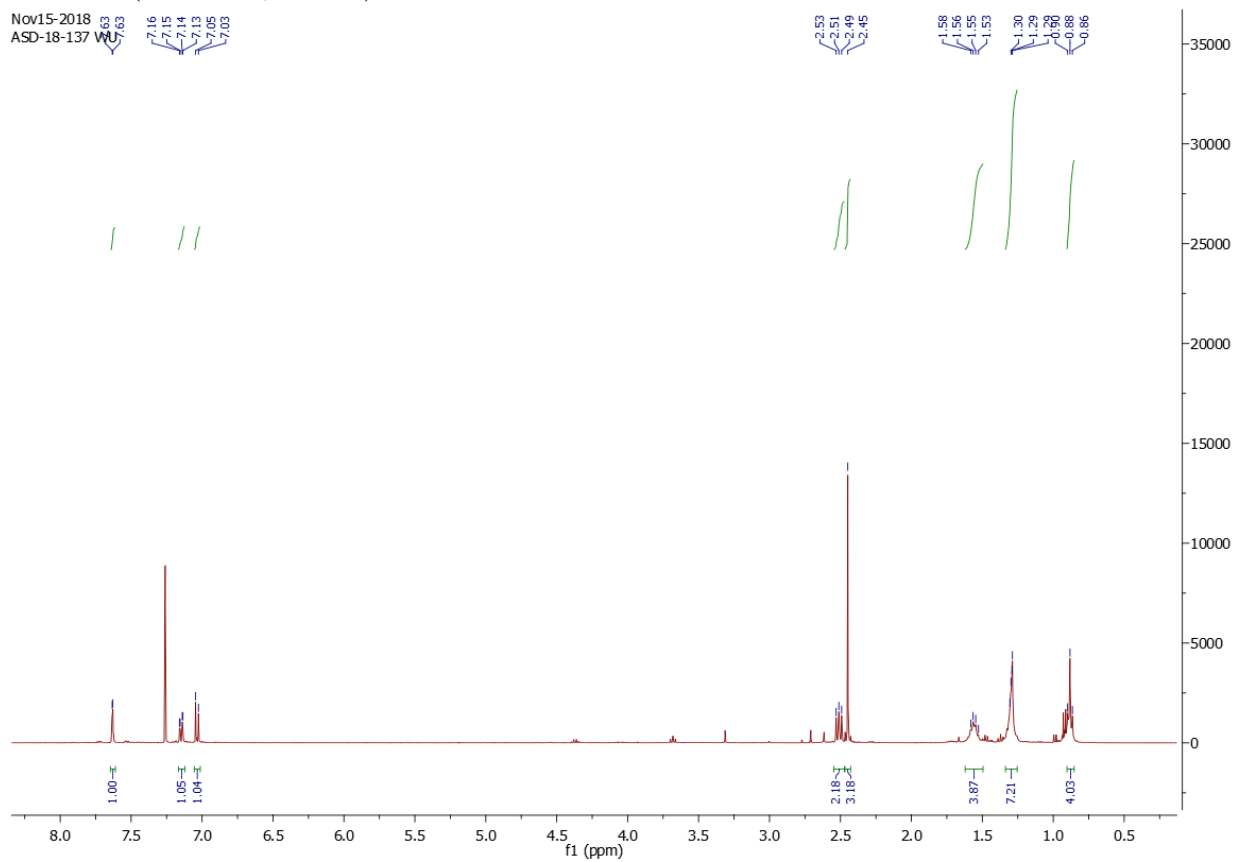
Nov19-2018
 ASD-18-132 CNMR



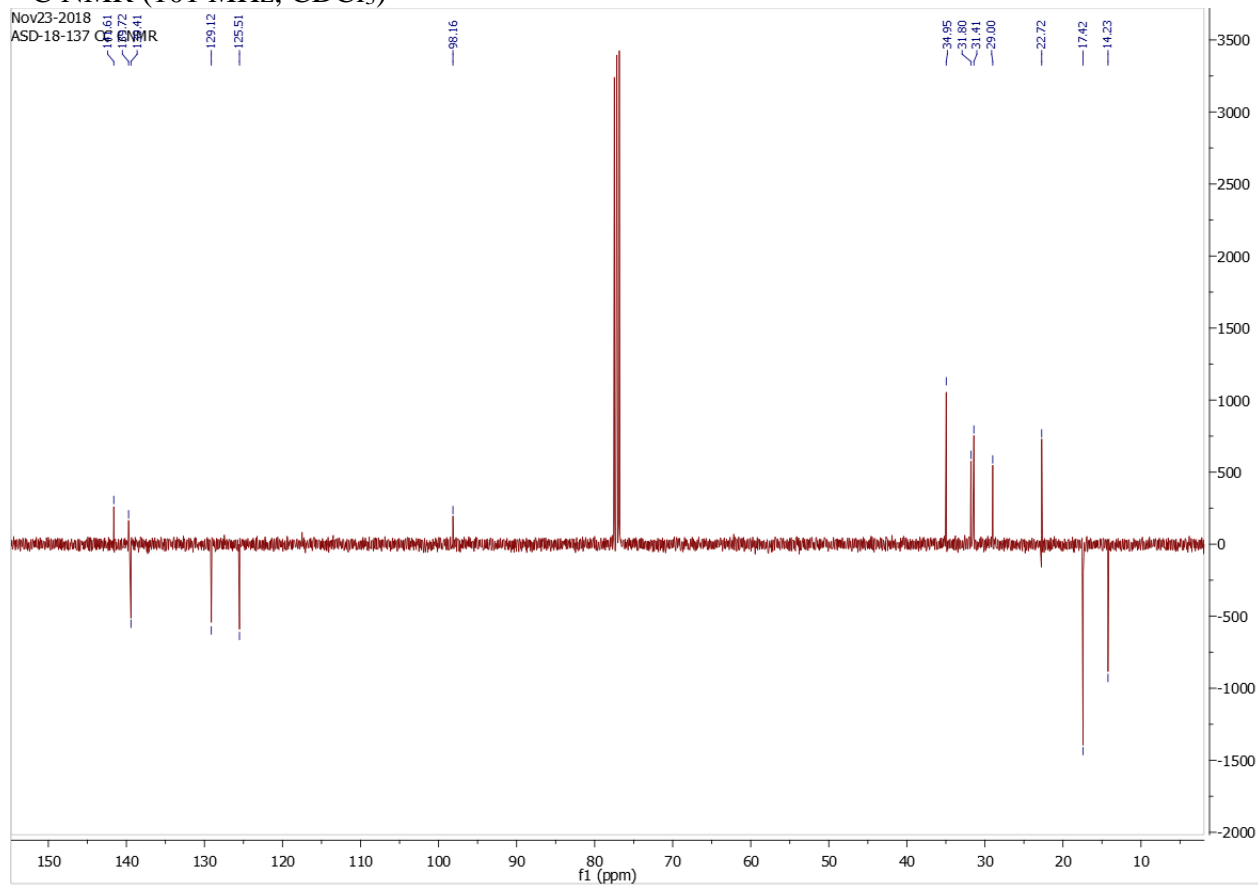
Chapter 6



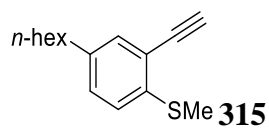
^1H NMR (401 MHz, CDCl_3)



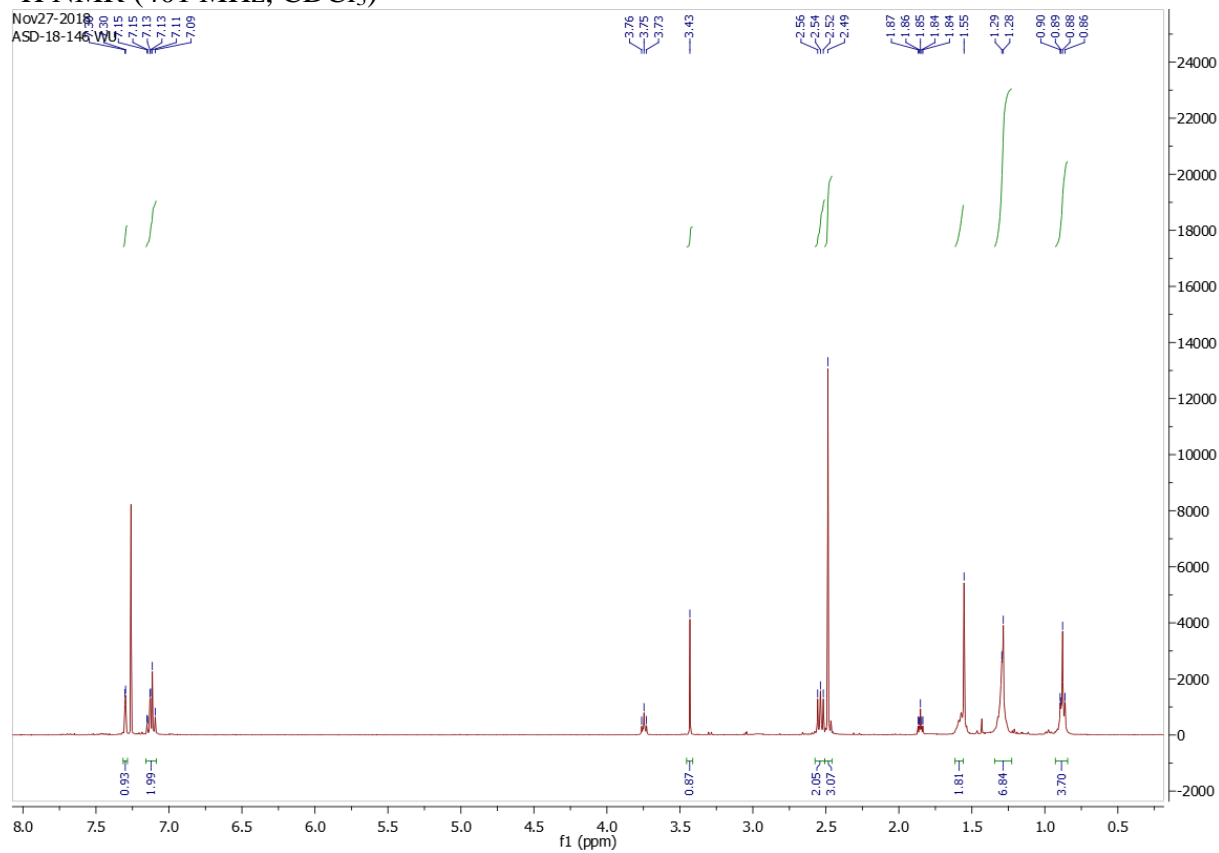
^{13}C NMR (101 MHz, CDCl_3)



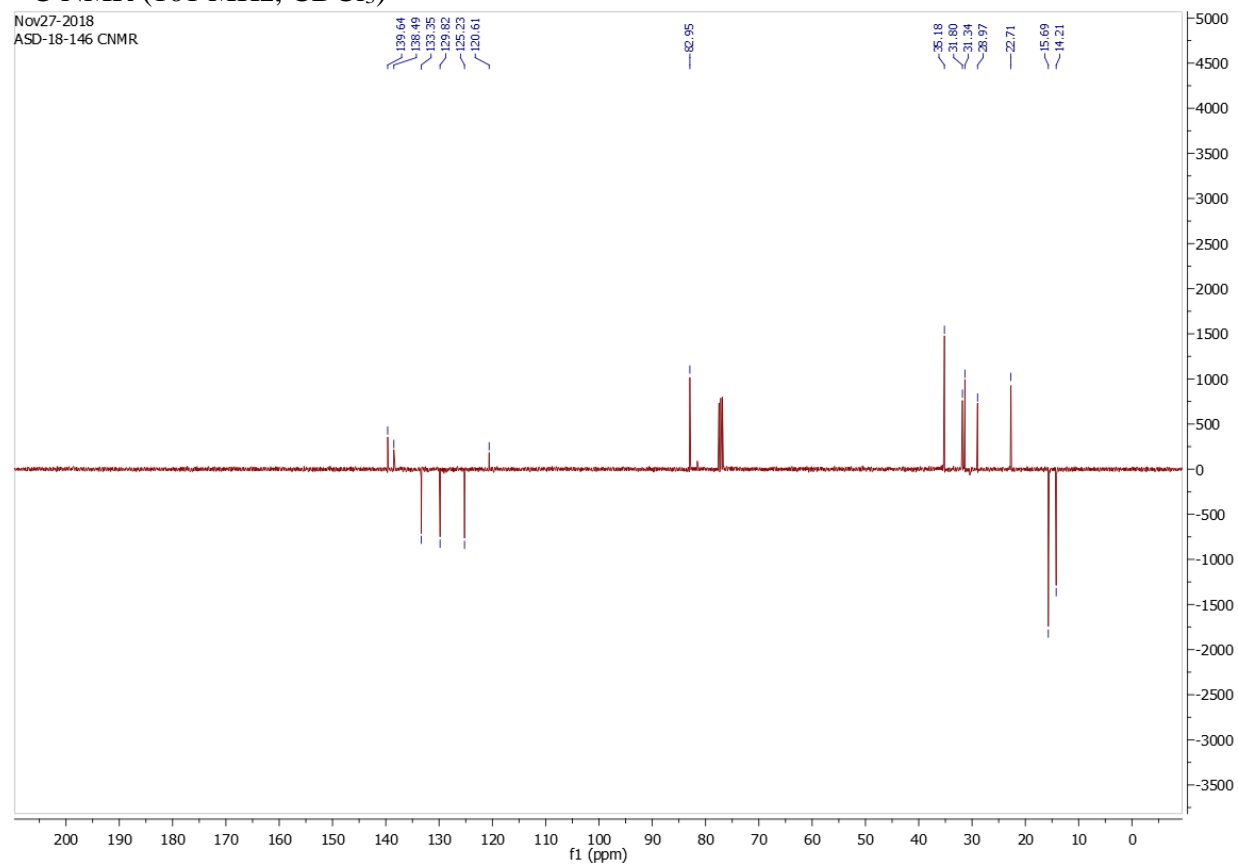
Chapter 6



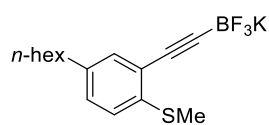
^1H NMR (401 MHz, CDCl_3)



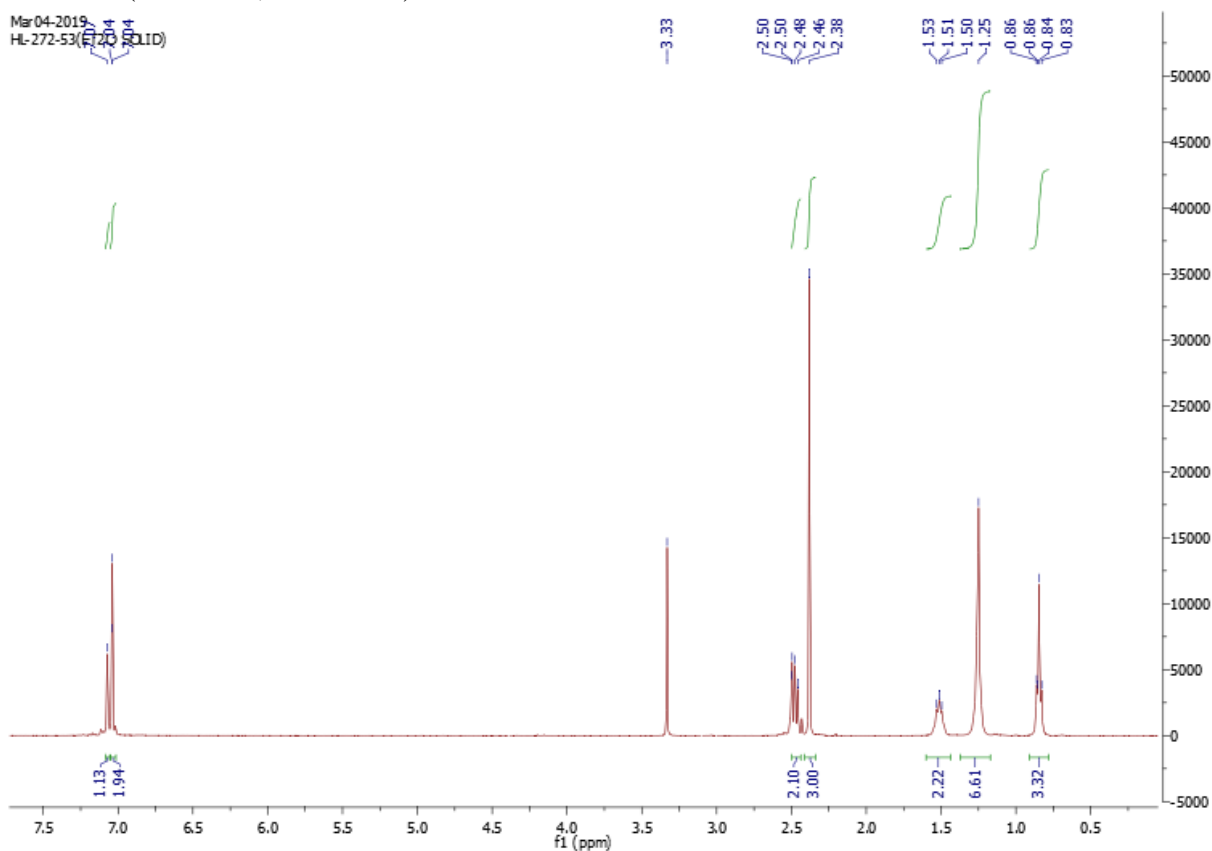
^{13}C NMR (101 MHz, CDCl_3)



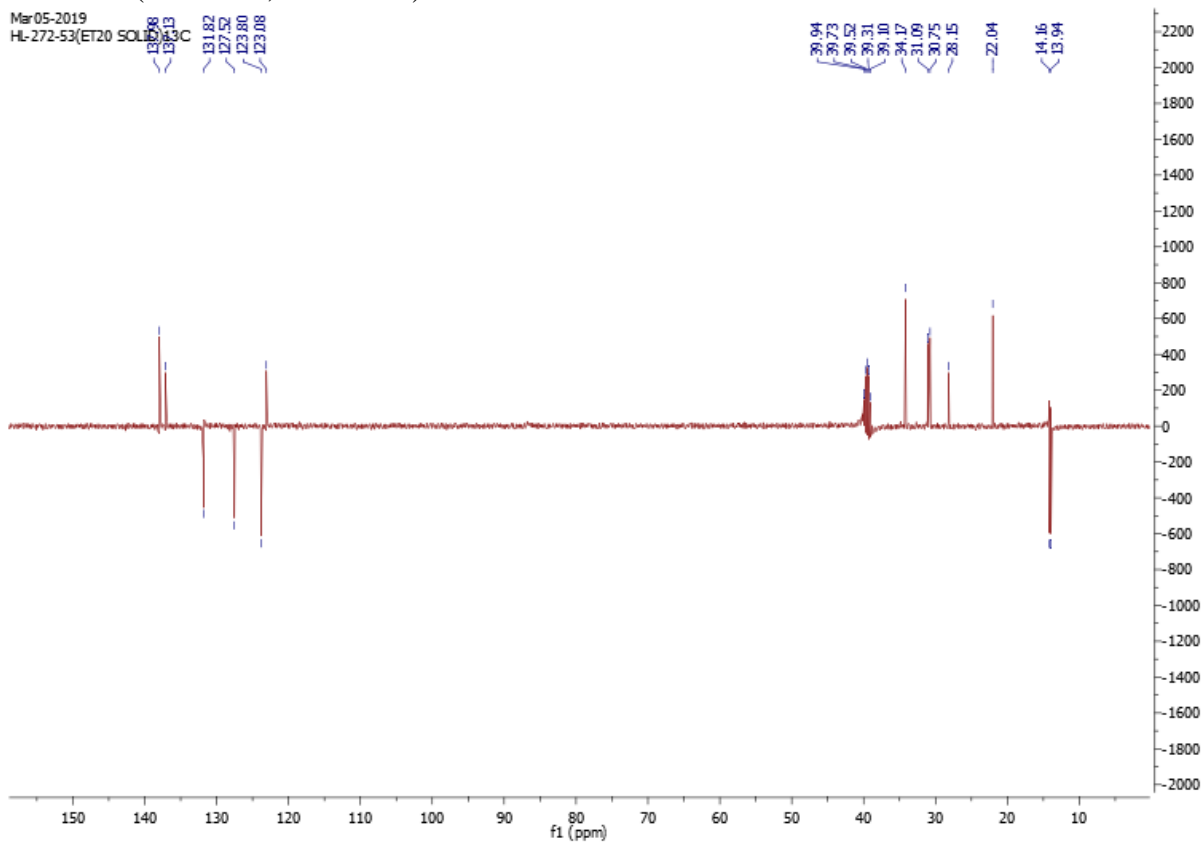
Chapter 6



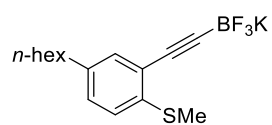
¹H NMR (401 MHz, DMSO-d₆)



¹³C NMR (101 MHz, DMSO-d₆)



Chapter 6

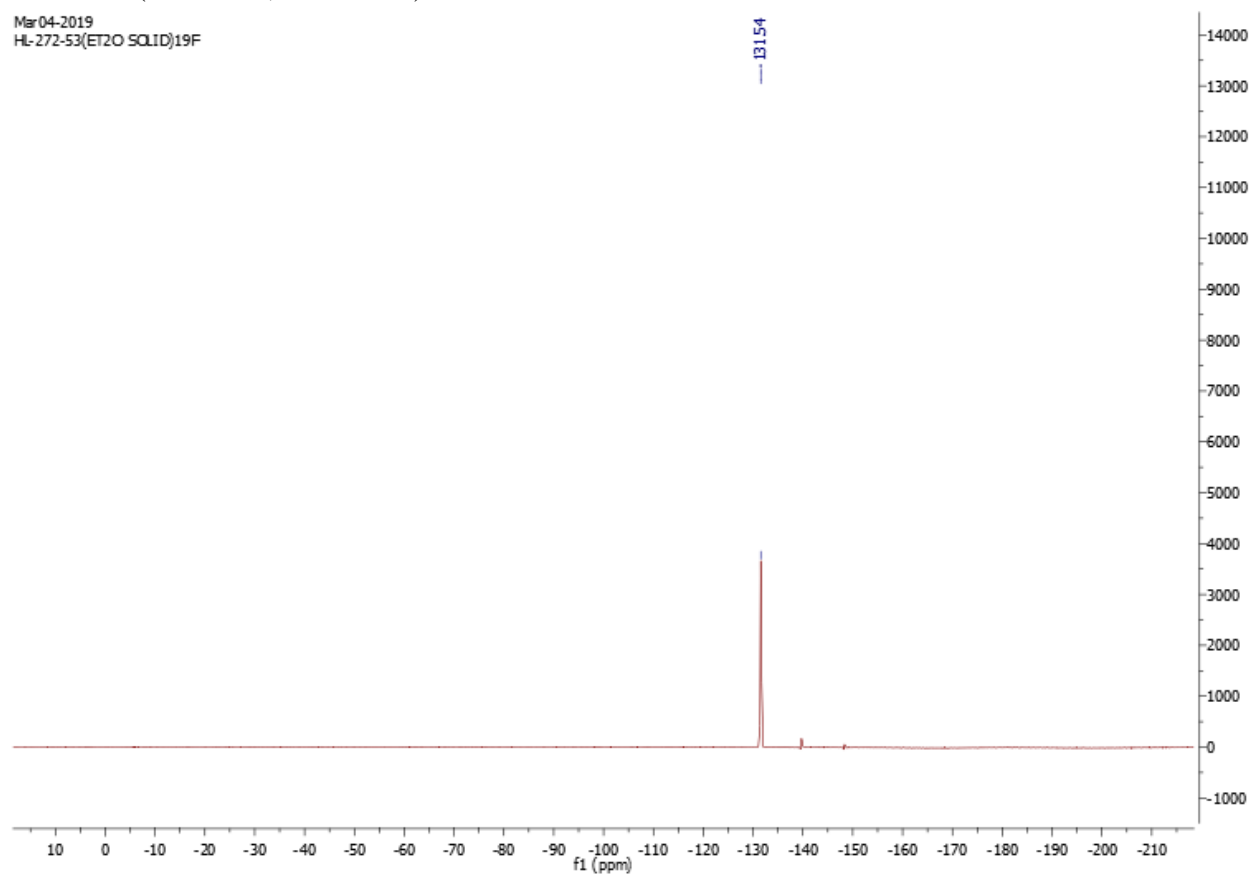


315-BF₃K

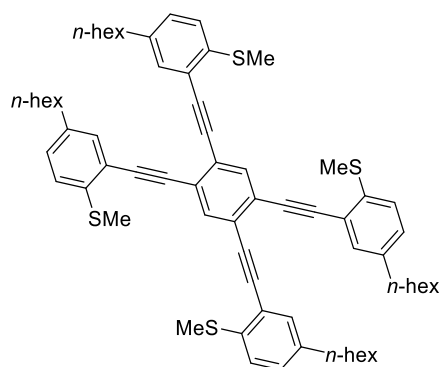
¹⁹F NMR (377 MHz, DMSO-d₆)

Mar04-2019

HL-272-53(ET2O SOLID)19F

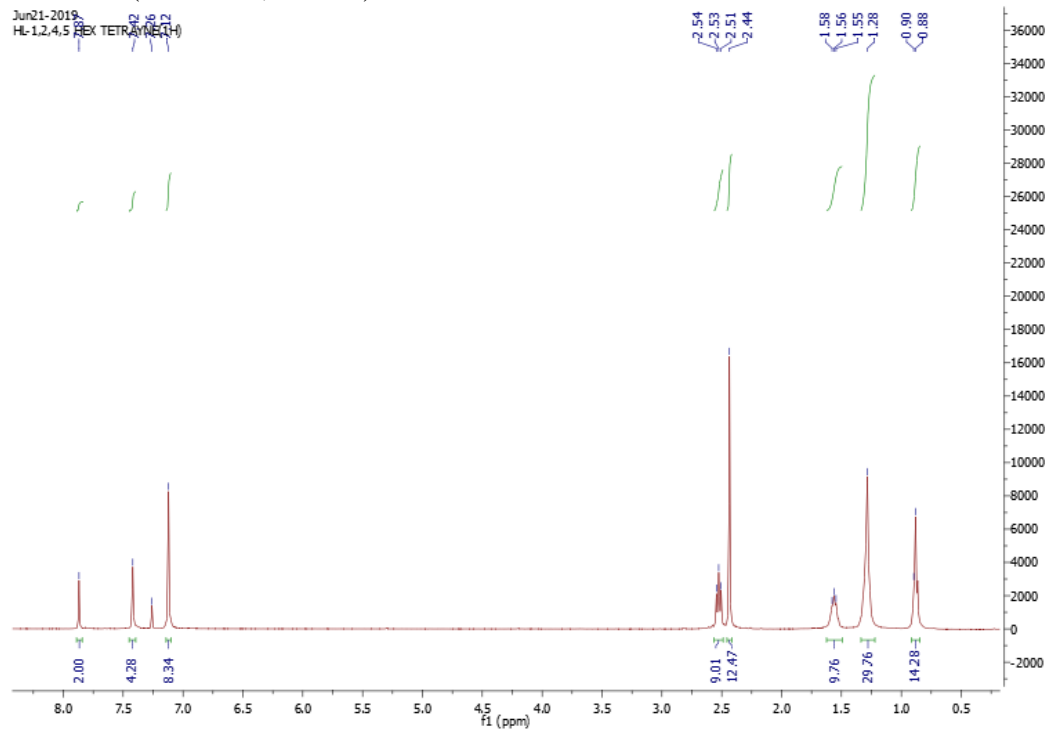


Chapter 6

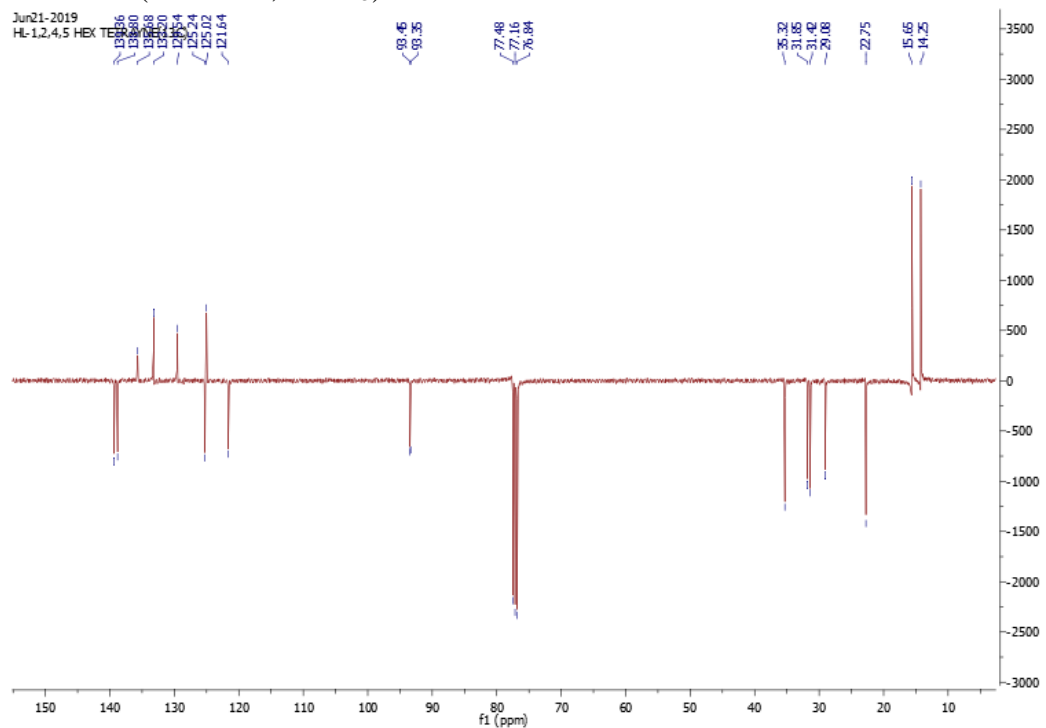


317

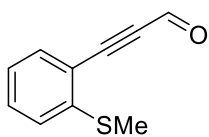
^1H NMR (401 MHz, CDCl_3)



^{13}C NMR (101 MHz, CDCl_3)

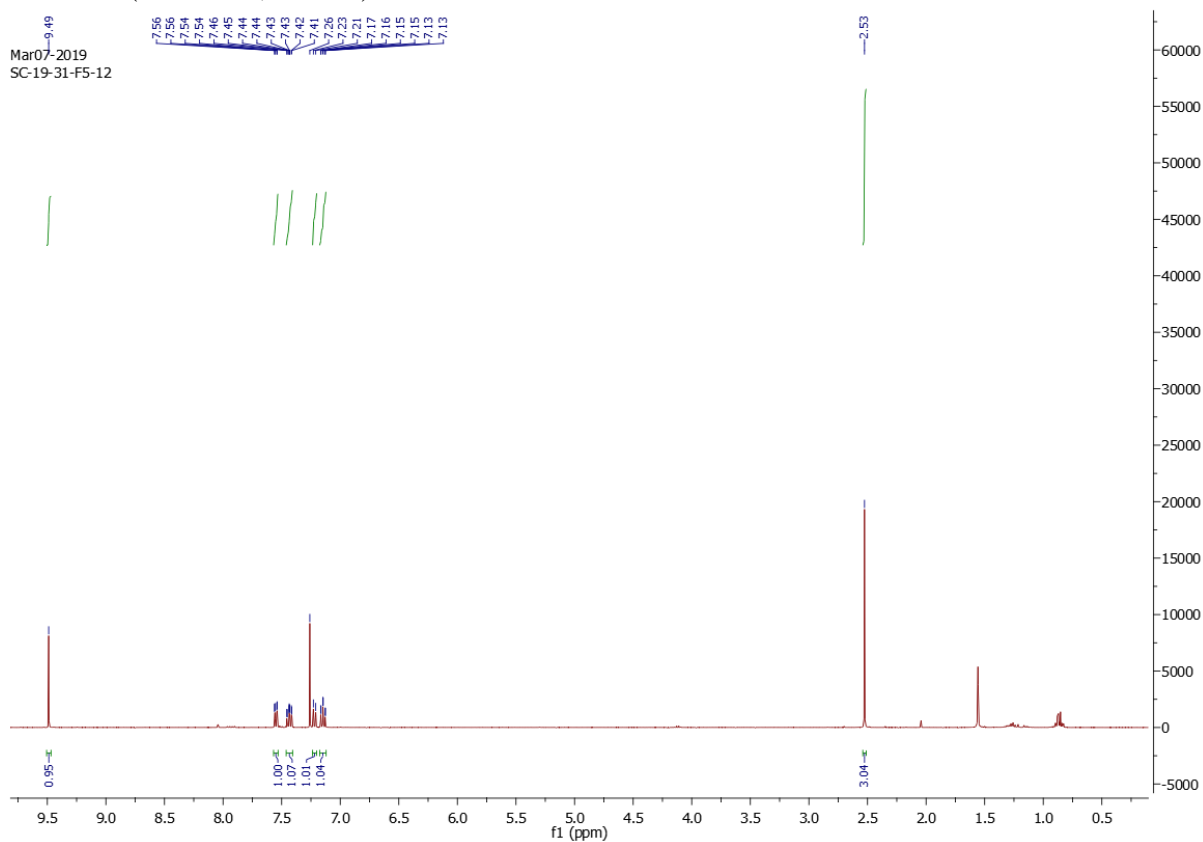


Chapter 6

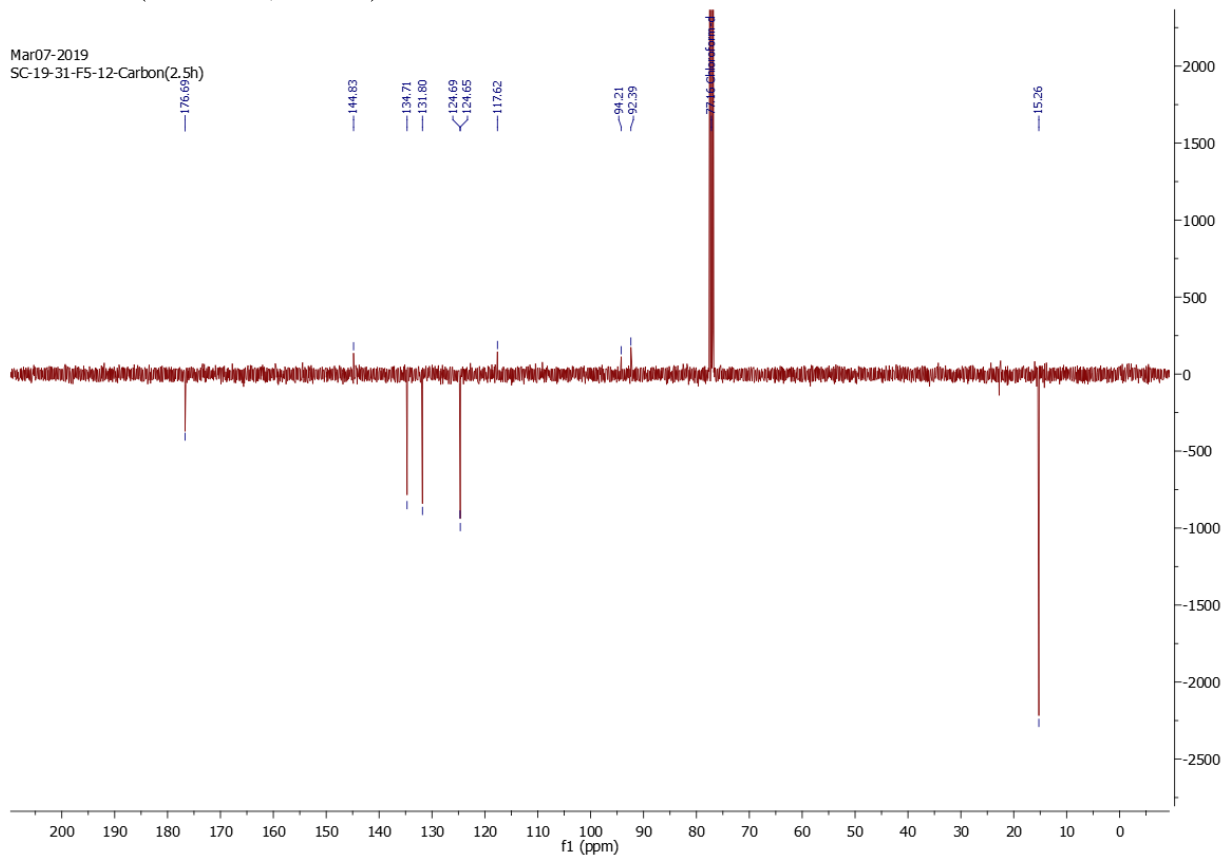


325

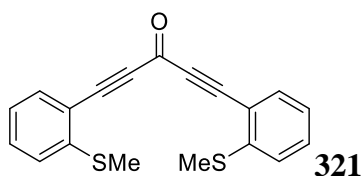
^1H NMR (401 MHz, CDCl_3)



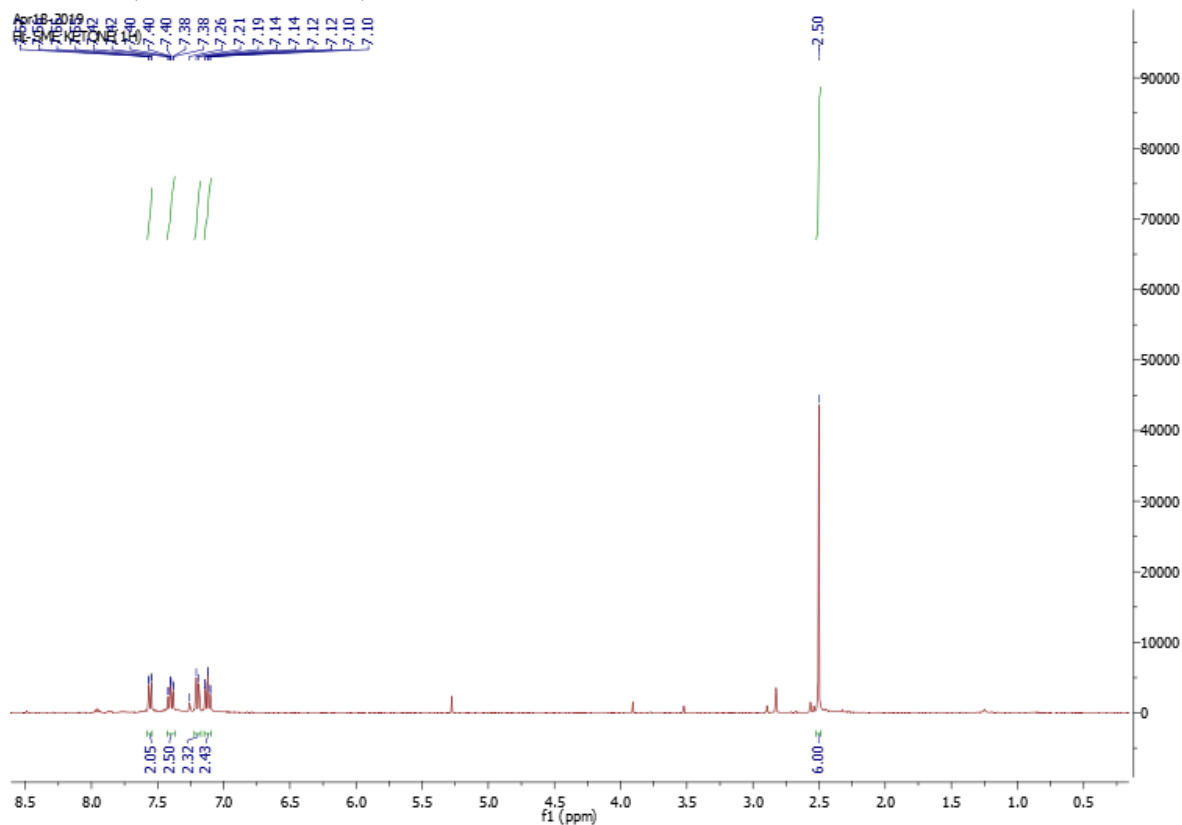
^{13}C NMR (101 MHz, CDCl_3)



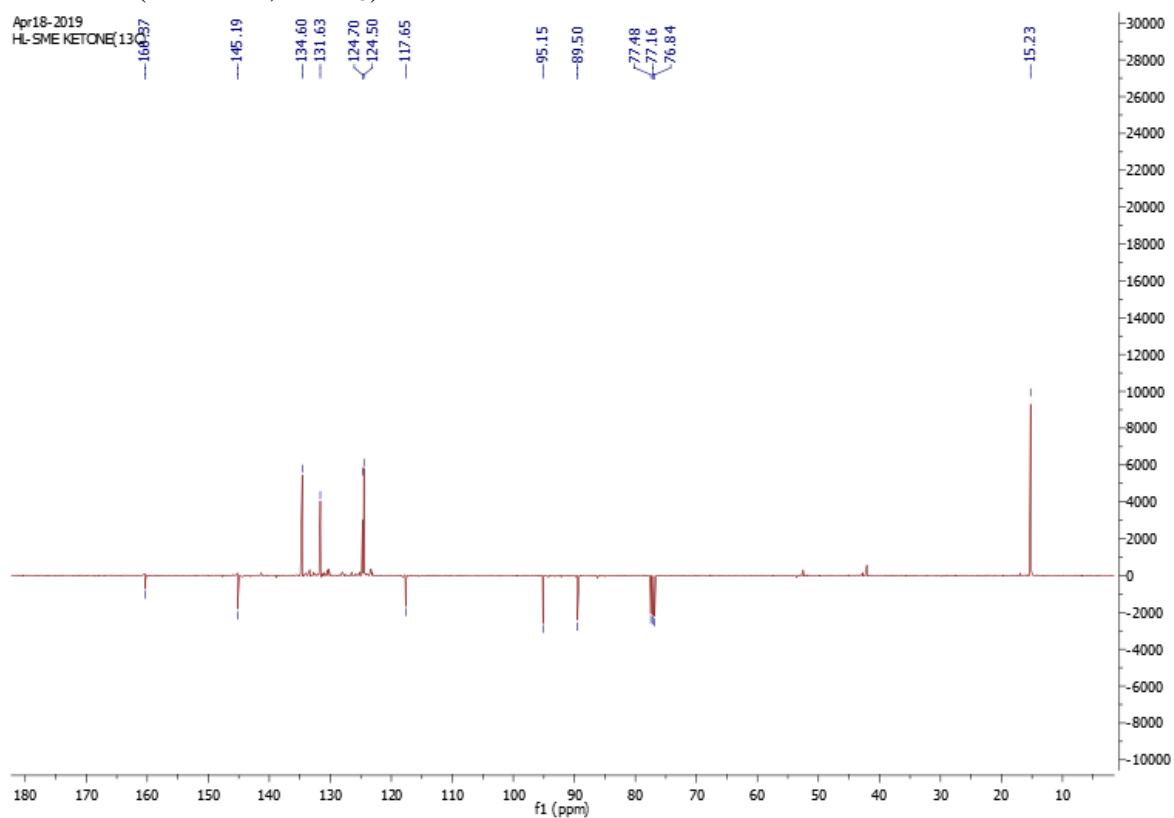
Chapter 6



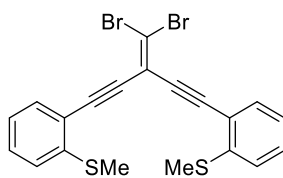
^1H NMR (401 MHz, CDCl_3)



^{13}C NMR (101 MHz, CDCl_3)

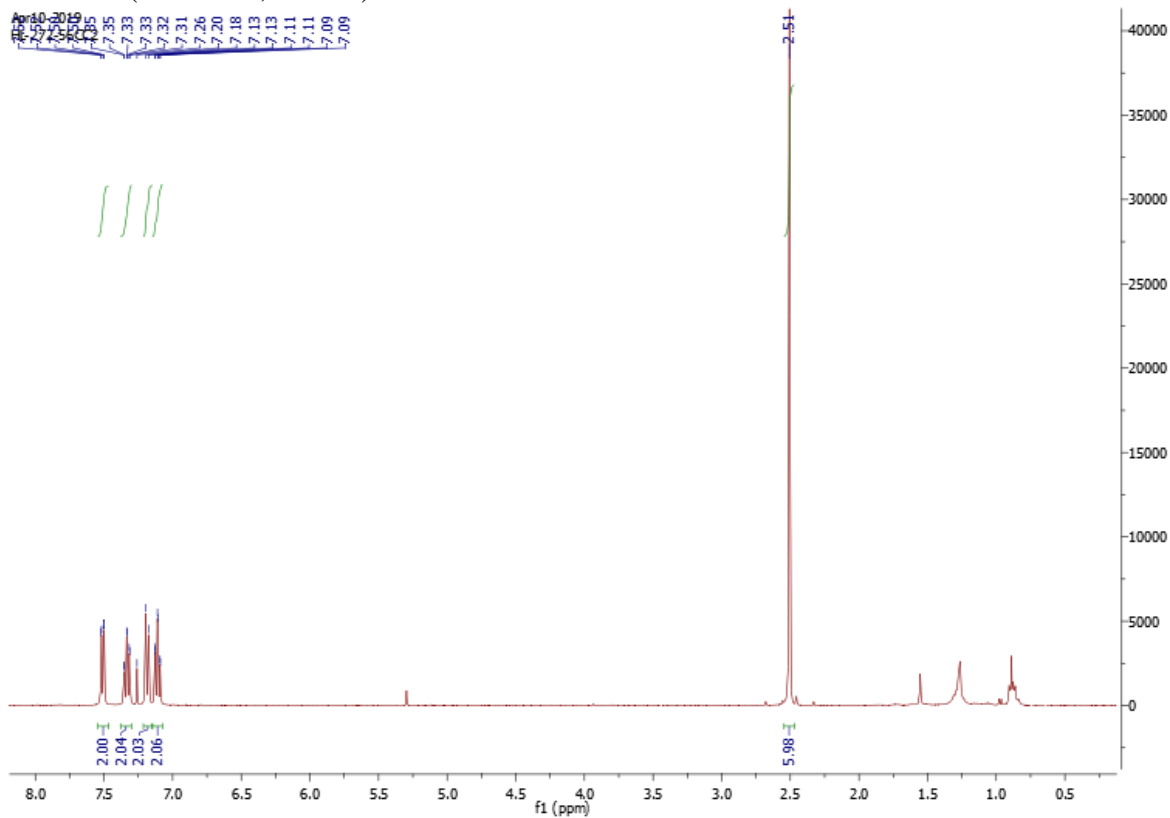


Chapter 6

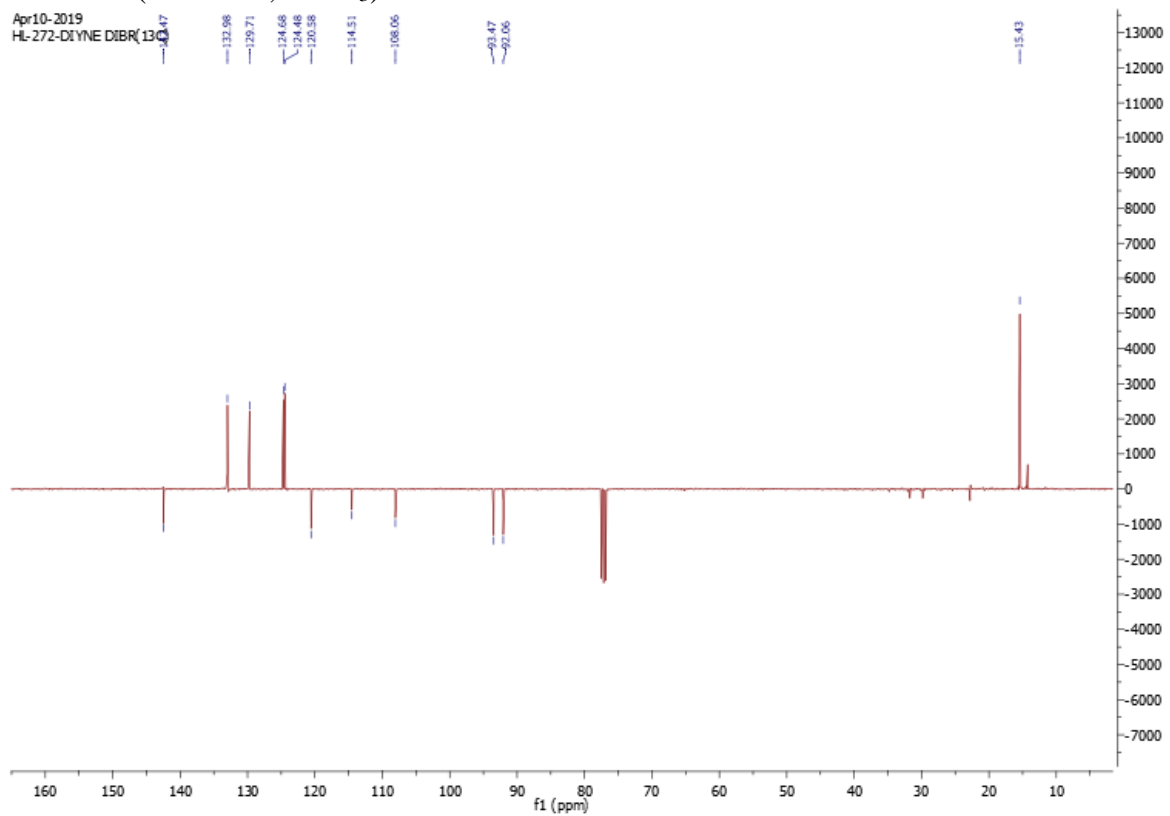


322

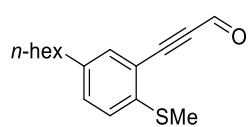
^1H NMR (401 MHz, CDCl_3)



^{13}C NMR (101 MHz, CDCl_3)



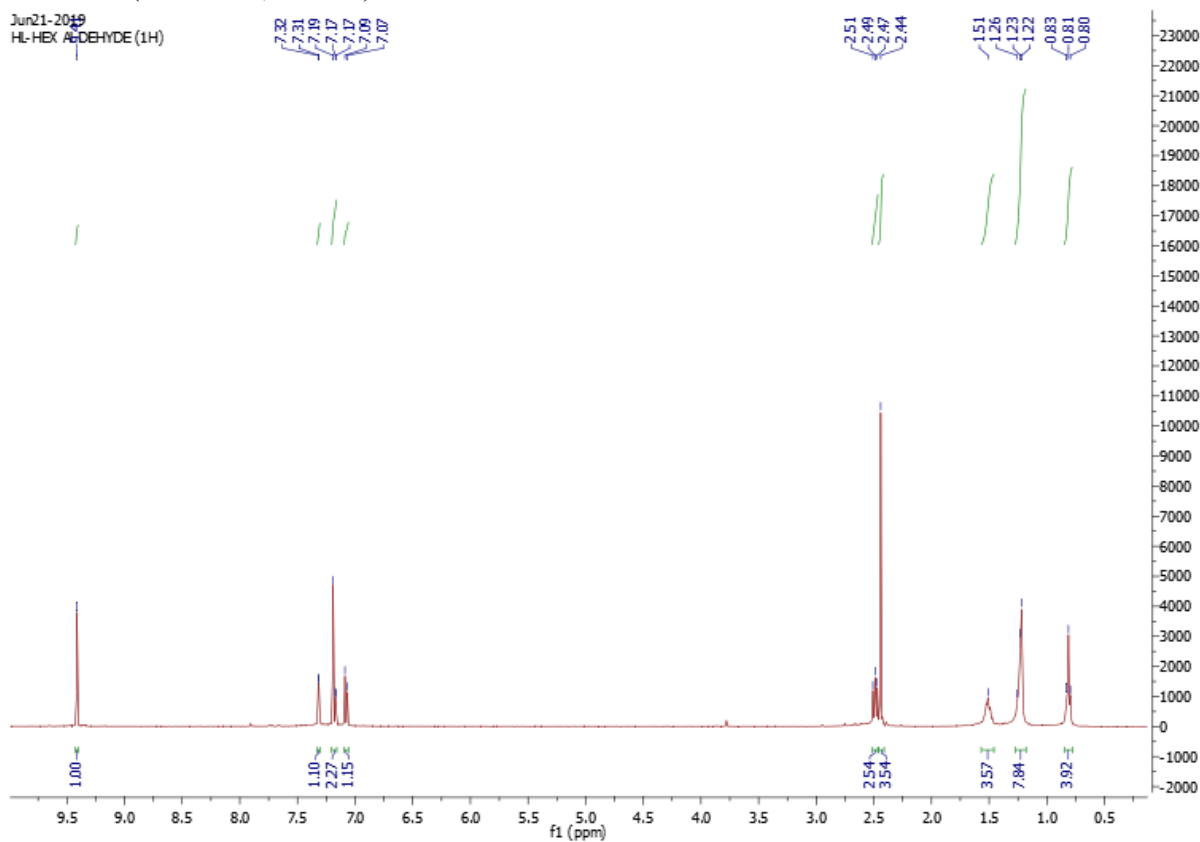
Chapter 6



332

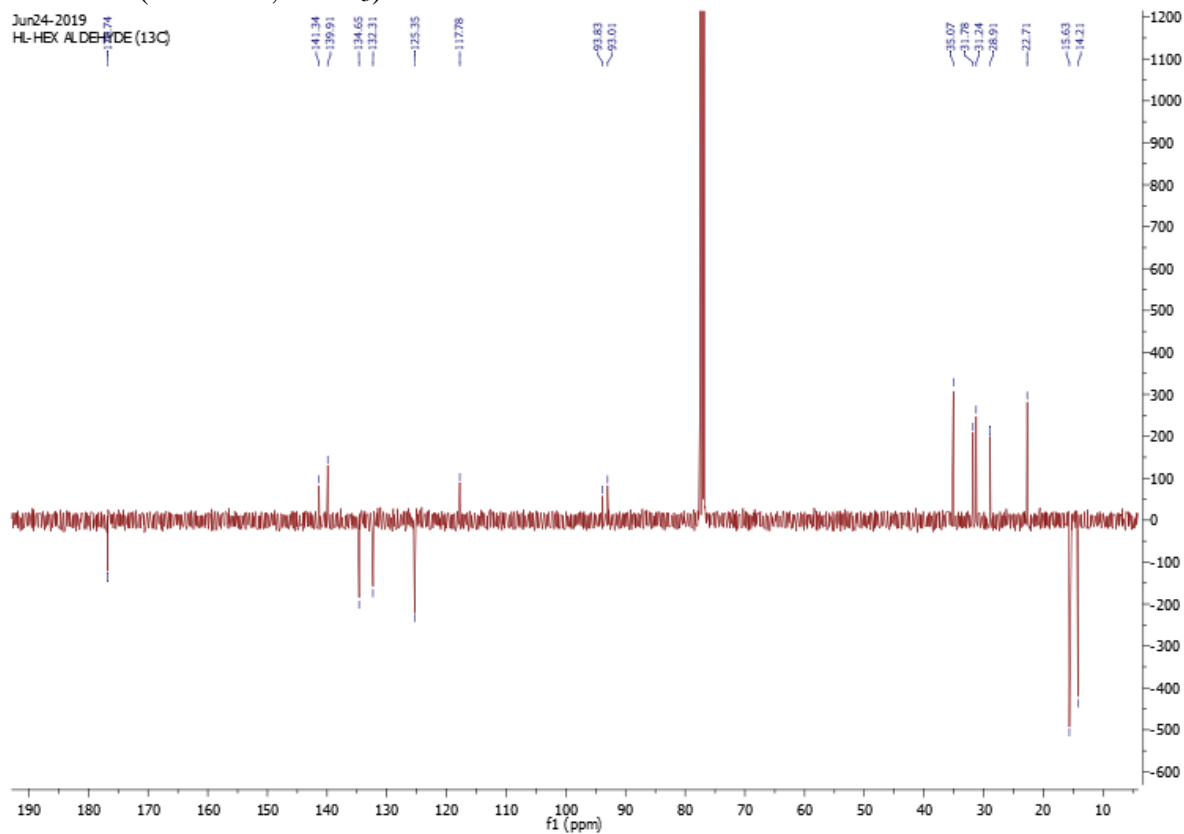
^1H NMR (401 MHz, CDCl_3)

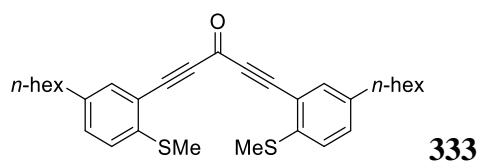
Jun21-2019
HL-HEX ALDEHYDE (1H)



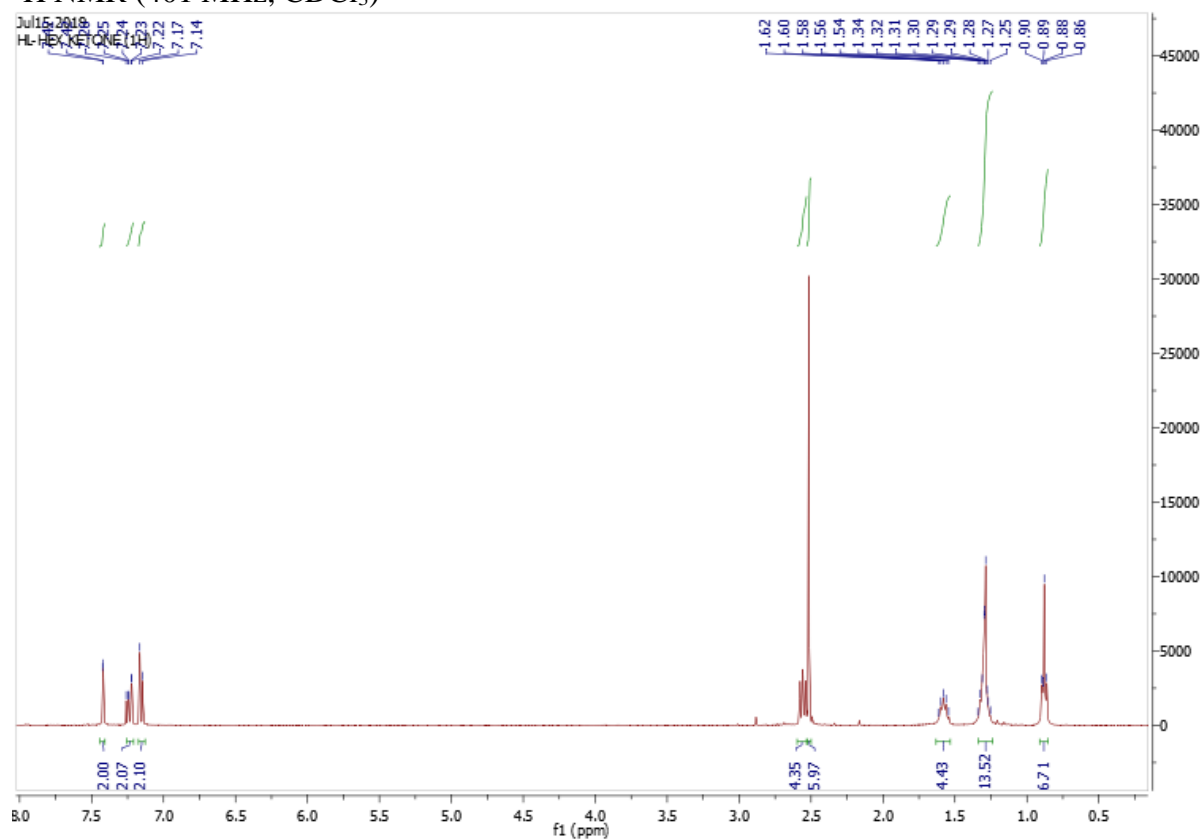
^{13}C NMR (101 MHz, CDCl_3)

Jun24-2019
HL-HEX ALDEHYDE (13C)

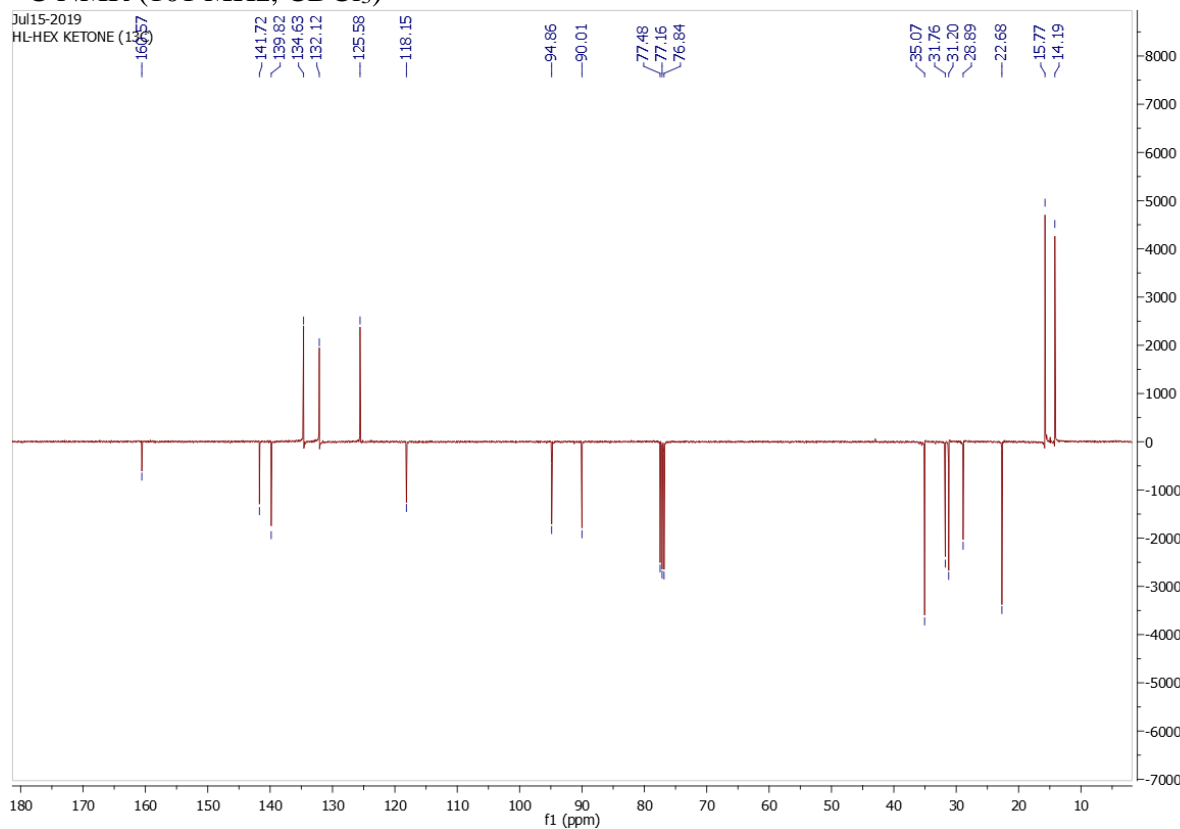


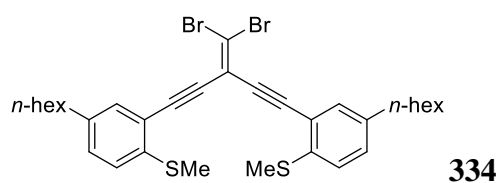


^1H NMR (401 MHz, CDCl_3)



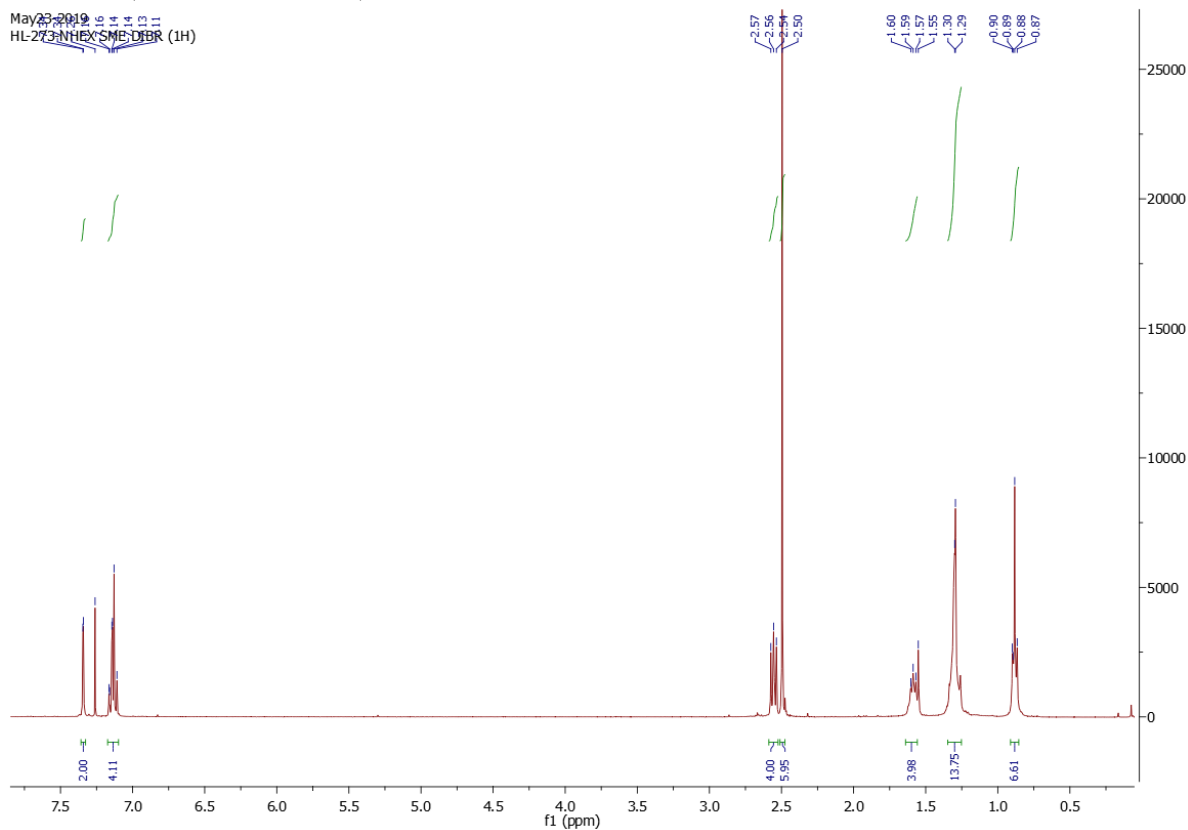
^{13}C NMR (101 MHz, CDCl_3)





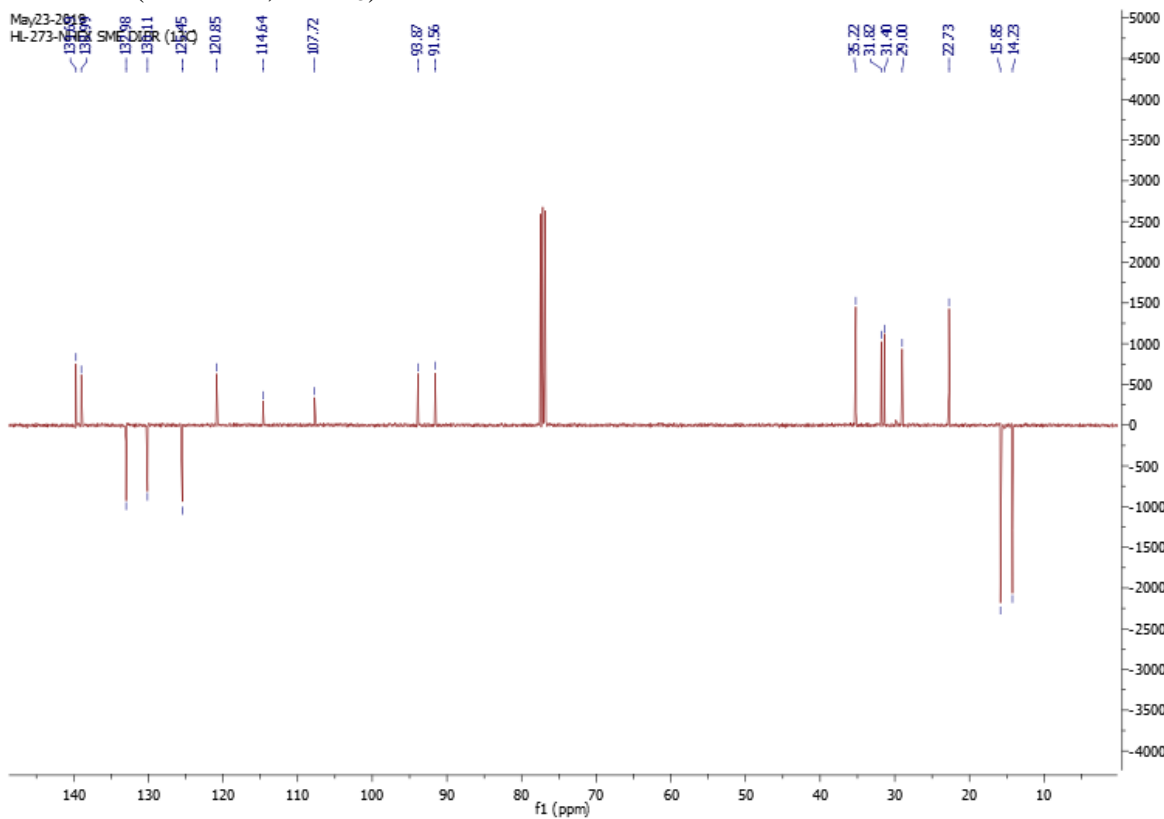
^1H NMR (401 MHz, CDCl_3)

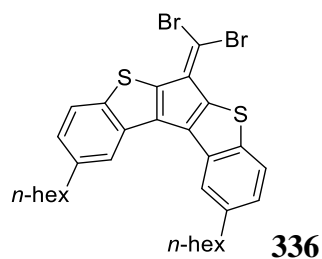
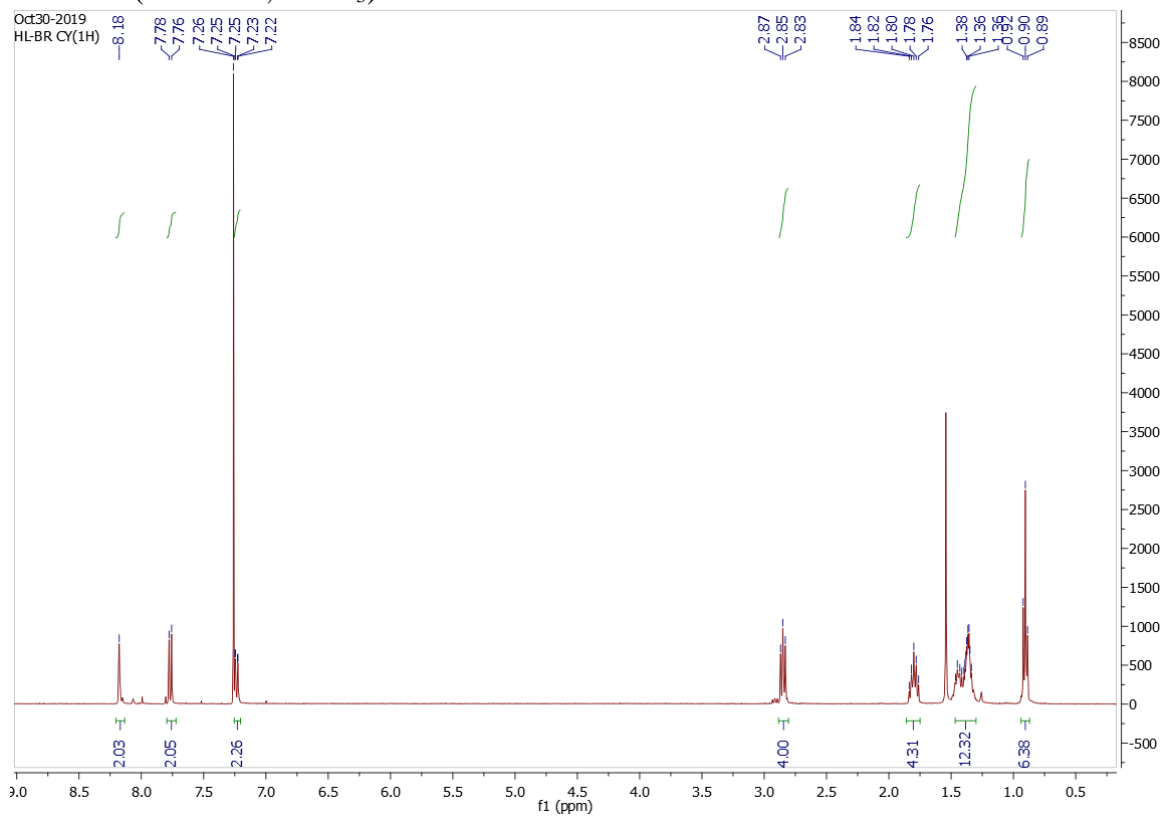
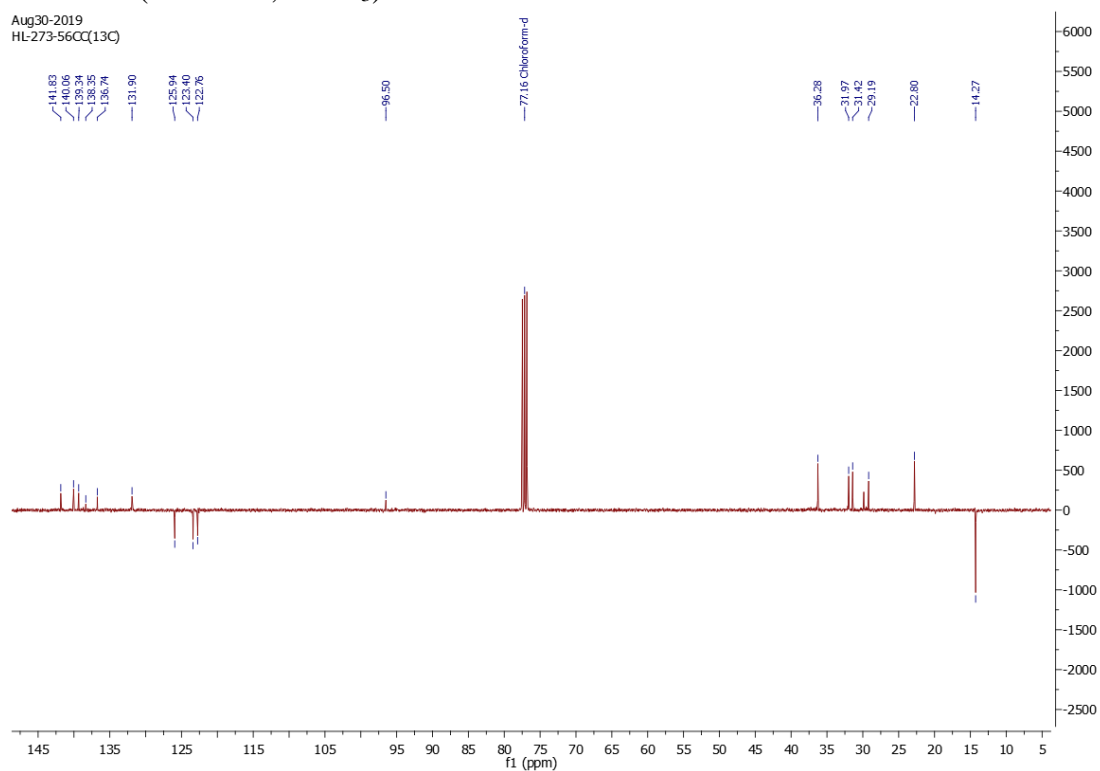
May23-2019
HL-273-NHEX-SME-DIBR (1H)

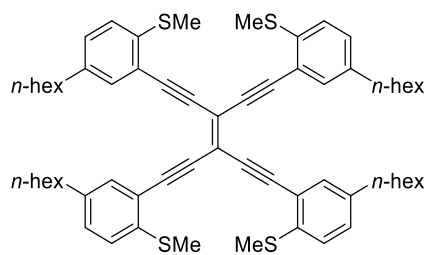


^{13}C NMR (101 MHz, CDCl_3)

May23-2019
HL-273-NHEX-SME-DIBR (13C)

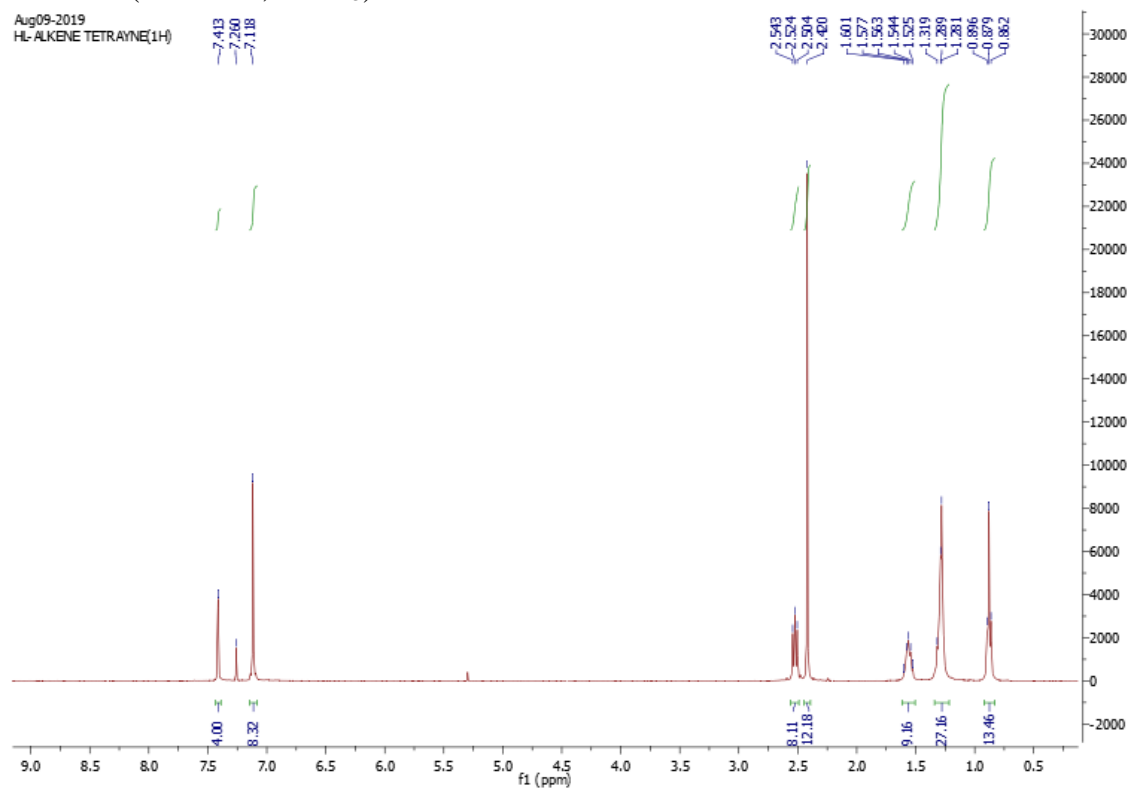


**336** ^1H NMR (401 MHz, CDCl_3) ^{13}C NMR (101 MHz, CDCl_3)

**335**¹H NMR (401 MHz, CDCl₃)

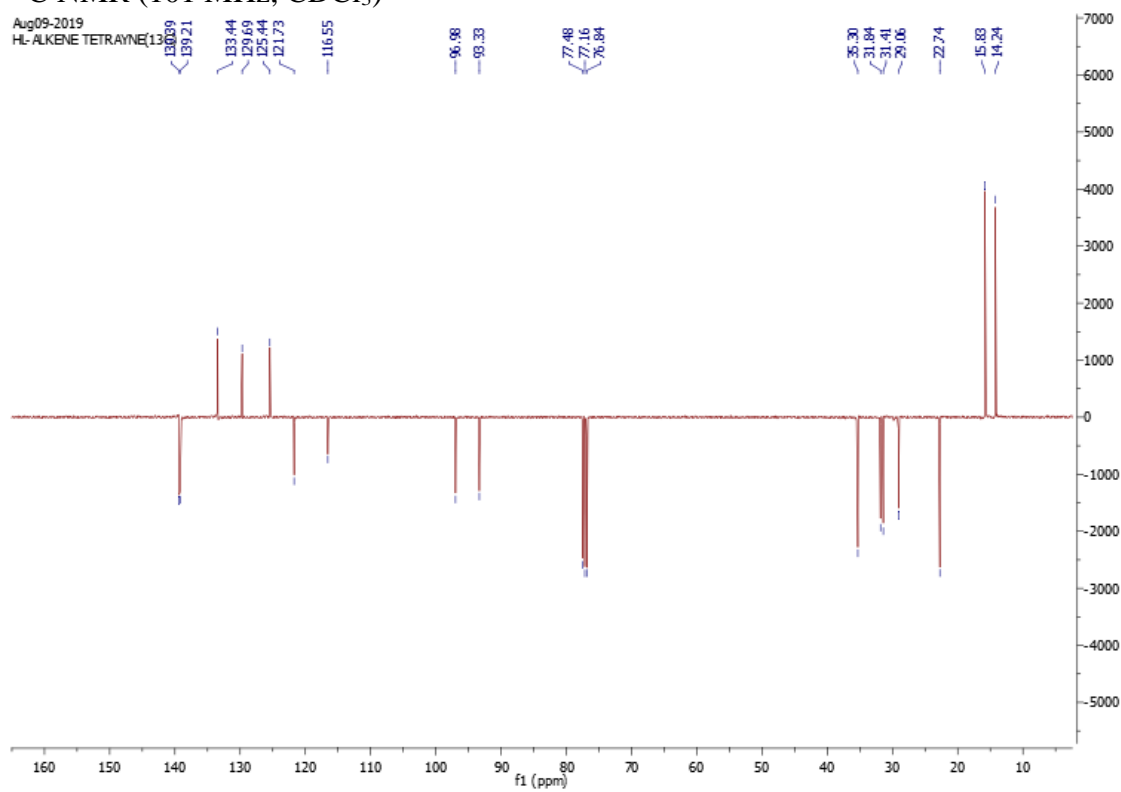
Aug09-2019

HL-ALKENE TETRAYNE(1H)

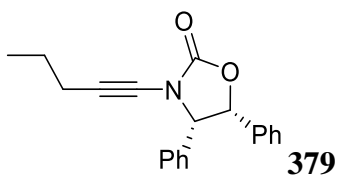
¹³C NMR (101 MHz, CDCl₃)

Aug09-2019

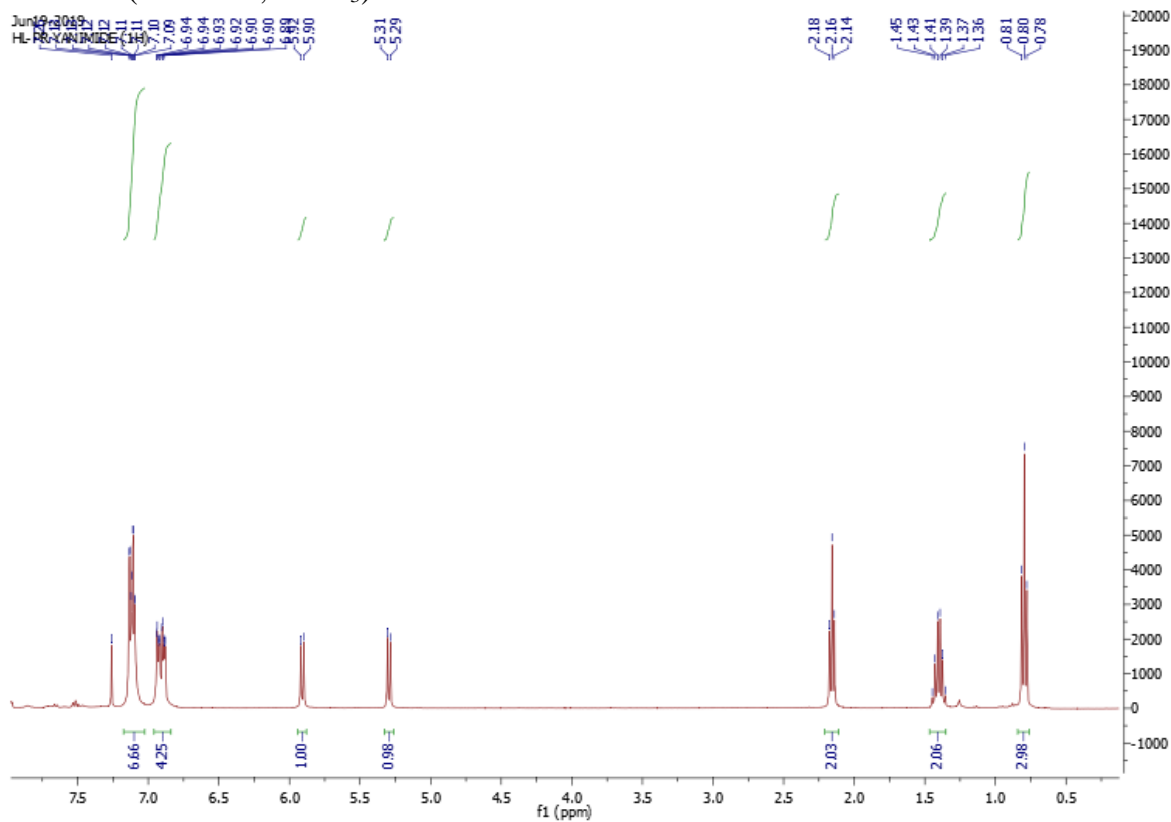
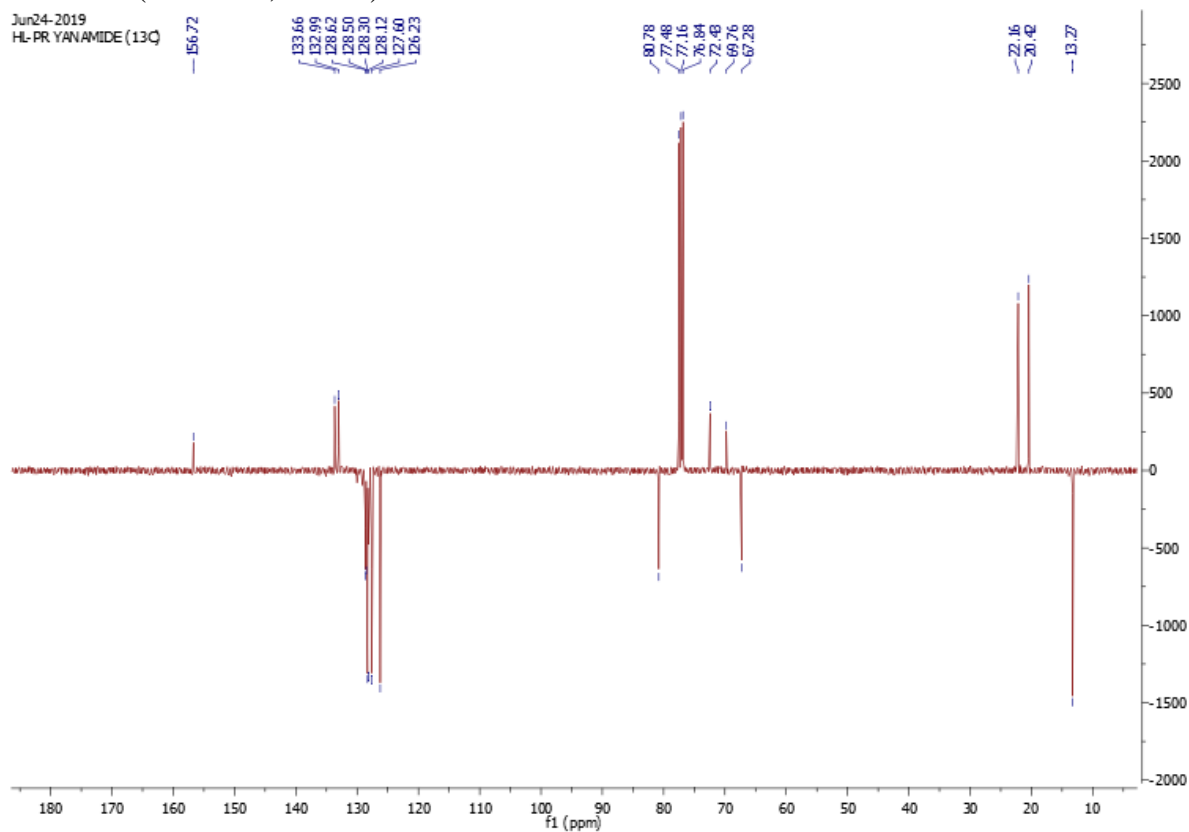
HL-ALKENE TETRAYNE(1H)

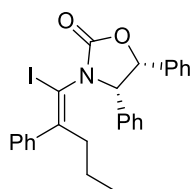
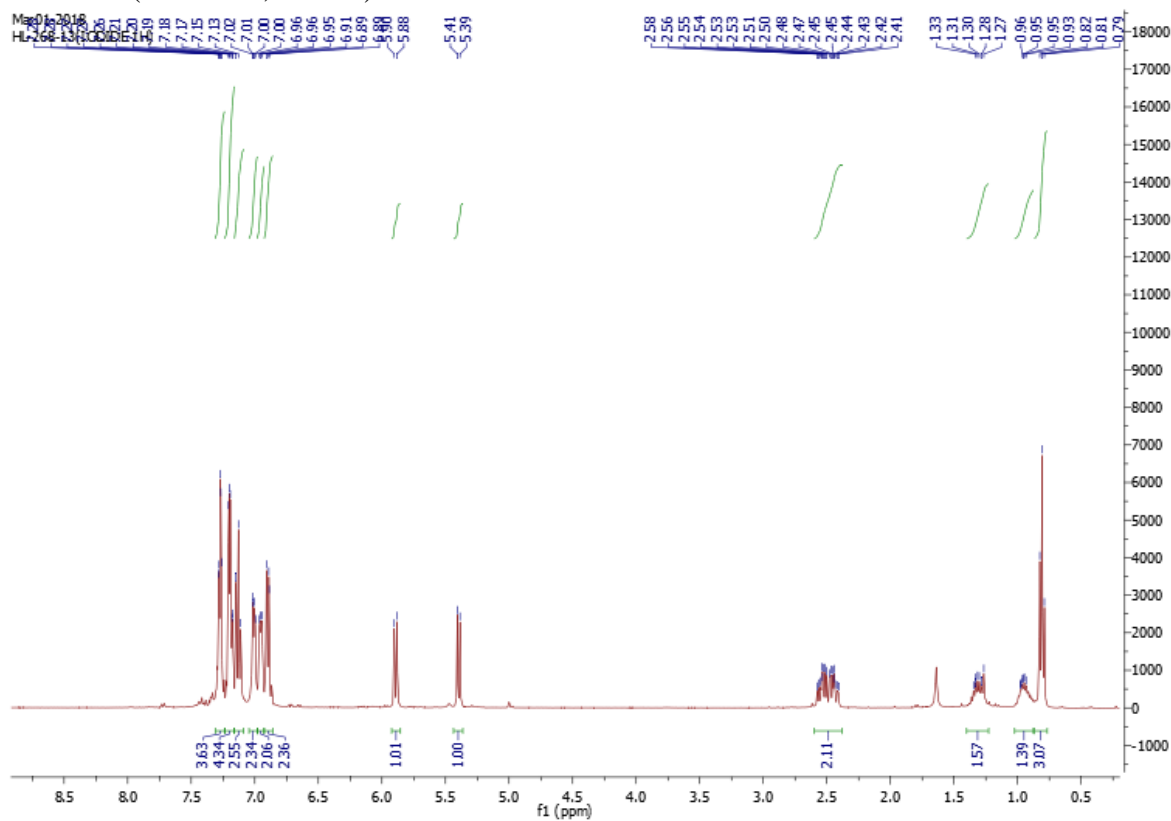
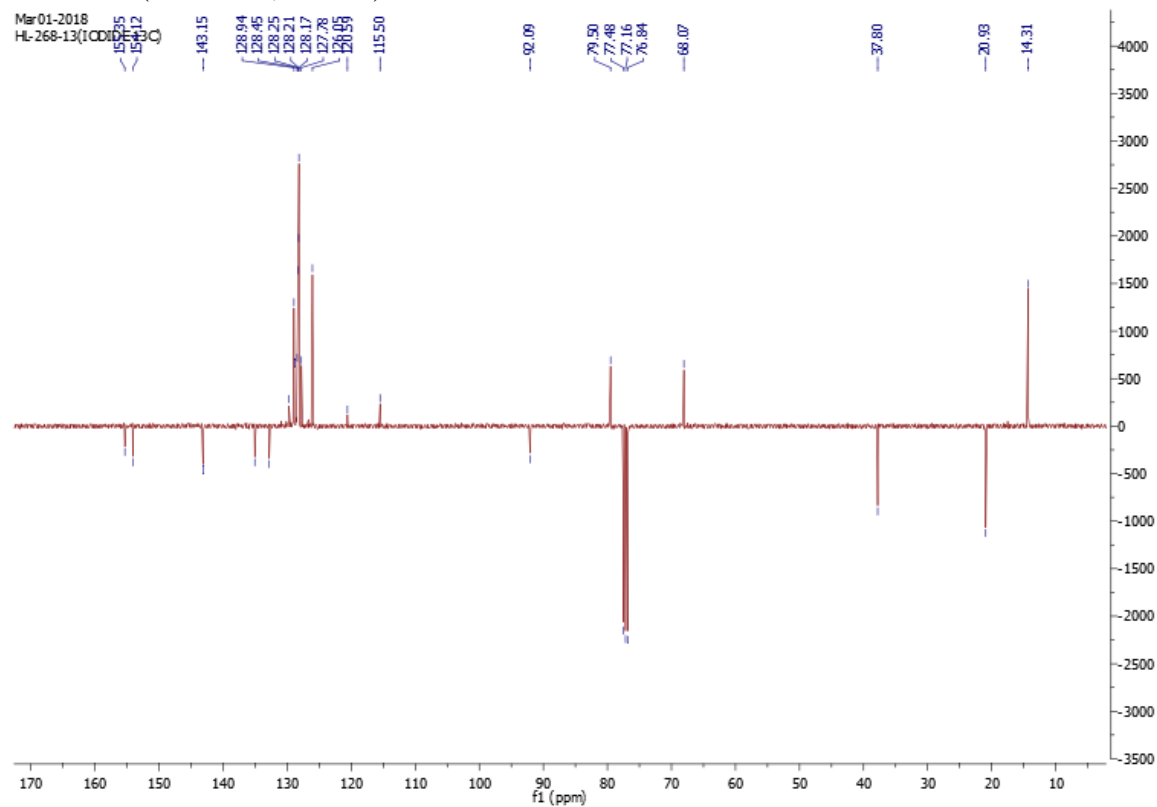


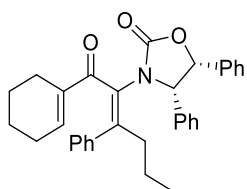
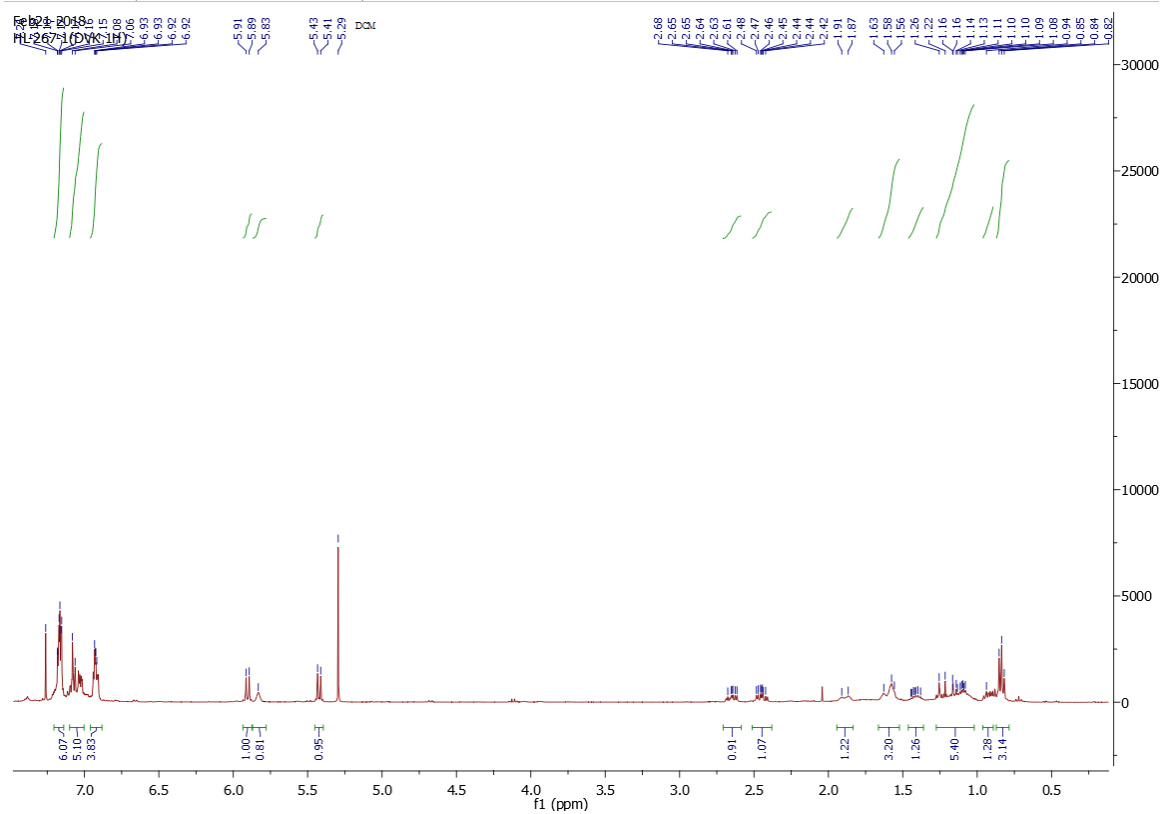
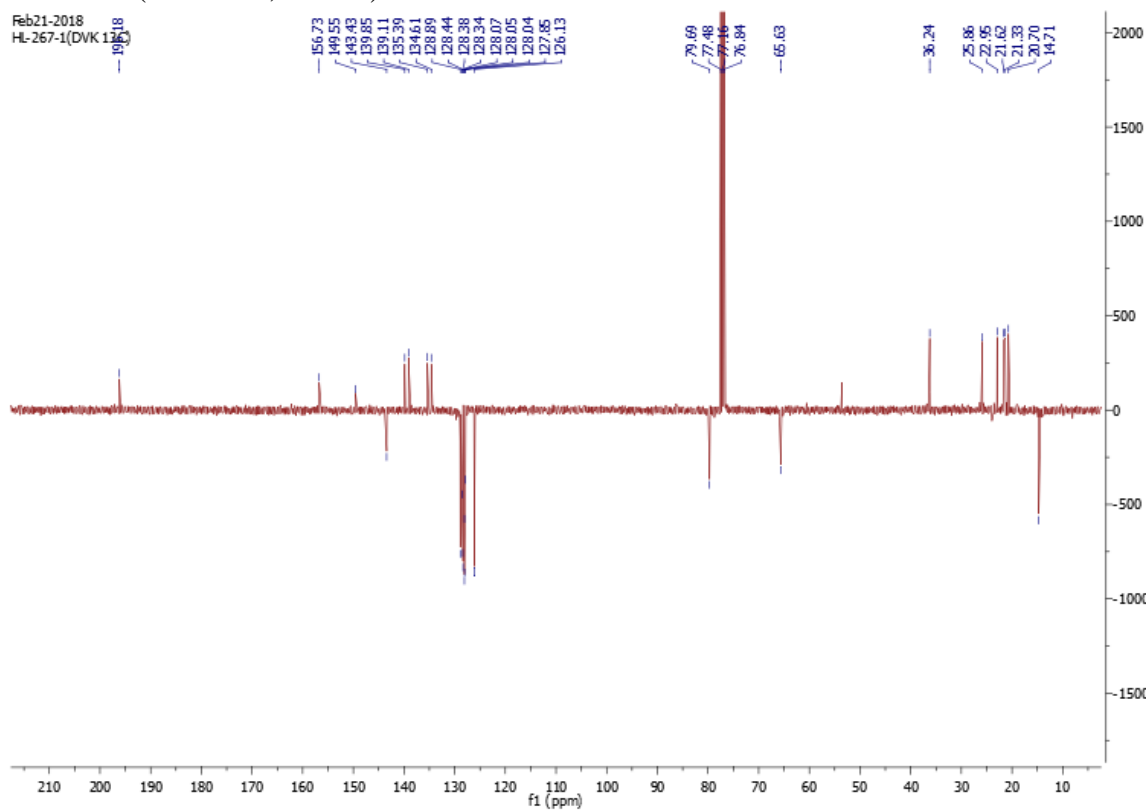
¹H NMR (401 MHz, CDCl₃)

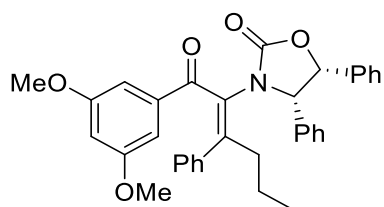
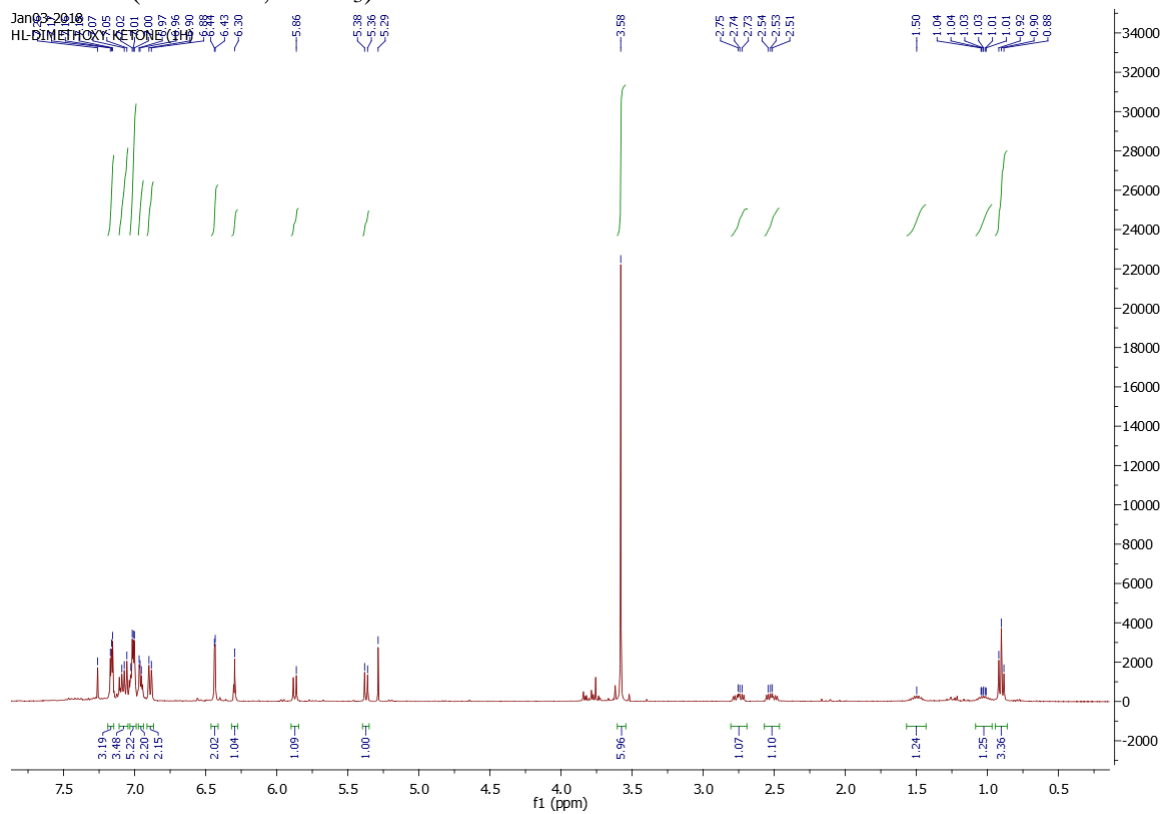
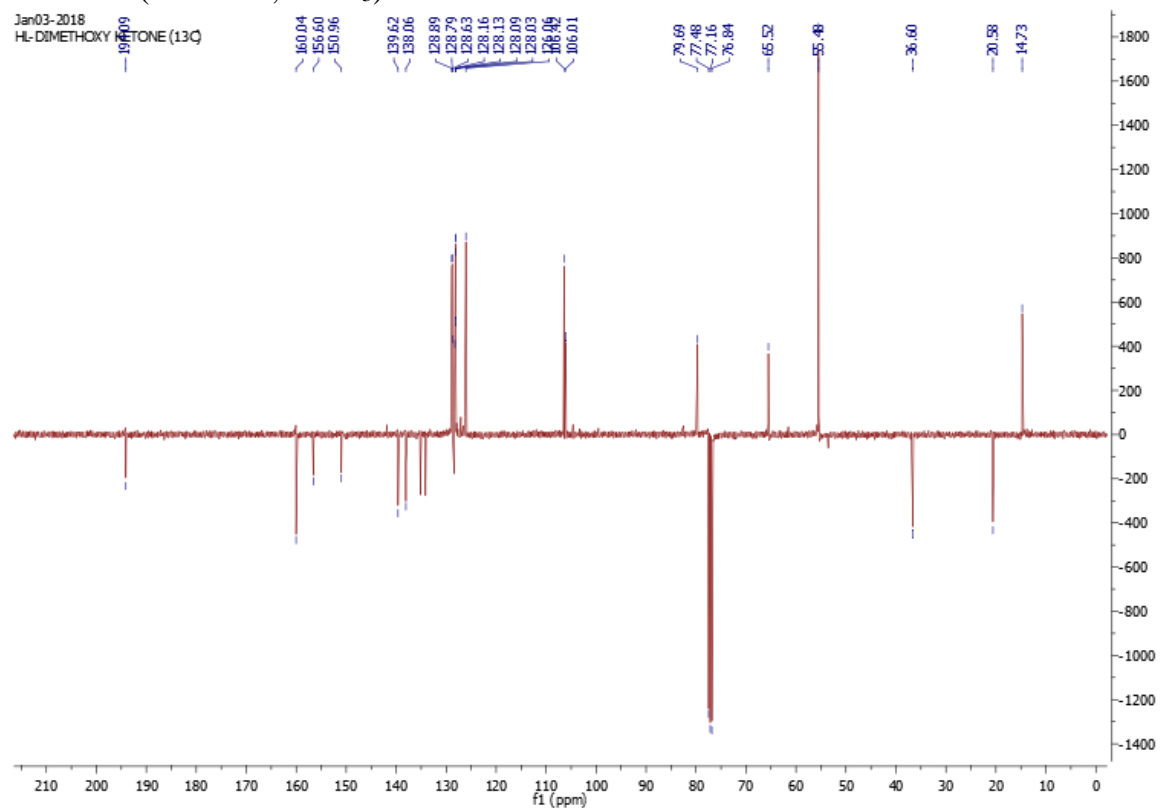


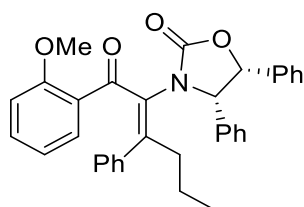
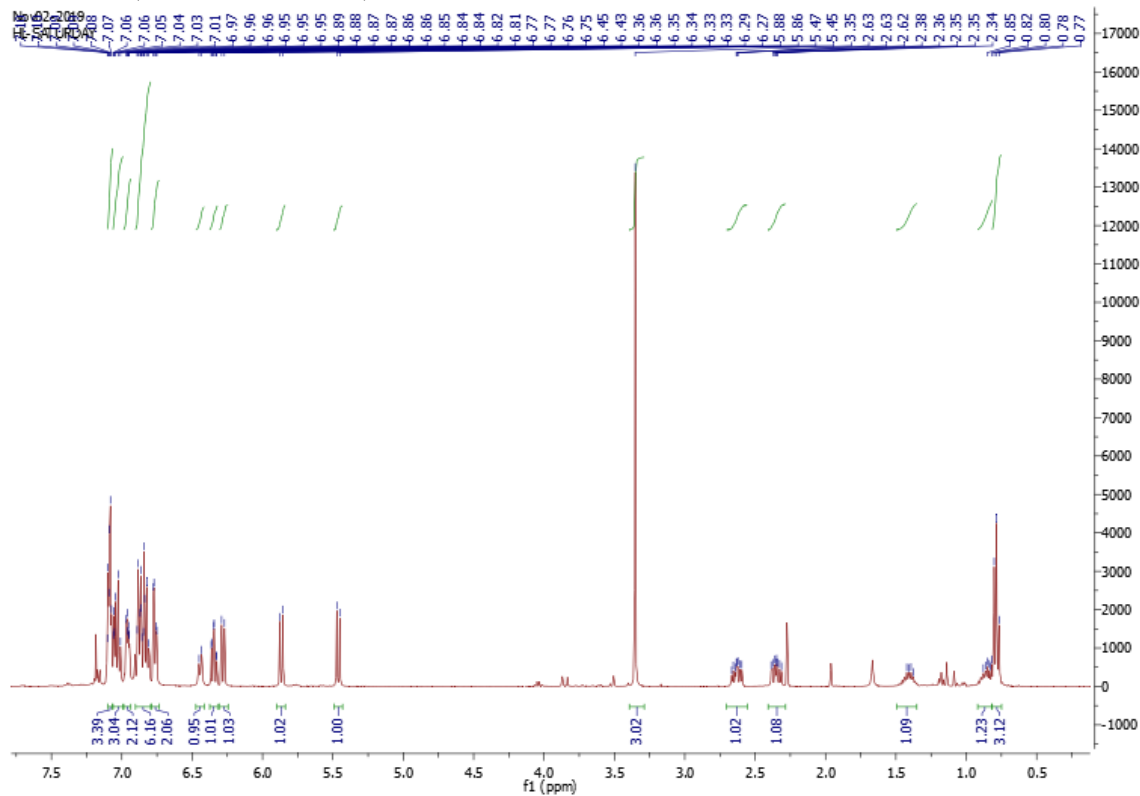
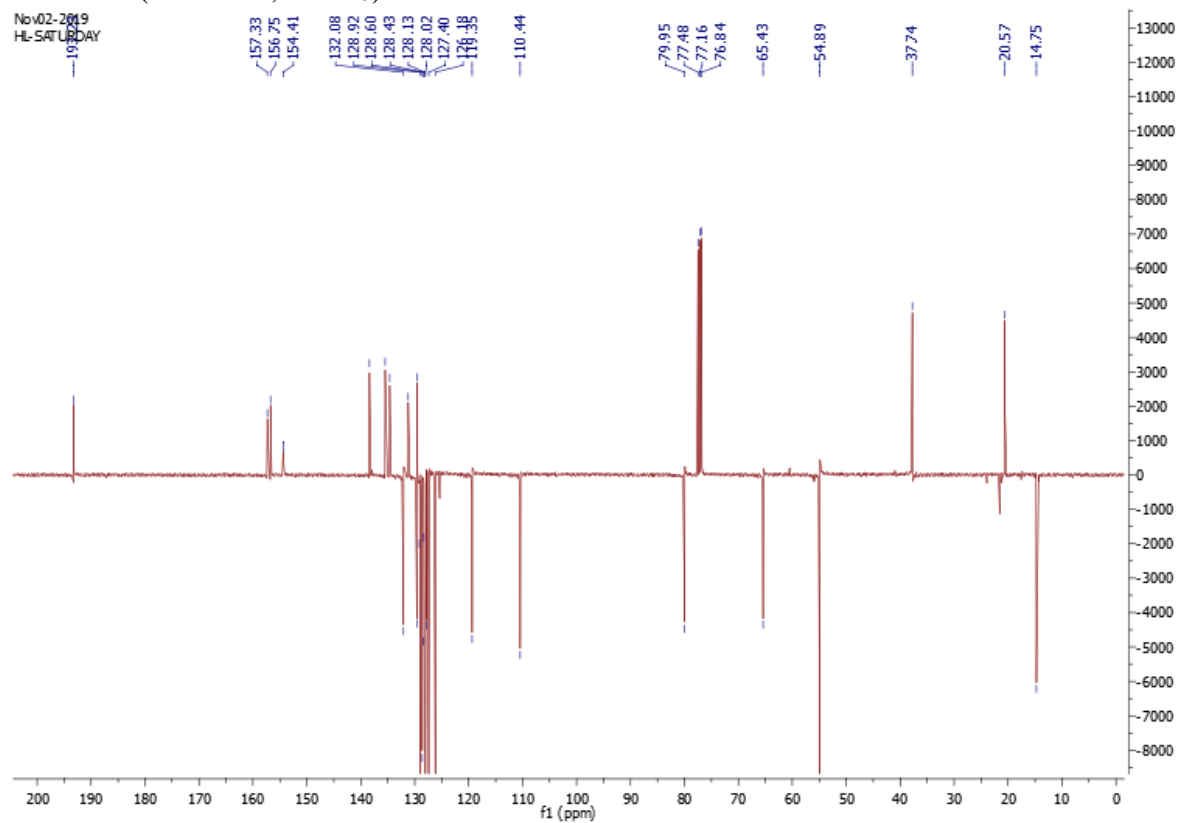
379

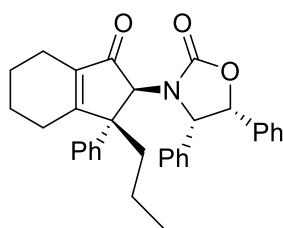
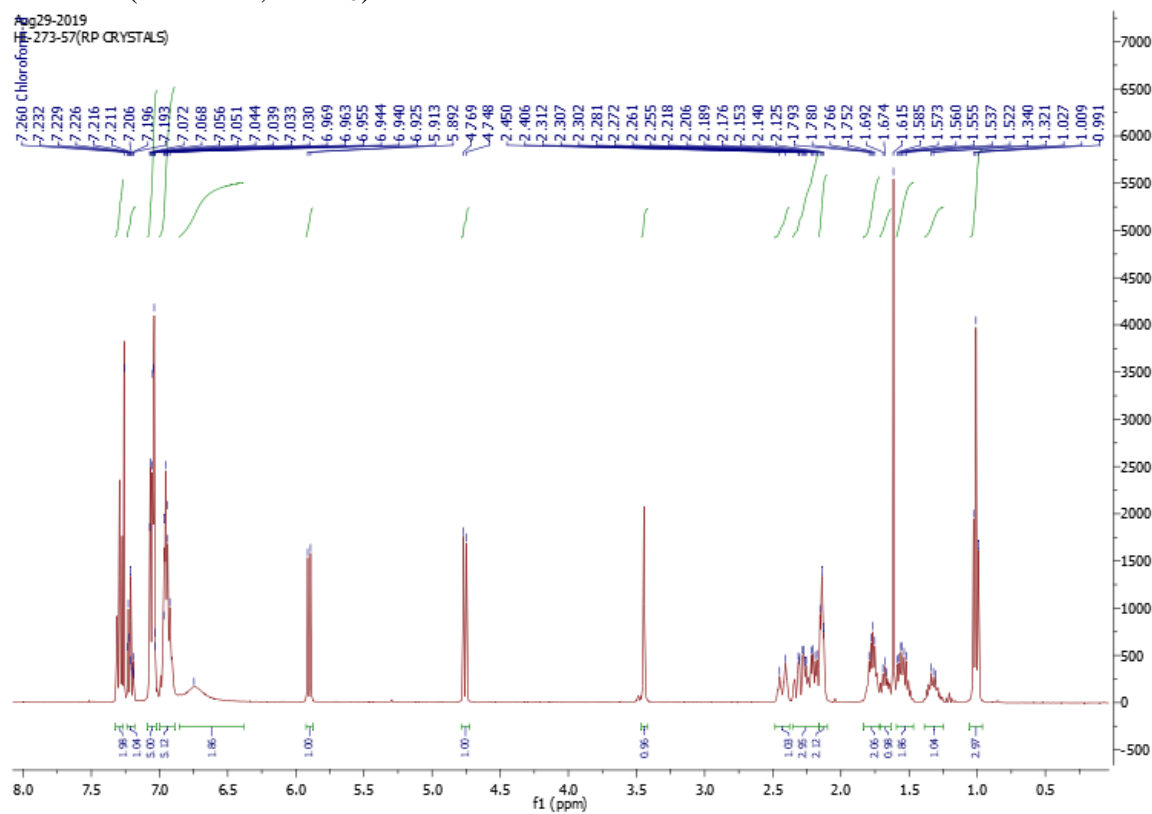
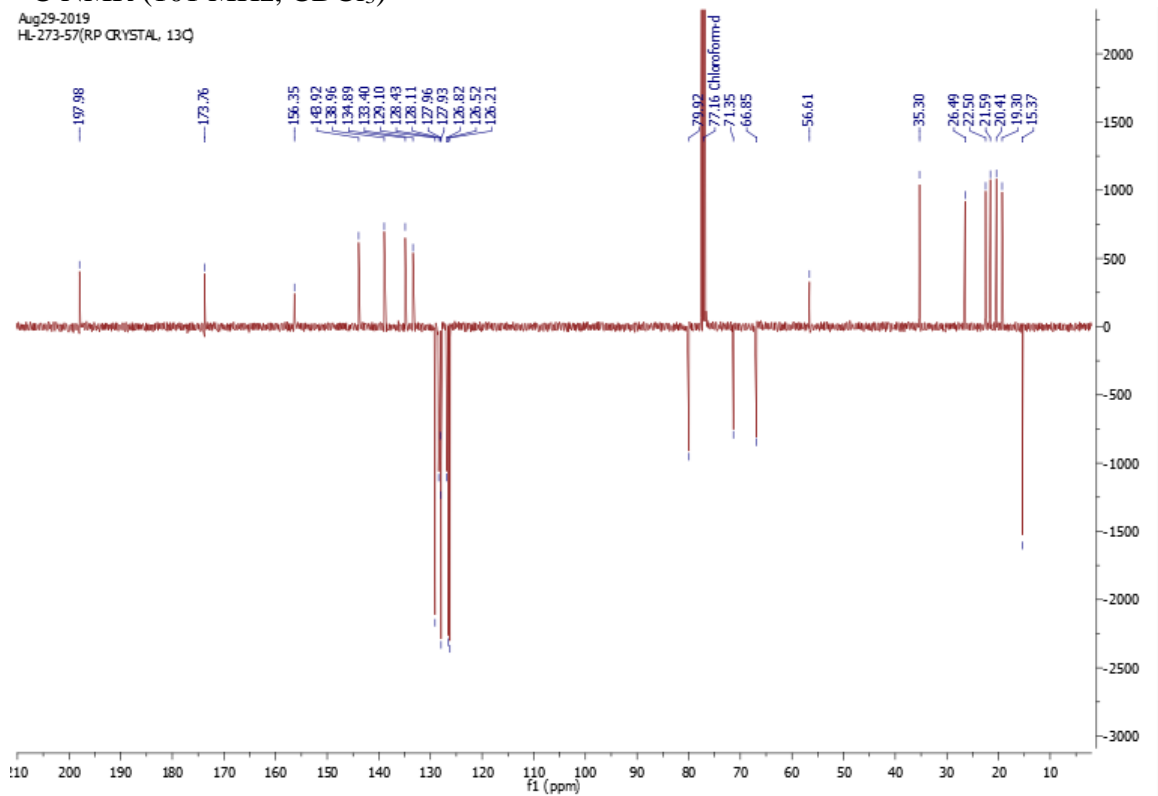
¹H NMR (401 MHz, CDCl₃)¹³C NMR (101 MHz, CDCl₃)

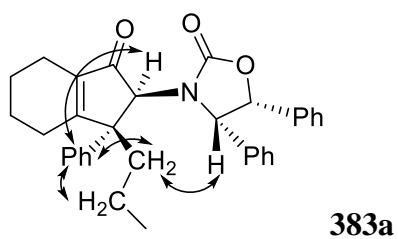
**381** ^1H NMR (401 MHz, CDCl_3) ^{13}C NMR (101 MHz, CDCl_3)

**382a** ^1H NMR (401 MHz, CDCl_3) ^{13}C NMR (101 MHz, CDCl_3)

**382b** ^1H NMR (401 MHz, CDCl_3) ^{13}C NMR (101 MHz, CDCl_3)

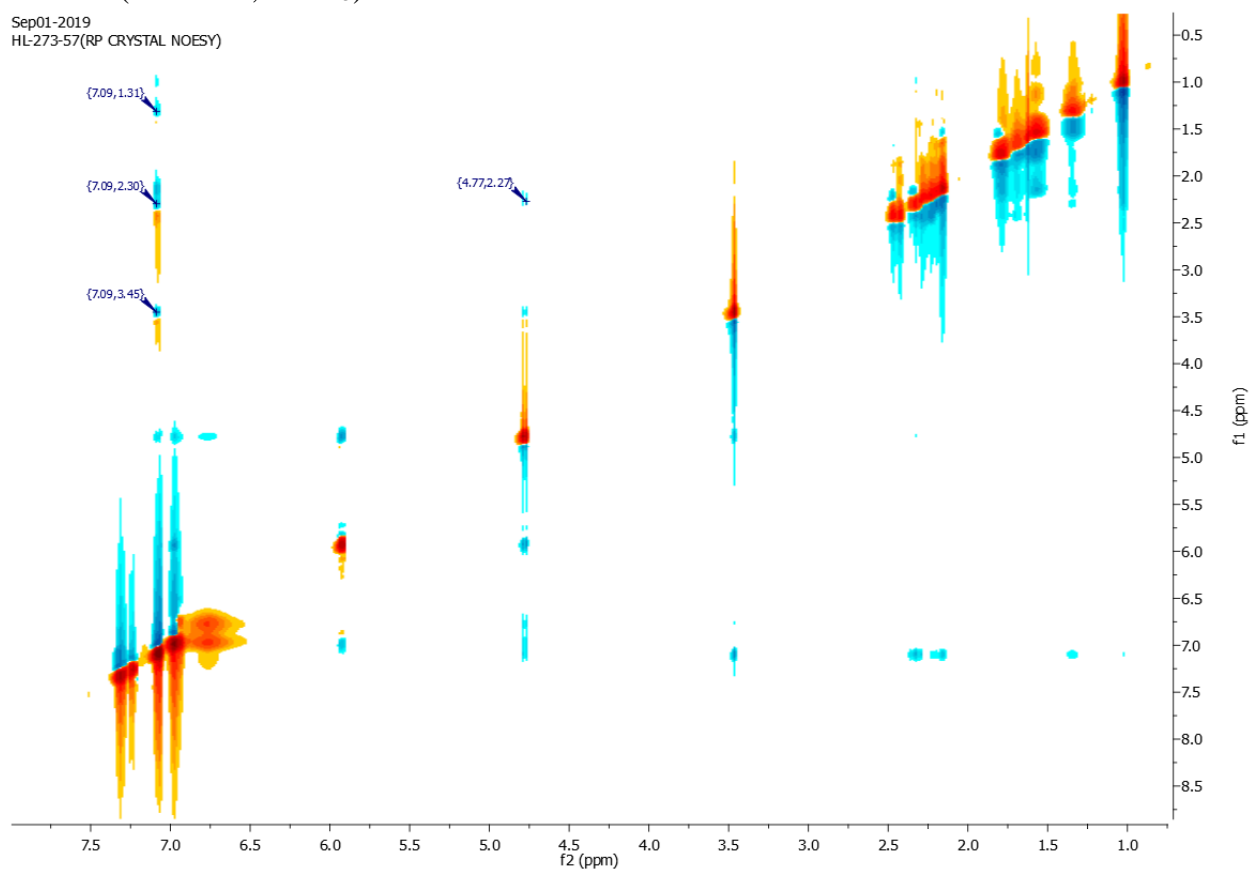
**382c** ^1H NMR (401 MHz, CDCl_3) ^{13}C NMR (101 MHz, CDCl_3)

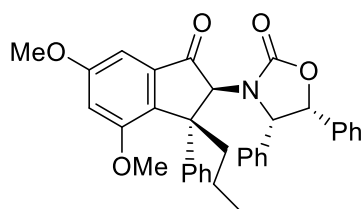
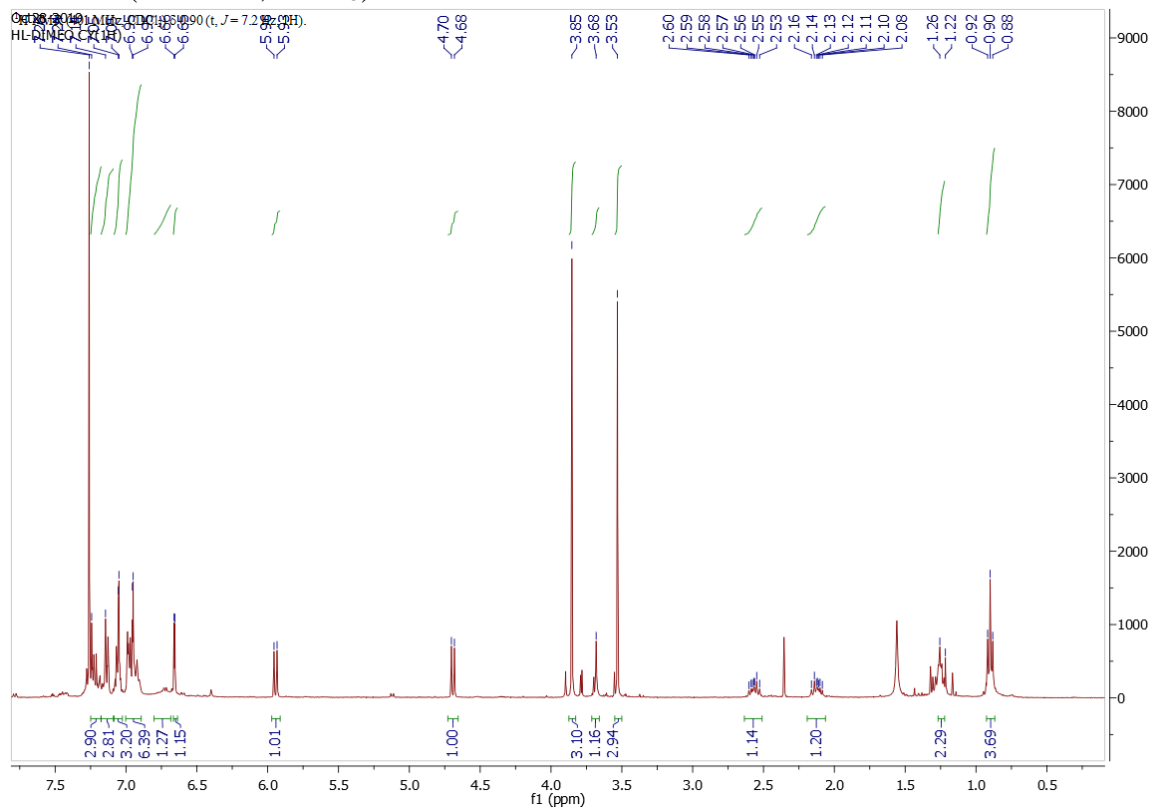
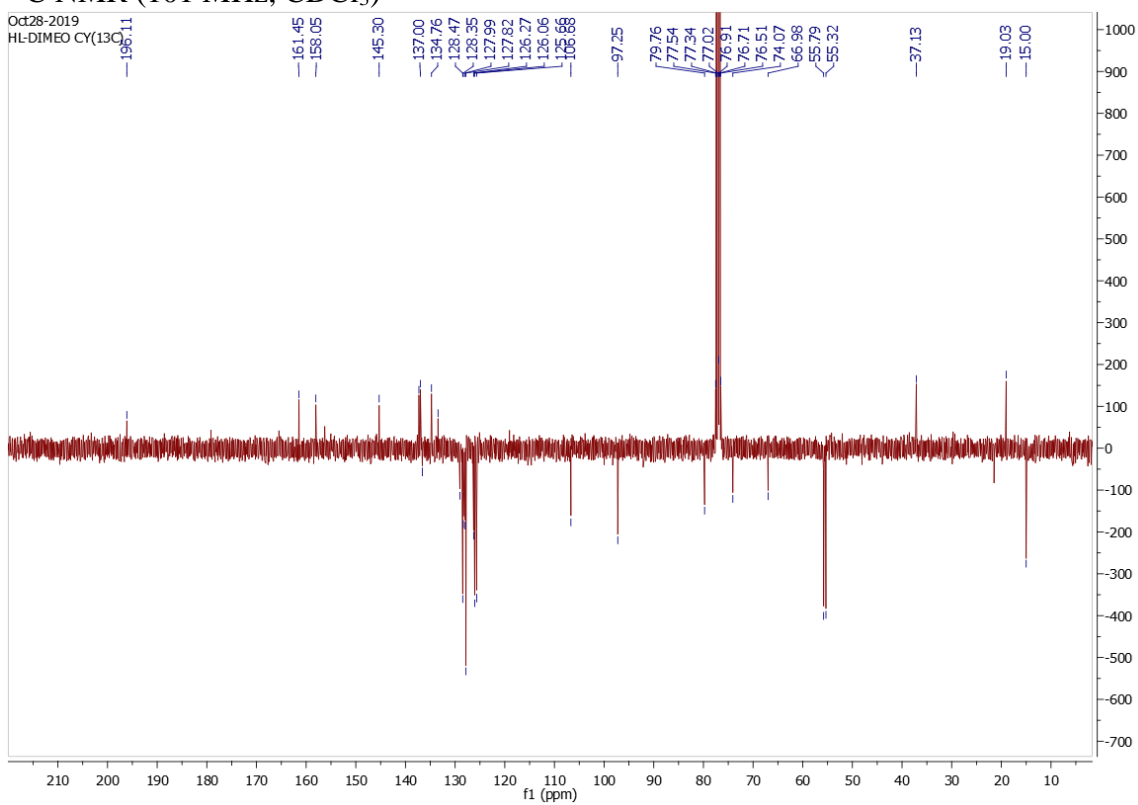
**383a** ^1H NMR (401 MHz, CDCl_3) ^{13}C NMR (101 MHz, CDCl_3)

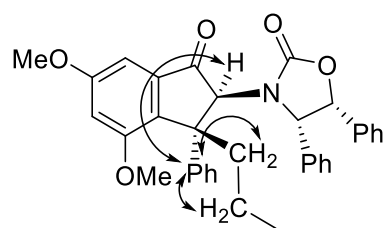
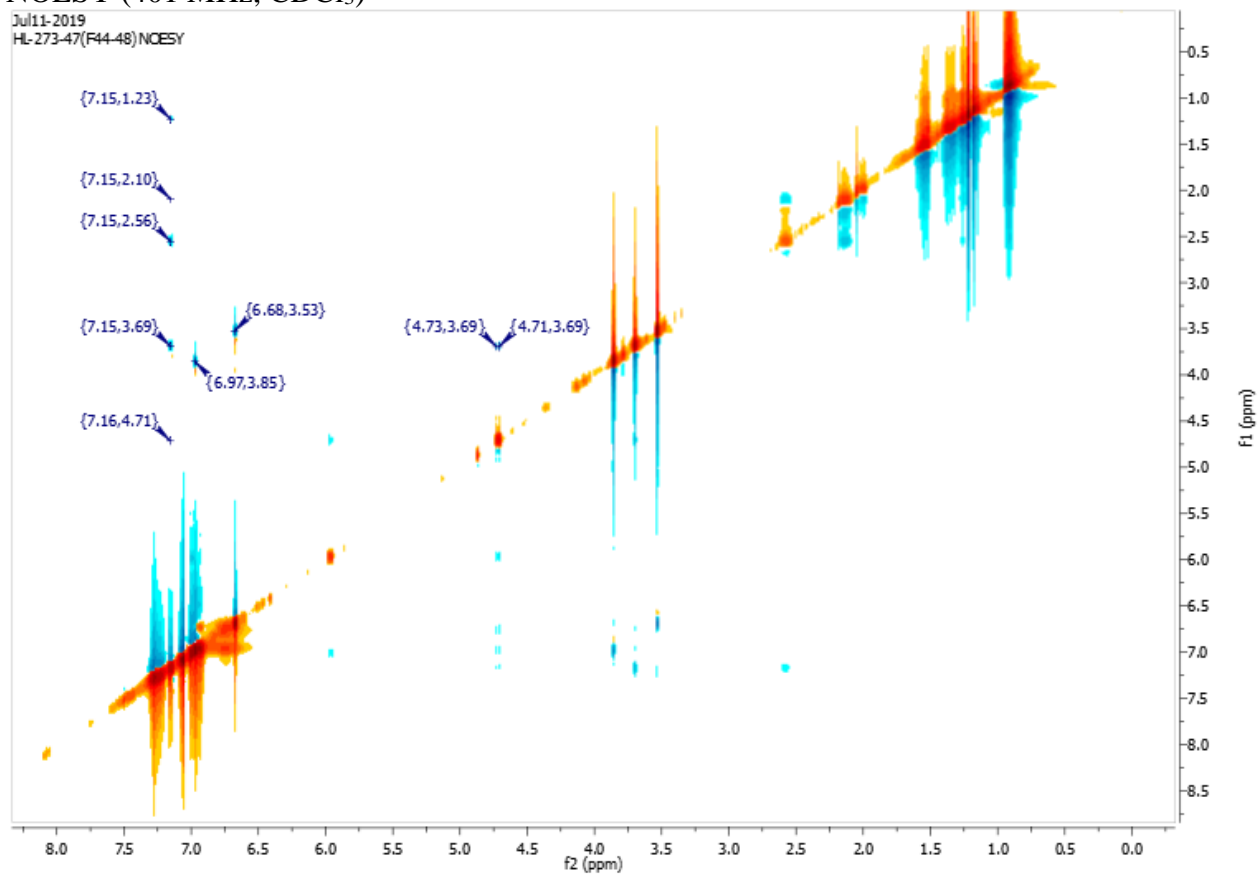
NOESY (401 MHz, CDCl₃)

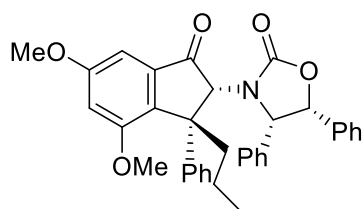
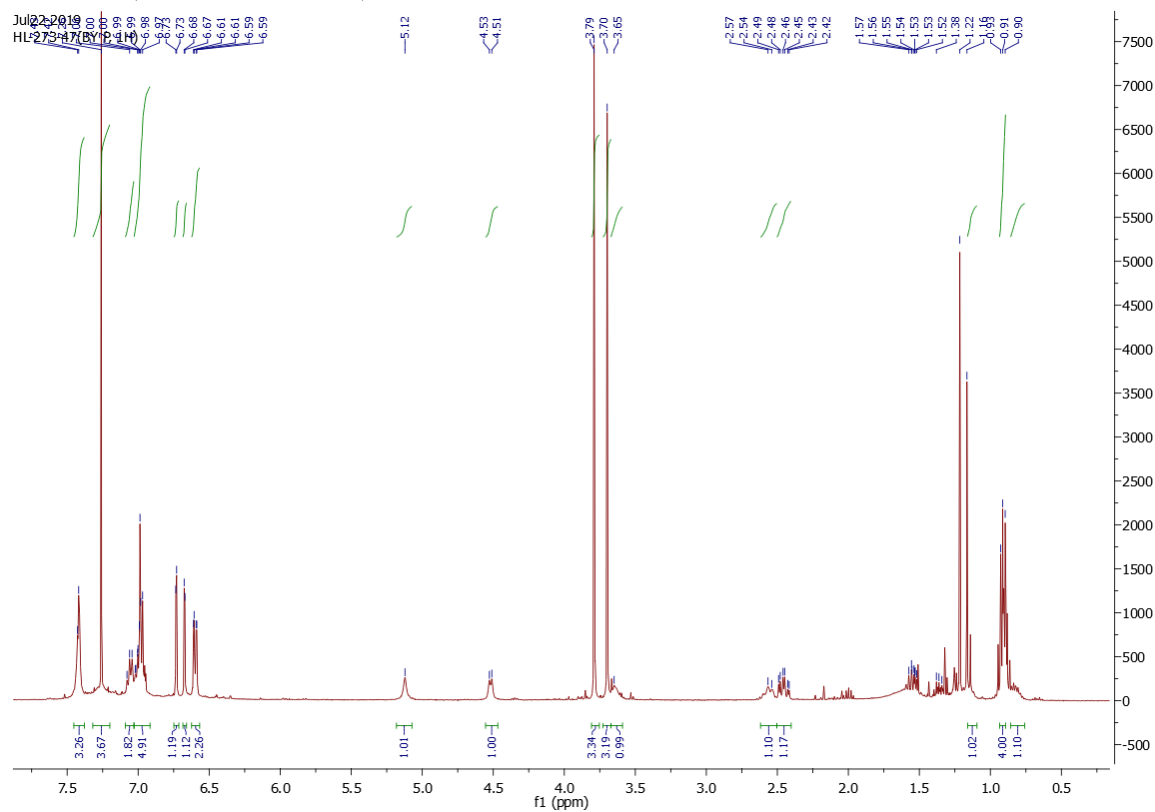
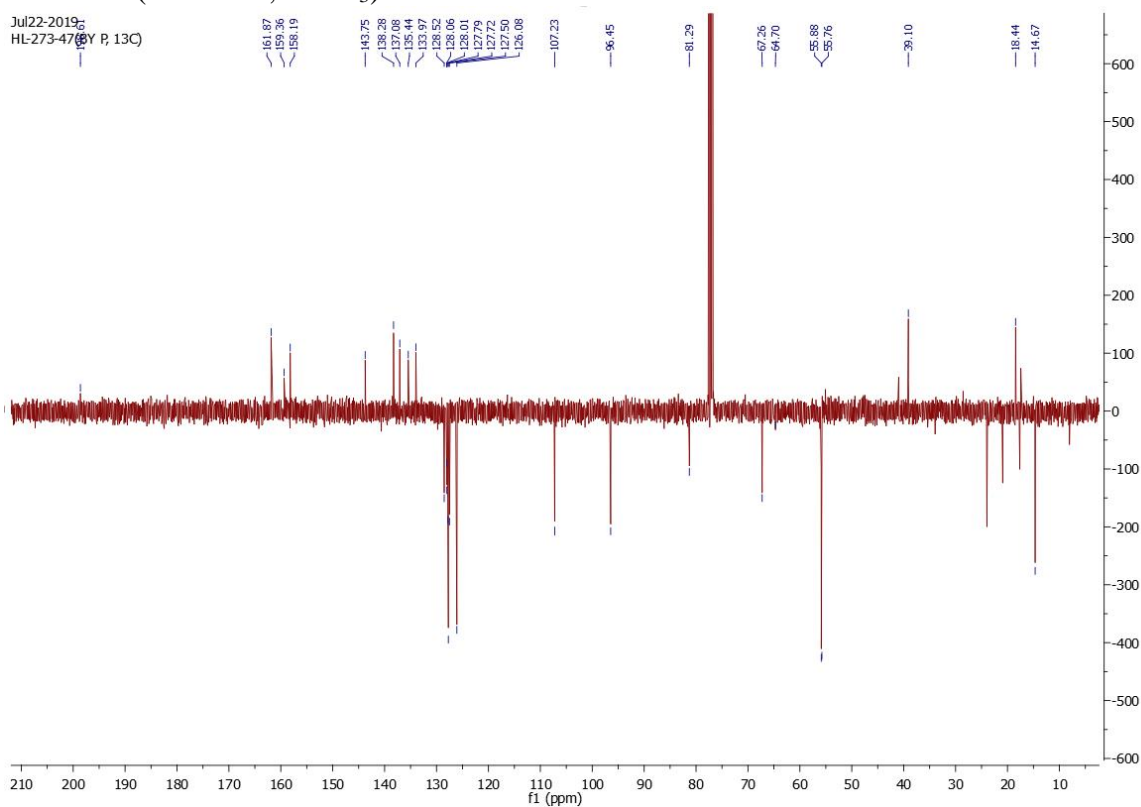
Sep01-2019

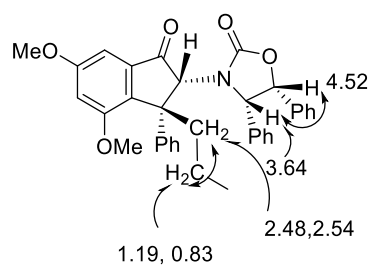
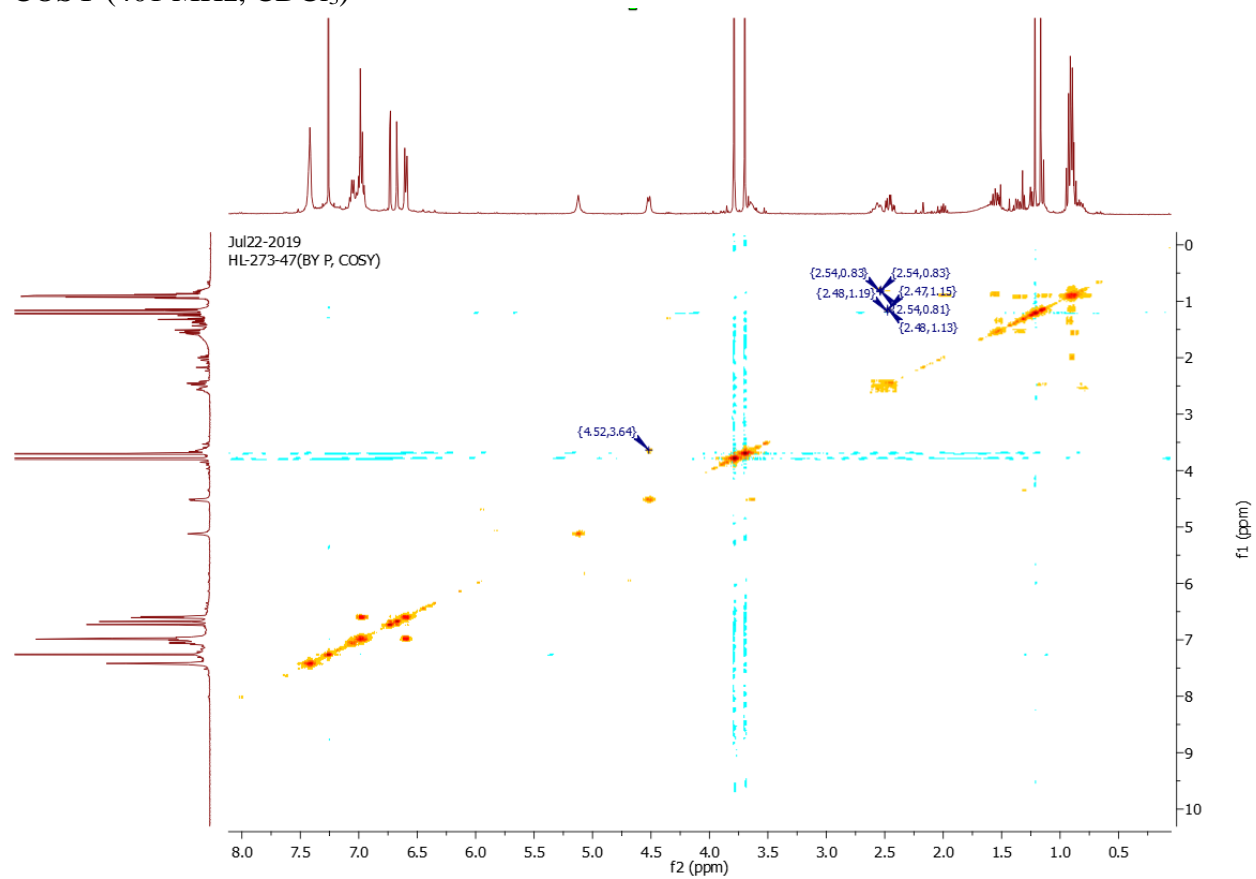
HL-273-57(RP CRYSTAL NOESY)

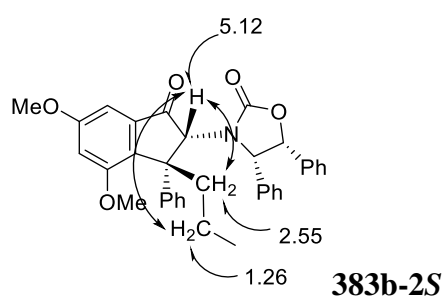
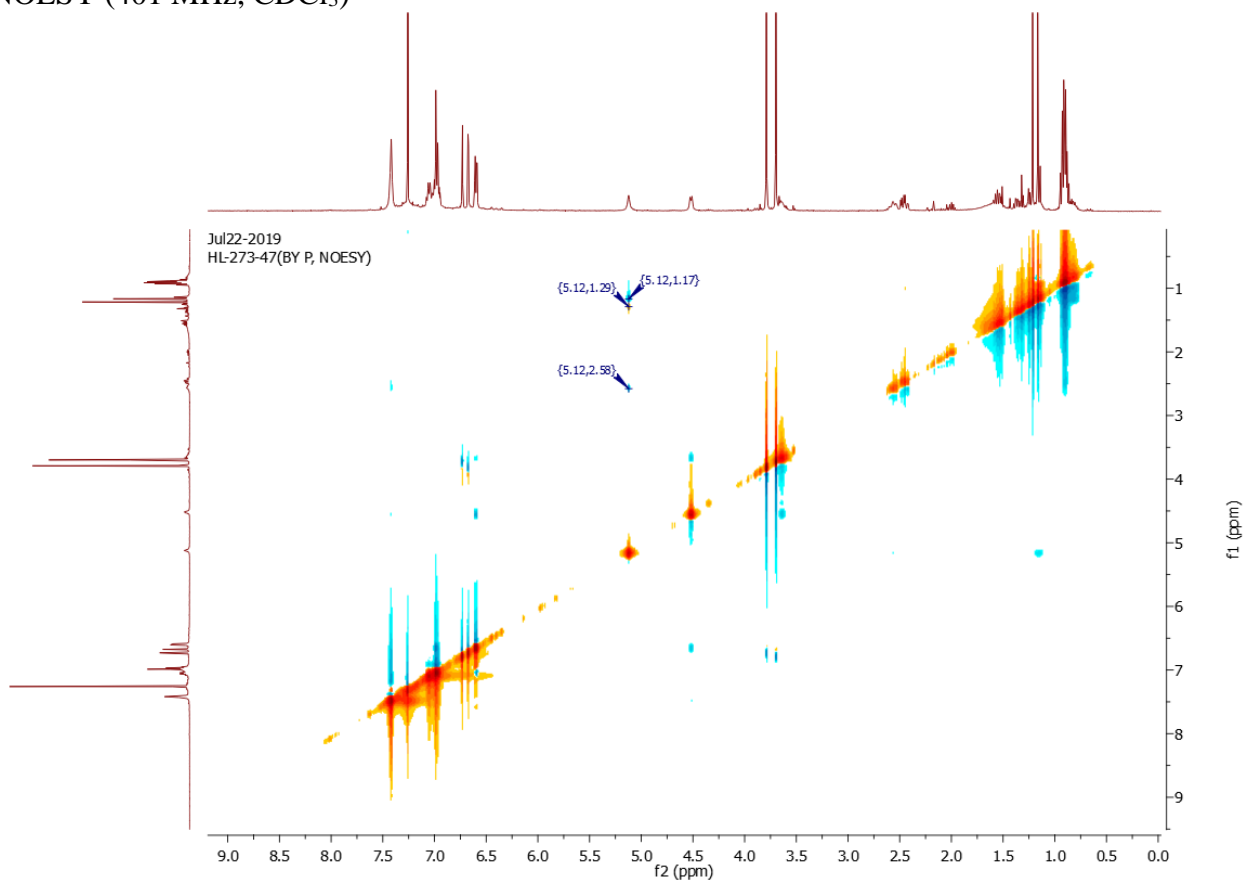


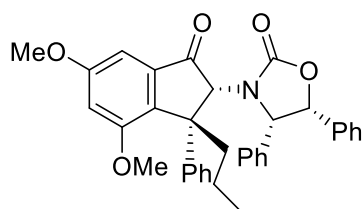
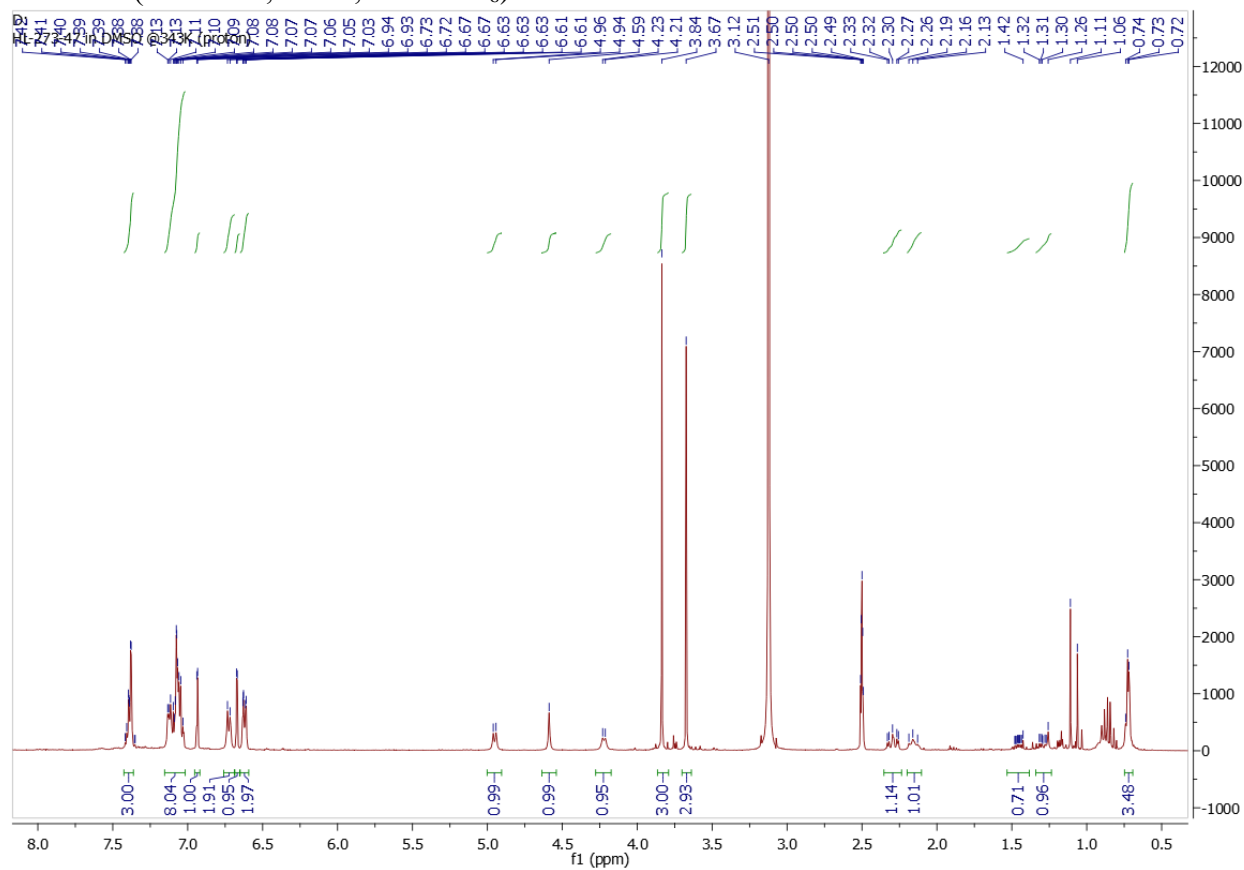
**383b-2R**¹H NMR (401 MHz, CDCl₃)¹³C NMR (101 MHz, CDCl₃)

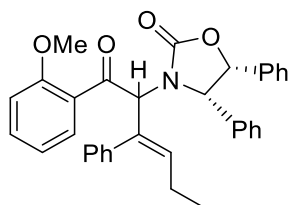
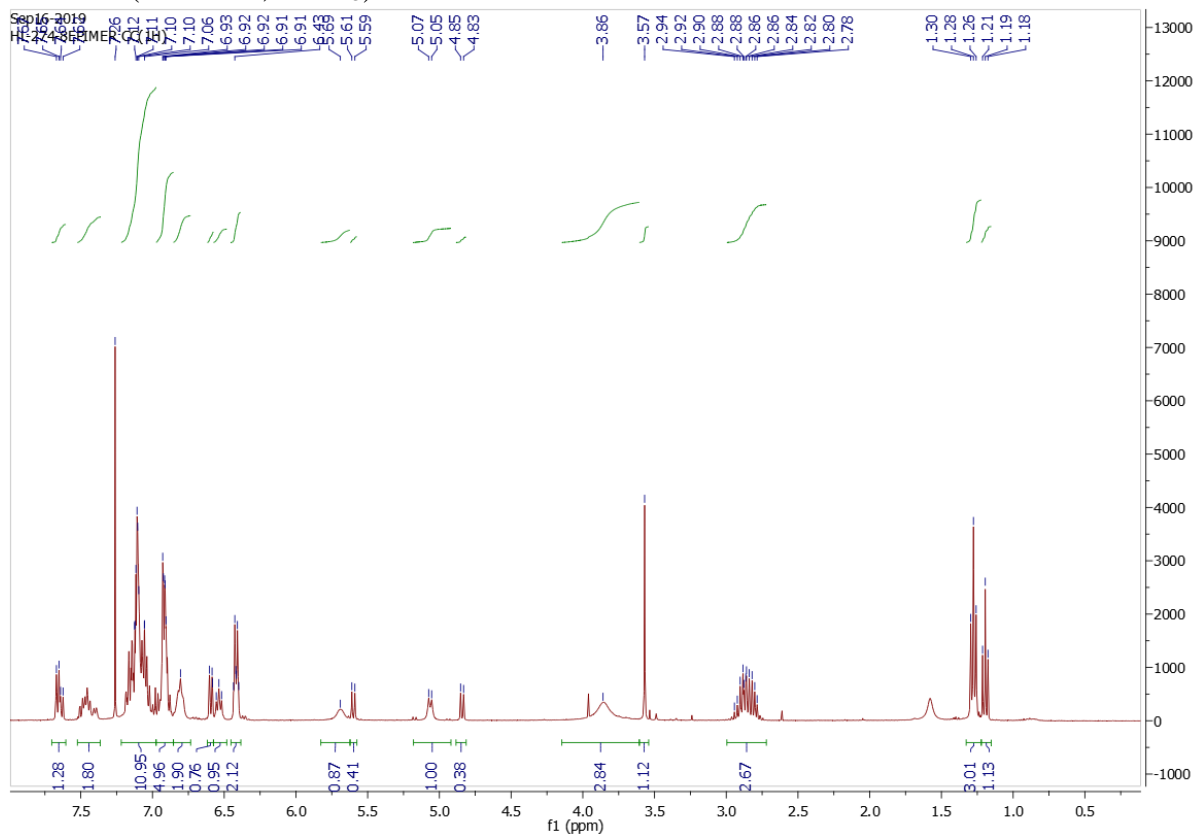
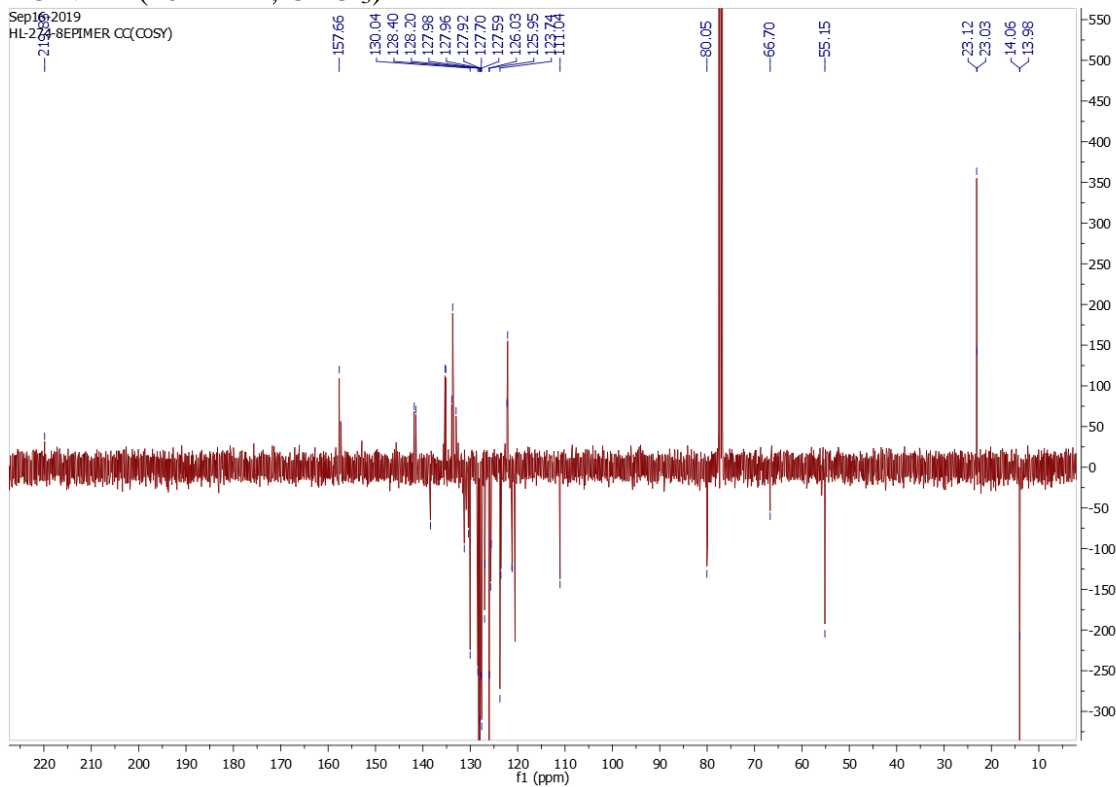
**383b-2R**NOESY (401 MHz, CDCl₃)

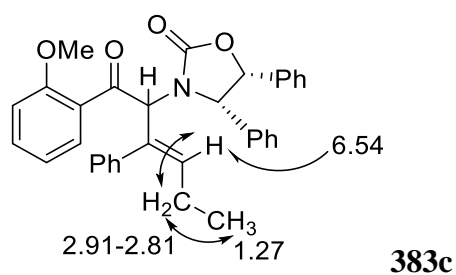
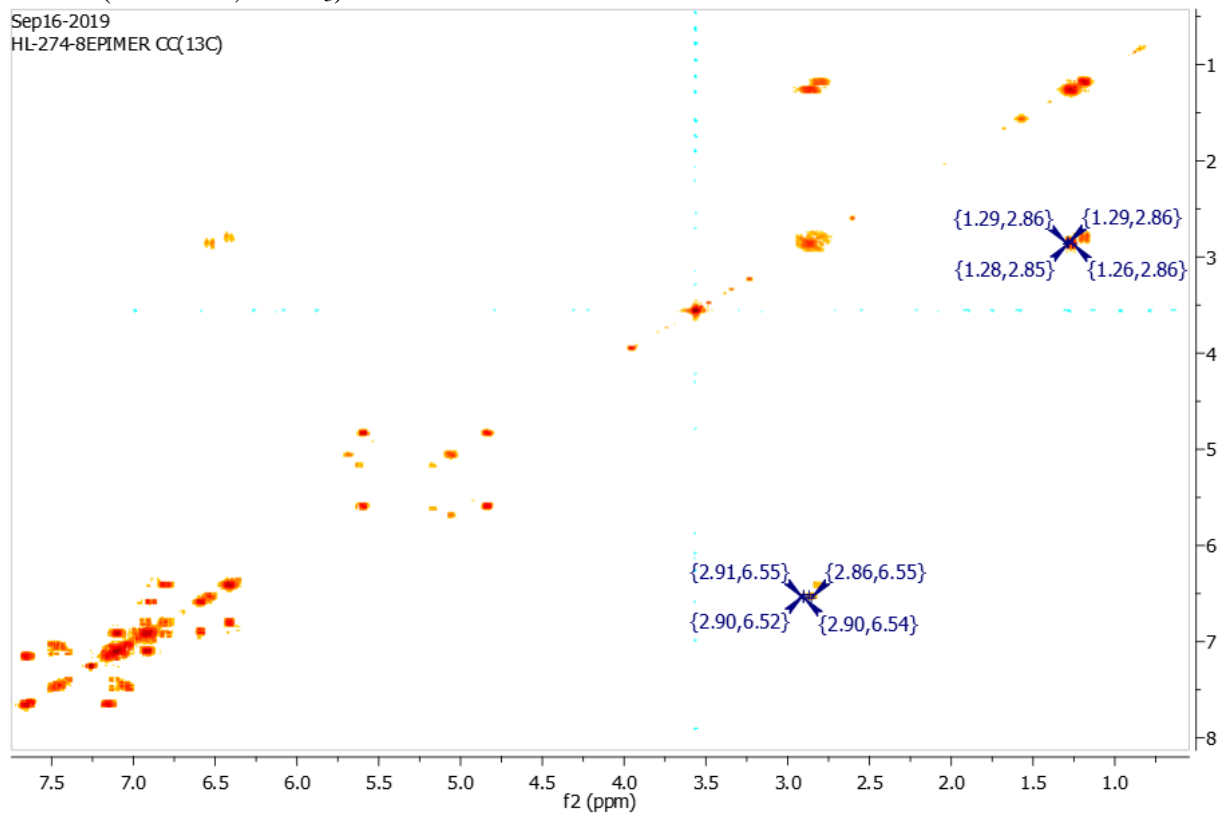
**383b-2S**¹H NMR (401 MHz, CDCl₃)¹³C NMR (101 MHz, CDCl₃)

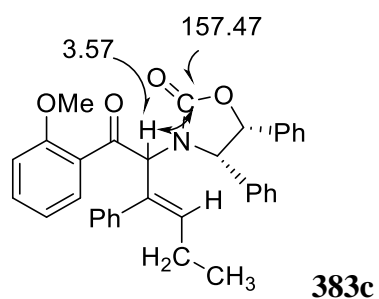
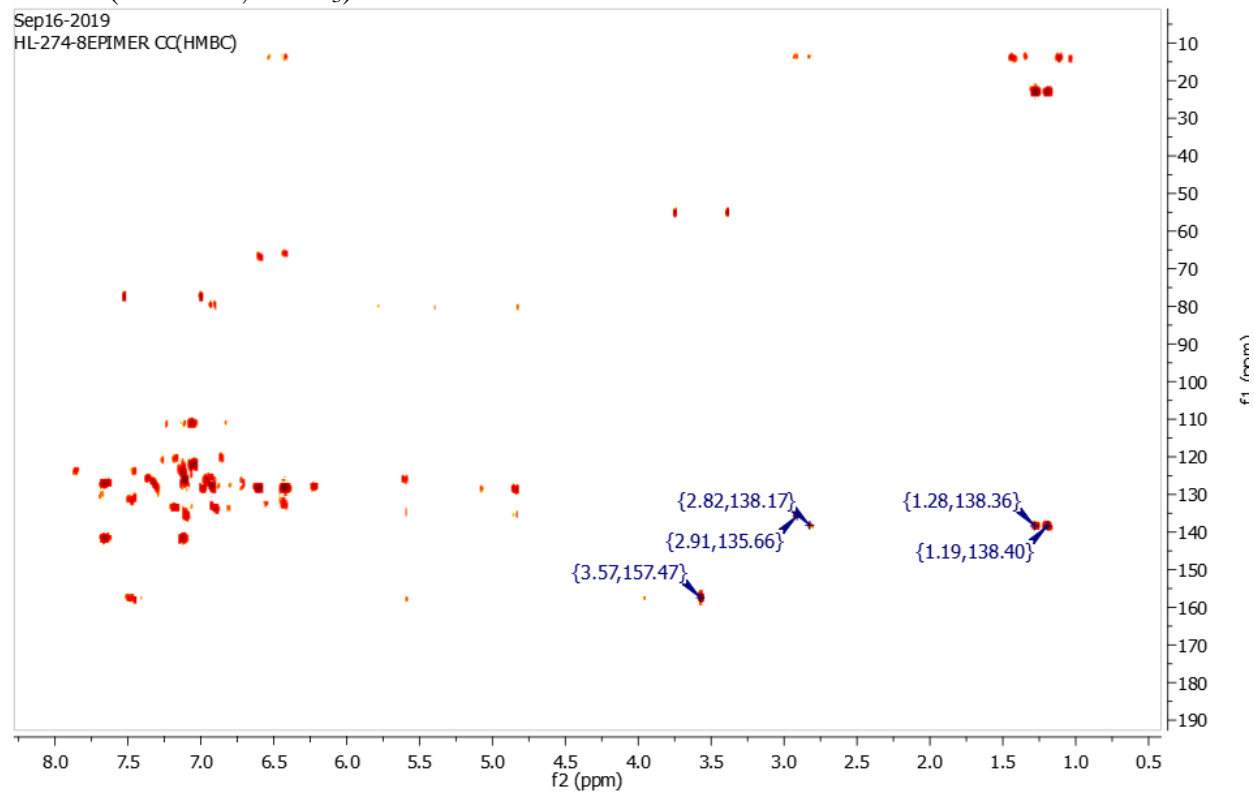
**383b-2S**COSY (401 MHz, CDCl₃)

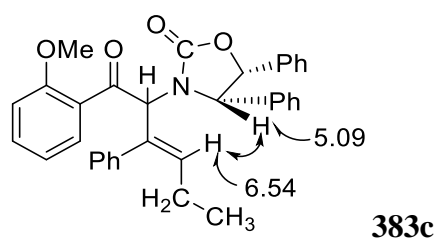
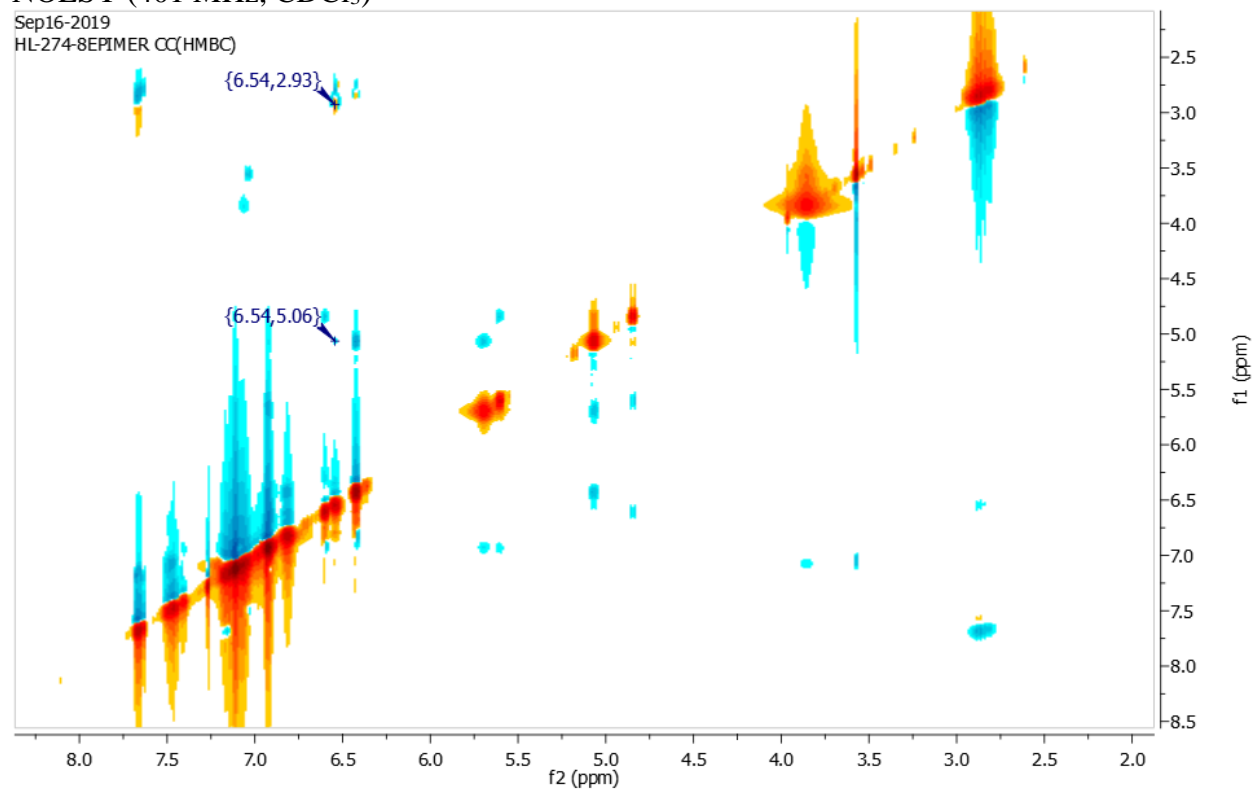
NOESY (401 MHz, CDCl₃)

**383b-2S** ^1H NMR (401 MHz, 70 °C, DMSO- d_6)

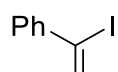
**383c** ^1H NMR (401 MHz, CDCl_3) ^{13}C NMR (101 MHz, CDCl_3)

COSY (401 MHz, CDCl₃)

HMBC (401 MHz, CDCl₃)

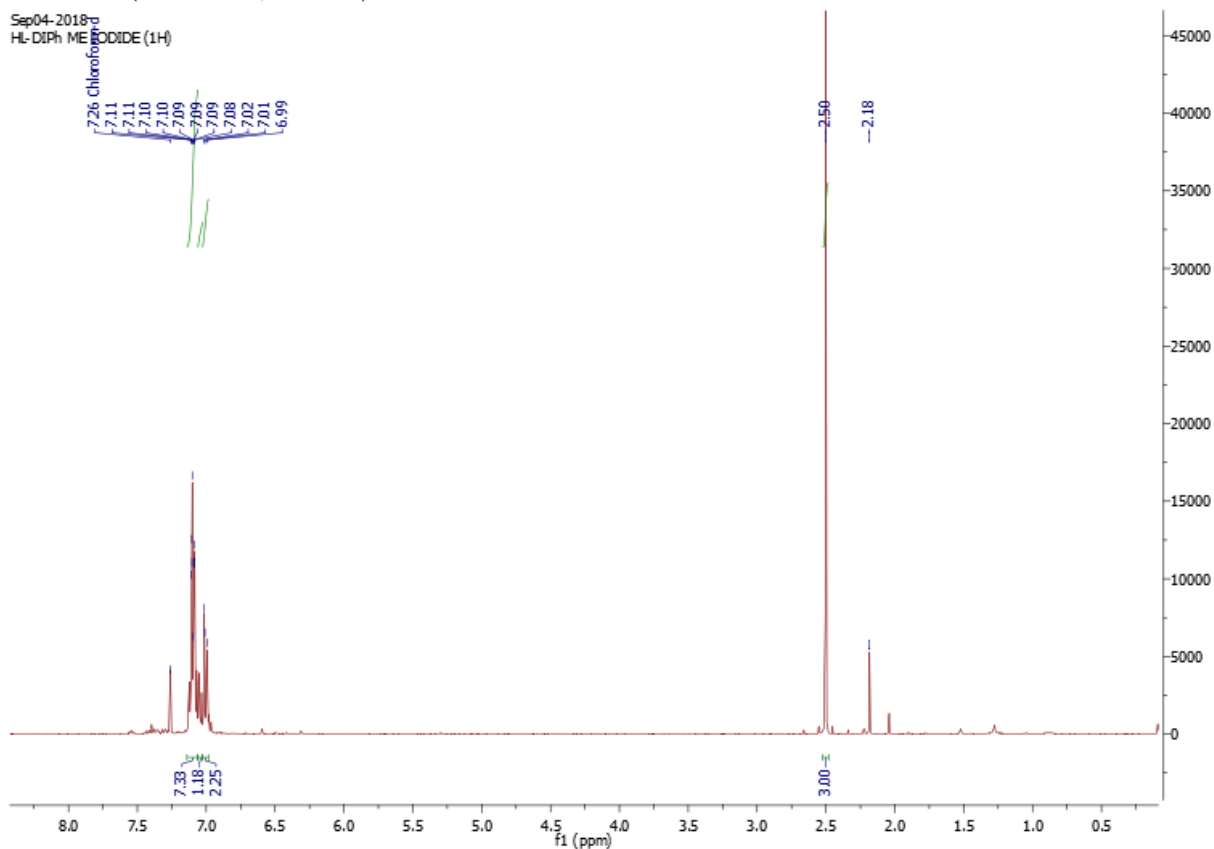
NOESY (401 MHz, CDCl₃)

Chapter 6

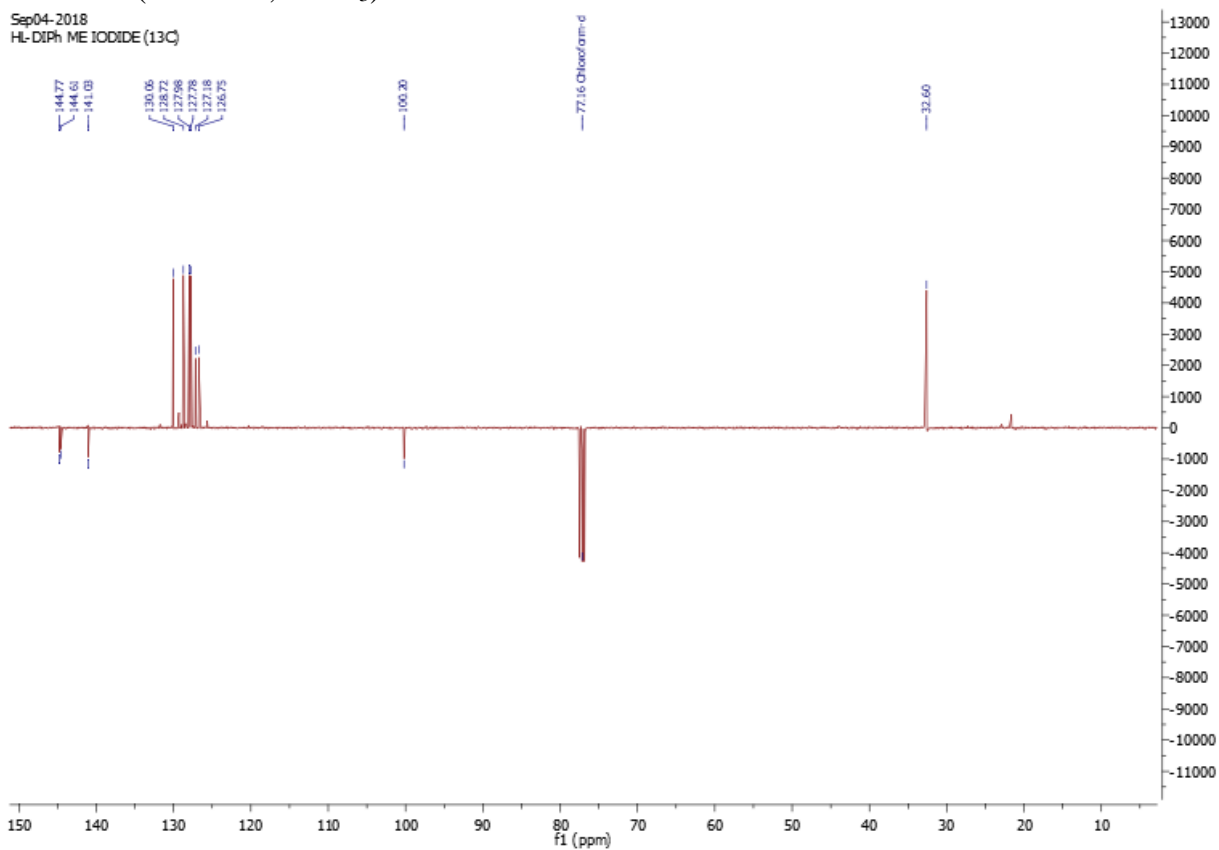


Ph **393**

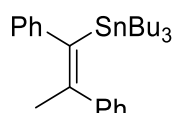
^1H NMR (401 MHz, CDCl_3)



^{13}C NMR (101 MHz, CDCl_3)

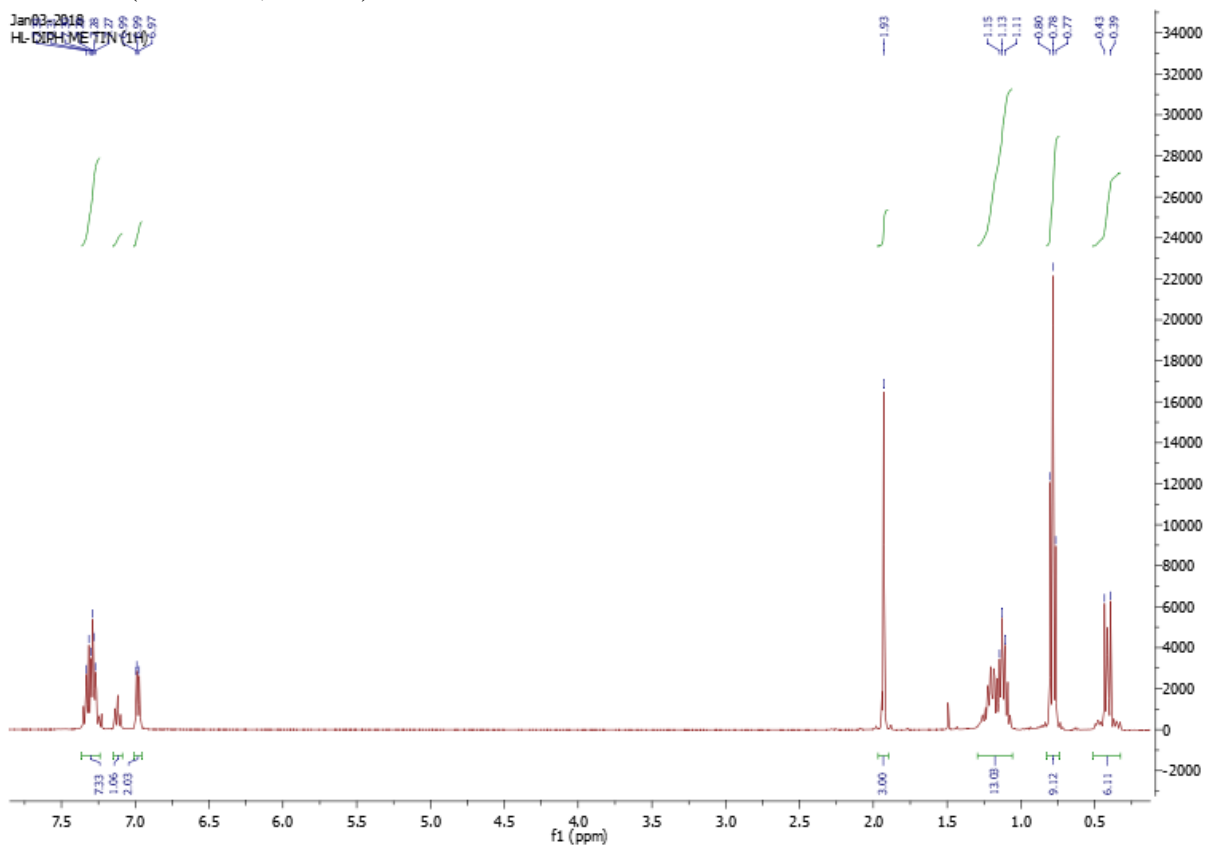


Chapter 6

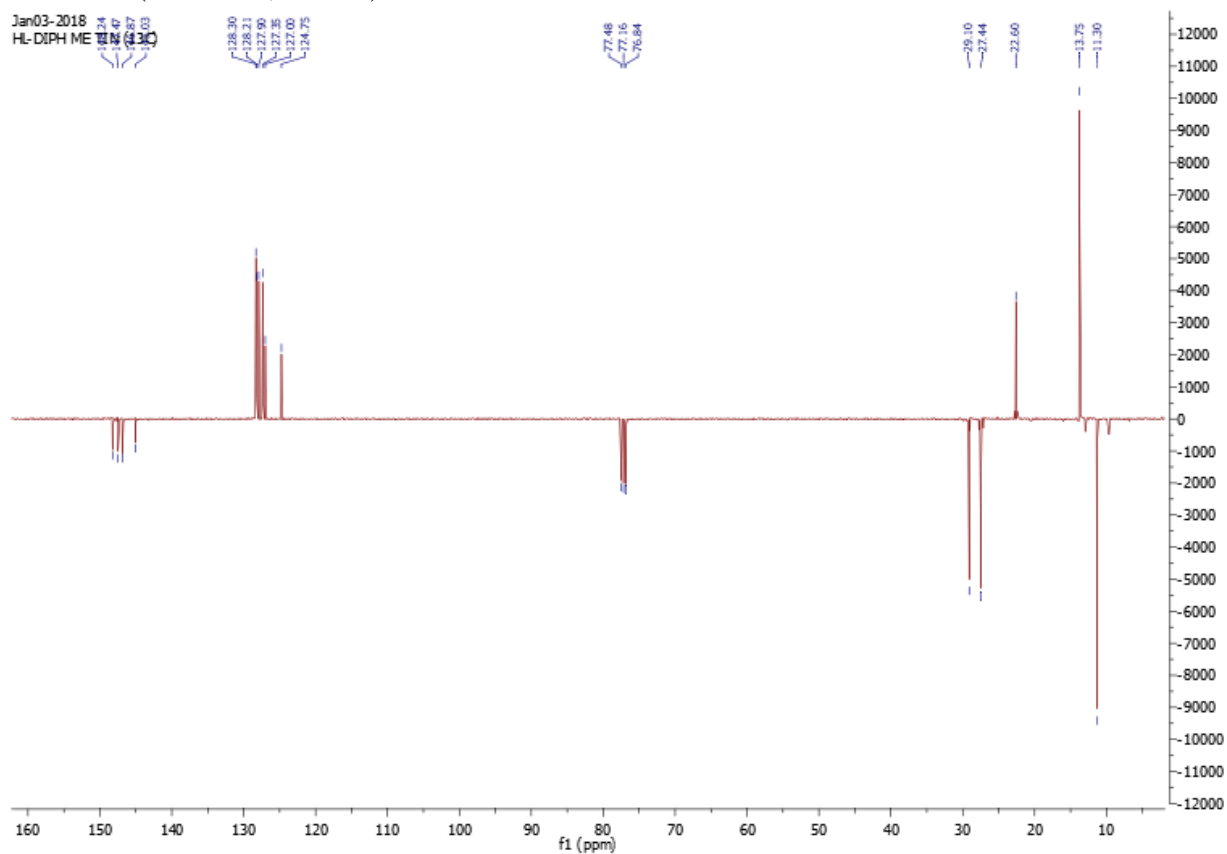


394Z

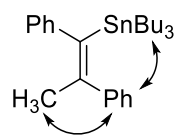
^1H NMR (401 MHz, CDCl_3)



^{13}C NMR (101 MHz, CDCl_3)

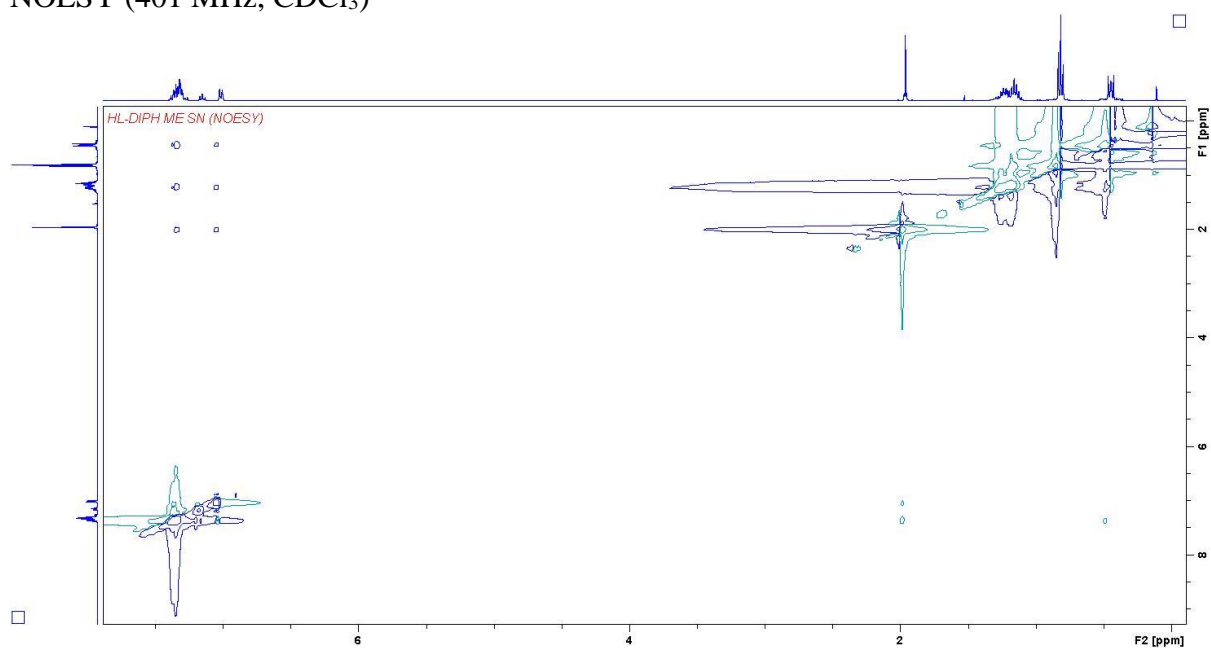


Chapter 6

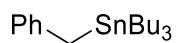


394Z

NOESY (401 MHz, CDCl₃)

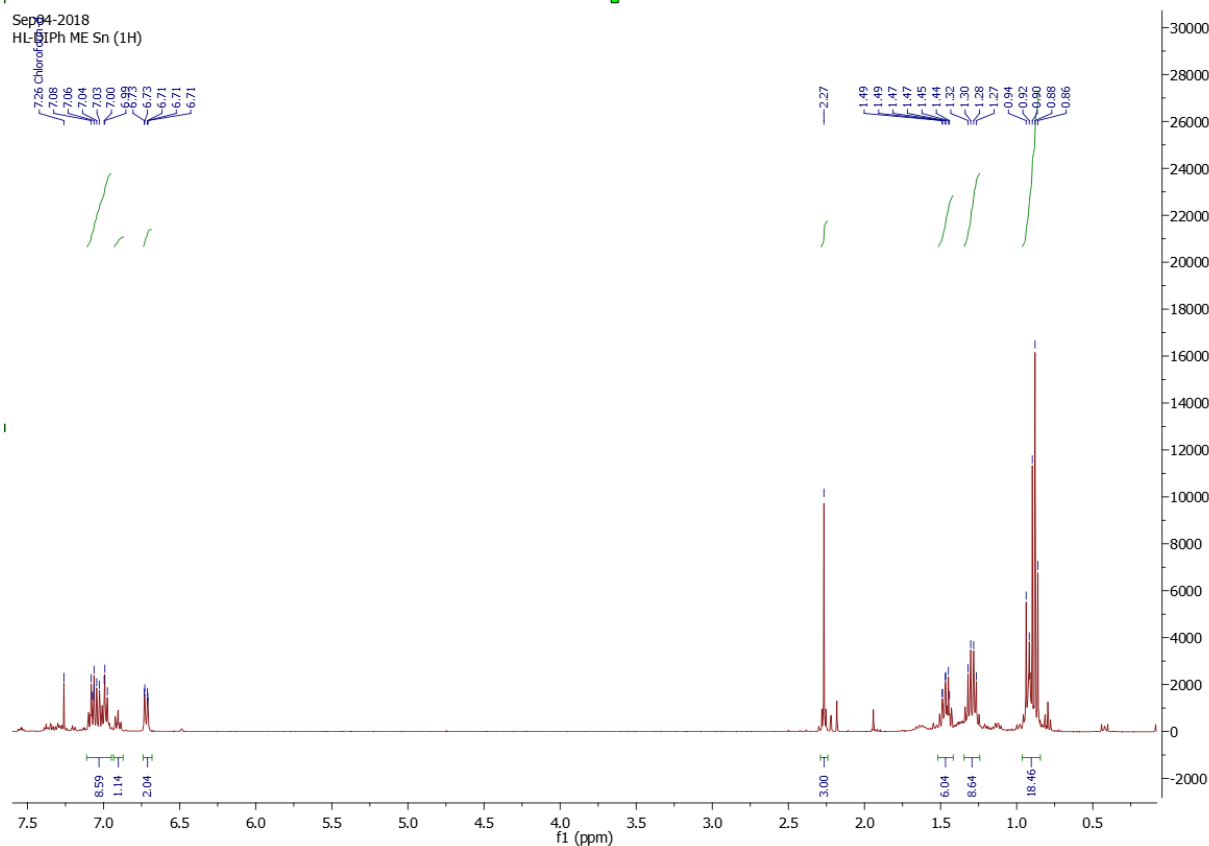


Chapter 6

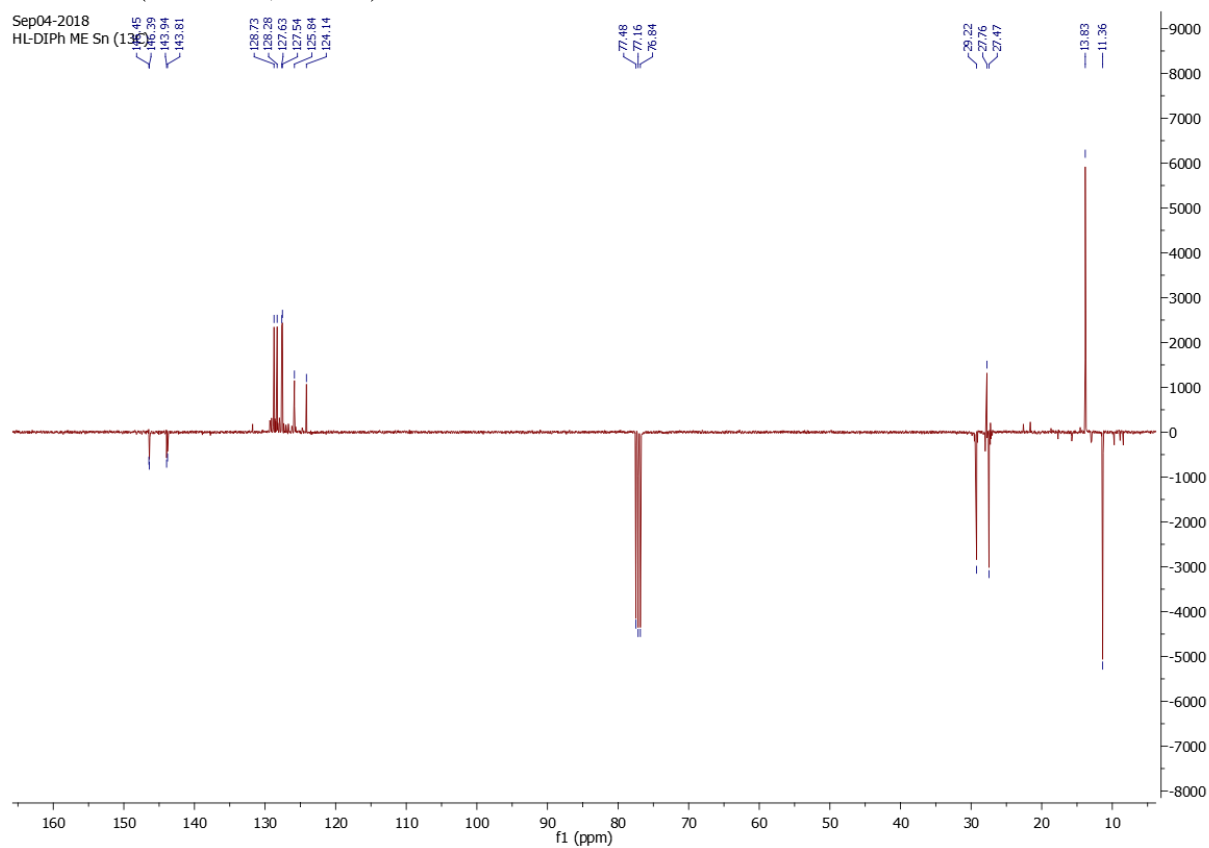


394E

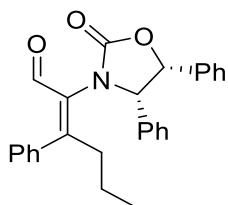
^1H NMR (401 MHz, CDCl_3)



^{13}C NMR (101 MHz, CDCl_3)

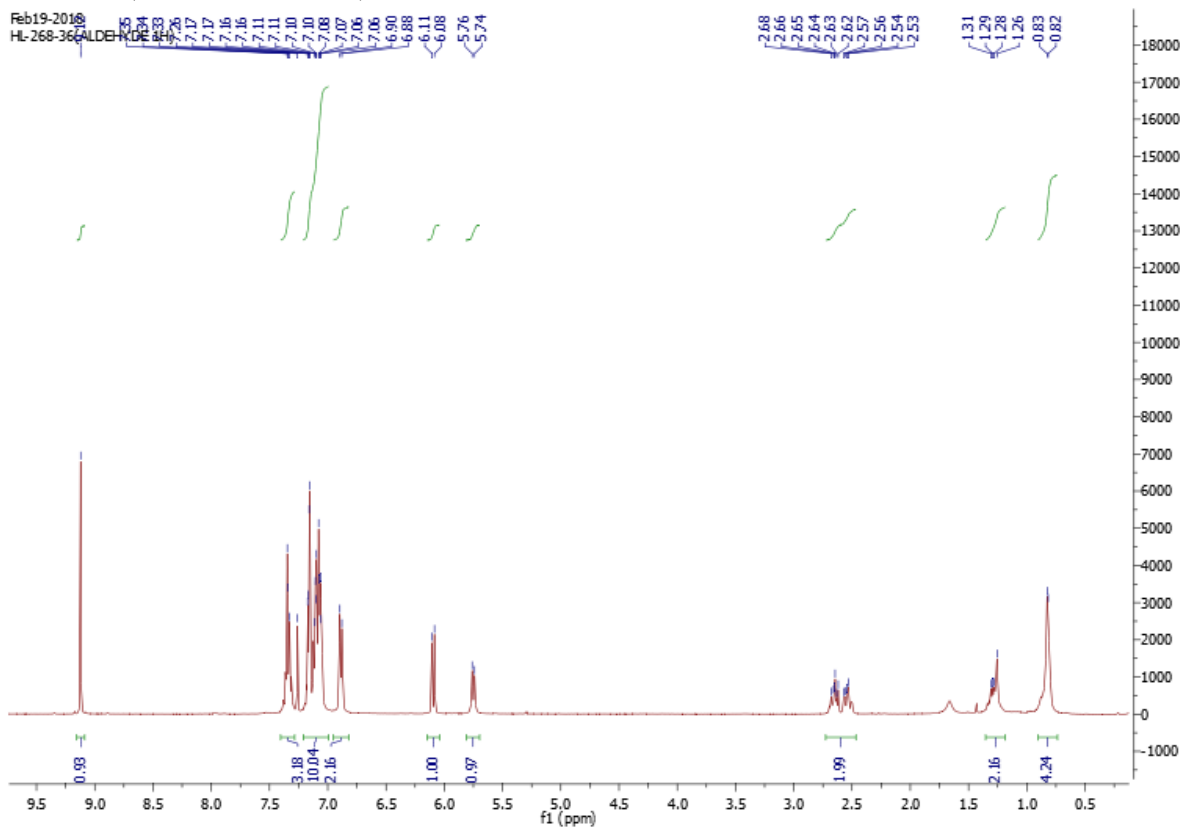


Chapter 6

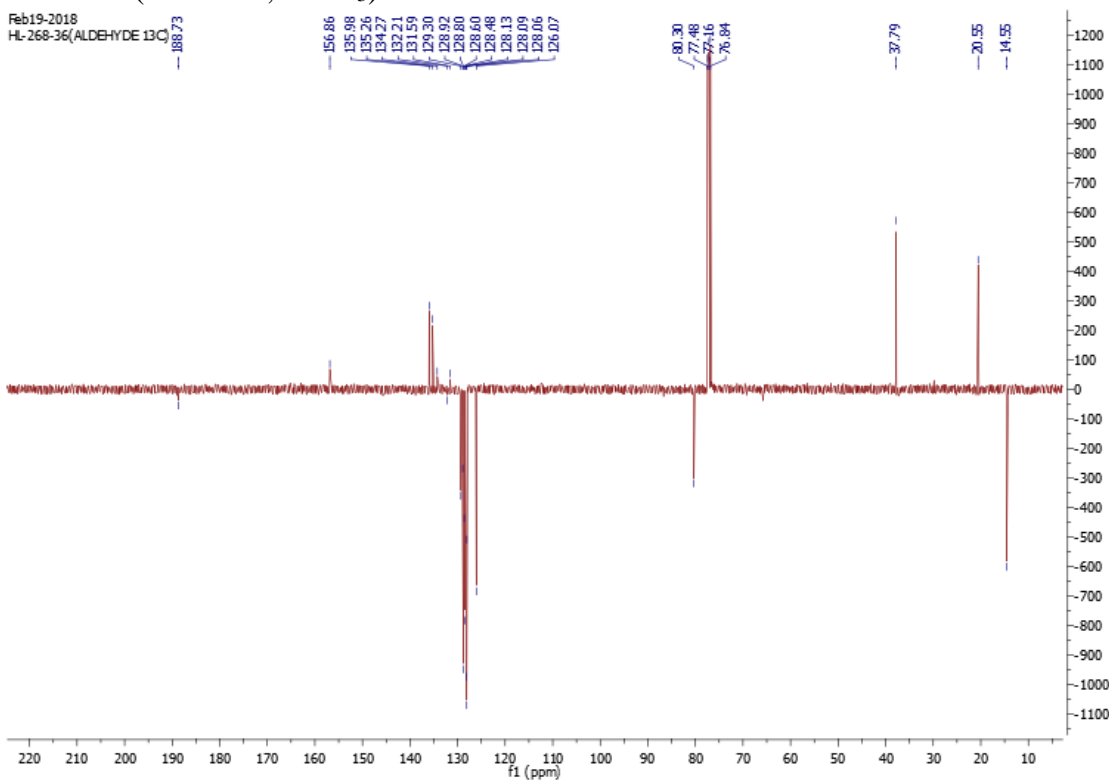


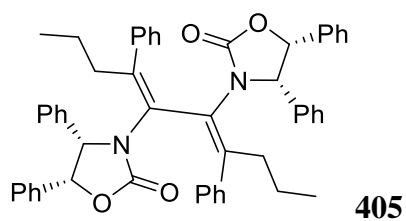
398

^1H NMR (401 MHz, CDCl_3)

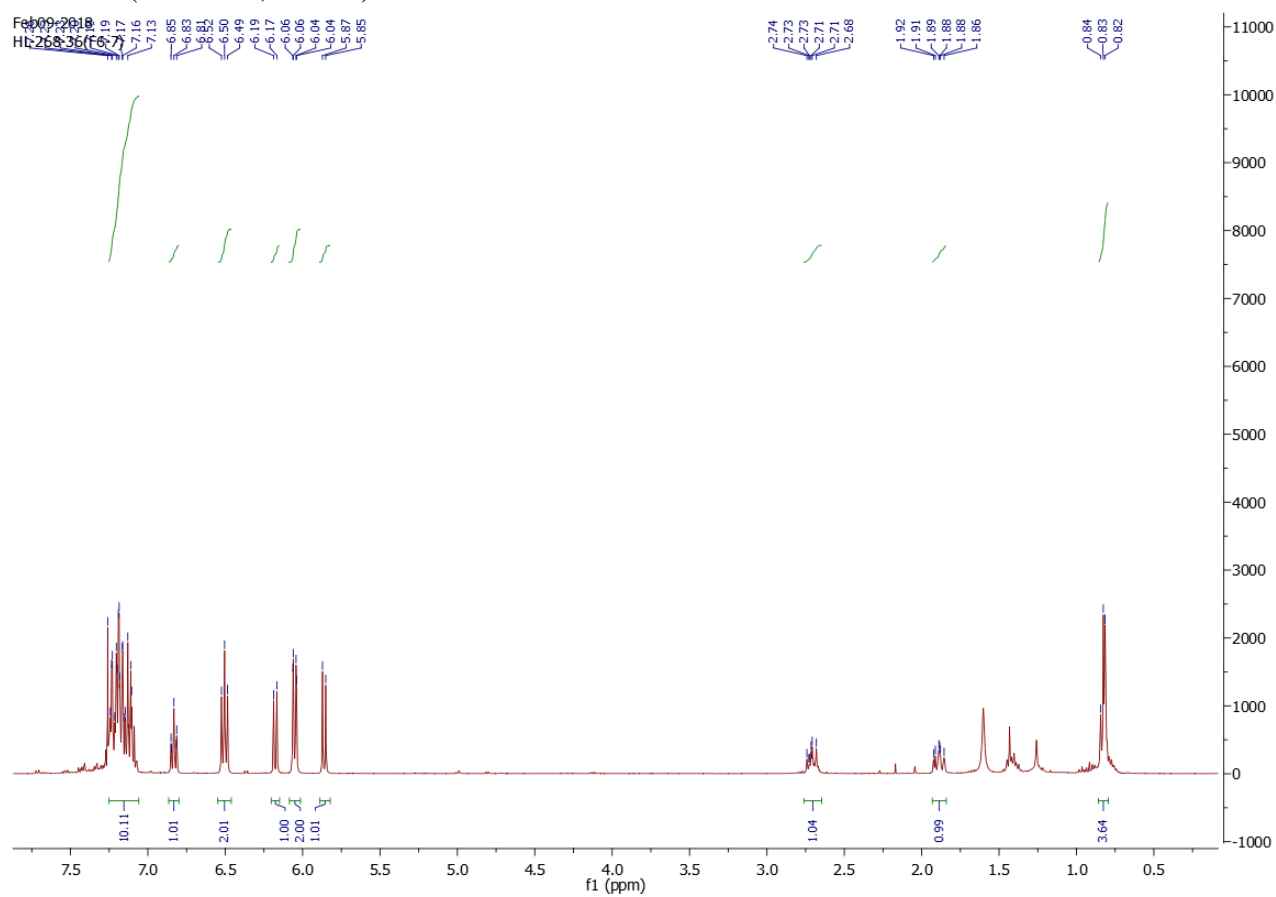


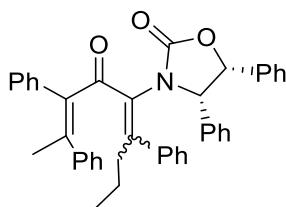
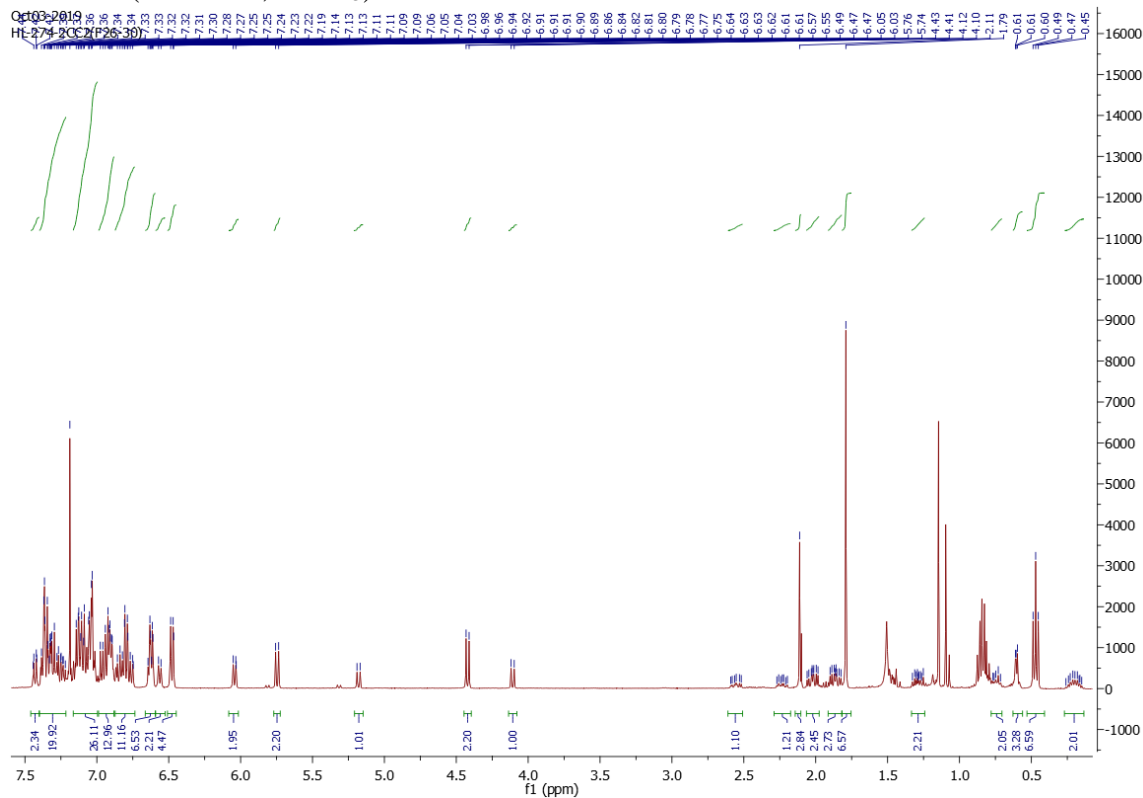
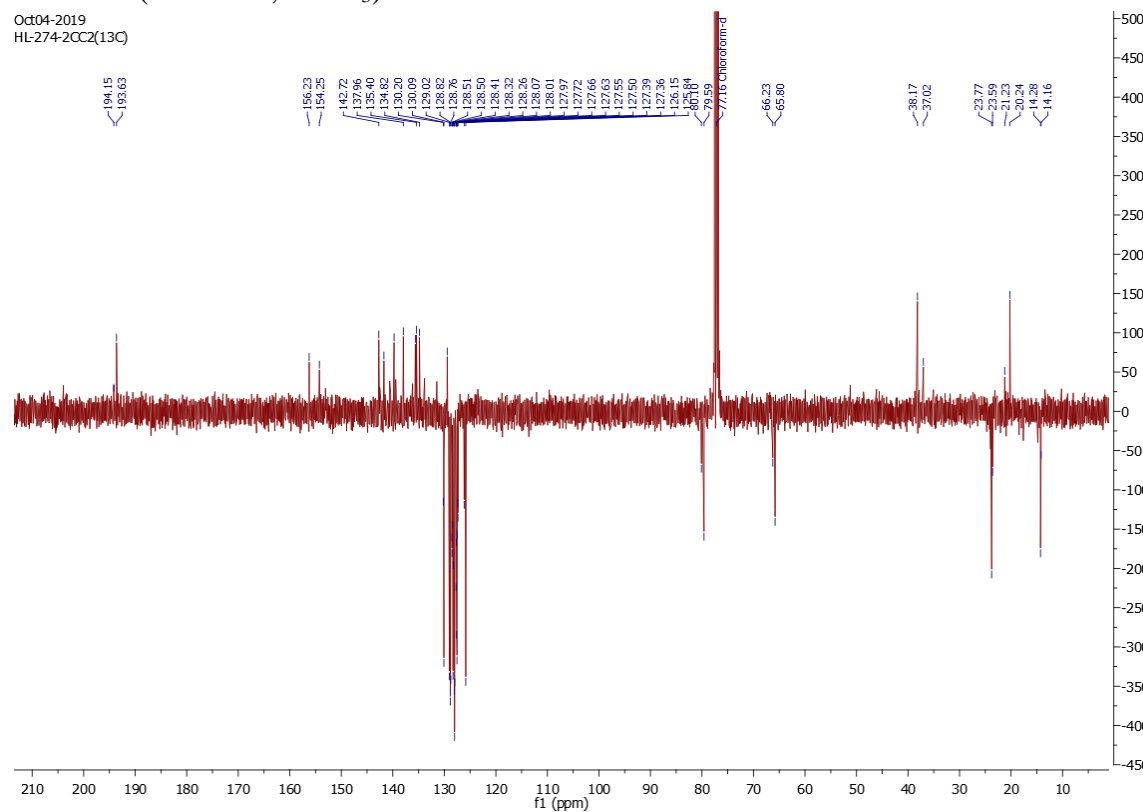
^{13}C NMR (101 MHz, CDCl_3)

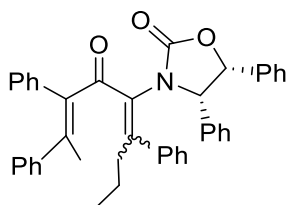
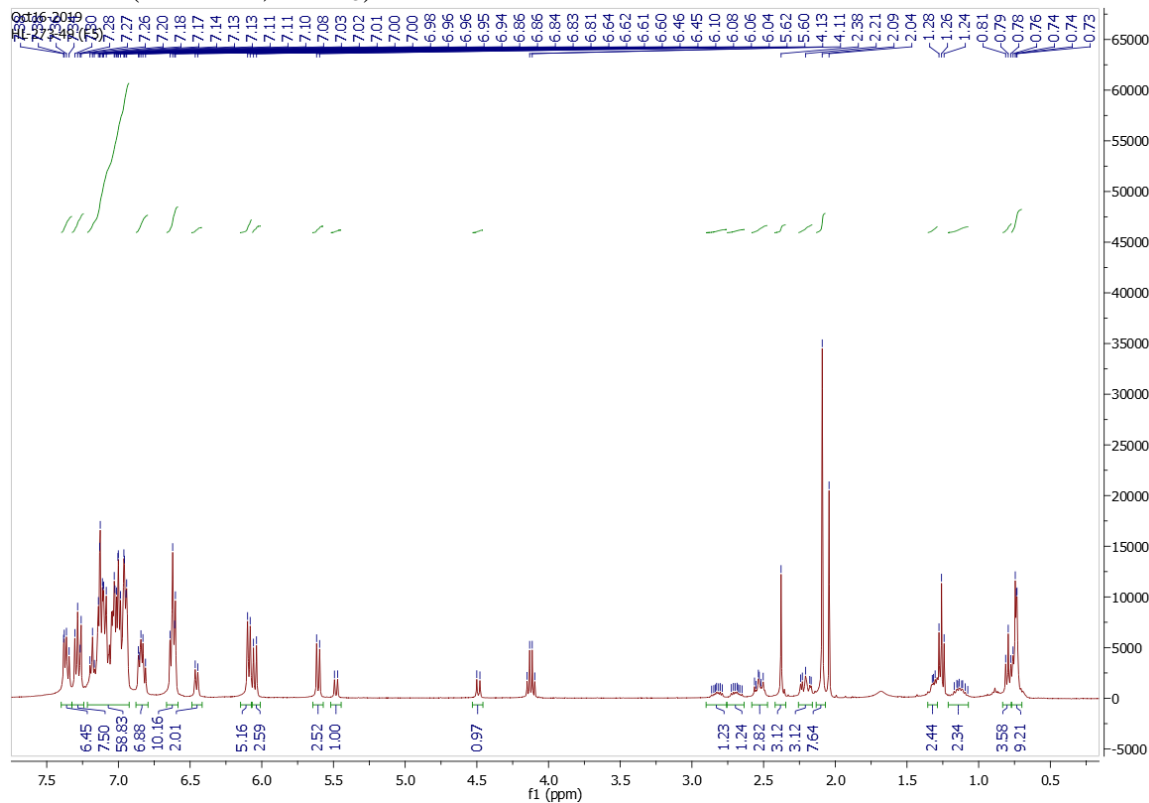
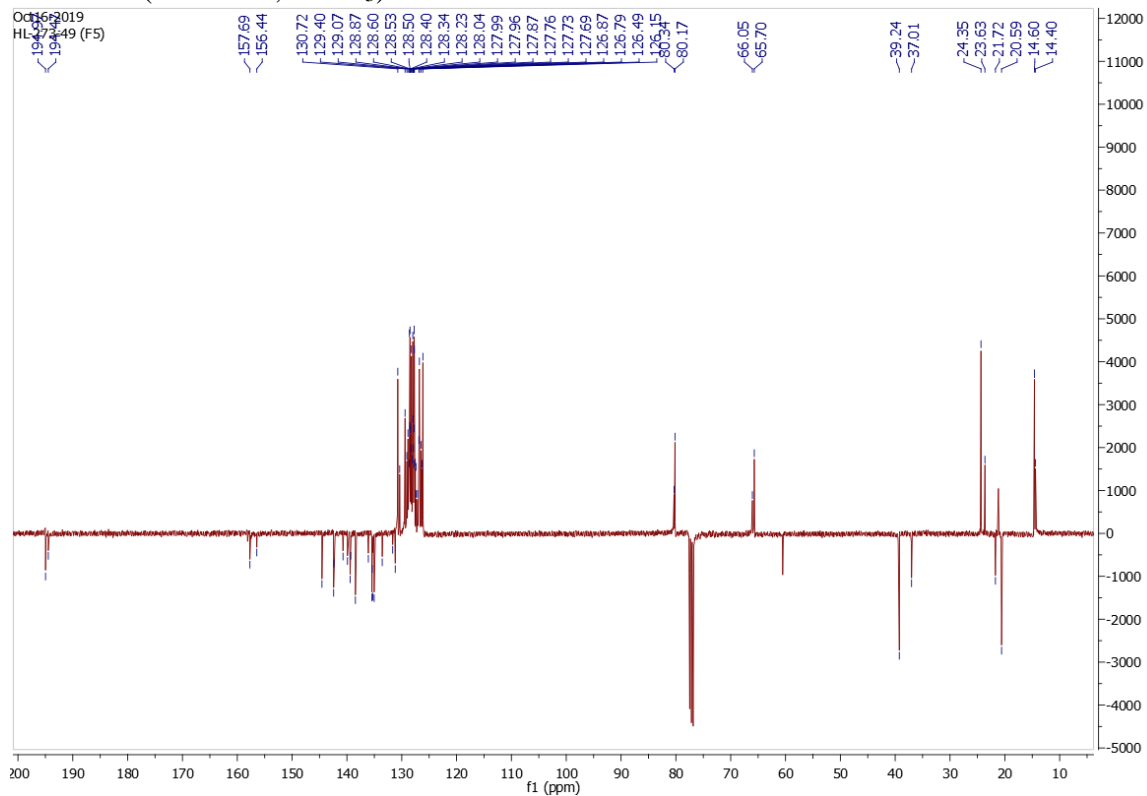




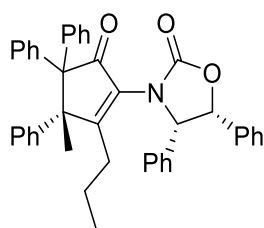
^1H NMR (401 MHz, CDCl_3)



**388a(5E/Z)**¹H NMR (401 MHz, CDCl₃)¹³C NMR (101 MHz, CDCl₃)

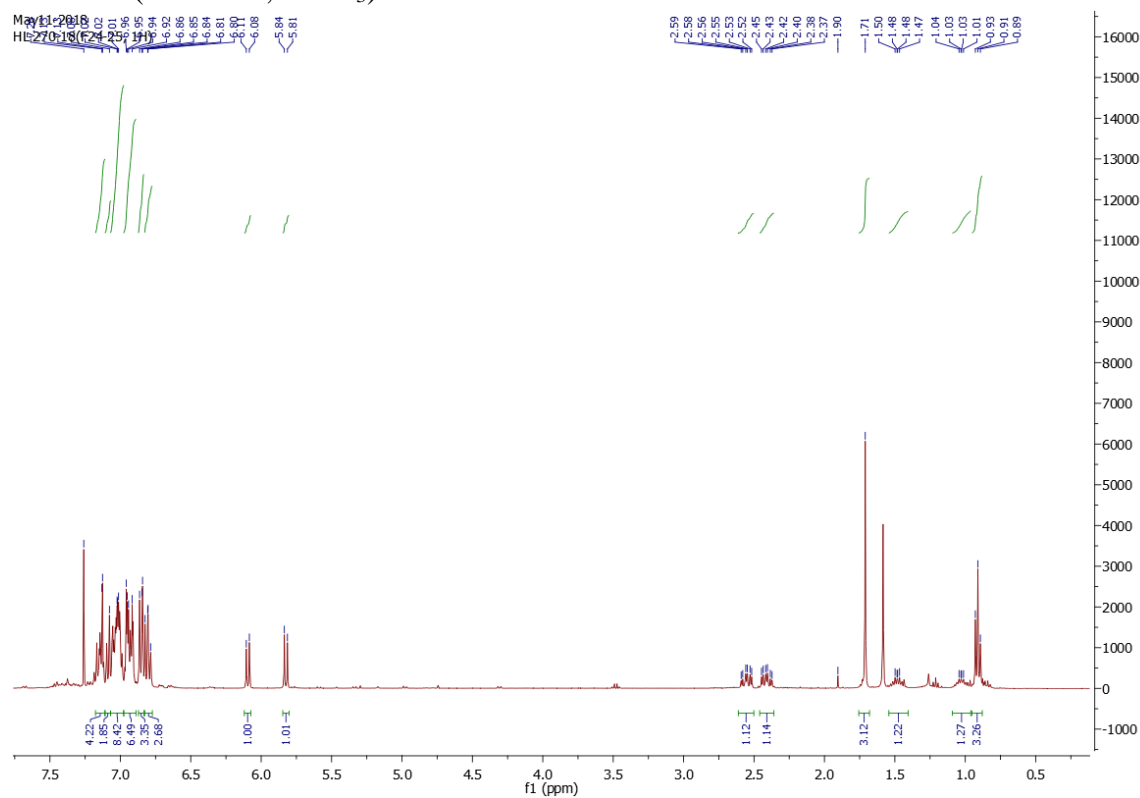
**388b(5E/Z)**¹H NMR (401 MHz, CDCl₃)¹³C NMR (101 MHz, CDCl₃)

Chapter 6

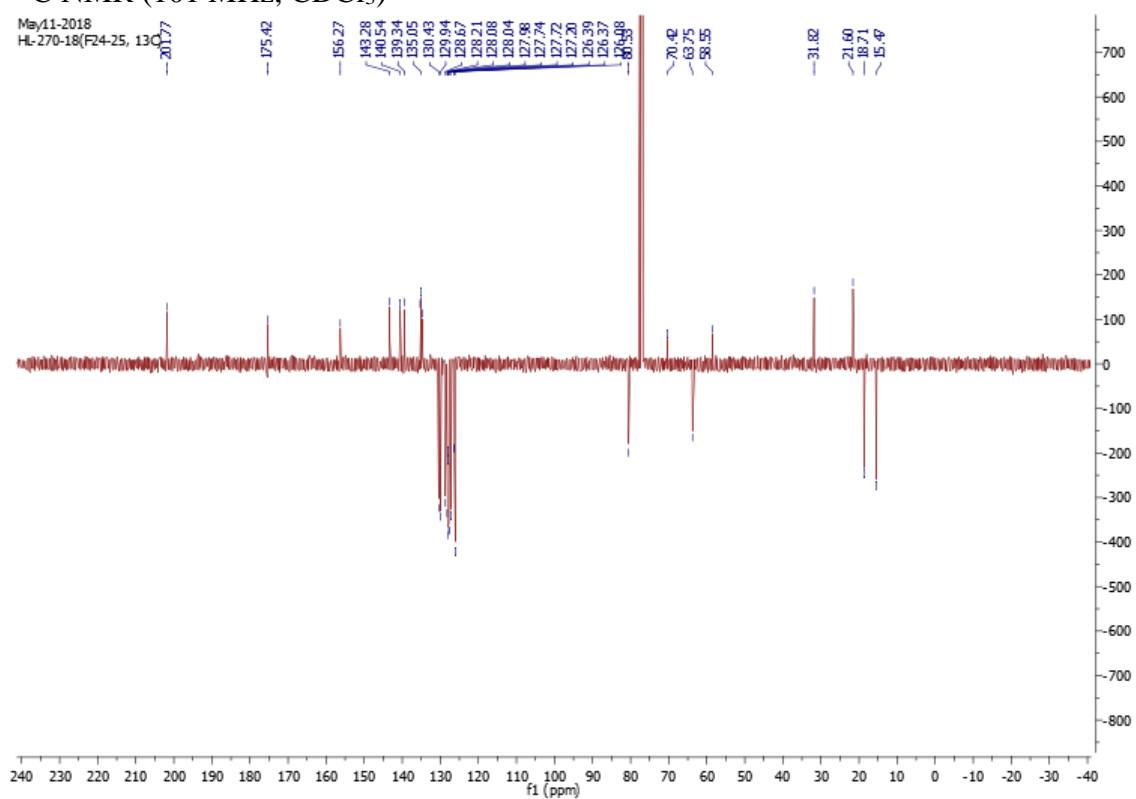


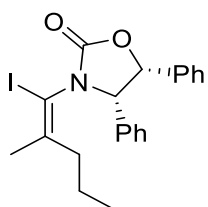
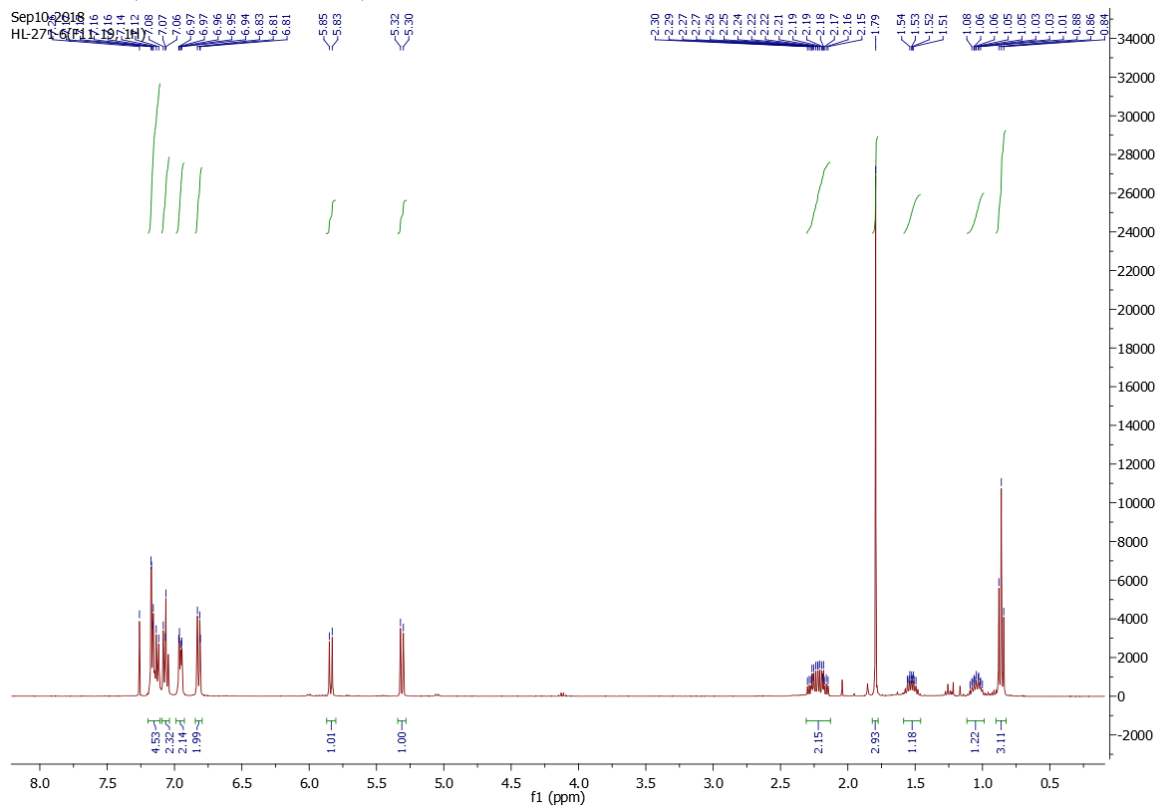
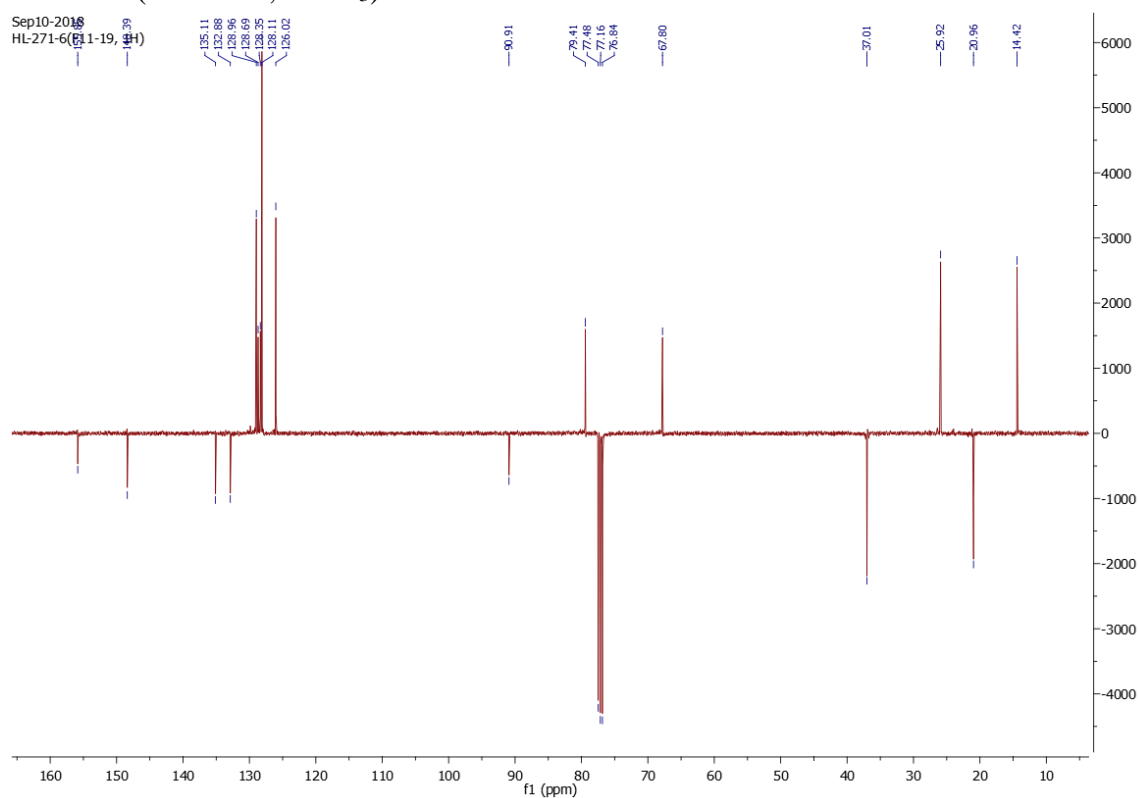
390

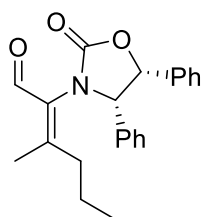
^1H NMR (401 MHz, CDCl_3)



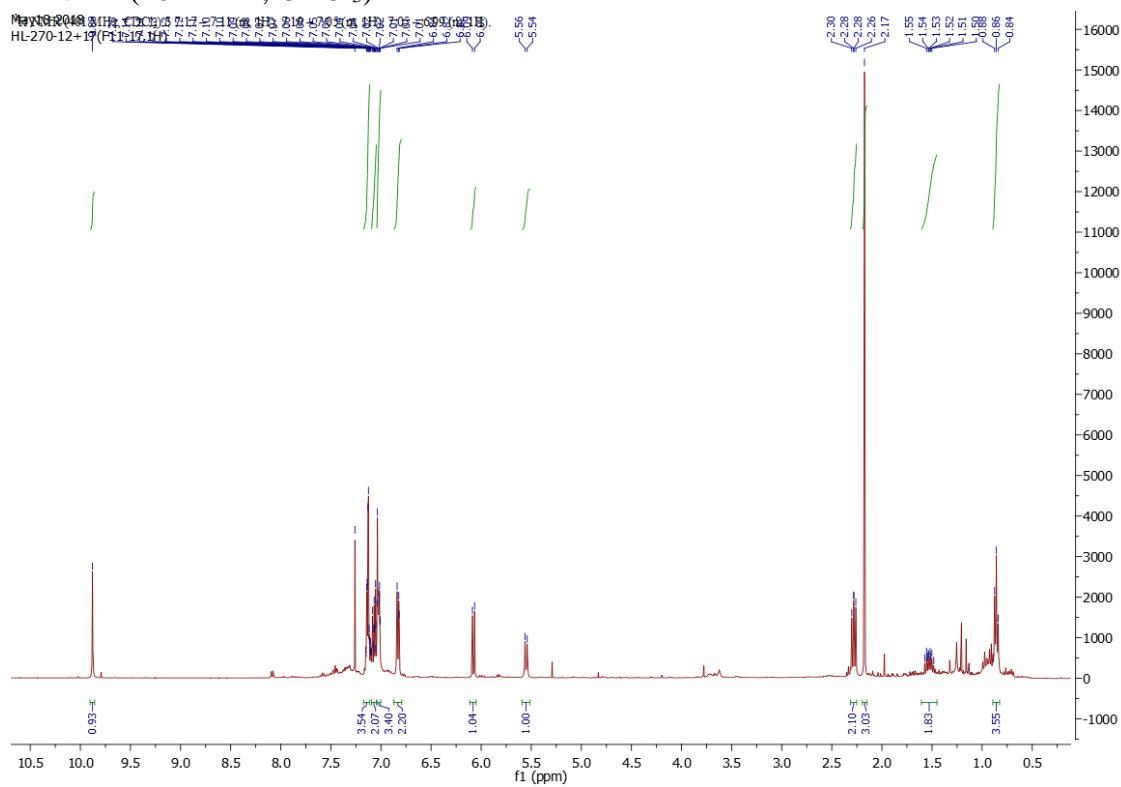
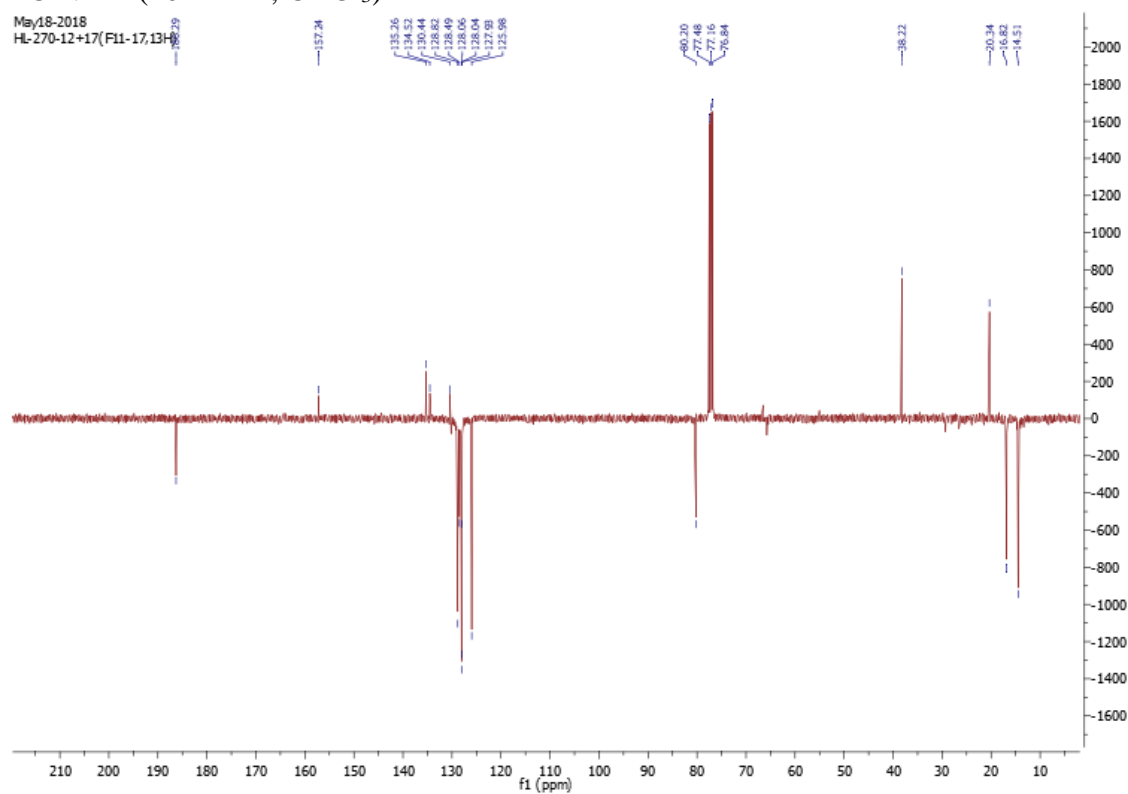
^{13}C NMR (101 MHz, CDCl_3)

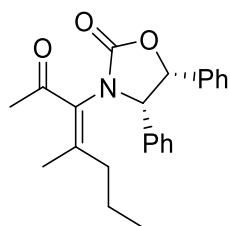
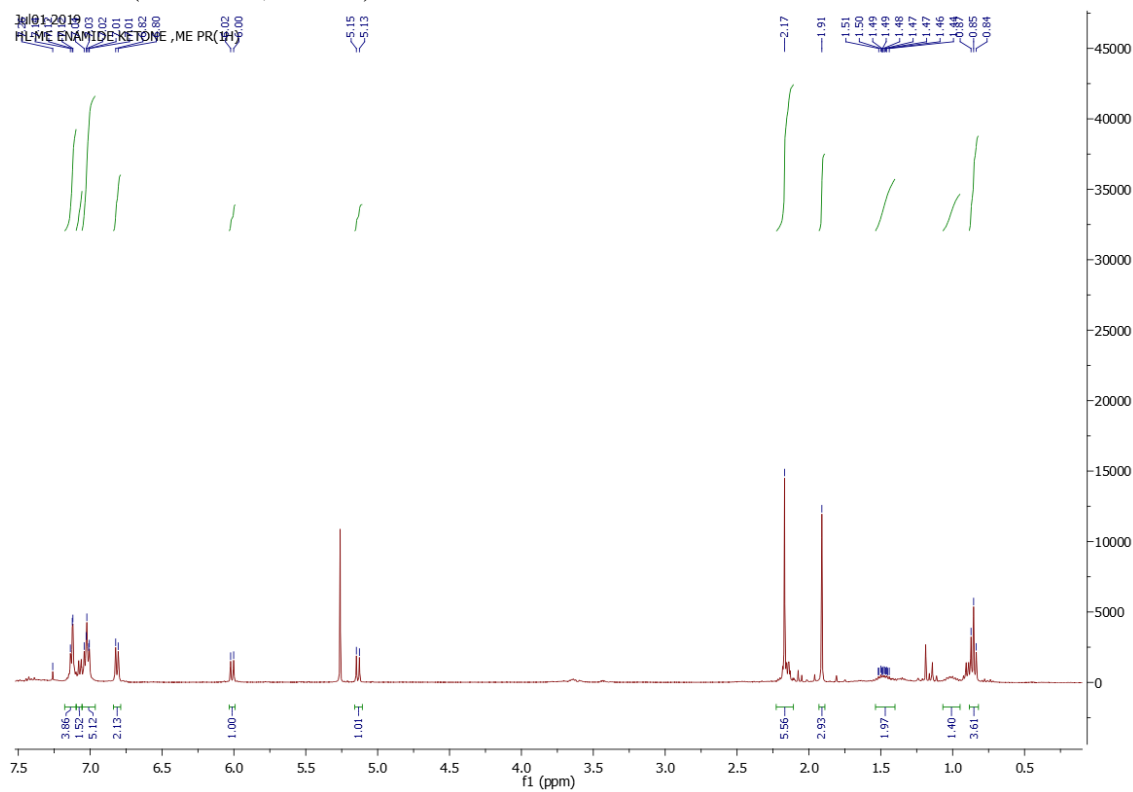
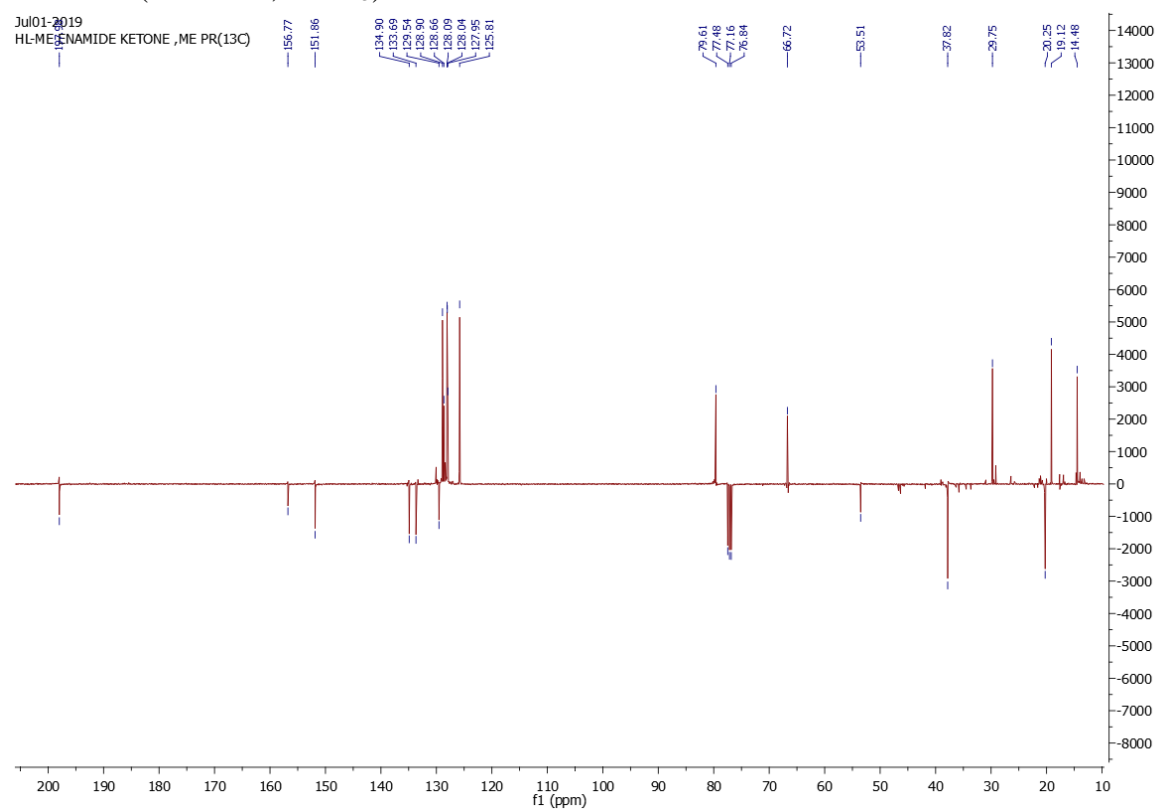


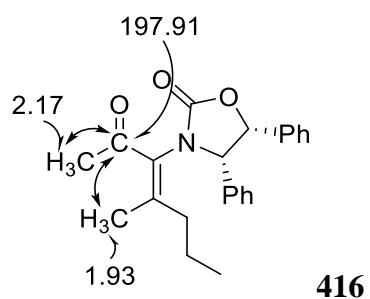
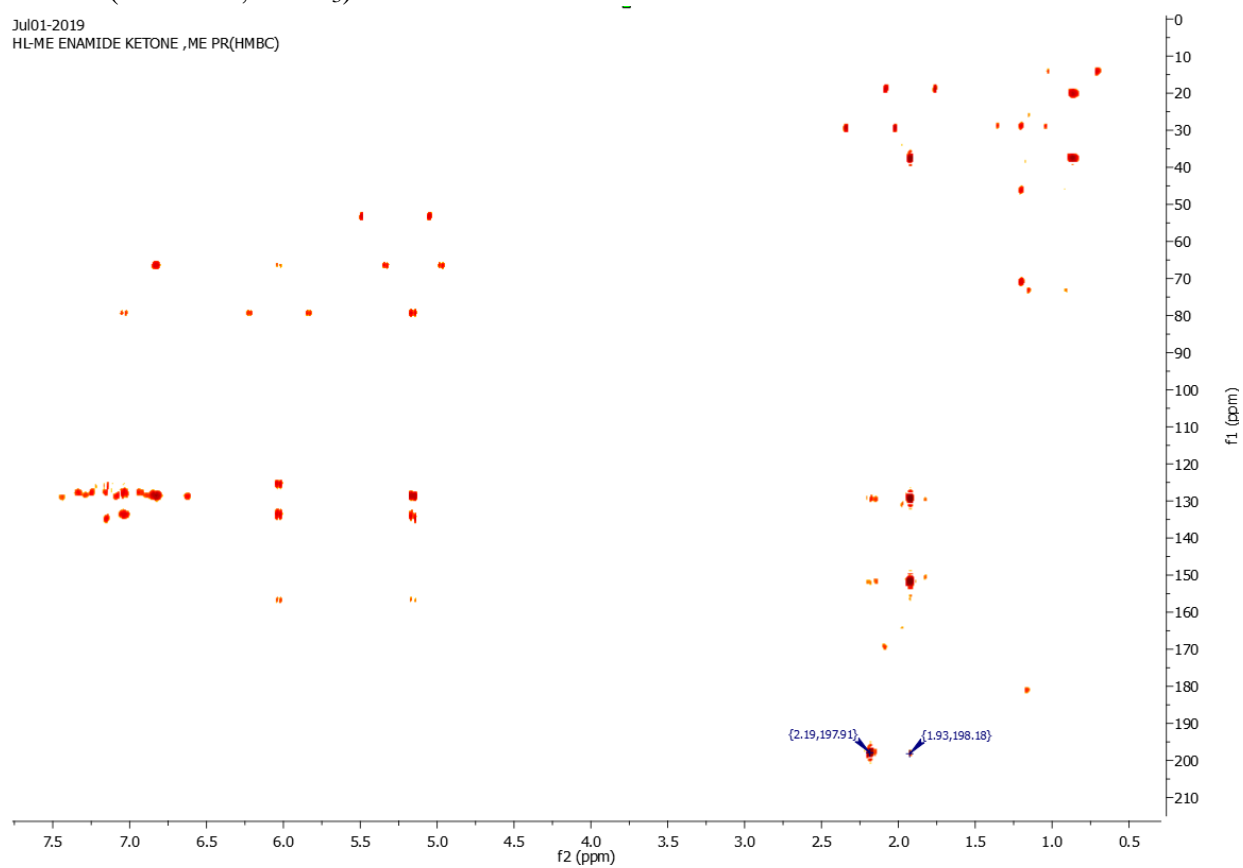
**409** ^1H NMR (401 MHz, CDCl_3) ^{13}C NMR (101 MHz, CDCl_3)



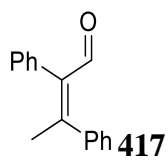
415

 ^1H NMR (401 MHz, CDCl_3) ^{13}C NMR (101 MHz, CDCl_3)

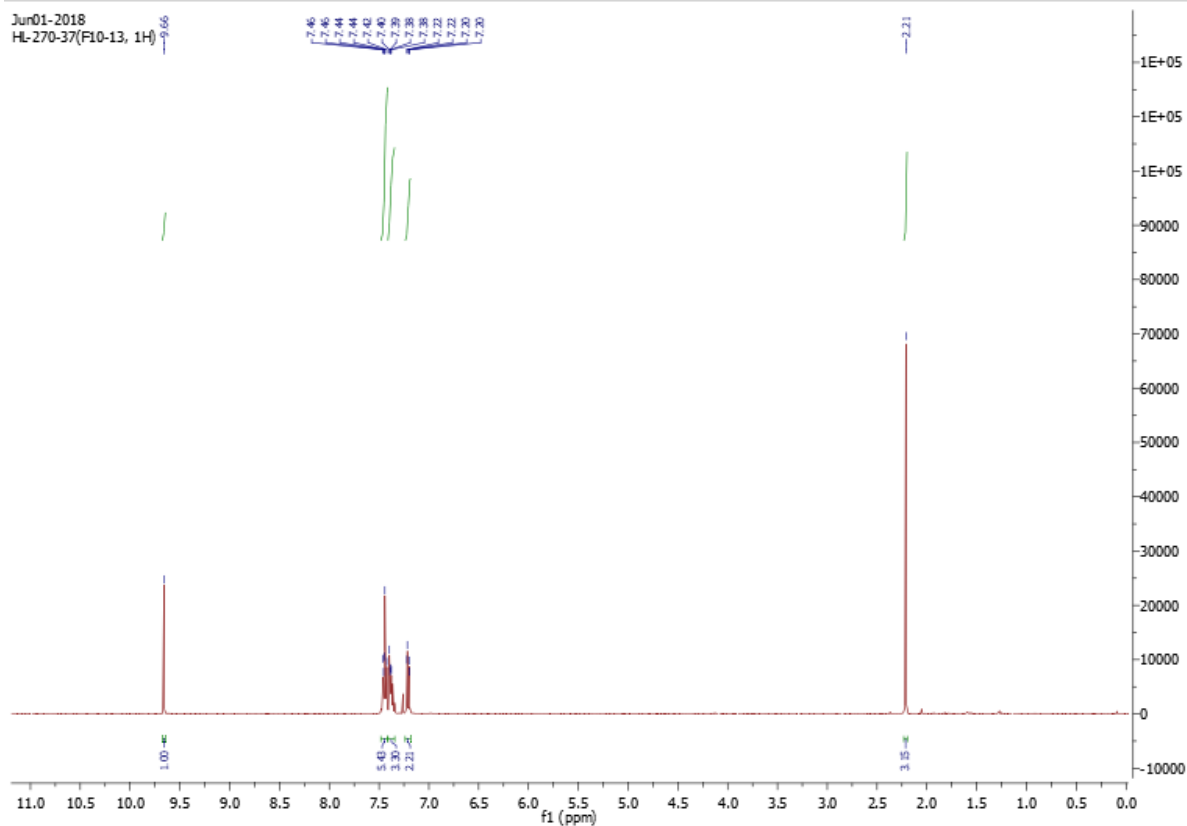
**416** ^1H NMR (401 MHz, CDCl_3) ^{13}C NMR (101 MHz, CDCl_3)

HMBC (401 MHz, CDCl₃)Jul01-2019
HL-ME ENAMIDE KETONE ,ME PR(HMBC)

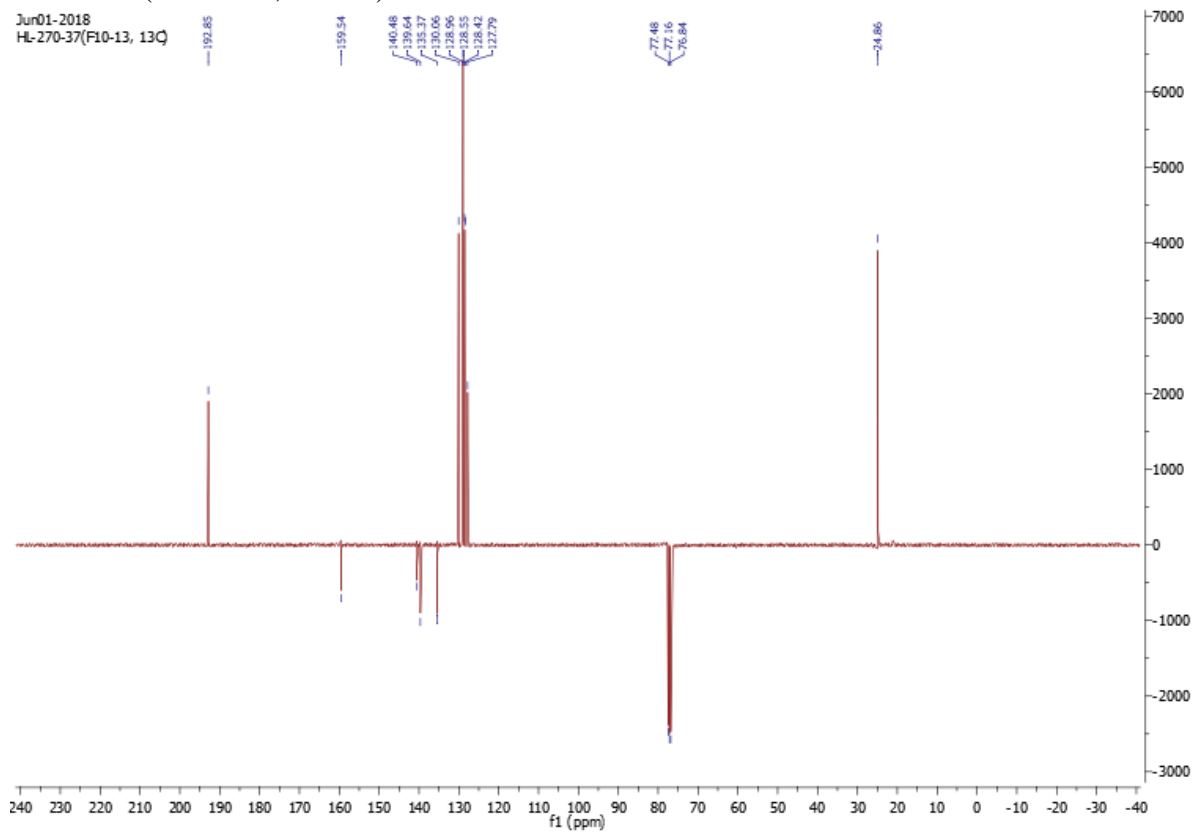
Chapter 6

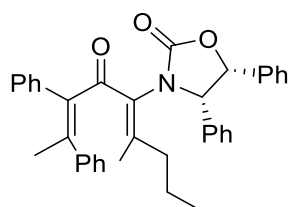
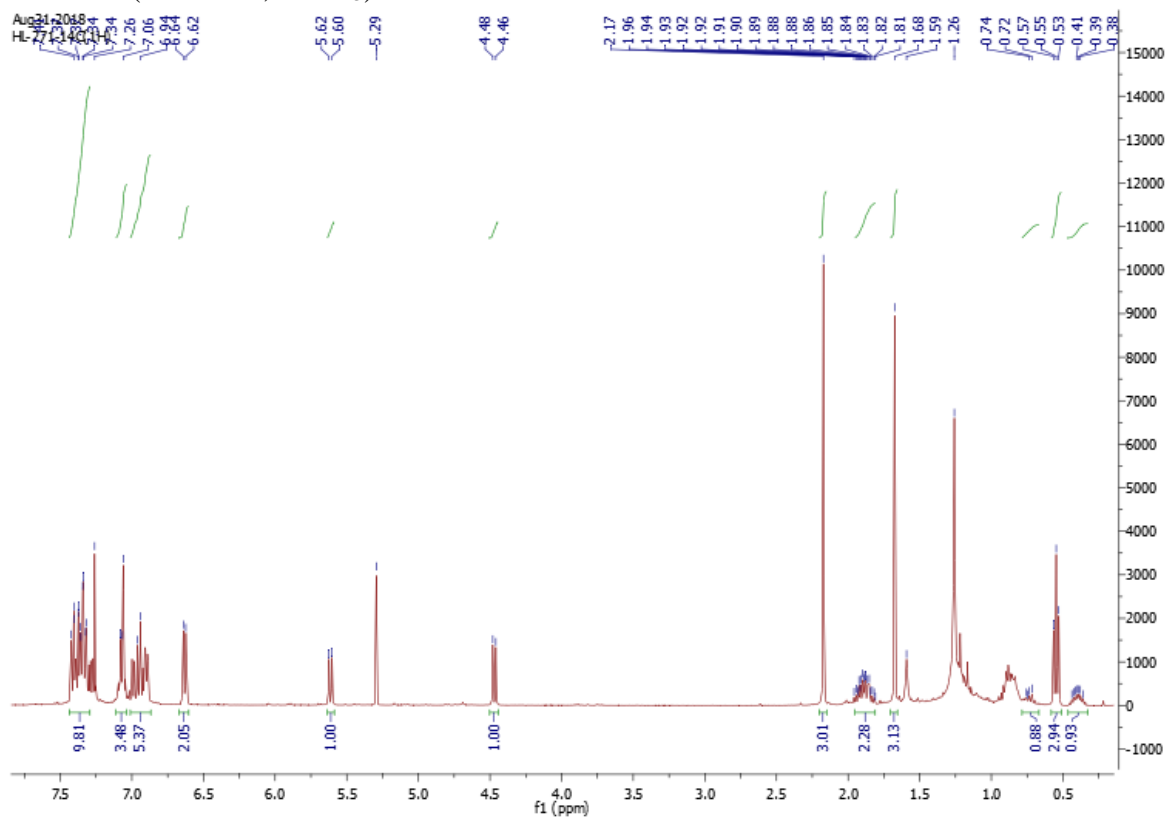
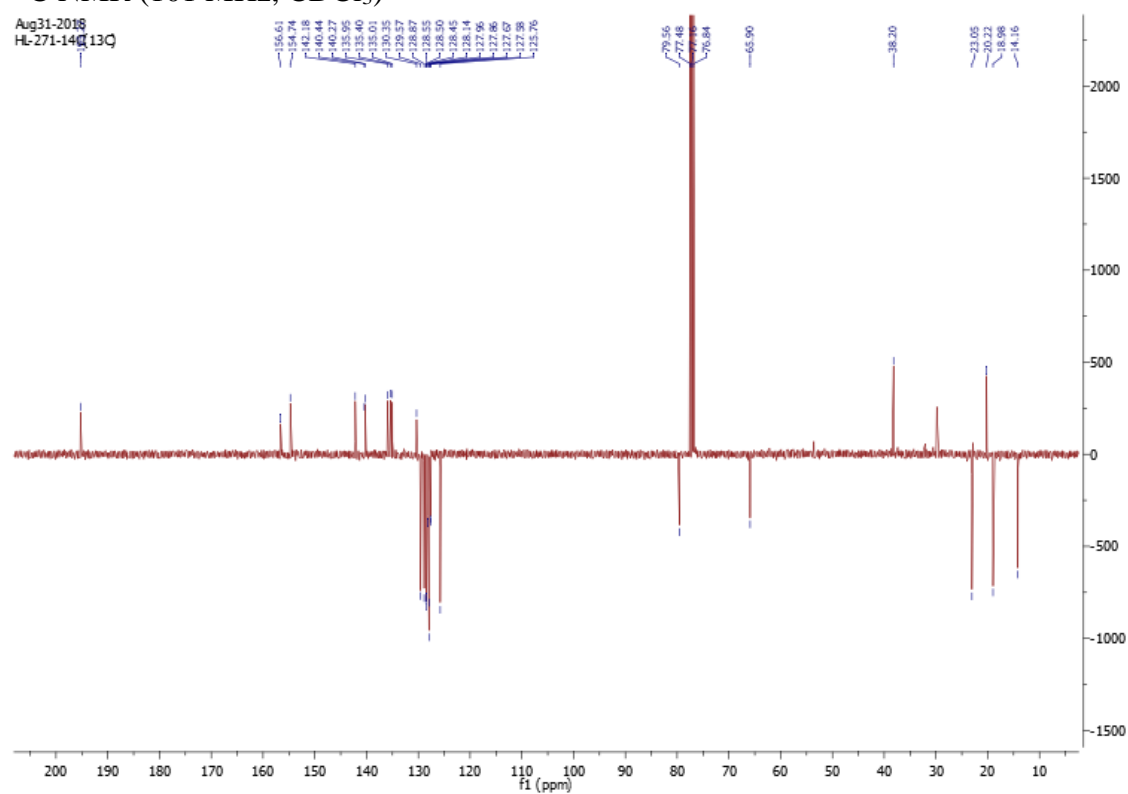


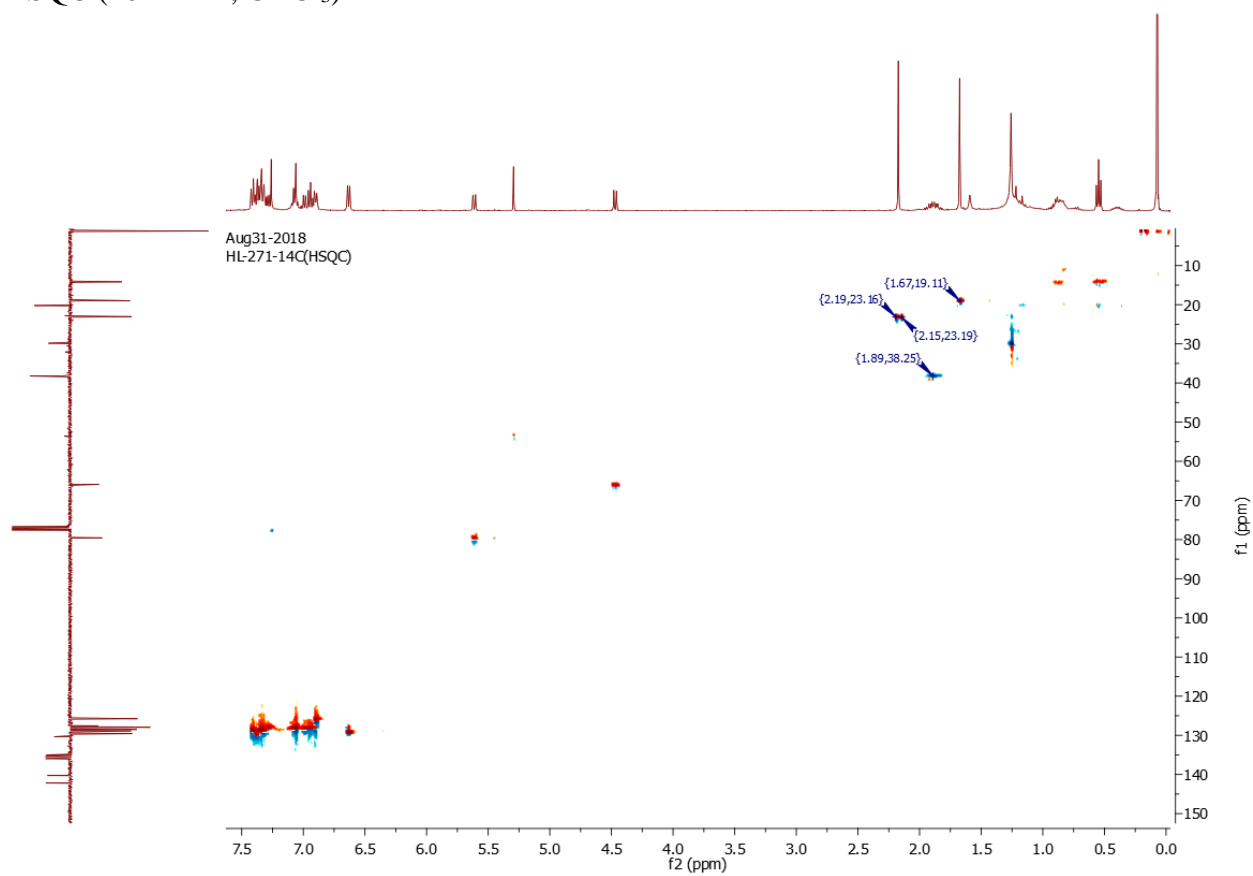
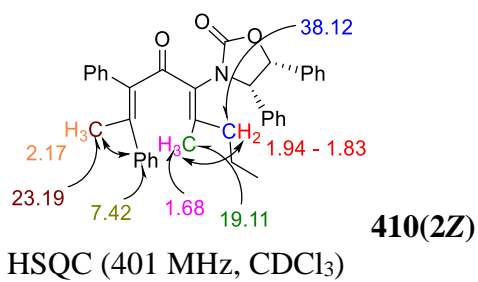
^1H NMR (401 MHz, CDCl_3)

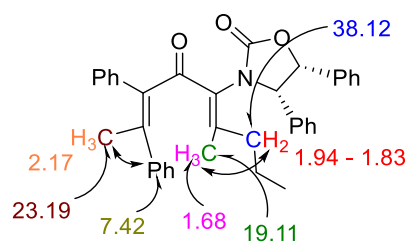
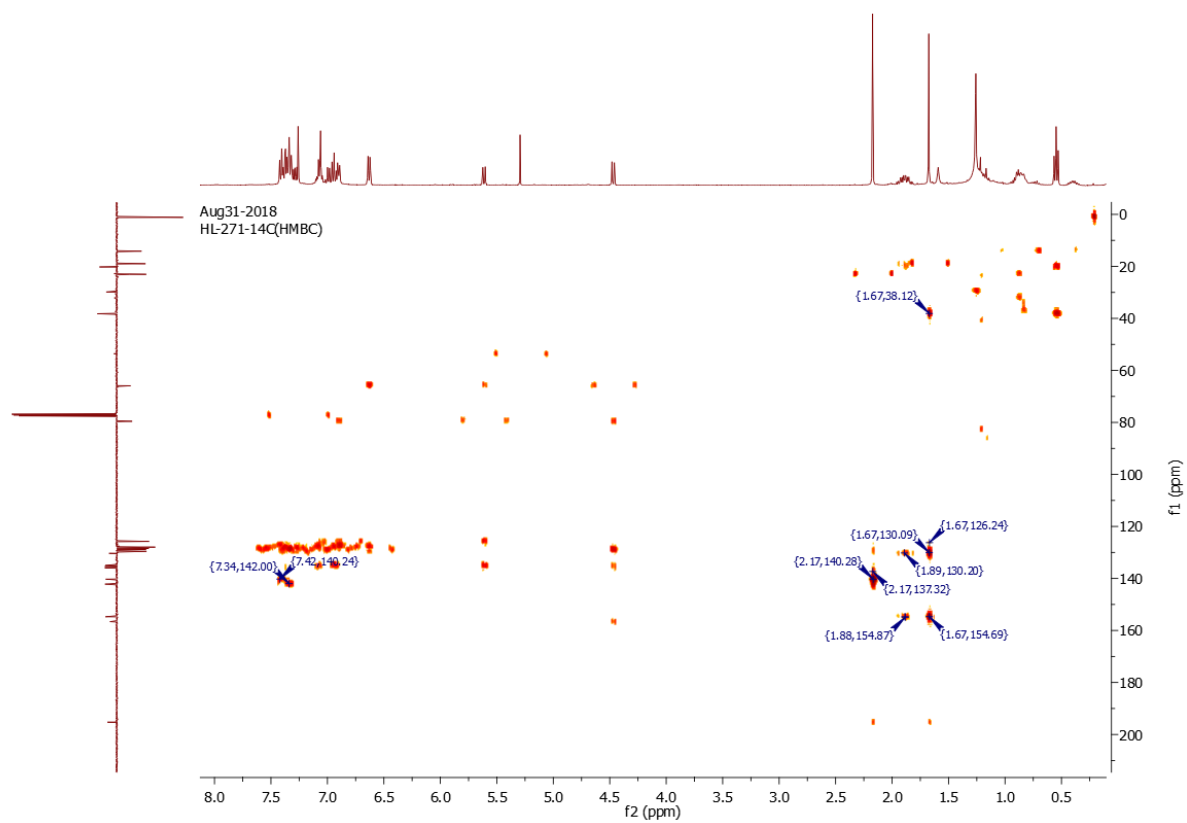


^{13}C NMR (101 MHz, CDCl_3)

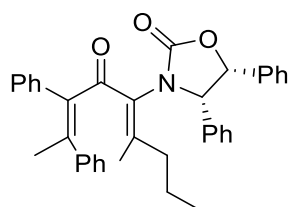


**410(2Z)**¹H NMR (401 MHz, CDCl₃)¹³C NMR (101 MHz, CDCl₃)



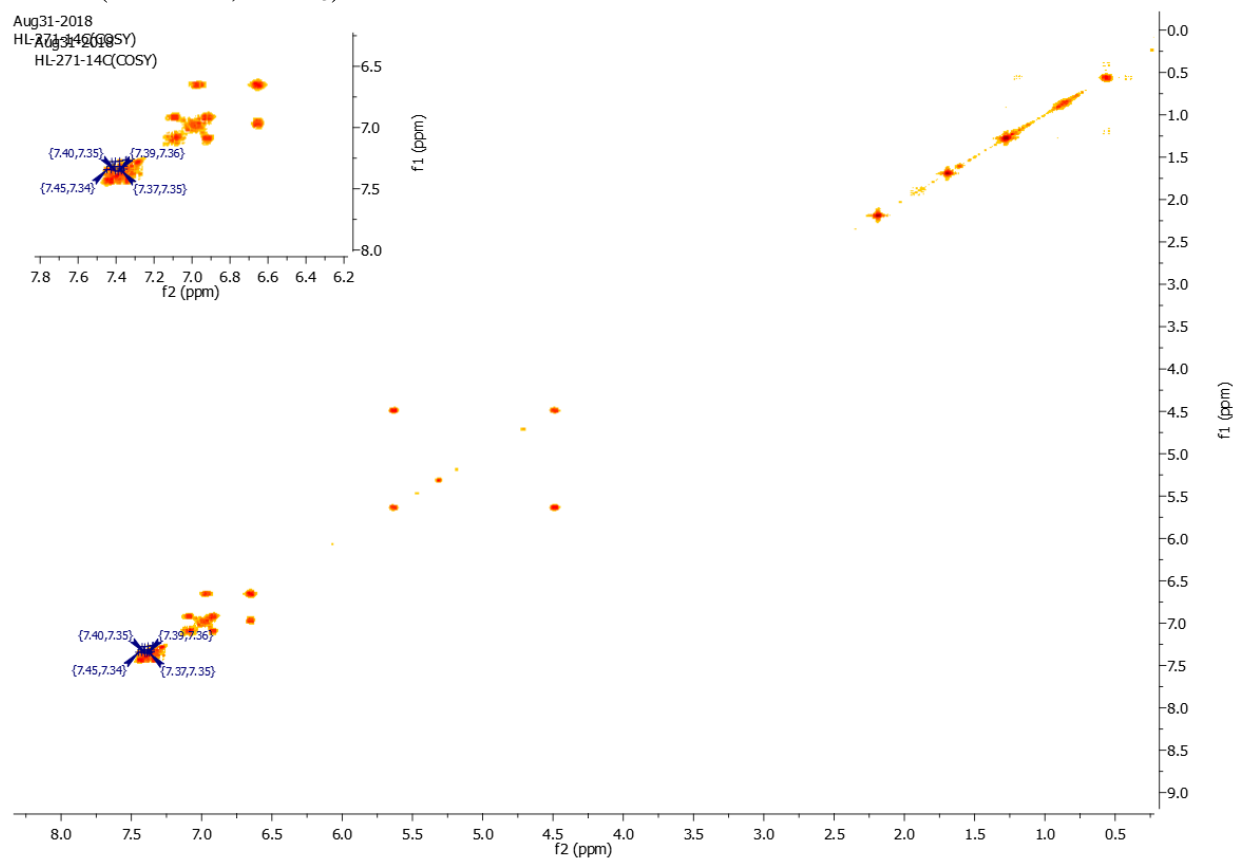
**410(2Z)**HMBC (401 MHz, CDCl_3)

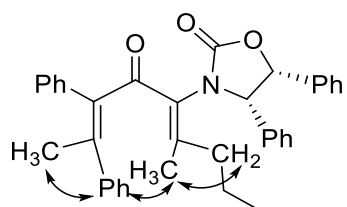
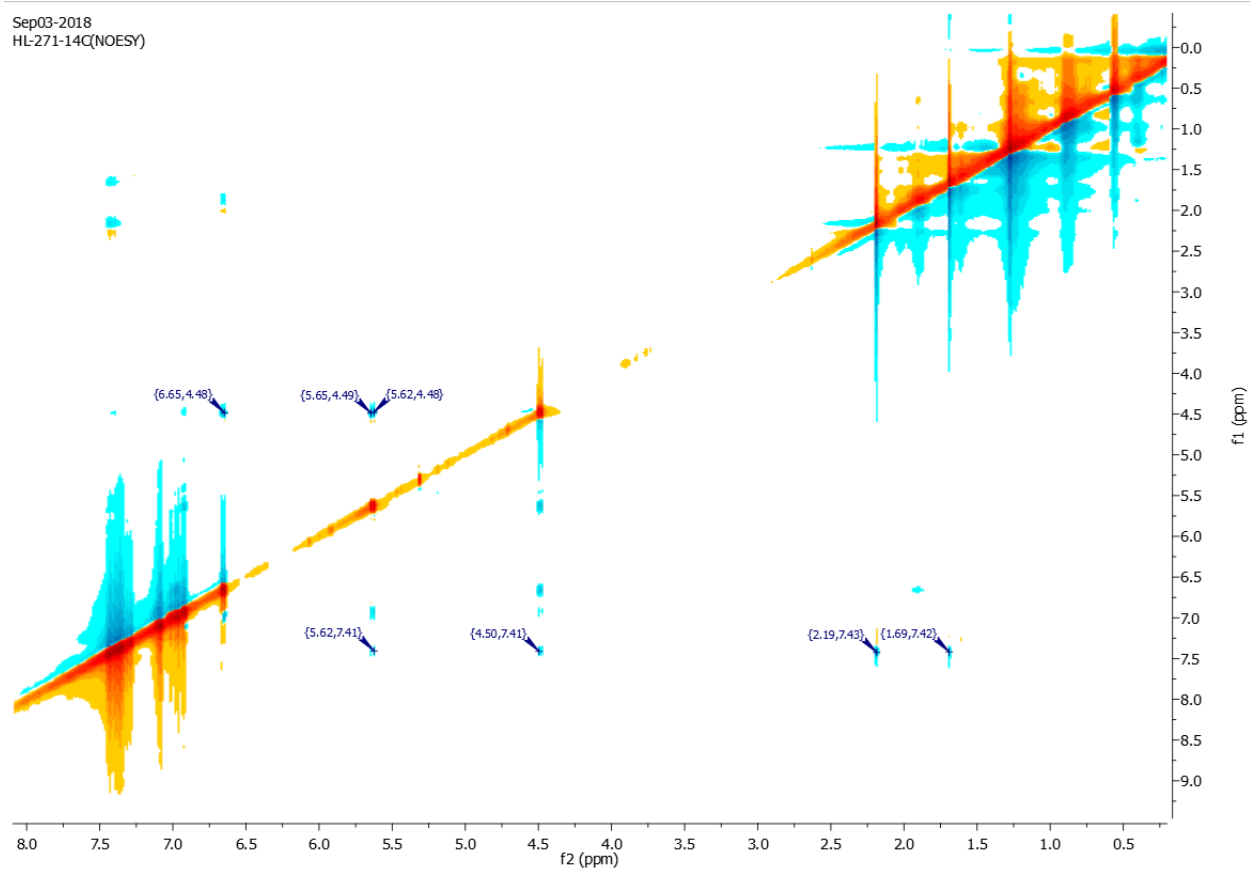
Chapter 6

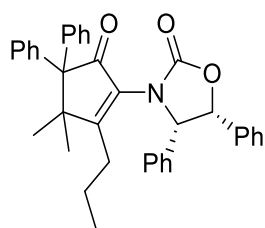
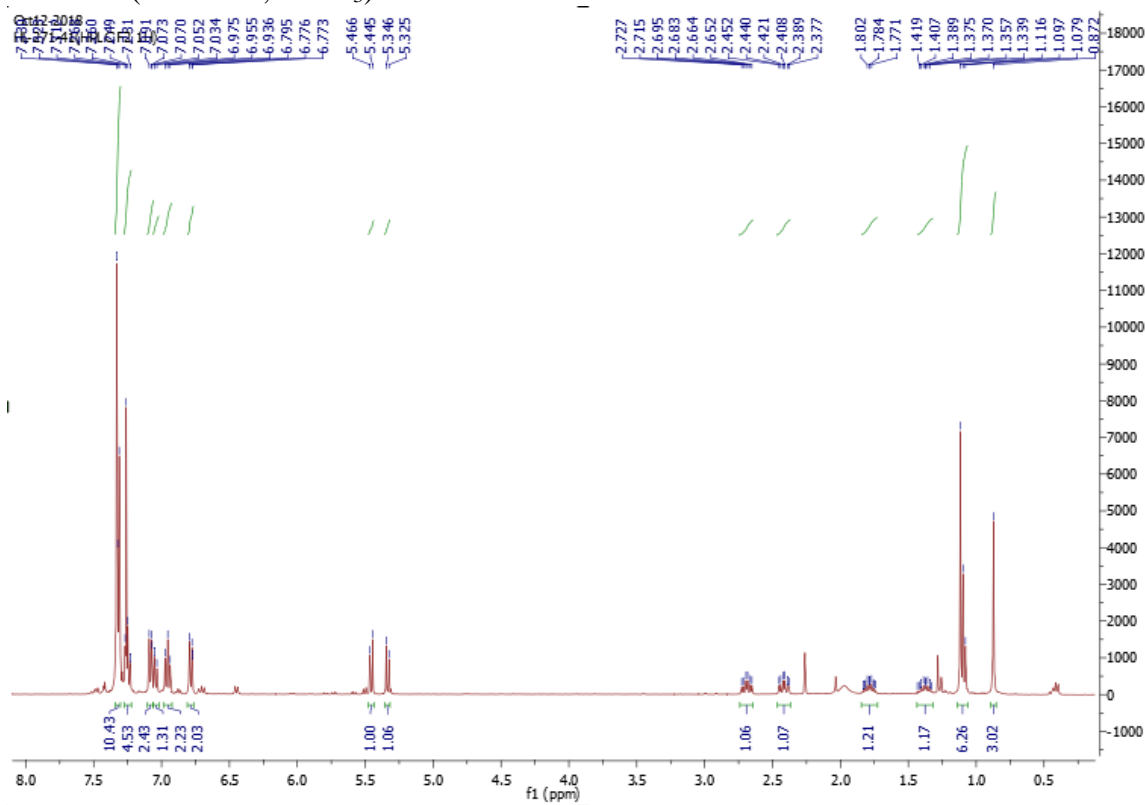
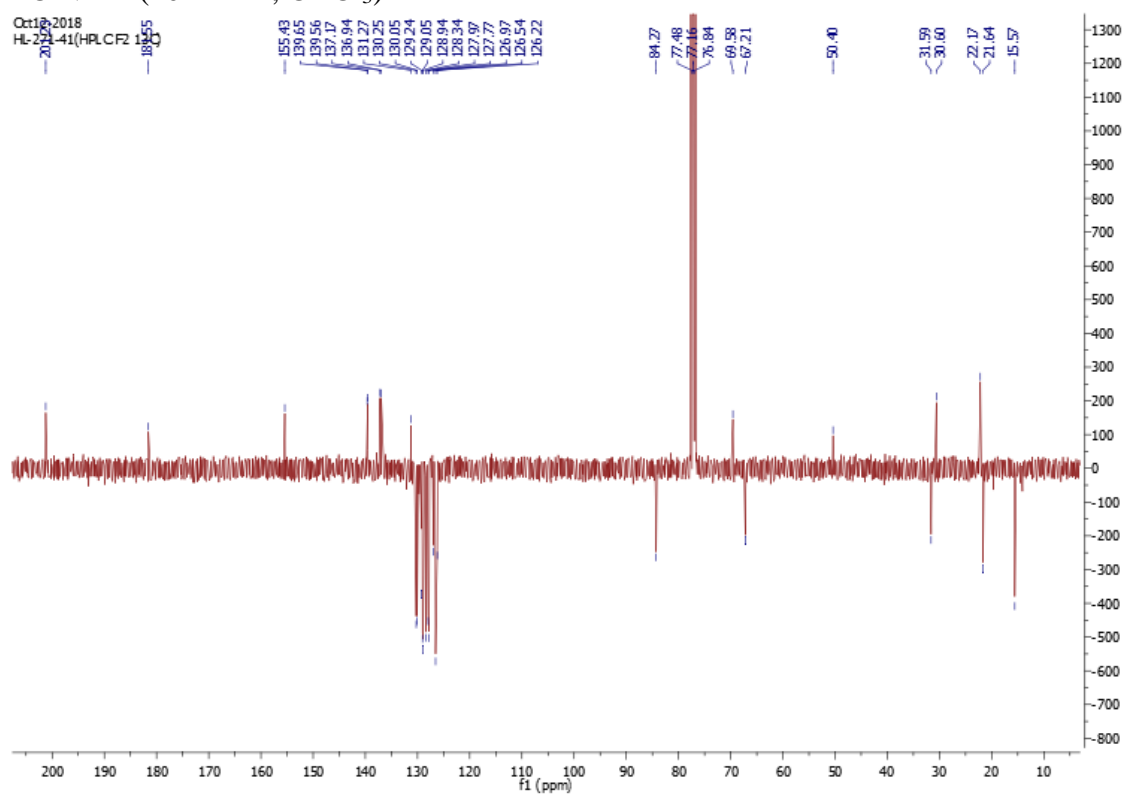


410(2Z)

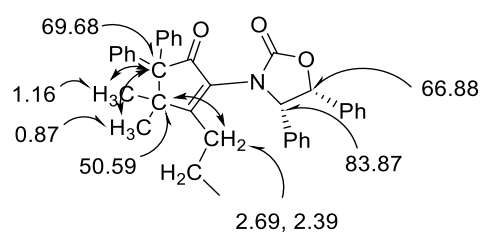
COSY (401 MHz, CDCl₃)



**410(2Z)**NOESY (401 MHz, CDCl₃)

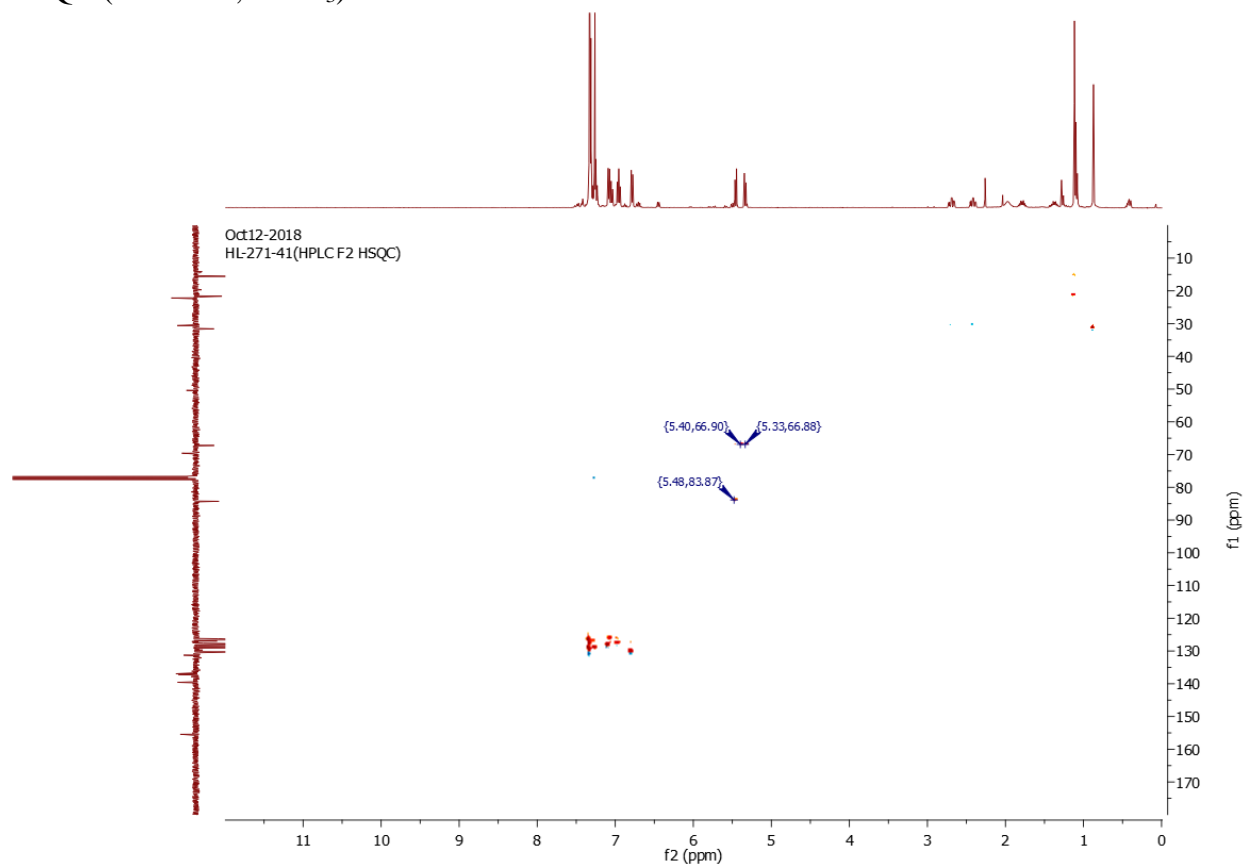
**422** ^1H NMR (401 MHz, CDCl_3) ^{13}C NMR (101 MHz, CDCl_3)

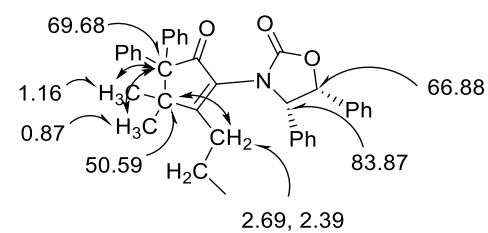
Chapter 6



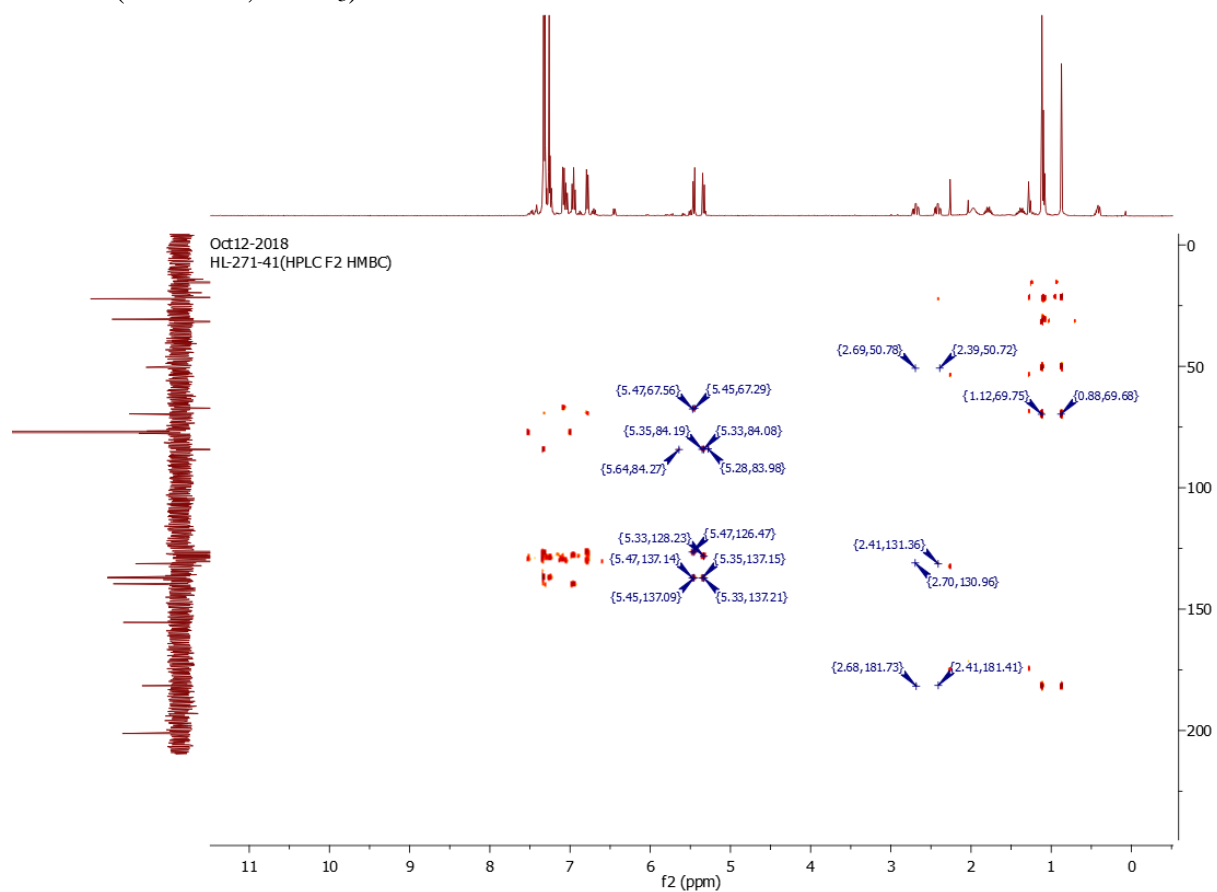
422

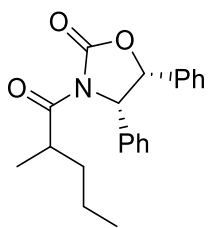
HSQC (401 MHz, CDCl_3)



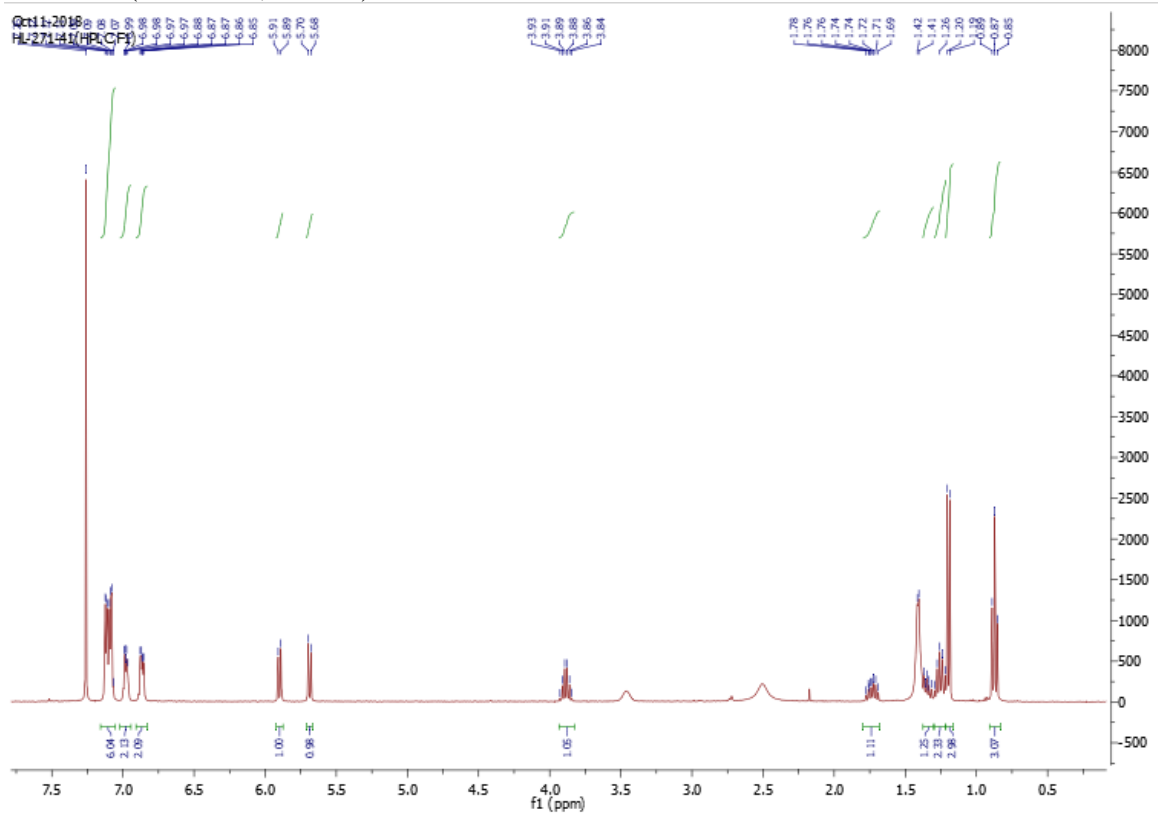
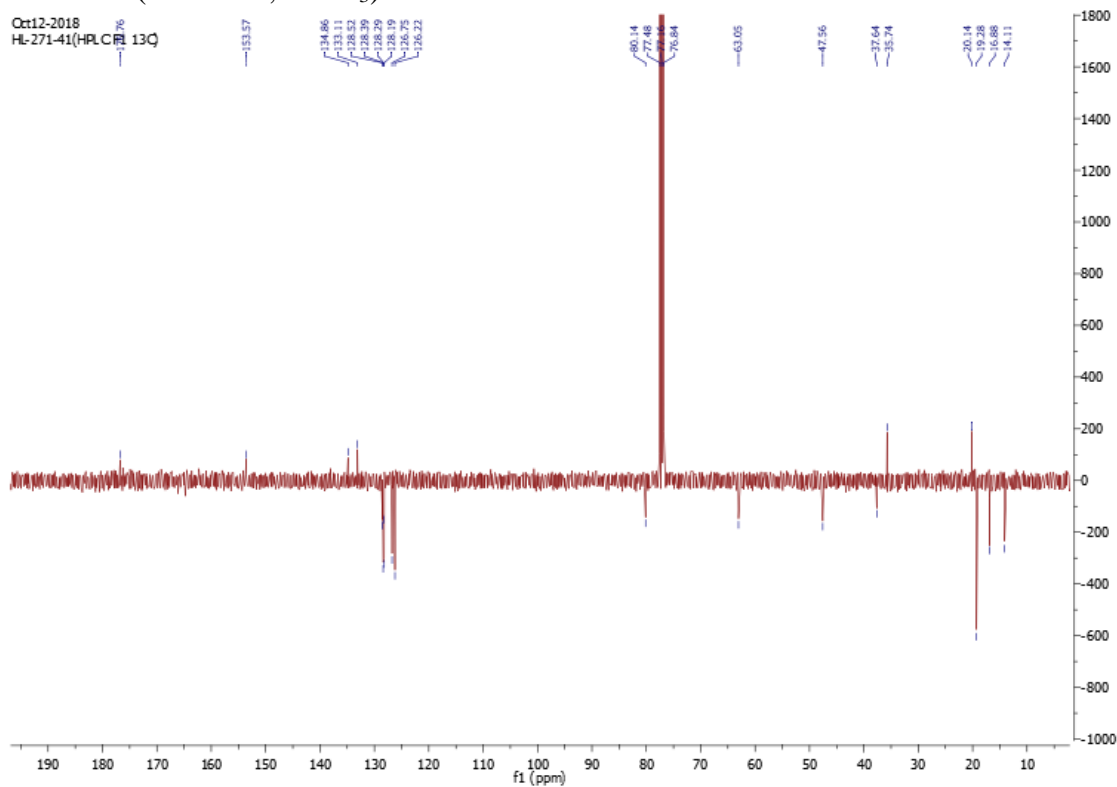


422

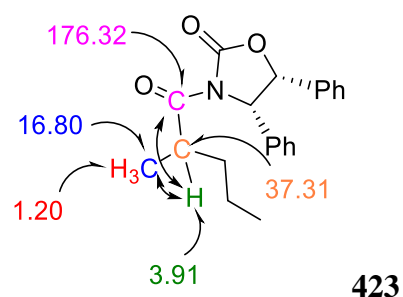
HMBC (401 MHz, CDCl₃)



423

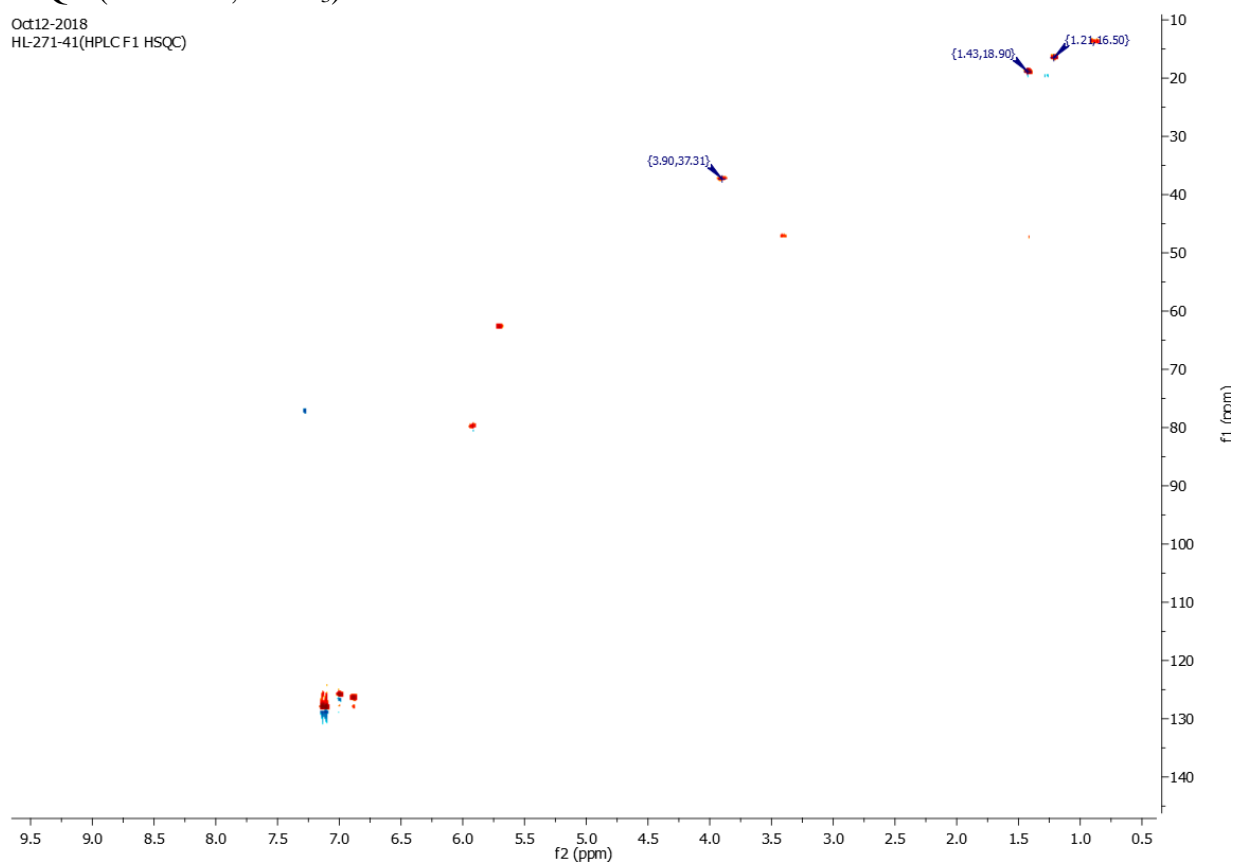
 ^1H NMR (401 MHz, CDCl_3) ^{13}C NMR (101 MHz, CDCl_3)

Chapter 6

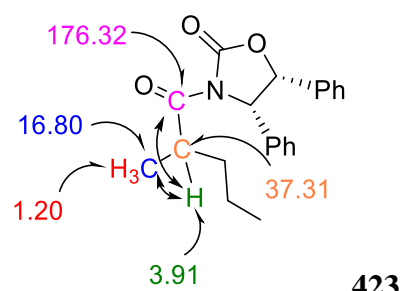


HSQC (401 MHz, CDCl₃)

Oct12-2018
HL-271-41(HPLC F1 HSQC)



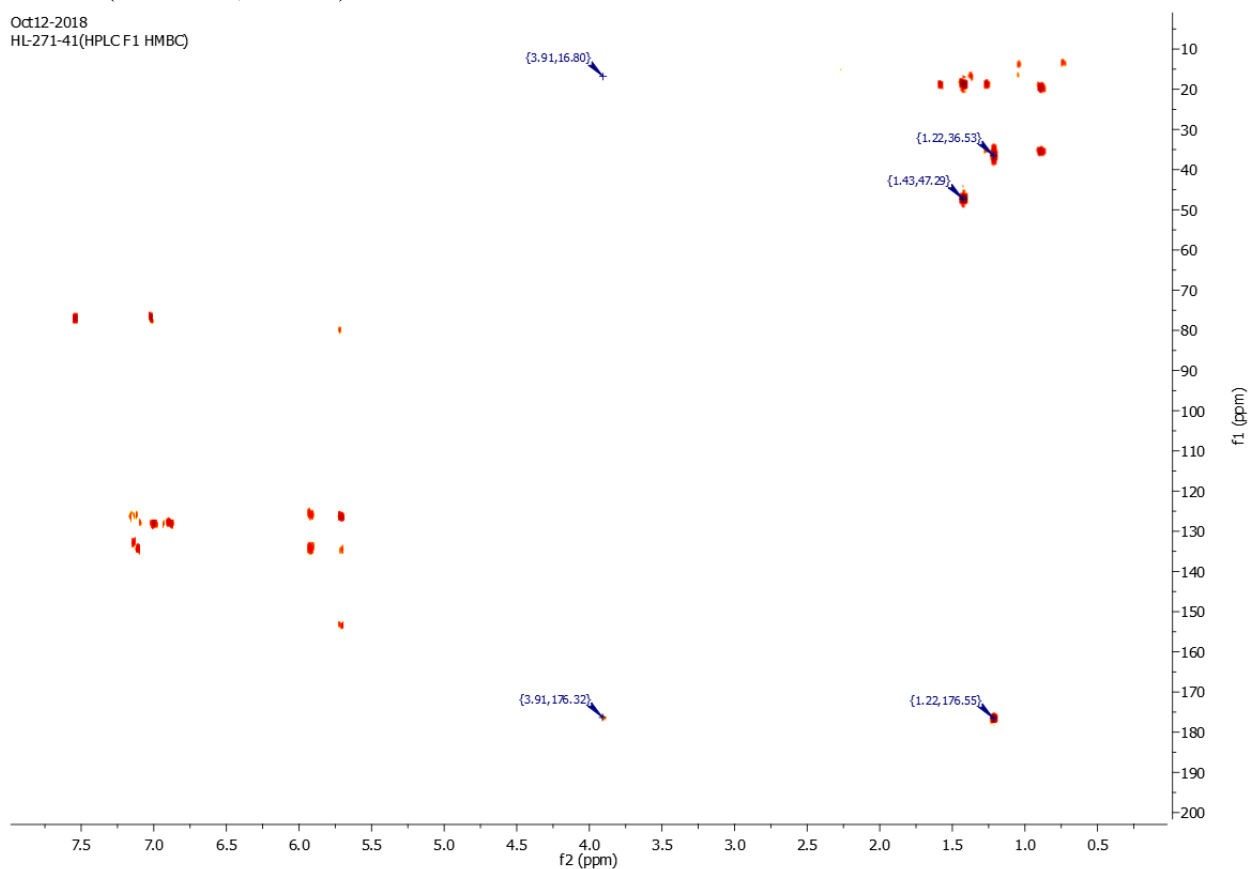
Chapter 6

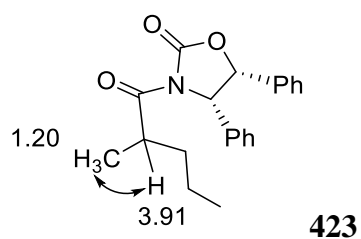
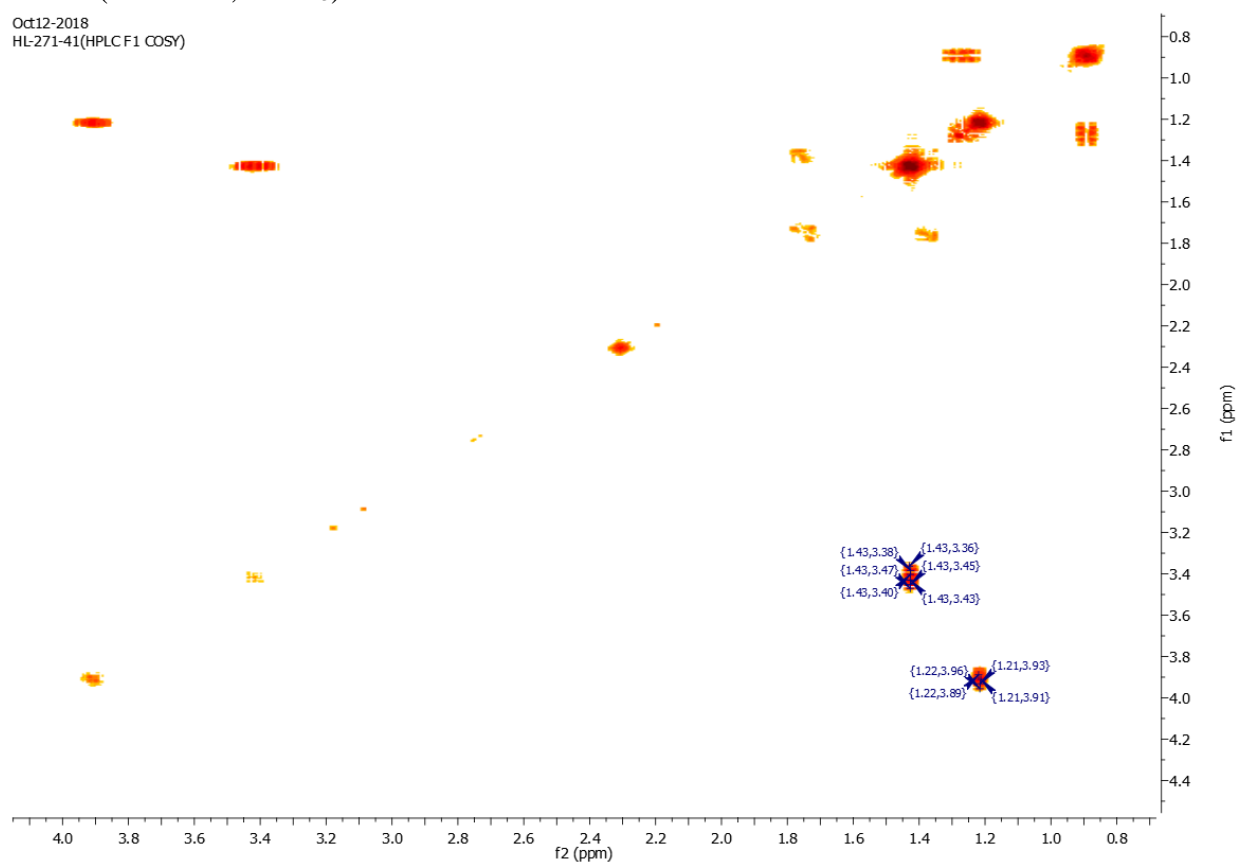


423

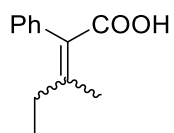
HMBC (401 MHz, CDCl₃)

Oct12-2018
HL-271-41(HPLC F1 HMBC)



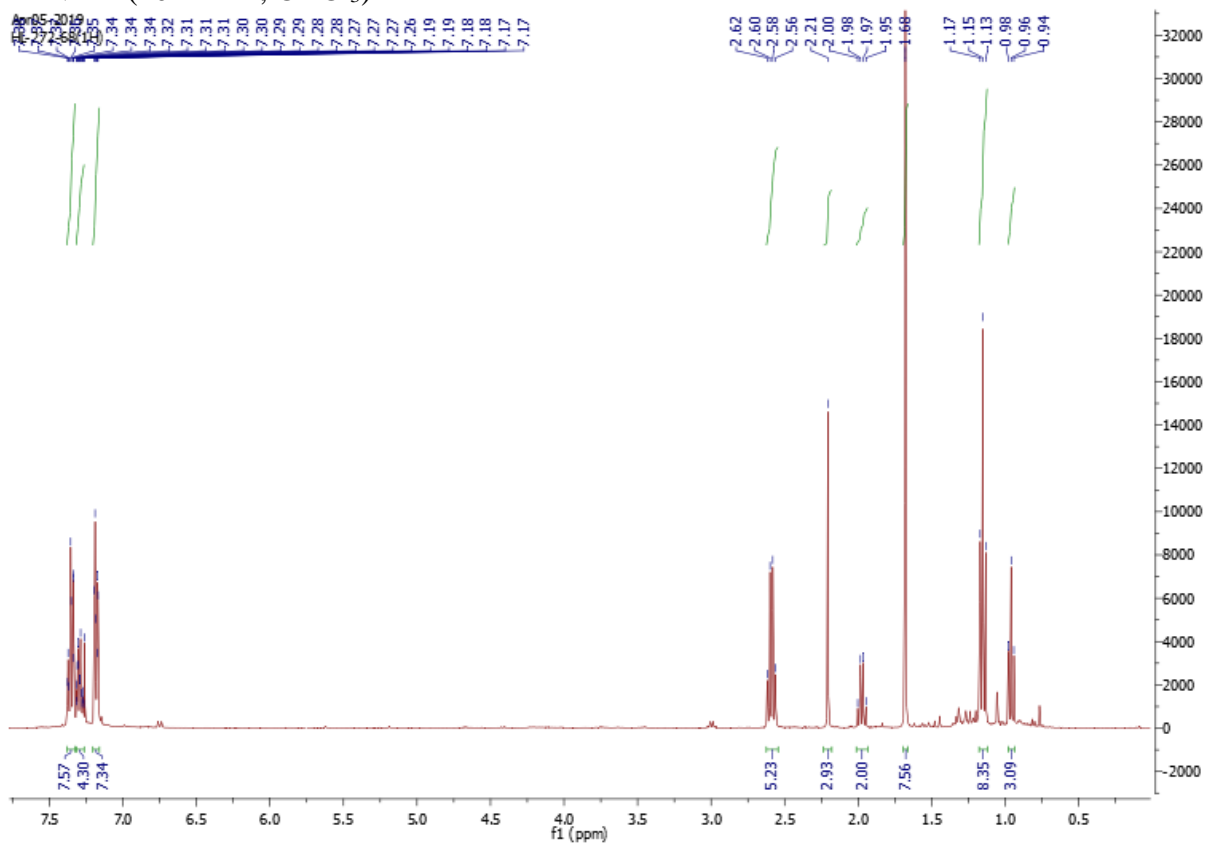
COSY (401 MHz, CDCl₃)Oct12-2018
HL-271-41(HPLC F1 COSY)

Chapter 6

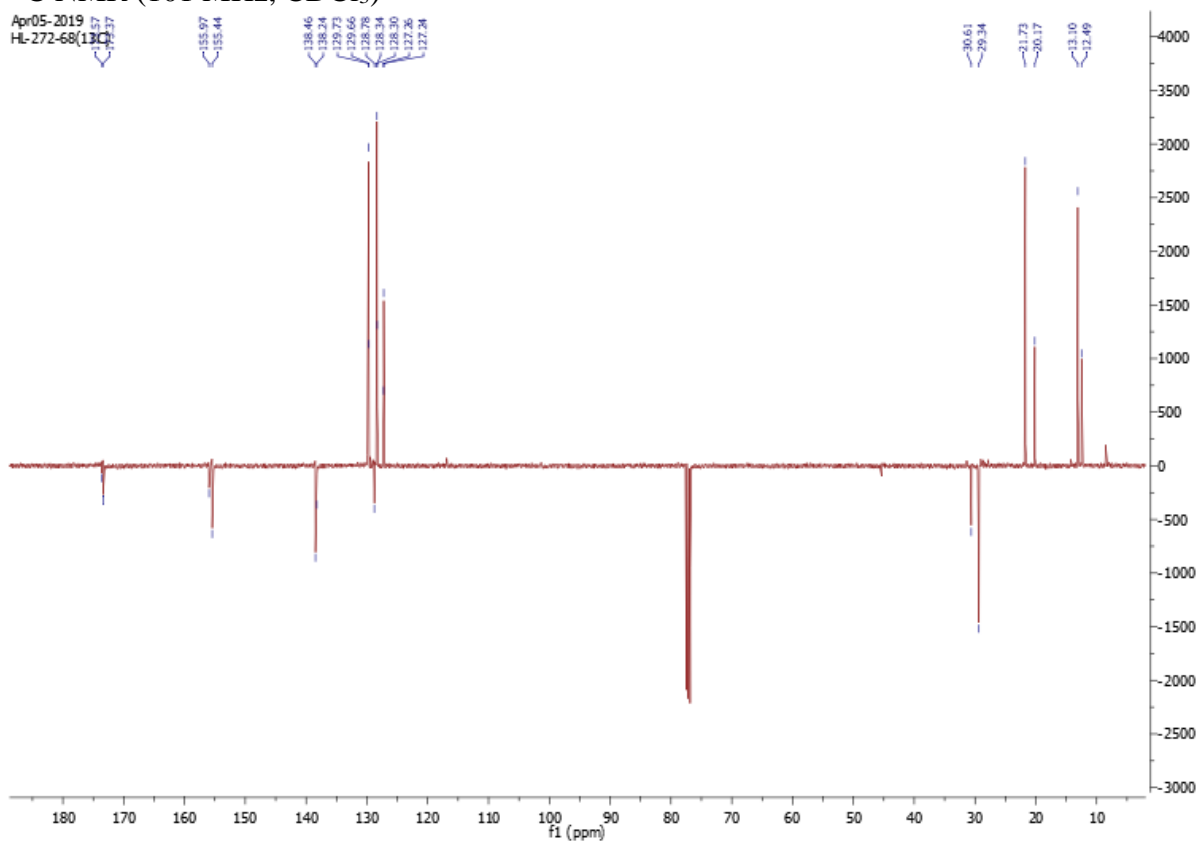


436

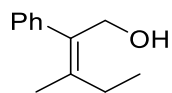
¹H NMR (401 MHz, CDCl₃)



¹³C NMR (101 MHz, CDCl₃)

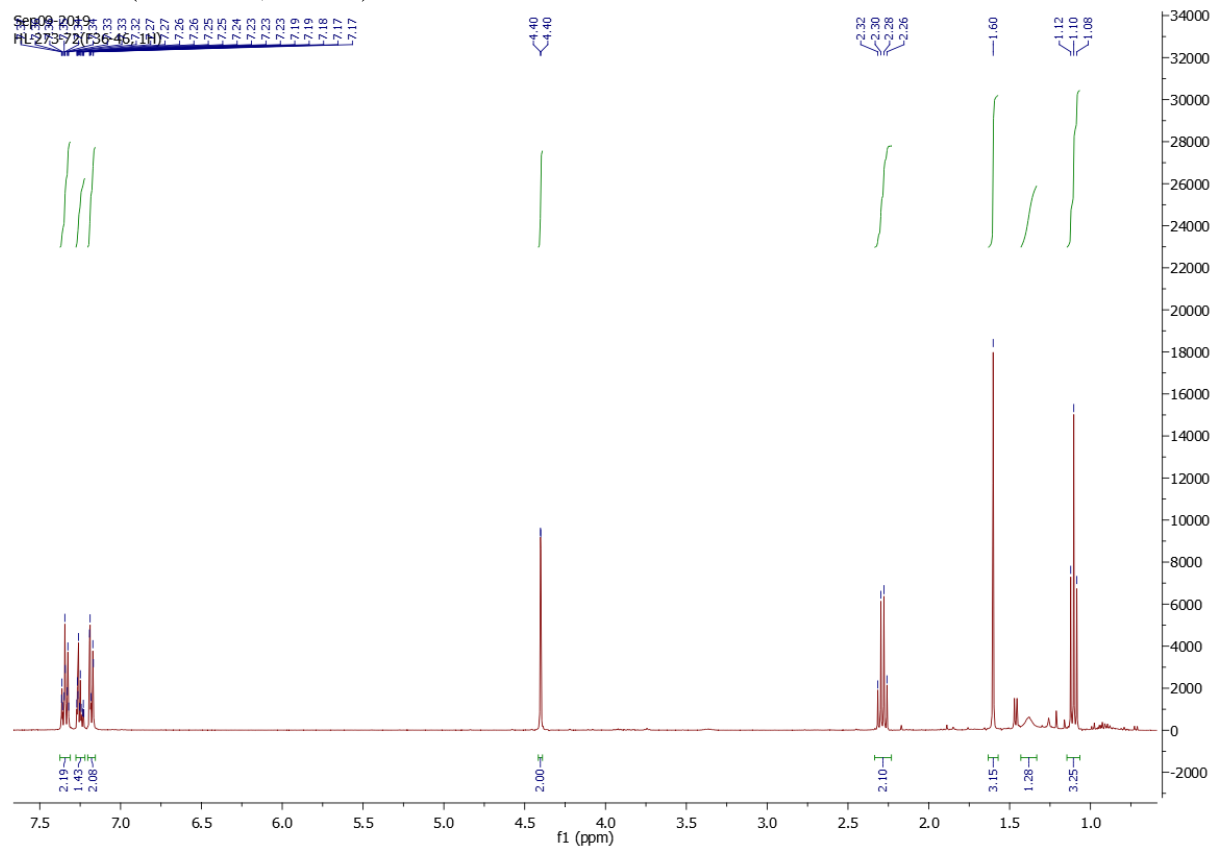


Chapter 6

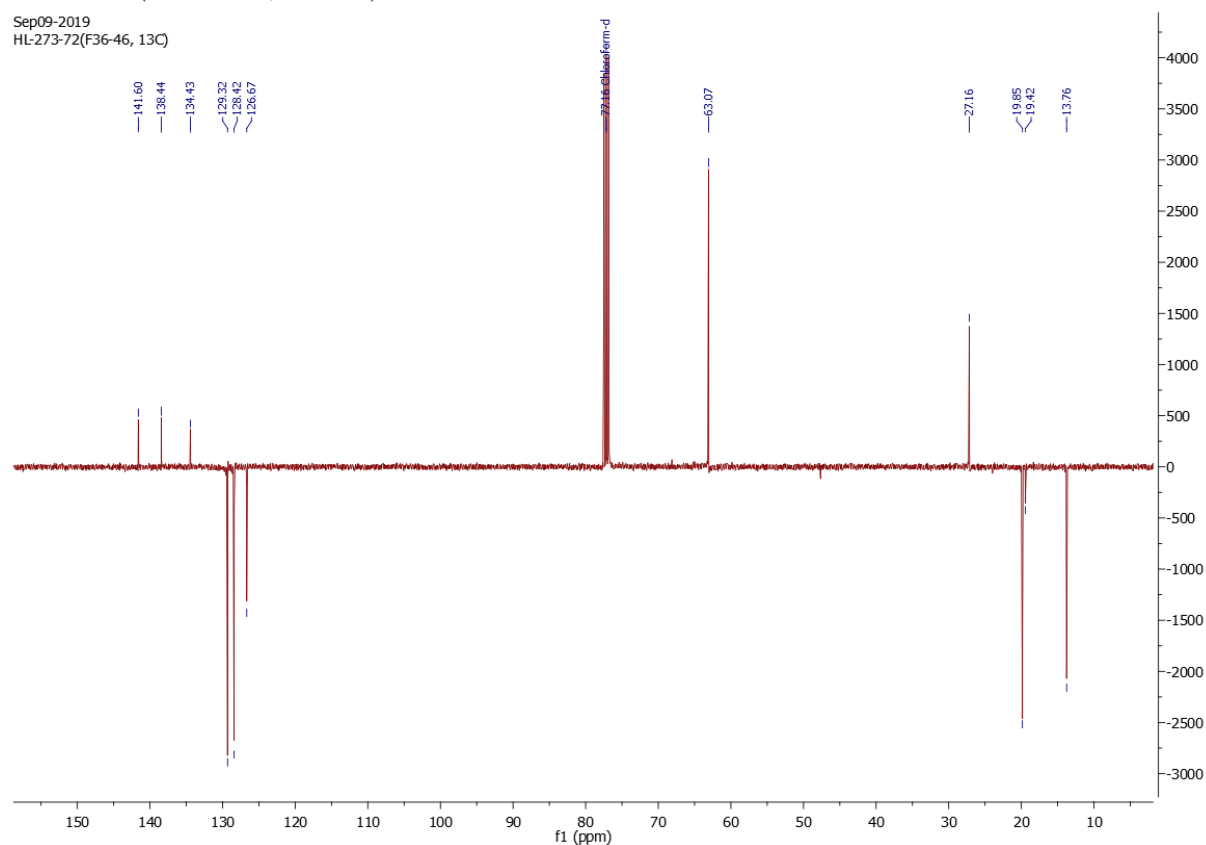


437Z

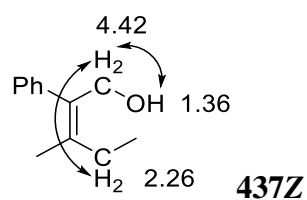
^1H NMR (401 MHz, CDCl_3)



^{13}C NMR (101 MHz, CDCl_3)



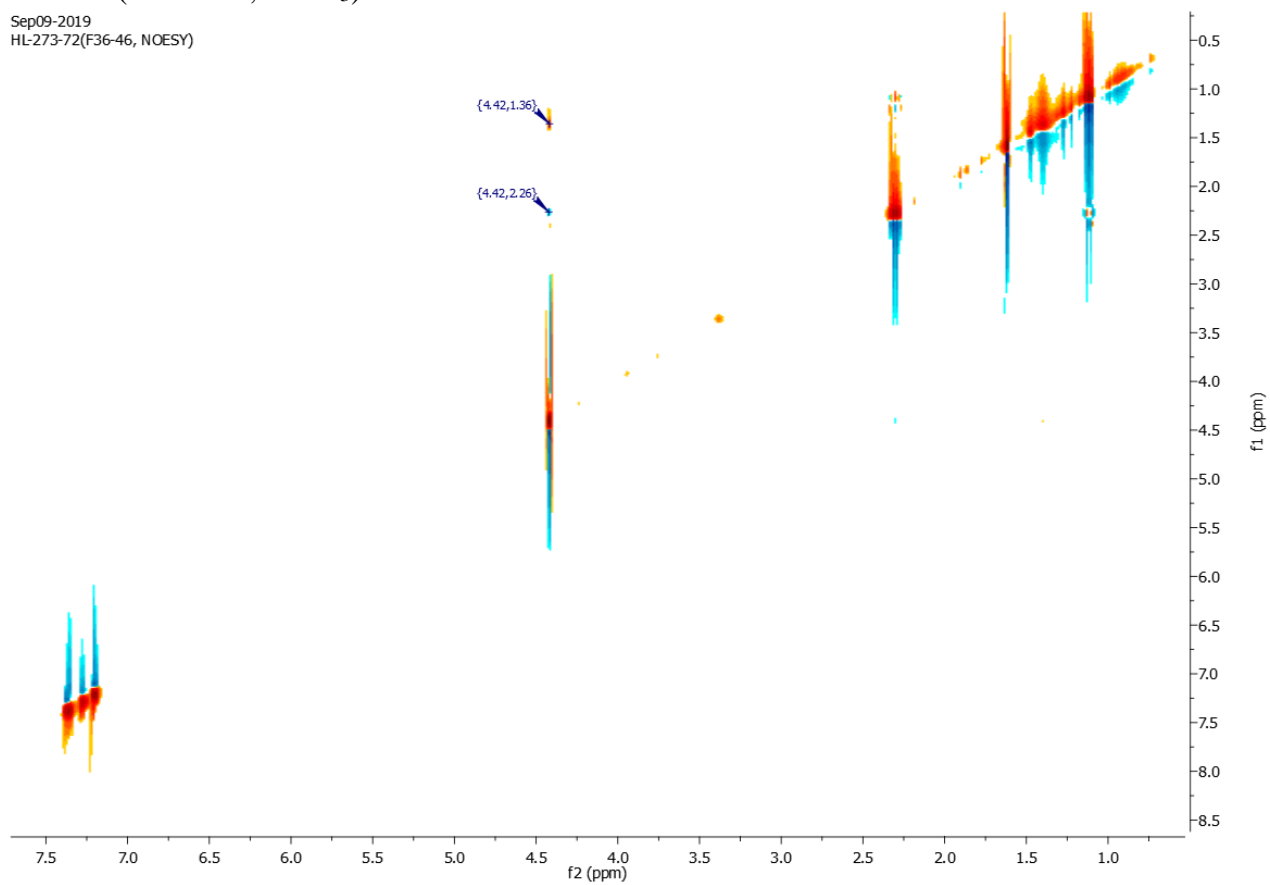
Chapter 6



NOESY (401 MHz, CDCl₃)

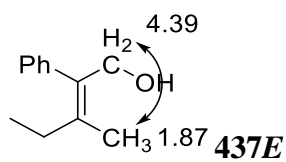
Sep09-2019

HL-273-72(F36-46, NOESY)



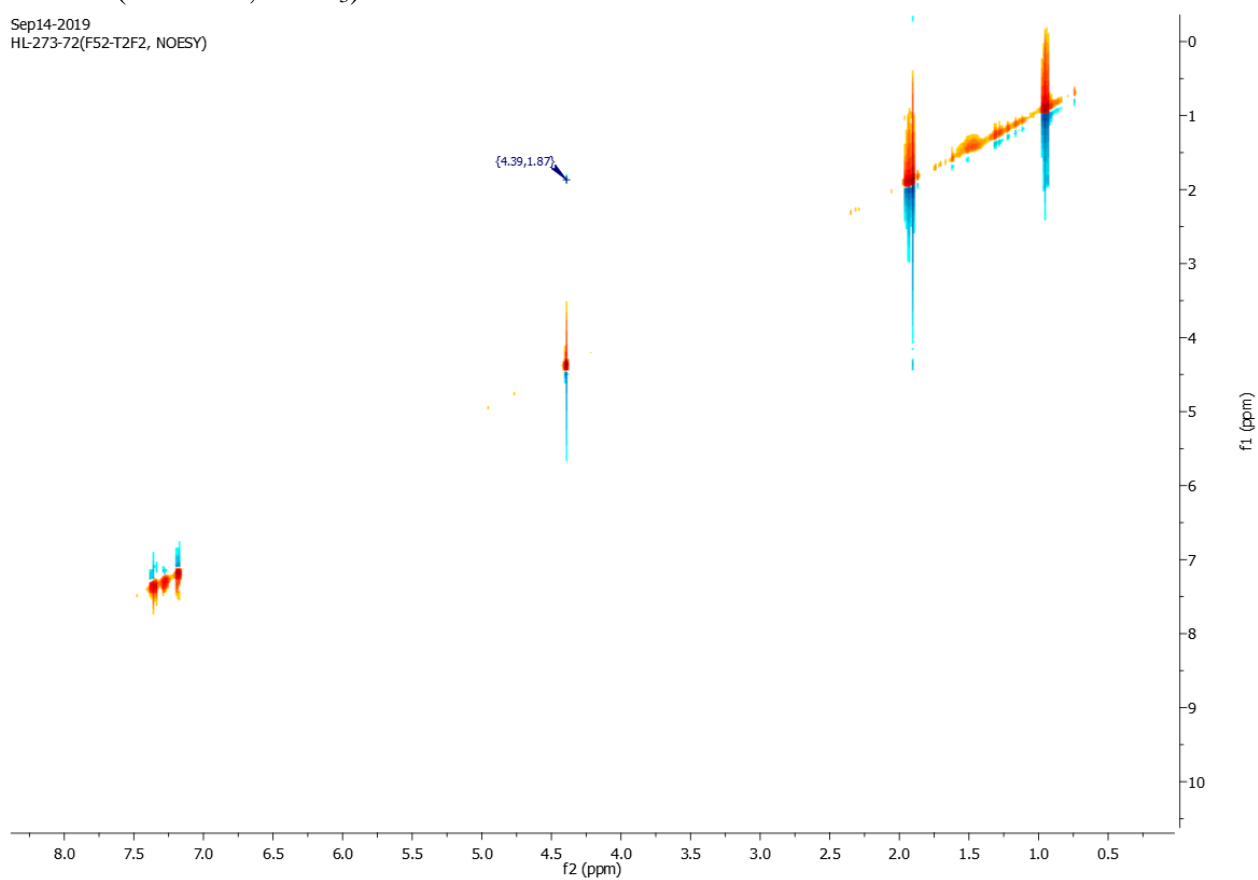
CC(C)=C(c1ccccc1)CO¹H NMR (401 MHz, CDCl₃)

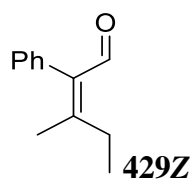
Chapter 6



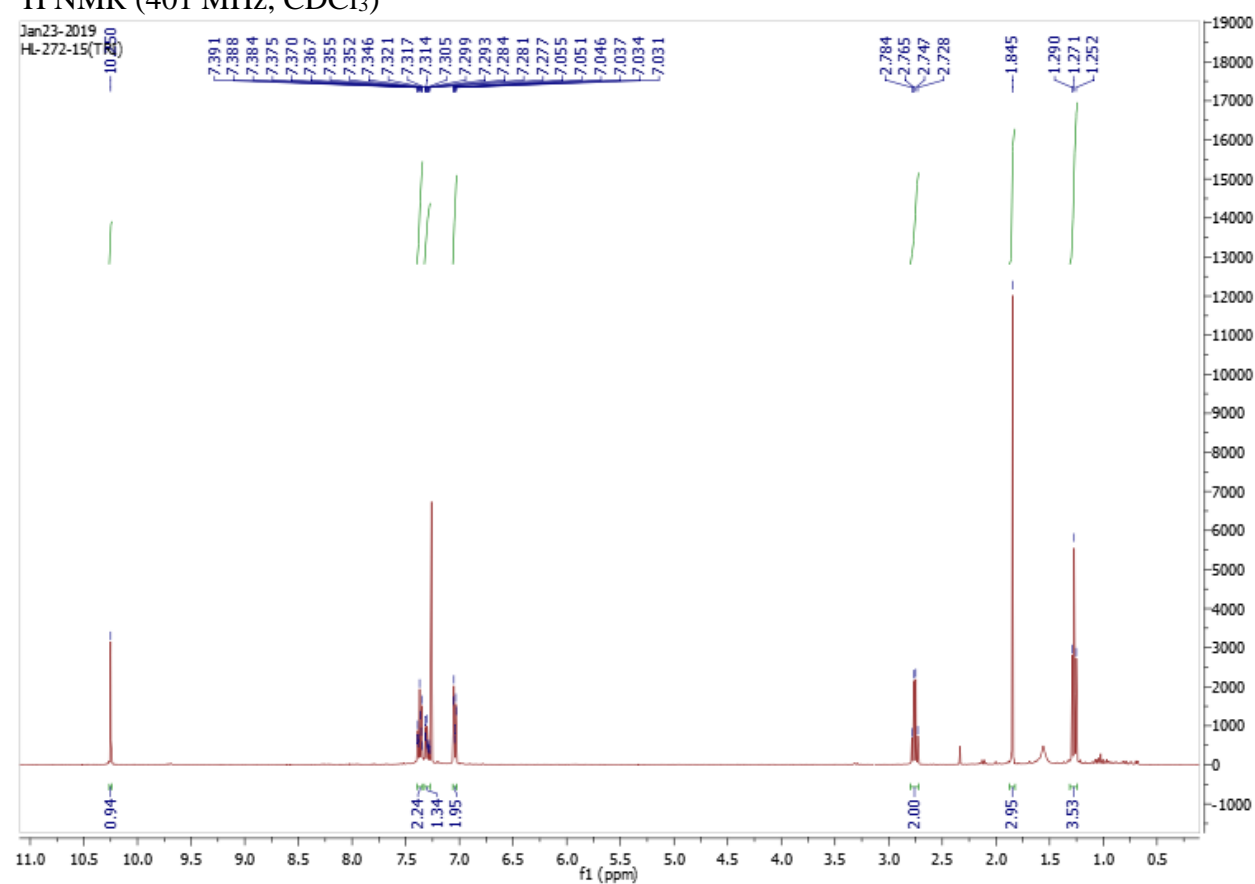
NOESY (401 MHz, CDCl₃)

Sep14-2019
HL-273-72(F52-T2F2, NOESY)

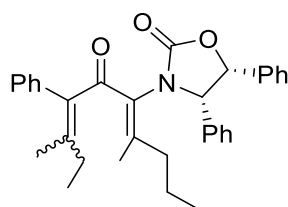




^1H NMR (401 MHz, CDCl_3)



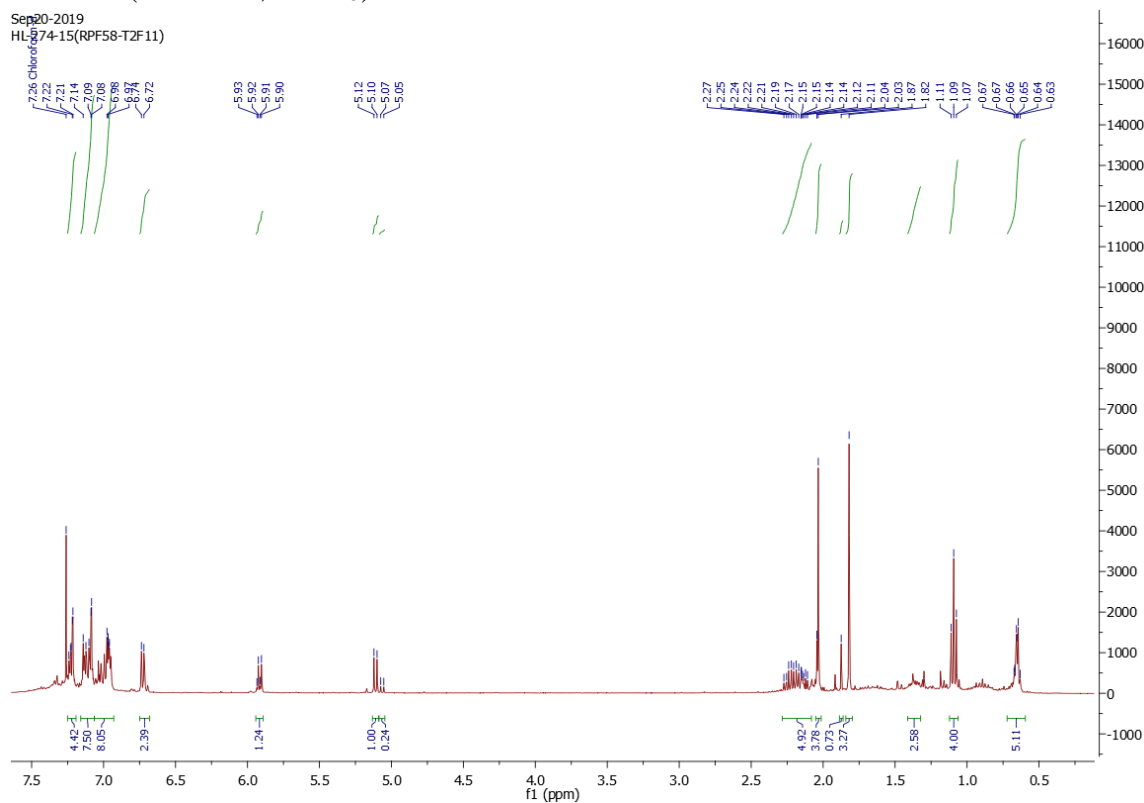
Chapter 6



430(7E/7Z)

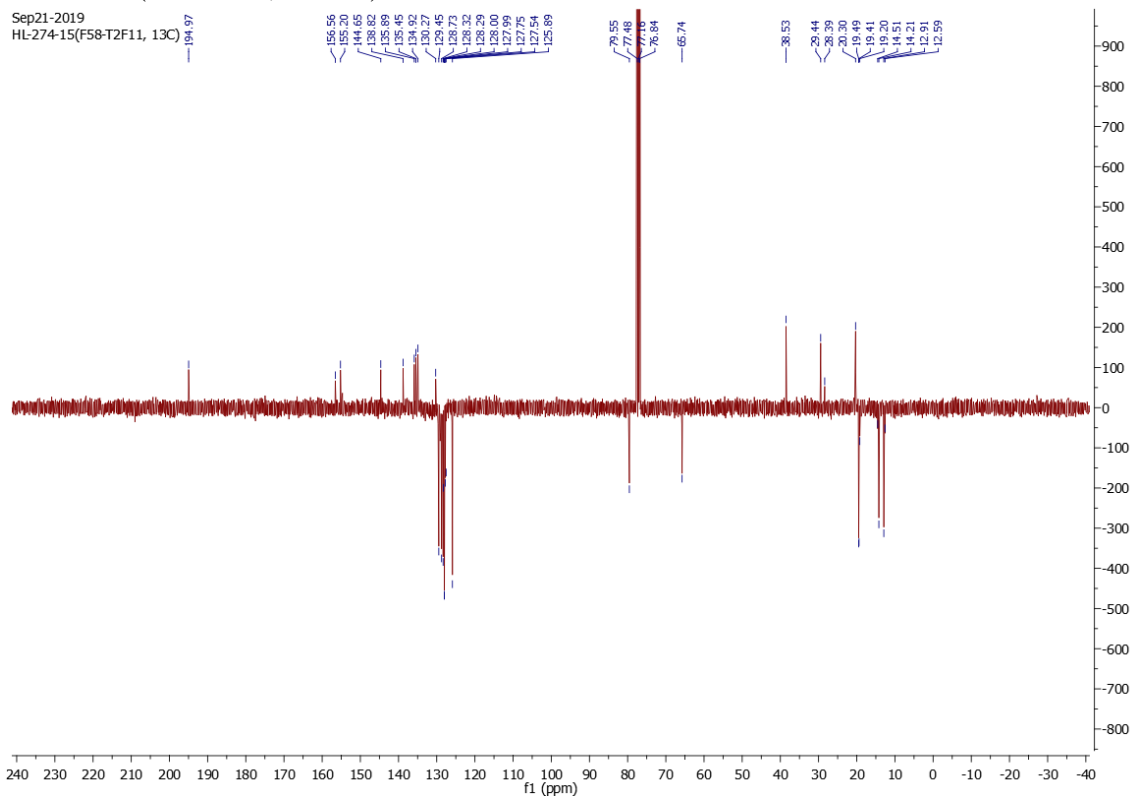
^1H NMR (401 MHz, CDCl_3)

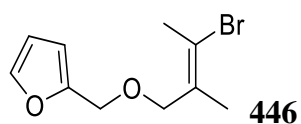
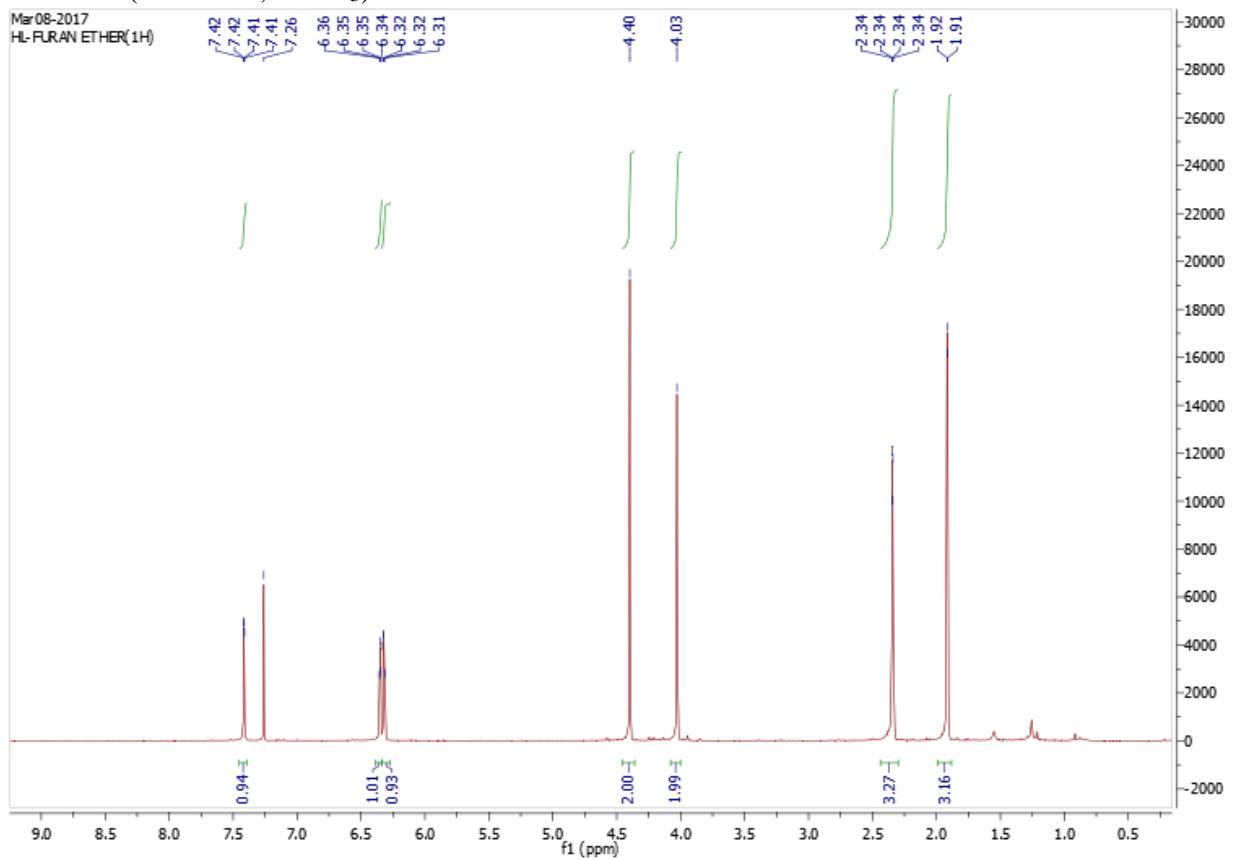
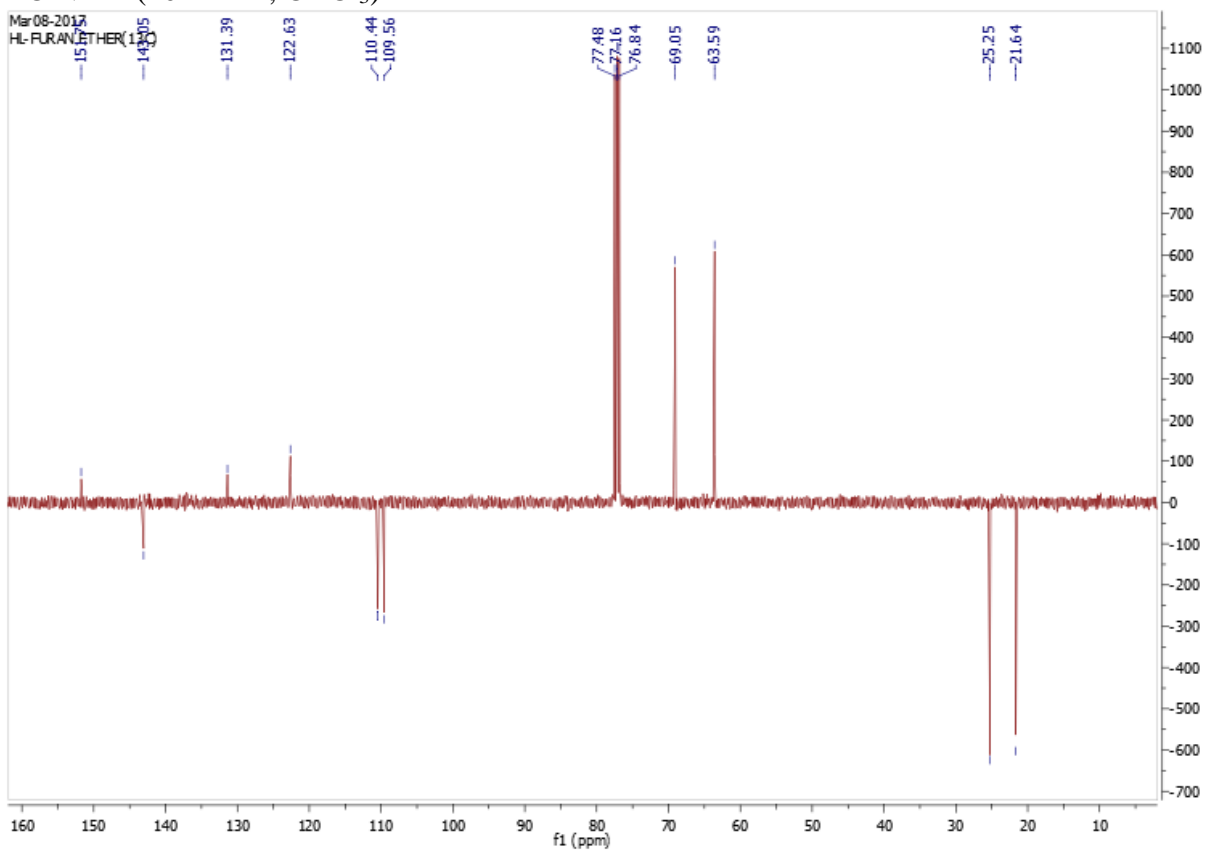
Sep20-2019
HL-274-15(RPF58-T2F11)

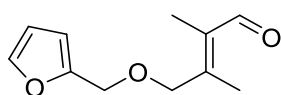
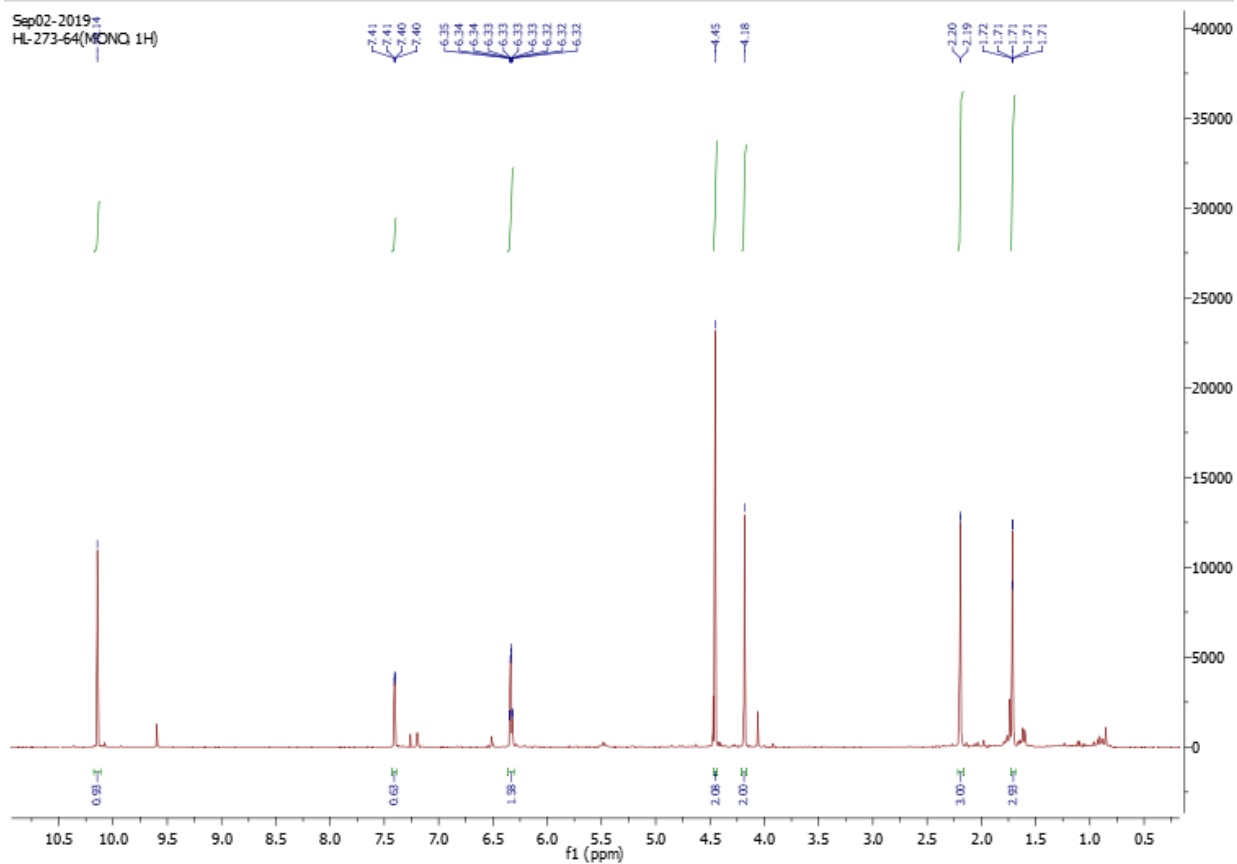
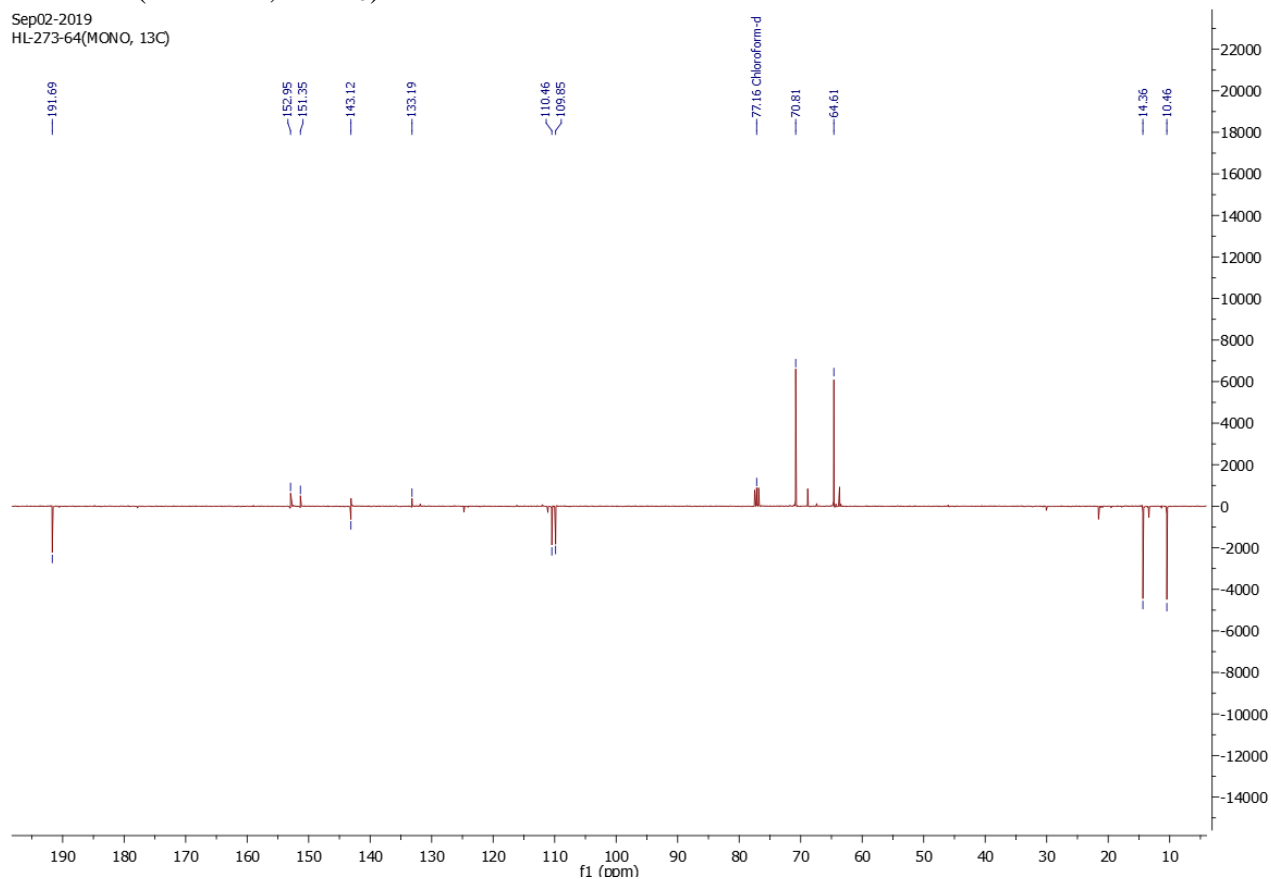


^{13}C NMR (101 MHz, CDCl_3)

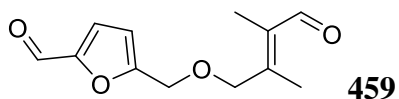
Sep21-2019
HL-274-15(F58-T2F11, ^{13}C)



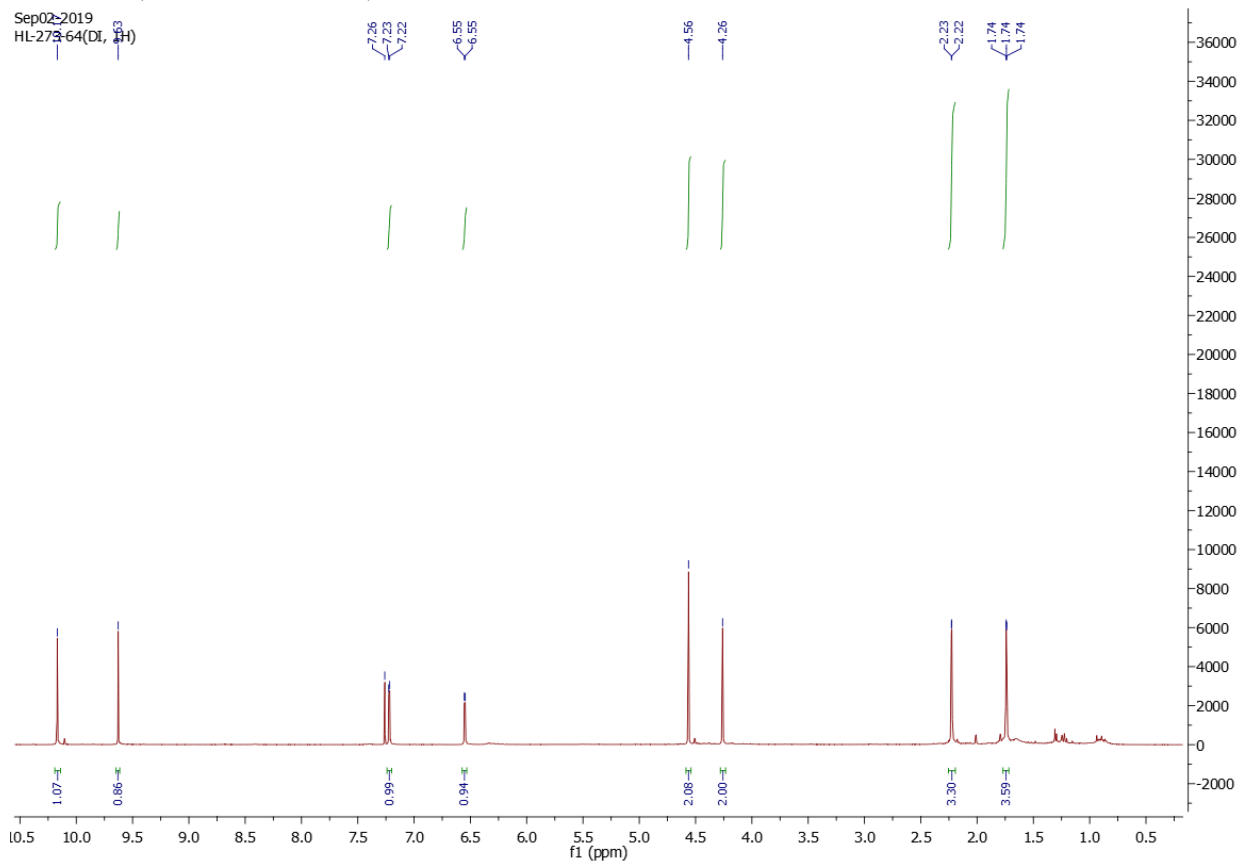
 ^1H NMR (401 MHz, CDCl_3) ^{13}C NMR (101 MHz, CDCl_3)

**458** ^1H NMR (401 MHz, CDCl_3) ^{13}C NMR (101 MHz, CDCl_3)

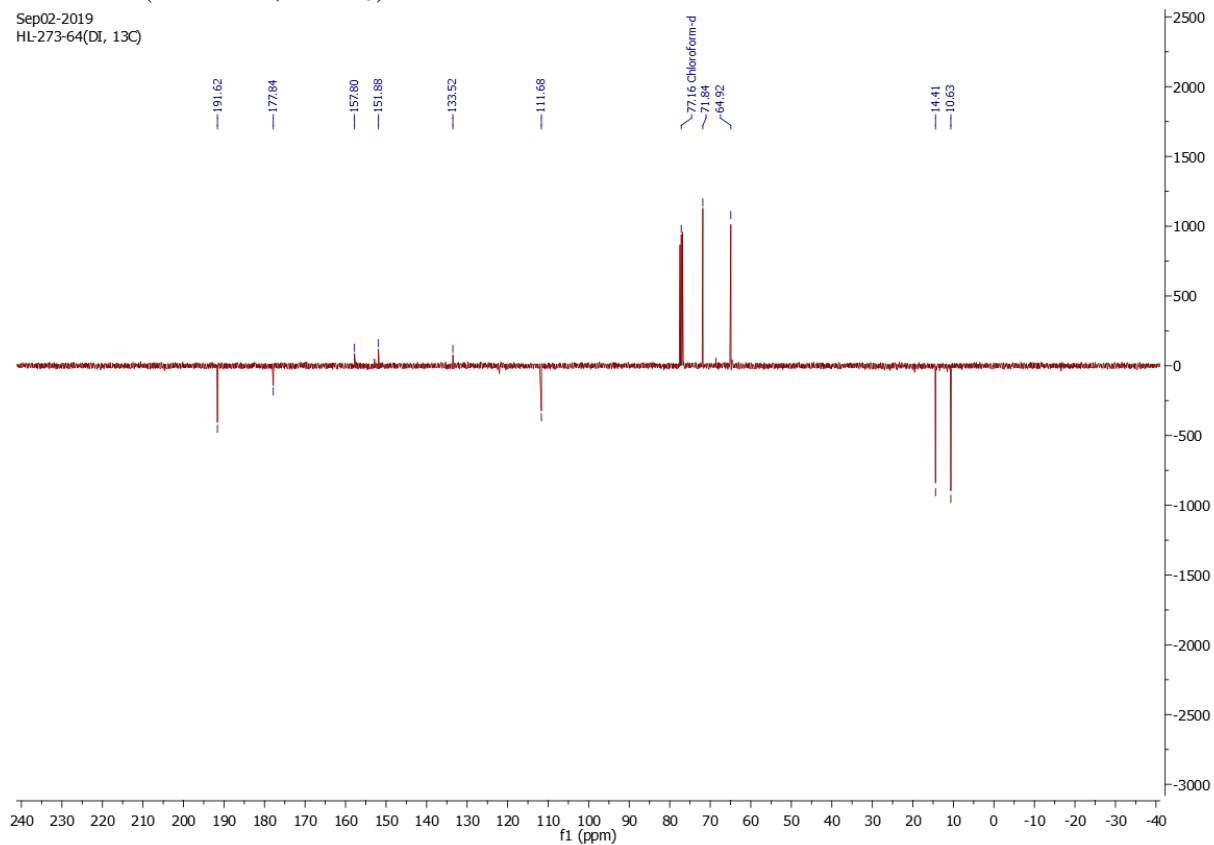
Chapter 6

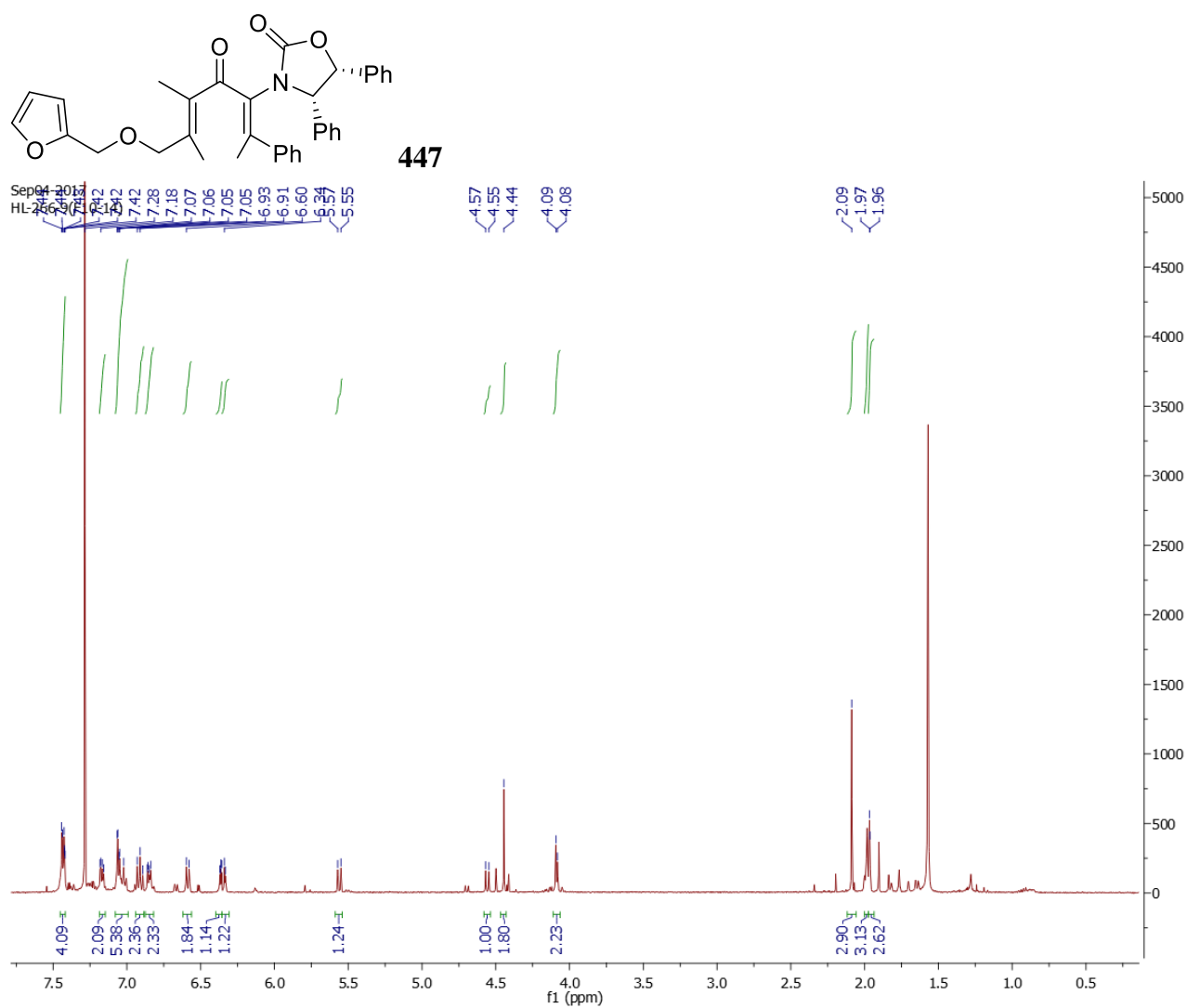


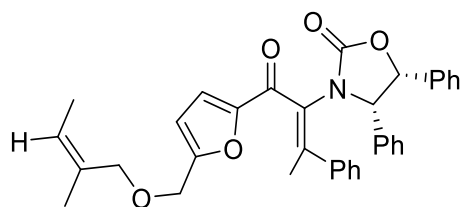
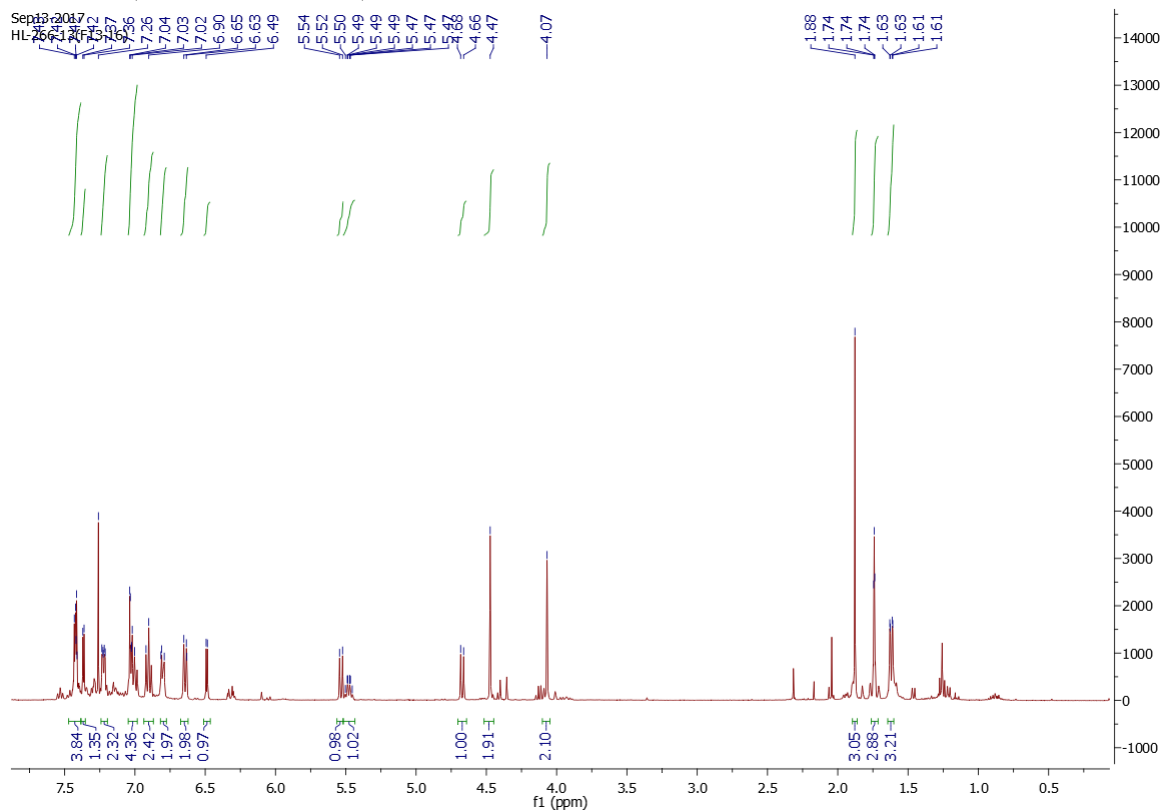
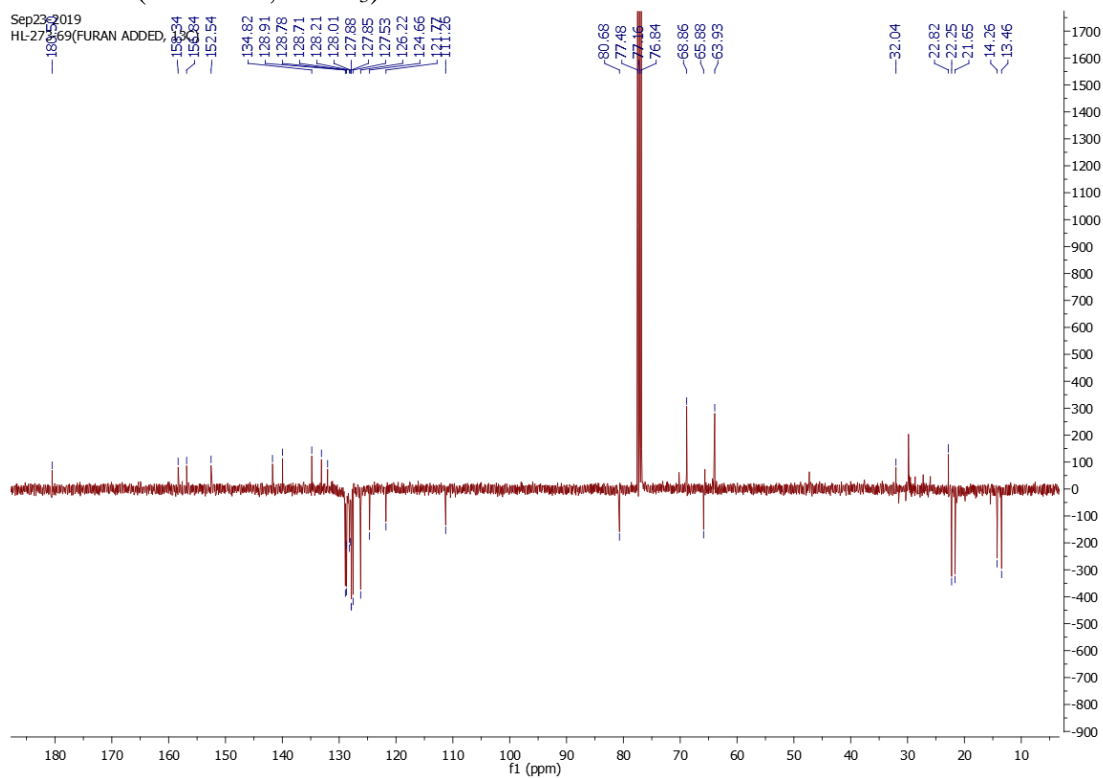
^1H NMR (401 MHz, CDCl_3)

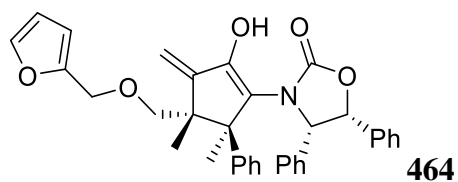


^{13}C NMR (101 MHz, CDCl_3)

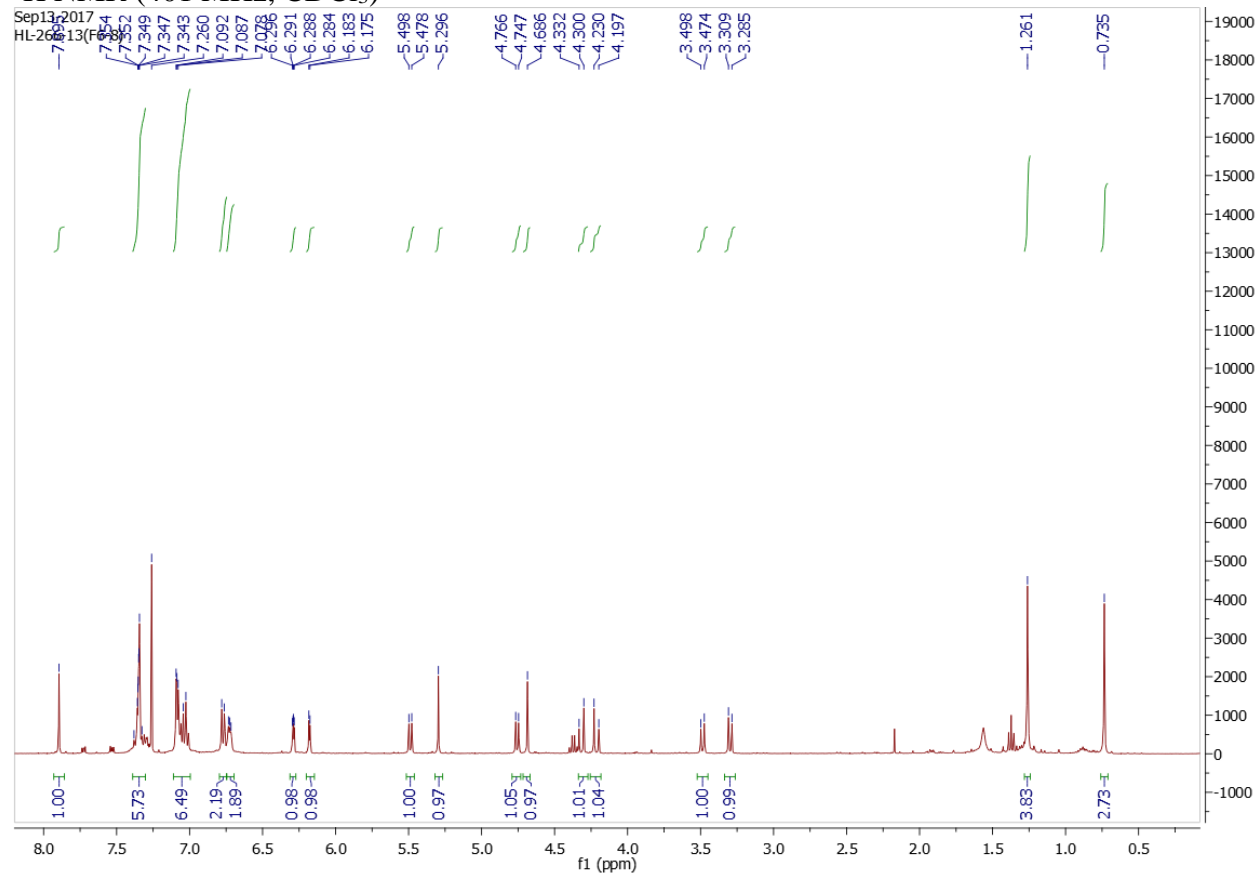




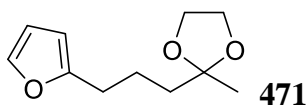
**462**¹H NMR (401 MHz, CDCl₃)¹³C NMR (101 MHz, CDCl₃)



^1H NMR (401 MHz, CDCl_3)

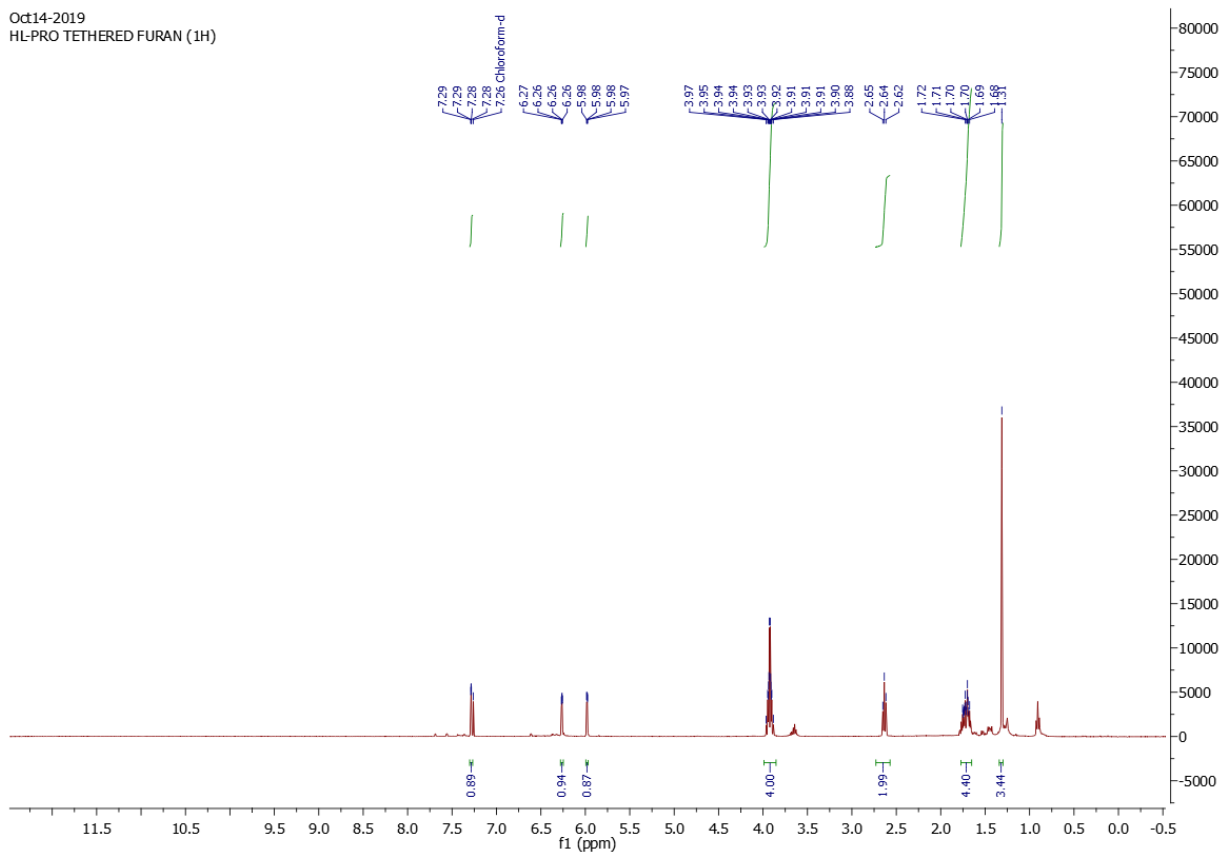


Chapter 6



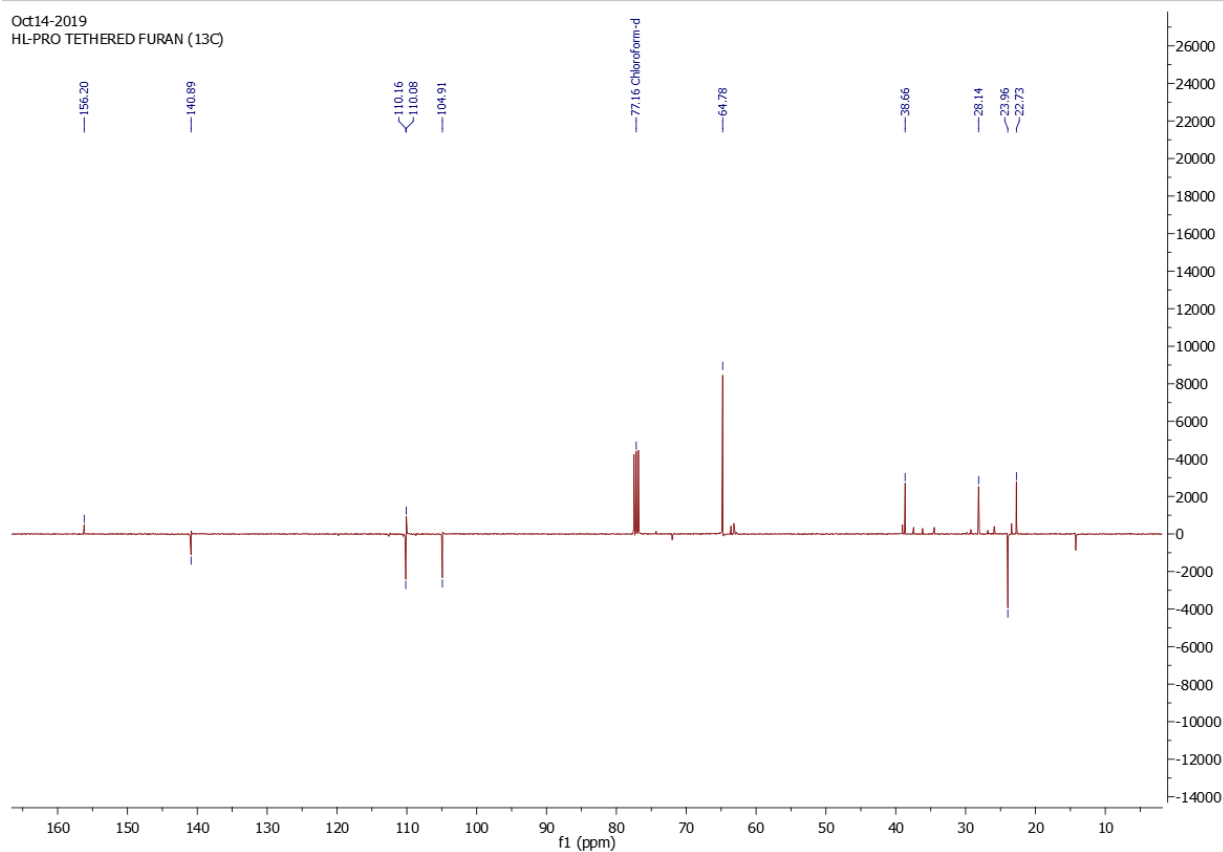
^1H NMR (401 MHz, CDCl_3)

Oct14-2019
HL-PRO TETHERED FURAN (^1H)

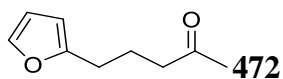


^{13}C NMR (101 MHz, CDCl_3)

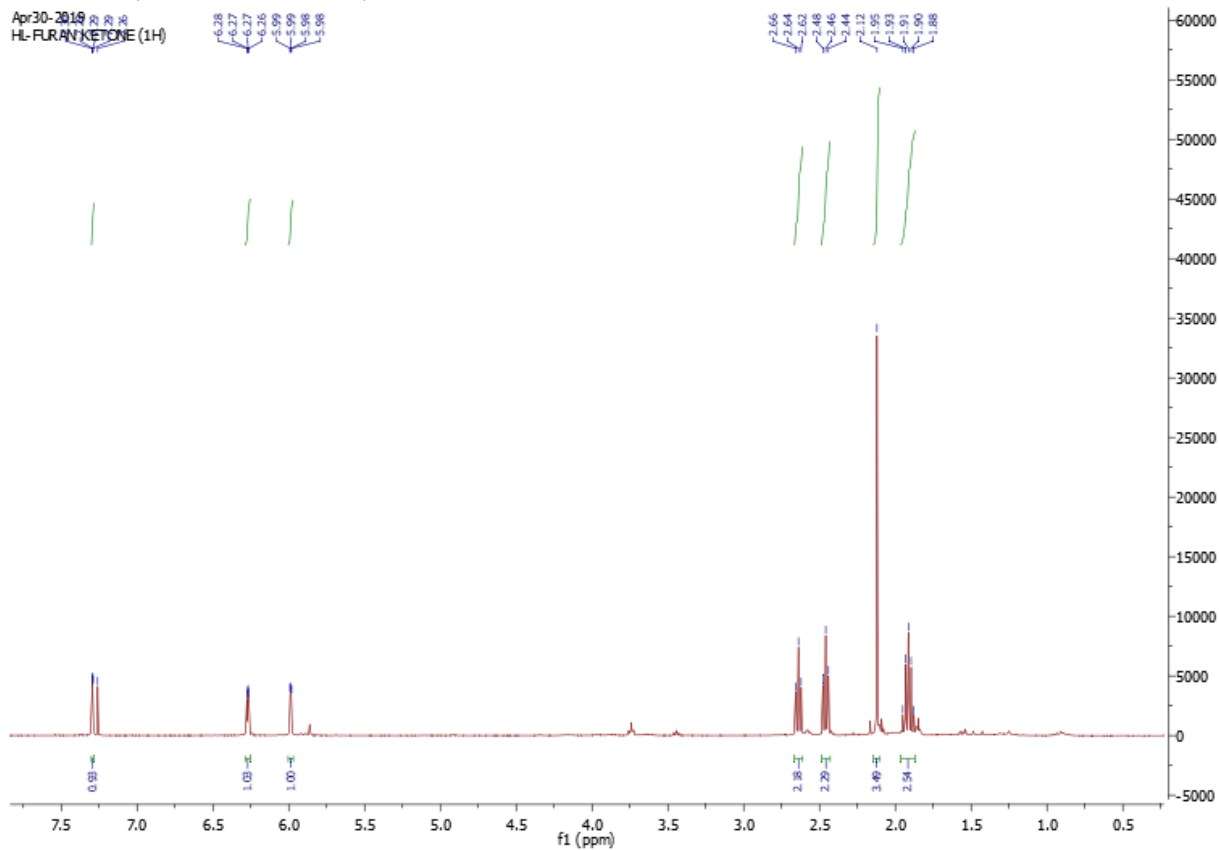
Oct14-2019
HL-PRO TETHERED FURAN (^{13}C)



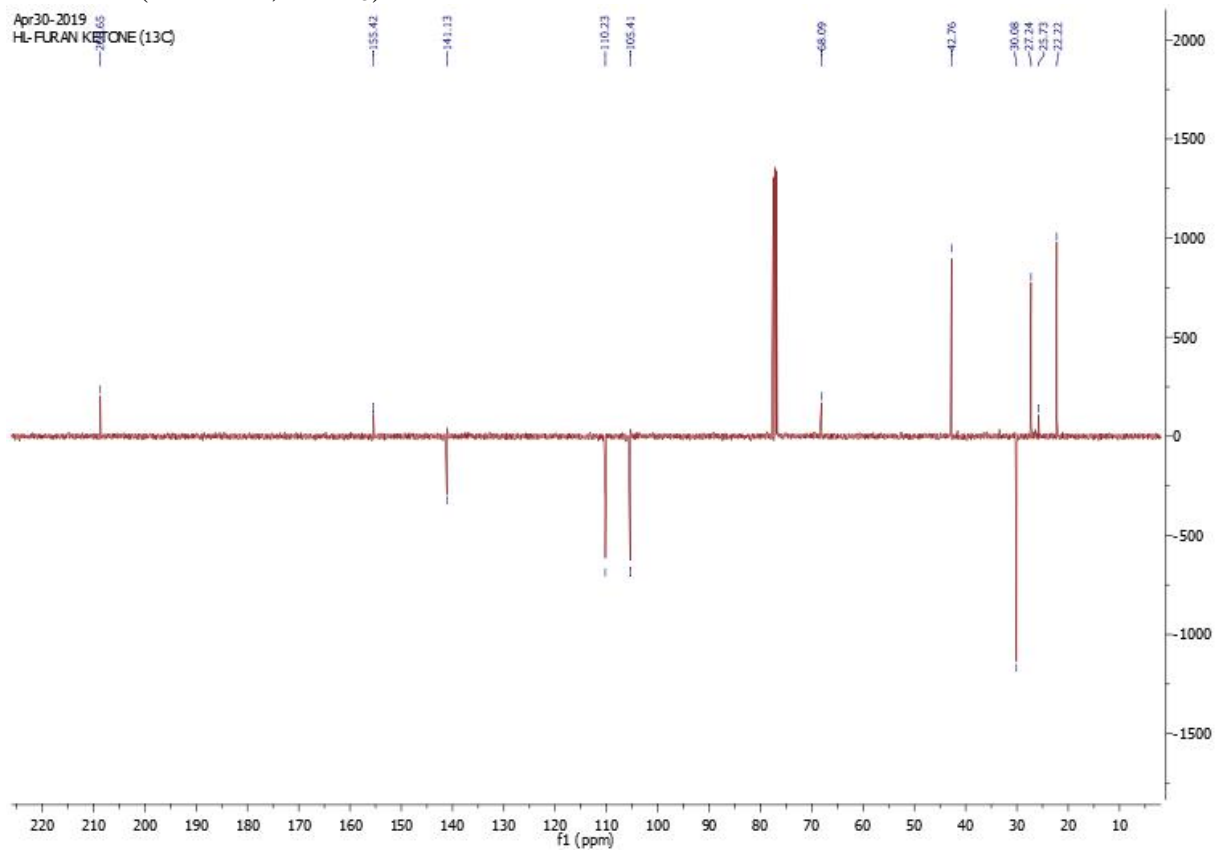
Chapter 6



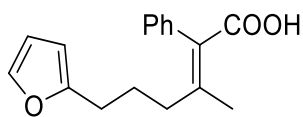
^1H NMR (401 MHz, CDCl_3)



^{13}C NMR (101 MHz, CDCl_3)

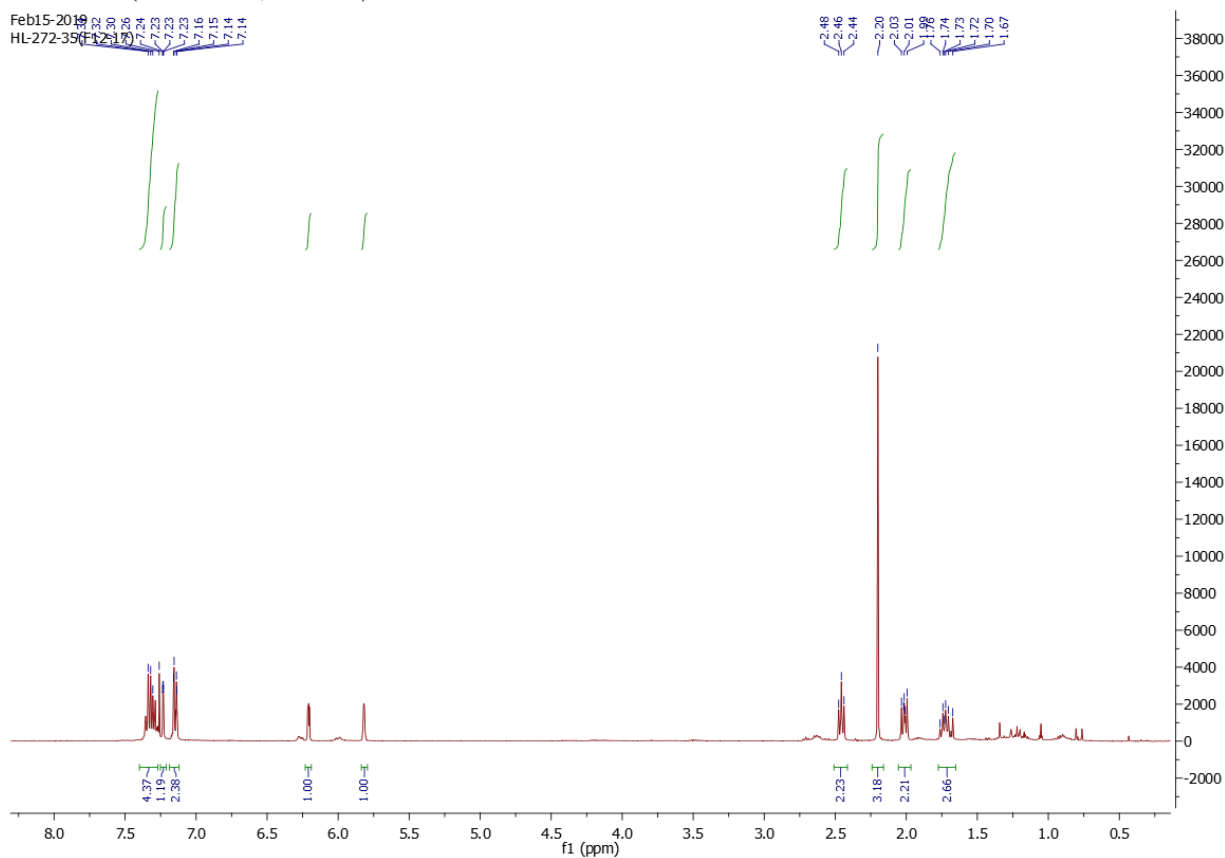


Chapter 6

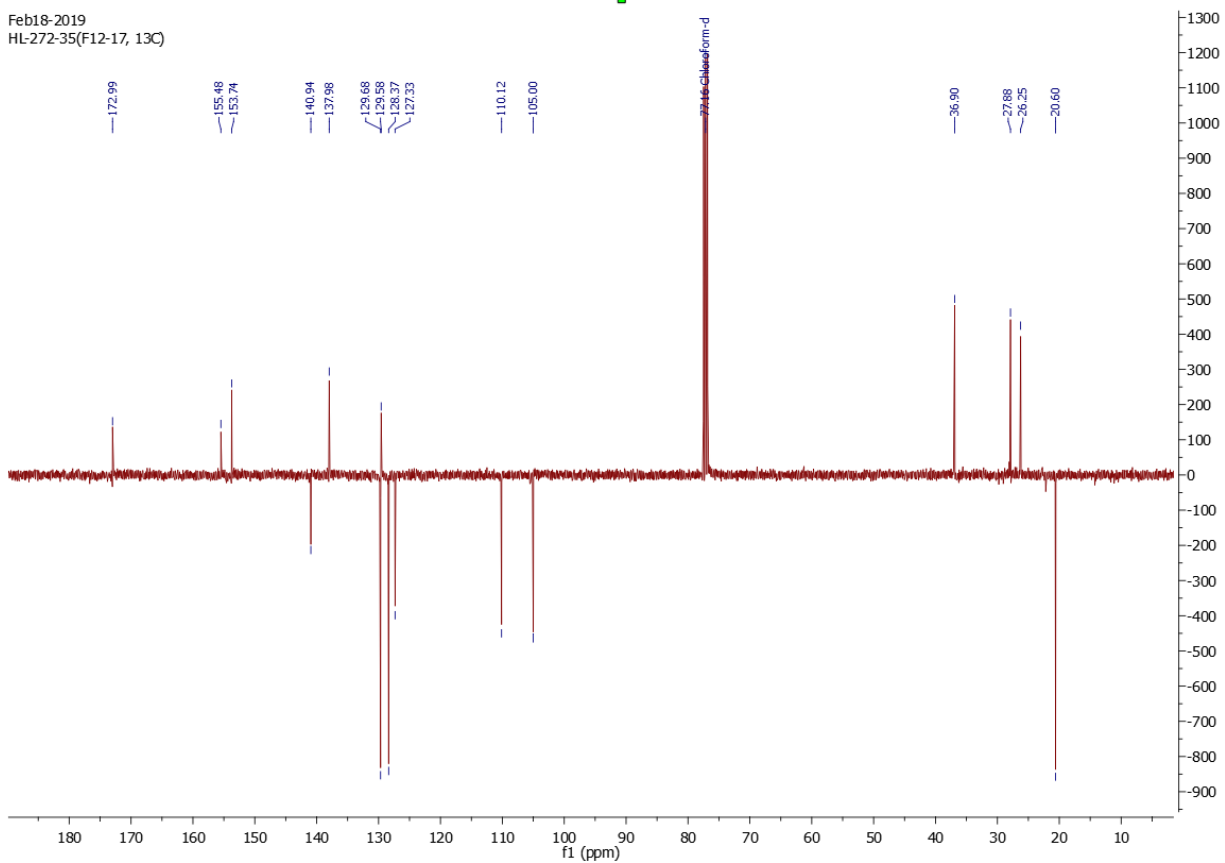


473E

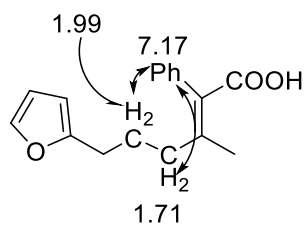
^1H NMR (401 MHz, CDCl_3)



^{13}C NMR (101 MHz, CDCl_3)



Chapter 6

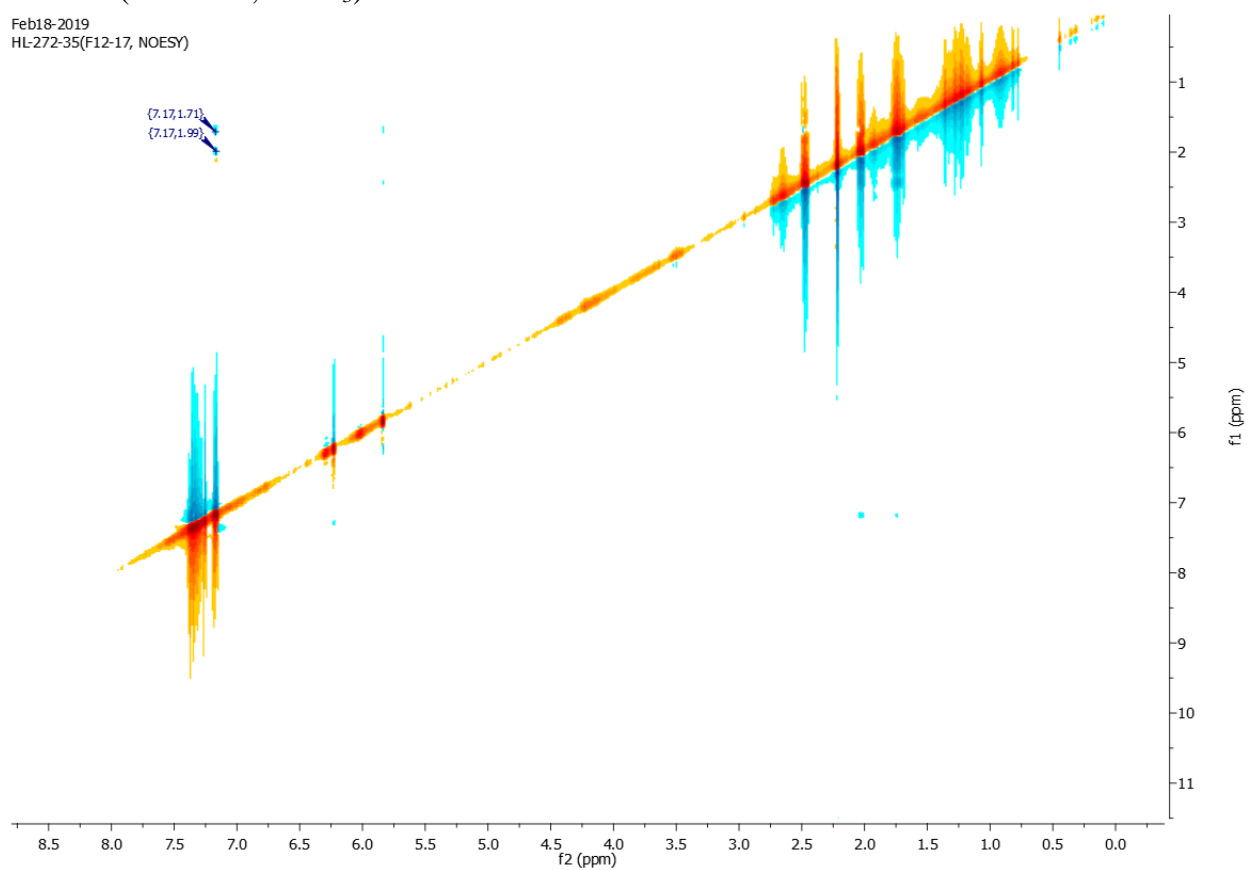


473E

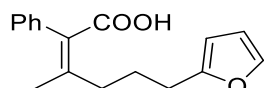
NOESY (401 MHz, CDCl₃)

Feb18-2019

HL-272-35(F12-17, NOESY)

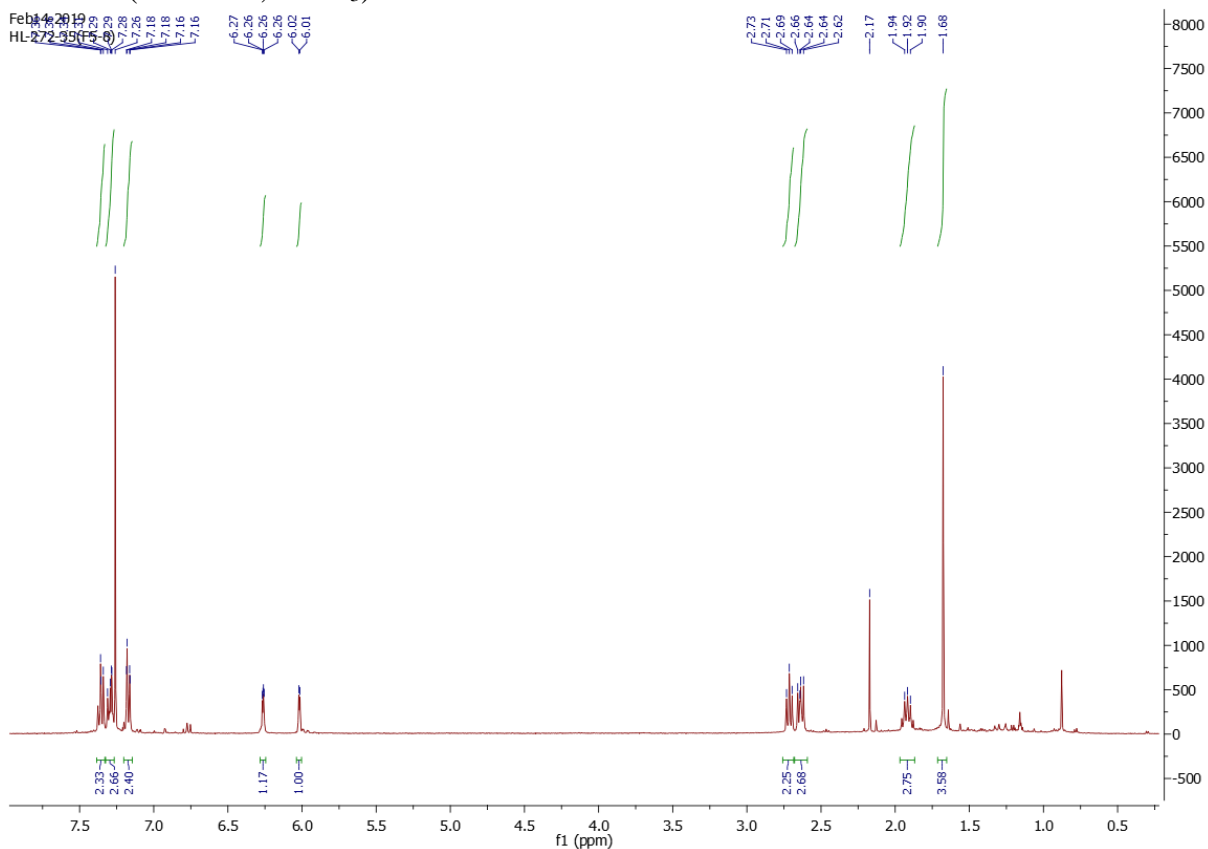


Chapter 6

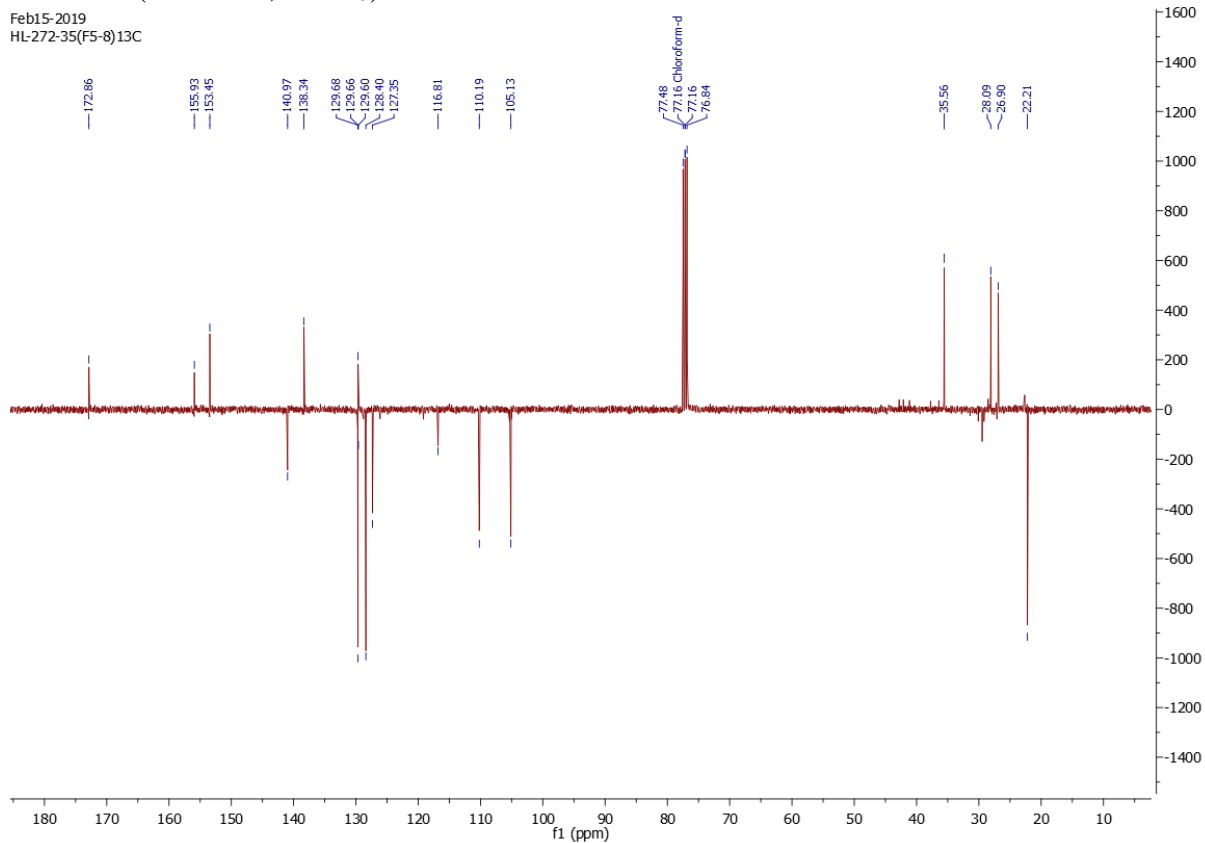


473Z

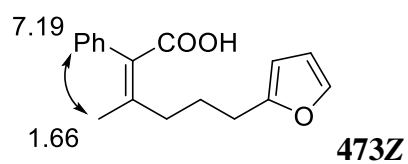
^1H NMR (401 MHz, CDCl_3)



^{13}C NMR (101 MHz, CDCl_3)

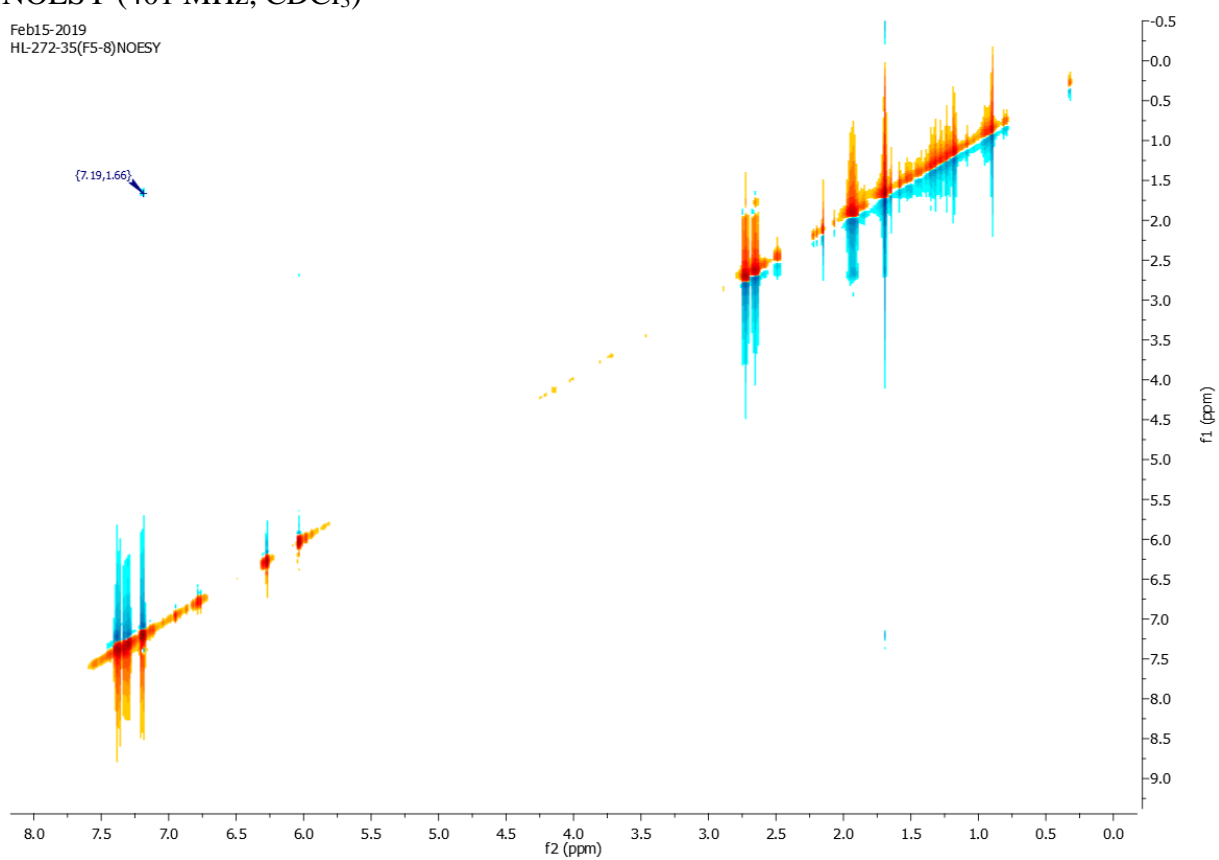


Chapter 6



NOESY (401 MHz, CDCl₃)

Feb15-2019
HL-272-35(F5-8)NOESY

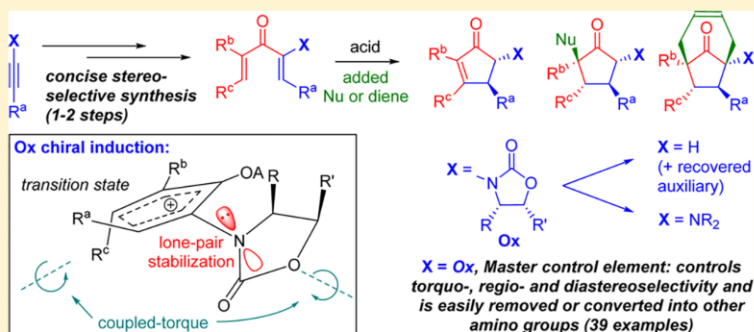


6.2 Appendix B- published journal article

Multistereocenter-Containing Cyclopentanoids from Ynamides via Oxazolidinone-Controlled Nazarov Cyclization

Narasimhulu Manchala,[†] Hanson Y. L. Law,[†] Daniel J. Kerr,[†] Rohan Volpe,[†] Romain J. Lepage,^{§,⊥} Jonathan M. White,^{‡,⊥} Elizabeth H. Krenske,^{§,⊥} and Bernard L. Flynn^{*,†,⊥}[†]Medicinal Chemistry, Monash Institute of Pharmaceutical Sciences, Monash University, 381 Royal Parade, Parkville, Victoria 3052, Australia[‡]Bio21 Institute, School of Chemistry, University of Melbourne, Parkville, Victoria 3010, Australia[§]School of Chemistry and Molecular Biosciences, The University of Queensland, Brisbane, Queensland 4072, Australia

S Supporting Information



ABSTRACT: Achieving ready-enantioselective access to multistereocenter-containing cyclopentyl rings is an area of great significance to organic synthesis. In this work, we describe a general protocol for accessing multistereocenter-containing cyclopentanoids from simple *N*-alkynyloxazolidinones (**Ox**-ynamides). This protocol involves conversion of **Ox**-ynamides into **Ox**-activated divinyl and aryl vinyl ketones that undergo facile Nazarov cyclization with excellent chemo-, regio-, and stereocontrol. The **Ox** auxiliary directs all aspects of reactivity and selectivity, both in the electrocyclization and in the subsequent transformations of the resulting oxyallyl intermediate. Stereoinduction in the electrocyclization results from a “coupled-torque” mechanism in which rotation of the **Ox** group, driven by increasing orbital overlap of the nitrogen lone pair with the incipient oxyallyl cation, is coupled with the rotation of the termini of the pentadienyl cation, favoring a particular direction of conrotatory ring closure (torquoselectivity). The associated lone-pair stabilization of the transition state by **Ox** promotes cyclization of traditionally resistant substrates, broadening the scope of this asymmetric Nazarov cyclization. The **Ox** group also facilitates the stereo- and regioselective incorporation of nucleophiles (**Nu**) and dienes, giving more complex, multistereocenter-containing cyclopentanoids. Finally, the **Ox** group is readily removed and recovered or can be converted into other amine functionalities.

INTRODUCTION

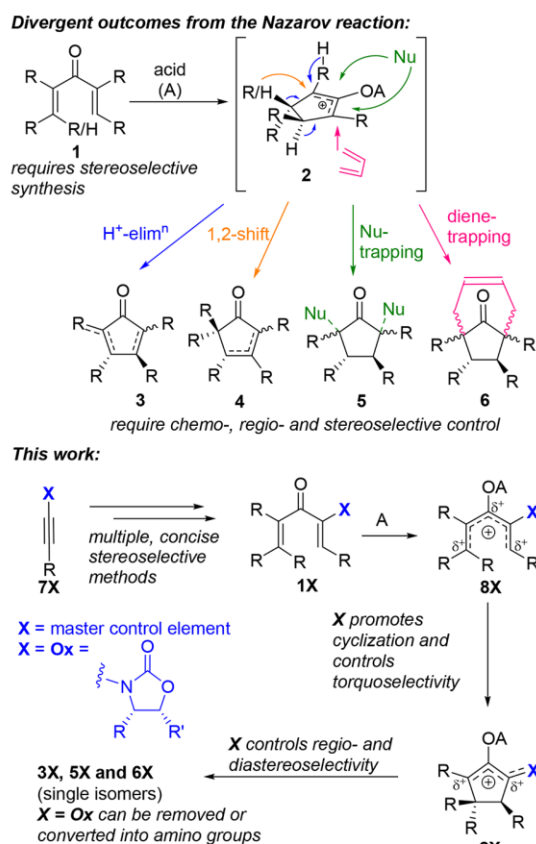
Versatile methods for accessing cyclopentyl rings are highly desirable given the preponderance of cyclopentyl rings in bioactive natural products and the potential utility of cyclopentyl rings as *sp*³-rich scaffolds in *de novo* drug design and compound-library screening.^{1,2} Nazarov cyclizations of divinyl and aryl vinyl ketones **1** to give cyclopentenones and indenones **3** have attracted considerable attention as the basis for developing general methods for the enantioselective synthesis of cyclopentyl rings, which if suitably controlled, could rival or even surpass the versatility that the Diels–Alder reaction holds for the synthesis of cyclohexyl rings (Scheme 1).^{3,4} The Nazarov cyclization is potentially enriched by the number of ways in which the reaction pathway can be terminated through the cationic intermediate **2**. Depending on the substitution pattern and the presence of suitable additives,

cation **2** may undergo an α -proton elimination to give **3**, [1,2]-sigmatropic shift to give **4**,⁵ nucleophilic trapping to give **5**,⁶ (4 + 3)-cycloaddition to give **6**,⁷ or a cationic reaction cascade to generate a polycycle (not shown).⁸ In order to effectively harness this extraordinary potential of the Nazarov reaction in multistereocenter (*sp*³-rich) scaffold synthesis, a number of challenges need to be overcome:⁹ (i) concise stereoselective access to a structurally diverse array of substrates **1**; (ii) a capacity to cyclize conventionally resistant substrates; (iii) chemoselective control over the competing outcomes **3**–**6**; (iv) regiochemical control over the double-bond placement in **3/4** and of the **Nu** in **5**; and (v) control of relative and absolute stereochemistry in **3**–**6**. Herein, we describe our studies toward

Received: January 31, 2017

Published: May 16, 2017

Scheme 1. Use of a Master-Control Element X To Achieve Regio-, Diastereo- And Enantioselective Control in the Nazarov Reaction



the identification of a master-control group X that can be readily incorporated into substrates 1X from simple alkynes 7X and which is highly effective in addressing the various chemo-, regio-, and stereoselectivity issues confronting the Nazarov reaction (Scheme 1).¹⁰ These studies have identified Evans' oxazolidinone (Ox) as an excellent control element X ($\text{X} = \text{Ox}$) that promotes Nazarov cyclization of resistant substrates by stabilizing the charge redistribution (δ^+) in the transition state of the conversion of the pentadienyl cation 8X to (oxy)allylic cation 2X . The Ox auxiliary has a strong influence on the torquoselectivity of the Nazarov reaction, resulting in essentially complete diastereoselectivity across a broad range of substrates.

The charge stabilization afforded in 2X by $\text{X} = \text{Ox}$ strongly influences its fate. It tends to favor regioselective proton elimination from 2X , relative to [1,2]-shifts, and facilitates the regio- and stereoselective trapping of 2X by nucleophiles and dienes. The Ox group is readily removed and recovered or can be further diversified by conversion into other amine functionalities.

RESULTS AND DISCUSSION

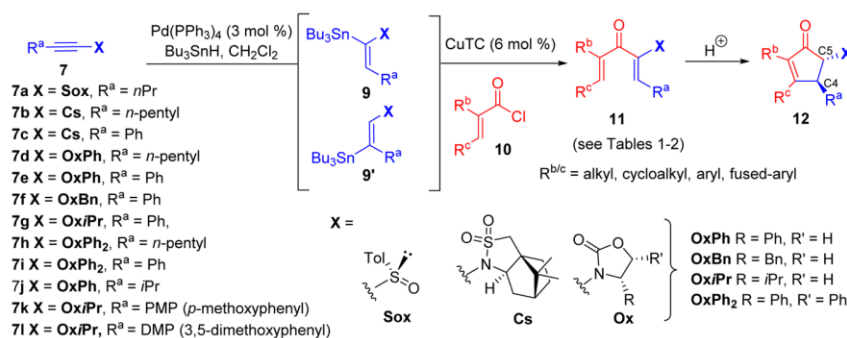
Identification of Suitable Control Elements X . Even though both electron-withdrawing and electron-donating groups X in 1X have been proposed to be effective in promoting the Nazarov reaction, we examined both as chiral-activating groups X .¹¹ The chiral sulfoxide ($\text{X} = \text{Sox}$) was employed as a chiral electron-withdrawing group, whereas Oppolzer's camphorsultam ($\text{X} = \text{Cs}$) and several Evans' oxazolidinones ($\text{X} = \text{Ox}$) were employed as chiral electron-donating groups (Scheme 2). Ready access to aryl vinyl and divinyl ketones bearing X groups was achieved using a reductive-coupling protocol (Scheme 2).¹² This involves initial Pd-mediated hydrostannylation of the alkyne 7 followed by in situ cross-coupling to an acid chloride: $7 \rightarrow 9 + 10 \rightarrow 11$. A series of alkynes 7 bearing different groups X and R^a were initially coupled to tigloyl chloride 10 ($\text{R}^b = \text{R}^c = \text{Me}$) for a preliminary evaluation of their synthetic utility in the formation of divinyl ketones 11 and for their capacity to induce torquoselectivity in the Nazarov cyclization to give 12 (Scheme 2 and Table 1). The regioselectivity of the hydrostannylation step in the reductive-coupling varied for the different alkynes 7 . The α -directing effect of the X -group dominated in all cases

Table 1. Evaluation of Control Elements X

entry	7	X	R^a	11, yield ^a	12, yield (dr) ^b
1	7a	Sox	<i>n</i> Pr	11a, 79%	no reaction
2	7b	Cs	<i>n</i> -pentyl	11b, 68%	12b, 80% (>20:1)
3	7c	Cs	Ph	11c, 15%	12c, 99% (>20:1)
4	7d	OxPh	<i>n</i> -pentyl	11d, 91%	12d, 99% (>20:1)
5	7e	OxPh	Ph	11e, 51%	12e, 75% (>20:1)
6	7f	OxBn	Ph	11f, 67%	12f, 85% (>20:1)
7	7g	OxiPr	Ph	11g, 83%	12g, 80% (>20:1)
8	7h	OxPh ₂	<i>n</i> -pentyl	11h, 93%	12h, 98% (>20:1)
9	7i	OxPh ₂	Ph	11i, 78%	12i, 84% (>20:1)

^a11a–i were formed by reductive-coupling with tigloyl chloride 10 ($\text{R}^b = \text{R}^c = \text{Me}$) (see Scheme 2). ^bAll reactions were performed using MeSO_3H (10 equiv) in CH_2Cl_2 at 0°C –rt.

Scheme 2. Synthesis of Various X-Substituted Divinyl Ketones and Their Nazarov Cyclization Products

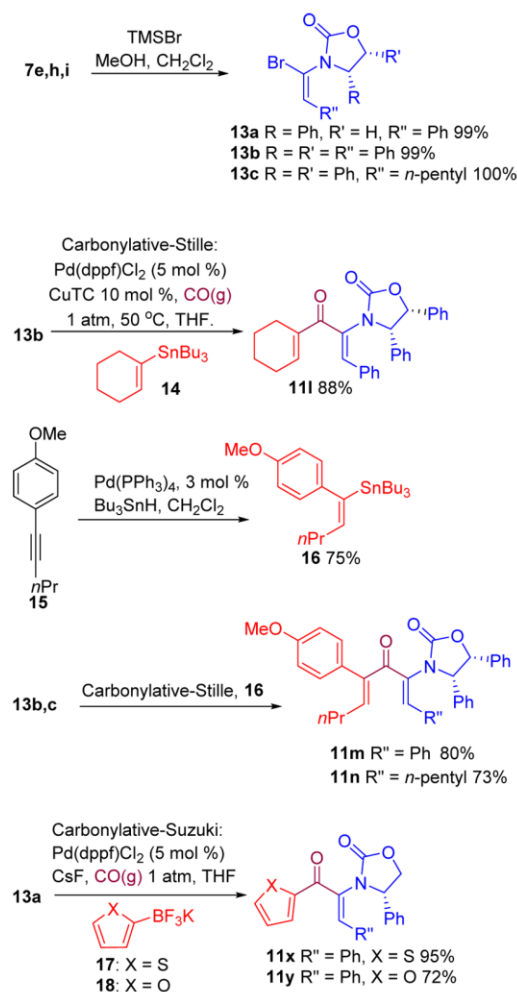


where R^a = alkyl, giving exclusively the desired regioisomer **9**. However, because aryl groups are also α -directing groups in the Pd-mediated hydrostannylation of aryl alkynes, the capacity of **X** to favor **9** over **9'** in cases in which R^a = aryl became an additional consideration in identifying preferred **X** groups. The order of the regioselectivity (ratio of **9** to **9'**) for the different **X** groups in the hydrostannylation of **7X** (R^a = Ar) was found to be $\text{OxPh}_2 \sim \text{OxiPr} (\sim 9:1) > \text{OxBn} (\sim 5:1) > \text{OxPh} (\sim 3:1) \gg \text{Cs} (\sim 2:3)$.¹³ The modest regioselectivities seen in the hydrostannylation of **7c** (**X** = **Cs**) (2:3) and **7e** (**X** = **OxPh**) (3:1) account for the lower yields achieved in their reductive-couplings with tigloyl chloride: **11c** (15%) and **11e** (51%), respectively (Table 1).

The Nazarov cyclizations of **11a–i** were undertaken using MeSO_3H (10 equiv = 1 M in CH_2Cl_2 , 0 °C–rt) (Table 1). During the course of these studies, Salom–Roig and Sun reported the Nazarov cyclizations of some aryl vinyl and divinyl ketones bearing a chiral sulfoxide (**Sox**).^{4d,e} These cyclizations require the involvement other electron-rich substituents in order to offset the electron-withdrawing nature of the sulfoxide.^{4d,e} In the case of sulfoxide **11a**, which does not bear such an electron-donating group, no cyclization was observed under the conditions used in this study (1 M MeSO_3H in CH_2Cl_2 , rt, 24 h). By contrast, the chiral electron-donating **Cs**- and **Ox**-activated systems all cyclized efficiently (75–99% yield) with excellent diastereoselectivity favoring the $\text{C4}\beta$ -stereochemistry [diastereomeric ratio (dr) > 20:1 (no $\text{C4}\alpha$ -diastereomer observable by ^1H NMR)]. Even though the substrate activation of **11b–i** by **Ox** and **Cs** is sufficient to enable cyclizations to be conducted at much lower temperatures (<0 °C) with catalytic amounts of acid (3 mol %), the higher acid concentrations (1 M) and sustained reaction at rt (24 h) were necessary to facilitate the epimerization at **C5** to exclusively give the thermodynamically favored C4,C5-trans isomer. The cyclizations of divinyl ketones **11b–i** produced only one double-bond regioisomer **12b–i**, favoring placement of the double-bond distal to the auxiliary **X**. X-ray crystal structure analysis of **12c**, **12e**, and a number of other products (**12j** and **23**, see below) confirmed the $\text{C4}\beta$ -stereochemistry, and all other isomers have also been assigned this stereochemistry.^{10,13} In light of their superior utility in the reductive-coupling protocol and their high levels of regio- and stereocontrol in the Nazarov reaction, **Ox** groups emerged as the preferred control elements **X** in the further development of this protocol.

Substituent Variation in the Ox-Controlled Nazarov Cyclization. A series of other divinyl and aryl vinyl ketones **11j–aa** containing **Ox** groups were accessed using either the reductive-coupling (Scheme 2) or a carbonylative cross-coupling protocol and were subjected to the Nazarov cyclization (Scheme 3 and Table 2; see legend for method of synthesis of **11**). Generally speaking, the reductive-coupling protocol worked well in all cases where it was applied (Table 2), except for those involving 2,3-dimethylcinnamoyl chloride (Table 2 entries 7 and 8), which suffer from the increased steric hindrance associated with the *cis*-methyl group. As a complement to hydrostannylation of **7**, the regio- and stereoselective hydrobromination of ynamides **7e,h,i** to give **13a–c** (99–100% yield) using TMSBr and MeOH in dichloromethane afforded access to Nazarov substrates **11** via carbonylative cross-coupling (Scheme 3). Carbonylative Stille coupling of **13b** with **14** to give **11l** (88%) was achieved using $\text{Pd}(\text{dppf})\text{Cl}_2$ and copper 2-thiophenecarboxylate (**CuTC**) in THF under 1 atm of

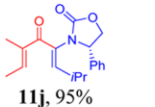
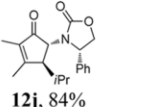
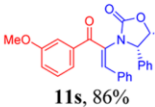
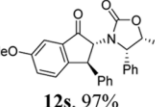
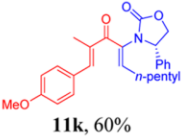
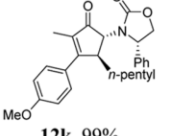

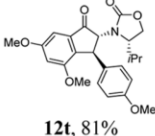
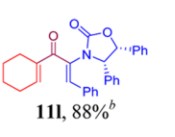
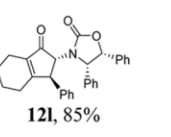

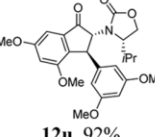
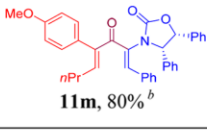
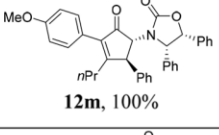
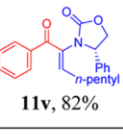
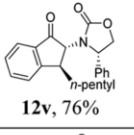
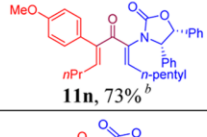
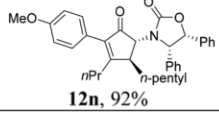
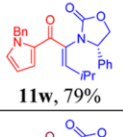
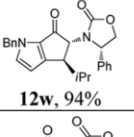
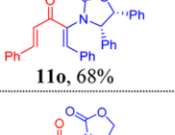
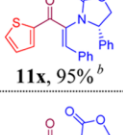
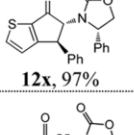
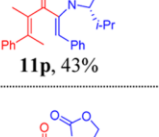
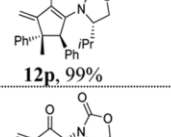
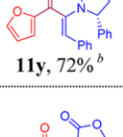
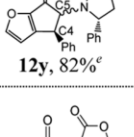
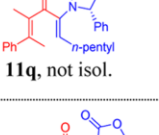
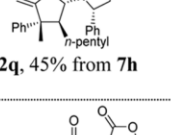
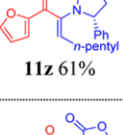
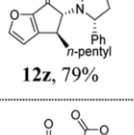
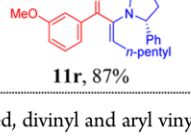
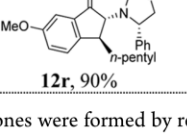
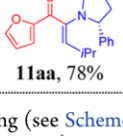
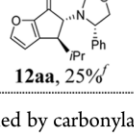
Scheme 3. Carbonylative Coupling Approaches to Ox-Substituted Divinyl Ketones



CO(g) .¹⁴ Hydrostannylation of the arylalkyne **15** to give **16** (75%), followed by carbonylative Stille cross-coupling of **16** with **13b** and **13c** gave **11m** (80%) and **11n** (73%), respectively, demonstrating a convergent synthesis of divinyl ketones **11** from two alkyne substrates (Scheme 2). Albeit, initial attempts to couple **13a** to arylboronic acids under standard, aqueous, carbonylative Suzuki–Miyaura conditions led only to the carboxylation of **13a** (not shown), we identified an alternative set of anhydrous conditions that could be performed at room temperature under just 1 atm of CO(g) using organotrifluoroborate salts, **CsF** and $\text{Pd}(\text{dppf})\text{Cl}_2$ in THF to give exclusively the coupled products **11x** (95%) and **11y** (72%).¹⁵

Nazarov cyclizations of divinyl ketones and aryl vinyl ketones depicted in Table 2 proceeded smoothly, except for **11o**, which gave a complex mixture of products (entry 6). Surprisingly, Nazarov cyclization of the same substrate, **11o**, in the presence of furan gave a good yield of furan-trapped products (see below), indicating that the Nazarov cyclization itself is facile but the product (or oxallyl cation) are subject to further reaction under these conditions. As in the examples reported above in Table 1, the **Ox** group favors the $\text{C4}\beta$ -stereochemistry (dr >20:1) and the C4,S-trans -stereochemistry. The modest overall yield of **12q** (45% from ynamide **7h**) is associated with a low

Table 2. Nazarov Cyclizations of Divinyl and Aryl Vinyl Ketones

entry	7 + 10 → 11, yield ^a	12, yield (dr) ^{c,d}	entry	7 + 10 → 11, yield ^a	12, yield (dr) ^{c,d}
1	 11j, 95%	 12j, 84%	10	 11s, 86%	 12s, 97%
2	 11k, 60%	 12k, 99%	11	 11t, 67%	 12t, 81%
3	 11l, 88% ^b	 12l, 85%	12	 11u, 75%	 12u, 92%
4	 11m, 80% ^b	 12m, 100%	13	 11v, 82%	 12v, 76%
5	 11n, 73% ^b	 12n, 92%	14	 11w, 79%	 12w, 94%
6	 11o, 68%	Complex mixture	15	 11x, 95% ^b	 12x, 97%
7	 11p, 43%	 12p, 99%	16	 11y, 72% ^b	 12y, 82% ^e
8	 11q, not isol.	 12q, 45% from 7h	17	 11z, 61%	 12z, 79%
9	 11r, 87%	 12r, 90%	18	 11aa, 78%	 12aa, 25% ^f

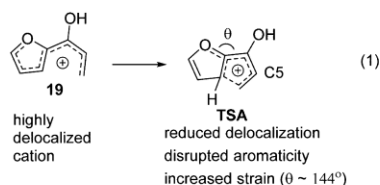
^aUnless otherwise stated, divinyl and aryl vinyl ketones were formed by reductive-coupling (see Scheme 2). ^bFormed by carbonylative coupling (see Scheme 3). ^cUnless otherwise stated, all reactions were performed using MeSO₃H (2–10 equiv) in dichloromethane, 1,2-dichloroethane, or toluene at rt or heating, depending on substrate (see Supporting Information for details). ^dUnless otherwise stated, all reactions proceeded with dr > 20:1, with no other diastereomer observable by ¹H NMR. ^eFormed as a mixture of C5 epimers each with dr = 18:1. ^fCyclized using 2 equiv of TfOH in dichloromethane at 40 °C.

yield in the reductive-coupling step. In this case 11q was not isolated but the crude reaction mixture resulting from reductive-coupling of 7h and 2,3-dimethylcinnamoyl chloride was treated directly with MeSO₃H. Again, as in the earlier examples, the regiochemical placement of the double bond in cyclopentenones 12j–q is always to the distal side of the ring with respect to Ox (Table 1, entries 1–8).

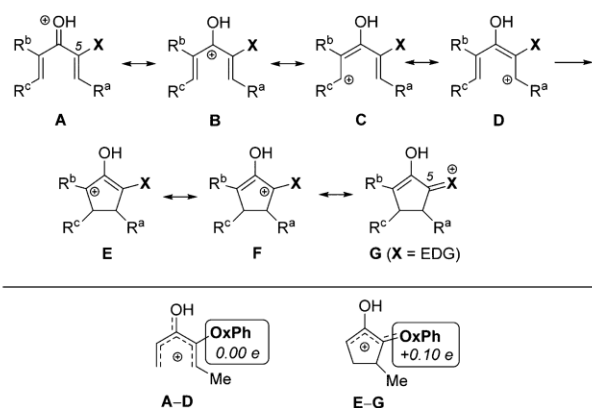
Even though the cyclizations of divinyl ketones were generally quite rapid, proceeding at <0 °C, cyclizations of some aryl vinyl ketones were usually slower with some

examples requiring moderate heating (40–80 °C). Importantly, the necessity to heat these Nazarov cyclizations had little effect on the level of chiral induction, which remained high in all cases (dr > 20:1). For example, the cyclization of the phenyl vinyl ketone 11v, which required 10 equiv of MeSO₃H in refluxing chloroform (65 °C) still afforded 12v in 76% yield and dr > 20:1 (entry 13). Furan-2-yl vinyl ketones are well-known to be resistant to Nazarov cyclization¹⁶ and the cyclization of 11y to 12y (82%) and 11z to 12z (79%), the former at rt, are indicative of the powerful activating capacity of Ox in

promoting the Nazarov reaction (Table 2 entries 16 and 17). All of the products could be isolated as a single C4,5-*trans* product after C5-epimerization, except for **12y**, which was resistant to C5-epimerization and attempts to achieve this through more forceful reaction conditions led to some C4 epimerization and loss of overall stereoinduction. Accordingly, **12y** was isolated as a mixture of C5-epimers. This inability to equilibrate **12y** to a single C5-epimer is of no consequence in instances where the **OxPh** group is subsequently cleaved from the epimeric mixture to give a single product (see below).



Scheme 4. Charge-Stabilization by X = EDG = Ox

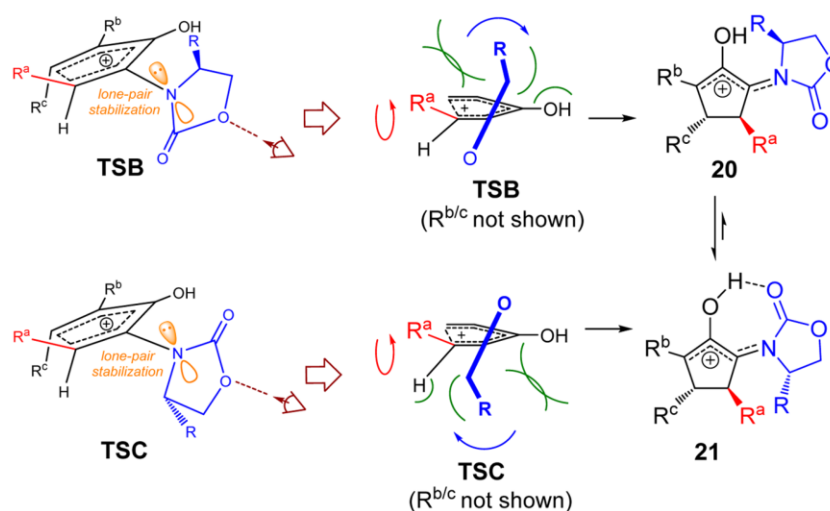


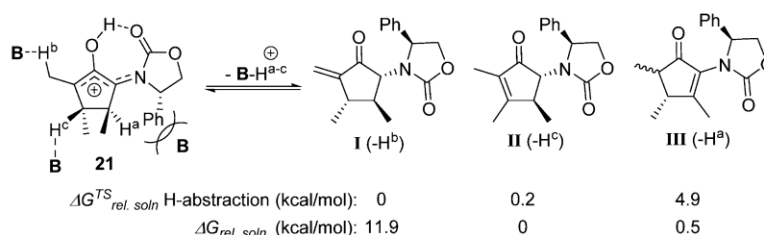
The Nazarov cyclization of isopropyl-substituted furanyl vinyl ketone **11aa** was sluggish and required treatment with triflic acid (2 equiv) in refluxing 1,2-dichloroethane (80 °C) to give **12aa** in low yield (25%) (Table 2, entry 18). Presumably, the combination of the furan ring and a sterically hindering *i*Pr

group combine to retard cyclization. This outcome stands in contrast to the corresponding pyrrole **11w**, which cyclized efficiently to **12w** (94%) upon treatment with 10 equiv of MeSO₃H in refluxing dichloromethane (40 °C). The resistance of furan-2-yl vinyl ketones to cyclization most likely arises from the conflation of several factors (eq 1): (i) disruption of furan aromaticity; (ii) a significant reduction in charge stabilization (delocalization) in progression of **19** to the transition state TSA (eq 1); and accumulating strain in TSA due to a widened bond angle ($\theta \sim 144^\circ$). These effects are less pronounced in equivalent pyrrol-2-yl and thiophen-2-yl systems because the disruption in aromaticity is less in the case of the pyrrole and bond-angle strain is less in the case of the thiophene because of the large size of the sulfur atom. Presumably, the presence of the C5 **Ox** substituent (π -electron-donor) in the furan-2-yl vinyl ketones **11y** and **11z** compensates to some extent for these unfavorable features by increasing charge stabilization in TSA. In general, the Nazarov cyclization of a divinyl (or aryl vinyl) ketone has the effect of concentrating the positive charge as shown in Scheme 4. The positive charge is initially delocalized across the oxygen and the five carbons (resonance contributors A–D), but upon electrocyclization the charge is delocalized across a three-carbon system (resonance contributors E and F). An electron-donating substituent, such as **OxPh**, at the C5 position introduces the additional resonance contributor G. Calculations on the model system shown in Scheme 4 indicate that upon cyclization, about +0.1 *e* of positive charge is transferred onto the oxazolidinone as it comes into resonance with the oxallyl cation.¹³ The cyclization transition state also derives stabilization from the incipient resonance stabilization by X = **OxPh**. In the model system, the **OxPh** substituent is calculated to lower the electrocyclization barrier by approximately 5 kcal/mol.¹³

We have previously examined the strong preference for the C4 β -stereochemistry in the **Ox**-promoted Nazarov cyclization using density functional theory (DFT).¹⁷ DFT calculations revealed that stereoinduction by **Ox** follows a unique “coupled-torque” mechanism. There are two low-lying transition states for the cyclization, wherein the **Ox** group adopts opposing conformations (TSB and TSC, Scheme 5). In both transition states, the **Ox** group exists at a relatively oblique angle ($\sim 40^\circ$)

Scheme 5. “Coupled-Torque” Mechanism of Chiral Induction in the Ox-Promoted Nazarov Cyclization

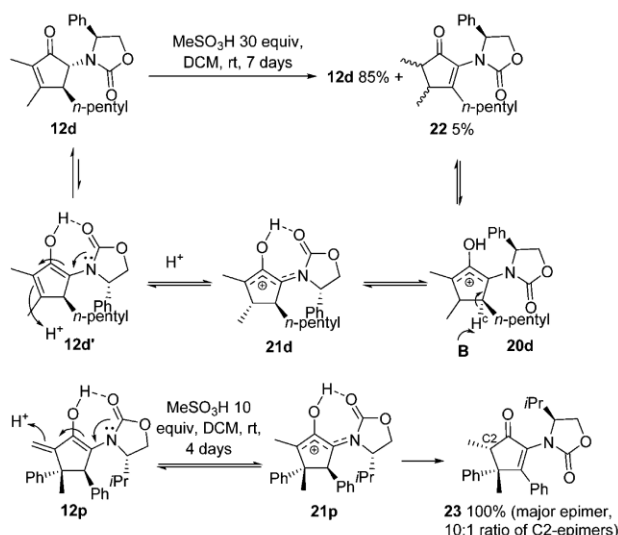


Scheme 6. Ox-Directed Regioselective Placement of the Double-Bond¹⁷

with respect to the pentadienyl cation, and as the reaction proceeds further along the reaction coordinate, the **Ox** rotates (blue arrows) thereby increasing orbital overlap of the electron-lone-pair on nitrogen with the emerging allylic π -cation in intermediates **20** and **21**. In each case, **TSB** \rightarrow **20** and **TSC** \rightarrow **21**, the sense of rotation of **Ox** is the same: clockwise. This unidirectional rotation by **Ox** minimizes steric clashing between the **Ox** R-group and the semiplanar pentadienyl cation. In turn, steric interactions between **Ox** and R^a determine the torquoselectivity of the conrotatory ring closure. The termini of the divinyl ketone rotate anticlockwise (red arrows), as this is the direction that minimizes clashing between R^a and the **Ox**-carbonyl (in **TSB**) or R^a and the **Ox**-CHR group (in **TSC**). Both cases lead to the same stereochemical outcome: the formation of the C4 β stereoisomer.

DFT calculations also explained the regioselectivity of the double-bond placement in the **Ox**-activated Nazarov cyclization (Scheme 6).¹⁷ The double bond is consistently delivered to the distal side of the cyclopentenone ring with respect to **Ox** (**12d–q**). DFT calculations predicted that the intramolecularly H-bonded species **21** is the preferred conformation of the intermediate oxyallyl cation (Scheme 5). Assuming that the proton is transferred to another molecule acting as a base **B** (**B** = solvent, counterion, substrate or product molecule), the calculations indicated that the preference for H^{a-c} in **21** is likely to result from a combination of thermodynamic and kinetic effects (Scheme 6). Kinetically, **I** and **II** are both favored over **III**, but thermodynamically **II** and **III** are favored over **I**. The strong preference for **II** that was observed experimentally can be rationalized as resulting from a rapid equilibration of the kinetically accessible isomers **I** and **II** through reversible formation of **21**, which favors **II** thermodynamically, specifically under conditions where **III** is kinetically inaccessible.

To further explore the kinetic barriers to double-bond isomerization, we treated **12d** with a large concentration of MeSO₃H (5 M/30 equiv) for an extended period (Scheme 7). Under these conditions, a small amount of the thermodynamic double-bond isomer **22** was detected by NMR after 7 days.¹⁸ DFT calculations reveal that the relatively high barrier to H^a-abstraction arises from the steric effects imposed by the **Ox** substituent in **21**, which blocks access to H^a by the base **B** (Scheme 6). Abstraction of H^a requires that the **Ox** group adopts a higher-energy conformation involving loss of H-bonding (i.e. **21d** \rightarrow **20d** Scheme 7). The necessity to form the enol **12d'** in order to reaccess the allylic cation **21d** is also likely to contribute to the low rate of equilibration of **12d** and **22**. Double-bond isomerization of **12p** was also studied (Scheme 7). In this case, reformation of the allylic cation **21p** is more facile because of the higher electron density in the double bond in **12p**. Nonetheless, its conversion to the thermodynamically preferred isomer **23** was still very slow, being notable only after 16 h and complete after 4 days. By contrast, the Nazarov

Scheme 7. Thermodynamic Double-Bond Isomerization of **12d** and **12p**

cyclization of **11p** to **12p** is complete in <5 min under these conditions. Compound **23** was obtained as a 10:1 mixture of C2Me-epimers, favoring the C2 α -epimer as determined by X-ray crystallography.¹³ The experimental studies (Scheme 7) are consistent with our earlier theoretical studies (Scheme 6)¹⁷ demonstrating significant kinetic barriers to H^a-abstraction during the Nazarov reaction, which are responsible for the regioselectivity favoring **I/II** over **III**. These barriers are important, because although the **Ox**-promoted Nazarov cyclization to form cyclopentenones is very fast (usually complete within minutes), the epimerization at C5 is slower, requiring up to 1–2 h in the presence of 3–10 equiv (0.3–1.0 M) of MeSO₃H. Thus, the low barrier for the conversion **I** \rightarrow **II**, the thermodynamic preference for **II** relative to **I**, and the significant thermodynamic difficulty associated with formation of **III** ensure that the Nazarov cyclization of **11Ox** to **12Ox** can be achieved under conditions that enable thermodynamic equilibration of the **Ox** group to the lower energy *trans*-isomer **II** without competing double-bond isomerization of **II** to **III**. Of additional significance is that no [1,2]-sigmatropic shifts were observed in these Nazarov cyclizations, even in cases where the group adjacent to the oxyallyl cation has a relatively high migratory aptitude, such as the Me and Ph groups attached to the quaternary center in **12p** and **12q**. This is attributed to the **Ox**-stabilization of the allylic cation, disfavoring the formation of higher energy cations via [1,2]-migration. This further underscores the master-control role played by the **Ox** auxiliary in ensuring a predictable, chemoselective outcome.

Scheme 8. Oxyallyl Trapping of Nucleophiles and Dienes

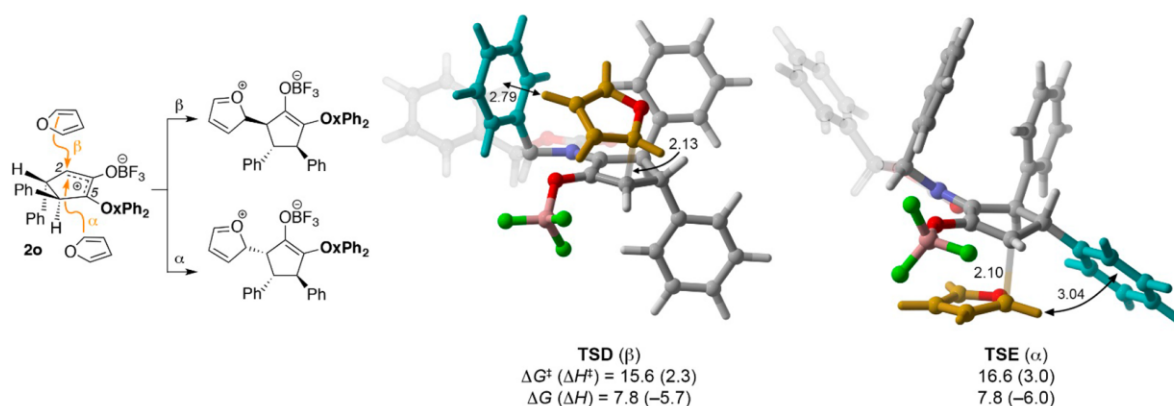
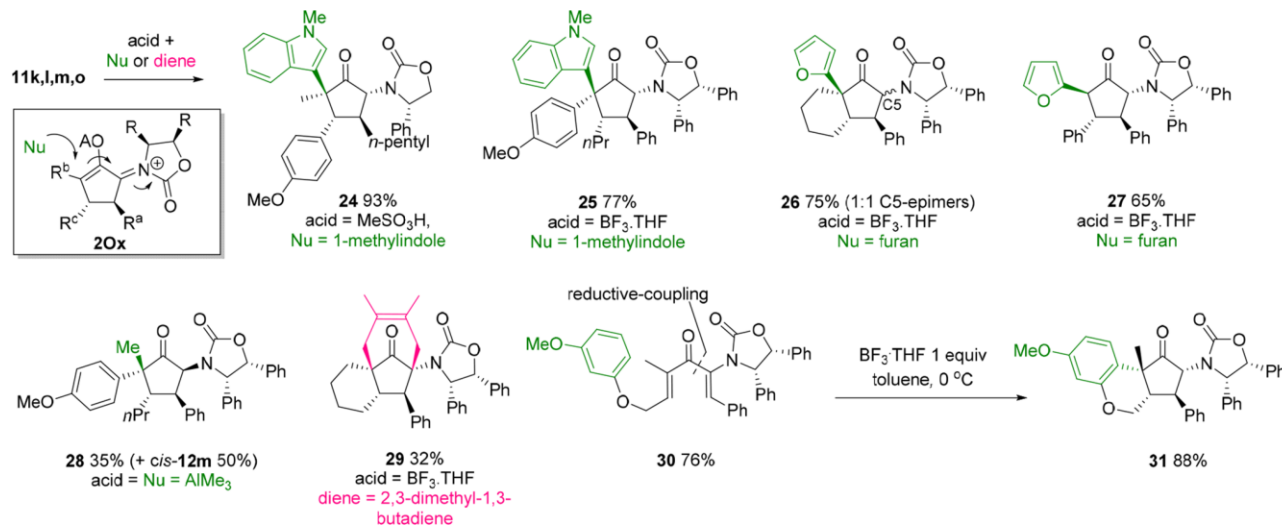


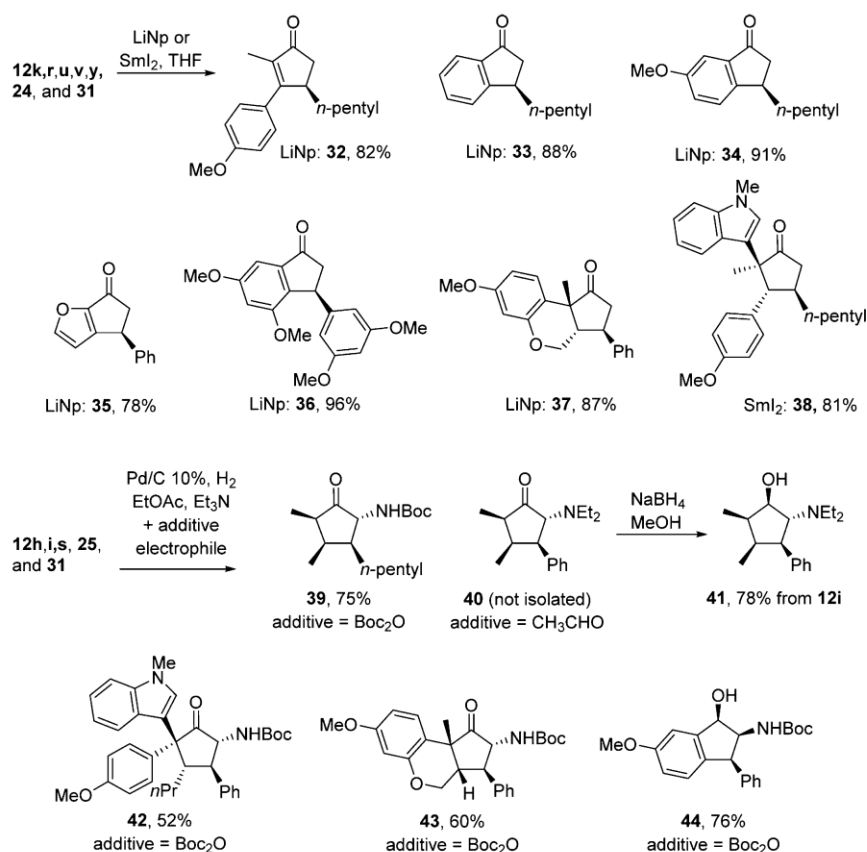
Figure 1. Transition states for addition of furan (highlighted in gold) to the α or β face of oxyallyl intermediate **2o** ($X = \text{OxPh}_2$, $A = \text{BF}_3$), computed with M06-2X/6-311+G(d,p)-SMD(CH_2Cl_2)/M06-2X/6-31G(d). Distances in Å. Energies (kcal/mol) are reported with respect to **2o** plus furan.

Oxyallyl-Cation Trapping. One of the most significant innovations in the Nazarov cyclization has been the effective trapping of the intermediate oxyallyl cations with a range of nucleophiles and dienes.^{5–7} We have investigated the utility of the **Ox**-promoted Nazarov cyclization for the regio- and stereoselective incorporation of nucleophiles and dienes [alkylation, arylation, or (4 + 3)-cycloaddition] (Scheme 8). Nazarov cyclizations of **11k** and **11m** in the presence of *N*-methylindole and of **11l** and **11o** in the presence of furan exclusively gave the trapped products **24** (93%), **25** (77%), **26** (75%), and **27** (65%), respectively.¹⁹ West and co-workers have previously shown that the use of AlMe_3 as a Lewis acid in the Nazarov cyclization results in oxyallyl-cation trapping through methyl transfer from aluminum.^{6d} Cyclization of **11m** with AlMe_3 afforded a modest yield of the trapped material **28** (35%), which was isolated as the kinetically favored *cis*-isomer, plus a significant amount of the cyclopentenone *cis*-**12m**. The **Ox**-group plays a key role in the regioselectivity of these intermolecular trapping reactions, favoring a 1,4-type addition to the α,β -unsaturated **Ox**-iminium ion **2Ox** (Scheme 8 box). At first glance, the stereochemistry of Nu incorporation might appear to be attributed to steric interactions between Nu and the neighboring $\alpha\text{-R}^c$ group of **2Ox**; however, computational studies of the furan-trapping suggest that the stereoselectivity

depends on CH– π interactions (see below). Trapping of **11l** with 1,3-butadiene produced the (4 + 3)-cycloadduct **29** in modest yield (32%). Lastly, intramolecular trapping of a tethered arene was achieved upon treatment of **30** (accessed in 76% yield by reductive-coupling)¹³ with $\text{BF}_3\cdot\text{THF}$ to give **31** (88%). These trapping reactions have enabled four contiguous stereocenters to be generated enantioselectively, including chiral quaternary stereocenters.

The trapping of furan in **26** and **27** by a Friedel–Crafts reaction rather than a (4 + 3)-cycloaddition contrasts with previous studies, which have suggested that stabilized oxyallyl cations arising from Nazarov cyclizations are biased toward asynchronous (4 + 3)-cycloadditions with furans, whereas less-stabilized, more-electrophilic, oxyallyl cations prefer to undergo nucleophilic trapping.^{7d} It also contrasts with other studies on the reactions of furans with acyclic **Ox**-stabilized oxyallyl intermediates, which led to (4 + 3) cycloadducts.²⁰ To gain a better understanding of the factors controlling the chemo- and stereoselectivity of the trapping of furans in the **Ox**-controlled Nazarov reaction, we performed DFT calculations. Computations with M06-2X²¹ were performed on the reaction of furan with oxyallyl intermediate **2o** ($X = \text{OxPh}_2$, $A = \text{BF}_3$) which leads to **27** (Figure 1). The computations show that the transition states for the addition of furan to the top and bottom

Scheme 9. Ox-Group Removal or Elaboration



faces of **2o** (TSD and TSE, respectively) differ in energy by 1.0 kcal/mol ($\Delta\Delta G^\ddagger$), favoring addition to the top (β) face.¹³ Although the molecular conformations of TSD and TSE resemble those of (4 + 3)-cycloaddition transition states,^{20c,d} the products contain only one C–C bond, that is the bond between furan and C2 of oxallyl **2o**. The interaction between furan and C5 of **2o** in the TS is stabilizing but does not lead to bond formation. This result is similar to that reported by West et al.^{7d} in their DFT studies on nonstabilized oxallyl cations. Computations predict that ring closure of the C2(β)-furan-trapped intermediate via formation of a bond to C5, which would lead to a (4 + 3)-cycloadduct, has a barrier (ΔG^\ddagger) of 21.3 kcal/mol, which is 5.7 kcal/mol higher than the barrier for the first C–C bond-forming step (15.6 kcal/mol, TSD) (see the Supporting Information). This provides the opportunity for the initially formed furan-trapped intermediate to undergo deprotonation leading to **27**, rather than ring closure leading to the (4 + 3)-cycloadduct. The stereoselectivity of the addition of furan to **2o** can be traced to CH– π interactions occurring within the transition states. The TS for addition to the top face (TSD) contains a CH– π interaction between furan and one of the Ph groups of **OxPh₂**, whereas the TS for addition to the bottom face (TSE) contains a CH– π interaction between furan and the C3-Ph group of **2o**. The phenyl rings involved in these CH– π interactions are highlighted in blue in Figure 1. In TSD, H3 of the furan lies 2.79 Å from the center of the nearby Ph ring of **OxPh₂**, but in TSE, H2 of the furan lies 3.04 Å from the center of the nearby Ph ring of **2o**. The stronger CH– π interaction in TSD explains the lower energy of TSD, which leads to the preference for the formation of the C4 β product.

Related CH– π interactions have previously been observed in both the nucleophilic and the cycloaddition pathways of oxallyl trapping,^{7d,20c} including the aforementioned (4 + 3)-cycloadditions of furans to acyclic **Ox**-stabilized oxallyl cations.^{20a}

Auxiliary Cleavage. The **Ox** group can be cleaved using either lithium naphthalenide (LiNp) or SmI₂ as demonstrated for a sample set of Nazarov cyclization products **12**, **24**, and **31**, giving **32–38** in good yields (78–96%) (Scheme 9). If desired, the cleaved **Ox** group can be recovered from these reactions for recycling, adding to the atom efficiency of the protocol. The diphenyloxazolidinone **OxPh₂** also serves as a masked amine, which can be revealed upon Pd/C hydrogenation (Scheme 9).²² Since the Nazarov cyclization products contain a ketone, it proved necessary to perform these hydrogenations in the presence of an electrophile (Boc₂O or CH₃CHO) in order to avoid the formation of dimers and oligomers through reductive-amination reactions. Accordingly, a sample set of **OxPh₂**-containing Nazarov products **12**, **25**, and **31** was converted to a series of substituted amines **39–44** (52–78%). In the case of **12h** and **12i**, the double bond was also stereoselectively hydrogenated to give **39** (75%) and **40**, respectively. Isolation of **40** proved to be difficult as the product was prone to decomposition during chromatography; however, diastereoselective reduction of the ketone with NaBH₄ gave the more stable alcohol **41**, which was isolated in 78% yield from **12i**. The stereochemistry of **41** was assigned by NOESY NMR, revealing that the stereoselective delivery of the hydrogen from hydrogenation (Pd/C, H₂) and the hydride from NaBH₄ had occurred from the bottom face. Hydrogenation of **12s** to give

44 (76%) is presumed to involve stereoselective hydrogenation of the enol tautomer of **12s** to give a hydroxyl group, followed by hydrogenation of **OxPh₂**. This explanation is supported by the observation that both the pure *trans*-isomer **12s** (formed under conditions of thermodynamic control) and a mixture of *cis*- and *trans*-**12s** (formed under conditions of kinetic control) both gave the same product **44** upon hydrogenation. The stereochemistry of **44** is tentatively assigned as all *cis*, assuming that delivery of the hydrogen to the enol occurs from the face opposite the C4-Ph group.

■ CONCLUSION

The stereoselective *syn*-hydrostannylation and *syn*-hydrobromination of readily accessible ynamides **7**, in conjunction with palladium-mediated coupling techniques (in particular reductive-coupling and carbonylative-coupling), provides concise, stereoselective access to a range of aryl vinyl and divinyl ketones **11**. The **Ox** group has emerged as a highly effective, multifunctional, master-control element in the Nazarov cyclization, enabling access to a broad range of cyclopentanoid structures with high levels of chemo-, regio- and stereoselectivity. The capacity of the **Ox** group to alleviate the otherwise unfavorable charge-concentrating effect of the Nazarov cyclization (**8X** → **2X**, Scheme 1) through nitrogen lone-pair donation in **2Ox**, enables it to be effectively employed in the cyclization of traditionally resistant substrates, such as furan-2-yl vinyl ketones (**19** → **TSA**, eq 1). The **Ox** in the oxyallyl intermediate **2Ox** also plays a critical role in controlling the regioselectivity of double-bond formation or nucleophilic trapping, and in avoiding competing [1,2]-sigmatropic shifts. The **Ox**-groups can be reductively cleaved from the products and recycled or, in the case of **OxPh₂**, converted into other amine functionalities by hydrogenation (Scheme 9). In short, the **Ox**-controlled Nazarov cyclization represents a broadly applicable method for the synthesis of enantiopure, multi-stereocenter-containing cyclopentanoids from readily accessible **Ox**-ynamides.

■ EXPERIMENTAL SECTION

General. All experiments were performed under an anhydrous atmosphere of nitrogen in flame-dried glassware except where indicated. Melting points were recorded with an electrothermal melting-point apparatus. Proton (¹H) and carbon (¹³C) NMR spectra were recorded using a Fourier transform instrument at the frequencies indicated. The protonicities of the carbon atoms observed in the carbon NMR were determined using J-modulated spin-echo (jmod) experiments. High-resolution mass spectra (HRMS) were recorded on a time-of-flight mass spectrometer fitted with either an electrospray (ESI) or atmospheric-pressure ionization (APCI) ion source. Tetrahydrofuran (THF) and dichloromethane (DCM) were purified using a commercial solvent-purification system. Analytical and preparative TLC were conducted on aluminum-backed 0.2 mm thick silica gel 60 GF254 plates, and the chromatograms were visualized under a 254 nm UV lamp and/or by treatment with a reagent solution [phosphomolybdic acid/95% ethanol (4g:100 mL) dip] or anisaldehyde dip (214 mL EtOH, 8 mL H₂SO₄, 2.4 mL AcOH, 5.9 mL anisaldehyde) followed by heating. Flash column chromatography was performed using silica, 40–63 μm. The synthesis and spectral data of the following compounds has been previously reported: **7d**,²³ **7l**,²³ **11d**,²³ **11e**,²³ **11f**,²³ **11g**,²³ **11h**,²³ **11i**,²³ **11j**,²³ **11k**,²³ **11l**,²³ **11m**,²³ **11n**,²³ **11o**,²³ **11p**,²³ **11q**,²³ **11r**,²³ **11s**,²³ **11t**,²³ **11u**,²³ **11v**,²³ **11w**,²³ **11x**,²³ **11y**,²³ **11z**,²³ **12a**,²³ **12b**,²³ **12c**,²³ **12d**,²³ **12e**,²³ **12f**,²³ **12g**,²³ **12h**,²³ **12i**,²³ **12j**,²³ **12k**,²³ **12l**,²³ **12m**,²³ **12n**,²³ **12o**,²³ **12p**,²³ **12q**,²³ **12r**,²³ **12s**,²³ **12t**,²³ **12u**,²³ **12v**,²³ **12w**,²³ **12x**,²³ **12y**,²³ **12z**,²³ **13a**,¹⁰ **16**,¹⁰ **24**,¹⁰ **32**,¹⁰ **35**,¹⁰ **36**,²³ and **37**–**38**.¹⁰

General Method A, Copper(II)-Catalyzed Ynamide Formation. Using a modification of the procedure previously described,²⁴ a mixture of camphorsultam or oxazolidinone (NH-substrate) (1.0 equiv), ground K₂CO₃ (2.0 equiv), ground CuSO₄·H₂O (0.1 equiv),

1,10-phenanthroline (0.2 equiv), and bromoalkyne (1.2 equiv) in toluene (1 M in NH-substrate) was heated at 90 °C until ¹H NMR (aliquot) indicated complete consumption of the NH-substrate, typically after 24–48 h. After this time, the reaction was cooled to rt, filtered through Celite (rinsing with EtOAc), concentrated under reduced pressure, and chromatographed.

General Method B, Reductive Coupling. To a stirred solution of alkyne **7** (1.0 equiv) and Pd(PPh₃)₄ (3–5 mol %) in dichloromethane (0.1–0.2 M, relative to **7**) at 0 °C was added Bu₃SnH (1.05 equiv) dropwise over 2 min. The solution was then warmed to rt over 0.5 h, and to it were added sequentially the acid chloride **10** (1.0–1.2 equiv) and copper(I) thiophenecarboxylate (CuTC) or CuCl (10 mol %). The reaction mixture was stirred until TLC revealed complete consumption of the intermediate vinylstannane (2–16 h, typically run overnight). The solvent was removed under reduced pressure and the residue dissolved in Et₂O (or EtOAc for solubility). KF solution (20% w/v, aq) was added, and the resultant mixture stirred for 1–2 h. The liquid phases were separated (some solid particulate matter may remain suspended in the organic phase, presumably Bu₃SnF, which is removed upon later filtration), and the aqueous phase was re-extracted twice with Et₂O (or EtOAc). The combined organic extracts were dried over MgSO₄, concentrated under reduced pressure, and the crude product was purified by flash chromatography.

General Method C, Nazarov Reaction. MeSO₃H (10 equiv) was added to a stirred solution of divinyl or aryl vinyl ketone **11** in dichloromethane (0.1–0.2 M) at 0 °C, and the reaction mixture was then allowed to warm to rt over 1 h. After this time, the reaction was monitored by TLC until completion and then quenched by careful addition of saturated NaHCO₃ aq solution. The mixture was transferred to a separatory funnel and the phases separated. The aqueous phase was extracted twice with dichloromethane, and the combined organic phases were dried over MgSO₄ and concentrated under reduced pressure. Where necessary, the crude compounds were purified by flash chromatography.

General Method D, Reductive Cleavage of Ox. Lithium naphthalenide solution (0.7–1.0 M, ~2 equiv, freshly prepared from addition of lithium metal into a solution naphthalene in THF), was added dropwise to a stirred solution of **Ox**-cyclopentanoid (1.0 equivalent) in THF (0.05–0.1 M) at –78 °C until the dark color persisted. The reaction was quenched at –78 °C by the addition of saturated aqueous NH₄Cl solution. After the reaction mixture was warmed to rt, it was partitioned between Et₂O and H₂O, and the aqueous phase was re-extracted with Et₂O. The combined organic extracts were washed with brine, dried over MgSO₄, concentrated under reduced pressure, and purified by flash chromatography.

General Method E, Hydrogenation of OxPh₂. Triethylamine (3 drops) and the desired electrophile (Boc anhydride or acetaldehyde) (5 equiv) was added to a solution of **OxPh₂**-cyclopentanoid (1 equiv) in EtOAc or THF (0.1 M in cyclopentanoid) and Pd/C (10%) (1:1 weight ratio with cyclopentanoid). The reaction mixture was evacuated and backfilled with hydrogen three times and stirred at rt for 2 days. After this time, the reaction was filtered through Celite (rinsing with EtOAc), concentrated under reduced pressure, and chromatographed.

(**3aS,6R,7aR**)-1-(Hept-1-yn-1-yl)-8,8-dimethylhexahydro-1H-3a,6-methanobenzo[c]isothiazole 2,2-dioxide (**7b**). This was prepared according to General Method A using (1S)-(-)-2,10-camphorsultam (754 mg, 3.5 mmol), 1-bromo-1-heptyne (674 mg, 3.85 mmol), CuSO₄·H₂O (62 mg, 0.35 mmol), 1,10-phenanthroline (126 mg, 0.70 mmol), and K₂CO₃ (967 mg, 7.0 mmol) in toluene (3.5 mL). Flash chromatography (silica gel, 12:88 EtOAc/hexanes) gave the title compound **7b** as a thick oil (939 mg, 87%): ¹H NMR (400 MHz, CDCl₃) δ 3.51 (dd, *J* = 7.8, 4.2 Hz, 1H), 3.21 (s, 2H), 2.29 (t, *J* = 6.9 Hz, 2H), 2.18 (m, 1H), 1.95–1.82 (m, 3H), 1.74 (dd, *J* = 13.5, 8.1 Hz, 1H), 1.52 (pent., *J* = 7.2 Hz, 2H), 1.42 (m, 1H), 1.47–1.25 (m, 5H), 1.10 (s, 3H), 0.93 (s, 3H), 0.89 (t, *J* = 6.9 Hz, 3H). This NMR spectra is consistent with that previously reported.²⁵

(**3aS,6R,7aR**)-8,8-Dimethyl-1-(phenylethynyl)hexahydro-1H-3a,6-methanobenzo[c]isothiazole 2,2-dioxide (**7c**). This was prepared according to General Method A using (1S)-(-)-2,10-camphorsultam (754 mg, 3.5 mmol), 1-bromo-2-phenylethyne (697 mg, 3.85 mmol),

from phenylacetylene), $\text{CuSO}_4 \cdot \text{H}_2\text{O}$ (62 mg, 0.35 mmol), 1,10-phenanthroline (126 mg, 0.70 mmol), and K_2CO_3 (967 mg, 7.0 mmol) in toluene (3.5 mL). Flash chromatography (silica gel, 15:85 EtOAc/hexanes) gave the title compound **7c** as a thick oil (939 mg, 87%): ^1H NMR (400 MHz, CDCl_3) δ 3.51 (dd, $J = 7.8, 4.2$ Hz, 1H), 3.21 (s, 2H), 2.29 (t, $J = 6.9$ Hz, 2H), 2.18 (m, 1H), 1.95–1.82 (m, 3H), 1.74 (dd, $J = 13.5, 8.1$ Hz, 1H), 1.52 (pent., $J = 7.2$ Hz, 2H), 1.42 (m, 1H), 1.47–1.25 (m, 5H), 1.10 (s, 3H), 0.93 (s, 3H), 0.89 (t, $J = 6.9$ Hz, 3H). This NMR spectra is consistent with what was previously reported.²⁵

(*S*)-4-Benzyl-3-(phenylethynyl)oxazolidin-2-one (**7f**). This was prepared according to General Method A using (*S*)-4-benzylloxazolidin-2-one (1.42 g, 8.00 mmol), 1-bromo-2-phenylethyne (1.73 g, 9.56 mmol, from phenylacetylene), $\text{CuSO}_4 \cdot \text{H}_2\text{O}$ (142 mg, 0.80 mmol), 1,10-phenanthroline (288 mg, 1.60 mmol), and K_2CO_3 (2.21 g, 16.0 mmol) in toluene (8 mL). Flash chromatography (silica gel, 2:49:49 Et_2O /DCM/hexanes) gave the title compound **7f** as a white solid (1.82 g, 82%): ^1H NMR (400 MHz, CDCl_3) δ 7.46 (m, 2H), 7.39–7.22 (m, 8H), 4.42–4.31 (m, 2H), 4.18 (m, 1H), 3.30 (dd, $J = 14.0, 3.7$ Hz, 1H), 3.02 (m, 1H). This NMR spectra is consistent with that previously reported.²⁶

(4*S*,5*R*)-3-(Hept-1-yn-1-yl)-4,5-diphenyloxazolidin-2-one (**7h**). This was prepared according to General Method A using (4*S*,5*R*)-4,5-diphenyloxazolidin-2-one (1.0 g, 4.18 mmol), 1-bromoheptyne (0.946 g, 5.44 mmol, from 1-heptyne), $\text{CuSO}_4 \cdot \text{H}_2\text{O}$ (66.7 mg, 0.418 mmol), 1,10-phenanthroline (150.8 mg, 0.837 mmol), and K_2CO_3 (1.154 g, 8.362 mmol) in toluene (5 mL). Flash chromatography (silica gel, 2:48:48 Et_2O /DCM/hexanes) gave the title compound as a thick oil (1.142 g, 82%): ^1H NMR (400 MHz, CDCl_3) δ 7.18–7.04 (m, 6H), 6.98–6.83 (m, 4H), 5.91 (d, $J = 8.2$ Hz, 1H), 5.29 (d, $J = 8.2$ Hz, 1H), 2.18 (t, $J = 7.0$ Hz, 2H), 1.43–1.30 (m, 2H), 1.22–1.09 (m, 4H), 0.79 (t, $J = 6.9$ Hz, 3H); ^{13}C NMR (101 MHz, CDCl_3) δ 156.7, 133.6, 133.0, 128.6, 128.44, 128.2, 128.1, 127.6, 126.2, 80.7, 72.56, 69.6, 67.2, 30.8, 28.32, 22.1, 18.4, 134.0; HRMS (ESI-TOF) m/z : $[\text{M} + \text{H}]^+$ calcd for $\text{C}_{22}\text{H}_{24}\text{NO}_2^+$: 334.1802, found: 334.1804.

(4*S*,5*R*)-4,5-Diphenyl-3-(phenylethynyl)oxazolidin-2-one (**7i**). This was prepared according to General Method A using (4*S*,5*R*)-4,5-diphenyloxazolidin-2-one (3 g, 12.552 mmol), 1-bromo-2-phenylethyne (2.83 g, 15.64 mmol), $\text{CuSO}_4 \cdot \text{H}_2\text{O}$ (200 mg, 1.29 mmol), 1,10-phenanthroline (452 mg, 2.51 mmol), and K_2CO_3 (3.46 g, 25.07 mmol) in toluene (15 mL). Flash chromatography (silica gel, 2:48:48 Et_2O /DCM/hexanes) gave the title compound as a white solid (3.80 g, 90%): mp = 158–162 °C; ^1H NMR (400 MHz, CDCl_3) δ 7.26 (m, 5H), 7.14 (m, 6H), 6.96 (m, 4H), 5.99 (d, $J = 8.1$ Hz, 1H), 5.44 (d, $J = 8.1$ Hz, 1H); ^{13}C NMR (101 MHz, CDCl_3) δ 156.0, 133.4, 132.8, 131.7, 128.8, 128.6, 128.4, 128.3, 128.2, 127.6, 126.2, 122.2, 81.1, 78.6, 72.5, 67.4; HRMS (ESI-TOF) m/z : $[\text{M} + \text{H}]^+$ calcd for $\text{C}_{23}\text{H}_{18}\text{NO}_2^+$: 340.1332, found: 340.1335.

(*S*)-4-Isopropyl-3-[(4-methoxyphenyl)ethynyl]oxazolidin-2-one (**7k**). This was prepared according to General Method A using (*S*)-4-isopropylloxazolidin-2-one (1.21 g, 9.39 mmol), 1-(bromoethynyl)-4-methoxybenzene (2.08 g, 9.86 mmol), $\text{CuSO}_4 \cdot \text{H}_2\text{O}$ (167 mg, 0.94 mmol), 1,10-phenanthroline (339 mg, 1.88 mmol), and K_2CO_3 (2.60 g, 18.8 mmol) in toluene (9.4 mL). Flash chromatography (silica gel, 3:49:48 Et_2O /DCM/hexanes) gave the title compound **7k** as a white solid (1.48 g, 61%): mp = 121–123 °C; ^1H NMR (400 MHz, CDCl_3) δ 7.38 (d, $J = 8.9$ Hz, 2H), 6.83 (d, $J = 8.9$ Hz, 2H), 4.41 (t, $J = 9.0$ Hz, 1H), 4.19 (dd, $J = 9.0, 5.8$ Hz, 1H), 4.03 (ddd, $J = 8.8, 5.8, 4.1$ Hz, 1H), 3.81 (s, 3H), 2.29 (septet, $J = 6.9, 4.1$ Hz, 1H), 1.03 (d, $J = 6.9$ Hz, 3H), 1.02 (d, $J = 6.9$ Hz, 3H); ^{13}C NMR (100 MHz, CDCl_3) δ 159.5 (C), 156.0 (C), 133.1 (CH), 114.1 (C), 113.7 (CH), 77.0 (C), 71.7 (C), 64.7 (CH₂), 61.9 (CH), 55.1 (CH₃), 29.1 (CH), 17.0 (CH₃), 15.1 (CH₃); HRMS (ESI-TOF) m/z : $[\text{M} + \text{H}]^+$ calcd for $\text{C}_{15}\text{H}_{18}\text{NO}_3^+$: 260.1281, found: 260.1278.

(4*S*,5*R*)-3-[(*E*)-1-Bromo-2-phenylvinyl]-4,5-diphenyloxazolidin-2-one (**13b**). This was prepared as for **13a** above: TMS-Br (221.29 mg, 1.445 mmol), MeOH (0.058 mL, 1.445 mmol), and (4*S*,5*R*)-4,5-diphenyl-3-(phenylethynyl)oxazolidin-2-one **7i** (500 mg, 1.474 mmol) in DCM (10 mL), gave **13b** 99% (610 mg, 100%) as white solid: mp 138–143 °C; ^1H NMR (400 MHz, CDCl_3) δ 7.37 (d, $J = 2.8$ Hz, 5H),

7.14–7.01 (m, 4H), 6.95 (s, 1H), 6.86 (m, 4H), 6.44 (d, $J = 7.3$ Hz, 2H), 5.80 (d, $J = 8.4$ Hz, 1H), 5.42 (d, $J = 8.4$ Hz, 1H); ^{13}C NMR (101 MHz, CDCl_3) δ 156.7, 136.9, 134.3, 134.3, 131.7, 128.9, 128.8, 128.6, 128.6, 128.5, 128.4, 128.0, 127.9, 126.1, 116.7, 80.2, 67.3; HRMS (APCI-TOF) m/z : $[\text{M} + \text{H}]^+$ calcd for $\text{C}_{23}\text{H}_{19}\text{BrNO}_2^+$: 420.0594, found: 420.0588.

(4*S*,5*R*)-3-[(*E*)-1-Bromohept-1-en-1-yl]-4,5-diphenyloxazolidin-2-one (**13c**). This was prepared as for **13a** above: TMS-Br (150.03 mg, 0.98 mmol), MeOH (0.0395 mL, 0.98 mmol), and **7h** (333 mg, 1 mmol) in DCM (7 mL) gave **13c** (410 mg, 100%) as a thick oil: ^1H NMR (400 MHz, CDCl_3) δ 7.22–7.00 (m, 6H), 6.95 (dd, $J = 6.3, 2.8$ Hz, 2H), 6.89–6.76 (m, 2H), 5.96–5.81 (m, 2H), 5.45 (d, $J = 8.6$ Hz, 1H), 2.29–1.91 (m, 2H), 1.51–1.03 (m, 6H), 0.88 (t, $J = 7.0$ Hz, 3H); ^{13}C NMR (101 MHz, CDCl_3) δ 172.80, 153.9, 134.7, 133.0, 128.5, 128.4, 128.23, 128.1, 126.6, 126.2, 80.39, 62.8, 35.8, 31.636, 28.8, 24.3, 22.6, 14.1; HRMS (APCI-TOF) m/z : $[\text{M} + \text{H}]^+$ calcd for $\text{C}_{22}\text{H}_{25}\text{NO}_2^+$: 414.1063, found: 414.1063.

(2*E*,5*Z*)-3-Methyl-5-[(*S*)-*p*-tolylsulfanyl]nona-2,5-dien-4-one (**11a**). This was prepared according to General Method B using alkynyl sulfoxide **7a**²⁷ (103 mg, 0.500 mmol), $\text{Pd}(\text{PPh}_3)_4$ (16 mg, 0.014 mmol), Bu_3SnH (140 μL , 0.500 mmol), tigloyl chloride (0.50 mmol), and CuCl (40 mg, 0.40 mmol) in THF (3.5 mL). Flash chromatography (silica gel, 84:16 hexane/EtOAc) yielded the title compound **11a** as a discolored oil (114 mg, 79%): ^1H NMR (300 MHz, CDCl_3) δ 7.39 (d, $J = 8.1$ Hz, 2H), 7.23 (d, $J = 8.1$ Hz, 2H), 6.60 (t, $J = 7.7$ Hz, 1H), 6.42 (q, $J = 7.1$ Hz, 1H), 2.37 (s, 3H), 2.14 (app. q, $J_{\text{app}} = 7.4$ Hz, 2H), 1.75 (d, $J = 7.1$ Hz, 3H), 1.62 (s, 3H), 1.49 (app. sext, $J_{\text{app}} = 7.3$ Hz, 2H), 0.91 (t, $J = 7.4$ Hz, 3H); ^{13}C NMR (JMOD, 75 MHz, CDCl_3) δ 193.5 (C), 145.4 (C), 144.8 (CH), 141.9 (C), 139.08 (C), 139.07 (C), 137.6 (CH), 129.7 (CH), 125.1 (CH), 31.7 (CH₂), 22.0 (CH₂), 21.4 (CH₃), 15.0 (CH₃), 13.7 (CH₃), 10.3 (CH₃); LRMS m/z (%): 313.2 (40, $\text{M} + \text{Na}^+$), 291.2 (100, MH^+); IR (cm^{-1}): 2959, 2929, 1632, 1242, 1083, 1055, 809; HRMS (ESI-TOF) m/z : $[\text{M} + \text{H}]^+$ calcd for $\text{C}_{17}\text{H}_{22}\text{NaO}_2\text{S}^+$: 313.1238, found: 313.1235.

(2*E*,5*Z*)-5-[(3*aS*,6*R*,7*aR*)-8,8-Dimethyl-2,2-dioxidohexahydro-1*H*-3*a*,6-methanobenzo[*c*]isothiazol-1-yl]-3-methylundeca-2,5-dien-4-one (**11b**). This was prepared according to General Method B using ynamide **7b** (464 mg, 1.5 mmol), DCM (15 mL), $\text{Pd}(\text{PPh}_3)_4$ (87 mg, 0.075 mmol), Bu_3SnH (0.42 mL, 1.58 mmol), tigloyl chloride (181 μL , 1.65 mmol), and CuTC (29 mg, 0.15 mmol). Flash chromatography (silica gel, 12:88 EtOAc/hexanes) gave the title compound as a low-melting solid (404 mg, 68%): ^1H NMR (400 MHz, CDCl_3) δ 6.42 (m, 1H), 6.28 (dd, $J = 8.8, 6.4$ Hz, 1H), 3.86 (dd, $J = 7.8, 4.2$ Hz, 1H), 3.16 (s, 2H), 2.44 (m, 1H), 2.32 (m, 1H), 1.83–1.74 (m, 10H), 1.54 (dd, $J = 12.0, 8.0$ Hz, 1H), 1.45–1.35 (m, 2H), 1.32–1.17 (m, 6H), 1.15 (s, 3H), 0.87 (s, 3H), 0.80 (t, $J = 7.0$ Hz, 3H); ^{13}C NMR (100 MHz, CDCl_3) δ 195.0 (C), 147.4 (CH), 139.7 (CH), 137.7 (C), 129.4 (C), 64.9 (CH), 49.83 (C), 49.76 (CH₂), 47.3 (C), 44.5 (CH), 35.1 (CH₂), 32.2 (CH₂), 31.4 (CH₂), 28.6 (CH₂), 28.5 (CH₂), 26.6 (CH₂), 22.1 (CH₂), 20.5 (CH₃), 19.9 (CH₃), 14.5 (CH₃), 13.7 (CH₃), 11.9 (CH₃); HRMS (ESI-TOF) m/z : $[\text{M} + \text{H}]^+$ calcd for $\text{C}_{22}\text{H}_{36}\text{NO}_3\text{S}^+$: 394.2410, found: 394.2412.

(1*Z*,4*E*)-2-[(3*aS*,6*R*,7*aR*)-8,8-Dimethyl-2,2-dioxidohexahydro-1*H*-3*a*,6-methanobenzo[*c*]isothiazol-1-yl]-4-methyl-1-phenylhexa-1,4-dien-3-one (**11c**). This was prepared according to General Method B using ynamide **7c** (473 mg, 1.5 mmol), DCM (15 mL), $\text{Pd}(\text{PPh}_3)_4$ (87 mg, 0.075 mmol), Bu_3SnH (0.420 mL, 1.58 mmol), tigloyl chloride (181 μL , 1.65 mmol), and CuTC (29 mg, 0.15 mmol). Flash chromatography (silica gel, hexanes/toluene/EtOAc) gave the title compound **11c** as a white solid (91.2 mg, 15%): mp 143–146 °C; ^1H NMR (400 MHz, CDCl_3) δ 7.56 (d, $J = 4.0$ Hz, 2H), 7.40–7.28 (m, 3H), 6.90 (s, 1H), 6.88 (q, $J = 7.2$ Hz, 1H), 3.70 (br. s, 1H), 3.19 (s, 1H), 1.89 (s, 3H), 1.87 (d, $J = 7.2$ Hz, 3H), 1.85–1.55 (m, 4H), 1.33 (m, 1H), 1.15 (s, 3H), 1.05–0.90 (m, 3H), 0.86 (s, 3H); ^{13}C NMR (100 MHz, CDCl_3) δ 196.0 (C), 143.4 (CH), 137.9 (C), 133.1 (C), 129.7 (C), 129.4 (CH), 128.9 (CH), 127.9 (CH, 2C), 65.6 (CH, broad), 50.6 (C), 49.8 (CH₂), 47.5 (C), 44.3 (CH), 35.0 (CH₃), 32.7 (CH₂), 26.6 (CH₂), 20.4 (CH₃), 20.3 (CH₃), 15.0 (CH₃), 11.7 (CH₃); HRMS (ESI-TOF) m/z : $[\text{M} + \text{H}]^+$ calcd for $\text{C}_{23}\text{H}_{30}\text{NO}_3\text{S}^+$: 400.1941, found: 400.1944.

(*S*)-4-Benzyl-3-[(1*Z*,4*E*)-4-methyl-3-oxo-1-phenylhexa-1,4-dien-2-yl]oxazolidin-2-one (**11f**). This was prepared according to General Method B using ynamide **7f** (418 mg, 1.51 mmol), DCM (10 mL), Pd(PPh₃)₄ (52 mg, 0.045 mmol), Bu₃SnH (0.43 mL, 1.58 mmol), tigloyl chloride (144 μL, 1.31 mmol), and CuTC (29 mg, 0.15 mmol). Flash chromatography (silica gel, 17:82:1 EtOAc/hexanes/Et₃N) gave the title compound **11f** as a white solid (366 mg, 67%): mp = 130–132 °C; ¹H NMR (400 MHz, CDCl₃) δ 7.53 (m, 2H), 7.48–7.38 (m, 3H), 7.19–7.12 (m, 3H), 7.00 (s, 1H), 6.77 (m, 2H), 6.66 (qq, *J* = 6.9, 1.3 Hz, 1H), 4.25 (m, 1H), 4.17–4.06 (m, 2H), 2.81 (dd, *J* = 13.6, 4.5 Hz, 1H), 2.65 (dd, *J* = 13.6, 9.5 Hz, 1H), 1.94 (m, *J* < 1.3 Hz, 3H), 1.88 (dq, *J* = 6.9, 1.0 Hz, 3H); ¹³C NMR (100 MHz, CDCl₃) δ 194.2 (C), 156.8 (C), 140.9 (CH), 137.0 (C), 135.63 (C), 135.56 (CH), 133.2 (C), 132.4 (C), 129.7 (CH), 129.3 (CH), 128.8 (CH), 128.7 (CH), 128.6 (CH), 126.8 (CH), 68.4 (CH₂), 56.2 (CH), 38.4 (CH₂), 14.7 (CH₃), 12.3 (CH₃); HRMS (ESI-TOF) *m/z*: [M + H]⁺ calcd for C₂₃H₂₄NO₃⁺: 362.1751, found: 362.1758.

(4*S*,5*R*)-3-[(2*E*,5*Z*)-3-Methyl-4-oxoundeca-2,5-dien-5-yl]-4,5-diphenyloxazolidin-2-one (**11h**). This was prepared according to General Method B using ynamide **7h** (1.00 g, 3.003 mmol), DCM (30 mL), Pd(PPh₃)₄ (173 mg, 5 mol %), Bu₃SnH (0.848 mL, 3.15 mmol), tigloyl chloride (395 μL, 3.609 mmol), and CuTC (57.26 mg, 0.3 mmol). Flash chromatography (silica gel, 12:88 EtOAc/hexanes) gave the title compound **11h** as a thick oil. (1.158 g, 93%): ¹H NMR (400 MHz, CDCl₃) δ 7.19–6.92 (m, 8H), 6.80–6.70 (m, 2H), 6.23 (dd, *J* = 8.9, 5.6 Hz, 1H), 5.93 (d, *J* = 8.7 Hz, 1H), 5.68 (qd, *J* = 6.9, 1.4 Hz, 1H), 5.53 (d, *J* = 8.7 Hz, 1H), 2.47–2.17 (m, 2H), 1.76–1.68 (m, 3H), 1.61 (dd, *J* = 6.9, 1.1 Hz, 3H), 1.52–1.38 (m, 1H), 1.36–1.16 (m, 5H), 0.88 (t, *J* = 6.9 Hz, 3H); ¹³C NMR (101 MHz, CDCl₃) δ 194.0, 156.2, 144.8, 138.5, 137.1, 135.4, 134.2, 132.7, 128.7, 128.5, 128.1, 128.0, 126.1, 79.8, 64.7, 31.9, 29.1, 28.0, 22.5, 14.5, 14.1, 12.4; HRMS (ESI-TOF) *m/z*: [M + H]⁺ calcd for C₂₇H₃₂NO₃⁺: 418.2377, found: 418.2381.

(4*S*,5*R*)-3-[(1*Z*,4*E*)-4-Methyl-3-oxo-1-phenylhexa-1,4-dien-2-yl]-4,5-diphenyloxazolidin-2-one (**11i**). This was prepared according to General Method B using ynamide **7i** (678 mg, 2.5 mmol), DCM (20 mL), Pd(PPh₃)₄ (115.55 mg, 0.1 mmol), Bu₃SnH (0.565 mL, 2.1 mmol), tigloyl chloride (241 μL, 2.193 mmol), and CuTC (38.13 mg, 0.2 mmol). Flash chromatography (silica gel, 19:81 EtOAc/hexanes) gave the title compound **11i** as a low-melting solid. 424.191 (658 mg, 78%): mp = 66–68 °C; ¹H NMR (400 MHz, CDCl₃) δ 7.42–7.30 (m, 5H), 7.15–7.10 (m, 3H), 6.98 (m, 3H), 6.84 (dd, *J* = 13.5, 6.0 Hz, 3H), 6.53 (dd, *J* = 8.2, 1.0 Hz, 2H), 6.35 (qd, *J* = 6.9, 1.3 Hz, 1H), 5.83 (d, *J* = 8.8 Hz, 1H), 5.41 (d, *J* = 8.7 Hz, 1H), 1.87–1.85 (m, 3H), 1.76 (dd, *J* = 6.9, 1.1 Hz, 3H); ¹³C NMR (101 MHz, CDCl₃) δ 193.91, 156.77, 140.57, 137.36, 135.8, 135.3, 133.6, 132.9, 132.2, 129.5, 129.5, 128.7, 128.6, 128.2, 128.1, 127.869, 127.6, 126.3, 80.4, 65.0, 14.8, 12.5. HRMS (ESI-TOF) *m/z*: [M + H]⁺ calcd for C₂₈H₂₆NO₃⁺: 424.1907, found: 424.1910.

Tributyl(cyclohex-1-en-1-yl)stannane (**14**). *t*-BuLi (1.31 M in pentane, 5.7 mL, 7.45 mmol) was added slowly to a solution of 1-bromocyclohex-1-ene (0.42 mL, 3.726 mmol) and anhydrous THF (6.2 mL) at –78 °C, and the reaction was stirred for 1 h at –78 °C. Bu₃SnCl (1.1 mL, 3.912 mmol) was slowly added, and the reaction was allowed to warm to rt and stir for 18 h. K₂CO₃ aq (10% w/v, 12 mL) was added to the reaction. The mixture was extracted with Et₂O (2 × 12 mL), washed with H₂O (2 × 12 mL), and brine (2 × 12 mL). It was then dried over MgSO₄ and concentrated under reduced pressure, yielding tributyl(cyclohex-1-en-1-yl)stannane as a colorless liquid (1.33 g, 96%): ¹H NMR (401 MHz, CDCl₃) δ 5.79 (m, 1H), 2.20–2.10 (m, 2H), 2.09–1.99 (m, 2H), 1.66–1.57 (m, 4H), 1.53–1.42 (m, 6H), 1.37–1.25 (m, 6H), 0.92–0.81 (m, 15H).²⁸

(4*S*,5*R*)-3-[(*Z*)-3-(Cyclohex-1-en-1-yl)-3-oxo-1-phenylprop-1-en-2-yl]-4,5-diphenyloxazolidin-2-one (**11l**). Bromoenamide **13b** (461.6 mg, 1.10 mmol), cyclohexenyl stannane **14** (530 mg, 1.4277 mmol), Pd(dppf)Cl₂ (44.8 mg, 0.0549 mmol), CuTC (20.9 mg, 0.11 mmol), and anhydrous THF (11 mL) were added to a flame-dried round-bottom flask. The reaction was evacuated and backfilled with CO(g) 3 times and then heated to 50 °C overnight under CO(g) (balloon). The reaction was then diluted with water (15 mL), extracted with

EtOAc (2 × 15 mL), and washed with water (2 × 15 mL) and brine (2 × 15 mL). It was dried over MgSO₄ and concentrated under reduced pressure. Flash chromatography (NEt₃ treated silica gel, 15:85 EtOAc/hexanes) yielded the title compound **11l** as an off-white syrup (432.3 mg, 88%): ¹H NMR (400 MHz, CDCl₃) δ 7.40–7.38 (m, 3H), 7.32–7.29 (m, 2H), 7.11–7.09 (m, 3H), 6.98–6.94 (m, 3H), 6.84–6.81 (m, 3H), 6.56–6.54 (m, 1H), 6.52 (dd, *J* = 8.17, 0.97 Hz, 2H), 5.82 (d, *J* = 8.77 Hz, 1H), 5.39 (d, *J* = 8.75 Hz, 1H), 2.57–2.51 (m, 1H), 2.17–2.03 (m, 3H), 1.68–1.57 (m, 4H); ¹³C NMR (101 MHz, CDCl₃) δ 193.1, 156.8, 143.19, 138.6, 135.6, 135.3, 133.7, 132.8, 132.2, 129.5, 129.4, 128.7, 128.6, 128.2, 128.1, 127.9, 127.6, 126.3, 80.5, 65.0, 26.1, 24.1, 22.0, 21.6; HRMS (ESI-TOF) *m/z*: [M + H]⁺ calcd for C₃₀H₂₇NO₃⁺: 450.2064, found: 450.2058.

(4*S*,5*R*)-3-[(1*Z*,4*E*)-4-(4-Methoxyphenyl)-3-oxo-1-phenylocta-1,4-dien-2-yl]-4,5-diphenyloxazolidin-2-one (**11m**). To a solution of bromoenamide **13b** (700 mg, 1.67 mmol) in THF (20 mL), the vinyl stannane **16** (1012 mg, 2.171 mmol) was added along with CuTC (31.9 mg, 0.167 mmol) and Pd(dppf)Cl₂ (68.2 mg, 0.083 mmol). The reaction was heated for 15 h at 50 °C under an atmosphere of CO (g) (balloon), after which TLC revealed complete consumption of **13b**. The reaction mixture was diluted with water and extracted with EtOAc, dried over MgSO₄, evaporated in vacuo and chromatographed (silica gel, 30% EtOAc in hexane). This gave the product as a yellow solid (728 mg, 80.2%): mp = 115–118 °C; ¹H NMR (400 MHz, CDCl₃) δ 7.45–7.28 (m, 5H), 7.10 (dd, *J* = 8.4, 4.8 Hz, 4H), 7.05–6.92 (m, 5H), 6.91–6.74 (m, 4H), 6.50 (d, *J* = 7.2 Hz, 2H), 6.30 (t, *J* = 7.5 Hz, 1H), 5.85 (d, *J* = 8.7 Hz, 1H), 5.55 (d, *J* = 8.7 Hz, 1H), 3.78 (s, 3H), 2.16 (ddd, *J* = 14.7, 7.3, 1.5 Hz, 2H), 1.37 (h, *J* = 7.4 Hz, 2H), 0.83 (t, *J* = 7.4 Hz, 3H); ¹³C NMR (101 MHz, CDCl₃) δ 193.0, 158.9, 157.2, 143.8, 140.4, 139.6, 135.2, 133.3, 133.0, 133.0, 130.6, 129.8, 129.6, 128.6, 128.5, 128.3, 128.2, 128.0, 127.8, 127.7, 126.2, 113.7, 80.2, 65.3, 55.2, 31.5, 22.4, 13.9; HRMS (ESI-TOF) *m/z*: [M + H]⁺ calcd for C₃₆H₃₄NO₄⁺: 544.2482, found: 544.2486.

(4*S*,5*R*)-3-[(4*E*,7*Z*)-5-(4-Methoxyphenyl)-6-oxotrideca-4,7-dien-7-yl]-4,5-diphenyloxazolidin-2-one (**11n**). This was prepared according to the procedure described for **11m**: bromoenamide **13c** (400 mg, 0.969 mmol), vinyl stannane **16** (587 mg, 1.26 mmol), CuTC (18.4 mg, 0.10 mmol), Pd(dppf)Cl₂ (40 mg, 0.48 mmol), and THF (10 mL). Flash chromatography (silica gel, 30% EtOAc in hexane) gave the product **11n** as a thick oil (380 mg, 73.1%): ¹H NMR (400 MHz, CDCl₃) δ 7.21–6.90 (m, 8H), 6.73 (m, 6H), 6.37 (dd, *J* = 9.4, 4.9 Hz, 1H), 5.98–5.83 (m, 2H), 5.77 (d, *J* = 8.7 Hz, 1H), 3.75 (s, 3H), 2.45–2.30 (m, 1H), 2.20 (tt, *J* = 14.7, 7.3 Hz, 1H), 2.05 (q, *J* = 7.5 Hz, 2H), 1.38–0.93 (m, 8H), 0.81 (dt, *J* = 12.3, 7.3 Hz, 6H); ¹³C NMR (101 MHz, CDCl₃) δ 207.4, 192.9, 158.82, 156.40, 147.7, 142.45, 140.40, 135.5, 134.3, 133.4, 130.4, 128.8, 128.5, 128.3, 128.1, 128.0, 128.0, 126.0, 113.7, 79.8, 64.6, 55.2, 31.7, 31.3, 30.7, 30.5, 30.3, 30.1, 29.9, 29.18, 27.9, 22.57, 22.4, 14.0, 13.9. HRMS (ESI-TOF) *m/z*: [M + H]⁺ calcd for C₃₅H₄₀NO₄⁺: 538.2952, found: 538.2956.

(4*S*,5*R*)-3-[(1*Z*,4*E*)-3-Oxo-1,5-diphenylpenta-1,4-dien-2-yl]-4,5-diphenyloxazolidin-2-one (**11o**). This was prepared according to General Method B using ynamide **7i** (300 mg, 0.884 mmol), Pd(PPh₃)₄ (30.6 mg, 0.027 mmol), Bu₃SnH (0.23 mL, 0.884 mmol), cinnamoyl chloride (147.3 mg, 0.884 mmol), CuTC (10.1 mg, 0.0530 mmol), and DCM (4.4 mL). Flash chromatography (silica gel, 15:85 EtOAc/hexanes) yielded **11o** as yellow oil (284.2 mg, 68%): ¹H NMR (401 MHz, CDCl₃) δ 7.72 (d, *J* = 15.7 Hz, 1H), 7.56 (dd, *J* = 6.7, 2.8 Hz, 2H), 7.47–7.37 (m, 9H), 7.21 (d, *J* = 15.7 Hz, 1H), 7.15–7.08 (m, 3H), 7.01–6.94 (m, 3H), 6.81 (t, *J* = 7.8 Hz, 2H), 6.46 (d, *J* = 7.2 Hz, 2H), 5.88 (d, *J* = 8.7 Hz, 1H), 5.46 (d, *J* = 8.7 Hz, 1H); ¹³C NMR (101 MHz, CDCl₃) δ 186.8, 157.5, 145.3, 137.9, 135.2, 134.7, 134.3, 133.4, 132.8, 130.7, 130.0, 129.6, 129.0, 128.7, 128.7, 128.6, 128.3, 128.1, 127.9, 127.7, 126.2, 121.4, 80.5, 65.6; HRMS (ESI-TOF) *m/z*: [M + H]⁺ calcd for C₃₂H₂₆NO₃⁺: 472.1907, found: 472.1907.

(*S*,*Z*)-3-[1-(3-Methoxyphenyl)-1-oxooct-2-en-2-yl]-4-phenyloxazolidin-2-one (**11r**). This was prepared according to General Method B using ynamide **7d** (515 mg, 2.0 mmol), DCM (10 mL), Pd(PPh₃)₄ (116 mg, 0.10 mmol), Bu₃SnH (0.56 mL, 2.1 mmol), 3-methoxybenzoyl chloride (310 μL, 2.2 mmol), and CuTC (38.2 mg, 0.10 mmol). Flash chromatography (silica gel, 18:82 EtOAc/hexanes)

gave the title compound as a thick oil (687 mg, 87%): ^1H NMR (400 MHz, CDCl_3) δ 7.38–7.27 (m, 5H), 7.23 (t, J = 7.8 Hz, 1H), 7.02 (ddd, J = 8.3, 2.7, 0.9 Hz, 1H), 6.87–6.83 (m, 2H), 6.36 (dd, J = 8.8, 5.6 Hz, 1H), 5.28 (t_{app} , J = 8.8 Hz, 1H), 4.78 (t_{app} , J = 8.8 Hz, 1H), 4.38 (t_{app} , J = 9.0 Hz, 1H), 3.74 (s, 3H), 2.34 (m, 1H), 2.20 (m, 1H), 1.37 (m, 1H), 1.30–1.10 (m, 5H), 0.86 (t, J = 7.0 Hz, 3H); ^{13}C NMR (100 MHz, CDCl_3) δ 191.7 (C), 159.0 (C), 155.7 (C), 148.6 (CH), 138.6 (C), 136.6 (C), 132.5 (C), 128.93 (CH), 128.89 (CH), 128.7 (CH), 127.6 (CH), 121.1 (CH), 118.4 (CH), 113.1 (CH), 69.7 (CH₂), 59.7 (CH), 54.9 (CH₃), 31.3 (CH₃), 28.8 (CH₃), 27.5 (CH₃), 22.0 (CH₃), 13.6 (CH₃); HRMS (ESI-TOF) m/z : $[\text{M} + \text{H}]^+$ calcd for $\text{C}_{24}\text{H}_{28}\text{NO}_4^+$: 394.2013, found: 394.2011.

(4*S*,5*R*)-3-[(*Z*)-3-(3-Methoxyphenyl)-3-oxo-1-phenylprop-1-en-2-yl]-4,5-diphenyloxazolidin-2-one (**11s**). This was prepared according to General Method B using ynamide **7i** (577 mg, 1.70 mmol), DCM (15 mL), $\text{Pd}(\text{PPh}_3)_4$ (98 mg, 0.085 mmol), Bu_3SnH (0.50 mL, 1.79 mmol), 3-methoxybenzoyl chloride (225 μL , 1.60 mmol), and CuTC (32 mg, 0.17 mmol). Flash chromatography (silica gel, 21:79 EtOAc/hexanes) gave the title compound **11s** as a thick gum (610 mg, 75%): ^1H NMR (400 MHz, CDCl_3) δ 7.46–7.38 (m, 5H), 7.30–7.23 (m, 1H), 7.18–7.12 (m, 5H), 7.09–7.00 (m, 4H), 6.99 (s, 1H), 6.92–6.83 (m, 2H), 6.57 (dd, J = 8.2, 1.0 Hz, 2H), 5.91 (d, J = 8.7 Hz, 1H), 5.57 (d, J = 8.7 Hz, 1H), 3.77 (s, 3H); ^{13}C NMR (100 MHz, CDCl_3) δ 192.2 (C), 159.4 (C), 156.8 (C), 139.8 (CH), 138.7 (C), 135.1 (C), 133.1 (C), 132.7 (C), 132.4 (C), 129.9 (CH), 129.6 (CH), 129.2 (CH), 128.6 (CH), 128.5 (CH), 128.3 (CH), 128.0 (CH), 127.8 (CH), 127.6 (CH), 126.1 (CH), 122.3 (CH), 119.0 (CH), 113.7 (CH), 80.3 (CH), 65.1 (CH), 55.4 (CH₃); HRMS (ESI-TOF) m/z : $[\text{M} + \text{H}]^+$ calcd for $\text{C}_{31}\text{H}_{26}\text{NO}_4^+$: 476.1856, found: 476.1852.

(*S*,*Z*)-3-[(3,5-Dimethoxyphenyl)-1-(4-methoxyphenyl)-3-oxoprop-1-en-2-yl]-4-isopropoxyloxazolidin-2-one (**11t**). This was prepared according to General Method B using ynamide **7k** (324 mg, 1.25 mmol), DCM (12 mL), $\text{Pd}(\text{PPh}_3)_4$ (72 mg, 0.063 mmol), Bu_3SnH (0.37 mL, 1.31 mmol), 3,5-dimethoxybenzoyl chloride (231 mg, 1.15 mmol), and CuTC (24 mg, 0.13 mmol). Flash chromatography (silica gel, 27:73 EtOAc/hexanes) gave the title compound **11t** as a yellow gum (358 mg, 67%): ^1H NMR (400 MHz, CDCl_3) δ 7.56 (d, J = 8.7 Hz, 2H), 7.32 (s, 1H), 6.91 (d, J = 8.7 Hz, 2H), 6.90 (d, J = 2.3 Hz, 2H), 6.65 (t, J = 2.3 Hz, 1H), 4.47 (t, J = 8.7 Hz, 1H), 4.21 (dd, J = 8.5, 7.3 Hz, 1H), 3.92 (ddd, J = 8.8, 7.3, 5.7 Hz, 1H), 3.84 (s, 3H), 3.82 (s, 6H), 1.82 (septet, J = 6.9, 5.7 Hz, 1H), 0.87 (d, J = 6.9 Hz, 3H), 0.85 (d, J = 6.9 Hz, 3H); ^{13}C NMR (100 MHz, CDCl_3) δ 192.4 (C), 161.5 (C), 160.6 (C), 157.6 (C), 142.3 (CH), 139.7 (C), 132.4 (CH), 131.3 (C), 125.3 (C), 114.3 (CH), 107.2 (CH), 104.4 (CH), 65.8 (CH₂), 61.4 (CH), 55.6 (CH₃), 55.3 (CH₃), 30.9 (CH), 18.7 (CH₃), 16.8 (CH₃); HRMS (ESI-TOF) m/z : $[\text{M} + \text{H}]^+$ calcd for $\text{C}_{24}\text{H}_{28}\text{NO}_6^+$: 426.1911, found: 426.1913.

(*S*,*Z*)-3-[1-(Furan-2-yl)-4-methyl-1-oxopent-2-en-2-yl]-4-phenyloxazolidin-2-one (**11aa**). This was prepared according to General Method B using ynamide **7j** (229 mg, 1.00 mmol), DCM (10 mL), $\text{Pd}(\text{PPh}_3)_4$ (35 mg, 0.030 mmol), Bu_3SnH (0.28 mL, 1.05 mmol), furanoyl chloride (108 μL , 1.10 mmol) and CuTC (19 mg, 0.10 mmol). Flash chromatography (silica gel, 25:75 EtOAc/hexanes) gave the title compound as a discolored solid (254 mg, 78%): (mp = 138–140 °C); ^1H NMR (400 MHz, CDCl_3) δ 7.59 (d, J = 1.6 Hz, 1H), 7.40–7.22 (m, 5H), 6.92 (d, J = 3.4 Hz, 1H), 6.64 (d, J = 10.8 Hz, 1H), 6.48 (dd, J = 3.4, 1.6 Hz, 1H), 5.13 (t_{app} , J = 8.6 Hz, 1H), 4.77 (t_{app} , J = 8.9 Hz, 1H), 4.39 (t_{app} , J = 8.5 Hz, 1H), 2.68 (m, 1H), 1.10 (d, J = 6.6 Hz, 3H), 0.66 (d, J = 6.6 Hz, 3H); ^{13}C NMR (100 MHz, CDCl_3) δ 178.0 (C), 156.7 (C), 153.8 (CH), 151.6 (C), 146.9 (CH), 137.2 (C), 129.8 (C), 129.1 (CH), 129.0 (CH), 127.8 (CH), 119.9 (CH), 112.0 (CH), 69.9 (CH₂), 60.5 (CH), 28.8 (CH), 21.7 (CH₃), 21.2 (CH₃); HRMS calcd for $\text{C}_{21}\text{H}_{24}\text{NO}_4^+$: 326.1387, found: 326.1387.

(4*S*,5*R*)-5-[(3*aS*,6*R*,7*aR*)-8,8-Dimethyl-2,2-dioxidotetrahydro-3*H*-3*a*,6-methanobenzo[*c*]isothiazol-1(4*H*)-yl]-2,3-dimethyl-4-pentylcyclopent-2-en-1-one (**12b**). This was prepared according to General Method C using **11b** (5.9 mg, 0.015 mmol) in DCM (1.5 mL) with MeSO_3H (0.1 M in DCM, 1.5 mL, 0.15 mmol), warmed to rt, and stirred overnight. Preparative TLC (silica gel, 15:85 EtOAc/hexanes) gave the title compound as an oil (4.7 mg, 80%): ^1H NMR (400 MHz,

CDCl_3) δ 3.79 (dd, J = 7.8, 4.6 Hz, 1H), 3.57 (d, J = 3.2 Hz, 1H), 3.23–3.12 (m, 3H), 2.01 (s, 3H), 1.93–1.78 (m, 5H), 1.71 (d, J = 0.8 Hz, 3H), 1.54–1.43 (m, 3H), 1.38–1.13 (m, 7H), 1.21 (s, 3H), 0.91 (s, 3H), 0.87 (t, J = 6.8 Hz, 3H); ^{13}C NMR (100 MHz, CDCl_3) δ 205.4 (C), 171.1 (C), 135.9 (C), 64.8 (CH), 59.0 (CH), 50.1 (CH₂), 49.7 (C), 47.6 (C), 44.9 (CH), 43.5 (CH), 35.0 (CH₂), 32.5 (CH₂), 32.0 (CH₂), 30.5 (CH₂), 26.8 (CH₂), 25.2 (CH₂), 22.5 (CH₂), 20.3 (CH₃), 20.1 (CH₃), 15.2 (CH₃), 14.0 (CH₃), 8.2 (CH₃). HRMS (ESI-TOF) m/z : $[\text{M} + \text{H}]^+$ calcd for $\text{C}_{22}\text{H}_{36}\text{NO}_3\text{S}^+$: 394.2410, found: 394.2412.

5-[(3*aS*,6*R*,7*aR*)-8,8-Dimethyl-2,2-dioxidohexahydro-1*H*-3*a*,6-methanobenzo[*c*]isothiazol-1-yl]-2,3-dimethyl-4-phenylcyclopent-2-enone (**12c**). This was prepared according to General Method C using **11c** (87 mg, 0.217 mmol) in DCM (2.2 mL) with MeSO_3H (140 μL , 2.17 mmol) and stirred at rt for 24h. The crude product was of good purity (86 mg, 99%), and further purification by flash chromatography (silica gel, 6:94 EtOAc/hexanes) gave a cleaner product but with significant loss of mass (54 mg, 63%): mp = 102–104 °C; ^1H NMR (400 MHz, CDCl_3) δ 7.32 (t, J = 7.2 Hz, 2H), 7.26 (t, J = 7.4 Hz, 1H), 7.13 (d, J = 7.6 Hz, 2H), 4.35 (br. s, 1H), 3.89 (dd, J = 7.6, 4.8 Hz, 1H), 3.65 (d, J = 3.2 Hz, 1H), 3.19 (s, 2H), 1.87 (s, 3H), 1.85–1.80 (m, 4H), 1.78 (m, 1H), 1.63 (m, 1H), 1.52–1.43 (m, 2H), 1.30–1.20 (m, 2H), 1.11 (s, 3H), 0.90 (s, 3H); ^{13}C NMR (100 MHz, CDCl_3) δ 205.2 (C), 169.5 (C), 139.8 (C), 136.7 (C), 128.9 (CH), 127.8 (CH), 127.3 (CH), 65.1 (CH), 63.9 (CH), 50.7 (CH), 50.4 (CH₂), 49.9 (C), 47.5 (C), 44.8 (CH), 35.0 (CH₂), 32.3 (CH₂), 26.7 (CH₂), 20.3 (CH₃), 20.0 (CH₃), 15.7 (CH₃), 8.4 (CH₃); HRMS (ESI-TOF) m/z : $[\text{M} + \text{H}]^+$ calcd for $\text{C}_{23}\text{H}_{30}\text{NO}_3\text{S}^+$: 400.1941, found: 400.1948.

(5)-4-Benzyl-3-[(1*R*,5*S*)-3,4-dimethyl-2-oxo-5-phenylcyclopent-3-en-1-yl]oxazolidin-2-one (**12f**). This was prepared according to General Method C using **11f** (50 mg, 0.138 mmol) in DCM (1.4 mL) with MeSO_3H (90 μL , 1.38 mmol). It was warmed to rt and stirred for 3 days. Trituration with 4:1 hexanes/Et₂O gave the title compound as a white solid (42.5 mg, 85%): mp = 240–242 °C; ^1H NMR (400 MHz, CDCl_3) δ 7.38 (m, 2H), 7.30 (m, 1H), 7.23–7.13 (m, 5H), 6.87 (m, 2H), 4.34–4.16 (m, 3H), 3.97 (dd, J = 8.2, 6.7 Hz, 1H), 3.63 (d, J = 4.2 Hz, 1H), 2.44 (dd, J = 13.8, 4.4 Hz, 1H), 2.32 (dd, J = 13.8, 9.1 Hz, 1H), 1.84 (s, 6H); ^{13}C NMR (100 MHz, CDCl_3) δ 202.8 (C), 168.5 (C), 157.3 (C), 139.7 (C), 136.0 (C), 135.0 (C), 129.1 (CH), 128.7 (CH), 128.6 (CH), 127.9 (CH), 127.6 (CH), 126.9 (CH), 67.6 (CH₂), 66.4 (CH), 58.5 (CH), 53.0 (CH), 39.7 (CH₂), 15.4 (CH₃), 8.4 (CH₃); HRMS (ESI-TOF) m/z : $[\text{M} + \text{H}]^+$ calcd for $\text{C}_{23}\text{H}_{24}\text{NO}_3^+$: 362.1751, found: 362.1746.

(4*S*,5*R*)-3-[(1*R*,5*S*)-3,4-Dimethyl-2-oxo-5-pentylcyclopent-3-en-1-yl]-4,5-diphenyloxazolidin-2-one (**12h**). This was prepared according to General Method C using **11h** (400 mg, 0.959 mmol) in DCM (9.5 mL) with MeSO_3H (621 μL , 9.59 mmol). It was warmed to rt and stirred overnight. Flash chromatography (silica gel, 15% EtOAc in hexane) gave the title compound as yellow solid (391.2 mg, 98%): mp = 126–127 °C. ^1H NMR (400 MHz, CDCl_3) δ 7.18–7.02 (m, 6H), 7.03–6.86 (m, 4H), 5.95 (d, J = 8.8 Hz, 1H), 5.49 (d, J = 8.8 Hz, 1H), 3.41 (d, J = 1.2 Hz, 1H), 3.25 (d, J = 3.7 Hz, 1H), 1.94 (s, 3H), 1.67 (d, J = 1.0 Hz, 3H), 1.46–1.21 (m, 3H), 1.11–0.90 (m, 4H), 0.74 (t, J = 7.1 Hz, 4H); ^{13}C NMR (101 MHz, CDCl_3) δ 193.91, 156.77, 140.57, 137.36, 135.80, 135.3, 133.6, 132.9, 132.2, 129.5, 129.4, 128.6, 128.5, 128.2, 128.0, 127.8, 127.6, 126.2, 80.4, 64.9, 14.7, 12.4; HRMS (ESI-TOF) m/z : $[\text{M} + \text{H}]^+$ calcd for $\text{C}_{27}\text{H}_{32}\text{NO}_3^+$: 418.2377, found: 418.2382.

(4*S*,5*R*)-3-[(1*R*,5*S*)-3,4-Dimethyl-2-oxo-5-phenylcyclopent-3-en-1-yl]-4,5-diphenyloxazolidin-2-one (**12i**). This was prepared according to General Method C using **11i** (200 mg, 0.428 mmol) in DCM (5 mL) with MeSO_3H (306 μL , 4.73 mmol). It was warmed to rt and stirred for 2 days. Flash chromatography (silica gel, 20% EtOAc in hexane) gave the title compound as clear resin (196 mg, 98%): ^1H NMR (400 MHz, CDCl_3) δ 7.22–7.15 (m, 3H), 7.09–7.02 (m, 3H), 6.96 (dd, J = 6.6, 2.9 Hz, 2H), 6.86 (m, 3H), 6.64 (t, J = 7.6 Hz, 2H), 6.41 (d, J = 7.2 Hz, 2H), 5.85 (d, J = 8.7 Hz, 1H), 5.58 (d, J = 8.7 Hz, 1H), 4.64–4.55 (m, 1H), 3.36 (d, J = 4.4 Hz, 1H), 1.81 (d, J = 2.8 Hz, 6H); ^{13}C NMR (101 MHz, CDCl_3) δ 204.0, 169.2, 158.1, 139.8,

136.0, 135.1, 133.1, 129.0, 128.2, 128.1, 128.0, 128.0, 127.9 (2C), 127.5, 126.2, 79.9, 67.8, 66.8, 52.6, 15.6, 8.6; HRMS (ESI-TOF) m/z : $[M + H]^+$ calcd for $C_{28}H_{26}NO_3^+$: 424.1907, found: 424.1913.

(4*S*,5*R*)-3-((2*R*,3*S*)-1-oxo-3-pentyl-2,3,4,5,6,7-hexahydro-1*H*-inden-2-yl)-4,5-diphenyloxazolidin-2-one (**12l**). This was prepared according to General Method C using **11l** (87.0 mg, 0.194 mmol) DCM (1.9 mL), and $MeSO_3H$ (0.13 mL, 1.94 mmol). It was kept at rt for 48 h. Flash chromatography (silica gel, 20:80 EtOAc/hexanes) gave **12l** as pale yellow oil (73.7 mg, 85%): 1H NMR (401 MHz, $CDCl_3$) δ 7.21–7.17 (m, 3H), 7.07–7.03 (m, 3H), 6.97–6.95 (m, 2H), 6.90–6.82 (m, 3H), 6.64 (t, J = 7.6 Hz, 2H), 6.41 (d, J = 7.2 Hz, 2H), 5.85 (d, J = 8.7 Hz, 1H), 5.57 (d, J = 8.7 Hz, 1H), 4.64 (d, J = 1.6 Hz, 1H), 3.38 (d, J = 4.3 Hz, 1H), 2.39–1.90 (m, 4H), 1.74–1.57 (m, 4H); ^{13}C NMR (101 MHz, $CDCl_3$) δ 203.0, 172.4, 185.1, 139.5, 138.0, 135.1, 133.1, 128.9, 128.1, 128.0, 127.9, 127.8, 127.3, 126.1, 79.7, 67.7, 67.1, 51.5, 26.3, 22.2, 21.4, 20.1; HRMS (ESI-TOF) m/z : $[M + H]^+$ calcd for $C_{30}H_{37}NO_3^+$: 450.2064, found: 450.207.

(4*S*,5*R*)-3-((1*R*,5*S*)-3-(4-methoxyphenyl)-2-oxo-5-phenyl-4-propylcyclopent-3-en-1-yl)-4,5-diphenyloxazolidin-2-one (**12m**). This was prepared according to General Method C using **11m** (350 mg, 0.644 mmol) in DCM (6 mL) with $MeSO_3H$ (417 μ L, 6.44 mmol). It was heated to 50 °C for 2 days. Flash chromatography (silica gel, 20% EtOAc in hexane) gave the title compound as an oil (346 mg, 100%, including 7% of the minor *cis*-isomer): 1H NMR (400 MHz, $CDCl_3$) δ 7.25 (m, 5H), 7.08 (m, 5H), 6.95 (d, J = 8.8 Hz, 2H), 6.92–6.85 (m, 3H), 6.67 (t, J = 7.6 Hz, 2H), 6.44 (d, J = 7.1 Hz, 2H), 5.85 (d, J = 8.7 Hz, 1H), 5.61 (d, J = 8.6 Hz, 1H), 3.83 (s, 3H), 3.50 (d, J = 4.5 Hz, 1H), 2.64–2.51 (m, 1H), 2.10–1.97 (m, 1H), 1.44 (m, 2H), 0.80 (t, J = 7.4 Hz, 3H); ^{13}C NMR (101 MHz, $CDCl_3$) δ 202.7, 173.4, 159.4, 158.2, 139.9, 139.8, 135.1, 133.1, 130.5, 129.1, 128.3, 128.2, 128.3, 128.2, 127.9, 127.9, 127.5, 126.2, 123.7, 113.9, 79.9, 67.6, 67.2, 55.4, 50.1, 31.3, 20.7, 13.9; HRMS (ESI-TOF) m/z : $[M + H]^+$ calcd for $C_{36}H_{44}NO_4^+$: 544.2482, found: 544.2486.

(4*S*,5*R*)-3-((1*R*,5*S*)-3-(4-methoxyphenyl)-2-oxo-5-pentyl-4-propylcyclopent-3-en-1-yl)-4,5-diphenyloxazolidin-2-one (**12n**). This was prepared according to General Method C using **11n** (26 mg, 0.048 mmol) in DCM (0.5 mL) with $MeSO_3H$ (32 μ L, 0.48 mmol). It was warmed to rt and stirred for 5 days. Flash chromatography (silica gel, 20% EtOAc in hexane) gave the title compound as an oil (24 mg, 92.3%): 1H NMR (400 MHz, $CDCl_3$) δ 7.17–7.04 (m, 8H), 6.95 (m, 6H), 5.95 (d, J = 8.7 Hz, 1H), 5.53 (d, J = 8.7 Hz, 1H), 3.81 (s, 3H), 3.58 (dd, J = 8.9, 4.8 Hz, 1H), 3.49 (d, J = 3.7 Hz, 1H), 2.68–2.56 (m, 1H), 2.21 (ddd, J = 13.9, 9.0, 5.1 Hz, 1H), 1.50–1.39 (m, 3H), 1.17–1.06 (m, 4H), 0.91–0.81 (m, 7H), 0.78 (t, J = 6.9 Hz, 3H); ^{13}C NMR (101 MHz, $CDCl_3$) δ 203.1, 175.3, 159.3, 157.9, 139.8, 135.3, 134.9, 130.5, 128.9, 128.8, 128.2, 128.2, 128.0, 126.1, 123.9, 113.8, 79.6, 67.4, 61.2, 55.4, 42.7, 32.1, 31.0, 29.6, 24.7, 22.4, 21.0, 14.11, 14.08; HRMS (ESI-TOF) m/z : $[M + H]^+$ calcd for $C_{35}H_{40}NO_4^+$: 538.2952, found: 538.2956.

(*S*)-3-[(1*R*,2*S*,3*R*)-3-methyl-4-methylene-5-oxo-2-pentyl-3-phenylcyclopentyl]-4-phenyloxazolidin-2-one (**12q**). This was prepared as a two-step one-pot procedure. The divinyl ketone **11q** was prepared according to General Method B using ynamide **7d** (51.5 mg, 0.20 mmol), DCM (1.3 mL), $Pd(PPh_3)_4$ (12 mg, 0.010 mmol), Bu_3SnH (0.056 mL, 0.21 mmol), (*E*)-2-methyl-3-phenylbut-2-enoyl chloride (41 mg, 0.21 mmol), and $CuTC$ (4.0 mg, 0.010 mmol). The crude product was dissolved in DCM (1.0 mL) and treated with $MeSO_3H$ (32 μ L, 0.48 mmol) for 1 h. A solution of $NaHCO_3$ aq (10% w/v, 3 mL) was added to the reaction mixture, followed by extraction with EtOAc (2 \times 10 mL). The organic layer was dried ($MgSO_4$) and concentrated under reduced pressure. Flash chromatography (silica gel, 20:80 EtOAc/hexanes) gave the title compound **12q** as a thick gum (37.5 mg, 45% from **7d**): 1H NMR (400 MHz, $CDCl_3$) δ 7.42 (s, 5H), 7.32–7.16 (m, 5H), 6.01 (s, 1H), 5.09 (t, J = 9.1 Hz, 1H), 4.78 (s, 1H), 4.71 (t, J = 8.7 Hz, 1H), 4.27 (t, J = 9.2 Hz, 1H), 3.55 (d, J = 12.2 Hz, 1H), 3.13 (dt, J = 12.2, 6.7 Hz, 1H), 1.31 (s, 3H), 1.27–1.13 (m, 2H), 1.13–0.86 (m, 6H), 0.72 (t, J = 7.0 Hz, 3H); ^{13}C NMR (100 MHz, $CDCl_3$) δ 201.6 (C), 158.4 (C), 154.7 (C), 146.7 (C), 136.2 (C), 129.5 (CH), 129.0 (CH), 128.7 (CH), 127.9 (CH), 127.4 (CH), 126.4 (CH), 120.6 (CH₂), 70.1 (CH₂), 63.9 (CH), 62.6 (CH), 47.7

(C), 45.9 (CH), 31.7 (CH₂), 28.6 (CH₂), 27.1 (CH₂), 22.1 (CH₂), 20.8 (CH₃), 13.8 (CH₃); HRMS (ESI-TOF) m/z : $[M + H]^+$ calcd for $C_{27}H_{32}NO_3^+$: 418.2377, found: 418.2389.

(*S*)-3-[(1*S*,2*R*)-5-methoxy-3-oxo-1-pentyl-2,3-dihydro-1*H*-inden-2-yl]-4-phenyloxazolidin-2-one (**12r**). This was prepared according to General Method C using **11r** (78.6, 0.2 mmol) in DCM (1.6 mL) with $MeSO_3H$ (32.7 μ L, 0.51 mmol). It was warmed to rt and stirred 3 h. Flash chromatography (silica gel, 20/80 EtOAc/hexanes) gave the product **12r** as a clear gum (71 mg, 90%): 1H NMR (400 MHz, $CDCl_3$) δ 7.48–7.37 (m, 5H), 7.29 (d, J = 8.4 Hz, 1H), 7.18 (dd, J = 8.4, 2.4 Hz, 1H), 7.11 (d, J = 2.4 Hz, 1H), 5.20 (t_{app}, J = 8.8 Hz, 1H), 4.76 (t_{app}, $J = 8.8 Hz, 1H), 4.31 (t_{app}, $J = 9.0 Hz, 1H), 3.81 (s, 3H), 3.80 (m, 1H), 3.49 (d, J = 5.6 Hz, 1H), 1.64–1.47 (m, 2H), 1.17–0.70 (m, 6H), 0.78 (t, J = 7.2 Hz, 3H); ^{13}C NMR (100 MHz, $CDCl_3$) δ 202.2 (C), 159.4 (C), 157.8 (C), 147.4 (C), 137.0 (C), 135.9 (C), 129.6 (CH), 129.2 (CH), 128.3 (CH), 125.9 (CH), 124.8 (CH), 104.9 (CH), 70.2 (CH₂), 63.2 (CH), 63.1 (CH), 56.0 (CH₃), 40.7 (CH), 32.0 (CH₂), 30.7 (CH₂), 24.5 (CH₂), 22.3 (CH₂), 14.0 (CH₃); HRMS (ESI-TOF) m/z : $[M + H]^+$ calcd for $C_{24}H_{28}NO_4^+$: 394.2013, found: 394.2010.$$

(4*S*,5*R*)-3-[(1*S*,2*R*)-5-methoxy-3-oxo-1-phenyl-2,3-dihydro-1*H*-inden-2-yl]-4,5-diphenyloxazolidin-2-one (**12s**). This was prepared according to General Method C using **11s** (800 mg, 1.684 mmol) in DCM (16 mL) with $MeSO_3H$ (327 μ L, 5.05 mmol). It was warmed to rt and stirred for 3 h. The crude shows mixture of *cis* and *trans* products (792 mg, 100%) (used for hydrogenation studies). The crude (200 mg) was then treated with $MeSO_3H$ (10 equiv) to give the *trans* compound (193 mg, 97%): mp = 104–106 °C. IR: 1H NMR (400 MHz, $CDCl_3$) δ 7.25–7.19 (m, 4H), 7.16 (dd, J = 8.5, 2.6 Hz, 1H), 7.12–7.01 (m, 6H), 6.87 (ddd, J = 8.6, 3.9, 1.6 Hz, 3H), 6.65 (d, J = 7.6 Hz, 2H), 6.38 (d, J = 6.2 Hz, 2H), 5.87 (d, J = 8.6 Hz, 1H), 5.67 (d, J = 8.6 Hz, 1H), 5.20 (d, J = 6.1 Hz, 1H), 3.85 (s, 3H), 3.64 (d, J = 6.1 Hz, 1H); ^{13}C NMR (101 MHz, $CDCl_3$) δ 201.6, 159.9, 158.5, 147.3, 141.0, 135.6, 135.0, 132.7, 128.9, 128.7, 128.2, 128.1, 128.1, 127.9, 127.9, 127.6, 127.5, 126.2, 125.2, 104.8, 80.1, 69.5, 67.8, 55.8, 47.9; HRMS (ESI-TOF) m/z : $[M + H]^+$ calcd for $C_{31}H_{26}NO_4^+$: 476.1856, found: 476.1863.

(*S*)-3-[(2*R*,3*S*)-4,6-dimethoxy-3-(4-methoxyphenyl)-1-oxo-2,3-dihydro-1*H*-inden-2-yl]-4-isopropoxyloxazolidin-2-one (**12t**). This was prepared according to General Method C using **11t** (192 mg, 0.451 mmol) in DCM (9 mL) with $MeSO_3H$ (290 μ L, 4.51 mmol). It was warmed to reflux and stirred overnight. Flash chromatography (silica gel, 10:45:45 Et₂O/DCM/hexanes) gave the title compound **12t** as a discolored solid (155 mg, 81%): mp = 183–185 °C; 1H NMR (400 MHz, $CDCl_3$) δ 7.06 (d, J = 8.7 Hz, 2H), 6.85 (d, J = 2.2 Hz, 1H), 6.81 (d, J = 8.7 Hz, 2H), 6.62 (d, J = 2.2 Hz, 1H), 4.75 (d, J = 4.8 Hz, 1H), 4.38 (t, J = 9.0 Hz, 1H), 4.08 (dd, J = 8.9, 6.1 Hz, 1H), 3.92 (ddd, J = 9.2, 6.1, 3.5 Hz, 1H), 3.83 (s, 3H), 3.79 (s, 3H), 3.74 (d, J = 4.8 Hz, 1H), 3.52 (s, 3H), 1.40 (septet, J = 6.8, 3.5 Hz, 1H), 0.71 (d, J = 7.0 Hz, 3H), 0.69 (d, J = 6.7 Hz, 3H); ^{13}C NMR (100 MHz, $CDCl_3$) δ 201.6 (C), 161.6 (C), 158.3 (C), 158.0 (C), 157.9 (C), 136.7 (C), 136.3 (C), 134.5 (C), 128.4 (CH), 113.7 (CH), 107.2 (CH), 96.1 (CH), 69.4 (CH), 63.6 (CH₂), 62.4 (CH), 55.7 (CH₃), 55.5 (CH₃), 55.2 (CH₃), 46.0 (CH), 28.7 (CH), 17.7 (CH₃), 14.2 (CH₃); HRMS (ESI-TOF) m/z : $[M + H]^+$ calcd for $C_{24}H_{28}NO_6^+$: 426.1911; found: 426.1910.

(*S*)-3-[(4*S*,5*R*)-4-isopropyl-6-oxo-5,6-dihydro-4*H*-cyclopenta[b]furan-5-yl]-4-phenyloxazolidin-2-one (**12aa**). Triflic acid (45 μ L, 0.507 mmol) was added to a stirred solution of **11aa** (66.0 mg, 0.203 mmol) in DCE (4 mL), and the reaction was refluxed for 2 h. The bath temperature was then lowered to 60 °C, and the reaction was stirred for a further 16 h. After this time, the reaction was quenched with saturated $NaHCO_3$ and extracted twice with DCM. The combined organic phases were dried over $MgSO_4$ and concentrated under reduced pressure. Flash chromatography (silica gel, 30:70 EtOAc/hexanes) gave the title compound as a white solid (16.3 mg, 25%): mp = 137–140 °C; 1H NMR (400 MHz, $CDCl_3$) δ 7.74 (d, J = 1.8 Hz, 1H), 7.45–7.33 (m, 5H), 6.46 (d, J = 1.8 Hz, 1H), 5.21 (t_{app}, $J = 8.9 Hz, 1H), 4.73 (t_{app}, $J = 8.8 Hz, 1H), 4.30 (t_{app}, $J = 8.9 Hz, 1H), 3.66 (d, J = 3.5 Hz, 1H), 3.57 (t_{app}, $J = 3.8 Hz, 1H), 1.56 (m, 1H),$$$$

0.96 (d, $J = 7.0$ Hz, 3H), 0.49 (d, $J = 6.8$ Hz, 3H); ^{13}C NMR (100 MHz, CDCl_3) δ 184.7 (C), 157.7 (C), 154.6 (C), 153.5 (CH), 152.6 (C), 136.6 (C), 129.7 (CH), 129.2 (CH), 128.3 (CH), 110.4 (CH), 70.0 (CH_2), 64.9 (CH), 62.9 (CH), 44.1 (CH), 28.4 (CH), 21.1 (CH_3), 17.1 (CH_3); HRMS (ESI-TOF) m/z : $[\text{M} + \text{H}]^+$ calcd for $\text{C}_{19}\text{H}_{20}\text{NO}_4^+$: 326.1387, found: 326.1388.

(*S*)-3-((3*S*,4*S*)-3,4-Dimethyl-5-oxo-2,3-diphenylcyclopent-1-en-1-yl)-4-isopropylloxazolidin-2-one (**23**). MeSO_3H (91 μL , 1.4 mmol) was added to a solution of divinyl ketone **11j** (54 mg, 0.14 mmol) in DCM (1.4 mL), and the reaction was stirred at rt for 4 days. A solution of NaHCO_3 aq (10% w/v, 3 mL) was added to the reaction mixture, followed by extraction with EtOAc (2×10 mL). The organic layer was dried over MgSO_4 and concentrated under reduced pressure. Flash chromatography (silica gel, 20:80 EtOAc/hexanes) gave the title compound **23** as a white powder (37.5 mg, 100%). This material recrystallized from chloroform and petroleum spirit by vapor diffusion method to afford a suitable crystal for X-ray crystal structure analysis (above): ^1H NMR (401 MHz, CDCl_3) δ 7.40–7.27 (m, 5H), 7.25–7.18 (m, 3H), 6.98–6.94 (m, 2H), 4.24 (t, $J = 8.8$ Hz, 1H), 4.12 (dd, $J = 8.7$, 7.0 Hz, 1H), 3.81 (s, br, 1H), 2.68 (q, $J = 7.1$ Hz, 1H), 1.79–1.70 (m, 1H), 1.58 (s, 3H), 0.96 (d, $J = 6.8$ Hz, 3H), 0.71 (d, $J = 7.1$ Hz, 6H); ^{13}C NMR (101 MHz, CDCl_3) δ 204.31, 156.0, 140.8, 133.9, 133.3, 129.6, 128.8, 128.9, 128.4, 127.7, 127.3, 127.2, 126.5, 64.8, 64.6, 59.051, 54.6, 51.9, 23.5, 18.22, 14.9, 9.9; HRMS (ESI-TOF) m/z : $[\text{M} + \text{H}]^+$ calcd for $\text{C}_{25}\text{H}_{27}\text{NO}_3^+$: 390.2064, found 390.2068.

(4*S*,5*R*)-3-((1*R*,3*R*,4*S*,5*R*)-3-(4-Methoxyphenyl)-3-(1-methyl-1*H*-indol-3-yl)-2-oxo-5-phenyl-4-propylcyclopentyl)-4,5-diphenyloxazolidin-2-one (**25**). $\text{BF}_3 \cdot \text{THF}$ (30.4 μL , 0.276 mmol) was added to a solution of **11m** (150 mg, 0.276 mmol) and *N*-methylindole (362.3 mg, 2.76 mmol) in DCM (2.8 mL) at -78°C . The reaction mixture was then allowed to warm to rt for 1 h. After this time, the reaction was quenched with saturated NaHCO_3 and extracted twice with DCM (2×10 mL). The combined organic phases were dried over MgSO_4 and concentrated under reduced pressure. The crude material was purified using flash chromatography (silica gel, 15% EtOAc in hexane), giving the title compound as a light-brown solid (127.2 mg, 77%): mp = 134.2–137.8; ^1H NMR (400 MHz, acetone- d_6) δ 7.63 (s, 1H), 7.49 (d, $J = 7.1$ Hz, 2H), 7.42 (t, $J = 7.3$ Hz, 2H), 7.32 (m, 5H), 7.15–7.07 (m, 1H), 7.05–6.98 (m, 3H), 6.91 (t, $J = 7.4$ Hz, 1H), 6.83 (m, 5H), 6.69 (t, $J = 7.6$ Hz, 2H), 6.13 (s, 2H), 5.88 (d, $J = 8.7$ Hz, 1H), 5.38 (d, $J = 8.7$ Hz, 1H), 4.46 (t, $J = 12.6$ Hz, 1H), 3.87 (d, $J = 13.2$ Hz, 1H), 3.79 (d, $J = 1.0$ Hz, 6H), 3.49–3.35 (m, 1H), 1.23–0.91 (m, 4H), 0.49 (t, $J = 6.9$ Hz, 3H); ^{13}C NMR (101 MHz, acetone- d_6) δ 212.7, 206.2, 159.6, 159.3, 140.8, 139.2, 136.6, 134.3, 134.2, 131.71, 129.8, 129.6, 129.4, 129.0, 128.5, 128.6, 128.5, 128.4, 128.2, 127.6, 127.1, 124.9, 122.4, 119.2, 116.6, 113.4, 110.0, 80.283, 68.3, 67.4, 60.0, 55.4, 47.4, 47.1, 33.6, 32.9, 22.0, 14.7; HRMS (ESI-TOF) m/z : $[\text{M} + \text{H}]^+$ calcd for $\text{C}_{45}\text{H}_{43}\text{N}_2\text{O}_4^+$: 675.3217, found 675.3224.

(4*S*,5*R*)-3-((1*R*,2*S*,4*S*,7*aS*)-3*a*-(Furan-2-yl)-3-oxo-1-phenyloctahydro-1*H*-inden-2-yl)-4,5-diphenyloxazolidin-2-one (*trans*-**26**). $\text{BF}_3 \cdot \text{THF}$ (0.02 mL, 27.1 mg, 0.1937 mmol) was added to a stirring solution of divinyl ketone **11l** (87.1 mg, 0.194 mmol) and furan (0.28 mL, 263.7 mg, 3.874 mmol) in anhydrous DCM (1.9 mL) at -78°C . It was then allowed to slowly warm up to rt for 16 h. The reaction mixture was quenched with NaHCO_3 aq (sat., 3 mL), extracted with DCM (2×5 mL), washed with water (2×5 mL) and brine (2×5 mL), dried over MgSO_4 , and concentrated under reduced pressure. Flash chromatography (NEt_3 treated silica gel, 15–25% EtOAc in PS, 10% step gradient) yielded *cis*-**26** as a yellow oil (36.9 mg, 36.8%) and *trans*-**26** as a tan oil (38.1 mg, 37.8%). Both isomers were obtained in a combined yield of 75%. *cis*-**26**: ^1H NMR (401 MHz, CDCl_3) δ 7.33 (dd, $J = 1.8$, 0.7 Hz, 1H), 7.32–7.27 (m, 3H), 7.25–7.22 (m, 2H), 7.07–6.98 (m, 3H), 6.94 (tt, $J = 7.4$, 1.1 Hz, 1H), 6.79 (dd, $J = 7.5$, 1.5 Hz, 2H), 6.71 (t, $J = 6.7$ Hz, 2H), 6.36 (dd, $J = 3.3$, 1.8 Hz, 1H), 6.32 (dd, $J = 3.3$, 0.7 Hz, 1H), 6.14 (s, br, 2H), 5.72 (d, $J = 8.8$ Hz, 1H), 5.44 (d, $J = 8.7$ Hz, 1H), 4.48 (t, $J = 12.3$ Hz, 1H), 3.58 (d, $J = 12.0$ Hz, 1H), 2.90 (d, $J = 12.5$ Hz, 1H), 2.16–2.01 (m, 2H), 1.76–1.60 (m, 2H), 1.56–1.23 (m, 4H); ^{13}C NMR (101 MHz, CDCl_3) δ 211.0, 158.3, 154.0, 142.0, 138.9, 135.1, 132.73, 129.0, 128.4, 128.3, 128.2, 128.1, 128.0, 127.8, 127.6, 126.2, 110.6, 107.5, 79.6, 68.6, 67.5, 51.4,

42.3, 41.1, 27.0, 22.1, 21.4, 20.4; HRMS (ESI-TOF) m/z : $[\text{M} + \text{H}]^+$ calcd for $\text{C}_{34}\text{H}_{31}\text{NO}_4^+$: 518.2326, found 518.2329. *trans*-**26**: ^1H NMR (401 MHz, CDCl_3) δ 7.30–7.27 (m, 3H), 7.17 (dd, $J = 6.6$, 2.9 Hz, 2H), 7.05–6.98 (m, 3H), 6.92 (tt, $J = 7.4$, 1.1 Hz, 1H), 6.78 (dd, $J = 7.8$, 1.3 Hz, 2H), 6.69 (t, $J = 6.5$ Hz, 2H), 6.23 (s, 1H), 6.14 (s, br, 2H), 5.71 (d, $J = 8.7$ Hz, 1H), 5.41 (d, $J = 8.7$ Hz, 1H), 4.44 (t, $J = 12.2$ Hz, 1H), 3.52 (d, $J = 12.0$ Hz, 1H), 2.73 (d, $J = 12.4$ Hz, 1H), 2.15–1.95 (m, 2H), 1.66 (d, $J = 13.0$ Hz, 1H), 1.54–1.41 (m, 4H), 1.28–1.22 (m, 1H); ^{13}C NMR (101 MHz, CDCl_3) δ 210.6, 158.3, 153.4, 138.8, 135.0, 132.7, 129.0, 128.3, 128.2, 128.1, 128.1, 127.8, 127.6, 126.2, 107.5, 79.6, 68.1, 67.5, 51.3, 42.4, 41.4, 28.1, 22.0, 21.5, 20.4; HRMS (ESI-TOF) m/z : $[\text{M} + \text{Na}]^+$ calcd for $\text{C}_{34}\text{H}_{31}\text{NNaO}_4^+$: 540.2151, found 540.2150.

(4*S*,5*R*)-3-((1*R*,3*S*,4*S*,5*R*)-3-(Furan-2-yl)-2-oxo-4,5-diphenylcyclopentyl)-4,5-diphenyloxazolidin-2-one (**27**). $\text{BF}_3 \cdot \text{THF}$ (0.02 mL, 0.197 mmol) was added to a solution of **11o** (92.9 mg, 0.1970 mmol) and furan (0.29 mL, 3.94 mmol) in anhydrous DCM (2.0 mL) at -78°C . The reaction was allowed to warm to rt and to stir for 2 h. To this, NaHCO_3 aq (sat., 2.0 mL) was added, and the mixture was extracted with DCM (2×4 mL), washed with water (2×4 mL) and brine (2×4 mL), dried over MgSO_4 , and concentrated under reduced pressure. Flash chromatography (silica gel, 20% EtOAc/hexanes) gave **27** as pink oil (69.5 mg, 65%): ^1H NMR (401 MHz, CDCl_3) δ 7.32 (dd, $J = 1.8$, 0.7 Hz, 1H), 7.21–7.11 (m, 10H), 7.08–6.99 (m, 3H), 6.96 (tt, $J = 7.4$, 1.0 Hz, 1H), 6.81 (dd, $J = 7.6$, 1.4 Hz, 2H), 6.71 (t, $J = 8.0$ Hz, 1H), 6.26 (dd, $J = 3.2$, 1.9 Hz, 1H), 6.18–6.10 (m, 3H), 5.76 (d, $J = 8.6$ Hz, 1H), 5.55 (d, $J = 8.6$ Hz, 1H), 4.60 (t, $J = 11.9$ Hz, 1H), 3.93 (d, $J = 11.9$ Hz, 1H), 3.72 (t, $J = 11.9$ Hz, 1H), 3.68 (dd, $J = 11.9$ Hz, 1H). ^{13}C NMR (101 MHz, CDCl_3) δ 208.8, 158.9, 149.1, 142.5, 138.8, 138.1, 134.8, 132.4, 128.8, 128.6, 128.3, 128.3, 128.1, 128.0, 127.8, 127.7, 127.5, 127.3, 126.2, 110.6, 109.1, 80.0, 68.0, 67.7, 55.7, 49.9, 48.9; HRMS (ESI-TOF) m/z : $[\text{M} + \text{H}]^+$ calcd for $\text{C}_{36}\text{H}_{30}\text{NO}_4^+$: 540.2169, found 540.2172.

(4*S*,5*R*)-3-((1*S*,3*R*,4*S*,5*R*)-3-(4-Methoxyphenyl)-3-methyl-2-oxo-5-phenyl-4-propylcyclopentyl)-4,5-diphenyloxazolidin-2-one (**28**). To a solution of **11m** (50 mg, 0.092 mmol) in DCM (0.9 mL, 0.1 M) with activated 4 Å MS (100 mg), was added 2.5 equiv of AlMe_3 (0.115 mL, 2.0 M solution in toluene) at -78°C . The reaction mixture was warmed to room temperature and stirred overnight. The reaction was quenched with 2 M aq HCl (1 mL) at 0°C and warmed to room temperature. After separation of the phases, the aqueous layer was extracted with DCM (3×5 mL). The combined organic extracts were washed with brine and dried over MgSO_4 , filtered, and concentrated in vacuo. Flash column chromatography (silica gel, 20:80 EtOAc/hexanes) provided the desired product **28** (18 mg, 35%): ^1H NMR (400 MHz, CDCl_3) δ 7.34–7.15 (m, 7H), 7.09–6.90 (m, 5H), 6.85 (d, $J = 8.9$ Hz, 2H), 6.80–6.65 (m, 4H), 6.10 (s, 1H), 5.69 (d, $J = 8.7$ Hz, 1H), 5.45 (d, $J = 8.8$ Hz, 1H), 4.11 (t, $J = 12.0$ Hz, 1H), 3.78 (s, 3H), 3.57 (d, $J = 12.3$ Hz, 1H), 2.68–2.53 (m, 1H), 1.51 (s, 3H), 1.47–1.24 (m, 2H), 0.95–0.80 (m, 1H), 0.71 (ddd, $J = 19.7$, 12.8, 7.5 Hz, 1H), 0.55 (t, $J = 7.2$ Hz, 3H); ^{13}C NMR (101 MHz, CDCl_3) δ 215.9, 158.4, 158.3, 140.1, 136.0, 135.1, 132.7, 128.9, 128.4, 128.3, 128.1, 128.0, 128.0, 127.929, 127.8, 127.5, 126.2, 113.9, 79.7, 69.4, 67.4, 55.4, 54.3, 49.3, 46.8, 31.3, 21.4, 17.0, 14.4; HRMS (ESI-TOF) m/z : $[\text{M} + \text{H}]^+$ calcd for $\text{C}_{37}\text{H}_{38}\text{NO}_4^+$: 560.2795, found: 560.2793.

(4*S*,5*R*)-3-((4*aR*,9*S*,10*R*,10*aS*)-6,7-Dimethyl-11-oxo-10-phenyl-1,2,3,4,5,8,10,10*a*-octahydro-9*H*-4*a*,9-methanobenzo[8]annulen-9-yl)-4,5-diphenyloxazolidin-2-one (**29**). $\text{BF}_3 \cdot \text{THF}$ (0.03 mL, 39.6 mg, 0.2834 mmol) was added to a stirring solution of **11i** (127.4 mg, 0.2834 mmol) and 2,3-dimethyl-1,3-butadiene (0.64 mL, 465.6 mg, 5.668 mmol) in anhydrous DCM (2.8 mL) at -10°C . The reaction mixture was at -10°C for 1.5 h, whereupon TLC revealed that **11j** was fully consumed. The reaction was then quenched with saturated NaHCO_3 (3 mL), extracted with DCM (2×5 mL), washed with water (2×5 mL) and brine (2×5 mL), dried over MgSO_4 , and concentrated. Flash chromatography (treated silica gel pretreated with 1% Et_3N , 1:9 EtOAc/hexanes) gave the product as white solid (48.2 mg, 32%): mp = 187–9 $^\circ\text{C}$; ^1H NMR (400 MHz, CDCl_3) δ 7.19–7.14 (m, 5H), 7.05–7.03 (m, 3H), 6.91–6.88 (m, 2H), 6.82 (tt, $J = 7.4$, 1.1 Hz, 1H), 6.65 (t, $J = 7.4$ Hz, 2H), 6.41 (d, $J = 7.3$ Hz, 2H),

5.87 (d, $J = 8.7$ Hz, 1H), 5.36 (d, $J = 8.8$ Hz, 1H), 4.58 (dd, $J = 10.9$, 1.3 Hz, 1H), 2.37 (dt, $J = 11.4$, 5.8 Hz, 1H), 2.26 (q, $J = 17.1$ Hz, 2H), 2.08 (d, $J = 17.1$ Hz, 1H), 2.02–1.94 (m, 1H), 1.80–1.70 (m, 3H), 1.66 (s, 3H), 1.60–1.46 (m, 3H), 1.42–1.32 (m, 5H); ^{13}C NMR (101 MHz, CDCl_3) δ 219.6, 158.6, 138.7, 136.6, 135.4, 130.3, 128.2, 127.9, 127.8, 127.7, 127.6, 127.4, 127.2, 126.3, 126.2, 123.8, 79.5, 74.1, 65.2, 49.8, 49.0, 47.2, 41.6, 40.3, 26.8, 23.5, 23.0, 22.9, 17.2, 16.8; HRMS (ESI-TOF) m/z : $[\text{M} + \text{H}]^+$ calcd for $\text{C}_{36}\text{H}_{37}\text{NO}_3$ ($\text{M} + \text{H}$): 532.2846, found: 532.2855.

(4*S*,5*R*)-3-[(1*Z*,4*E*)-6-(3-Methoxyphenoxy)-4-methyl-3-oxo-1-phenylhexa-1,4-dien-2-yl]-4,5-diphenyloxazolidin-2-one (**30**). This was prepared according to General Method B using ynamide **7i** (982 mg, 2.89 mmol), DCM (29 mL), $\text{Pd}(\text{PPh}_3)_4$ (100 mg, 0.087 mmol), Bu_3SnH (0.82 mL, 3.04 mmol), (*E*)-4-(3-methoxyphenoxy)-2-methylbut-2-enoyl chloride¹² (708 mg, 2.74 mmol), and CuTC (55 mg, 0.29 mmol). Flash chromatography (silica gel, 22:78 EtOAc/hexanes) gave the title compound as a white solid (1.20 g, 76%); mp = 59–62 °C; ^1H NMR (400 MHz, CDCl_3) δ 7.43–7.38 (m, 3H), 7.35–7.28 (m, 2H), 7.15–7.10 (m, 4H), 7.01–6.94 (m, 3H), 6.93 (s, 1H), 6.83 (t, $J = 7.7$ Hz, 2H), 6.55–6.46 (m, 3H), 6.42 (ddd, $J = 8.1$, 2.3, 0.6 Hz, 1H), 6.39 (t, $J = 2.3$ Hz, 1H), 6.27 (td, $J = 5.7$, 1.2 Hz, 1H), 5.85 (d, $J = 8.7$ Hz, 1H), 5.43 (d, $J = 8.7$ Hz, 1H), 4.72 (ddq, $J = 14.3$, 5.9, 0.8 Hz, 1H), 4.59 (ddq, $J = 14.3$, 5.1, 1.0 Hz, 1H), 3.73 (s, 3H), 1.94 (q, $J = 1.0$ Hz, 3H); ^{13}C NMR (100 MHz, CDCl_3) δ 193.1 (C), 160.8 (C), 159.3 (C), 156.6 (C), 138.5 (CH), 137.6 (CH), 137.5 (C), 135.0 (C), 133.1 (C), 132.6 (C), 131.7 (C), 129.9 (CH), 129.6 (CH), 129.5 (CH), 128.5 (CH), 128.4 (CH), 128.3 (CH), 128.0 (CH), 127.7 (CH), 127.5 (CH), 126.1 (CH), 106.8 (CH), 106.7 (CH), 101.3 (CH), 80.3 (CH), 64.9 (CH), 64.7 (CH_2), 55.2 (CH_3), 13.4 (CH_3); HRMS (ESI-TOF) m/z : $[\text{M} + \text{H}]^+$ calcd for $\text{C}_{35}\text{H}_{32}\text{NO}_5$: 546.2275, found: 546.2280.

(4*S*,5*R*)-3-[(2*R*,3*R*,3*aS*,9*bR*)-7-Methoxy-9*b*-methyl-1-oxo-3-phenyl-1,2,3,3*a*,4,9*b*-hexahydrocyclopenta[*c*]chromen-2-yl]-4,5-diphenyloxazolidin-2-one (**31**). $\text{BF}_3 \cdot \text{THF}$ (101 μL , 0.917 mmol) was added to a solution of **30** (500 mg, 0.917 mmol) in toluene (9 mL) and was stirred at 0 °C for 1 h. The reaction was then quenched with saturated NaHCO_3 (20 mL), extracted with EtOAc (2 \times 15 mL), washed with water (2 \times 10 mL) and brine (2 \times 10 mL), dried over MgSO_4 , and concentrated. Flash chromatography (silica gel, 8:46:46 Et₂O/DCM/hexanes) gave the title compound as a yellow gum (440 mg, 88% including 5% of the minor *cis*-isomer); ^1H NMR (400 MHz, CDCl_3) δ 7.43–7.27 (m, 5H), 7.20 (d, $J = 8.8$ Hz, 1H), 7.04–6.94 (m, 3H), 6.82 (tt, $J = 7.5$, 1.2 Hz, 1H), 6.80–6.73 (m, 2H), 6.66 (t, $J = 7.3$ Hz, 2H), 6.40 (dd, $J = 8.8$, 2.6 Hz, 1H), 6.33 (br. s., 2H), 6.24 (d, $J = 2.5$ Hz, 1H), 5.56 (d, $J = 8.7$ Hz, 1H), 5.09 (d, $J = 8.7$ Hz, 1H), 4.33 (d, $J = 13.2$ Hz, 1H), 3.99 (dd, $J = 11.6$, 1.9 Hz, 1H), 3.86–3.76 (m, 2H), 3.74 (s, 3H), 2.10 (dt, $J = 11.6$, 1.9 Hz, 1H), 1.48 (s, 3H); ^{13}C NMR (100 MHz, CDCl_3) δ 211.9 (C), 159.5 (C), 158.2 (C), 154.0 (C), 137.6 (C), 134.7 (C), 132.3 (C), 129.7 (CH), 129.2 (CH), 128.0 (CH), 127.9 (CH), 127.8 (CH), 127.8 (CH), 127.7 (CH), 127.61 (CH), 127.59 (CH), 125.9 (CH), 112.6 (C), 109.2 (CH), 101.5 (CH), 79.4 (CH), 65.5 (CH), 65.0 (CH), 60.7 (CH_2), 55.1 (CH_3), 47.2 (CH), 45.7 (C), 41.7 (CH), 27.0 (CH_3); HRMS (ESI-TOF) m/z : $[\text{M} + \text{H}]^+$ calcd for $\text{C}_{35}\text{H}_{32}\text{NO}_5$: 546.2275, found: 546.2282.

(*R*)-6-Methoxy-3-pentyl-2,3-dihydro-1*H*-inden-1-one (**34**). This was prepared according to General Method D using **12r** (113 mg, 0.35 mmol) in THF (4 mL) using lithium naphthalenide in THF (~1.0 M, 0.8 mL). Flash chromatography (silica gel, 5% EtOAc in hexane) gave the title compound as a clear oil (74 mg, 91%); ^1H NMR (400 MHz, CDCl_3) δ 7.35 (d, $J = 7.31$ Hz, 1H), 7.38–7.36 (m, 1H), 3.79 (s, 3H), 3.24–3.21 (m, 1H), 2.85 (dd, $J = 18.3$, 6.7 Hz, 1H), 2.36 (dd, $J = 18.3$, 2.3 Hz, 1H), 1.90–1.86 (m, 1H), 1.44–1.18 (m, 8H), 0.8 (m, 3H); ^{13}C NMR δ 205.2 (C), 158.8 (C), 150.2 (C), 137.6 (C), 127.0 (CH), 123.2 (CH), 108.1 (CH), 56.6 (CH_3), 45.6 (CH), 38.1 (CH), 36.0 (CH_2), 31.8 (CH_2), 26.1 (CH_2), 21.8 (CH), 13.4 (CH_3); HRMS (ESI-TOF) m/z : $[\text{M} + \text{H}]^+$ calcd for $\text{C}_{15}\text{H}_{21}\text{O}_2$: 233.1542, found: 233.1546; Optical rotation: $T = 22.78$ °C, $[\alpha]_D = -0.03$ ($c = 1$, MeOH).

(3*R*,3*aS*,9*bR*)-7-Methoxy-9*b*-methyl-3-phenyl-2,3,3*a*,4-tetrahydrocyclopenta[*c*]chromen-1(9*bH*)-one (**37**). This was prepared

according to General Method D using **31** (87.1 mg, 0.200 mmol), THF (4 mL), and lithium naphthalenide (~0.89 M, 0.46 mL, 0.41 mmol). Flash chromatography (silica gel, 6:47:47 Et₂O/DCM/hexanes) gave the title compound as a white solid (56.4 mg, 91%); mp = 92–95 °C; ^1H NMR (400 MHz, CDCl_3) δ 7.42–7.26 (m, 6H), 6.55 (dd, $J = 8.7$, 2.6 Hz, 1H), 6.44 (d, $J = 2.6$ Hz, 1H), 4.12 (dd, $J = 11.4$, 1.9 Hz, 1H), 3.99 (dd, $J = 11.4$, 2.0 Hz, 1H), 3.78 (s, 3H), 3.42 (td, $J = 11.6$, 8.6 Hz, 1H), 2.79 (dd, $J = 19.1$, 8.6 Hz, 1H), 2.55 (dd, $J = 19.1$, 12.0 Hz, 1H), 2.23 (dt, $J = 11.4$, 1.9 Hz, 1H), 1.52 (s, 3H). The spectral data of this material are identical to that previously reported.¹⁰

tert-Butyl [(1*R*,5*S*)-3,4-Dimethyl-2-oxo-5-pentylcyclopent-3-en-1-yl]carbamate (**39**). This was prepared according to General Method E using **12h** (50 mg, 0.12 mmol), THF (4 mL), Pd/C (10%) (50 mg), and Boc anhydride (157 mg, 0.72 mmol). Flash chromatography (silica gel, 10% EtOAc in hexanes) gave the title compound **39** as a tan oil (27 mg, 75%); ^1H NMR (400 MHz, CDCl_3) δ 4.75 (d, $J = 5.5$ Hz, 1H), 3.55–3.38 (m, 1H), 2.54–2.31 (m, 2H), 2.05 (m, 1H), 1.70–1.55 (m, 1H), 1.43 (s, 9H), 1.31 (m, 6H), 1.15 (m, 1H), 1.06 (d, $J = 7.0$ Hz, 3H), 0.89 (t, $J = 6.6$ Hz, 3H), 0.77 (d, $J = 7.3$ Hz, 3H); ^{13}C NMR (101 MHz, CDCl_3) δ 217.6, 155.8, 80.1, 60.6, 48.0, 44.3, 32.8, 32.1, 28.9, 28.4, 27.0, 22.7, 14.2, 10.0, 9.1; HRMS (ESI-TOF) m/z : $[\text{M} + \text{H}]^+$ calcd for $\text{C}_{17}\text{H}_{32}\text{NO}_3$: 298.2377, found: 298.2368; $[\alpha]_D -44.19$ ($c = 1$, DCM).

(1*S*,2*R*,3*R*,4*R*,5*R*)-2-(Diethylamino)-4,5-dimethyl-3-phenylcyclopentan-1-ol (**41**). This was prepared according to General Method E using **12i** (50 mg, 0.118 mmol), Pd/C (10%) (50 mg), and acetaldehyde (52.1 mg, 1.18 mmol). After the solution was filtered through Celite, the combined organic phases were concentrated under reduced pressure. The crude residue was dissolved in methanol (2 mL) and NaBH_4 (25 mg, 0.661 mmol) was added. The reaction mixture stirred at rt for 6 h. The reaction mixture was then diluted with H_2O (8 mL) and extracted into EtOAc (2 \times 5 mL). The combined organic layers were dried over anhydrous MgSO_4 and concentrated under reduced pressure. The crude was chromatographed (silica gel, 10% EtOAc in hexane), and it gave the title compound **41** as clear oil (24.1 mg, 78%); ^1H NMR (400 MHz, acetone- d_6) δ 7.38–7.12 (m, 5H), 3.77 (dd, $J = 10.5$, 7.6 Hz, 1H), 3.70–3.58 (m, 1H), 3.51 (dd, $J = 10.5$, 7.5 Hz, 1H), 2.83 (s, 1H), 2.74–2.43 (m, 4H), 2.25 (dq, $J = 14.6$, 7.2 Hz, 1H), 2.00 (dt, $J = 12.9$, 6.6 Hz, 1H), 1.04 (d, $J = 7.1$ Hz, 3H), 0.91 (t, $J = 7.1$ Hz, 6H), 0.50 (d, $J = 7.6$ Hz, 3H); ^{13}C NMR (101 MHz, acetone- d_6) δ 143.04, 129.63, 128.9, 126.8, 76.1, 65.8, 51.3, 46.7, 45.7, 40.9, 14.9, 13.7, 12.0; HRMS (ESI-TOF) m/z : $[\text{M} + \text{H}]^+$ calcd for $\text{C}_{17}\text{H}_{27}\text{NO}$: 261.2087, found: 261.2051; $[\alpha]_D + 42.25$ ($c = 1$, DCM).

tert-Butyl [(1*R*,3*R*,4*S*,5*R*)-3-(4-Methoxyphenyl)-3-(1-methyl-1*H*-indol-3-yl)-2-oxo-5-phenyl-4-propylcyclopentyl]carbamate (**42**). This was prepared according to General Method E using **28** (45 mg, 0.0667 mmol), EtOAc (2 mL), Pd/C (10%) (45 mg) and Boc anhydride (87.42 mg, 0.4 mmol). Flash chromatography (silica gel, 20:80 EtOAc/hexanes) gave the title compound **42** as yellow oil (18.9 mg, 52%); ^1H NMR (400 MHz, acetone- d_6) δ 7.53 (s, 1H), 7.35 (d, $J = 7.4$ Hz, 2H), 7.28–7.09 (m, 5H), 6.96 (t, $J = 7.1$ Hz, 3H), 6.67 (t, $J = 8.9$ Hz, 2H), 6.31 (d, $J = 8.5$ Hz, 1H), 4.67–4.44 (m, 1H), 3.75 (s, 3H), 3.64 (s, 3H), 3.23 (d, $J = 7.9$ Hz, 2H), 1.15 (s, 9H), 1.05–0.94 (m, 2H), 0.92–0.82 (m, 2H), 0.36 (t, $J = 7.1$ Hz, 3H); ^{13}C NMR (101 MHz, acetone- d_6) δ 213.5, 206.3, 159.2, 156.6, 141.5, 139.3, 134.2, 131.7, 129.5, 129.3, 129.2, 127.8, 127.8, 124.81, 122.3, 119.1, 117.1, 113.4, 109.9, 78.9, 64.4, 60.4, 55.4, 51.1, 48.7, 33.5, 323.0, 28.2, 22.0, 14.7; HRMS (ESI-TOF) m/z : $[\text{M} + \text{H}]^+$ Calcd for $\text{C}_{35}\text{H}_{41}\text{N}_2\text{O}_4$: 553.3066, found: 553.3059; $[\alpha]_D + 24.3$ ($c = 1$, DCM).

tert-Butyl [(2*R*,3*R*,3*aS*,9*bR*)-7-Methoxy-9*b*-methyl-1-oxo-3-phenyl-1,2,3,3*a*,4,9*b*-hexahydrocyclopenta[*c*]chromen-2-yl]carbamate (**43**). This was prepared according to General Method E using **31** (200 mg, 0.3668 mmol), THF (10 mL), Pd/C (10%) (200 mg), and Boc anhydride (480 mg, 2.197 mmol). Flash chromatography (silica gel, 20:80 EtOAc in hexanes) gave the product **43** as a white solid (93 mg, 60%); mp = 79–84 °C; ^1H NMR (400 MHz, CDCl_3) δ 7.50 (d, $J = 8.8$ Hz, 1H), 7.42–7.27 (m, 5H), 6.56 (dd, $J = 8.8$, 2.6 Hz, 1H), 6.39 (d, $J = 2.6$ Hz, 1H), 4.74 (s, 1H), 4.50 (s, 1H), 4.09 (d, $J = 10.5$ Hz, 1H), 3.92 (dd, $J = 11.5$, 2.0 Hz, 1H), 3.76 (s, 3H), 3.07 (t, $J = 12.2$ Hz,

1H), 2.20 (d, $J = 11.7$ Hz, 1H), 1.57 (s, 3H), 1.28 (s, 9H); ^{13}C NMR (101 MHz, CDCl_3) δ 213.6, 159.9, 155.7, 154.7, 137.7, 130.4, 128.9, 128.1, 127.6, 113.4, 109.2, 101.9, 80.1, 61.1, 55.4, 47.0, 46.8, 45.5, 28.2, 27.1; HRMS (ESI-TOF) m/z : $[\text{M} + \text{Na}]^+$ calcd for $\text{C}_{25}\text{H}_{29}\text{NNaO}_5$: 446.1938, found: 446.1945; $[\alpha]_{\text{D}}^{25} +23.5$ ($c = 1$, DCM).

tert-Butyl [(1*S*,2*R*,3*S*)-3-Hydroxy-5-methoxy-1-phenyl-2,3-dihydro-1*H*-inden-2-yl]carbamate (44). This was prepared according to General Method E using **12s** (68 mg, 0.143 mmol) EtOAc (2 mL), Pd/C (10%) (68 mg), and Boc anhydride (131 mg, 0.6 mmol). Flash chromatography (silica gel, 20:80 EtOAc/hexanes) gave the title compound **44** as clear oil (30.5 mg, 76%): ^1H NMR (400 MHz, CDCl_3) δ 7.42–7.29 (m, 3H), 7.26 (d, $J = 7.3$ Hz, 2H), 7.04 (d, $J = 2.1$ Hz, 1H), 6.77 (dd, $J = 8.4$, 2.1 Hz, 1H), 6.69 (d, $J = 8.4$ Hz, 1H), 5.24 (br. s., 1H), 5.15 (d, $J = 6.2$ Hz, 1H), 5.01 (br. s., 1H), 3.97 (ddd, $J = 9.5$, 6.2, 2.8 Hz, 1H), 3.91 (d, $J = 9.5$ Hz, 1H), 3.83 (s, 3H), 1.44 (s, 9H); ^{13}C NMR (100 MHz, CDCl_3) δ 159.9 (C), 133.3 (C), 128.9 (CH), 128.6 (CH), 127.6 (CH), 125.2 (CH), 115.5 (CH), 108.1 (CH), 80.7 (C), 80.0 (CH), 70.7 (CH), 55.5 (CH_3), 53.3 (CH), 28.3 (CH_3); HRMS (ESI-TOF) m/z : $[\text{M} + \text{H}]^+$ calcd for $\text{C}_{17}\text{H}_{16}\text{NO}_3$: 282.1125, found: 282.1110; $[\alpha]_{\text{D}}^{25} +8.1$ ($c = 1$, DCM).

■ ASSOCIATED CONTENT

● Supporting Information

The Supporting Information is available free of charge on the ACS Publications website at DOI: 10.1021/acs.joc.7b00082.

X-ray crystal structure data for **12c** and **23**. Copies of ^1H NMR and ^{13}C NMR spectra for all new compounds. Chiral HPLC data and 2D NMR data on **27**, **29** and **41**. Details of computational methods, and computational data. (PDF)

X-ray data (**12c**) (CIF)

X-ray data (**23**) (CIF)

■ AUTHOR INFORMATION

Corresponding Author

*E-mail: bernard.flynn@monash.edu

ORCID

Jonathan M. White: 0000-0002-0707-6257

Elizabeth H. Krenske: 0000-0003-1911-0501

Bernard L. Flynn: 0000-0003-4410-2423

Present Address

[†]R.J.L.: Visiting PhD student from Griffith Institute for Drug Discovery, Griffith University, Brisbane, QLD 4111, Australia.

Notes

The authors declare no competing financial interest.

■ ACKNOWLEDGMENTS

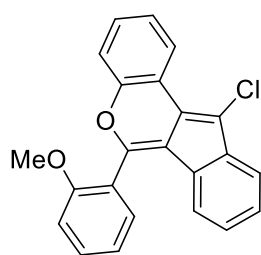
This research has been supported by the Australian Research Council (DP150103131 and FT120100632). Computer resources were provided by the Australian National Computational Infrastructure National Facility and by the University of Queensland Research Computing Centre.

■ REFERENCES

- (1) For reviews on cyclopentyl ring synthesis, see: (a) Simeonov, S. P.; Nunes, J. P. M.; Guerra, K.; Kurteva, V. B.; Afonso, C. A. M. *Chem. Rev.* **2016**, *116*, 5744–5893. (b) Gabriele, B.; Mancuso, R.; Veltri, L. *Chem. - Eur. J.* **2016**, *22*, 5056–5094.
- (2) For reviews on sp^3 -scaffolds in drug discovery, see: (a) Ritchie, T.; MacDonald, S. J. F. *Drug Discovery Today* **2009**, *14*, 1011–1020. (b) Lovering, F.; Bikker, C. J.; Humblet, J. J. *Med. Chem.* **2009**, *52*, 6752–6756. (c) Lovering, F. *MedChemComm* **2013**, *4*, 515–519.
- (3) For general reviews on the Nazarov reactions, see: (a) Denmark, S. E. Nazarov and Related Cationic Cyclizations. In *Comprehensive Organic Synthesis*; Trost, B. M., Fleming, I., Eds.; Pergamon: New York, 1991; Volume 5, pp 751. (b) Tius, M. A. *Acc. Chem. Res.* **2003**, *36*, 284–290. (c) Tius, M. A. *Eur. J. Org. Chem.* **2005**, *2005*, 2193–2206. (d) Pellissier, H. *Tetrahedron* **2005**, *61*, 6479–6517. (e) Frontier, A. J.; Collison, C. *Tetrahedron* **2005**, *61*, 7577–7606. (f) Vaidya, T.; Eisenberg, R.; Frontier, A. *ChemCatChem* **2011**, *3*, 1531–1548. (g) Shimada, N.; Stewart, C.; Tius, M. A. *Tetrahedron* **2011**, *67*, 5851–5870. (h) West, F. G.; Scadeng, O.; Wu, Y.-K.; Fradette, R. J.; Joy, S. The Nazarov Cyclization. In *Comprehensive Organic Synthesis*, 2nd ed.; Knochel, P., Molander, G. A., Eds.; Elsevier: Amsterdam, 2014; Vol. 5, pp 827. (i) Tius, M. A. *Chem. Soc. Rev.* **2014**, *43*, 2979–3002.
- (4) For reviews on the enantioselective Nazarov reaction: (a) Vaidya, T.; Eisenberg, R.; Frontier, A. J. *ChemCatChem* **2011**, *3*, 1531–1548. (b) Shimada, N.; Stewart, C.; Tius, M. A. *Tetrahedron* **2011**, *67*, 5851–5870. For selected papers see: (c) Jolit, A.; Walleiser, P. M.; Yap, G. P. A.; Tius, M. A. *Angew. Chem., Int. Ed.* **2014**, *53*, 6180–6183. (d) Grenet, E.; Martínez, J.; Salom-Roig, X. J. *Chem. - Eur. J.* **2016**, *22*, 16770–16773. (e) Tang, M.-L.; Peng, P.; Liu, Z.-Y.; Zhang, J.; Yu, J.-M.; Sun, X. *Chem. - Eur. J.* **2016**, *22*, 14535–14539.
- (5) (a) Huang, J.; Lebœuf, D.; Frontier, A. J. *J. Am. Chem. Soc.* **2011**, *133*, 6307–6317. (b) Lebœuf, D.; Huang, J.; Gandon, V.; Frontier, A. J. *Angew. Chem., Int. Ed.* **2011**, *50*, 10981–10985. (c) Yang, B.-M.; Cai, P.-J.; Tu, Y.-Q.; Yu, Z.-X.; Chen, Z.-M.; Wang, S.-H.; Wang, S.-H.; Zhang, F.-M. *J. Am. Chem. Soc.* **2015**, *137*, 8344–8347. (d) Lebœuf, D.; Gandon, V.; Ciesielski, J.; Frontier, A. J. *J. Am. Chem. Soc.* **2012**, *134*, 6296–6308.
- (6) (a) Grant, T. N.; Rieder, C. J.; West, F. G. *Chem. Commun.* **2009**, 5676–5688. (b) Wu, Y. K.; McDonald, R.; West, F. G. *Org. Lett.* **2011**, *13*, 3584–3587. (c) Wu, Y. K.; West, F. G. *Org. Lett.* **2014**, *16*, 2534–2537. (d) Kwon, Y.; McDonald, R.; West, F. G. *Angew. Chem., Int. Ed.* **2013**, *52*, 8616–8619 and refs cited therein.
- (7) (a) Wang, Y.; Arif, A. M.; West, F. G. *J. Am. Chem. Soc.* **1999**, *121*, 876–877. (b) Wang, Y.; Schill, B. D.; Arif, A. M.; West, F. G. *Org. Lett.* **2003**, *5*, 2747–2750. (c) LeFort, F. M.; Mishra, V.; Dexter, G. D.; Morgan, T. D. R.; Burnell, D. J. *J. Org. Chem.* **2015**, *80*, 5877–5886. (d) Wu, Y.-K.; Dunbar, C. R.; McDonald, R.; Ferguson, M. J.; West, F. G. *J. Am. Chem. Soc.* **2014**, *136*, 14903–14911. (e) Marx, V. M.; Burnell, D. J. *J. Am. Chem. Soc.* **2010**, *132*, 1685–1689.
- (8) Bender, J. A.; Arif, A. M.; West, F. G. *J. Am. Chem. Soc.* **1999**, *121*, 7443–7444.
- (9) Atesin, T. A. *Organic Chem. Curr. Res.* [Online]. **2014**, Volume 3, 1000e130, <https://www.omicsonline.org/open-access/nazarov-cyclization-reaction-challenges-and-opportunities-2161-0401.1000e130.php?aid=22440>.
- (10) Elements of this work have been previously described in a short communication: Kerr, D. J.; Miletic, M.; Chaplin, J. H.; White, J. M.; Flynn, B. L. *Org. Lett.* **2012**, *14*, 1732–1735.
- (11) (a) He, W.; Sun, X.; Frontier, A. J. *J. Am. Chem. Soc.* **2003**, *125*, 14278–14279. (b) He, W.; Herrick, I. R.; Atesin, T. A.; Caruana, P. A.; Kellenberger, C. A.; Frontier, A. J. *J. Am. Chem. Soc.* **2008**, *130*, 1003–1011. (c) Denmark, S. E.; Habermas, K. L.; Hite, G. A. *Helv. Chim. Acta* **1988**, *71*, 168–194. (d) Polo, V.; Andrés, J. J. *Chem. Theory Comput.* **2007**, *3*, 816–823.
- (12) (a) Kerr, D. J.; Metje, C.; Flynn, B. L. *Chem. Commun.* **2003**, *34*, 1380–1381. (b) Kerr, D. J.; White, J. M.; Flynn, B. L. *J. Org. Chem.* **2010**, *75*, 7073–7084.
- (13) See [Supporting Information](#) for details.
- (14) Mazzola, R. D., Jr.; Giese, S.; Benson, C. L.; West, F. G. *J. Org. Chem.* **2004**, *69*, 220–223.
- (15) For carbonylative Suzuki–Miyaura couplings using ArBF_3K salts under more forcing conditions, see: Wu, X.-F.; Neumann, H.; Beller, M. *Adv. Synth. Catal.* **2011**, *353*, 788–792 and references cited therein.
- (16) (a) Denmark, S. E.; Habermas, K. L.; Hite, G. A. *Helv. Chim. Acta* **1988**, *71*, 168–194. (b) Koltunov, K. Yu.; Walspurger, S.; Sommer, J. *Tetrahedron Lett.* **2005**, *46*, 8391–8394. (c) Malona, J. A.; Colbourne, J. M.; Frontier, A. J. *Org. Lett.* **2006**, *8*, 5661–5664. (d) Vaidya, T.; Manbeck, G. F.; Chen, S.; Frontier, A. J.; Eisenberg, R. *J. Am. Chem. Soc.* **2011**, *133*, 3300–3303.

- (17) Flynn, B. L.; Manchala, N.; Krenske, E. H. *J. Am. Chem. Soc.* **2013**, *135*, 9156–9163.
- (18) Compound **22** was detected as a set of two methyl doublets and two doublets of quartets for the two ring protons in the ^1H NMR of the crude-reaction mixture (stereochemistry not determined). The level of conversion was determined by integration.
- (19) The stereochemistry of arene incorporation, *trans* to the adjacent (vicinal) substituent is based on NOESY spectra of **26**, see [Supporting Information](#).
- (20) (a) Xiong, H.; Hsung, R. P.; Berry, C. R.; Rameshkumar, C. *J. Am. Chem. Soc.* **2001**, *123*, 7174–7177. (b) Huang, J.; Hsung, R. P. *J. Am. Chem. Soc.* **2005**, *127*, 50–51. (c) Antoline, J. E.; Krenske, E. H.; Lohse, A. G.; Houk, K. N.; Hsung, R. P. *J. Am. Chem. Soc.* **2011**, *133*, 14443–14451. (d) Cramer, C. J.; Barrows, S. E. *J. Phys. Org. Chem.* **2000**, *13*, 176–186.
- (21) Zhao, Y.; Truhlar, D. G. *Theor. Chem. Acc.* **2008**, *120*, 215–241.
- (22) Lucet, D.; Sabelle, S.; Kostelitz, O.; Le Gall, T.; Mioskowski, C. *Eur. J. Org. Chem.* **1999**, *1999*, 2583–2591.
- (23) Kerr, D. J.; Miletic, M.; Manchala, N.; White, J. M.; Flynn, B. L. *Org. Lett.* **2013**, *15*, 4118–4121.
- (24) Zhang, X.; Zhang, Y.; Huang, J.; Hsung, R. P.; Kurtz, K. C. M.; Oppenheimer, J.; Petersen, M. E.; Sagamanova, I. K.; Shen, L.; Tracey, M. R. *J. Org. Chem.* **2006**, *71*, 4170–4177.
- (25) Villeneuve, K.; Riddell, N.; Tam, W. *Tetrahedron* **2006**, *62*, 3823–3836.
- (26) Wei, L.-L.; Mulder, J. A.; Xiong, H.; Zifcsak, C. A.; Douglas, C. J.; Hsung, R. P. *Tetrahedron* **2001**, *57*, 459–466.
- (27) Kosugi, H.; Kitaoka, M.; Tagami, K.; Takahashi, A.; Uda, H. *J. Org. Chem.* **1987**, *52*, 1078.
- (28) Duboudin, J. G.; Petraud, M.; Ratier, M.; Trouve, B. *J. Organomet. Chem.* **1985**, *288*, C6–C8.

6.3 Appendices C- X-ray crystallography data

compound **275**Table 1. Crystal data and structure refinement for compound **275**.

Identification code	shelx
Empirical formula	C ₂₃ H ₁₅ Cl O ₂
Formula weight	358.80
Temperature	100.00(10) K
Wavelength	1.54184 Å
Crystal system	Monoclinic
Space group	P 21/c
Unit cell dimensions	a = 8.11170(10) Å $\alpha = 90^\circ$. b = 14.62620(10) Å $\beta = 100.2150(10)^\circ$. c = 14.5010(2) Å $\gamma = 90^\circ$.
Volume	1693.18(3) Å ³
Z	4
Density (calculated)	1.408 Mg/m ³
Absorption coefficient	2.109 mm ⁻¹
F(000)	744
Crystal size	0.313 x 0.218 x 0.184 mm ³
Theta range for data collection	4.328 to 77.117°.
Index ranges	-9<=h<=10, -18<=k<=17, -18<=l<=17
Reflections collected	20393
Independent reflections	3552 [R(int) = 0.0514]
Completeness to theta = 67.684°	100.0 %
Absorption correction	Semi-empirical from equivalents
Max. and min. transmission	1.00000 and 0.79000
Refinement method	Full-matrix least-squares on F ²
Data / restraints / parameters	3552 / 0 / 236
Goodness-of-fit on F ²	1.082
Final R indices [I>2sigma(I)]	R1 = 0.0412, wR2 = 0.1111
R indices (all data)	R1 = 0.0430, wR2 = 0.1130
Extinction coefficient	n/a
Largest diff. peak and hole	0.253 and -0.381 e.Å ⁻³

Table 2. Atomic coordinates ($\times 10^4$) and equivalent isotropic displacement parameters ($\text{\AA}^2 \times 10^3$) for compound **275**. $U(\text{eq})$ is defined as one third of the trace of the orthogonalized U_{ij} tensor.

	x	y	z	$U(\text{eq})$
C(1)	3136(2)	5715(1)	4822(1)	23(1)
C(2)	3647(2)	5493(1)	5759(1)	27(1)
C(3)	3109(2)	4683(1)	6098(1)	29(1)
C(4)	2063(2)	4099(1)	5495(1)	30(1)
C(5)	1537(2)	4333(1)	4567(1)	27(1)
C(6)	2056(2)	5157(1)	4205(1)	24(1)
C(7)	1565(2)	5483(1)	3254(1)	22(1)
C(8)	509(2)	5173(1)	2478(1)	24(1)
C(9)	479(2)	5806(1)	1708(1)	23(1)
C(10)	-431(2)	5786(1)	795(1)	26(1)
C(11)	-240(2)	6510(1)	201(1)	27(1)
C(12)	843(2)	7231(1)	507(1)	26(1)
C(13)	1766(2)	7252(1)	1411(1)	24(1)
C(14)	1586(2)	6535(1)	2019(1)	22(1)
C(15)	2301(2)	6342(1)	2999(1)	22(1)
C(16)	3407(2)	6809(1)	3635(1)	22(1)
C(17)	4303(2)	7666(1)	3504(1)	23(1)
C(18)	5394(2)	7731(1)	2853(1)	24(1)
C(19)	6223(2)	8548(1)	2757(1)	27(1)
C(20)	5941(2)	9305(1)	3288(1)	30(1)
C(21)	4877(2)	9246(1)	3931(1)	30(1)
C(22)	4088(2)	8424(1)	4052(1)	26(1)
C(23)	6589(2)	7016(1)	1641(1)	39(1)
O(1)	3789(1)	6524(1)	4547(1)	24(1)
O(2)	5566(1)	6963(1)	2349(1)	28(1)
Cl(1)	-649(1)	4180(1)	2358(1)	30(1)

Table 3. Bond lengths [\AA] and angles [$^\circ$] for compound **275**.

C(1)-O(1)	1.3842(17)
C(1)-C(2)	1.387(2)
C(1)-C(6)	1.398(2)
C(2)-C(3)	1.382(2)
C(2)-H(2)	0.9300
C(3)-C(4)	1.396(2)
C(3)-H(3)	0.9300
C(4)-C(5)	1.380(2)
C(4)-H(4)	0.9300
C(5)-C(6)	1.409(2)
C(5)-H(5)	0.9300
C(6)-C(7)	1.447(2)
C(7)-C(8)	1.364(2)
C(7)-C(15)	1.4665(19)
C(8)-C(9)	1.447(2)
C(8)-Cl(1)	1.7228(14)
C(9)-C(10)	1.397(2)
C(9)-C(14)	1.415(2)
C(10)-C(11)	1.389(2)
C(10)-H(10)	0.9300
C(11)-C(12)	1.394(2)
C(11)-H(11)	0.9300
C(12)-C(13)	1.390(2)
C(12)-H(12)	0.9300
C(13)-C(14)	1.394(2)
C(13)-H(13)	0.9300
C(14)-C(15)	1.4633(19)
C(15)-C(16)	1.352(2)
C(16)-O(1)	1.3685(17)
C(16)-C(17)	1.477(2)
C(17)-C(22)	1.393(2)
C(17)-C(18)	1.407(2)
C(18)-O(2)	1.3607(18)
C(18)-C(19)	1.390(2)
C(19)-C(20)	1.391(2)
C(19)-H(19)	0.9300
C(20)-C(21)	1.382(2)

Chapter 6

C(20)-H(20)	0.9300
C(21)-C(22)	1.387(2)
C(21)-H(21)	0.9300
C(22)-H(22)	0.9300
C(23)-O(2)	1.4315(19)
C(23)-H(23A)	0.9600
C(23)-H(23B)	0.9600
C(23)-H(23C)	0.9600

O(1)-C(1)-C(2)	114.78(13)
O(1)-C(1)-C(6)	122.90(13)
C(2)-C(1)-C(6)	122.32(14)
C(3)-C(2)-C(1)	119.37(14)
C(3)-C(2)-H(2)	120.3
C(1)-C(2)-H(2)	120.3
C(2)-C(3)-C(4)	119.77(14)
C(2)-C(3)-H(3)	120.1
C(4)-C(3)-H(3)	120.1
C(5)-C(4)-C(3)	120.49(14)
C(5)-C(4)-H(4)	119.8
C(3)-C(4)-H(4)	119.8
C(4)-C(5)-C(6)	120.94(15)
C(4)-C(5)-H(5)	119.5
C(6)-C(5)-H(5)	119.5
C(1)-C(6)-C(5)	117.08(13)
C(1)-C(6)-C(7)	116.92(13)
C(5)-C(6)-C(7)	126.00(14)
C(8)-C(7)-C(6)	134.63(13)
C(8)-C(7)-C(15)	107.51(12)
C(6)-C(7)-C(15)	117.86(12)
C(7)-C(8)-C(9)	110.26(13)
C(7)-C(8)-Cl(1)	127.96(12)
C(9)-C(8)-Cl(1)	121.77(11)
C(10)-C(9)-C(14)	121.06(13)
C(10)-C(9)-C(8)	130.74(13)
C(14)-C(9)-C(8)	108.20(13)
C(11)-C(10)-C(9)	118.27(14)
C(11)-C(10)-H(10)	120.9
C(9)-C(10)-H(10)	120.9

Chapter 6

C(10)-C(11)-C(12)	120.80(14)
C(10)-C(11)-H(11)	119.6
C(12)-C(11)-H(11)	119.6
C(13)-C(12)-C(11)	121.36(14)
C(13)-C(12)-H(12)	119.3
C(11)-C(12)-H(12)	119.3
C(12)-C(13)-C(14)	118.71(14)
C(12)-C(13)-H(13)	120.6
C(14)-C(13)-H(13)	120.6
C(13)-C(14)-C(9)	119.80(13)
C(13)-C(14)-C(15)	133.65(13)
C(9)-C(14)-C(15)	106.53(12)
C(16)-C(15)-C(14)	131.78(13)
C(16)-C(15)-C(7)	120.73(13)
C(14)-C(15)-C(7)	107.48(12)
C(15)-C(16)-O(1)	120.98(13)
C(15)-C(16)-C(17)	128.47(13)
O(1)-C(16)-C(17)	110.50(12)
C(22)-C(17)-C(18)	119.05(13)
C(22)-C(17)-C(16)	119.21(13)
C(18)-C(17)-C(16)	121.72(12)
O(2)-C(18)-C(19)	123.96(13)
O(2)-C(18)-C(17)	116.16(12)
C(19)-C(18)-C(17)	119.87(13)
C(18)-C(19)-C(20)	119.96(14)
C(18)-C(19)-H(19)	120.0
C(20)-C(19)-H(19)	120.0
C(21)-C(20)-C(19)	120.52(14)
C(21)-C(20)-H(20)	119.7
C(19)-C(20)-H(20)	119.7
C(20)-C(21)-C(22)	119.77(14)
C(20)-C(21)-H(21)	120.1
C(22)-C(21)-H(21)	120.1
C(21)-C(22)-C(17)	120.74(14)
C(21)-C(22)-H(22)	119.6
C(17)-C(22)-H(22)	119.6
O(2)-C(23)-H(23A)	109.5
O(2)-C(23)-H(23B)	109.5
H(23A)-C(23)-H(23B)	109.5

Chapter 6

O(2)-C(23)-H(23C)	109.5
H(23A)-C(23)-H(23C)	109.5
H(23B)-C(23)-H(23C)	109.5
C(16)-O(1)-C(1)	120.39(11)
C(18)-O(2)-C(23)	117.87(12)

Symmetry transformations used to generate equivalent atoms:

Table 4. Anisotropic displacement parameters ($\text{\AA}^2 \times 10^3$) for compound **275**. The anisotropic displacement factor exponent takes the form: $-2\pi^2 [h^2 a^{*2} U^{11} + \dots + 2 h k a^* b^* U^{12}]$

	U ¹¹	U ²²	U ³³	U ²³	U ¹³	U ¹²
C(1)	24(1)	20(1)	28(1)	1(1)	7(1)	2(1)
C(2)	29(1)	26(1)	25(1)	-1(1)	4(1)	3(1)
C(3)	31(1)	30(1)	27(1)	5(1)	7(1)	6(1)
C(4)	31(1)	25(1)	35(1)	6(1)	9(1)	2(1)
C(5)	27(1)	23(1)	32(1)	1(1)	6(1)	-1(1)
C(6)	22(1)	22(1)	27(1)	1(1)	6(1)	2(1)
C(7)	22(1)	18(1)	28(1)	-1(1)	7(1)	1(1)
C(8)	23(1)	21(1)	29(1)	-2(1)	6(1)	-1(1)
C(9)	21(1)	23(1)	27(1)	-2(1)	7(1)	2(1)
C(10)	23(1)	26(1)	28(1)	-6(1)	4(1)	1(1)
C(11)	26(1)	32(1)	23(1)	-3(1)	3(1)	5(1)
C(12)	28(1)	26(1)	26(1)	2(1)	7(1)	6(1)
C(13)	23(1)	22(1)	27(1)	-1(1)	6(1)	2(1)
C(14)	21(1)	22(1)	24(1)	-2(1)	5(1)	3(1)
C(15)	21(1)	21(1)	25(1)	0(1)	5(1)	2(1)
C(16)	22(1)	22(1)	23(1)	1(1)	5(1)	2(1)
C(17)	21(1)	22(1)	23(1)	1(1)	0(1)	0(1)
C(18)	21(1)	24(1)	25(1)	1(1)	1(1)	1(1)
C(19)	22(1)	29(1)	28(1)	4(1)	2(1)	-3(1)
C(20)	31(1)	26(1)	31(1)	2(1)	0(1)	-9(1)
C(21)	36(1)	24(1)	27(1)	-5(1)	1(1)	-5(1)
C(22)	28(1)	26(1)	24(1)	-2(1)	4(1)	-2(1)
C(23)	40(1)	37(1)	45(1)	-5(1)	22(1)	1(1)
O(1)	27(1)	21(1)	23(1)	1(1)	3(1)	-2(1)
O(2)	29(1)	24(1)	33(1)	-2(1)	12(1)	2(1)
Cl(1)	30(1)	26(1)	34(1)	-3(1)	6(1)	-8(1)

Table 5. Hydrogen coordinates ($\times 10^4$) and isotropic displacement parameters ($\text{\AA}^2 \times 10^3$) for compound **275**.

	x	y	z	U(eq)
H(2)	4346	5885	6155	32
H(3)	3443	4527	6725	35
H(4)	1719	3549	5720	36
H(5)	829	3941	4176	33
H(10)	-1146	5302	590	31
H(11)	-842	6512	-407	33
H(12)	950	7708	98	32
H(13)	2490	7735	1607	29
H(19)	6965	8588	2338	32
H(20)	6472	9855	3209	36
H(21)	4691	9755	4283	36
H(22)	3409	8379	4503	31
H(23A)	6155	7478	1193	58
H(23B)	6583	6436	1330	58
H(23C)	7715	7169	1926	58

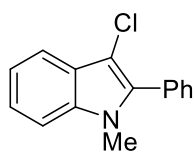
Table 6. Torsion angles [°] for compound **275**.

O(1)-C(1)-C(2)-C(3)	-177.92(13)
C(6)-C(1)-C(2)-C(3)	1.5(2)
C(1)-C(2)-C(3)-C(4)	0.1(2)
C(2)-C(3)-C(4)-C(5)	-1.2(2)
C(3)-C(4)-C(5)-C(6)	0.8(2)
O(1)-C(1)-C(6)-C(5)	177.48(13)
C(2)-C(1)-C(6)-C(5)	-1.9(2)
O(1)-C(1)-C(6)-C(7)	-3.0(2)
C(2)-C(1)-C(6)-C(7)	177.62(13)
C(4)-C(5)-C(6)-C(1)	0.8(2)
C(4)-C(5)-C(6)-C(7)	-178.73(14)
C(1)-C(6)-C(7)-C(8)	-176.55(15)
C(5)-C(6)-C(7)-C(8)	2.9(3)
C(1)-C(6)-C(7)-C(15)	3.17(19)
C(5)-C(6)-C(7)-C(15)	-177.33(13)
C(6)-C(7)-C(8)-C(9)	178.59(15)
C(15)-C(7)-C(8)-C(9)	-1.16(16)
C(6)-C(7)-C(8)-Cl(1)	-2.2(2)
C(15)-C(7)-C(8)-Cl(1)	178.01(11)
C(7)-C(8)-C(9)-C(10)	-178.49(14)
Cl(1)-C(8)-C(9)-C(10)	2.3(2)
C(7)-C(8)-C(9)-C(14)	0.85(16)
Cl(1)-C(8)-C(9)-C(14)	-178.38(10)
C(14)-C(9)-C(10)-C(11)	-0.9(2)
C(8)-C(9)-C(10)-C(11)	178.36(14)
C(9)-C(10)-C(11)-C(12)	0.6(2)
C(10)-C(11)-C(12)-C(13)	0.1(2)
C(11)-C(12)-C(13)-C(14)	-0.4(2)
C(12)-C(13)-C(14)-C(9)	0.0(2)
C(12)-C(13)-C(14)-C(15)	-178.18(14)
C(10)-C(9)-C(14)-C(13)	0.6(2)
C(8)-C(9)-C(14)-C(13)	-178.79(12)
C(10)-C(9)-C(14)-C(15)	179.26(13)
C(8)-C(9)-C(14)-C(15)	-0.15(15)
C(13)-C(14)-C(15)-C(16)	-1.0(3)
C(9)-C(14)-C(15)-C(16)	-179.40(15)
C(13)-C(14)-C(15)-C(7)	177.83(14)

Chapter 6

C(9)-C(14)-C(15)-C(7)	-0.53(15)
C(8)-C(7)-C(15)-C(16)	-179.93(13)
C(6)-C(7)-C(15)-C(16)	0.3(2)
C(8)-C(7)-C(15)-C(14)	1.05(15)
C(6)-C(7)-C(15)-C(14)	-178.75(12)
C(14)-C(15)-C(16)-O(1)	174.54(13)
C(7)-C(15)-C(16)-O(1)	-4.2(2)
C(14)-C(15)-C(16)-C(17)	-2.9(3)
C(7)-C(15)-C(16)-C(17)	178.38(13)
C(15)-C(16)-C(17)-C(22)	121.01(17)
O(1)-C(16)-C(17)-C(22)	-56.63(17)
C(15)-C(16)-C(17)-C(18)	-60.3(2)
O(1)-C(16)-C(17)-C(18)	122.09(14)
C(22)-C(17)-C(18)-O(2)	179.14(13)
C(16)-C(17)-C(18)-O(2)	0.41(19)
C(22)-C(17)-C(18)-C(19)	-0.8(2)
C(16)-C(17)-C(18)-C(19)	-179.49(13)
O(2)-C(18)-C(19)-C(20)	178.56(13)
C(17)-C(18)-C(19)-C(20)	-1.5(2)
C(18)-C(19)-C(20)-C(21)	1.8(2)
C(19)-C(20)-C(21)-C(22)	0.2(2)
C(20)-C(21)-C(22)-C(17)	-2.6(2)
C(18)-C(17)-C(22)-C(21)	2.8(2)
C(16)-C(17)-C(22)-C(21)	-178.41(13)
C(15)-C(16)-O(1)-C(1)	4.5(2)
C(17)-C(16)-O(1)-C(1)	-177.61(11)
C(2)-C(1)-O(1)-C(16)	178.62(12)
C(6)-C(1)-O(1)-C(16)	-0.8(2)
C(19)-C(18)-O(2)-C(23)	-3.6(2)
C(17)-C(18)-O(2)-C(23)	176.47(13)

Symmetry transformations used to generate equivalent atoms:

compound **295a**Table 7. Crystal data and structure refinement for compound **295a**.

Identification code	shelx
Empirical formula	C ₁₅ H ₁₂ Cl N
Formula weight	241.71
Temperature	100.00(10) K
Wavelength	0.71073 Å
Crystal system	Monoclinic
Space group	P 2 ₁ /n
Unit cell dimensions	a = 11.9505(3) Å $\alpha = 90^\circ$. b = 10.1422(3) Å $\beta = 91.866(3)^\circ$. c = 19.8545(7) Å $\gamma = 90^\circ$.
Volume	2405.18(13) Å ³
Z	8
Density (calculated)	1.335 Mg/m ³
Absorption coefficient	0.292 mm ⁻¹
F(000)	1008
Crystal size	0.584 x 0.349 x 0.293 mm ³
Theta range for data collection	2.255 to 37.240°.
Index ranges	-19 ≤ h ≤ 19, -17 ≤ k ≤ 11, -24 ≤ l ≤ 32
Reflections collected	30215
Independent reflections	11191 [R(int) = 0.0408]
Completeness to theta = 25.242°	99.5 %
Absorption correction	Gaussian
Max. and min. transmission	1.000 and 0.195
Refinement method	Full-matrix least-squares on F ²
Data / restraints / parameters	11191 / 0 / 309
Goodness-of-fit on F ²	1.054
Final R indices [I > 2σ(I)]	R1 = 0.0481, wR2 = 0.1169
R indices (all data)	R1 = 0.0761, wR2 = 0.1314
Extinction coefficient	n/a
Largest diff. peak and hole	0.814 and -0.454 e.Å ⁻³

Table 8. Atomic coordinates ($\times 10^4$) and equivalent isotropic displacement parameters ($\text{\AA}^2 \times 10^3$)
 For compound **295a**. U(eq) is defined as one third of the trace of the orthogonalized U^{ij} tensor.

	x	y	z	U(eq)
C(1)	3035(1)	8956(1)	5126(1)	21(1)
C(1A)	7902(1)	6019(1)	5305(1)	20(1)
C(2)	2588(1)	9358(1)	4510(1)	25(1)
C(2A)	7495(1)	5807(1)	4657(1)	22(1)
C(3)	3405(1)	9184(1)	4013(1)	27(1)
C(3A)	8346(1)	6116(1)	4198(1)	23(1)
C(4)	4368(1)	8688(1)	4358(1)	24(1)
C(4A)	9287(1)	6493(1)	4604(1)	21(1)
C(5)	5375(1)	8483(1)	4034(1)	31(1)
C(5A)	10313(1)	6810(1)	4323(1)	26(1)
C(6)	5385(2)	8751(1)	3350(1)	40(1)
C(6A)	10362(1)	6786(1)	3630(1)	34(1)
C(7)	4429(2)	9195(1)	2996(1)	45(1)
C(7A)	9425(1)	6452(1)	3219(1)	34(1)
C(8)	3437(1)	9424(1)	3317(1)	37(1)
C(8A)	8420(1)	6111(1)	3495(1)	30(1)
C(9)	2504(1)	8924(1)	5782(1)	21(1)
C(9A)	7315(1)	5884(1)	5940(1)	22(1)
C(10)	1870(1)	10003(1)	5994(1)	28(1)
C(10A)	7237(1)	6950(1)	6383(1)	26(1)
C(11)	1344(1)	9967(1)	6607(1)	32(1)
C(11A)	6629(1)	6837(1)	6963(1)	33(1)
C(12)	1433(1)	8863(1)	7017(1)	31(1)
C(12A)	6098(1)	5658(2)	7109(1)	36(1)
C(13)	2065(1)	7790(1)	6815(1)	28(1)
C(13A)	6179(1)	4593(1)	6676(1)	35(1)
C(14)	2590(1)	7817(1)	6203(1)	23(1)
C(14A)	6781(1)	4702(1)	6093(1)	28(1)
C(15)	4950(1)	8139(1)	5546(1)	23(1)
C(15A)	9785(1)	6693(1)	5832(1)	23(1)
N(1)	4128(1)	8540(1)	5029(1)	20(1)
N(1A)	9002(1)	6449(1)	5270(1)	19(1)
Cl(1)	1249(1)	9960(1)	4347(1)	34(1)
Cl(1A)	6150(1)	5329(1)	4423(1)	29(1)

Table 9. Bond lengths [\AA] and angles [$^\circ$] for compound **295a**.

C(1)-C(2)	1.3798(16)
C(1)-N(1)	1.3916(13)
C(1)-C(9)	1.4683(16)
C(1A)-C(2A)	1.3788(15)
C(1A)-N(1A)	1.3885(13)
C(1A)-C(9A)	1.4689(16)
C(2)-C(3)	1.4211(18)
C(2)-Cl(1)	1.7341(11)
C(2A)-C(3A)	1.4212(17)
C(2A)-Cl(1A)	1.7276(10)
C(3)-C(8)	1.4055(18)
C(3)-C(4)	1.4128(17)
C(3A)-C(8A)	1.4022(17)
C(3A)-C(4A)	1.4158(15)
C(4)-N(1)	1.3798(15)
C(4)-C(5)	1.3989(17)
C(4A)-N(1A)	1.3763(14)
C(4A)-C(5A)	1.4004(16)
C(5)-C(6)	1.385(2)
C(5)-H(5)	0.9300
C(5A)-C(6A)	1.3792(19)
C(5A)-H(5A)	0.9300
C(6)-C(7)	1.396(2)
C(6)-H(6)	0.9300
C(6A)-C(7A)	1.405(2)
C(6A)-H(6A)	0.9300
C(7)-C(8)	1.383(2)
C(7)-H(7)	0.9300
C(7A)-C(8A)	1.380(2)
C(7A)-H(7A)	0.9300
C(8)-H(8)	0.9300
C(8A)-H(8A)	0.9300
C(9)-C(10)	1.4024(15)
C(9)-C(14)	1.4024(15)
C(9A)-C(14A)	1.3963(15)
C(9A)-C(10A)	1.3981(16)
C(10)-C(11)	1.3889(19)

Chapter 6

C(10)-H(10)	0.9300
C(10A)-C(11A)	1.3860(18)
C(10A)-H(10A)	0.9300
C(11)-C(12)	1.387(2)
C(11)-H(11)	0.9300
C(11A)-C(12A)	1.3889(19)
C(11A)-H(11A)	0.9300
C(12)-C(13)	1.3913(17)
C(12)-H(12)	0.9300
C(12A)-C(13A)	1.387(2)
C(12A)-H(12A)	0.9300
C(13)-C(14)	1.3857(17)
C(13)-H(13)	0.9300
C(13A)-C(14A)	1.3868(19)
C(13A)-H(13A)	0.9300
C(14)-H(14)	0.9300
C(14A)-H(14A)	0.9300
C(15)-N(1)	1.4559(14)
C(15)-H(15D)	0.9600
C(15)-H(15E)	0.9600
C(15)-H(15F)	0.9600
C(15A)-N(1A)	1.4534(13)
C(15A)-H(15A)	0.9600
C(15A)-H(15B)	0.9600
C(15A)-H(15C)	0.9600
C(2)-C(1)-N(1)	107.78(10)
C(2)-C(1)-C(9)	128.81(10)
N(1)-C(1)-C(9)	123.40(9)
C(2A)-C(1A)-N(1A)	107.90(10)
C(2A)-C(1A)-C(9A)	128.58(9)
N(1A)-C(1A)-C(9A)	123.48(9)
C(1)-C(2)-C(3)	108.91(10)
C(1)-C(2)-Cl(1)	126.71(10)
C(3)-C(2)-Cl(1)	124.38(9)
C(1A)-C(2A)-C(3A)	109.02(9)
C(1A)-C(2A)-Cl(1A)	126.27(9)
C(3A)-C(2A)-Cl(1A)	124.62(9)
C(8)-C(3)-C(4)	119.40(13)

Chapter 6

C(8)-C(3)-C(2)	134.68(13)
C(4)-C(3)-C(2)	105.90(10)
C(8A)-C(3A)-C(4A)	119.55(11)
C(8A)-C(3A)-C(2A)	134.98(11)
C(4A)-C(3A)-C(2A)	105.47(10)
N(1)-C(4)-C(5)	129.55(12)
N(1)-C(4)-C(3)	108.42(10)
C(5)-C(4)-C(3)	121.94(12)
N(1A)-C(4A)-C(5A)	129.64(11)
N(1A)-C(4A)-C(3A)	108.70(10)
C(5A)-C(4A)-C(3A)	121.64(11)
C(6)-C(5)-C(4)	117.18(14)
C(6)-C(5)-H(5)	121.4
C(4)-C(5)-H(5)	121.4
C(6A)-C(5A)-C(4A)	117.38(12)
C(6A)-C(5A)-H(5A)	121.3
C(4A)-C(5A)-H(5A)	121.3
C(5)-C(6)-C(7)	121.59(14)
C(5)-C(6)-H(6)	119.2
C(7)-C(6)-H(6)	119.2
C(5A)-C(6A)-C(7A)	121.66(12)
C(5A)-C(6A)-H(6A)	119.2
C(7A)-C(6A)-H(6A)	119.2
C(8)-C(7)-C(6)	121.45(14)
C(8)-C(7)-H(7)	119.3
C(6)-C(7)-H(7)	119.3
C(8A)-C(7A)-C(6A)	121.13(12)
C(8A)-C(7A)-H(7A)	119.4
C(6A)-C(7A)-H(7A)	119.4
C(7)-C(8)-C(3)	118.36(15)
C(7)-C(8)-H(8)	120.8
C(3)-C(8)-H(8)	120.8
C(7A)-C(8A)-C(3A)	118.59(12)
C(7A)-C(8A)-H(8A)	120.7
C(3A)-C(8A)-H(8A)	120.7
C(10)-C(9)-C(14)	118.42(11)
C(10)-C(9)-C(1)	120.17(10)
C(14)-C(9)-C(1)	121.39(9)
C(14A)-C(9A)-C(10A)	119.17(11)

Chapter 6

C(14A)-C(9A)-C(1A)	120.00(10)
C(10A)-C(9A)-C(1A)	120.76(9)
C(11)-C(10)-C(9)	120.48(11)
C(11)-C(10)-H(10)	119.8
C(9)-C(10)-H(10)	119.8
C(11A)-C(10A)-C(9A)	120.37(11)
C(11A)-C(10A)-H(10A)	119.8
C(9A)-C(10A)-H(10A)	119.8
C(12)-C(11)-C(10)	120.50(11)
C(12)-C(11)-H(11)	119.8
C(10)-C(11)-H(11)	119.8
C(10A)-C(11A)-C(12A)	120.04(12)
C(10A)-C(11A)-H(11A)	120.0
C(12A)-C(11A)-H(11A)	120.0
C(11)-C(12)-C(13)	119.58(12)
C(11)-C(12)-H(12)	120.2
C(13)-C(12)-H(12)	120.2
C(13A)-C(12A)-C(11A)	119.95(13)
C(13A)-C(12A)-H(12A)	120.0
C(11A)-C(12A)-H(12A)	120.0
C(14)-C(13)-C(12)	120.28(12)
C(14)-C(13)-H(13)	119.9
C(12)-C(13)-H(13)	119.9
C(12A)-C(13A)-C(14A)	120.29(12)
C(12A)-C(13A)-H(13A)	119.9
C(14A)-C(13A)-H(13A)	119.9
C(13)-C(14)-C(9)	120.74(10)
C(13)-C(14)-H(14)	119.6
C(9)-C(14)-H(14)	119.6
C(13A)-C(14A)-C(9A)	120.18(12)
C(13A)-C(14A)-H(14A)	119.9
C(9A)-C(14A)-H(14A)	119.9
N(1)-C(15)-H(15D)	109.5
N(1)-C(15)-H(15E)	109.5
H(15D)-C(15)-H(15E)	109.5
N(1)-C(15)-H(15F)	109.5
H(15D)-C(15)-H(15F)	109.5
H(15E)-C(15)-H(15F)	109.5
N(1A)-C(15A)-H(15A)	109.5

Chapter 6

N(1A)-C(15A)-H(15B)	109.5
H(15A)-C(15A)-H(15B)	109.5
N(1A)-C(15A)-H(15C)	109.5
H(15A)-C(15A)-H(15C)	109.5
H(15B)-C(15A)-H(15C)	109.5
C(4)-N(1)-C(1)	108.98(9)
C(4)-N(1)-C(15)	123.69(9)
C(1)-N(1)-C(15)	127.04(9)
C(4A)-N(1A)-C(1A)	108.88(9)
C(4A)-N(1A)-C(15A)	123.88(9)
C(1A)-N(1A)-C(15A)	126.97(9)

Symmetry transformations used to generate equivalent atoms:

Table 10. Anisotropic displacement parameters ($\text{\AA}^2 \times 10^3$) for compound **295a**. The anisotropic displacement factor exponent takes the form: $-2\pi^2 [h^2 a^{*2} U^{11} + \dots + 2 h k a^* b^* U^{12}]$

	U ¹¹	U ²²	U ³³	U ²³	U ¹³	U ¹²
C(1)	17(1)	17(1)	29(1)	2(1)	-3(1)	-2(1)
C(1A)	16(1)	17(1)	26(1)	-2(1)	-2(1)	1(1)
C(2)	22(1)	20(1)	32(1)	5(1)	-7(1)	-4(1)
C(2A)	18(1)	19(1)	28(1)	-5(1)	-6(1)	2(1)
C(3)	34(1)	20(1)	26(1)	1(1)	-5(1)	-10(1)
C(3A)	25(1)	18(1)	25(1)	-2(1)	-4(1)	5(1)
C(4)	27(1)	17(1)	26(1)	-3(1)	1(1)	-6(1)
C(4A)	23(1)	16(1)	24(1)	0(1)	-1(1)	2(1)
C(5)	35(1)	22(1)	35(1)	-7(1)	10(1)	-7(1)
C(5A)	25(1)	21(1)	32(1)	3(1)	4(1)	1(1)
C(6)	56(1)	30(1)	36(1)	-10(1)	19(1)	-14(1)
C(6A)	39(1)	28(1)	35(1)	5(1)	12(1)	4(1)
C(7)	74(1)	35(1)	26(1)	-5(1)	7(1)	-21(1)
C(7A)	49(1)	29(1)	25(1)	2(1)	5(1)	9(1)
C(8)	55(1)	28(1)	28(1)	2(1)	-8(1)	-15(1)
C(8A)	39(1)	25(1)	25(1)	-1(1)	-6(1)	8(1)
C(9)	16(1)	18(1)	30(1)	-1(1)	-1(1)	0(1)
C(9A)	16(1)	21(1)	27(1)	1(1)	-2(1)	-1(1)
C(10)	21(1)	20(1)	41(1)	-1(1)	1(1)	3(1)
C(10A)	27(1)	24(1)	28(1)	-1(1)	1(1)	-1(1)
C(11)	22(1)	31(1)	44(1)	-10(1)	4(1)	4(1)
C(11A)	33(1)	37(1)	28(1)	-2(1)	3(1)	1(1)
C(12)	22(1)	40(1)	31(1)	-7(1)	3(1)	1(1)
C(12A)	25(1)	52(1)	31(1)	5(1)	4(1)	-5(1)
C(13)	25(1)	32(1)	27(1)	2(1)	1(1)	1(1)
C(13A)	25(1)	39(1)	40(1)	8(1)	-1(1)	-11(1)
C(14)	20(1)	21(1)	28(1)	0(1)	0(1)	2(1)
C(14A)	22(1)	26(1)	37(1)	1(1)	-1(1)	-6(1)
C(15)	17(1)	20(1)	30(1)	-1(1)	-3(1)	1(1)
C(15A)	19(1)	24(1)	26(1)	0(1)	-5(1)	-1(1)
N(1)	17(1)	19(1)	25(1)	-1(1)	0(1)	-1(1)
N(1A)	16(1)	20(1)	22(1)	0(1)	-2(1)	-1(1)
Cl(1)	25(1)	25(1)	50(1)	11(1)	-13(1)	-3(1)
Cl(1A)	18(1)	22(1)	45(1)	-10(1)	-8(1)	1(1)

Table 11. Hydrogen coordinates ($\times 10^4$) and isotropic displacement parameters ($\text{\AA}^2 \times 10^3$) for compound **295a**.

	x	y	z	U(eq)
H(5)	6011	8180	4268	37
H(5A)	10936	7029	4593	31
H(6)	6044	8633	3121	48
H(6A)	11032	6995	3430	40
H(7)	4460	9340	2534	54
H(7A)	9484	6460	2753	41
H(8)	2807	9729	3077	45
H(8A)	7805	5883	3220	36
H(10)	1803	10747	5722	33
H(10A)	7595	7740	6288	31
H(11)	929	10689	6744	39
H(11A)	6576	7551	7254	39
H(12)	1073	8840	7425	37
H(12A)	5689	5582	7498	43
H(13)	2134	7052	7091	33
H(13A)	5828	3801	6776	41
H(14)	3006	7092	6070	28
H(14A)	6828	3986	5802	34
H(15D)	4952	7196	5584	34
H(15E)	4761	8522	5970	34
H(15F)	5679	8437	5426	34
H(15A)	10471	6231	5759	34
H(15B)	9467	6389	6241	34
H(15C)	9933	7622	5865	34

Table 12. Torsion angles [°] for compound **295a**.

N(1)-C(1)-C(2)-C(3)	0.53(12)
C(9)-C(1)-C(2)-C(3)	-178.58(10)
N(1)-C(1)-C(2)-Cl(1)	179.70(8)
C(9)-C(1)-C(2)-Cl(1)	0.59(16)
N(1A)-C(1A)-C(2A)-C(3A)	-0.42(11)
C(9A)-C(1A)-C(2A)-C(3A)	177.34(10)
N(1A)-C(1A)-C(2A)-Cl(1A)	-177.16(8)
C(9A)-C(1A)-C(2A)-Cl(1A)	0.60(16)
C(1)-C(2)-C(3)-C(8)	-179.31(12)
Cl(1)-C(2)-C(3)-C(8)	1.49(19)
C(1)-C(2)-C(3)-C(4)	-1.22(12)
Cl(1)-C(2)-C(3)-C(4)	179.59(8)
C(1A)-C(2A)-C(3A)-C(8A)	-179.04(11)
Cl(1A)-C(2A)-C(3A)-C(8A)	-2.23(18)
C(1A)-C(2A)-C(3A)-C(4A)	1.30(11)
Cl(1A)-C(2A)-C(3A)-C(4A)	178.11(8)
C(8)-C(3)-C(4)-N(1)	179.90(10)
C(2)-C(3)-C(4)-N(1)	1.45(11)
C(8)-C(3)-C(4)-C(5)	3.01(16)
C(2)-C(3)-C(4)-C(5)	-175.44(10)
C(8A)-C(3A)-C(4A)-N(1A)	178.57(9)
C(2A)-C(3A)-C(4A)-N(1A)	-1.70(11)
C(8A)-C(3A)-C(4A)-C(5A)	-2.77(15)
C(2A)-C(3A)-C(4A)-C(5A)	176.95(10)
N(1)-C(4)-C(5)-C(6)	-178.01(11)
C(3)-C(4)-C(5)-C(6)	-1.84(16)
N(1A)-C(4A)-C(5A)-C(6A)	-179.48(10)
C(3A)-C(4A)-C(5A)-C(6A)	2.18(16)
C(4)-C(5)-C(6)-C(7)	-0.60(18)
C(4A)-C(5A)-C(6A)-C(7A)	-0.22(17)
C(5)-C(6)-C(7)-C(8)	1.9(2)
C(5A)-C(6A)-C(7A)-C(8A)	-1.17(19)
C(6)-C(7)-C(8)-C(3)	-0.71(19)
C(4)-C(3)-C(8)-C(7)	-1.67(17)
C(2)-C(3)-C(8)-C(7)	176.23(12)
C(6A)-C(7A)-C(8A)-C(3A)	0.58(18)
C(4A)-C(3A)-C(8A)-C(7A)	1.33(16)

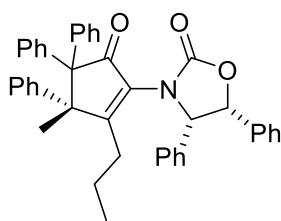
Chapter 6

C(2A)-C(3A)-C(8A)-C(7A)	-178.30(12)
C(2)-C(1)-C(9)-C(10)	-45.04(16)
N(1)-C(1)-C(9)-C(10)	135.98(11)
C(2)-C(1)-C(9)-C(14)	133.46(12)
N(1)-C(1)-C(9)-C(14)	-45.53(15)
C(2A)-C(1A)-C(9A)-C(14A)	54.46(15)
N(1A)-C(1A)-C(9A)-C(14A)	-128.09(11)
C(2A)-C(1A)-C(9A)-C(10A)	-122.40(12)
N(1A)-C(1A)-C(9A)-C(10A)	55.04(14)
C(14)-C(9)-C(10)-C(11)	-0.02(17)
C(1)-C(9)-C(10)-C(11)	178.51(11)
C(14A)-C(9A)-C(10A)-C(11A)	-0.50(17)
C(1A)-C(9A)-C(10A)-C(11A)	176.40(11)
C(9)-C(10)-C(11)-C(12)	-0.26(19)
C(9A)-C(10A)-C(11A)-C(12A)	0.37(19)
C(10)-C(11)-C(12)-C(13)	0.68(19)
C(10A)-C(11A)-C(12A)-C(13A)	0.1(2)
C(11)-C(12)-C(13)-C(14)	-0.82(19)
C(11A)-C(12A)-C(13A)-C(14A)	-0.5(2)
C(12)-C(13)-C(14)-C(9)	0.55(18)
C(10)-C(9)-C(14)-C(13)	-0.12(16)
C(1)-C(9)-C(14)-C(13)	-178.64(10)
C(12A)-C(13A)-C(14A)-C(9A)	0.41(19)
C(10A)-C(9A)-C(14A)-C(13A)	0.10(17)
C(1A)-C(9A)-C(14A)-C(13A)	-176.81(11)
C(5)-C(4)-N(1)-C(1)	175.41(11)
C(3)-C(4)-N(1)-C(1)	-1.17(11)
C(5)-C(4)-N(1)-C(15)	1.17(17)
C(3)-C(4)-N(1)-C(15)	-175.41(9)
C(2)-C(1)-N(1)-C(4)	0.40(11)
C(9)-C(1)-N(1)-C(4)	179.57(9)
C(2)-C(1)-N(1)-C(15)	174.39(9)
C(9)-C(1)-N(1)-C(15)	-6.45(15)
C(5A)-C(4A)-N(1A)-C(1A)	-177.01(10)
C(3A)-C(4A)-N(1A)-C(1A)	1.50(11)
C(5A)-C(4A)-N(1A)-C(15A)	-2.64(17)
C(3A)-C(4A)-N(1A)-C(15A)	175.87(9)
C(2A)-C(1A)-N(1A)-C(4A)	-0.67(11)
C(9A)-C(1A)-N(1A)-C(4A)	-178.57(9)

Chapter 6

C(2A)-C(1A)-N(1A)-C(15A)	-174.81(9)
C(9A)-C(1A)-N(1A)-C(15A)	7.28(15)

Symmetry transformations used to generate equivalent atoms:

compound **390**Table 13. Crystal data and structure refinement for compound **390**.

Identification code	shelx
Empirical formula	C ₄₂ H ₃₇ N O ₃
Formula weight	603.72
Temperature	100.0(1) K
Wavelength	1.54184 Å
Crystal system	Triclinic
Space group	P 1
Unit cell dimensions	a = 9.4983(2) Å $\alpha = 79.202(2)^\circ$ b = 11.1047(2) Å $\beta = 76.189(2)^\circ$ c = 16.2802(3) Å $\gamma = 78.716(2)^\circ$
Volume	1617.36(6) Å ³
Z	2
Density (calculated)	1.240 Mg/m ³
Absorption coefficient	0.604 mm ⁻¹
F(000)	640
Crystal size	0.500 x 0.352 x 0.206 mm ³
Theta range for data collection	2.826 to 78.191°.
Index ranges	-11 ≤ h ≤ 12, -14 ≤ k ≤ 13, -20 ≤ l ≤ 20
Reflections collected	57926
Independent reflections	12942 [R(int) = 0.0400]
Completeness to theta = 67.684°	100.0 %
Absorption correction	Semi-empirical from equivalents
Max. and min. transmission	1.00000 and 0.64560
Refinement method	Full-matrix least-squares on F ²
Data / restraints / parameters	12942 / 3 / 833
Goodness-of-fit on F ²	1.049
Final R indices [I > 2σ(I)]	R1 = 0.0339, wR2 = 0.0906
R indices (all data)	R1 = 0.0343, wR2 = 0.0910
Absolute structure parameter	-0.07(6)
Extinction coefficient	n/a
Largest diff. peak and hole	0.175 and -0.201 e.Å ⁻³

Table 14. Atomic coordinates ($\times 10^4$) and equivalent isotropic displacement parameters ($\text{\AA}^2 \times 10^3$) for compound **390**. U(eq) is defined as one third of the trace of the orthogonalized U^{ij} tensor.

	x	y	z	U(eq)
C(1)	2645(2)	3684(2)	8115(1)	20(1)
C(1A)	6859(2)	8972(2)	3226(1)	19(1)
C(1B)	7791(2)	-359(2)	6900(2)	31(1)
C(2)	3221(2)	2397(2)	7955(1)	19(1)
C(2A)	7539(2)	7772(2)	2940(1)	18(1)
C(3)	4507(2)	2314(2)	7391(1)	19(1)
C(3A)	8830(2)	7832(2)	2389(1)	19(1)
C(4)	5038(2)	3573(2)	7140(1)	20(1)
C(4A)	9227(2)	9135(2)	2242(1)	19(1)
C(5)	5352(2)	10315(2)	951(1)	26(1)
C(5A)	7716(2)	9967(2)	2643(1)	19(1)
C(6)	5383(2)	1173(2)	7049(1)	22(1)
C(6A)	9851(2)	6767(2)	2020(1)	24(1)
C(7)	3556(2)	4526(2)	7408(1)	20(1)
C(7A)	9719(3)	6620(2)	1126(1)	31(1)
C(8)	6912(2)	795(2)	7267(2)	26(1)
C(8A)	10678(3)	5444(2)	843(2)	43(1)
C(9)	6110(2)	3637(2)	7716(1)	21(1)
C(9A)	10410(2)	9082(2)	2768(1)	20(1)
C(10)	5943(2)	3029(2)	8562(1)	22(1)
C(10A)	10368(2)	8326(2)	3561(1)	22(1)
C(11)	6838(2)	3171(2)	9090(1)	24(1)
C(11A)	11375(2)	8329(2)	4056(1)	24(1)
C(12)	7923(2)	3918(2)	8788(2)	26(1)
C(12A)	12453(2)	9085(2)	3770(1)	24(1)
C(13)	8111(2)	4510(2)	7946(2)	27(1)
C(13A)	12529(2)	9820(2)	2975(1)	25(1)
C(14)	7226(2)	4370(2)	7419(1)	23(1)
C(14A)	11515(2)	9817(2)	2484(1)	23(1)
C(15)	5787(2)	3812(2)	6189(1)	25(1)
C(15A)	9816(2)	9585(2)	1292(1)	24(1)
C(16)	3915(2)	5655(2)	7672(1)	21(1)
C(16A)	8009(2)	10924(2)	3117(1)	19(1)
C(17)	3802(2)	5788(2)	8514(1)	24(1)

Chapter 6

C(17A)	7820(2)	10756(2)	4001(1)	22(1)
C(18)	4278(3)	6788(2)	8711(2)	30(1)
C(18A)	8211(2)	11591(2)	4411(1)	25(1)
C(19)	4898(2)	7654(2)	8063(2)	30(1)
C(19A)	8809(2)	12619(2)	3939(2)	26(1)
C(20)	5010(2)	7535(2)	7221(2)	28(1)
C(20A)	9013(2)	12792(2)	3058(1)	24(1)
C(21)	4514(2)	6555(2)	7024(1)	24(1)
C(21A)	8611(2)	11963(2)	2647(1)	22(1)
C(22)	2544(2)	4923(2)	6755(1)	21(1)
C(22A)	6681(2)	10540(2)	2009(1)	20(1)
C(23)	2379(2)	4142(2)	6216(1)	24(1)
C(23A)	6390(2)	9833(2)	1452(1)	23(1)
C(24)	1363(3)	4514(2)	5691(1)	28(1)
C(24A)	4569(2)	11498(2)	995(1)	27(1)
C(25)	456(3)	5645(2)	5706(1)	30(1)
C(26)	572(2)	6424(2)	6260(1)	29(1)
C(26A)	4820(2)	12201(2)	1549(1)	26(1)
C(27)	1600(2)	6065(2)	6775(1)	23(1)
C(27A)	5857(2)	11720(2)	2056(1)	23(1)
C(28)	3018(2)	483(2)	8966(1)	20(1)
C(28A)	7325(2)	5837(2)	3923(1)	21(1)
C(29)	618(2)	275(2)	9079(1)	20(1)
C(29A)	4934(2)	5648(2)	3977(1)	21(1)
C(30)	1021(2)	1265(2)	8280(1)	19(1)
C(30A)	5404(2)	6620(2)	3179(1)	19(1)
C(31)	-208(2)	-721(2)	9018(1)	20(1)
C(31A)	5470(2)	6280(2)	2314(1)	20(1)
C(32)	511(2)	-1884(2)	8824(1)	24(1)
C(32A)	6372(2)	5216(2)	2042(1)	24(1)
C(33)	-287(2)	-2799(2)	8810(1)	25(1)
C(33A)	6421(2)	4921(2)	1243(1)	27(1)
C(34)	-1806(2)	-2564(2)	8990(1)	26(1)
C(34A)	5561(3)	5684(2)	711(2)	35(1)
C(35)	-2532(2)	-1413(2)	9193(2)	28(1)
C(35A)	4661(3)	6737(3)	981(2)	41(1)
C(36)	-1734(2)	-498(2)	9211(1)	24(1)
C(36A)	4619(3)	7037(2)	1777(1)	30(1)
C(37)	1113(2)	962(2)	7398(1)	19(1)

Chapter 6

C(37A)	4152(2)	4660(2)	3855(1)	20(1)
C(38)	2011(2)	-82(2)	7098(1)	24(1)
C(38A)	2843(2)	5021(2)	3563(1)	24(1)
C(39)	2111(2)	-298(2)	6272(1)	29(1)
C(39A)	2063(2)	4130(2)	3480(1)	26(1)
C(40)	1317(3)	541(2)	5730(1)	29(1)
C(40A)	2577(2)	2877(2)	3689(1)	26(1)
C(41)	434(2)	1578(2)	6025(1)	27(1)
C(41A)	3876(2)	2517(2)	3980(1)	26(1)
C(42)	326(2)	1794(2)	6854(1)	22(1)
C(42A)	4667(2)	3406(2)	4060(1)	23(1)
N(1)	2459(2)	1414(2)	8402(1)	19(1)
N(1A)	6859(2)	6712(2)	3300(1)	19(1)
O(1)	1600(2)	4009(1)	8667(1)	24(1)
O(1A)	5796(2)	9138(1)	3803(1)	22(1)
O(2)	4200(2)	319(1)	9157(1)	26(1)
O(3)	2017(2)	-293(1)	9304(1)	23(1)
O(2A)	8470(2)	5684(1)	4155(1)	29(1)
O(3A)	6289(2)	5089(1)	4256(1)	25(1)

Table 15. Bond lengths [\AA] and angles [$^\circ$] for compound **390**.

C(1)-O(1)	1.217(3)
C(1)-C(2)	1.475(3)
C(1)-C(7)	1.544(3)
C(1A)-O(1A)	1.215(2)
C(1A)-C(2A)	1.471(3)
C(1A)-C(5A)	1.540(2)
C(1B)-C(8)	1.525(3)
C(1B)-H(1B1)	0.9600
C(1B)-H(1B2)	0.9600
C(1B)-H(1B3)	0.9600
C(2)-C(3)	1.340(3)
C(2)-N(1)	1.416(2)
C(2A)-C(3A)	1.341(3)
C(2A)-N(1A)	1.415(2)
C(3)-C(6)	1.496(3)
C(3)-C(4)	1.530(3)
C(3A)-C(6A)	1.496(3)
C(3A)-C(4A)	1.528(3)
C(4)-C(15)	1.539(3)
C(4)-C(9)	1.559(3)
C(4)-C(7)	1.609(3)
C(4A)-C(15A)	1.537(3)
C(4A)-C(9A)	1.553(3)
C(4A)-C(5A)	1.612(3)
C(5)-C(24A)	1.383(3)
C(5)-C(23A)	1.392(3)
C(5)-H(5)	0.9300
C(5A)-C(16A)	1.526(3)
C(5A)-C(22A)	1.558(3)
C(6)-C(8)	1.536(3)
C(6)-H(6A)	0.9700
C(6)-H(6B)	0.9700
C(6A)-C(7A)	1.532(3)
C(6A)-H(6A1)	0.9700
C(6A)-H(6A2)	0.9700
C(7)-C(16)	1.520(3)
C(7)-C(22)	1.548(3)

Chapter 6

C(7A)-C(8A)	1.519(3)
C(7A)-H(7A1)	0.9700
C(7A)-H(7A2)	0.9700
C(8)-H(8A)	0.9700
C(8)-H(8B)	0.9700
C(8A)-H(8A1)	0.9600
C(8A)-H(8A2)	0.9600
C(8A)-H(8A3)	0.9600
C(9)-C(14)	1.402(3)
C(9)-C(10)	1.403(3)
C(9A)-C(14A)	1.394(3)
C(9A)-C(10A)	1.399(3)
C(10)-C(11)	1.391(3)
C(10)-H(10)	0.9300
C(10A)-C(11A)	1.391(3)
C(10A)-H(10A)	0.9300
C(11)-C(12)	1.390(3)
C(11)-H(11)	0.9300
C(11A)-C(12A)	1.390(3)
C(11A)-H(11A)	0.9300
C(12)-C(13)	1.391(3)
C(12)-H(12)	0.9300
C(12A)-C(13A)	1.389(3)
C(12A)-H(12A)	0.9300
C(13)-C(14)	1.383(3)
C(13)-H(13)	0.9300
C(13A)-C(14A)	1.392(3)
C(13A)-H(13A)	0.9300
C(14)-H(14)	0.9300
C(14A)-H(14A)	0.9300
C(15)-H(15D)	0.9600
C(15)-H(15E)	0.9600
C(15)-H(15F)	0.9600
C(15A)-H(15A)	0.9600
C(15A)-H(15B)	0.9600
C(15A)-H(15C)	0.9600
C(16)-C(17)	1.383(3)
C(16)-C(21)	1.405(3)
C(16A)-C(17A)	1.388(3)

Chapter 6

C(16A)-C(21A)	1.402(3)
C(17)-C(18)	1.393(3)
C(17)-H(17)	0.9300
C(17A)-C(18A)	1.389(3)
C(17A)-H(17A)	0.9300
C(18)-C(19)	1.389(3)
C(18)-H(18)	0.9300
C(18A)-C(19A)	1.390(3)
C(18A)-H(18A)	0.9300
C(19)-C(20)	1.377(3)
C(19)-H(19)	0.9300
C(19A)-C(20A)	1.383(3)
C(19A)-H(19A)	0.9300
C(20)-C(21)	1.383(3)
C(20)-H(20)	0.9300
C(20A)-C(21A)	1.389(3)
C(20A)-H(20A)	0.9300
C(21)-H(21)	0.9300
C(21A)-H(21A)	0.9300
C(22)-C(23)	1.397(3)
C(22)-C(27)	1.404(3)
C(22A)-C(27A)	1.395(3)
C(22A)-C(23A)	1.410(3)
C(23)-C(24)	1.391(3)
C(23)-H(23)	0.9300
C(23A)-H(23A)	0.9300
C(24)-C(25)	1.378(4)
C(24)-H(24)	0.9300
C(24A)-C(26A)	1.386(3)
C(24A)-H(24A)	0.9300
C(25)-C(26)	1.395(3)
C(25)-H(25)	0.9300
C(26)-C(27)	1.389(3)
C(26)-H(26)	0.9300
C(26A)-C(27A)	1.397(3)
C(26A)-H(26A)	0.9300
C(27)-H(27)	0.9300
C(27A)-H(27A)	0.9300
C(28)-O(2)	1.206(2)

Chapter 6

C(28)-O(3)	1.357(2)
C(28)-N(1)	1.363(2)
C(28A)-O(2A)	1.205(3)
C(28A)-N(1A)	1.359(3)
C(28A)-O(3A)	1.360(2)
C(29)-O(3)	1.454(2)
C(29)-C(31)	1.506(3)
C(29)-C(30)	1.562(3)
C(29)-H(29)	0.9800
C(29A)-O(3A)	1.451(2)
C(29A)-C(37A)	1.505(3)
C(29A)-C(30A)	1.562(3)
C(29A)-H(29A)	0.9800
C(30)-N(1)	1.470(2)
C(30)-C(37)	1.515(3)
C(30)-H(30)	0.9800
C(30A)-N(1A)	1.466(2)
C(30A)-C(31A)	1.510(3)
C(30A)-H(30A)	0.9800
C(31)-C(36)	1.390(3)
C(31)-C(32)	1.392(3)
C(31A)-C(36A)	1.386(3)
C(31A)-C(32A)	1.395(3)
C(32)-C(33)	1.389(3)
C(32)-H(32)	0.9300
C(32A)-C(33A)	1.387(3)
C(32A)-H(32A)	0.9300
C(33)-C(34)	1.383(3)
C(33)-H(33)	0.9300
C(33A)-C(34A)	1.388(3)
C(33A)-H(33A)	0.9300
C(34)-C(35)	1.387(3)
C(34)-H(34)	0.9300
C(34A)-C(35A)	1.383(4)
C(34A)-H(34A)	0.9300
C(35)-C(36)	1.389(3)
C(35)-H(35)	0.9300
C(35A)-C(36A)	1.387(3)
C(35A)-H(35A)	0.9300

Chapter 6

C(36)-H(36)	0.9300
C(36A)-H(36A)	0.9300
C(37)-C(42)	1.391(3)
C(37)-C(38)	1.391(3)
C(37A)-C(42A)	1.388(3)
C(37A)-C(38A)	1.395(3)
C(38)-C(39)	1.387(3)
C(38)-H(38)	0.9300
C(38A)-C(39A)	1.390(3)
C(38A)-H(38A)	0.9300
C(39)-C(40)	1.397(3)
C(39)-H(39)	0.9300
C(39A)-C(40A)	1.388(3)
C(39A)-H(39A)	0.9300
C(40)-C(41)	1.377(3)
C(40)-H(40)	0.9300
C(40A)-C(41A)	1.386(3)
C(40A)-H(40A)	0.9300
C(41)-C(42)	1.391(3)
C(41)-H(41)	0.9300
C(41A)-C(42A)	1.393(3)
C(41A)-H(41A)	0.9300
C(42)-H(42)	0.9300
C(42A)-H(42A)	0.9300

O(1)-C(1)-C(2)	125.99(18)
O(1)-C(1)-C(7)	127.32(19)
C(2)-C(1)-C(7)	106.56(16)
O(1A)-C(1A)-C(2A)	125.66(17)
O(1A)-C(1A)-C(5A)	127.03(18)
C(2A)-C(1A)-C(5A)	107.28(16)
C(8)-C(1B)-H(1B1)	109.5
C(8)-C(1B)-H(1B2)	109.5
H(1B1)-C(1B)-H(1B2)	109.5
C(8)-C(1B)-H(1B3)	109.5
H(1B1)-C(1B)-H(1B3)	109.5
H(1B2)-C(1B)-H(1B3)	109.5
C(3)-C(2)-N(1)	127.40(18)
C(3)-C(2)-C(1)	112.03(17)

Chapter 6

N(1)-C(2)-C(1)	120.52(17)
C(3A)-C(2A)-N(1A)	128.13(19)
C(3A)-C(2A)-C(1A)	112.47(17)
N(1A)-C(2A)-C(1A)	119.24(17)
C(2)-C(3)-C(6)	127.13(18)
C(2)-C(3)-C(4)	110.68(18)
C(6)-C(3)-C(4)	122.17(17)
C(2A)-C(3A)-C(6A)	126.24(18)
C(2A)-C(3A)-C(4A)	110.81(18)
C(6A)-C(3A)-C(4A)	122.68(17)
C(3)-C(4)-C(15)	112.50(17)
C(3)-C(4)-C(9)	108.79(15)
C(15)-C(4)-C(9)	110.43(16)
C(3)-C(4)-C(7)	102.55(15)
C(15)-C(4)-C(7)	114.15(16)
C(9)-C(4)-C(7)	108.02(16)
C(3A)-C(4A)-C(15A)	112.16(16)
C(3A)-C(4A)-C(9A)	107.09(15)
C(15A)-C(4A)-C(9A)	110.18(16)
C(3A)-C(4A)-C(5A)	103.57(15)
C(15A)-C(4A)-C(5A)	113.26(15)
C(9A)-C(4A)-C(5A)	110.24(15)
C(24A)-C(5)-C(23A)	120.7(2)
C(24A)-C(5)-H(5)	119.7
C(23A)-C(5)-H(5)	119.7
C(16A)-C(5A)-C(1A)	113.94(16)
C(16A)-C(5A)-C(22A)	112.96(16)
C(1A)-C(5A)-C(22A)	101.19(14)
C(16A)-C(5A)-C(4A)	110.95(15)
C(1A)-C(5A)-C(4A)	101.79(15)
C(22A)-C(5A)-C(4A)	115.19(15)
C(3)-C(6)-C(8)	114.45(17)
C(3)-C(6)-H(6A)	108.6
C(8)-C(6)-H(6A)	108.6
C(3)-C(6)-H(6B)	108.6
C(8)-C(6)-H(6B)	108.6
H(6A)-C(6)-H(6B)	107.6
C(3A)-C(6A)-C(7A)	114.91(17)
C(3A)-C(6A)-H(6A1)	108.5

Chapter 6

C(7A)-C(6A)-H(6A1)	108.5
C(3A)-C(6A)-H(6A2)	108.5
C(7A)-C(6A)-H(6A2)	108.5
H(6A1)-C(6A)-H(6A2)	107.5
C(16)-C(7)-C(1)	116.54(17)
C(16)-C(7)-C(22)	110.88(16)
C(1)-C(7)-C(22)	101.19(15)
C(16)-C(7)-C(4)	110.05(15)
C(1)-C(7)-C(4)	101.21(15)
C(22)-C(7)-C(4)	116.66(17)
C(8A)-C(7A)-C(6A)	111.2(2)
C(8A)-C(7A)-H(7A1)	109.4
C(6A)-C(7A)-H(7A1)	109.4
C(8A)-C(7A)-H(7A2)	109.4
C(6A)-C(7A)-H(7A2)	109.4
H(7A1)-C(7A)-H(7A2)	108.0
C(1B)-C(8)-C(6)	113.42(18)
C(1B)-C(8)-H(8A)	108.9
C(6)-C(8)-H(8A)	108.9
C(1B)-C(8)-H(8B)	108.9
C(6)-C(8)-H(8B)	108.9
H(8A)-C(8)-H(8B)	107.7
C(7A)-C(8A)-H(8A1)	109.5
C(7A)-C(8A)-H(8A2)	109.5
H(8A1)-C(8A)-H(8A2)	109.5
C(7A)-C(8A)-H(8A3)	109.5
H(8A1)-C(8A)-H(8A3)	109.5
H(8A2)-C(8A)-H(8A3)	109.5
C(14)-C(9)-C(10)	117.62(19)
C(14)-C(9)-C(4)	120.70(18)
C(10)-C(9)-C(4)	121.58(17)
C(14A)-C(9A)-C(10A)	117.65(18)
C(14A)-C(9A)-C(4A)	121.47(17)
C(10A)-C(9A)-C(4A)	120.84(17)
C(11)-C(10)-C(9)	120.96(18)
C(11)-C(10)-H(10)	119.5
C(9)-C(10)-H(10)	119.5
C(11A)-C(10A)-C(9A)	121.04(18)
C(11A)-C(10A)-H(10A)	119.5

Chapter 6

C(9A)-C(10A)-H(10A)	119.5
C(12)-C(11)-C(10)	120.6(2)
C(12)-C(11)-H(11)	119.7
C(10)-C(11)-H(11)	119.7
C(12A)-C(11A)-C(10A)	120.56(19)
C(12A)-C(11A)-H(11A)	119.7
C(10A)-C(11A)-H(11A)	119.7
C(11)-C(12)-C(13)	118.8(2)
C(11)-C(12)-H(12)	120.6
C(13)-C(12)-H(12)	120.6
C(13A)-C(12A)-C(11A)	119.04(19)
C(13A)-C(12A)-H(12A)	120.5
C(11A)-C(12A)-H(12A)	120.5
C(14)-C(13)-C(12)	120.78(19)
C(14)-C(13)-H(13)	119.6
C(12)-C(13)-H(13)	119.6
C(12A)-C(13A)-C(14A)	120.18(18)
C(12A)-C(13A)-H(13A)	119.9
C(14A)-C(13A)-H(13A)	119.9
C(13)-C(14)-C(9)	121.19(19)
C(13)-C(14)-H(14)	119.4
C(9)-C(14)-H(14)	119.4
C(13A)-C(14A)-C(9A)	121.51(19)
C(13A)-C(14A)-H(14A)	119.2
C(9A)-C(14A)-H(14A)	119.2
C(4)-C(15)-H(15D)	109.5
C(4)-C(15)-H(15E)	109.5
H(15D)-C(15)-H(15E)	109.5
C(4)-C(15)-H(15F)	109.5
H(15D)-C(15)-H(15F)	109.5
H(15E)-C(15)-H(15F)	109.5
C(4A)-C(15A)-H(15A)	109.5
C(4A)-C(15A)-H(15B)	109.5
H(15A)-C(15A)-H(15B)	109.5
C(4A)-C(15A)-H(15C)	109.5
H(15A)-C(15A)-H(15C)	109.5
H(15B)-C(15A)-H(15C)	109.5
C(17)-C(16)-C(21)	118.37(19)
C(17)-C(16)-C(7)	123.30(18)

Chapter 6

C(21)-C(16)-C(7)	118.08(18)
C(17A)-C(16A)-C(21A)	118.00(19)
C(17A)-C(16A)-C(5A)	122.48(17)
C(21A)-C(16A)-C(5A)	119.29(17)
C(16)-C(17)-C(18)	120.5(2)
C(16)-C(17)-H(17)	119.8
C(18)-C(17)-H(17)	119.8
C(16A)-C(17A)-C(18A)	121.25(19)
C(16A)-C(17A)-H(17A)	119.4
C(18A)-C(17A)-H(17A)	119.4
C(19)-C(18)-C(17)	120.4(2)
C(19)-C(18)-H(18)	119.8
C(17)-C(18)-H(18)	119.8
C(17A)-C(18A)-C(19A)	120.4(2)
C(17A)-C(18A)-H(18A)	119.8
C(19A)-C(18A)-H(18A)	119.8
C(20)-C(19)-C(18)	119.6(2)
C(20)-C(19)-H(19)	120.2
C(18)-C(19)-H(19)	120.2
C(20A)-C(19A)-C(18A)	118.93(19)
C(20A)-C(19A)-H(19A)	120.5
C(18A)-C(19A)-H(19A)	120.5
C(19)-C(20)-C(21)	120.1(2)
C(19)-C(20)-H(20)	120.0
C(21)-C(20)-H(20)	120.0
C(19A)-C(20A)-C(21A)	120.77(19)
C(19A)-C(20A)-H(20A)	119.6
C(21A)-C(20A)-H(20A)	119.6
C(20)-C(21)-C(16)	121.0(2)
C(20)-C(21)-H(21)	119.5
C(16)-C(21)-H(21)	119.5
C(20A)-C(21A)-C(16A)	120.68(19)
C(20A)-C(21A)-H(21A)	119.7
C(16A)-C(21A)-H(21A)	119.7
C(23)-C(22)-C(27)	117.36(18)
C(23)-C(22)-C(7)	123.52(18)
C(27)-C(22)-C(7)	118.62(18)
C(27A)-C(22A)-C(23A)	117.30(18)
C(27A)-C(22A)-C(5A)	120.59(18)

Chapter 6

C(23A)-C(22A)-C(5A)	121.56(18)
C(24)-C(23)-C(22)	120.9(2)
C(24)-C(23)-H(23)	119.5
C(22)-C(23)-H(23)	119.5
C(5)-C(23A)-C(22A)	121.0(2)
C(5)-C(23A)-H(23A)	119.5
C(22A)-C(23A)-H(23A)	119.5
C(25)-C(24)-C(23)	121.2(2)
C(25)-C(24)-H(24)	119.4
C(23)-C(24)-H(24)	119.4
C(5)-C(24A)-C(26A)	119.25(19)
C(5)-C(24A)-H(24A)	120.4
C(26A)-C(24A)-H(24A)	120.4
C(24)-C(25)-C(26)	118.8(2)
C(24)-C(25)-H(25)	120.6
C(26)-C(25)-H(25)	120.6
C(27)-C(26)-C(25)	120.3(2)
C(27)-C(26)-H(26)	119.9
C(25)-C(26)-H(26)	119.9
C(24A)-C(26A)-C(27A)	120.3(2)
C(24A)-C(26A)-H(26A)	119.8
C(27A)-C(26A)-H(26A)	119.8
C(26)-C(27)-C(22)	121.4(2)
C(26)-C(27)-H(27)	119.3
C(22)-C(27)-H(27)	119.3
C(22A)-C(27A)-C(26A)	121.4(2)
C(22A)-C(27A)-H(27A)	119.3
C(26A)-C(27A)-H(27A)	119.3
O(2)-C(28)-O(3)	122.79(18)
O(2)-C(28)-N(1)	128.26(18)
O(3)-C(28)-N(1)	108.95(16)
O(2A)-C(28A)-N(1A)	128.07(18)
O(2A)-C(28A)-O(3A)	122.98(18)
N(1A)-C(28A)-O(3A)	108.93(16)
O(3)-C(29)-C(31)	109.66(16)
O(3)-C(29)-C(30)	104.57(14)
C(31)-C(29)-C(30)	119.41(16)
O(3)-C(29)-H(29)	107.6
C(31)-C(29)-H(29)	107.6

Chapter 6

C(30)-C(29)-H(29)	107.6
O(3A)-C(29A)-C(37A)	110.46(16)
O(3A)-C(29A)-C(30A)	104.67(15)
C(37A)-C(29A)-C(30A)	117.19(16)
O(3A)-C(29A)-H(29A)	108.1
C(37A)-C(29A)-H(29A)	108.1
C(30A)-C(29A)-H(29A)	108.1
N(1)-C(30)-C(37)	111.82(16)
N(1)-C(30)-C(29)	98.72(14)
C(37)-C(30)-C(29)	119.17(16)
N(1)-C(30)-H(30)	108.8
C(37)-C(30)-H(30)	108.8
C(29)-C(30)-H(30)	108.8
N(1A)-C(30A)-C(31A)	112.06(16)
N(1A)-C(30A)-C(29A)	99.59(14)
C(31A)-C(30A)-C(29A)	116.93(16)
N(1A)-C(30A)-H(30A)	109.3
C(31A)-C(30A)-H(30A)	109.3
C(29A)-C(30A)-H(30A)	109.3
C(36)-C(31)-C(32)	119.06(19)
C(36)-C(31)-C(29)	118.95(19)
C(32)-C(31)-C(29)	121.87(18)
C(36A)-C(31A)-C(32A)	119.10(19)
C(36A)-C(31A)-C(30A)	119.58(19)
C(32A)-C(31A)-C(30A)	121.32(17)
C(33)-C(32)-C(31)	120.34(19)
C(33)-C(32)-H(32)	119.8
C(31)-C(32)-H(32)	119.8
C(33A)-C(32A)-C(31A)	120.50(19)
C(33A)-C(32A)-H(32A)	119.8
C(31A)-C(32A)-H(32A)	119.8
C(34)-C(33)-C(32)	120.2(2)
C(34)-C(33)-H(33)	119.9
C(32)-C(33)-H(33)	119.9
C(32A)-C(33A)-C(34A)	119.9(2)
C(32A)-C(33A)-H(33A)	120.0
C(34A)-C(33A)-H(33A)	120.0
C(33)-C(34)-C(35)	119.8(2)
C(33)-C(34)-H(34)	120.1

Chapter 6

C(35)-C(34)-H(34)	120.1
C(35A)-C(34A)-C(33A)	119.7(2)
C(35A)-C(34A)-H(34A)	120.1
C(33A)-C(34A)-H(34A)	120.1
C(34)-C(35)-C(36)	120.00(19)
C(34)-C(35)-H(35)	120.0
C(36)-C(35)-H(35)	120.0
C(34A)-C(35A)-C(36A)	120.3(2)
C(34A)-C(35A)-H(35A)	119.8
C(36A)-C(35A)-H(35A)	119.8
C(35)-C(36)-C(31)	120.5(2)
C(35)-C(36)-H(36)	119.7
C(31)-C(36)-H(36)	119.7
C(31A)-C(36A)-C(35A)	120.4(2)
C(31A)-C(36A)-H(36A)	119.8
C(35A)-C(36A)-H(36A)	119.8
C(42)-C(37)-C(38)	119.00(19)
C(42)-C(37)-C(30)	118.50(18)
C(38)-C(37)-C(30)	122.42(17)
C(42A)-C(37A)-C(38A)	119.49(18)
C(42A)-C(37A)-C(29A)	121.63(18)
C(38A)-C(37A)-C(29A)	118.82(18)
C(39)-C(38)-C(37)	120.59(19)
C(39)-C(38)-H(38)	119.7
C(37)-C(38)-H(38)	119.7
C(39A)-C(38A)-C(37A)	120.13(19)
C(39A)-C(38A)-H(38A)	119.9
C(37A)-C(38A)-H(38A)	119.9
C(38)-C(39)-C(40)	120.1(2)
C(38)-C(39)-H(39)	120.0
C(40)-C(39)-H(39)	120.0
C(40A)-C(39A)-C(38A)	120.29(19)
C(40A)-C(39A)-H(39A)	119.9
C(38A)-C(39A)-H(39A)	119.9
C(41)-C(40)-C(39)	119.3(2)
C(41)-C(40)-H(40)	120.3
C(39)-C(40)-H(40)	120.3
C(41A)-C(40A)-C(39A)	119.60(19)
C(41A)-C(40A)-H(40A)	120.2

Chapter 6

C(39A)-C(40A)-H(40A)	120.2
C(40)-C(41)-C(42)	120.7(2)
C(40)-C(41)-H(41)	119.7
C(42)-C(41)-H(41)	119.7
C(40A)-C(41A)-C(42A)	120.3(2)
C(40A)-C(41A)-H(41A)	119.8
C(42A)-C(41A)-H(41A)	119.8
C(37)-C(42)-C(41)	120.3(2)
C(37)-C(42)-H(42)	119.9
C(41)-C(42)-H(42)	119.9
C(37A)-C(42A)-C(41A)	120.16(18)
C(37A)-C(42A)-H(42A)	119.9
C(41A)-C(42A)-H(42A)	119.9
C(28)-N(1)-C(2)	122.98(16)
C(28)-N(1)-C(30)	113.27(15)
C(2)-N(1)-C(30)	123.71(15)
C(28A)-N(1A)-C(2A)	123.03(16)
C(28A)-N(1A)-C(30A)	113.53(15)
C(2A)-N(1A)-C(30A)	121.96(15)
C(28)-O(3)-C(29)	109.50(14)
C(28A)-O(3A)-C(29A)	109.82(15)

Symmetry transformations used to generate equivalent atoms:

Table 16. Anisotropic displacement parameters ($\text{\AA}^2 \times 10^3$) for compound **390**. The anisotropic displacement factor exponent takes the form: $-2\pi^2 [h^2 a^{*2} U^{11} + \dots + 2 h k a^* b^* U^{12}]$

	U ¹¹	U ²²	U ³³	U ²³	U ¹³	U ¹²
C(1)	23(1)	20(1)	19(1)	-1(1)	-7(1)	-6(1)
C(1A)	21(1)	18(1)	20(1)	0(1)	-10(1)	-7(1)
C(1B)	27(1)	23(1)	41(1)	-6(1)	-3(1)	-4(1)
C(2)	25(1)	17(1)	18(1)	1(1)	-7(1)	-8(1)
C(2A)	24(1)	15(1)	19(1)	-1(1)	-7(1)	-6(1)
C(3)	23(1)	18(1)	18(1)	-2(1)	-7(1)	-6(1)
C(3A)	23(1)	19(1)	18(1)	-1(1)	-8(1)	-7(1)
C(4)	24(1)	17(1)	20(1)	-1(1)	-5(1)	-7(1)
C(4A)	21(1)	18(1)	18(1)	-1(1)	-5(1)	-5(1)
C(5)	29(1)	31(1)	22(1)	-1(1)	-10(1)	-10(1)
C(5A)	21(1)	15(1)	20(1)	0(1)	-6(1)	-6(1)
C(6)	25(1)	19(1)	24(1)	-4(1)	-4(1)	-6(1)
C(6A)	25(1)	20(1)	26(1)	-4(1)	-5(1)	-2(1)
C(7)	25(1)	17(1)	21(1)	-1(1)	-7(1)	-7(1)
C(7A)	42(1)	25(1)	25(1)	-6(1)	-3(1)	-5(1)
C(8)	23(1)	22(1)	35(1)	-7(1)	-5(1)	-3(1)
C(8A)	63(2)	30(1)	31(1)	-10(1)	-1(1)	0(1)
C(9)	20(1)	16(1)	26(1)	-4(1)	-4(1)	-5(1)
C(9A)	20(1)	17(1)	23(1)	-3(1)	-4(1)	-4(1)
C(10)	23(1)	20(1)	25(1)	-3(1)	-5(1)	-6(1)
C(10A)	22(1)	22(1)	23(1)	-1(1)	-6(1)	-6(1)
C(11)	25(1)	23(1)	26(1)	-4(1)	-7(1)	-4(1)
C(11A)	26(1)	22(1)	24(1)	-2(1)	-6(1)	-6(1)
C(12)	24(1)	25(1)	34(1)	-10(1)	-9(1)	-4(1)
C(12A)	19(1)	25(1)	30(1)	-9(1)	-7(1)	-2(1)
C(13)	23(1)	21(1)	37(1)	-6(1)	-3(1)	-7(1)
C(13A)	21(1)	23(1)	33(1)	-6(1)	-2(1)	-8(1)
C(14)	23(1)	19(1)	27(1)	-3(1)	-1(1)	-6(1)
C(14A)	22(1)	20(1)	25(1)	-2(1)	-2(1)	-6(1)
C(15)	31(1)	21(1)	24(1)	-3(1)	-2(1)	-9(1)
C(15A)	27(1)	23(1)	21(1)	1(1)	-3(1)	-9(1)
C(16)	20(1)	18(1)	26(1)	-3(1)	-8(1)	-3(1)
C(16A)	18(1)	14(1)	25(1)	-2(1)	-7(1)	-3(1)
C(17)	25(1)	20(1)	29(1)	-3(1)	-11(1)	1(1)

Chapter 6

C(17A)	23(1)	19(1)	25(1)	-1(1)	-8(1)	-5(1)
C(18)	33(1)	28(1)	33(1)	-11(1)	-17(1)	4(1)
C(18A)	29(1)	23(1)	26(1)	-4(1)	-11(1)	-3(1)
C(19)	30(1)	19(1)	45(1)	-9(1)	-18(1)	1(1)
C(19A)	26(1)	19(1)	37(1)	-7(1)	-14(1)	-4(1)
C(20)	26(1)	19(1)	40(1)	-2(1)	-11(1)	-4(1)
C(20A)	24(1)	16(1)	35(1)	0(1)	-11(1)	-5(1)
C(21)	26(1)	19(1)	28(1)	-3(1)	-8(1)	-5(1)
C(21A)	24(1)	19(1)	26(1)	0(1)	-7(1)	-6(1)
C(22)	24(1)	21(1)	19(1)	0(1)	-5(1)	-9(1)
C(22A)	21(1)	20(1)	20(1)	2(1)	-4(1)	-7(1)
C(23)	31(1)	23(1)	22(1)	0(1)	-8(1)	-10(1)
C(23A)	26(1)	22(1)	22(1)	-1(1)	-7(1)	-7(1)
C(24)	37(1)	30(1)	22(1)	1(1)	-11(1)	-16(1)
C(24A)	26(1)	30(1)	24(1)	6(1)	-10(1)	-8(1)
C(25)	34(1)	35(1)	26(1)	5(1)	-15(1)	-14(1)
C(26)	31(1)	26(1)	28(1)	5(1)	-11(1)	-7(1)
C(26A)	26(1)	23(1)	29(1)	3(1)	-9(1)	-4(1)
C(27)	25(1)	23(1)	23(1)	-1(1)	-7(1)	-8(1)
C(27A)	24(1)	21(1)	25(1)	1(1)	-7(1)	-7(1)
C(28)	25(1)	18(1)	18(1)	-2(1)	-5(1)	-6(1)
C(28A)	27(1)	19(1)	22(1)	-2(1)	-8(1)	-9(1)
C(29)	21(1)	20(1)	19(1)	-1(1)	-4(1)	-5(1)
C(29A)	24(1)	23(1)	20(1)	-3(1)	-4(1)	-8(1)
C(30)	19(1)	16(1)	22(1)	-2(1)	-5(1)	-6(1)
C(30A)	21(1)	16(1)	24(1)	-3(1)	-7(1)	-5(1)
C(31)	22(1)	22(1)	17(1)	1(1)	-3(1)	-8(1)
C(31A)	23(1)	16(1)	20(1)	0(1)	-5(1)	-7(1)
C(32)	23(1)	23(1)	27(1)	-1(1)	-5(1)	-3(1)
C(32A)	27(1)	20(1)	25(1)	-2(1)	-8(1)	-3(1)
C(33)	27(1)	19(1)	27(1)	-3(1)	-3(1)	-3(1)
C(33A)	36(1)	19(1)	27(1)	-6(1)	-5(1)	-3(1)
C(34)	29(1)	24(1)	28(1)	-4(1)	-6(1)	-9(1)
C(34A)	52(1)	30(1)	23(1)	-6(1)	-13(1)	-2(1)
C(35)	22(1)	29(1)	34(1)	-7(1)	-6(1)	-5(1)
C(35A)	61(2)	35(1)	29(1)	-6(1)	-24(1)	10(1)
C(36)	24(1)	21(1)	26(1)	-4(1)	-5(1)	-3(1)
C(36A)	40(1)	23(1)	27(1)	-4(1)	-13(1)	2(1)
C(37)	20(1)	18(1)	20(1)	0(1)	-4(1)	-8(1)

Chapter 6

C(37A)	21(1)	22(1)	18(1)	-3(1)	-2(1)	-8(1)
C(38)	26(1)	22(1)	24(1)	-1(1)	-6(1)	-3(1)
C(38A)	25(1)	21(1)	26(1)	-1(1)	-6(1)	-6(1)
C(39)	31(1)	26(1)	28(1)	-8(1)	-3(1)	-4(1)
C(39A)	23(1)	26(1)	30(1)	-3(1)	-8(1)	-6(1)
C(40)	35(1)	33(1)	21(1)	-5(1)	-5(1)	-12(1)
C(40A)	26(1)	22(1)	32(1)	-7(1)	-5(1)	-9(1)
C(41)	32(1)	27(1)	24(1)	1(1)	-12(1)	-10(1)
C(41A)	26(1)	19(1)	31(1)	-4(1)	-4(1)	-5(1)
C(42)	23(1)	19(1)	26(1)	-2(1)	-7(1)	-6(1)
C(42A)	21(1)	23(1)	24(1)	-3(1)	-4(1)	-4(1)
N(1)	19(1)	18(1)	22(1)	2(1)	-6(1)	-7(1)
N(1A)	21(1)	16(1)	23(1)	2(1)	-8(1)	-8(1)
O(1)	26(1)	23(1)	24(1)	-4(1)	-2(1)	-3(1)
O(1A)	22(1)	23(1)	22(1)	-3(1)	-3(1)	-8(1)
O(2)	26(1)	26(1)	28(1)	0(1)	-12(1)	-7(1)
O(3)	24(1)	22(1)	24(1)	4(1)	-9(1)	-9(1)
O(2A)	33(1)	26(1)	32(1)	5(1)	-18(1)	-12(1)
O(3A)	30(1)	26(1)	24(1)	6(1)	-12(1)	-15(1)

Table 17. Hydrogen coordinates ($\times 10^4$) and isotropic displacement parameters ($\text{\AA}^2 \times 10^3$) for compound **390**.

	x	y	z	U(eq)
H(1B1)	7303	-1060	7155	46
H(1B2)	8756	-513	7022	46
H(1B3)	7868	-231	6292	46
H(5)	5183	9836	584	31
H(6A)	5499	1310	6432	27
H(6B)	4835	489	7274	27
H(6A1)	9670	6007	2404	28
H(6A2)	10851	6871	1996	28
H(7A1)	8703	6590	1129	37
H(7A2)	10010	7333	721	37
H(8A)	7460	1480	7048	32
H(8B)	6800	642	7884	32
H(8A1)	11679	5461	855	64
H(8A2)	10609	5393	272	64
H(8A3)	10351	4734	1223	64
H(10)	5224	2524	8774	27
H(10A)	9656	7813	3760	26
H(11)	6710	2761	9649	29
H(11A)	11327	7822	4582	29
H(12)	8513	4020	9143	31
H(12A)	13115	9098	4106	28
H(13)	8839	5006	7736	32
H(13A)	13259	10316	2771	30
H(14)	7375	4769	6856	28
H(14A)	11577	10316	1954	27
H(15D)	6737	3306	6096	37
H(15E)	5894	4672	6030	37
H(15F)	5196	3607	5848	37
H(15A)	10772	9124	1109	36
H(15B)	9882	10452	1215	36
H(15C)	9162	9459	959	36
H(17)	3405	5204	8952	29
H(17A)	7424	10071	4325	26

Chapter 6

H(18)	4181	6876	9279	36
H(18A)	8071	11462	5004	30
H(19)	5234	8310	8196	36
H(19A)	9068	13182	4213	31
H(20)	5421	8114	6785	33
H(20A)	9425	13471	2736	29
H(21)	4578	6490	6455	29
H(21A)	8743	12100	2055	27
H(23)	2956	3362	6208	29
H(23A)	6900	9033	1418	28
H(24)	1295	3989	5324	34
H(24A)	3881	11818	656	32
H(25)	-221	5885	5354	36
H(26)	-41	7185	6284	34
H(26A)	4297	12997	1584	31
H(27)	1665	6594	7140	28
H(27A)	6000	12198	2432	28
H(29)	39	720	9547	24
H(29A)	4296	6097	4427	26
H(30)	338	2041	8355	23
H(30A)	4757	7416	3240	23
H(32)	1532	-2048	8704	29
H(32A)	6945	4700	2398	29
H(33)	200	-3573	8679	30
H(33A)	7029	4212	1065	33
H(34)	-2338	-3176	8975	32
H(34A)	5591	5489	176	41
H(35)	-3552	-1254	9318	33
H(35A)	4079	7247	626	50
H(36)	-2225	270	9352	29
H(36A)	4017	7751	1951	36
H(38)	2550	-640	7454	29
H(38A)	2492	5860	3425	28
H(39)	2707	-1003	6080	34
H(39A)	1194	4375	3283	31
H(40)	1383	400	5176	34
H(40A)	2053	2282	3634	31
H(41)	-95	2140	5666	32
H(41A)	4220	1679	4123	31

Chapter 6

H(42)	-274	2497	7045	27
H(42A)	5542	3159	4250	27

Table 18. Torsion angles [°] for compound **390**.

O(1)-C(1)-C(2)-C(3)	-170.59(19)
C(7)-C(1)-C(2)-C(3)	13.3(2)
O(1)-C(1)-C(2)-N(1)	7.0(3)
C(7)-C(1)-C(2)-N(1)	-169.10(16)
O(1A)-C(1A)-C(2A)-C(3A)	-169.78(18)
C(5A)-C(1A)-C(2A)-C(3A)	11.8(2)
O(1A)-C(1A)-C(2A)-N(1A)	5.9(3)
C(5A)-C(1A)-C(2A)-N(1A)	-172.46(15)
N(1)-C(2)-C(3)-C(6)	5.3(3)
C(1)-C(2)-C(3)-C(6)	-177.38(18)
N(1)-C(2)-C(3)-C(4)	-172.97(17)
C(1)-C(2)-C(3)-C(4)	4.4(2)
N(1A)-C(2A)-C(3A)-C(6A)	0.5(3)
C(1A)-C(2A)-C(3A)-C(6A)	175.76(18)
N(1A)-C(2A)-C(3A)-C(4A)	-173.67(17)
C(1A)-C(2A)-C(3A)-C(4A)	1.6(2)
C(2)-C(3)-C(4)-C(15)	-142.33(18)
C(6)-C(3)-C(4)-C(15)	39.3(2)
C(2)-C(3)-C(4)-C(9)	94.98(19)
C(6)-C(3)-C(4)-C(9)	-83.4(2)
C(2)-C(3)-C(4)-C(7)	-19.2(2)
C(6)-C(3)-C(4)-C(7)	162.42(17)
C(2A)-C(3A)-C(4A)-C(15A)	-135.97(18)
C(6A)-C(3A)-C(4A)-C(15A)	49.6(2)
C(2A)-C(3A)-C(4A)-C(9A)	103.04(18)
C(6A)-C(3A)-C(4A)-C(9A)	-71.4(2)
C(2A)-C(3A)-C(4A)-C(5A)	-13.5(2)
C(6A)-C(3A)-C(4A)-C(5A)	172.09(17)
O(1A)-C(1A)-C(5A)-C(16A)	43.4(3)
C(2A)-C(1A)-C(5A)-C(16A)	-138.24(16)
O(1A)-C(1A)-C(5A)-C(22A)	-78.1(2)
C(2A)-C(1A)-C(5A)-C(22A)	100.23(17)
O(1A)-C(1A)-C(5A)-C(4A)	162.90(18)
C(2A)-C(1A)-C(5A)-C(4A)	-18.74(18)
C(3A)-C(4A)-C(5A)-C(16A)	140.59(15)
C(15A)-C(4A)-C(5A)-C(16A)	-97.65(18)
C(9A)-C(4A)-C(5A)-C(16A)	26.3(2)

Chapter 6

C(3A)-C(4A)-C(5A)-C(1A)	19.01(17)
C(15A)-C(4A)-C(5A)-C(1A)	140.76(16)
C(9A)-C(4A)-C(5A)-C(1A)	-95.27(17)
C(3A)-C(4A)-C(5A)-C(22A)	-89.49(18)
C(15A)-C(4A)-C(5A)-C(22A)	32.3(2)
C(9A)-C(4A)-C(5A)-C(22A)	156.23(15)
C(2)-C(3)-C(6)-C(8)	-117.8(2)
C(4)-C(3)-C(6)-C(8)	60.2(2)
C(2A)-C(3A)-C(6A)-C(7A)	97.6(2)
C(4A)-C(3A)-C(6A)-C(7A)	-88.8(2)
O(1)-C(1)-C(7)-C(16)	41.1(3)
C(2)-C(1)-C(7)-C(16)	-142.94(16)
O(1)-C(1)-C(7)-C(22)	-79.3(2)
C(2)-C(1)-C(7)-C(22)	96.74(17)
O(1)-C(1)-C(7)-C(4)	160.37(19)
C(2)-C(1)-C(7)-C(4)	-23.62(19)
C(3)-C(4)-C(7)-C(16)	149.02(16)
C(15)-C(4)-C(7)-C(16)	-89.0(2)
C(9)-C(4)-C(7)-C(16)	34.2(2)
C(3)-C(4)-C(7)-C(1)	25.15(18)
C(15)-C(4)-C(7)-C(1)	147.12(16)
C(9)-C(4)-C(7)-C(1)	-89.64(17)
C(3)-C(4)-C(7)-C(22)	-83.56(19)
C(15)-C(4)-C(7)-C(22)	38.4(2)
C(9)-C(4)-C(7)-C(22)	161.65(16)
C(3A)-C(6A)-C(7A)-C(8A)	-174.09(19)
C(3)-C(6)-C(8)-C(1B)	-179.17(18)
C(3)-C(4)-C(9)-C(14)	151.71(18)
C(15)-C(4)-C(9)-C(14)	27.8(3)
C(7)-C(4)-C(9)-C(14)	-97.7(2)
C(3)-C(4)-C(9)-C(10)	-32.2(3)
C(15)-C(4)-C(9)-C(10)	-156.12(19)
C(7)-C(4)-C(9)-C(10)	78.4(2)
C(3A)-C(4A)-C(9A)-C(14A)	146.87(19)
C(15A)-C(4A)-C(9A)-C(14A)	24.6(3)
C(5A)-C(4A)-C(9A)-C(14A)	-101.1(2)
C(3A)-C(4A)-C(9A)-C(10A)	-35.5(2)
C(15A)-C(4A)-C(9A)-C(10A)	-157.76(18)
C(5A)-C(4A)-C(9A)-C(10A)	76.5(2)

Chapter 6

C(14)-C(9)-C(10)-C(11)	1.2(3)
C(4)-C(9)-C(10)-C(11)	-175.03(19)
C(14A)-C(9A)-C(10A)-C(11A)	1.4(3)
C(4A)-C(9A)-C(10A)-C(11A)	-176.30(19)
C(9)-C(10)-C(11)-C(12)	-0.1(3)
C(9A)-C(10A)-C(11A)-C(12A)	-0.2(3)
C(10)-C(11)-C(12)-C(13)	-0.8(3)
C(10A)-C(11A)-C(12A)-C(13A)	-1.2(3)
C(11)-C(12)-C(13)-C(14)	0.6(3)
C(11A)-C(12A)-C(13A)-C(14A)	1.5(3)
C(12)-C(13)-C(14)-C(9)	0.5(3)
C(10)-C(9)-C(14)-C(13)	-1.4(3)
C(4)-C(9)-C(14)-C(13)	174.89(19)
C(12A)-C(13A)-C(14A)-C(9A)	-0.3(3)
C(10A)-C(9A)-C(14A)-C(13A)	-1.2(3)
C(4A)-C(9A)-C(14A)-C(13A)	176.53(19)
C(1)-C(7)-C(16)-C(17)	16.7(3)
C(22)-C(7)-C(16)-C(17)	131.67(19)
C(4)-C(7)-C(16)-C(17)	-97.8(2)
C(1)-C(7)-C(16)-C(21)	-169.14(17)
C(22)-C(7)-C(16)-C(21)	-54.1(2)
C(4)-C(7)-C(16)-C(21)	76.4(2)
C(1A)-C(5A)-C(16A)-C(17A)	13.7(3)
C(22A)-C(5A)-C(16A)-C(17A)	128.47(19)
C(4A)-C(5A)-C(16A)-C(17A)	-100.5(2)
C(1A)-C(5A)-C(16A)-C(21A)	-171.90(17)
C(22A)-C(5A)-C(16A)-C(21A)	-57.1(2)
C(4A)-C(5A)-C(16A)-C(21A)	73.9(2)
C(21)-C(16)-C(17)-C(18)	-0.3(3)
C(7)-C(16)-C(17)-C(18)	173.91(18)
C(21A)-C(16A)-C(17A)-C(18A)	0.1(3)
C(5A)-C(16A)-C(17A)-C(18A)	174.57(18)
C(16)-C(17)-C(18)-C(19)	-1.2(3)
C(16A)-C(17A)-C(18A)-C(19A)	-0.2(3)
C(17)-C(18)-C(19)-C(20)	1.4(3)
C(17A)-C(18A)-C(19A)-C(20A)	-0.3(3)
C(18)-C(19)-C(20)-C(21)	-0.3(3)
C(18A)-C(19A)-C(20A)-C(21A)	0.8(3)
C(19)-C(20)-C(21)-C(16)	-1.2(3)

Chapter 6

C(17)-C(16)-C(21)-C(20)	1.4(3)
C(7)-C(16)-C(21)-C(20)	-173.05(18)
C(19A)-C(20A)-C(21A)-C(16A)	-0.9(3)
C(17A)-C(16A)-C(21A)-C(20A)	0.5(3)
C(5A)-C(16A)-C(21A)-C(20A)	-174.19(18)
C(16)-C(7)-C(22)-C(23)	160.50(18)
C(1)-C(7)-C(22)-C(23)	-75.2(2)
C(4)-C(7)-C(22)-C(23)	33.5(3)
C(16)-C(7)-C(22)-C(27)	-27.8(2)
C(1)-C(7)-C(22)-C(27)	96.4(2)
C(4)-C(7)-C(22)-C(27)	-154.84(17)
C(16A)-C(5A)-C(22A)-C(27A)	-14.9(2)
C(1A)-C(5A)-C(22A)-C(27A)	107.34(19)
C(4A)-C(5A)-C(22A)-C(27A)	-143.80(18)
C(16A)-C(5A)-C(22A)-C(23A)	173.82(17)
C(1A)-C(5A)-C(22A)-C(23A)	-64.0(2)
C(4A)-C(5A)-C(22A)-C(23A)	44.9(2)
C(27)-C(22)-C(23)-C(24)	2.9(3)
C(7)-C(22)-C(23)-C(24)	174.70(18)
C(24A)-C(5)-C(23A)-C(22A)	-0.6(3)
C(27A)-C(22A)-C(23A)-C(5)	1.9(3)
C(5A)-C(22A)-C(23A)-C(5)	173.43(18)
C(22)-C(23)-C(24)-C(25)	-2.1(3)
C(23A)-C(5)-C(24A)-C(26A)	-0.5(3)
C(23)-C(24)-C(25)-C(26)	0.1(3)
C(24)-C(25)-C(26)-C(27)	0.9(3)
C(5)-C(24A)-C(26A)-C(27A)	0.2(3)
C(25)-C(26)-C(27)-C(22)	0.0(3)
C(23)-C(22)-C(27)-C(26)	-1.9(3)
C(7)-C(22)-C(27)-C(26)	-174.09(18)
C(23A)-C(22A)-C(27A)-C(26A)	-2.2(3)
C(5A)-C(22A)-C(27A)-C(26A)	-173.82(18)
C(24A)-C(26A)-C(27A)-C(22A)	1.2(3)
O(3)-C(29)-C(30)-N(1)	-21.00(18)
C(31)-C(29)-C(30)-N(1)	-144.07(18)
O(3)-C(29)-C(30)-C(37)	100.09(19)
C(31)-C(29)-C(30)-C(37)	-23.0(3)
O(3A)-C(29A)-C(30A)-N(1A)	-16.49(19)
C(37A)-C(29A)-C(30A)-N(1A)	-139.22(18)

Chapter 6

O(3A)-C(29A)-C(30A)-C(31A)	104.39(18)
C(37A)-C(29A)-C(30A)-C(31A)	-18.3(3)
O(3)-C(29)-C(31)-C(36)	149.98(17)
C(30)-C(29)-C(31)-C(36)	-89.5(2)
O(3)-C(29)-C(31)-C(32)	-26.1(3)
C(30)-C(29)-C(31)-C(32)	94.5(2)
N(1A)-C(30A)-C(31A)-C(36A)	-124.4(2)
C(29A)-C(30A)-C(31A)-C(36A)	121.5(2)
N(1A)-C(30A)-C(31A)-C(32A)	55.6(2)
C(29A)-C(30A)-C(31A)-C(32A)	-58.4(2)
C(36)-C(31)-C(32)-C(33)	1.1(3)
C(29)-C(31)-C(32)-C(33)	177.13(19)
C(36A)-C(31A)-C(32A)-C(33A)	0.2(3)
C(30A)-C(31A)-C(32A)-C(33A)	-179.82(18)
C(31)-C(32)-C(33)-C(34)	-0.2(3)
C(31A)-C(32A)-C(33A)-C(34A)	-0.4(3)
C(32)-C(33)-C(34)-C(35)	-0.6(3)
C(32A)-C(33A)-C(34A)-C(35A)	0.0(4)
C(33)-C(34)-C(35)-C(36)	0.4(3)
C(33A)-C(34A)-C(35A)-C(36A)	0.4(4)
C(34)-C(35)-C(36)-C(31)	0.6(3)
C(32)-C(31)-C(36)-C(35)	-1.3(3)
C(29)-C(31)-C(36)-C(35)	-177.46(19)
C(32A)-C(31A)-C(36A)-C(35A)	0.2(3)
C(30A)-C(31A)-C(36A)-C(35A)	-179.7(2)
C(34A)-C(35A)-C(36A)-C(31A)	-0.6(4)
N(1)-C(30)-C(37)-C(42)	-117.67(19)
C(29)-C(30)-C(37)-C(42)	128.09(19)
N(1)-C(30)-C(37)-C(38)	59.0(2)
C(29)-C(30)-C(37)-C(38)	-55.3(3)
O(3A)-C(29A)-C(37A)-C(42A)	4.7(3)
C(30A)-C(29A)-C(37A)-C(42A)	124.4(2)
O(3A)-C(29A)-C(37A)-C(38A)	-178.17(17)
C(30A)-C(29A)-C(37A)-C(38A)	-58.5(2)
C(42)-C(37)-C(38)-C(39)	-0.7(3)
C(30)-C(37)-C(38)-C(39)	-177.28(18)
C(42A)-C(37A)-C(38A)-C(39A)	0.0(3)
C(29A)-C(37A)-C(38A)-C(39A)	-177.20(19)
C(37)-C(38)-C(39)-C(40)	0.6(3)

Chapter 6

C(37A)-C(38A)-C(39A)-C(40A)	0.3(3)
C(38)-C(39)-C(40)-C(41)	-0.2(3)
C(38A)-C(39A)-C(40A)-C(41A)	-0.1(3)
C(39)-C(40)-C(41)-C(42)	-0.1(3)
C(39A)-C(40A)-C(41A)-C(42A)	-0.3(3)
C(38)-C(37)-C(42)-C(41)	0.3(3)
C(30)-C(37)-C(42)-C(41)	177.05(17)
C(40)-C(41)-C(42)-C(37)	0.1(3)
C(38A)-C(37A)-C(42A)-C(41A)	-0.5(3)
C(29A)-C(37A)-C(42A)-C(41A)	176.67(19)
C(40A)-C(41A)-C(42A)-C(37A)	0.6(3)
O(2)-C(28)-N(1)-C(2)	-2.1(3)
O(3)-C(28)-N(1)-C(2)	178.30(17)
O(2)-C(28)-N(1)-C(30)	175.6(2)
O(3)-C(28)-N(1)-C(30)	-4.0(2)
C(3)-C(2)-N(1)-C(28)	62.5(3)
C(1)-C(2)-N(1)-C(28)	-114.7(2)
C(3)-C(2)-N(1)-C(30)	-115.0(2)
C(1)-C(2)-N(1)-C(30)	67.9(2)
C(37)-C(30)-N(1)-C(28)	-110.50(19)
C(29)-C(30)-N(1)-C(28)	15.8(2)
C(37)-C(30)-N(1)-C(2)	67.2(2)
C(29)-C(30)-N(1)-C(2)	-166.47(18)
O(2A)-C(28A)-N(1A)-C(2A)	-14.2(4)
O(3A)-C(28A)-N(1A)-C(2A)	167.45(18)
O(2A)-C(28A)-N(1A)-C(30A)	179.4(2)
O(3A)-C(28A)-N(1A)-C(30A)	1.1(2)
C(3A)-C(2A)-N(1A)-C(28A)	74.0(3)
C(1A)-C(2A)-N(1A)-C(28A)	-101.0(2)
C(3A)-C(2A)-N(1A)-C(30A)	-120.8(2)
C(1A)-C(2A)-N(1A)-C(30A)	64.2(2)
C(31A)-C(30A)-N(1A)-C(28A)	-114.39(19)
C(29A)-C(30A)-N(1A)-C(28A)	10.0(2)
C(31A)-C(30A)-N(1A)-C(2A)	79.1(2)
C(29A)-C(30A)-N(1A)-C(2A)	-156.56(17)
O(2)-C(28)-O(3)-C(29)	168.98(19)
N(1)-C(28)-O(3)-C(29)	-11.4(2)
C(31)-C(29)-O(3)-C(28)	150.15(16)
C(30)-C(29)-O(3)-C(28)	21.0(2)

Chapter 6

O(2A)-C(28A)-O(3A)-C(29A)	168.5(2)
N(1A)-C(28A)-O(3A)-C(29A)	-13.0(2)
C(37A)-C(29A)-O(3A)-C(28A)	145.86(17)
C(30A)-C(29A)-O(3A)-C(28A)	18.9(2)

Symmetry transformations used to generate equivalent atoms: